A PRACTICAL GUIDE TO SELECTING GAMETES AND EMBRYOS

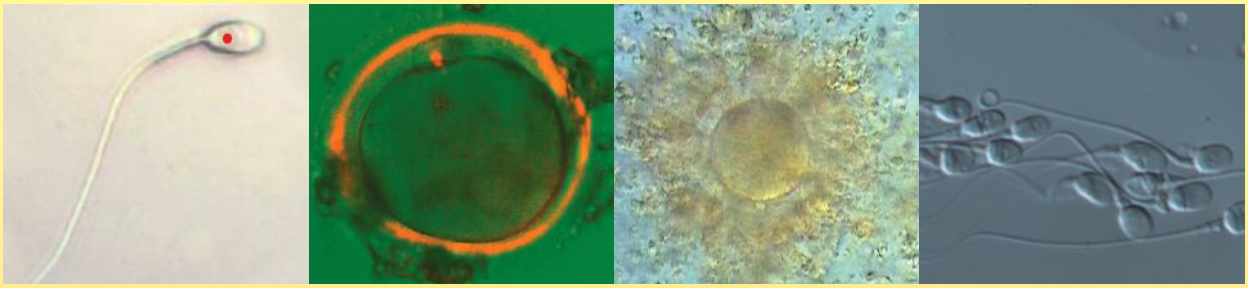

EDITED BY **MARKUS MONTAG**

CRC Press
Taylor & Francis Group

A PRACTICAL GUIDE TO SELECTING GAMETES AND EMBRYOS

A PRACTICAL GUIDE TO SELECTING GAMETES AND EMBRYOS

Edited by

Markus Montag, PhD
iLabCoMM GmbH, International Reprolab Consulting
St. Augustin, Germany

CRC Press
Taylor & Francis Group
Boca Raton London New York

CRC Press is an imprint of the
Taylor & Francis Group, an **informa** business

CRC Press
Taylor & Francis Group
6000 Broken Sound Parkway NW, Suite 300
Boca Raton, FL 33487-2742

Version Date: 20140224

International Standard Book Number-13: 978-1-84214-548-7 (eBook - PDF)

Contents

Preface

The development of current technologies to identify the most viable oocyte, sperm, or embryo is one of the most discussed topics in assisted reproduction conferences and symposia. However, most of these, sometimes fancy, technologies are yet to be introduced in the daily routine of an in vitro fertilization laboratory, and the reasons for this are many.

So, from the perspective of the laboratory, it would be helpful to have an overview of ready-to-use assisted reproduction technologies, with practical guidance from those who have knowledge and expertise in the relevant field. The resultant textbook, *A Practical Guide to Selecting Gametes and Embryos*, has compiled such practical tips, accompanied by numerous figures and descriptions of methods. This book differentiates between noninvasive and invasive techniques; however, to my understanding, even the most sophisticated selection strategies may fail if they are not based on a sound start. It happens frequently—that is, by looking at the most ideal endpoint, we simply overlook the way to reach that endpoint. Practically speaking, the starting point involves good practice in the laboratory setting in handling gametes and embryos with special focus on quality measures. This starting point is an absolute prerequisite to be able to apply selection strategies that make sense.

I thank all the authors who have devoted their time to contribute to this illustrated textbook. They are all active in their respective fields with numerous obligations; hence, taking on the additional task of contributing to this book is a commitment that cannot be praised enough.

I also thank Robert Peden (Senior Editor for Reproductive Medicine, CRC Press) for his enthusiasm, support, and continuous efforts in bringing this project to life.

Markus Montag

Contributors

Carmela Albert
Instituto Valenciano de Infertilidad
Universidad de Valencia
Valencia, Spain

Belén Aparicio
Instituto Valenciano de Infertilidad
Universidad de Valencia
Valencia, Spain

Magnus Bach
IVF Centers Prof. Zech
Bregenz, Austria

Başak Balaban
Assisted Reproduction Unit
VKF American Hospital
Istanbul, Turkey

Çağrı Beyazyürek
Reproductive Endocrinology and Genetics Center
Istanbul Memorial Hospital
Istanbul, Turkey

Alison Campbell
CARE Fertility
Nottingham, United Kingdom

Arancha Delgado
Instituto Valenciano de Infertilidad
Universidad de Valencia
Valencia, Spain

Anick De Vos
Centrum voor Reproductieve Geneeskunde
Universitair Ziekenhuis Brussel
Brussels, Belgium

Thomas Ebner
Landes-, Frauen- und Kinderklinik
Kinderwunsch Zentrum
Linz, Austria

Olivier Gaspard
Department of Gynaecology and Obstetrics
Centre of AMP (CPMA)
University of Liège
Liège, Belgium

Martin Greuner
Fertility Center IVF-Saar
Saarbrücken-Kaiserslautern, Germany

Darren Griffin
School of Biosciences
University of Kent
Canterbury, United Kingdom

Gary Harton
School of Biosciences
University of Kent
Canterbury, United Kingdom

Benedetta Iussig
GENERA Centres for Reproductive Medicine
Rome, Italy

Lars Johansson
Origio a/s
Måløv, Denmark

Gayle Jones
Centre for Human Reproduction
Genesis Hospital
Athens, Greece

and

Department of Anatomy and Developmental Biology
Monash University, Clayton
Victoria, Australia

Semra Kahraman
Reproductive Endocrinology and Genetics Center
Istanbul Memorial Hospital
Istanbul, Turkey

Sabine Kliesch
Department of Clinical Andrology
Centre of Reproductive Medicine and Andrology
University Hospital of Münster
Münster, Germany

Maria Köster
Department of Gynecological Endocrinology and Reproductive Medicine
University Women's Hospital Bonn
Bonn, Germany

Bernard Lejeune
Assisted Reproductive Department
Centre Hospitalier Inter Régional Cavell (CHIREC)
Braine l'Alleud, Belgium

Jana Liebenthron
Department of Gynecological Endocrinology and Reproductive Medicine
University Women's Hospital Bonn
Bonn, Germany

M. Cristina Magli
Società Italiana Studi Medicina della Riproduzione
Bologna, Italy

Con Mallidis
Centre of Reproductive Medicine and Andrology
University Hospital of Münster
Münster, Germany

Steve McArthur
Genea Fertility
Sydney, Australia

Marcos Meseguer
Instituto Valenciano de Infertilidad
Universidad de Valencia
Valencia, Spain

Markus Montag
iLabCoMM GmbH (International Reprolab Consulting)
St. Augustin, Germany

Anton Neyer
IVF Centers Prof. Zech
Bregenz, Austria

Verena Nordhoff
Department of Clinical Andrology
Centre of Reproductive Medicine and Andrology
University Hospital of Münster
Münster, Germany

Christian Ottolini
The London Bridge Fertility, Gynaecology and Genetics Centre
London, United Kingdom
and
School of Biosciences
University of Kent
Canterbury, United Kingdom

Françoise Puissant
Assisted Reproductive Department
Centre Hospitalier Inter Régional Cavell (CHIREC)
Braine l'Alleud, Belgium

Laura Rienzi
GENERA Centres for Reproductive Medicine
Rome, Italy

Victoria Sánchez
Centre of Reproductive Medicine and Andrology
University Hospital of Münster
Münster, Germany

Maximilian Schuff
IVF Centers Prof. Zech
Bregenz, Austria

Emre Seli
Department of Obstetrics, Gynecology, and Reproductive Sciences
Yale School of Medicine
New Haven, Connecticut

Astrid Stecher
IVF Centers Prof. Zech
Bregenz, Austria

Jason E. Swain
Fertility Lab Sciences
National Foundation for Fertility Research
Colorado Center for Reproductive Medicine
Lone Tree, Colorado

Alberto Tejera
Instituto Valenciano de Infertilidad
Universidad de Valencia
Valencia, Spain

Alan R. Thornhill
Assisted Conception Unit
Guy's Hospital
London, United Kingdom
and
School of Biosciences
University of Kent
Canterbury, United Kingdom

Filippo Maria Ubaldi
GENERA Centres for Reproductive Medicine
Rome, Italy

Asli Uyar
Department of Obstetrics, Gynecology, and Reproductive Sciences
Yale School of Medicine
New Haven, Connecticut

Pierre Vanderzwalmen
IVF Centers Prof. Zech
Bregenz, Austria
and
Assisted Reproductive Department
Centre Hospitalier Inter Régional Cavell (CHIREC)
Braine l'Alleud, Belgium

Sabine Vanderzwalmen
Assisted Reproductive Department
Centre Hospitalier Inter Régional Cavell (CHIREC)
Braine l'Alleud, Belgium

Barbara Wirleitner
IVF Centers Prof. Zech
Bregenz, Austria

Joachim Wistuba
Centre of Reproductive Medicine and Andrology
University Hospital of Münster
Münster, Germany

Nicolas H. Zech
IVF Centers Prof. Zech
Bregenz, Austria

1

Handling Gametes and Embryos: Sperm Collection and Preparation Techniques

Verena Nordhoff, Con Mallidis, and Sabine Kliesch

Introduction

Spermatozoa are an integral part of assisted reproduction techniques (ARTs). As such, the collection and preparation of spermatozoa should be of high quality standards to ensure the best possible treatment outcome. It is therefore important that the protocols for the preparation and the use of sperm are standardized and dependable. A series of such standards exists in the form of guidelines and procedures comprising the World Health Organization (WHO) laboratory manual [1].

It is important therefore that protocols for the preparation and the use of sperm are standardized and dependable.

The following sections provide a comprehensive description of the steps undertaken for the analysis of a semen sample. They are not meant to be as detailed as the WHO manual nor replace the same [1]; rather, they act as an adjunct. For specific details and explanations for the choice of techniques, the WHO manual should be referred to.

Semen Analysis

Semen consists of two major fractions: spermatozoa from the testis, making up a small fraction of the ejaculate, and seminal fluid from the accessory glands, making up the major portion of the ejaculate [2].

The proper analysis of the semen sample necessitates the evaluation of the following parameters:

- Volume (or weight)
- Liquefaction
- Viscosity
- Appearance
- pH
- Aggregation or agglutination
- Motility
- Concentration
- Morphology

For ARTs, the most important of the aforementioned parameters are motility, concentration, and morphology.

Normozoospermia is defined as a sample containing more than 39 million spermatozoa/ejaculate or 15 million/mL, with >32% of the spermatozoa being progressively motile (PR) and >4% having normal forms. If the total sperm count is below the reference value, the sample is classified as oligozoospermic (O); if motility is

lower, it is considered as asthenozoospermic (A), and if morphology is less than the defined cutoff, it is designated teratozoospermic (T). Combinations of the conditions exist and are classified accordingly (e.g., OA, OT, OAT).

The most important sperm parameters for ARTs are motility, concentration, and morphology.

Biochemical markers of seminal fluid can be determined to evaluate the function of the epididymis, seminal vesicles, and prostate [1]. Biochemical markers may help to differentiate between obstructive and nonobstructive restrictions of semen quality.

Analysis of the Native Ejaculate

For assisted reproduction, the native semen must be collected in a sterile container to allow either the exact measurement of the volume (e.g., a cylinder with scale) or the determination of the weight of a sample. Directly after collection, semen is normally coagulated, but it liquefies after 30–60 min at room temperature (37°C). If liquefaction takes >60 min, this should be noted. If no liquefaction is obvious, then the use of a proteolytic enzyme such as bromelain may be necessary. A process that involves mixing equal volumes of ejaculate and a 10 IU/mL bromelain/medium (e.g., an HEPES-buffered medium) solution followed by incubation at 37°C for 10 min. If this process is undertaken, it must be duly noted because it might affect other semen parameters, most notably motility and final sperm concentration (due to the dilution, the original concentration is halved).

Because semen is very heterogeneous, it is extremely important that the sample is mixed thoroughly before starting the different facets of the analysis. Only a very well mixed sample will provide data that are representative and reproducible (i.e., when duplicate samplings are taken). After liquefaction, the semen sample should be evaluated for its viscosity and appearance. Viscosity is determined by using a glass rod to mix the sample. If threads of >2 cm can be seen after pulling the rod out of the semen, then the viscosity is higher than what is considered normal, and represents a finding that should be recorded. Normal-appearing semen is gray-opalescent; any variation from this color must be noted because it can be indicative of some underlying pathology. For example, a brown color is symptomatic of the presence of blood cells. The final visual assessment is that of pH, an assessment that must be performed quickly after liquefaction because the pH of semen changes with time. The process involves placement of one drop of mixed semen unto pH paper with a range of 6.0–10.0. A pH value between 7.2 and 8.0 is accepted as normal.

Only a very well mixed semen sample will provide representative and reproducible data.

For the initial microscopic assessments, a wet preparation is performed whereby 10 μL of native ejaculate is placed onto a microscope slide, which is then covered by a 22 × 22 mm coverslip forming a 20 μm-deep chamber. It should be noted that all aliquoting of semen must be performed using a positive displacement pipette, because the viscosity of the ejaculate is such that accurate and reliable sampling is precluded by the use of other forms of pipettes. The microscope for evaluation has to be equipped with a phase contrast system and should have objectives of 4×, 10×, 40×, and 100× (oil) magnifications. The first microscopic evaluation entails noting the occurrence of cells other than spermatozoa (e.g., spermatogenic or epithelial cells) and the presence of sperm aggregation and agglutination. Although aggregation is rather unspecific and may be the incidental binding of spermatozoa to other cells or debris, agglutination refers to motile spermatozoa that adhere to one another. The extent and type of agglutination are of importance and must be noted, preferably using the four-grade classification system recommended by the WHO (for examples and illustrations, please refer to the relevant section of ref. [1]). If agglutinations are present, additional testing for antibodies against spermatozoa are indicated.

Next, sperm motility should be assessed. It must be kept in mind that if the sample is left on the bench (i.e., at room temperature) for a long time, changes in the sample may occur that could lead to mistaken

determinations of motility. Therefore, it is important that the assessment is performed quickly after liquefaction. Duplicate wet preparations (as described above) should be prepared and evaluated by counting and grading the motility or otherwise of 200 spermatozoa at 200× or 400× magnification. Three categories of movement may be detected: (1) spermatozoa that progress actively regardless of their type of movement are designated the PR fraction, (2) spermatozoa that have slow movements without any progression are designated the nonprogressive (NP) motile fraction, and (3) spermatozoa with no movement whatsoever are designated the immotile (IM) fraction. If the agreement of the duplicate measurements is not within an acceptable range (for tables, see ref. [1]), a new set of samples has to be prepared. For an accurate assessment, a minimum of five fields per slide should be evaluated. Often, the motile fraction is overestimated because the eye pays more attention to movements. A solution to this problem is to first count the immotile spermatozoa and then the motile fraction in the same field. The necessity of counting a minimum of 200 spermatozoa helps to minimize the sampling error to a 95% confidence interval (see ref. [1] for acceptable differences) and to fulfill internal quality-control standards. The lower normal reference limit for normozoospermia is determined by at least 32% PR spermatozoa (5% percentile).

For ARTs, only living spermatozoa are of importance and are assessed using dyes that are able to pass fragmented membranes (i.e., those of dead cells) but not intact membranes (i.e., living cells). Because the number of viable cells may vary over time, this assessment should be done quickly after liquefaction. The recommended stains are either eosin alone or eosin in combination with nigrosin (see ref. [1] for preparation of the staining dyes). As with motility, 2 × 200 spermatozoa are assessed to achieve a precise count and a low sampling error with the percentage of spermatozoa not stained constituting the living fraction. At least 58% vital spermatozoa should be available.

Sperm concentration and total sperm count are important parameters because they may give an indication as to which of the repertoire of ART techniques is to be used. The most important consideration for the determination of the concentration is the choice of counting chamber. The 100 µm-deep hemocytometer (i.e., improved Neubauer) chamber is highly recommended, although other deep chambers may also be used once certain considerations have been taken into account, namely the differences in chamber volumes, grid patterns, and calculations needed to derive the final concentration. Importantly, whatever the type of chamber to be used, it must first be validated against the approved improved Neubauer.

The improved Neubauer has two counting chambers with a grid in each chamber; when these are covered by a thick coverslip (i.e., 0.44 mm), an underlying chamber exactly 100 µm in depth is created. When Newton's rings can be seen between the chamber and the coverslip, it is ready for loading.

Sperm concentration and total sperm count may give an indication as to which of the repertoire of ART techniques is to be used.

The counting grids are 3 × 3 mm and contain nine large squares (Figure 1.1). The central of these nine squares has five rows containing five squares each, all of which are surrounded by three lines. The middle of the three lines represents the boundary of the square. Each of these 25 squares is further subdivided into 16 smaller squares. Normally, counting the number of sperm present in the central 25 squares is sufficient for a reliable measurement; however, if sperm numbers are low, then counts of the contents of the neighboring horizontal grids or even all nine big grids should be performed.

Only intact spermatozoa showing clearly distinguishable heads and tails are counted, and then only if more than half of the head lays over the boundary of a square. As mentioned, a minimum of 200 spermatozoa should be counted in each of the replicates (i.e., a total of 400 spermatozoa). To circumvent the distraction of moving sperm, an appropriate fixative (refer to ref. [1]) should be used, ideally at a 1:1 (1+1) dilution. Because semen samples with high concentrations may be difficult to count (e.g., spermatozoa may be lying on top of each other) and therefore a site of possible errors, the dilution can be adjusted (e.g., 1:5 [1+4], 1:20 [1+19], even 1:50 [1+49]) to provide numbers that are easily countable. If the chosen dilution results in numbers that are too high or too low, it can be amended (i.e., a higher or lower dilution can be used); in such cases, it is important that a new dilution of the sample must be prepared (i.e., not a dilution of the already diluted sample), otherwise counting errors can arise. Whatever dilution is used, it must be taken into account when calculating the final concentration of the sample.

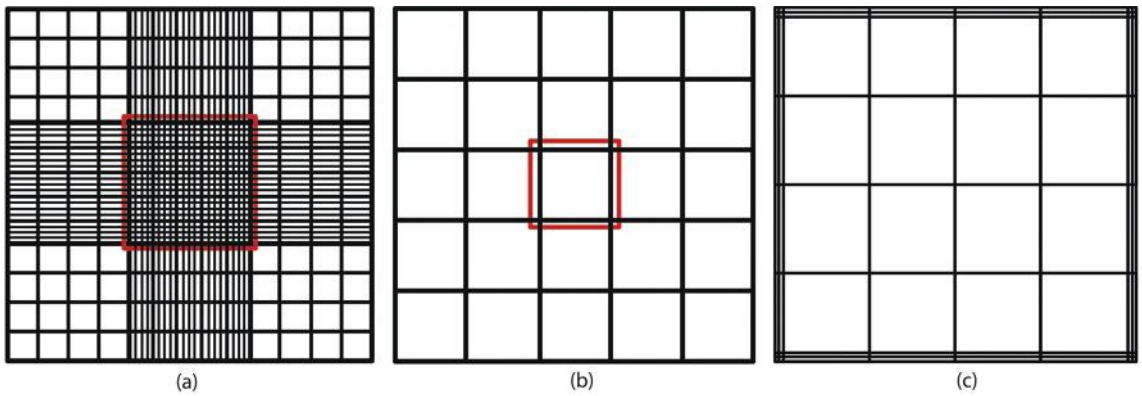

FIGURE 1.1 Grids of the improved Neubauer chamber. (a) All nine big grids. (b) Only the middle grid. (c) Twenty-five squares for counting concentration, keeping the middle of the three lines as the boundary of each small square.

Once the sample has been loaded into the chamber, the spermatozoa must be given time to settle onto the grid. The contents of each side of the chamber are then counted, with the process always finishing a row even if >200 spermatozoa are counted; stopping elsewhere will introduce counting errors. Each evaluation is repeated on the second side of the chamber, and if the difference between the counts is within acceptable levels (refer to ref. [1]), the concentration can be calculated. To calculate total sperm count per ejaculate, concentration is multiplied with seminal fluid; thus, correct measurements are prerequisites for further use of semen samples.

Low Sperm Numbers

If the initial inspection of the wet preparation shows the presence of any spermatozoa, then the sample might be azoospermic. For this suspicion to be substantiated, the sample must first be centrifuged at high velocity and force (e.g., 3000*g* for 15 min) so as to pellet the contents of the semen. After removal of the supernatant, the pellet should be resuspended in 50 µL of seminal plasma from which two aliquots of 10 µL each are placed under coverslips (22 × 22 mm) and the contents scanned for the presence of spermatozoa. Absence of spermatozoa most likely indicates azoospermia; however, for this finding to be confirmed, all the contents of the pellet need to be examined. If spermatozoa are found during this scanning procedure, the sample is most likely cryptozoospermic. The fewer the sperm found, the greater the sampling error and the more likely that it will exceed the acceptable 5%. If fewer than 25 spermatozoa are found, the concentration will most likely be <56,000 spermatozoa/mL [1], and as such a definite measure cannot be given in such cases but must be recorded in both the assessor's lab book and in the patient's file. If cryptozoospermic samples are to be used for ARTs, the absolute number of motile spermatozoa is decisive. To evaluate motile spermatozoa, high-speed centrifugation is contraindicated [1].

Azoospermia can be confirmed only after centrifugation and screening of the pellet for the presence of sperm.

The final analysis is the assessment of sperm morphology. For this purpose, replicate air-dried smears are prepared: one smear for evaluation and the other smear serving as a safeguard should an unforeseen incident occur (i.e., breakage of the slide or staining not working). The smears are made by quickly placing an aliquot of well-mixed semen onto the first slide. The replicate is similarly prepared but by using an aliquot of semen that has again been mixed. Aliquots of 5 µL should be used for samples with high concentrations, whereas larger volumes (up to 10 µL) should be used for low concentrations. If a sample has a very low concentration, it is advisable that it is first centrifuged (e.g., 600*g* for 10 min), the supernatant removed, and the pellet resuspended with a suitable volume of the supernatant. If the semen is too viscous, a washing step might be considered before

preparing the smear. The smear itself is prepared using a second glass slide that is pulled at an angle of about 45° over the slide with the aliquoted sample. Slides are then left to air dry for 1–4 hr before staining.

The staining methods recommended by the WHO [1] are Papanicolaou, Shorr, or Diff-Quik, all of which produce a pale blue staining in the acrosomal region and a dark blue staining in the post-acrosomal region. The midpiece might appear red and the tail red to blue. Excess cytoplasm in the area around the midpiece (i.e., cytoplasmic droplet) might occur on some sperm and will stain red with Papanicolaou and orange to red with the Shorr procedure. For more details regarding the preparation, staining, and particularly the exact grading of sperm morphology, please refer to the WHO manual [1]. As with all evaluations, duplicate counts of a minimum of 200 spermatozoa are needed to decrease the extent of possible counting error. The lower normal limit for morphology is as low as at least 4% of normal spermatozoa. Morphological criteria are strict and intend to define those spermatozoa as normal that are presumably capable of fertilizing [1].

Other tests that may be conducted are the differentiation of round cells using peroxidase staining. Because only leucocytes contain this enzyme, they can be recognized from other round cells (e.g., immature germ cells) that do not stain. The presence of antisperm antibodies can be detected using the mixed antiglobulin reaction (MAR) whereby immunoglobulin A (IgA)- and G (IgG)-coated beads attach to sperm possessing the antigen and thereby restrict their movement. 5 µl of native semen are mixed with 5 µl of anti-IgG/IgA and 5 µl of erythrocytes (0 Rh pos) and incubated for 3 minutes. After 3 and 10 minutes only motile spermatozoa are evaluated. The test is positive with at least 10% IgG- and/or IgA-bound spermatozoa. However, only >50% IgG- and/or IgA-bound spermatozoa are considered clinically relevant. Instead of erythrocytes, commercially available immunobeads can be used.

Preparation Techniques

In nature, the mucus of the female reproductive tract actively selects fertile spermatozoa, whereas debris, non-sperm cells, and the constituents of seminal plasma are excluded. In addition, the essential physiological change of a spermatozoon, capacitation, is initiated during passage through the cervical mucus. These important steps are omitted during ARTs, and as a consequence, sperm preparation techniques are necessary.

First, it is necessary to separate spermatozoa from the seminal fluid within 1 hr of ejaculation to minimize possible damage (e.g., oxidative attack) coming from nonspermatogenic cells contained in semen. The second aim of preparing the semen is to separate cells that would normally never enter the female tract because they cannot cross the cervical mucus. However, because ARTs circumvent this natural border, their presence must be dealt with accordingly. The third benefit is the separation and concentration of motile and normally formed spermatozoa that are most likely to fertilize an oocyte.

Several techniques for preparation of spermatozoa are available. The most commonly used techniques are simple washing, "swim-up," and density gradient (DG) centrifugation. The technique chosen greatly depends on the nature of the semen sample. If the sample is within the normal range, according to ref. [1] reference values, a swim-up is preferred. If the sample has low concentration, motility, or morphology, then often DG centrifugation is the method of choice (for comparison, see Table 1.1). It is important to note that swim-up does not give as high recovery rates of motile spermatozoa as centrifugation, but it is quick, easy to perform, and yields a fraction enriched with motile spermatozoa because it is dependent on the movement of the sperm for selection [3,4]. DG centrifugation yields high numbers of motile spermatozoa, but the choice of appropriate centrifugal force is often difficult because samples vary and the pellet containing the spermatozoa may be too loose and may detach too quickly from the bottom of the tube.

For all preparation techniques, a medium based on a balanced salt solution supplemented with proteins should be used. If the procedure is not conducted in an incubator of 37°C without CO_2, then the medium used should be supplemented with HEPES or a similar buffer for pH stability, and a preincubation of the medium without CO_2 should be performed. If a 37°C incubator with CO_2 is used, then the medium is usually buffered with sodium bicarbonate, and the cap of the tube should be loosely closed to allow gas exchange for optimal pH.

Simple Washing

This technique is often used for normozoospermic semen samples. It is quick, easy, and yields high quantities of spermatozoa (Figure 1.2).

TABLE 1.1

Comparison of Different Sperm Preparation Techniques

	Type of Ejaculate Quality	Pros	Cons
Washing (W)	Normozoospermia	Quick-and-easy technique Yields high numbers of spermatozoa	Only for sperm counts with high sperm numbers Not useful for samples with contamination with other cells, debris, or blood cells
Swim-up (SU)	Normozoospermia Moderate OAT	Quick and easy to perform High rates of highly progressive motile spermatozoa	Lower recovery rates compared with DG
Density gradient (DG)	Moderate-to-severe OAT	High numbers of motile spermatozoa Best removal of debris or other cell types occurring in the semen sample	Difficult to standardize High-molecular-weight compounds of unknown influence Costs more because DG solutions have to be purchased

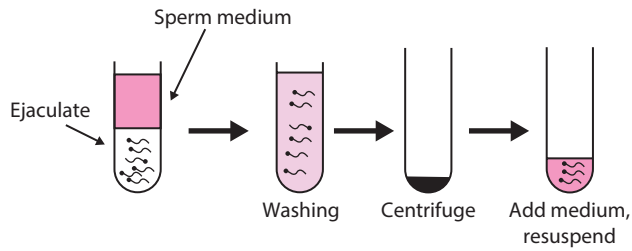

FIGURE 1.2 Sketch of protocol for simple washing.

BOX 1.1 SIMPLE SPERM WASHING

Materials

- A balanced salt solution or a commercially available sperm preparation medium supplemented with protein (usually human serum albumin [HSA]) according to the manufacturer's protocol; ready-for-use media are also available.
- Test tubes of 6 or 13 mL volume.
- A centrifuge that is able to reach at least 500*g*.
- Pipettes with variable volumes (e.g., 2–200 µL and 100–1000 µL).

Protocol

- The semen sample is mixed well (e.g., stirring with a glass rod).
- Transfer the sample to a test tube (if the sample is of high volume, more test tubes may be used).
- Add an equal amount of medium to the semen sample.
- Mix gently by tilting the closed test tube.
- Centrifuge the mixture at 300–500*g* for 5–10 min.
- Gently aspirate or decant the supernatant.
- Add 1 mL of preincubated equilibrated medium to the pellet.
- Gently resuspend the pellet by flicking the tube or by gentle pipetting of the pellet.
- Centrifuge again at 300–500*g* for 3–5 min.
- Again gently aspirate or decant the resulting supernatant.

- Resuspend the pellet with medium, normally the final volume is 0.5 mL. (The volume is important! If the sample has to be used for intrauterine insemination (IUI), the amount should not be >0.5 mL; for other purposes, higher volume can be used.)
- Determine sperm concentration and if necessary the motility and morphology (according to ref. [1]).

Direct Swim-Up

The direct swim-up is a quick-and-easy technique using the unique ability of spermatozoa to move forward. The basis of the procedure is the layering of a medium over the sample; the motile spermatozoa then swim into the medium. Although the final number of spermatozoa might be not very high, it is compensated by the enrichment of the number of spermatozoa with the highest forward progression (Figure 1.3).

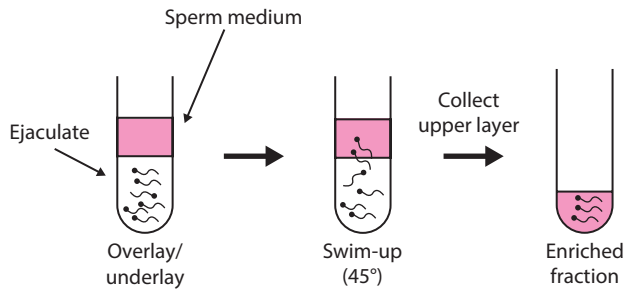

FIGURE 1.3 Sketch of protocol for direct swim-up.

BOX 1.2 DIRECT SWIM-UP

Materials

- A balanced salt solution or a commercially available sperm preparation medium supplemented with protein (usually HSA) according to the manufacturer's protocol; ready-for-use media are also available.
- Test tubes of 6 or 13 mL volume.
- A centrifuge that is able to reach at least 500*g*.
- Pipettes with variable volumes (e.g., 2–200 µL and 100–1000 µL).

Protocol

- The semen sample is mixed well by stirring with a glass rod.
- Ejaculate (1 mL) is transferred to a test tube (if the sample is of high volume, more tubes may be used).
- Medium (1.0–1.2 mL) is pipetted onto the semen sample (it is also possible to pipette the medium under the ejaculate; however, this is more difficult than overlaying it).
- Place the test tube bevelled at an angle of 45° in the incubator (this is necessary to reach a higher surface area where spermatozoa can swim into the medium).
- Incubate for 1 hr at 37°C. (The duration of incubation can be reduced if the semen sample is of very high concentration. Again, the final application will determine the time span: high concentration, low incubation time; low concentration, high incubation time. Regardless, it is prudent

not to exceed 1 hr because zinc and the other components of the seminal plasma may diffuse into the medium and, in turn, might create problems for the spermatozoa [5].)
- After incubation, gently aspirate the top 0.5–1.0 mL of the medium.
- If the sample is high in concentration, a dilution might be necessary. (Again, if the sample is used for IUI, it might be better to decrease the incubation time than to use an additional dilution because the amount of fluid that can be inseminated is limited.)
- A variation of the procedure is to centrifuge the sample at 300–500*g* for 5 min and to resuspend the pellet in 0.5 mL of medium.
- Determine sperm concentration and if necessary the motility and morphology (according to ref. [1]).

Swim-Up with an Additional Washing Step

This technique is equivalent to the direct swim-up and differs only in the introduction of a washing or dilution step (Figure 1.4). The washing step is an elegant way to minimize or remove substances from the seminal plasma (e.g., zinc) that may have a negative influence on spermatozoal quality.

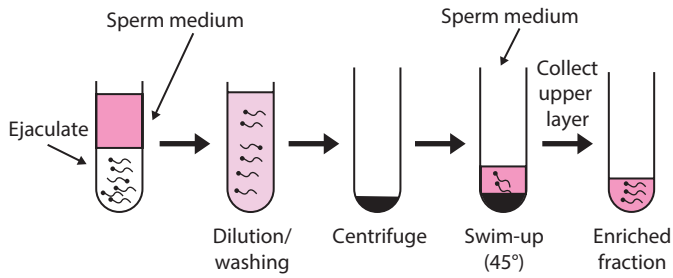

FIGURE 1.4 Sketch of protocol for swim-up with dilution/washing.

BOX 1.3 SWIM-UP WITH AN ADDITIONAL WASHING STEP

Materials

- A balanced salt solution or a commercially available sperm preparation medium supplemented with protein (usually HSA) according to the manufacturer's protocol; ready-for-use media are also available.
- Test tubes of 6 or 13 mL volume.
- A centrifuge that is able to reach at least 500*g*.
- Pipettes with variable volumes (e.g., 2–200 µL and 100–1000 µL).

Protocol

- The semen sample is mixed very well by stirring with a glass rod.
- Transfer the sample to a test tube.
- Add an equal amount of medium.
- Mix gently by tilting the closed test tube.
- Centrifuge the mixture at 300–500*g* for 5–10 min.
- Carefully aspirate or decant the supernatant.
- Add 1 mL of preincubated equilibrated medium to the pellet.
- Place the test tube bevelled at an angle of 45° in the incubator (this is necessary to reach a higher surface area where spermatozoa can swim into the medium).

- Incubate for 1 hr at 37°C. (The duration of incubation can be reduced if the semen sample is of very high concentration; again, the final application will determine the time span: high concentration, low incubation time; low concentration, high incubation time. Regardless, it is prudent not to exceed 1 hr because zinc and the other components of the seminal plasma may diffuse into the medium and, in turn, might create problems for the spermatozoa [5].)
- After incubation, gently aspirate the top 0.5–1.0 mL of the medium.
- If the sample is high in concentration, a dilution might be necessary. (Again, if the sample is used for IUI, it might be better to decrease the incubation time rather than use an additional dilution because the amount of fluid that can be inseminated is limited.)
- As with the previous method, the procedure can be varied, namely, centrifuge the sample at 300–500*g* for 5 min and then resuspend the pellet in 0.5 mL of medium.
- Determine concentration and if necessary also motility and morphology (according to ref. [1]).

Discontinuous Density Gradient (DG) Centrifugation

A discontinuous DG is often the method of choice if a sample is of low concentration and is to be used for in vitro fertilization (IVF) and intracytoplasmic sperm injection (ICSI). The technique yields the optimal selection of good spermatozoa while simultaneously reducing debris, leucocytes, and other cells present in the ejaculate.

For this preparation, two solutions of different densities are used, both consisting of colloidal silica coated with silane of high molecular mass and low osmolality. Usually, an upper gradient with 40% (v/v) and a lower gradient with 80% (v/v) are used, and the semen is placed on top. The layers are then centrifuged, and the enriched fraction of spermatozoa is retrieved from the loose pellet at the bottom of the tube (Figure 1.5).

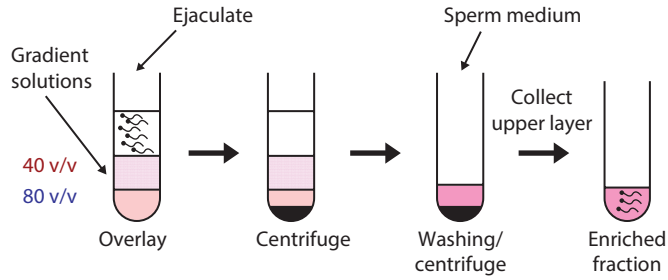

FIGURE 1.5 Sketch of protocol for density gradient centrifugation.

BOX 1.4 DISCONTINUOUS DG CENTRIFUGATION

Materials

- A balanced salt solution or a commercially available sperm preparation medium supplemented with protein (usually HSA) according to the manufacturer's protocol; ready-for-use media are also available.
- Gradient media (these are commercially available and should be used according to the manufacturer's protocol); often, they are ready to use or need to be diluted with an iso-osmotic medium that resembles the fluids of the female reproductive tract.
- Test tubes of 6 or 13 mL volume.
- A centrifuge that is able to reach at least 500*g*.
- Pipettes with variable volumes (e.g., 2–200 µL and 100–1000 µL).

Protocol

- First, prepare the DG layers: place 1 mL of the 80% gradient medium into a test tube and then 1 mL of the 40% medium on top of the first layer.
- The semen sample is mixed well by stirring with a glass rod.
- Semen (1 mL) is gently transferred to the prelayered gradient media (if the sample is of high volume, more tubes may be used).
- Place the test tube carefully into the apparatus and centrifuge at 300–400*g* for 15–30 min.
- Aspirate the supernatant leaving the sperm pellet.
- The sperm pellet is washed by adding 5 mL of preincubated equilibrated medium and resuspended gently by pipetting.
- Centrifuge again at 200*g* for 4–10 min.
- Resuspend the pellet in 0.5–1 mL of medium (depending on the ART to be performed).
- Determine concentration and if necessary also motility and morphology (according to ref. [1]).

Epididymal Spermatozoa

In cases of nonreconstructible obstructive azoospermia, it is possible to surgically retrieve spermatozoa by the aspiration of fluid from expanded epididymal tubules. This fluid should be harvested with as few as possible contaminating erythrocytes or other cell types originating from the operation site. The type of sample preparation technique depends on the number of spermatozoa retrieved, that is, if a high number has been found, a DG centrifugation or a swim-up can be undertaken. However, if only few spermatozoa are seen, then a simple washing step is adequate.

Testicular Spermatozoa

Spermatozoa can be harvested from material obtained by open biopsy using either the conventional *te*sticular *s*perm *e*xtraction (TESE) procedure in case of obstruction or its microsurgical variant mTESE in case of non-obstructive azoospermia with severe testicular damage (Figure 1.6) [6,7]. As TESE material is often contaminated with high numbers of erythrocytes, a washing step is always necessary.

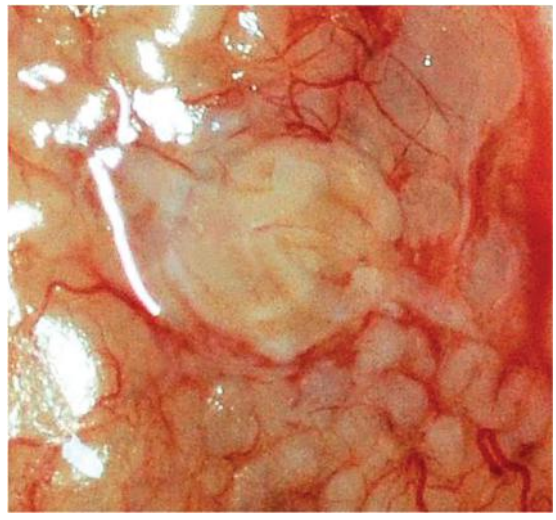

FIGURE 1.6 Microscopic picture of a testis during operation. Thicker tubuli (in the middle) are identified for mTESE.

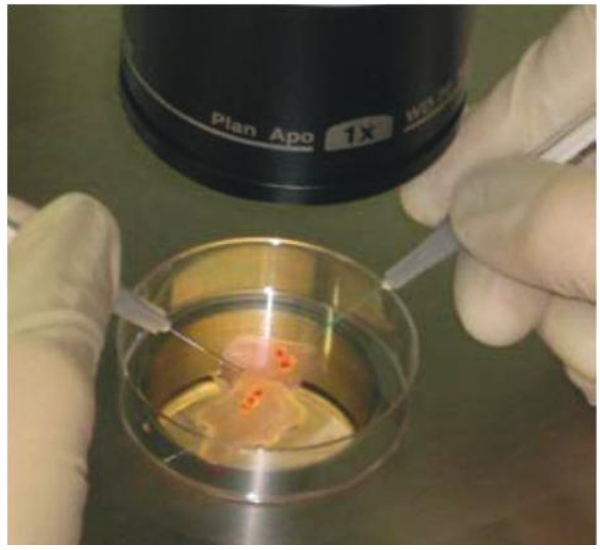

FIGURE 1.7 Mechanical maceration by fine needles.

During the operation, without applying force and squeezing, the testicular tissue is gently retrieved from different parts of the segmentally structured testis and placed by nontouch technique into a HEPES-buffered medium (e.g., a balanced salt solution with HEPES or a commercially available sperm preparation medium). To have several samples for cryopreservation and thawing, the tissue samples should be distributed to four to eight different tubes per testis. To release and collect the mostly tissue-bound spermatozoa, either a mechanical (Figure 1.7) or an enzymatic preparation technique is used.

Mechanical Preparation of Testicular Sperm

BOX 1.5 MECHANICAL PREPARATION OF TESTICULAR SPERM

Materials

- A balanced salt solution or a commercially available sperm preparation medium supplemented with protein (usually HSA) according to manufacturer's protocol; ready-for-use media are also available.
- Two tuberculin syringes with fine needles or glass slides.
- Test tubes of 6 or 13 mL volume.
- Petri dish of 6–10 cm.
- A centrifuge able to reach at least 500*g*.
- Pipettes with variable volumes (e.g., 2–200 µL and 100–1000 µL).

Protocol

- The freshly retrieved or frozen tissue is incubated in preequilibrated medium for up to 30 min to remove contaminating red blood and other cells.
- The tissue is removed from the test tube and placed into a Petri dish and if necessary the culture medium is augmented.
- The tissue is macerated either with the fine needles or by glass slides until a suspension of small pieces of tissue has been achieved.

- The suspension is transferred to tube and centrifuged at speed between 100 and 300*g* for 10 min.
- The supernatant is gently discarded.
- Gently resuspend the pellet by flicking the tube or by pipetting.
- Centrifuge again at speed between 100 and 300*g* for 10 min.
- Resuspend the pellet either in the remaining culture medium or by adding 0.2–0.5 mL of fresh medium.

Enzymatic Preparation of Testicular Sperm

An alternative procedure for the retrieval of testicular spermatozoa is digestion of either a piece of whole tissue or of single tubules with the enzyme collagenase (from *Clostridium histolyticum*, type 1A) (Figure 1.8).

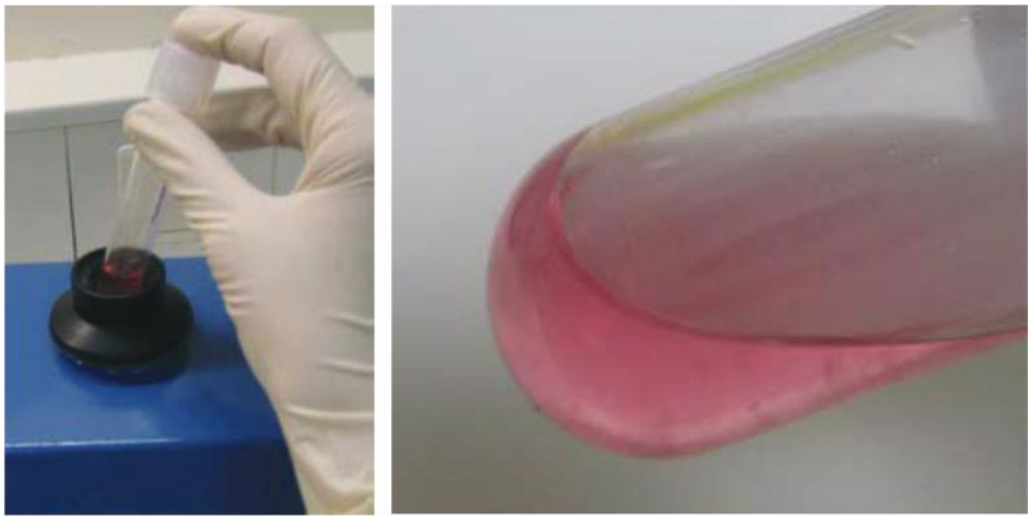

FIGURE 1.8 Digested testicular tissue after enzymatic treatment.

BOX 1.6 ENZYMATIC PREPARATION OF TESTICULAR SPERM

Materials

- Collagenase type 1A from *Clostridium histolyticum* (commercially available).
- A balanced salt solution or a commercially available sperm preparation medium supplemented with protein (usually HSA) according to manufacturer's protocol; ready-for-use media are also available.
- Test tubes of 6 or 13 mL volume.
- A centrifuge that is able to reach at least 500*g*.
- Pipettes with variable volumes (e.g., 2–200 μL and 100–1000 μL).

Protocol

- Incubate the freshly retrieved or frozen tissue in preequilibrated medium at 37°C for 30 min.
- Prepare the collagenase solution by dissolving 0.8 mg of collagenase type 1A in 1 mL of culture medium.

- Add the tissue to the collagenase and incubate at 37°C for 1.5–2 hr, vortex every 30 min (it might still be that remnants of the tissue are not resolved; often these are remnants of the tubular structure in cases of testicular dysfunction).
- Centrifuge at 100–300*g* for 10 min.
- The supernatant is gently discarded.
- Wash the pellet to remove any collagenase by adding 1 mL of culture medium.
- Gently resuspend the pellet by flicking at the tube or by pipetting.
- Centrifuge again at 100–300*g* for 10 min.
- Resuspend the pellet either in the remaining culture medium or by adding 0.2–0.5 mL of fresh medium.

Collecting Testicular Spermatozoa for ICSI

BOX 1.7 COLLECTING TESTICULAR SPERMATOZOA FOR ICSI (FIGURE 1.9)

Protocol

- Place 5–10 µL of the prepared suspension into an ICSI dish.
- Allow the suspension time to settle to the bottom of the dish.
- Retrieve motile, or if none are available, immotile spermatozoa (for rationale, see the following section) using an ICSI needle.
- Place into a drop of polyvinylpyrrolidone (PVP) until injected.

Vitality Tests for Immotile Spermatozoa

It has been shown that immotile spermatozoa either from the ejaculate [8] or extracted from a testicular biopsy [9] are capable of fertilizing an oocyte and producing viable healthy pregnancies.

Using light microscopy, dead spermatozoa are undistinguishable from spermatozoa that are alive but immotile; consequently, several tests have been developed to differentiate between them ([10]; for comparison, see Table 1.2). A long-established technique is the hypoosmotic swelling (HOS) test wherein viable spermatozoa are selected based on their response to exposure to a hypoosmotic medium [11,12]. In such medium, the tails of viable sperm become curved or swollen, thus making them recognizable for selection. This technique in combination with an ART has been successfully implemented with ejaculated and testicular samples [13,14]. The technique as such is useful, although the time frame in which spermatozoa are exposed to the hypoosmotic medium should be as low as possible. If spermatozoa are exposed too long, the curved tail will result in steric problems while getting the spermatozoon into an ICSI needle. In addition, this test is time-consuming and in cases of, for example, severe TESE-ICSI, the retrieval of every individual spermatozoon already is cumbersome and time-consuming and thus not applicable.

Oocytes can be fertilized by immotile sperms if these sperms are viable.

Other tests available use xanthine derivatives (e.g., pentoxifylline or theophylline) that induce tail movements of immotile ejaculated or testicular spermatozoa or that enhance the movement of spermatozoa with very low motility [15–18]. The application of such compounds is quite easy, but in humans it is not known whether their use might interfere with later embryonic development. Therefore, this procedure cannot be recommended for routine clinical use.

For experienced embryologists, the mechanical touch technique can be used, wherein spermatozoa are gently agitated with an ICSI needle and the flexibility of the tail is taken as a sign of vitality [19,20]. But for routine use,

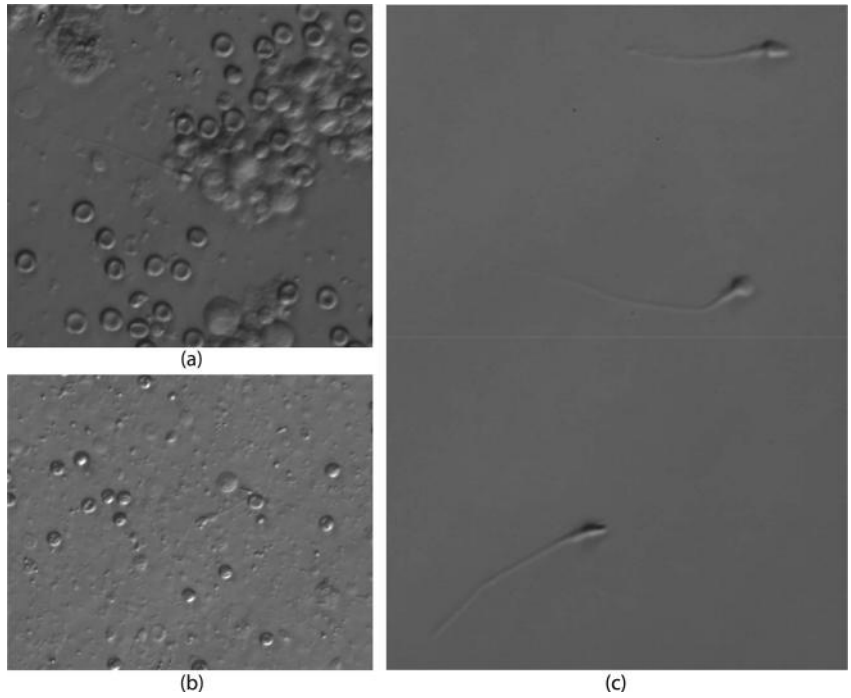

FIGURE 1.9 Mechanically derived suspension (a), enzymatic digestion (b), and collection of individual spermatozoa (c) in an ICSI dish.

TABLE 1.2

Pros and Cons of Different Spermatozoal Vitality Tests

	Type of Spermatozoa	Pros	Cons
HOS test	All types (ejaculate, MESA, TESE)	Easy recognition of living spermatozoa because their tails swell	Time of exposing spermatozoa to the hypo-osmotic medium should be low Steric problems from the tail swelling Solution has to be purchased
Chemical compounds	All types	Vital spermatozoa that are able to bend their tails can be visualized very quickly Useful for ejaculate and TESE spermatozoa	In humans, it is not known whether these compounds may have an influence on further development Solution has to be purchased Vital spermatozoa that are not able to bend their tails will not be identified
Mechanical touch technique	All types	Quick technique without need for further solutions	Only for experienced lab personnel
Laser-assisted immotile sperm selection	All types	Quick-and-easy technique without need for further solutions Easy to learn	ICSI microscope has to be equipped with a laser and a 40× laser objective

this technique is not reproducible enough. A refinement of this technique is the use of a laser that when directed onto the tip of the viable spermatozoon's flagellum causes it to coil at the site of impact [21,22]. This technique seems to be quick and easy, although the microscope has to have a laser and also a 40× laser objective has to be available. The laser-assisted TESE-ICSI in severe nonobstructive azoospermia has been recently introduced into clinical routine and results in increased fertilization rates [22].

Summary and Essentials

The analysis of a semen sample is a crucial point for the treatment decision in ARTs. The sequence of analyzing each individual parameter should always be the same because some parameters are susceptible to change. After liquefaction, the volume and appearance should be recorded. The next step should always be the measurement of the pH, followed by motility assessment, identification of aggregation or agglutination, and determination of vitality. Because these parameters may change over time, it is important to start with these measurements. Especially pH, motility, and vitality are prone to variation due to external influences, for example, temperature or air. The final steps are normally the evaluation of concentration and morphology. These factors are the least susceptible to change because sperm numbers are not affected by external influences and morphology is assessed on fixed, stained slides.

Only after appropriate analysis of the native semen sample can the right technique for its preparation be chosen. Sperm preparation is as important as that of oocytes. A preparation method that is able to select the most motile and morphologically normal spermatozoa from a semen sample is crucial, because the quality of the gametes used constitutes the determinants for the outcome of the ART treatment.

The most used techniques are simple washing, swim-up, and DG centrifugation. Semen samples that possess sperm with parameters within the normal range are processed primarily by swim-up; those with lower concentrations benefit from DG preparation. Although the swim-up procedure does not provide as high recovery rates as gradient centrifugation, it is quick, easy to perform, and yields a population enriched with the best motile spermatozoa. Gradient centrifugation results in the retrieval of high numbers of motile spermatozoa; however, standardization of the method is difficult due to the inherent variation of semen samples.

Testicular or epididymal spermatozoa can be retrieved relatively easily using standard surgical techniques. Sperm retrieval rates from testicular tissue depend on the surgical technique applied, the status of the testis, and its underlying spermatogenic state. In cases of obstructive azoospermia, high retrieval rates are achieved. The method of choice for surgical sperm retrieval in nonobstructive azoospermia is the microsurgical method wherein focal areas with spermatogenic activity are selected. In nonobstructive cases where spermatogenic abnormalities are the expected cause, spermatozoa retrieval might be laborious and time-consuming and should always be handled with care.

All sperm preparation methods are necessary and should be done in a quality-controlled manner. By preparing spermatozoa, the best selection is possible and guarantees high success rates in an ART program.

REFERENCES

1. WHO. *WHO Laboratory Manual for the Examination of Human Semen*, 5th edn. Cambridge: Cambridge University Press, 2010.
2. Björndahl L, Kvist U. Sequence of ejaculation affects the spermatozoon as a carrier and its message. *Reprod Biomed Online*. 2003;7:440–8.
3. Mortimer D. Laboratory standards in routine clinical andrology. *Reprod Med Rev*. 1994;3:97–111.
4. Mortimer D. *Practical Laboratory Andrology*. Oxford: Oxford University Press, 1994.
5. Björndahl L, Mohammadieh M, Pourian M, Söderlund I, Kvist U. Contamination by seminal plasma factors during sperm selection. *J Androl*. 2005;26:170–3.
6. Marconi M, Keudel A, Diemer T, Bergmann M, Steger K, Schuppe HC, et al. Combined trifocal and microsurgical testicular sperm extraction is the best technique for testicular sperm retrieval in "low-chance" nonobstructive azoospermia. *Eur Urol*. 2012;62:713–19.
7. Ramasamy R, Yagan N, Schlegel PN. Structural and functional changes to the testis after conventional versus microdissection testicular sperm extraction. *Urology*. 2005;65:1190–4.
8. Barros A, Sousa M, Andrade MJ, Oliveira C, Silva J, Beires J. Birth after electroejaculation coupled to intracytoplasmic sperm injection in a gun-shot spinal cord-injured man. *Arch Androl*. 1998;41:5–9.
9. Shulman A, Feldman B, Madgar I, Levron J, Mashiach S, Dor J. In-vitro fertilization treatment for severe male factor: The fertilization potential of immotile spermatozoa obtained by testicular extraction. *Hum Reprod*. 1999;14:749–52.

10. Ortega C, Verheyen G, Raick D, Camus M, Devroey P, Tournaye H. Absolute asthenozoospermia and ICSI: What are the options? *Hum Reprod Update*. 2011;17:684–92.
11. Bourne H, Richings N, Liu DY, Clarke GN, Harari O, Baker HW. Sperm preparation for intracytoplasmic sperm injection: Methods and relationship to fertilization results. *Reprod Fertil Dev*. 1995;7:177–83.
12. Casper RF, Meriano JS, Jarvi KA, Cowan L, Lucato ML. The hypo-osmotic swelling test for selection of viable sperm for intracytoplasmic sperm injection in men with complete asthenozoospermia. *Fertil Steril*. 1996;65:972–6.
13. Ved S, Montag M, Schmutzler A, Prietl G, Haid G, van der Ven H. Pregnancy following intracytoplasmic sperm injection of immotile spermatozoa selected by the hypo-osmotic swelling-test: A case report. *Andrologia*. 1997;29:241–2.
14. Sallam HN, Farrag A, Agameya AF, El-Garem Y, Ezzeldin F. The use of the modified hypo-osmotic swelling test for the selection of immotile testicular spermatozoa in patients treated with ICSI: A randomized controlled study. *Hum Reprod*. 2005;20:3435–40.
15. Nassar A, Mahony M, Morshedi M, Lin MH, Srisombut C, Oehninger S. Modulation of sperm tail protein tyrosine phosphorylation by pentoxifylline and its correlation with hyperactivated motility. *Fertil Steril*. 1999;71:919–23.
16. Kovacic B, Vlaisavljevic V, Reljic M. Clinical use of pentoxifylline for activation of immotile testicular sperm before ICSI in patients with azoospermia. *J Androl*. 2006;27:45–52.
17. Yildirim G, Ficicioglu C, Akcin O, Attar R, Tecellioglu N, Yencilek F. Can pentoxifylline improve the sperm motion and ICSI success in the primary ciliary dyskinesia? *Arch Gynecol Obstet*. 2009;279:213–15.
18. Ebner T, Tews G, Mayer RB, Ziehr S, Arzt W, Costamoling W, et al. Pharmacological stimulation of sperm motility in frozen and thawed testicular sperm using the dimethylxanthine theophylline. *Fertil Steril*. 2011;96:1331–6.
19. Soares JB, Glina S, Antunes N, Jr, Wonchockier R, Galuppo AG, Mizrahi FE. Sperm tail flexibility test: A simple test for selecting viable spermatozoa for intracytoplasmic sperm injection from semen samples without motile spermatozoa. *Rev Hosp Clin Fac Med Sao Paulo*. 2003;58:250–3.
20. de Oliveira NM, Vaca Sanchez R, Rodriguez Fiesta S, Lopez Salgado T, Rodriguez R, Bethencourt JC, et al. Pregnancy with frozen-thawed and fresh testicular biopsy after motile and immotile sperm microinjection, using the mechanical touch technique to assess viability. *Hum Reprod*. 2004;19:262–5.
21. Aktan TM, Montag M, Duman S, Gorkemli H, Rink K, Yurdakul T. Use of a laser to detect viable but immotile spermatozoa. *Andrologia*. 2004;36:366–9.
22. Nordhoff V, Schüring AN, Krallmann C, Zitzmann M, Schlatt S, Kiesel L, et al. Optimizing TESE-ICSI by laser-assisted selection of immotile spermatozoa and polarization microscopy for selection of oocytes. *Andrology*. 2013;1:67–74.

2

Handling Gametes and Embryos: Oocyte Collection and Embryo Culture

Lars Johansson

Introduction

A couple that undergoes a treatment in an assisted reproduction technique (ART) clinic expects that the clinic undertakes all necessary pre-cautions to ensure that their embryos are cultured in a clean and safe environment, generating embryos of a high implantation potential and the delivery of a healthy baby after a normal gestational period.

All efforts have been taken by the clinic to prevent the exposure of oocytes or embryos to embryo-toxic pollutants from the surrounding environment (e.g., traffic, industrial hazards) or from within the clinic (e.g., construction materials, ventilation system, furniture, lightning, gas cylinders, disposables, detergents, and cloths). Accumulation of toxins, especially volatile organic compounds (VOCs) [1–6], in the culture media could affect the embryos' developmental and implantation capacities, increasing miscarriage rates and reducing a couple's chances of a successful treatment.

Oocyte Collection

Clinical Part

For the best outcome, the clinic should implement a mild stimulation protocol promoting recovery of high-quality and mature oocytes from large follicles and an endometrium that supports implantation. In contrast, excessive stimulation and high serum estradiol levels influence oocyte quality, increase oocyte dysmorphism and epigenetic problems, decrease endometrial receptivity, and increase miscarriage rates [7–16]. The couple should also be informed about the age-dependent decline in oocyte quality and quantity and how it affects the outcome [17] before they sign the consent form.

Before an egg collection is undertaken, the nurse and the clinician verify together the identity of the patient and inform the laboratory. Furthermore, they control the settings and functions of the equipment in the oocyte collection room; this duty should at least include control of the pressure (90–120 mmHg) [16] and the flushing mechanism of the aspiration pump. The ultrasound machine and probes are controlled, and the test tube warmer is loaded with prewarmed test tubes which are kept at the correct temperature (36.5°C–36.9°C) [18]. Some clinics also preload the warm test tubes with a low volume of flushing media containing heparin, to avoid formation of blood clots.

The oocyte collection is usually performed 36–38 hours post–human chorionic gonadotropin (hpHCG), using a short-acting conscious sedation regime to avoid detrimental effects of anesthesia on oocytes, fertilization, embryo development, and pregnancy rates [19–30]. Just before the oocyte collection starts, the needle is rinsed with flushing media for removal of potential debris or contaminations from the manufacturing procedure. Be aware of not touching the needle tip against the wall of the test tube, because a blunt tip will negatively affect the ability to penetrate the follicle and may induce pain and bleeding in the patient.

Nowadays, most clinics retrieve the follicular fluid (FF) via transvaginal ultrasound guidance [31] and a thin single-lumen needle (17–21 gauge) [32] that is connected to a pressure-controlled aspiration pump, thus avoiding flushing of follicles.

FIGURE 2.1 Collection of follicular fluid (FF). Deep heat block is needed for keeping prewarmed test tubes at an acceptable temperature during the collection of the FF. Be sure also that the transparent plug is properly inserted into the test tube, so that the aspiration pressure can be maintained. Also, see to that the tubings between the needle and the FF collecting test tube are kept as short as possible to prevent a drop in temperature.

FIGURE 2.2 Flushing of follicles. Do not flush follicles with media in hand-held syringes because the media cool down quickly, and the lower temperature might damage the temperature-sensitive meiotic spindle in the oocyte.

Oocyte retrieval should be performed in a way that avoids damaging the oocyte via aspiration that is too strong or exposure to suboptimal temperatures.

The oocyte collection is therefore quick and efficient, and it reduces the costs for anesthesia, disposables, and flushing media. A thin aspiration needle also reduces the patient's experience of pain and causes less bleeding, thereby facilitating the laboratory being able to find and retrieve the cumulus–oophorous complexes (COCs) from the almost clear FF [33].

The length of the tubing between the aspiration needle and the prewarmed test tube should be as short as possible to reduce temperature fluctuations that damage the meiotic spindle [34], increase aneuploidy rates, or entrap the COC within a blood clot (Figure 2.1). If the latter occurs, the COC can be released from the blood clot by cutting it with two large cannulas.

Double-lumen aspiration needles can also be used as long as the temperature of the flushing solution can be kept within an acceptable range (36.5°C–36.9°C; [18]). Unfortunately, many clinics flush the follicles with media kept in hand-held syringes in which acceptable temperatures cannot be maintained, causing unnecessary damage to meiotic spindles and induction of aneuploidies (Figure 2.2) [35]. It also increases the risk of exposing the oocytes to toxic lubricants from the syringes; if not embryo tested, one-component syringes are used [36]. In addition, COCs are mechanically damaged due to excessive pressure [37]. There is also evidence that a brief exposure of the COCs to an inappropriate flushing buffer during the egg collection, such as phosphate-buffered saline (PBS), might compromise the function of the oocyte and reduce embryo development and implantation rate [38]. Regardless, a high proportion of clinics still use a double-lumen needle by which they seem to retrieve more oocytes [32].

Laboratory Part

Every morning, the laboratory staff changes their clothes and places all their personal belongings (e.g., mobile phones, jewelry, pens) in their lockers. After entry into the first coded, controlled prelaboratory room, the staff

change their shoes, dress in lint-free and antistatic nonwoven gowns that cover the skin and hair, and perform hand decontamination before entering the second prelaboratory room through an airlock chamber (air shower). In this room, the laboratory stores unwrapped and fumed-off embryo-tested disposables in ventilated cupboards and culture media in medical refrigerators.

From the latter room, the staff enter the cleanest, most sensitive and restricted area, the culture room, ideally via a foot-controlled door opener. First, the embryologist performs a quality control (QC) of the facility and the equipment (e.g., temperature, CO_2, O_2, pH, and gas inflow). The QC can either be performed via 24 hr surveillance systems or by physically writing down the numbers.

In the afternoon, on the day before the egg collection, the laboratory turns off the heating of the laminar airflow (LAF) bench and reduces its fan speed to prevent evaporation of media and potential increase in osmolality. Equally important is that a turned off LAF bench is not restarted at the time of the preparation of the dishes and disposables since the filter initially releases dirt that contaminates the bench surface area. If the LAF bench has been shut down overnight, it must run for at least 15–20 min before it is taken into use.

Clean the LAF bench surface area with water for injection and lint-free clean-room wipes. The embryologist puts on embryo-tested powder-free gloves, and another staff member retrieves fumed-off collection and culture dishes, round-bottomed FF collection test tubes, serological pipettes, and combi- and filter-tips and places them aseptically on the LAF bench. The number of test tubes and dishes (e.g., collection, insemination, denudation, holding, and culture dishes) (Figure 2.3) are prepared in accordance with the expected number of retrieved COCs, treatment, and culture techniques. Each disposable is labeled with the couple's specific nontoxic identity code by a diamond marker pen, cannula, or transparent name and barcoded sticker (www.mtg-de.com, www.fertgms.com, www.research-instruments.com). More recently, a new laser-engraving system of the patient's name and barcodes is available (www.ankdatasystems.com). Both the lid and the bottom of the dishes are labeled with the couple's specific identifier.

After labeling of all test tubes and dishes, one of the culture media products is retrieved from the refrigerator. The expire date of the product is entered into the QC overview of disposables and on the patient's protocol, and then the retrieved product is placed in the lid of a Petri dish to prevent the adherence of contaminants to the product. This is especially important if preincubated products, such as liquid paraffin oil (LPO), are to be returned back into the incubator. It is recommended that LPOs are stored at the dark and at 4°C–6°C to prevent excess formation of peroxides or VOCs that could affect embryo quality and reduce implantation rate [39,40]. Therefore,

FIGURE 2.3 Selection of embryo-tested disposables. (Courtesy of Thermo Fisher.)

avoid prolonged storage of large volumes of LPO in incubators. Equally important is to not aliquot and transfer media products into nonembryo-tested vials or flasks that potentially could contaminate or alter the product.

Prepare only one dish at a time if micro-drop cultures are to be used and avoid repeated retrieval of culture media from the vial or flask.

Prerinse all disposables with excess media, just before they are to be used, so that potential toxins from the manufacturing of the disposables are removed and the drying out of media, within the pipette, and a potential increase in osmolality are avoided. Preferably, a multipipette, fitted with a prerinsed DNA, RNA, and pyrogenic-free syringe, should be used for quick and safe dispensing of the culture media. Thus, because the multipipette is filled only twice, it reduces the risk for contamination of the vial or the flask, allows quick, reproducible pipetting of droplets from a sealed unit, thereby prevents increase in osmolality and reduces; and reduces the laboratory workload. If only one dish is prepared at a time, culture media droplets <40 μL–50 μL could be prepared, if the droplets are quickly covered with preincubated LPO [41,42]. Avoid a too thick overlay of LPO over the media droplets because this would require a longer preincubation of the media before it reaches its optimal pH. Be aware that variability in pH during egg collection disrupts mitochondrial filaments and actins [41], and during culture reduces cell numbers and formation and hatching of blastocysts, increases cell apoptosis, and decreases fetal weights [42–44].

Clinics collect and rinse COCs in many different types of embryo-tested dishes, in combination with either CO_2-dependent or bench work media. The CO_2-dependent media are preferably preincubated overnight in mini-incubators, at low oxygen tension, wherein the media in the center or four-well dishes have been covered with a thin film of LPO. In contrast, bench work media only need to be pipetted into test tubes; their corks should be properly pushed down and prewarmed overnight in a bacteriological cabinet.

The patient's dishes and test tubes are allocated to the patient's incubator and bacteriological cabinet, respectively, as noted in the patient's embryo protocol. A nonsticky magnetic labeler on the incubator, verifying the location of the dishes, reduces incubator openings and thereby negative effects on culture conditions.

Finally, the embryologist cleans the surface of the LAF workbench with water for injection and fumed off empty collection and rinsing dishes and collector devices (e.g., embryo-tested Pasteur pipettes, yellow Eppendorf Biopur filter tips, Stripper and glass denudation tips, and plastic tips or syringes) (Figure 2.4) are placed on its surface.

Use embryo-tested material for all steps.

The decision of what type and size of embryo-tested collection and rinsing dishes (e.g., Nunc, Corning, VitroWare) are to be used is that of the laboratory. For example, if a large dish is used, the full content of a test tube can be poured in giving a thin layer of FF for easy localization of the COCs. However, the large search area prolongs the search time and COCs might cool down. If a smaller Petri dish is used, the content of the test tube must be divided into two dishes, thereby generating a thicker layer of FF with less fluctuation in temperature; but again, this prolongs the search time. Remember that the surface temperature of the LAF bench is set such that it generates a temperature of approximately 37°C *within* the selected dishes. Fluctuation in temperature should be kept to a minimum because it causes irreversible damage to the meiotic spindle [35].

The optimal temperature must be checked at the location of the oocyte: in a dish/tube/….

On the oocyte collection day, the staff perform QC of the area and equipment, including a Køhler adjustment of stereomicroscopes. The stereomicroscopes should be set at their lowest magnification for a quicker overview, localization, and evaluation of the COCs within the FF. A light-emitting diode (LED) source, complemented

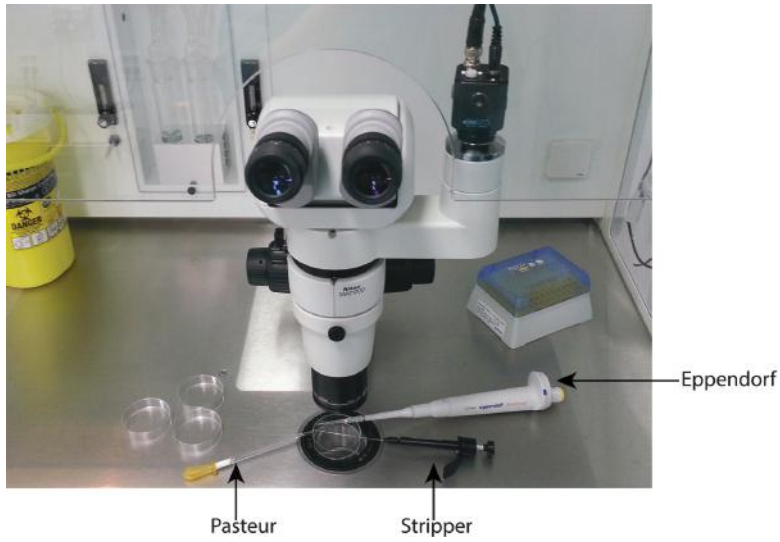

FIGURE 2.4 Devices for collection of cumulus–oophorous complexes (COCs). There are many different "collectors" of COCs available in the market. In the LAF, you see, from the left, a sterile Pasteur pipette, Eppendorf yellow filter tip connected to an Eppendorf pipette, and a Stripper with a large tip.

with different filters, reduces light-induced formation of reactive oxygen species (ROS) in the media, gives more individual options, and facilitates the evaluation of the COCs [45,46].

After verification of the identity of the patient (e.g., double identification via wristband), the gas humidifier (dish gasser), which delivers a media- and altitude-adjusted mix of humidified tri-gas over the preincubated dishes, is turned on in the LAF bench. The clinician prepares the patient for the oocyte collection and rinses the oocyte retrieval needle with flushing media. When the patient has been properly sedated, the laboratory staff put on embryo-tested gloves, control the identity (www.fertqms.com, www.research-instruments.com) of the two collection dishes (Figure 2.5), and place them under the dish gasser. Some clinics replace the media droplets with preincubated media to remove potential toxins that have accumulated in the culture media via the oil overlay.

When the first test tube with FF is placed in the block heater, the embryologist prerinses the collector and pours out the FF into a prewarmed collection dish. The temperature-controlled high-efficiency particulate air (HEPA) and VOC filter ventilation system might generate a slight draft through the hatch. The laboratory should therefore avoid placing any heated blocks for test tubes within the passage of the hatch because the overpressure and draft will cool them down. It is better to place the calibrated block heaters, for storage of FF-filled test tubes, below the hatch, close to the LAF bench.

The FF is scanned and when a COCs is found one of the dishes from underneath, the dish gasser is moved next to the collection dish. Preincubated media from the outer ring of the center-well dish is aspirated up into the collector and flushed over the COC to clear the area around it from debris. The COC is taken up in the collector and repeatedly washed in the outer ring of the center-well dish and when clean it is transferred into the center well.

The coloration of the FF is dependent on the nutritional status of the female, the vascularization of the follicle, and contamination within the FF (Figure 2.6). Good blood supply to the follicles generates more oxygenation and reduces aneuploidy rates and cytoplasmic abnormalities in the oocytes [47]. In fact, retrieval of FF from follicles with a good blood supply, via Doppler imaging, is correlated to high oocyte quality developing into top-quality embryos with high implantation rates [48].

Large blood clots attached to or entrapping the COC should be removed because they can reduce fertilization rates [49] (Figure 2.7), whereas blood within the cumulus, generated during folliculogenesis, is an indication of low oocyte quality and developmental capacity [50].

FIGURE 2.5 Follicular fluid. The color of the follicular fluid is dependent on the nutritional status, food intake, and blood content.

FIGURE 2.6 Blood clot in a cumulus–oophorous complex (COC). If a too slow aspiration of follicular fluid is performed, a long blood clot can be formed that adheres and entraps the COC.

The practice of reducing the cumulus cloud, by cutting, should be omitted because it increases the time that the COCs are exposed to the environment, but perhaps more seriously damages the transzonal projections (TZPs) that symbiotically and bidirectionally transfer information and nourishment between the cumulus and the oocyte [51] (Figure 2.8).

After prewash, the COC is transferred into the center well, and the dish is placed under the dish gasser. When the next COC is found, the second dish from underneath the dish gasser is used, thus alternating between the dishes until you have a maximum of five COCs per dish or the oocyte collection is finished. The number and quality of the COCs are evaluated (Table 2.1, Figures 2.8–2.15), and the dishes are placed in the patient's allocated mini-incubator that quickly recovers the temperature and pH of the culture media. The COCs are left in the incubator, awaiting in vitro fertilization (IVF) insemination or partial denudation for intracytoplasmic sperm injection (ICSI).

Work fast and concentrated and avoid too long exposure of COC/oocytes to the environment.

Retrieval of oocytes from small follicles, too early after HCG or to prevent OHSS, might generate morphologically good embryos, but it gives a much lower clinical pregnancy rate and a lower birth weight [52]. Cysts should be emptied last to avoid contamination of disposables and culture media [53]. Finally, the surface area of the LAF bench is cleaned with lint-free wipes and water for injection, gloves are discarded and all information is written down. The area and staff are ready for the next oocyte collection.

It is very important that the COCs, and the developing embryos and blastocysts, are cultured at low oxygen tensions, and preferably in mini-incubators with quick recovery of the culture conditions. Culture at low oxygen tension is very beneficial because it lowers ROS formation, aneuploidy rates, and apoptosis; improves embryonic gene expression, cleavage rate, and speed; generates a higher percentage of top quality embryos and blastocysts; and increases pregnancy, implantation, cryopreservation, and baby take-home rates [54–60]. For this to become successful, the clinic must adjust the number of incubators to the number of patients so that the frequency of incubator lid openings and embryo evaluation is kept to a minimum, or perhaps also by using a reliable 24 hr embryo culture surveillance system. However, it also requires that the CO_2 and O_2

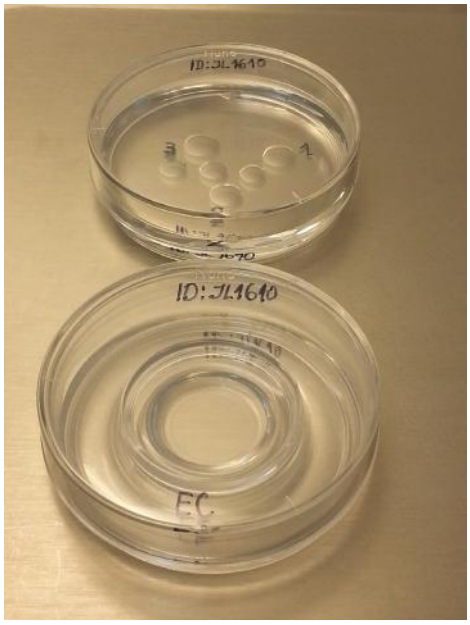

FIGURE 2.7 Culture techniques. Cultures can be performed in either small microdrops or in open large dishes.

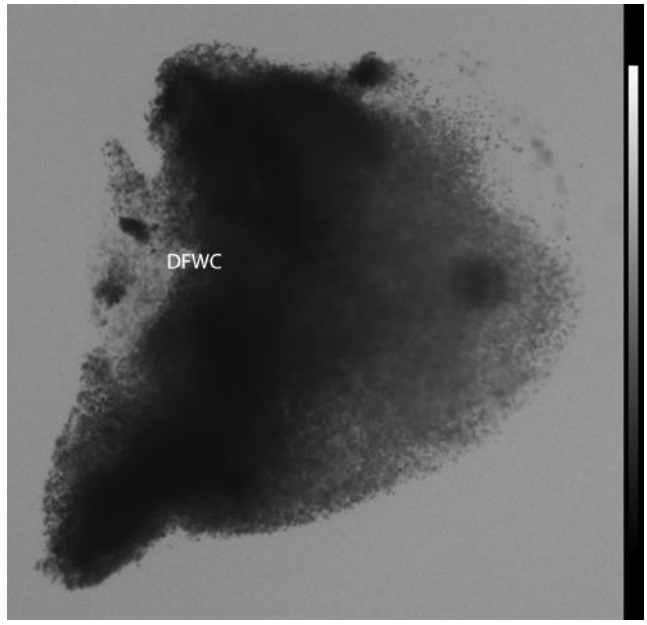

FIGURE 2.8 Immature (I) cumulus–oophorous complex (COC). Immature COC with a compact nonexpanded cumulus and a nonvisible oocyte. The COC is adhered to the dark follicle wall cells (DFWCs). (Courtesy of Dr. Maria Köster, University of Bonn.)

TABLE 2.1

Classification of Cumulus Oophorous Complexes

Quality	Cumulus	Corona	Oocyte
Immature (I) (Figure 2.8)	Small, compact, grey, non-expanded	Dark ring around the zona pellucida	Not visible, if visible GV stage
Mature (M) (Figure 2.9–2.11)	Small, bright, expanded	Not fully radiated	Partially visible
Excellent (E) (Figure 2.12–2.13)	Large, bright, expanded	Radiated	Clear and visible
Overmature (O) (Figure 2.14–2.15)	Small, thin, patches of dark cells	Light or dark	Visible, granular and dark
Atretic (A)	Patches of dark cells or absent	None or clumps	Dark

concentrations have been adjusted to the requirement of the culture media, stage of development, and altitude of the clinic.

Exposure of oocytes to variable pHs during handling, denudation, or ICSI affects embryo development and blastulation rates [44]. For example, completely denuded oocytes, before ICSI or cryopreservation, cannot regulate their intracellular pH (pHi) and are highly dependent on the extracellular pH (pHe), whereas the later stages of development are less sensitive, probably due to the formation of tight junctions [61–69]. In addition, prolonged exposure of oocytes to high concentrations of sperm in IVF lowers the fertilization rate because the metabolism and decomposition of sperm lowers the pHe [70] and excess formation of ROS affects the development of the embryo [60]. However, inclusion of amino acids in handling and culture media could preserve the pHi and protect gametes and embryos [71–73].

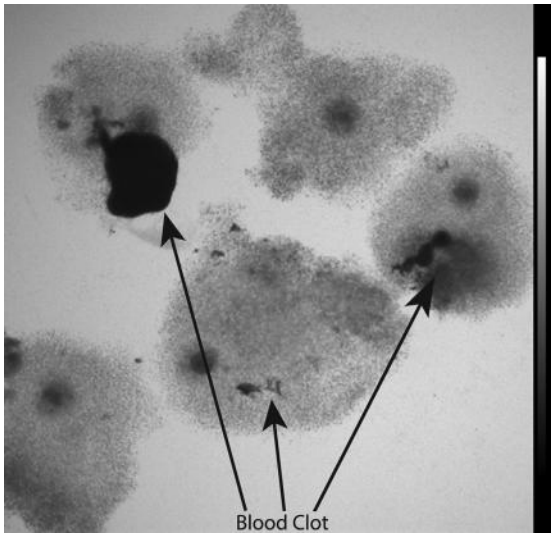

FIGURE 2.9 Mature (M) COC surrounded with expanded or nonexpanded cumulus. A mixture of mature COC with nonexpanded (MNE) or expanded (ME) cumulus. The dark patches within the cumulus cells represent blood (B). (Courtesy of Dr. Maria Köster, University of Bonn.)

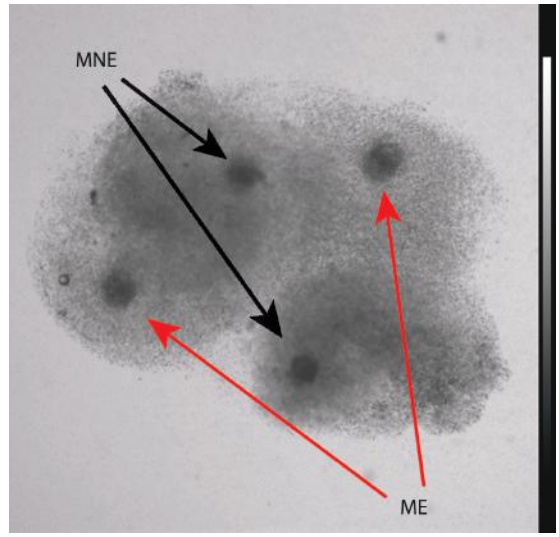

FIGURE 2.10 Mature (M) COC surrounded with expanded or nonexpanded cumulus. A mixture of mature COC with nonexpanded (MNE) or expanded (ME) cumulus. The dark patches within the cumulus cells represent blood (B). (Courtesy of Dr. Maria Köster, University of Bonn.)

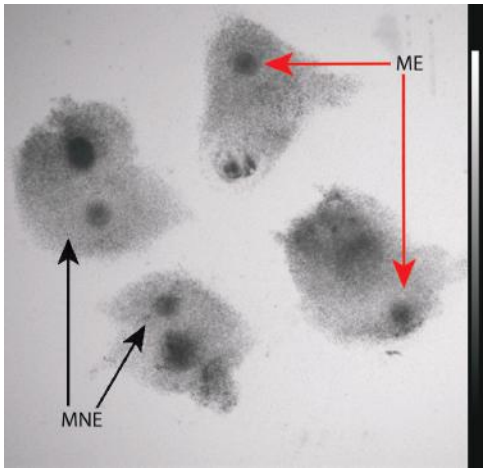

FIGURE 2.11 Mature (M) COC surrounded with expanded or nonexpanded cumulus. A mixture of mature COC with nonexpanded (MNE) or expanded (ME) cumulus. The dark patches within the cumulus cells represent blood (B). (Courtesy of Dr. Maria Köster, University of Bonn.)

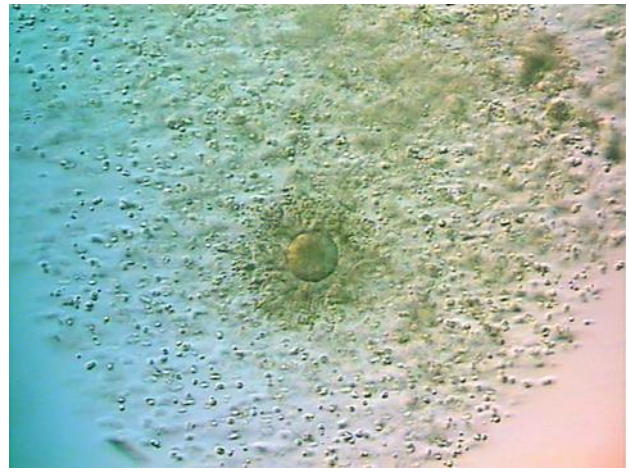

FIGURE 2.12 Excellent (E) mature COC. Large, bright expanded cumulus with radiated corona (CR) and visible oocyte with polar body (PB). (Courtesy of Lev Levkov.)

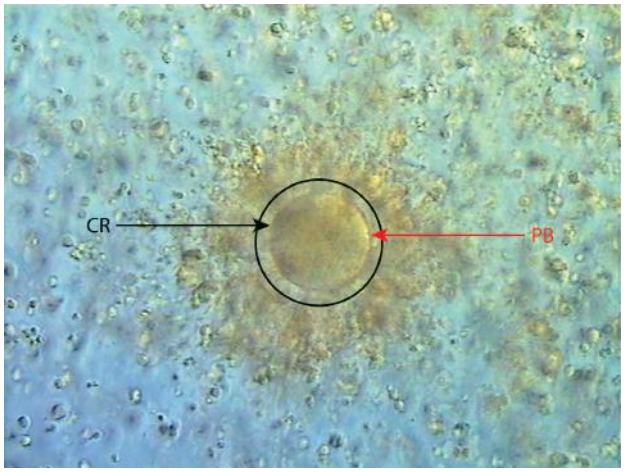

FIGURE 2.13 Excellent (E) mature COC. Large, bright expanded cumulus with radiated corona (CR) and visible oocyte with polar body (PB). (Courtesy of Lev Levkov.)

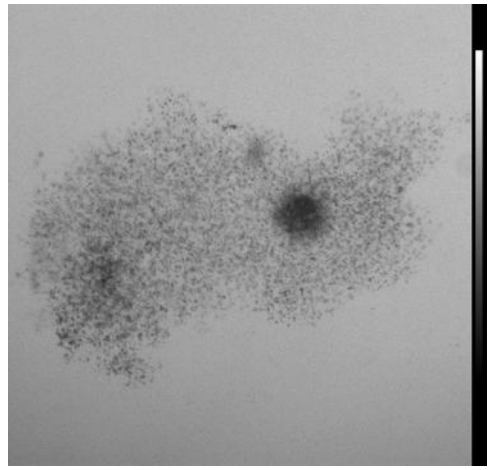

FIGURE 2.14 Overmature (O) COC. An overmature COC with a small cumulus, patches of dark cumulus cells (DCCs), and a visible oocyte. (Courtesy of Dr. Maria Köster, University of Bonn.)

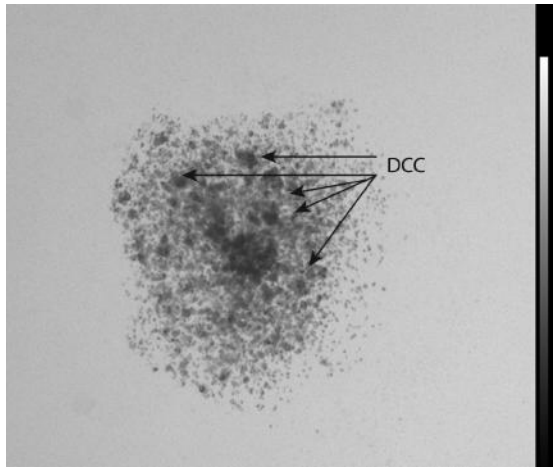

FIGURE 2.15 Overmature (O) COC. An overmature COC with a small cumulus, patches of dark cumulus cells (DCCs), and a visible oocyte. (Courtesy of Dr. Maria Köster, University of Bonn.)

Control and maintenance of proper pH and temperature are key to success.

If oocytes and embryos also are cultured in dishes with a flat surface that is in direct contact with the heated surface of the incubator, there will be less variation in temperature and less damage to meiotic spindles, aneuploidy rate, and delay in embryo development.

After fertilization and scoring of the quality of the zygotes, they are either cultured singly or in groups, and preferably in droplets. In single culture, the embryo development and quality can be successively evaluated, facilitating the selection of the best embryos for transfer. Group culture, in contrast, is

sought to improve implantation rate and to rescue borderline-quality embryos for cryopreservation [74]. Group culture in concavely shaped grooves separated by a low barrier allows both the exchange of nutrients between the embryos and the successive evaluation of embryos [75–79]. In this embryo-friendly culture environment, high concentrations of autocrine and paracrine embryotrophic and detoxifying factors surround the embryos [77], but the exchange of nutrients and metabolites is limited by diffusion, which is estimated to be 80 μm–120 μm [76]. The exchange of nutrients between the embryos and the proliferation of cells are thought to be enhanced by tilting the incubators or dishes and by mechanical or indirect vibration of dishes [80–82], thereby mimicking the movements of the fallopian tubes and the uterus [83,84] and generating a higher proportion of high-quality blastocysts and higher implantation and live birth rates. A high density of embryos generates higher concentrations of embryotrophic factors, but it also generates a potential enrichment of detrimental waste products that could be dependent on media product and on culture technique. The combination of group culture and coculture of embryos with autologous cumulus or endometrial cells mimics the microenvironment that surrounds the embryos; generates growth factors that induce better embryo growth and earlier compaction of embryos; reduces apoptosis; increases cell numbers, blastocyst formation, hatching ability and pregnancy rate; and makes the blastocysts more resistant to cryo-damage [85–94].

The choice of culture media products [95] or the day of embryo transfer [96,97] does not seem to affect the pregnancy rate, even though higher implantation and lower aneuploidy rates are seen in embryos that reach the blastocyst stage [98].

There is also insufficient clinical evidence favoring the single or the sequential media systems. The single-step culture media system decreases environmental stress and removal of valuable nutrition (e.g., autocrine and paracrine factors), it is less laborious and costly, and it generates more blastocysts. In contrast, a sequential media system takes into consideration the changes in metabolism and the environment that the embryo encounters during passage through the female reproductive tract [99,100].

Practical Guide in Preparation for Oocyte Collection and Culture Techniques

Every morning and before entering the restricted culture area, the staff must be properly dressed. In the pre entry room, staff redress according to the culture room dress code and perform hand decontamination. Upon entry into the culture room, the staff perform QC of the area and equipment *before* starting the day's work.

BOX 2.1 EQUIPMENT AND MATERIALS

The equipment and materials suggested give consistent, good results in clinics audited worldwide by the author.

The disposables are sterile, nonembryotoxic, and nonpyrogenic, but there are many additional regional alternatives that can be used.

The following protocols should be considered only as a guide to avoid the most frequent problems during egg collection and culture routines.

Equipment and materials

1. LAF bench, class II cabinet, or IVF chamber (hereafter called LAF bench)
   a. A dish gasser that purges a temperature-controlled, humidified, pH- and altitude-adjusted tri-gas mix over the dishes is recommended instead of using a small CO_2 incubator within the LAF bench. The recovery of the culture environment within the latter incubator type

is slow and affects the culture conditions, thereby potentially harming the COCs and the development of the embryos.

2. Labeling machine, diamond marker pen, or cannula
3. Incubators
   a. Large (60 L) with small inner doors and low oxygen
      i. Dishes kept in metal blocks for uniform heating
   b. Benchtop mini-incubator, premixed gas or gas mixer, and low oxygen
      i. Most types of dishes fit within the incubator, and they are in direct contact with the heated metal surface
4. Pipette aid, pipetter, and pipettes (www.eppendorf.de)
   a. EasyPet 4421: for transfer of preincubated oil or large volumes of culture media with serological pipettes (Nunc)
   b. Repeater Plus or Repeater Xstream: the pipette is used in combination with Combi Plus Tips of Biopur quality (RNA, DNA, and pyrogen free)
      i. Use single-wrapped repeater tips of 0.1–50 mL sizes
   c. Pipettes: Research Plus kit, possible to autoclave
      i. These pipettes are used with filter tips of Biopur quality

Materials

1. Gloves
   a. Embryo-tested, powder-free sterile gloves without chemical additives, accelerants, or emulsifiers
      i. BioClean N-Plus, sterile nitrile gloves for clean-room
      ii. Ansell, TNT 92-760
      iii. Ansell, Derma Prene Type 2-RT
      iv. Kimberly-Clark, Safeskin NXT 62992
2. Collection pipettes (hereafter called collectors)
   a. Pasteur pipettes with cotton plug (Humagen, Hunter), stripper, or Flexipet tips (600 µL); glass pipettes (Humagen), or Eppendorf Yellow Biopur filter tips
3. Cleaning solution for surfaces in-between patients
   a. Wipe only with water for injection
   b. Soiled surfaces are cleaned with embryo-tested detergents that should be used only after all work has been done to avoid exposure of gametes, embryos, and environment to potentially toxic components
      i. Oosafe, hydrogen peroxide, and 70% ethanol are the most frequently used detergents, but they need extensive cleaning with water for injection after use (Catt, ESHRE 2013, O–240).
4. Lint-free wipes for clean-room work (www.techniwipe.com)
5. Round-bottom test tubes for collection of FF
   a. Nunc, 150268, VitroWare, Corning
6. Serological pipettes
   a. 5 and 10 mL (Nunc, 159625 and 159633)
7. Collection and culture dishes
   a. Select the choice of preference as long as they are embryo tested with several different methods, preferably gamma-irradiated and of clear plastic, facilitating inspection and evaluation of gametes and embryos (e.g., Nunc, LifeGlobal, Corning, VitroWare).
8. Culture media of your choice

BOX 2.2 PROCEDURE

Day 1: Preparations on the day before oocyte collection

1. Turn off the heating of the LAF bench where the dishes are to be prepared.
   a. The ventilation of the LAF bench should have been turned on before the area is cleaned to prevent release of dirt from the filter during the initial start of the LAF bench.
   Note: *Use a low fan speed to reduce evaporation rate of the media during preparation of the dishes.*
   b. Clean the area with water for injection and lint-free clean-room wipes.
   c. Put on embryo-tested gloves and work aseptically.
2. Place fumed-off collection and culture dishes, round-bottom FF collection test tubes, serological pipettes, and Combitips and filter tips on the surface of the LAF bench.
   a. Clean the outer part of the Pipette Aid, Repeaters, and metal blocks (for large incubators) with wipes moist with water for injection.
   b. Adjust the number of dishes according to the number of expected COCs per patient and culture techniques.
   c. Label dishes, both lid and bottom, with the couple's specific barcode identifier.
   Note: *Prerinse all disposables, with their designated media, just before use to avoid drying of media and potential increases in osmolality.*
3. Take out the media of choice, one at a time, for rinsing of COCs, insemination (IVF), denudation (ICSI), and culture, from the refrigerator and place the vials, flasks, or bottles are placed in a Petri dish lid on the cold and clean surface of the LAF bench.
   a. Also, take out the preincubated liquid paraffin oil (PLPO) from the incubator.
4. **Preparation of rinsing and collection media**

   Bench work media (HEPES or MOPS)

   1. Place four round-bottomed test tubes in a metal heat block with holes of a depth that covers most of the length of the test tubes.
   2. Fill the test tubes completely with media for cleaning of the aspiration needle, before and after the oocyte collection, and for rinsing of the COCs during the collection.
   3. Push down the cork of the test tubes and place the metal block, containing the test tubes, for warming overnight in a bacteriological cabinet (37°C).
   Note: *The day before the egg collection, the nurse places round-bottom test tubes for prewarming in the bacteriological cabinet of the oocyte retrieval room. Additional test tubes with bench work media can be prepared for unforeseen additional work.*

   CO_2-dependent media

   1. Prepare and place two round-bottom test tubes in the metal block for cleaning of the aspiration needle before and after oocyte collection.
   2. Prepare, in accordance to the number of large follicles, several center-well dishes containing CO_2-dependent media for holding collected COCs.
      a. Aspirate and rinse a suitable-sized Combitip, refill it, and adjust the dispense volume.
      b. Fill the outer ring with 1.5 mL and the inner well with 600 µL of holding media, usually the fertilization media.
      c. Cover the inner center well with a thin layer of PLPO.
         i. Preincubate the dishes overnight or at least for 8 hr.
         ii. When five COCs have been collected in each dish, they are returned to the mini-incubator.
         Note: *These dishes are ready for insemination (IVF).*
         iii. Select a flat-bottom dish for insemination of COCs in microdrops. Number each droplet.

iv. Aspirate and rinse the selected Combitip, refill it, and adjust the dispense volume to the required droplet size (40 µL–50 µL).
v. Dispense the droplets according to your preference, preferably four prerinsing droplets in the middle and insemination droplets at the prelabeled numbers (1–5).
vi. Cover the droplets immediately with PLPO to avoid evaporation and detrimental changes in osmolality.
Note: *Only prepare one dish at a time!*
Note: *Do not place the droplets at the edge of the dish because it causes optical interference and a drop in temperature toward the edge of the dish.*

5. **For ICSI patients, you also prepare dishes for the following.**
   1. ***Denudation***
      a. ***Four-well dish***
         i. Aspirate and rinse a Combitip, refill it, and dispense 500 µL of fertilization medium in all four wells.
         Note: *One four-well dish per every five COCs.*
         ii. Place the dishes in the incubator for preincubation overnight.
      b. ***Flat-bottom 35 mm Petri dish***
         i. Rinse a Combitip with fertilization media, refill it, and adjust the volume to 100 µL–200 µL and dispense the media in the upper part of the dish.
         ii. Underneath the large droplet, dispense three additional 50 µL droplets of fertilization media to be used for rinsing and scoring of the partially denuded oocytes before they are transferred to the holding dish of the oocytes.
         iii. Cover the droplets immediately with PLPO.
         iv. The next day, the large upper droplet is aspirated with a yellow Eppendorf filter tip and is replaced with 100 µL–200 µL of prewarmed nontoxic hyaluronidase (ICSI Cumulase).
   2. ***Holding dishes for denuded oocytes****.*
   3. ***Oocyte injection dishes*** *(Nunc, Corning, or VitroWare)*
      Notes:
      - The ICSI Injection dishes can be prepared in many different ways, but the method should be standardized within the laboratory.
      - Select a flat-bottom ICSI dish that is in direct contact with the heated surface of the inverted microscope.
      - A dish with a low wall does not restrict the movement of the ICSI pipettes!
      - If the media droplets are placed in the middle of the dish, it is easier and quicker to perform the ICSI procedure.
      - Minimize the exposure of the oocytes to the outer environment by keeping the number of oocytes per dish at a minimum, which speeds up the ICSI procedure.
        a. Quickly cover the fertilization media droplets with PLPO.
        b. The next day, just before the ICSI procedure starts one of the droplets is replaced by prewarmed polyvinylpyrrolidone (PVP) or Sperm-Slow (SS).
        c. Return the dish to the incubator or preferably to the dish gasser for *short* rewarming and preincubation before the sperm and oocytes are introduced.
   4. Culture dishes for injected (ICSI) or short-time (1–4 hr) inseminated oocytes (IVF).
6. Place the dishes in the patient's allocated mini-incubator for preincubation overnight. Fill in the location of the dishes on the patient's embryo protocol (paper or software).
7. Confirm that you have enough FF collection dishes (Nunc, 35 mm) for warming and aeration on the heated and calibrated surface of the LAF bench.
   a. Warm additional back-up dishes in the bacteriological cabinet overnight.

8. Prepare the oocyte collectors and place them in the LAF bench for aeration overnight.
   Note: *Avoid mouth-pipetting, for safety reasons, and pulling of denudation pipettes, which will vary in dimensions, because they can damage oocytes and prevent standardization.*

BOX 2.3 OOCYTE COLLECTION AND INSEMINATION

Day 0: Oocyte collection and insemination

1. Adjust the light source and perform Køhler adjustment of the stereomicroscope.
   Note: *The more efficiently you work, the less exposure of the COCs to the outer environment and the better the embryo development.*
2. Verify the identity of the patient (double identification, wristband).
3. When anesthesia has been given, two prewarmed test tubes containing bench work media are placed in the test tube warmer in the oocyte retrieval room.
4. Turn on the gas humidifier in the LAF bench that delivers humidified, premixed gas to the dish gasser.
5. The clinician prerinses the aspiration needle with the bench work media and controls simultaneously the pump pressure.
   Note: *Perform oocyte collection 36–38 hpHCG*
6. Meanwhile, the embryologist puts on the correct-size embryo-tested nontoxic gloves and places two of the patient's center-well dishes under the dish gasser.
7. The embryologist prerinses one of the collectors with culture media, from the outer ring of the center-well dish, when the first test tube with FF is placed in the heat block next to or inside the LAF bench.
8. The contents of the test tube are poured out into prewarmed Petri collection dishes, and the test tube is discarded.
9. The FF is scanned through and when a COC is found
   A. CO_2-dependent media
      i. One of the dishes, underneath the dish gasser, is moved to the side of the collection dish, and preincubated media from the outer ring of the center-well dish is aspirated up into the prerinsed collector.
      ii. Preincubated media are flushed over the COC, to clear the area around the COC from debris, and the COC is taken up into the collector with as little contamination as possible.
      iii. The COC is *repeatedly* washed in the outer ring of the center-well dish and when clean, it is transferred into the center well.
      iv. The dish is then returned to its position under the dish gasser, and the collection dish is discarded in the waste bin.
      v. When the next COC is found, the second dish under the dish gasser is used, thus alternating between the dishes until you have a maximum of five COCs per dish or the oocyte collection is finished.
      vi. When the oocyte collection is finished, the number and quality of the COCs are evaluated (Table 2.1), and the dishes are placed in the patient's allocated mini-incubator.
      vii. The bench surface area is cleaned with lint-free wipes and water for injection, and the gloves are discarded.
      viii. Fill in all paper or software protocols.
      ix. The area and staff are ready for the next oocyte collection.

Alternatively you can use the following protocol.

B. Bench work media (HEPES or MOPS)
   i. Follow the instructions in points 7 and 8.
   ii. Pour out the FF of the first test tube in the prewarmed collection dishes.
   iii. Quickly pour in prewarmed media, from the bacteriological cabinet, into the outer and inner rings of a prewarmed center-well dish, for rinsing and collection of COCs.
   iv. Locate the COC and aspirate it with the prerinsed collector.
   v. Wash the COC *repeatedly* in the outer ring of the center-well dish, and when clean it is transferred into the center well.
   vi. When four or five COCs have been collected or when the dish has been on the LAF bench for 3–5 min, one of the patient's preincubated culture dishes is placed on the surface of the LAF bench.
      a. Wash the COCs *repeatedly* in the outer ring of the culture dish, and when clean they are transferred into the center well and placed in the patient's allocated mini-incubator.

10. Let the COCs "rest" in the mini-incubator until it is time for insemination (IVF) or denudation (ICSI).
11. Insemination (IVF)
   A. Short-time insemination (1–4 hr) in droplets (40–42 hpHCG)
      i. Verify the identity of the couple's prepared, diluted, and well-mixed sperm suspension.
      ii. Place one of the culture dishes with microdroplets on the heated surface of the LAF bench.
      iii. Prerinse a gray filter tip (1 µL–10 µL) and take up a standard aliquot of the sperm suspension and inseminate the microdroplets (20,000 motile sperm per droplet).
         a. Confirm that the droplets have been properly inseminated and incubate the dish for 30 min before the COCs are transferred into the droplets.
      iv. Place one culture and insemination dish close to each other on the heated surface of the LAF bench.
      v. Quickly prerinse a yellow filter tip (Biopur quality) with culture media from one of the centrally located droplets and aspirate one of the COCs from the center-well dish.
      vi. Wash the retrieved COC in two of the centrally located droplets, and then put it into one of the inseminated microdroplets.
      vii. Place the dish in the patient's allocated mini-incubator.
      viii. Incubate the dish in accordance to the preference of the laboratory.
      ix. After the selected insemination time, the dish is retrieved from the mini-incubator and placed on the heated surface of the LAF bench.
      x. Prerinse a stripper tip (175 µm), quickly aspirate the oocytes, and then expel them into the unused third centrally located droplet. Finally, place them in the fourth droplet with as little debris as possible.
         Note: *Do not denude the oocytes; just aspirate and transfer them to a clean droplet.*
      xi. Return the dish to the patient's allocated mini-incubator.
   B. Overnight insemination in a center-well dish
      i. Verify the identity of the couple's prepared, diluted. and well-mixed sperm suspension.
      ii. Prerinse a gray filter tip (1 µL–10 µL), aspirate a standard aliquot of the sperm suspension, and expel it into the collection dish containing the COCs (100,000 motile sperm per dish and five oocytes).
      iii. Place the dish in the patient's allocated mini-incubator overnight.

12. Denudation of oocytes (40–41 hpHCG) followed by ICSI within 30–60 min
    A. Four-well dish
        i. Prewarm a vial of ICSI Cumulase for 30 min in a block heater.
        ii. Retrieve the four-well dish containing the fertilization media from the incubator.
        iii. Quickly replace the fertilization media in the first well with prewarmed ICSI Cumulase and place the dish under the dish gasser.
        iv. Retrieve one of the patient's collection dishes with the COCs from the incubator and place it close to the light source of the LAF bench.
        v. Move the denudation dish from underneath the dish gasser, and put it close to the collection dish.
        vi. Quickly prerinse an Eppendorf yellow filter tip and a 150 µm Stripper tip with ICSI Cumulase.
        vii. Transfer the five COCs to the first well of the denudation dish, with the yellow filter tip, and gently denude the COCs by repeatedly aspirating and expelling the COCs into the ICSI Cumulase solution.
            – When a few layers of the cumulus are left, shift to the Stripper tip and transfer the partially denuded oocytes to the second well and continue the denudation.
            – Wash the partially denuded oocytes in the remaining wells.
            – Score the quality and maturation of the oocytes according to Table 2.2.
            – Take out a holding dish (see Holding dishes (2.4.5- CO_2 dependent media, page 32, #2) for denuded oocytes in Box 2.2) from the mini-incubator and transfer the denuded oocytes to the dish.
            – Place the dish in the patient's allocated space in the mini-incubator.
    B. Denudation of oocytes in droplets
        i. Prewarm a vial of ICSI Cumulase for 30 min in a block heater.
        ii. Retrieve the droplet denudation dish from the incubator.
        iii. Quickly replace the upper big fertilization media droplet with prewarmed ICSI Cumulase and place the dish under the dish gasser.
        iv. Retrieve one of the patient's collection dishes with the COCs from the incubator and place it close to the light source of the LAF bench.
        v. Move the denudation dish from underneath the dish gasser and put it close to the collection dish.
        vi. Quickly prerinse an Eppendorf yellow filter tip and a 150 µm Stripper tip with ICSI Cumulase.
        vii. Transfer five COCs to the large ICSI Cumulase droplet, with the yellow filter tip, and gently denude the COCs by repeatedly aspirating and expelling the COCs into the ICSI Cumulase solution.
            – When a few layers of the cumulus are left, shift to the Stripper tip and transfer the partially denuded oocytes to the first rinsing droplets and continue the denudation as described in "Four-well dish."

TABLE 2.2

Classification of the Oocyte Maturational Stages

Stage	Polar Body	Nucleus
Germinal vesicle (GV)	None	Large halo with nucleoli
Meiosis I (MI)	None	None
Meiosis II (MII)	Present	None

TABLE 2.3

Timing of Procedures in Relationship to Injection of HCG (hpHCG)

Procedure	Egg Collection	Oocyte Vitrification	Insemination (IVF)	Denudation	ICSI
hpHCG	36–38	38–40	40–41	40–41	41–42

13. Final preparation of the ICSI dishes
    Note: *The dishes can also be prepared the same day; the oocyte-holding droplets are replaced by prewarmed HEPES- or MOPS-buffered media.*
    A. Take out the preprepared ICSI dishes from the mini-incubator and exchange one of the droplets against PVP or SS.
    B. Add a low volume of highly motile sperm suspension to the edge of PVP or SS for swim-out and selection of sperm.
    C. Add a few partially denuded oocytes and perform ICSI as quickly as possible.
    D. After ICSI, the oocytes are transferred back to the patient's culture dish.
        i. Wash the oocytes in the centrally located droplets and keep the oocytes in the outer numbered droplets.
        ii. Place the dish in the patient's allocated incubator.
        iii. Repeat the procedure until all oocytes have been injected. (See Table 2.3, Timing of Procedures.)
14. Preparation of dishes for culture of fertilized oocytes (Zygotes, 2PN).
    A. The culture dishes are prepared in accordance to the steps discussed in Box 2.2, but for culture of zygotes to Day 2–3 or for Day 4–6 embryo (morula and blastocysts) cleavage, respectively, blastocyst culture media are used.
        i. There are also single-step media available that can be used from the zygote to the blastocyst stage without the need for changing of the media.

BOX 2.4 FERTILIZATION AND CLEAVAGE

Day +1: Control of fertilization (16–18 hpInsemination [hpInsem])

1. Clean the area with water for injection and lint-free clean-room wipes.
2. Verify the location of the couple's dishes.
3. Put on embryo-tested gloves and work aseptically.
4. Adhere a plastic or a glass denudation tip to a stripper (150 µm) or a Humagen handle.
5. Take out the patient dish from the incubator and verify the identity of the dish.
6. Place the dish under the dish gasser and retrieve the patient's preincubated culture dish, containing cleavage stage media, from the mini-incubator.
7. Prerinse the denudation pipette with media, from one of the droplets in the dish containing the oocytes and strip the oocytes of their remaining cumulus cells.
8. Gently roll the oocytes while evaluating the fertilization.
9. Retrieve all normally fertilized oocytes (2PN) and wash them in the centrally located droplets of the cleavage stage media and then group culture them in one of the outer droplets.
    i. Separate unfertilized, single and multinucleated oocytes and transfer them to their allocated droplets.
    ii. Note in which droplet they are cultured.
    iii. Score early cleavage 25–27 and 27–29 hpInsem for ICSI and IVF, respectively.

Day +2–3: Control of embryo cleavage and quality (43–45 resp. 67–69 hpInsem)
Day +4–5: Control of compaction and blastocyst stage (90–94 resp. 114–118 hpInsem)

For information on how to perform and morphologically evaluate oocytes and perform scoring of zygotes, embryos, and blastocysts, see Chapters 5 through 8 in this book.

REFERENCES

1. Doshi A, Karunakaran S, Worrilow K, et al. What makes an IVF laboratory successful? In: *A Practical Guide to Setting Up an IVF Lab, Embryo Culture Systems and Running the Unit* (eds. Varghese A, Sjoblom P, Jayaprakasan K). New Delhi: Jaypee Brothers Medical Publishers, 2013, pp. 13–23.
2. Johansson L. Establishment of an ART clinic: Location, construction and design. In: *A Practical Guide to Setting Up an IVF Lab, Embryo Culture Systems and Running the Unit* (eds. Varghese A, Sjoblom P, Jayaprakasan K). New Delhi: Jaypee Brothers Medical Publishers, 2013, pp. 24–30.
3. Schimmel T, Gilligan A, Garrisi GJ, et al. Removal of volatile organic compounds from incubators used for gamete and embryo culture. *Reprod Fertil* 1997;68(Suppl 1):S52–S53.
4. Khoudja RY, Xu Y, Li T, et al. Better IVF outcomes following improvements in laboratory air quality. *J Assist Reprod Genet* 2012;30(1):69–76.
5. Worrilow KC. *The Impact of UVC Irradiation on Clinical Pregnancy Rates in an ISO 5 Cleanroom In Vitro Fertilization Laboratory*. ASHRAE IAQ Guide, ASHRAE, Atlanta, 2009, pp. 4–6.
6. Worrilow KC, Huynh HT, Bower JB, et al. A retrospective analysis: Seasonal decline in implantation rates (IR) and its correlation with increased levels of volatile organic compounds (VOC). *Fertil Steril* 2002;78(Suppl 1):S39.
7. Baart EB, Martini E, Eijkemans MJ, et al. Milder ovarian simulation for in vitro fertilization reduces aneuploidy in the human preimplantation embryo: A randomized controlled trial. *Hum Reprod* 2007;22:980–988.
8. Pena JE, Chang PL, Chan LK, et al. Supraphysiological estradiol levels do not effect oocyte and embryo quality in oocyte donation cycles. *Hum Reprod* 2002;17:83–87.
9. Hohmann FP, Macklon NS, Fauser BC. A randomized comparison of two ovarian stimulation protocols with gonadotropin-releasing hormone antagonist cotreatment for in vitro fertilization commencing recombinant follicle stimulating hormone on cycle 2 or 5 with standard long GnRH agonist protocol. *J Clin Endocrinol Metab* 2003;88:166–173.
10. Fauser BC, Devroey P, Macklon NS. Multiple birth resulting from ovarian stimulation for subfertility treatment. *Lancet* 2005;365:1807–1816.
11. Macklon NS, Fauser BC. Impact of ovarian hyperstimulation on the luteal phase. *J Reprod Fertil* 2000;55:101–108.
12. Howles CM, Macnamee MC, Edward RG, et al. Effect of high tonic levels of luteinizing hormone on the outcome of in-vitro fertilization. *Lancet* 1986;2(8505):521–522.
13. Homburg R, Armar NA, Eshel A, et al. Influence of serum luteinizing hormone concentrations on ovulation, conception and early pregnancy loss in polycystic ovary syndrome. *Br Med J* 1988;297:1024–1026.
14. Regan L, Owen EJ, Jacobs HS. Hypersecretion of luteinizing hormone, infertility and miscarriage. *Lancet* 1990;336:1141–1144.
15. Outsuki J, Okada A, Morimoto K, et al. The relationship between pregnancy outcome and smooth endoplasmic reticulum clusters in MII human oocytes. *Hum Reprod* 2004;19:1591–1597.
16. Hassan-Ali H, Hisham-Saleh A, El-Gezeiry D, et al. Perivitelline space granularity: A sign of human menopausal gonadotropin overdose in intracytoplasmic sperm injection. *Hum Reprod* 1998;13:3425–3430.
17. Nagaoka I, Hassold TJ, Hunt PA. Human aneuploidy: Mechanisms and new insights into an age-old problem. *Nat Rev Genet* 2012;13:493–504.
18. Wikland M. Oocyte retrieval. In: *In Vitro Fertilization – A Practical Approach* (ed. Gardner D). New York: Informa Health Care Inc., 2007, pp. 117–126.
19. Higdon H, Blackhurst D, Boone W. Incubator management in an assisted reproductive technology laboratory. *Fertil Steril* 2008;89:703–710.
20. Endler GC, Stout M, Magyar DM, et al. Follicular fluid concentrations of thiopental and thiamylal during laparoscopy for oocyte retrieval. *Fertile Steril* 1987;48:828–833.

21. Hayez MF, Sacco AG, Savoy-Moore RT, et al. Effect of general anaesthesia on fertilization and cleavage of human oocytes in vitro. *Fertil Steril* 1987;48:975–981.
22. Gonen O, Schulman A, Gethler Y, et al. The impact of different types of anaesthesia on in vitro fertilization-embryo transfer treatment outcome. *J Assist Reprod Genet* 1995;12:678–682.
23. Matt DW, Steingold KA, Dastvan CM, et al. Effects of sera from patients given various anaesthetics on pre-implantation mouse embryo development in vitro. *J In Vitro Fert Embryo Transf* 1991;8:191–197.
24. Soussis I, Boyd O, Paraschos T, et al. Follicular levels of midazolam, fentanyl and alfentanil during transvaginal oocyte retrieval. *Fertil Steril* 1995;64:1003–1007.
25. Wilhelm W, Hammamed ME, White PF, et al. General anaesthesia versus monitored anaesthesia care with remifentanil for assisted reproductive technologies: Effect on pregnancy rate. *J Clin Anesthesia* 2002;14:1–5.
26. Bokhari A, Pollard BJ. Anaesthesia for assisted conception: A survey of UK practice. *Eur J Anesthesiol* 1999;16:225–230.
27. Wikland M, Evers H, Jacobsson AH, et al. The concentration of lidocaine in follicular fluid when used for paracervical block in a human IVF-ET programme. *Hum Reprod* 1990;5:920–923.
28. Ben-Shlomo I, Moskovich R, Golan J, et al. The effect of propofol anaesthesia on oocyte fertilization and early embryo quality. *Hum Reprod* 2000;15:2197–2199.
29. Hadimiglou N, Titz T, Dosemeci L, et al. Comparison of various sedation regimes for transvaginal oocyte retrieval. *Fertil Steril* 2002;78:648–649.
30. Jain D, Kohli A, Gupta L, et al. Anaesthesia for in vitro fertilization. *Indian J Anaesth* 2009;53(4):408–413.
31. Garg R, Dali JS. Assisted reproductive technology and anesthetic considerations: Review of literature. *Int J Anesthesia* 2008;18(2).
32. Steiner HP. Optimizing technique of follicular aspiration and flushing. In: *Minimal Stimulation IVF – Milder Mildest or Back to Nature* (eds. Chaves-Badiola A, Allahbadia GN). New Delhi: Jaypee Brothers Medical Publishers, 2011, pp. 98–102.
33. Awonuga A, Waterstone J, Ovesanya O, et al. A prospective randomized study comparing needles of different diameters for transvaginal ultrasound-directed follicle aspiration. *Fertil Steril* 1996;65:109–113.
34. Wikland M, Blad S, Bungum L, et al. A randomized controlled study comparing pain experience between a newly designed needle with a thin tip and a standard needle for oocyte aspiration. *Hum Reprod* 2011;26(6): 1377–1383.
35. Pickering SJ, Braude PR, Johnson MH, et al. Transient cooling to room temperature can cause irreversible disruption of the meiotic spindle in the human oocyte. *Fertil Steril* 2009;54:102–108.
36. Nijs M, Franssen K, Cox A, et al. Reprotoxicity of intrauterine insemination and in vitro fertilization-embryo transfer disposables and products: A 4-year survey. *Fertil Steril* 2009;92(2):527–535.
37. Cohen J, Avery S, Campbell S, et al. Follicular aspiration using a syringe suction system may damage the zona pellucida. *J In Vitro Fert Embryo Transf* 1986;3(4):224–226.
38. Will M, Clark N, Swain J. Biological pH buffers in IVF: Help or hindrance to success. *J Assist Reprod Genet* 2011;28(8):711–724.
39. Morbeck DE, Khan Z, Barnidge DR, et al. Washing mineral oil reduces contaminants and embryotoxicity. *Fertile Steril* 2010;94(7):2747–2752.
40. Otsuki J, Nagai Y, Chiba K. Damage of embryo development caused by peroxidized mineral oil and its association with albumin in culture. *Fertil Steril* 2009;91(5):1745–1749.
41. Wagner-Coughlin CM, Maravilla AE, Nikurs AR, et al. Microdroplets under oil improves embryo quality even when an isolette is used. *Fertil Steril* 1994;62(Suppl 1):S177.
42. Swain JE, Cabrera L, Xu X, et al. Microdrop preparation factors influence culture-media osmolality which can impair mouse embryo preimplantation development. *Reprod Biomed Online* 2012;24(2):142–147.
43. Swain JE. Media composition: pH and buffers. In: *Embryo Culture Methods and Protocols* (eds. Smith G, Swain JE, Pool TB). New York: Humana Press, Springer Science + Business Media, 2012, pp. 161–175.
44. Koustas G, Sjøblom Ø. Epigenetic consequences of pH stress in mouse embryos. *Hum Reprod* 2011;26:i78.
45. Ottesen LD, Hindkjaer J, Ingerslev J. Light exposure of the ovum and pre-implantation embryo during ART procedures. *J Assist Reprod Genet* 2007;24(2–3):99–103.
46. Takenaka M, Horiuchi T, Yanagimachi R. Effects of light on development of mammalian zygotes. *Proc Natl Acad Sci USA* 2007;105(36):14289–14293.

47. Van Blerkom J, Antczak M, Schrader R. The developmental potential of the human oocyte is related to the dissolved oxygen content of follicular fluid: Association with vascular endothelial growth factor levels and perifollicular blood flow characteristics. *Hum Reprod* 1997;12:1047–1055.
48. Huey S, Abuhamad A, Barros G, et al. Perifollicular blood flow Doppler indices, but not follicular pO2, pCO2 or pH predict oocyte developmental competence in in vitro fertilization. *Fertil Steril* 1999;72(4):707–712.
49. Daya S, Kohut J, Gunby J, et al. Influence of blood clots in the cumulus complex on oocyte fertilization and cleavage. *Hum Reprod* 1990;5:744–746.
50. Ebner T, Moser M, Shebl O, et al. Blood clots in the cumulus-oocyte complex predict poor oocyte quality and post-fertilization development. *Reprod Biomed Online* 2008;16:801–807.
51. Gilchrist RB, lane M, Thompson JG. Oocyte-secreted factors: Regulators of cumulus cell function and oocyte quality. *Hum Reprod Update* 2008;14(2):159–177.
52. Montag M, Køster M, Van der Ven H. Polarization microscopy. In: *Practical Manual of In Vitro Fertilization, Advanced Methods and Novel Devices* (eds. Nagy ZP, Varghese AC, Agarwal A). New York: Springer, 2012, pp. 121–125.
53. Pelzer ES, Allan JA, Cunningham K, et al. Microbial colonization of human follicular fluid: Alterations in cytokine expression and adverse assisted reproductive technology outcome. *Hum Reprod* 2011;26(7):1799–1812.
54. Kovacic B, Vlaisavljevic V. Influence of atmospheric versus reduced oxygen concentrations on development of human blastocysts in vitro: A prospective study on sibling oocytes. *Reprod Biomed Online* 2008;17:229–236.
55. Waldenstrøm U, Engstrøm A, Hellberg D, et al. Low-oxygen compared with high-oxygen atmosphere in blastocyst culture, a prospective randomized study. *Fertil Steril* 2009;91:2461–2465.
56. Meintjes M, Chantilis SJ, Douglas JD, et al. A controlled randomized trial evaluating the effect of lowered incubator oxygen tension on live births in a predominantly blastocyst transfer program. *Hum Reprod* 2009;24:300–307.
57. Catt J, Henman M. Toxic effects of oxygen on human embryo development. *Hum Reprod* 2000;15(Suppl 2): 199–206.
58. Gardner D, Lane M. Ex vivo early embryo development and effects on gene expression and imprinting. *Reprod Fertil Dev* 2005;17(3):361–370.
59. Katz-Jaffe MG, Linck DW, Schoolcraft WB, et al. A proteomic analysis of mammalian preimplantation embryonic development. *Reproduction* 2005;130(6):899–905.
60. Enkhmaa D, Kasai T, Hoshi K. Longtime exposure of mouse embryos to the sperm produces high levels of reactive oxygen species in culture medium and relates to poor embryo development. *Reprod Domest Anima* 2009;44:634–637.
61. Fitzharris G, Baltz KM. Granulosa cells regulate pH of the murine growing oocyte via gap junctions: Development of independent homeostasis during oocyte growth. *Development* 2006;133(4):591–599.
62. Fitzharris G, Sitanov V, Baltz KM. Granulosa cells regulate oocyte intracellular pH against acidosis in preantral follicles by multiple mechanisms. *Development* 2007;134(23):4283–4295.
63. Phillips KP, Petrunewich MA, Collins JL, et al. The intracellular pH-regulatory HCO3/Cl exchanger in the mouse oocyte is inactivated during the first meiotic metaphase and reactivated after egg activation via the MAP kinase pathway. *Mol Biol Cell* 2002;13(11):3800–3810.
64. Lane M, Lyons EA, Bavister BD. Cryopreservation reduces the ability of hamster 2-cell embryos to regulate intracellular pH. *Hum Reprod* 2000;15(2):389–394.
65. Phillips KP, Leveille MC, Claman P, et al. Intracellular pH regulation in human preimplantation embryos. *Hum Reprod* 2000;15(4):896–904.
66. Swain JE. Optimizing the culture environment in the IVF laboratory: Impact of pH and buffer capacity on gamete and embryo quality. *Reprod Biomed Online* 2010;21(1):6–16.
67. Swain JE, Pool TB. New pH-buffering system for media utilized during gamete and embryo manipulations for assisted reproduction. *Reprod Biomed Online* 2009;18(6):799–810.
68. Pool TB. Optimizing pH in clinical embryology. *Clin Embryol* 2004;7:1–7.
69. Ebner T, Moser M, Sommergruber M, et al. Incomplete denudation of oocytes prior to ICSI enhances embryo quality and blastocyst development. *Hum Reprod* 2006;21:2972–2977.
70. Cunningham KJ, McCarthy CB, Russell JB. The pH change in a microdroplet system under oil with different numbers of sperm added for insemination. *Fertil Steril* 1994;62(Suppl 1):S47.
71. Edwards LJ, Williams DA, Gardner DK. Intracellular pH of the mouse preimplantation embryo: Amino acids act as buffers of intracellular pH. *Hum Reprod* 1998;13(12):3441–3448.

72. Baltz JM. Media composition: Salts and osmolality. In: *Embryo Culture: Methods and Protocols* (eds. Smith GD, Swain JE, Pool TB). New York: Humana Press, Springer Science + Business Media, 2012, pp. 61–80.
73. Kolajora M, Baltz JM. Volume-regulated anion and organic osmolyte channels in mouse zygotes. *Biol Reprod* 1999;60:964–972.
74. Quinn P, Margalit R. Beneficial effects of co-culture with cumulus cells on blastocyst formation in a prospective trial with supernumerary human embryos. *J Assist Reprod Genet* 1996;13:9–14.
75. Ebner T, Shebl O, Moser M, et al. Group culture of human zygotes is superior to individual culture in terms of blastulation, implantation and life birth. *Reprod Biomed Online* 2010;21:762–768.
76. Brison DR, Schultz RM. Apoptosis during mouse blastocyst formation: Evidence for a role for survival factors including transforming growth factor alpha. *Biol Reprod* 1997;56(5):1088–1096.
77. Gardner DK, Lane M. Embryo culture. In: *Textbook of Assisted Reproductive Techniques. Laboratory and Clinical Perspectives* (eds. Gardner D, Weismann A, Howles CM, Shoham Z). London: Martin Dunitz, 2008; pp. 219–240.
78. Behr B, Pool TB, Milki AA, et al. Preliminary clinical experience with human blastocyst development in vitro without co-culture. *Hum Reprod* 1999;14:454–457.
79. Almagor M, Bejar C, Kaftka I, et al. Pregnancy rates after communal growth of preimplantation human embryos in vitro. *Fertil Steril* 1996;66:394–397.
80. Smith G, Bormann C, Takayama S. Microfluidics for gamete manipulation and embryo culture. In: *Practical Manual of In Vitro Fertilization: Advanced Methods and Novel Devices* (eds. Nagy ZP, Varghese AC, Agarwal A). New York: Springer Science + Business Media, 2012, pp. 171–181.
81. Swain JE, Smith GD. Advances in embryo culture platforms: Novel approaches to improve preimplantation embryo development through modifications of the microenvironment. *Hum Reprod Update* 2011;17:541–557.
82. Matsuura K, Hayashi N, Kuroda Y, et al. Improved development of mouse and human embryos using a tilting embryo culture system. *Reprod Biomed Online* 2010;20:358–364.
83. Isachenko E, Maettner R, Isachenko V, et al. Mechanical agitation during the in vitro culture of human preimplantation embryos drastically increases the pregnancy rate. *Clin Lab* 2010;56(11–12):569–576.
84. Isachenko V, Maettner R, Sterzik K, et al. In-vitro culture of human embryos with mechanical micro-vibration increases implantation rates. *Reprod Biomed Online* 2011;22(6):536–544.
85. Guerin P, El Mouatassim S, Menezo Y. Oxidative stress and protection against reactive oxygen species in the preimplantation embryo and its surroundings. *Hum Reprod Update* 2001;7:175–189.
86. Menezo Y, Sakkas D. Monozygotic winning, is it related to apoptosis in the embryo? *Fertil Steril* 2002;17:247–248.
87. Desai N, Kattal N, AbdelHafez F, et al. Granulocyte-macrophage colony-stimulating factor (GM-CSF) and co-culture can effect post thaw development and apoptosis in cryopreserved embryos. *J Assist Reprod Genet* 2007;24:215–222.
88. Sjøblom C, Wikland M, Robertson S. Granulocyte-macrophage colony-stimulating factor promotes human blastocyst development in vitro. *Hum Reprod* 1999;14:3069–3076.
89. Kaufman RA, Menezo Y, Hazout A, et al. Cocultured blastocyst cryopreservation: Experience of more than 500 transfer cycles. *Fertil Steril* 1995;64:1125–1129.
90. Kim D, Kim M, Kang H, et al. The supplementation of granulocyte-macrophage colony-stimulating factor (GM-CSF) in culture medium improves the pregnancy rate in human ART programs. *Fertil Steril* 2001;76:s6.
91. Shapiro B, Richter K, Daneshmand S, et al. Granulocyte-macrophage colony-stimulating factor enhances human embryo development to the blastocyst stage, a randomized study. *Fertil Steril* 2003;79:15–16.
92. Milki A, Jun S, Hickley M, et al. Incidence of monozygotic twinning with blastocyst transfer compared to cleavage-stage transfer. *Fertil Steril* 2003;79(3):503–506.
93. Behr B, Fisch J, Racowsky C, et al. Blastocyst-ET and monozygotic twinning. *J Assist Reprod Genet* 2000;17(6):349–351.
94. Wright V, Schieve L, Vahratian A, Reynolds M. Monozygotic twinning associated with day 5 embryo transfer in pregnancies conceived after IVF. *Hum Reprod* 2004;19(8):1831–1836.
95. Mantikou E, Youssef MA, van Wely M, et al. Embryo culture media and IVF/ICSI success rates: A systematic review. *Hum Reprod Update* 2013;19(3):210–220.
96. Aoki VW, Wilcox AL, Peterson CM. Comparison of four media types during 3-day human IVF embryo culture. *Reprod Biomed Online* 2005;10(5):600–606.

97. Kovacic B, Vlaisavljevic V, Reljic M, et al. Clinical outcome of day 2 versus day 5 transfer in cycles with one or two developed embryos. *Fertil Steril* 2002;77(3):529–536.
98. McArthur SJ, Leigh D, Marshall JT, et al. Blastocyst trophectoderm biopsy and preimplantation genetic diagnosis for familial monogenetic disorder and chromosomal translocations. *Prenat Diagn* 2008;28:434–442.
99. Reed ML, Hamic A, Thompson DJ, et al. Continuous uninterrupted single medium culture without medium renewal versus sequential media culture: A sibling embryo study. *Fertil Steril* 2009;92(5):1783–1786.
100. Sepulveda S, Garcia J, Arriaga E, et al. In vitro development and pregnancy outcomes for human embryos cultured in either a single medium or in a sequential media system. *Fertil Steril* 2009;91:1765–1770.

3

Handling Gametes and Embryos: Quality Control for Culture Conditions

Jason E. Swain

Introduction

Quality control (QC) in the culture system is a crucial factor in ensuring success within the in vitro fertilization (IVF) lab. Without proper QC or quality assurance (QA), no combination of culture media, protein, and novel culture platforms of implementation of cutting-edge lab technology will yield acceptably high outcomes. When it comes to optimizing results within the IVF laboratory, the devil really is in the details.

When optimizing IVF results in the laboratory, the devil really is in the details.

Listing all areas for QC and QA within the lab is a monumental task, and it is not feasible to address all of them within the confines of this chapter. However, a general area that deserves extra attention and focus is laboratory environmental control; specifically those environmental variables that directly affect the culture system. Various environmental parameters can act as stressors within the culture system and compromise gamete and embryo development and function. Only through accurate monitoring of these variables can proper implementation be achieved. Of particular importance are those variables that can be adjusted or altered directly within the laboratory, sometimes inadvertently, resulting in compromised embryo development.

Contact Material Testing

One of the most important aspects of laboratory QC and QA with respect to the culture system is the testing of all contact materials to avoid introduction of contamination or toxicity into the culture environment. It is well documented that not all products, despite being packaged or sold as sterile, are inert in terms of impact on embryo development [1,2]. Thus, verification of material safety is required before clinical use. This verification is usually performed using a relevant bioassay, such as the mouse embryo assay (MEA) (Appendix 3A) or the human sperm survival assay, also known as the human sperm motility assay (Appendix 3B).

Comparisons and the merits of these two assays have been discussed previously [3–9], and each can be useful in its own way, with factors such as cost and availability warranting attention. Perhaps more importantly, the sensitivity of the bioassay is imperative, and approaches can be modified to increase the sensitivity to ensure that subtle material toxicities can be detected. Examples of approaches used to increase sensitivity are the one-cell versus the two-cell MEA, outbred versus inbred versus hybrid mouse strains, blastocyst cell counts versus simple blastocyst formation, exclusion of protein from media versus protein inclusion, and simple media versus a more robust complex media [10–12]. Notably, thresholds must be set for an assay to "pass," and these thresholds should be set to ensure rigorous criteria. Each laboratory can determine which assay and threshold suit their needs regarding sensitivity and cost. A commonly used and often recommended sensitive assay includes using the one-cell MEA, noting time-appropriate embryo development with rate of expanded or hatching blastocyst >70% at 96 hr (4 days) of culture. Other useful endpoints to assess material biocompatibility may include early

APPENDIX 3A: CONTACT MATERIAL MEA ASSAY

Purpose: All contact materials that are used during the collection, incubation, and transfer of gametes and embryos must be tested before use for their ability to support mouse blastocyst development from the one-cell stage. Untested material must remain in packing boxes and not be placed into lab circulation until testing is complete and passed. If materials are pretested by the manufacturer using an approved assay with appropriate sensitivity, and the laboratory has confidence in the pretesting procedures from the manufacturer, these materials may be exempt from further laboratory testing (this decision is at the discretion of each laboratory).

Controls

A. Positive control
   1. A positive control is set up for each item being tested. This usually entails use of materials/lot numbers already in use, having previously passed screening (>70% blastocyst formation).

Materials and Equipment (not all inclusive)

Culture dishes
Collection dishes
Test tubes (all sizes)
Pipettes (all sizes)
Catheters
Specimen collection containers
Pipette tips
Filters and receivers
Syringes
Media (all types)
Mineral oil

Procedure

A. Grouping of items helps conserve resources and cost. No more than three items should be grouped together at one time to facilitate ease of retesting and identifying the offending item if a test has failed. An example procedure is as follows:
   1. Draw up culture media into new lot of serological pipettes. Hold for 5 min to allow adequate exposure.
   2. Expel media from pipette into new lot of test tubes. Hold media for 5 min.
   3. Draw up media from new test tubes and expel appropriate amount on new lot of culture dishes per laboratory protocol to permit embryo culture (i.e., 50 µL microdrop covered with 5 mL of oil).
   4. Place at least 10 one-cell mouse embryos into the test drop of media and culture for 96 hr, checking development at appropriate intervals to verify time-appropriate development. Embryos can be obtained fresh if a mouse colony is available, or frozen one-cell embryos may be used. The strain of mouse is flexible, although F1 hybrids are less sensitive.
   5. Prepare culture media using currently used, prior tested, or approved lots as per lab protocol to serve as the positive control. Place at least 10 embryos into the medium and incubate in the same incubator as the test sample made in step 4.

Results

A. If the tested material yields expanded and hatching blastocyst formation >70%, it passes the MEA. This should be within 10%–20% of the positive control results. Materials can be released into lab circulation. Also important to note is that time-appropriate development should be apparent between test and control materials, paying particular attention to the percentage of advanced cell development at each time point to ensure no lag is present with the new test lots (e.g., early compaction at 48 hr and early blast formation at 72 hr should be within 20% of controls).

B. If out of limits, various options can be explored:
   1. Retest in same manner/group
      a. If the test passes, materials can be released or used.
      b. If the test fails, items can be retested individually to identify the offending product.

If the toxic item is identified from the failed test, return the lot to the manufacturer and request new lot number.

If the specific item cannot be identified when testing individually, a more sensitive test can be performed (no protein, less robust medium) or all items from the failed test batch can be returned and new items ordered or tested.

C. Record all tests and results in a contact material log. Also note when new lots are placed into circulation or used to permit tracking.

D. Label tested material with test date and technologist's initials and place into circulation if passed.

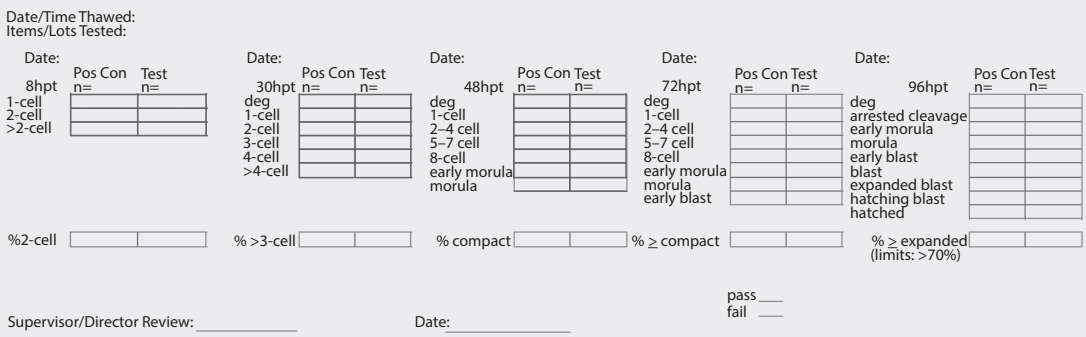

FIGURE 3A.1 Material testing and sample MEA development tracking form.

compaction or early blastocyst formation at 48 and 72 hr, respectively, to ensure new materials yield similar results to controls (Figure 3A.1). Indeed, real-time assessment of morphokinetics has been used to improve sensitivity of the MEA [13].

One point worthy of note is that many materials from manufacturers can now be purchased as "pretested," having passed some manner of bioassay. However, these manufacturers' bioassays may not meet the sensitivity criteria of individual labs. Furthermore, factors affecting material quality can convey detrimental effects at a point after the initial successful passing of the bioassay. For example, improper storage conditions in warehouses or delayed effects from prolonged storage can cause a "prescreened" item to later become toxic once received in the laboratory. A common example of this situation is the toxicity associated with mineral oil [1,13,14]. Also, potential toxicity from a single item could be very minor, but when used in the context of several sequential items in a particular laboratory culture system, this toxicity could be compounded due to interactions with other system components. This occurrence is noted anecdotally across several labs, where "tested" materials are later found to have a detrimental impact. Therefore, more stringent labs retest certain pretested materials, or they test them in a manner similar to their use within the lab to help ensure safety.

APPENDIX 3B: CONTACT MATERIAL HUMAN SPERM MOTILITY ASSAY

Principle: All contact materials that are used during the collection, incubation, and transfer of gametes and embryos must be tested before use for their effect on sperm motility. Untested material must remain in packing boxes and not be placed into lab circulation until testing is complete, with a positive outcome. If materials are pretested by the manufacturer using an approved assay with appropriate sensitivity, and the laboratory has confidence in the pretesting procedures from the manufacturer, these materials may be exempt from further laboratory testing (this is at the discretion of each laboratory).

Controls

A. Positive control
   1. A positive control is set up for each item being tested.
   2. The positive control is the current lot number being used.

B. Negative control
   1. A negative control is set up for each batch of material being tested.
   2. A small piece of powdered glove serves as the negative control.
   3. The glove piece is placed in a small snap top tube that contains a density gradient processed sperm sample (10×10^6/mL and ≥70% motility).
   4. Motility is observed after 24 hr incubation.
      a. Expected value: 0% motility

Materials and Equipment

Culture dishes
Collection dishes
Test tubes (all sizes)
Pipettes (all sizes)
Catheters
Specimen collection containers
Pipette tips
Filters and receivers
Syringes
Media (all types)
Mineral oil

Procedure: Sperm should be prepared using density gradient separation to obtain a final motility >70%. Several sperm samples can be combined to form a high concentration of a homogenous mixture and 1 mL aliquots made for testing of multiple items.

A. Culture dishes
   1. Fill dish with processed sperm sample (10×10^6/mL and ≥70% motility).
   2. Repeat for positive controls of each item being tested.
   3. For the small tissue culture dishes, place sperm sample on dish as microdrops and cover with oil.
   4. Incubate for 24 hr in CO_2 incubator.
   5. Check motility and forward progression.

B. Tubes
   1. Fill tubes with 1 mL of processed sperm sample (10×10^6/mL and ≥70% motility).
   2. Repeat for positive controls of each item being tested.
   3. Incubate for 24 hr in CO_2 incubator.
   4. Check motility and forward progression.

C. Pipettes, catheters, syringes, and pipette tips
   1. Aspirate processed sperm (10×10^6/mL and ≥70% motility) into material being tested.
   2. Repeat for positive controls of each item being tested.
   3. Allow to sit for 30 min.
   4. Expel sample into tested test tube.
   5. Incubate for 24 hr in CO_2 incubator.
   6. Check motility and forward progression.

D. Specimen containers
   1. Fill containers with 1 mL of processed sperm sample (10×10^6/mL and motility ≥70%).
   2. Repeat for positive controls for each item being tested.
   3. Allow to sit for 30 min.
   4. Transfer sample into tested small snap top tube (Falcon 2054).
   5. Incubate for 24 hr in CO_2 incubator.
   6. Check motility and forward progression.

E. Filter units
   1. Filter media through filter unit.
   2. Add appropriate amount of sperm with ≥70% motility to filtrate to obtain 10×10^6/mL.
   3. Repeat for positive controls of each item being tested.
   4. Allow to sit for 30 min.
   5. Transfer a portion of sample into tested small snap top tube (Falcon 2054).
   6. Incubate for 24 hr in CO_2 incubator.
   7. Check motility and forward progression.

Results

A. If the tested material has sperm motility within 10% of the positive control and the same forward progression, it is within acceptable limits for use.
B. If out of limits, perform the following steps.
   1. Retest.
   2. If material is still out of limits, return the lot to the manufacturer and request a new lot number.
C. Record all tests and results in a contact material log. Also note when new lots are placed into circulation or used to permit tracking.
D. Label tested material with test date and the technologist's initials and place into circulation if passed.

Air Quality

Air quality is another environmental variable that deserves attention when performing QC in the IVF laboratory culture system [15], and it can be inadvertently influenced. All modern IVF labs should have laminar flow hoods in which to prepare culture dishes or observe embryos to avoid possible contamination, and the these hoods should undergo routine annual maintenance to ensure proper functioning. Many labs also have specialized, dedicated air filtration units that not only provide positive pressure and limit particle counts through use of high-efficiency particulate absorption (HEPA) filters, but also are outfitted with charcoal or potassium permanganate filters to remove volatile organic compounds (VOCs) from circulation. Use of ultraviolet (UV) photocatalytic oxidation may also be used to reduce VOC levels [16,17]. The presence of VOCs, such as aldehydes or toluene, within the air of IVF labs has been well documented [18–20], and it is well accepted that poor air quality can compromise the culture system, whereas measures to improve air quality result in improved outcomes [21], presumably due to the detrimental effects of the VOCs on the preimplantation embryo [18,20,22,23]. Importantly, these VOCs may stem from materials used in lab construction or cleaning, such as cabinet or flooring materials, various adhesives,

TABLE 3.1

Recommended Monitoring and Filter Exchange Schedules to Maintain or Improve IVF Lab Air Quality

Equipment	Recommended Maintenance
Heating, ventilating, and air-conditioning (HVAC)/air handler (positive pressure, if present)	Confirm daily
HVAC/air handler (HEPA filters, charcoal/permanganate filters)	Replace 3–6 months or as needed
Incubator HEPA filters	Replace 6–12 months
Incubator/gas line VOC filters	Replace 3–6 months
Laminar flow hood prefilters	Replace or clean annually or as needed
Laminar flow hood (flow rate inspection)	Inspect annually
Lab air quality assessment (particle counts, VOC levels)	Inspect annually

Note: Lab air exchange rates may be modified to improve certain variables, such as particle counts. Additional maintenance may be required to maintain air quality if other systems are in place (i.e., UV photocatalytic oxidation).

solvents, cleansers, or paint or from plastics and other materials stored in the lab. Thus, careful selection of items used in and around the laboratory is essential to prevent accidental introduction of harmful VOCs.

Poor air quality in the lab can compromise embryo development and outcome, but air quality in the incubator should also be addressed.

An initial assessment of air quality within the IVF lab is recommended to determine whether a problem exists, and whether preventative measures are needed to improve air quality (i.e., reduce VOC levels). Methods for air quality assessment can be found elsewhere and include particle count testing, VOC level determination, and other methods [15,24]. Unfortunately, threshold limits for detrimental impact of air quality are difficult to verify. Particle counts are often recommended to fall below standards for International Organization for Standardization (ISO) class 7, and harmful levels of VOCs are undefined. Regardless of lab levels, regular assessment of laboratory air quality, including particle count and VOC levels, and routine replacement of relevant air filters and adjustment of air exchange rates is prudent to ensure air quality conditions have not changed or deteriorated dramatically over time; such assessments also may indicate inappropriate procedures (e.g., new cleaning agents, improper storage of lab supplies) or improper equipment or filter functioning (Table 3.1).

Perhaps, more importantly, air quality within the laboratory incubator should also be addressed. Air quality within the laboratory incubator, in part, is influenced by the quality of the room air. However, VOCs can accumulate inside of incubators due to presence of dishware at elevated temperatures and lack of routine or thorough air exchange within the closed environment. Interestingly, use of low-oxygen incubators entails the use of ~90% nitrogen in place of room air or premixed tri-gas cylinders. Thus, this may offer an opportunity to provide an initial purer gas quality within the laboratory incubator, if the gas supply is free from contaminants. However, this may not always be the case, because gas cylinders can be the source of harmful VOCs, such as benzenes or alcohols [18,19]. Thus, inclusion of specialized inline filters or filters placed within the incubator [23,25–27] are recommended to remove VOCs from the gas supply or incubator and to further improve air quality inside. These incubator filters should be replaced at regular intervals, with recommendations often being every 3–6 months (Table 3.1).

Dish Setup

It is known that media osmolality affects embryo development [28–32], although tolerances and optimal values vary between cell stages and are dependent upon media formulation. When osmolality increases >~300 mOsm, development is compromised. Thus, embryo culture media is usually formulated in the range of 260–290 mOsm. In addition, inclusion of organic osmolytes, including key amino acids, helps regulate cell volume and combat media osmolality changes [28–31,33–37]. Although it is not required to retest commercial media osmolality, because these media are generally pretested using an MEA before release by the manufacturer, QC measures should be taken to ensure that detrimental shifts in osmolality do not inadvertently occur within the laboratory.

This measure is achieved via avoidance of evaporation that can occur primarily during improper setup of culture dishes or improper culture conditions.

It has been shown that temperature, volume of media, and drop preparation technique during dish preparation with microdrops can influence media osmolality [32] (Figure 3.1). When combined with airflow inside the working sterile hood, these four variables can raise media osmolality to a point that capable of inhibiting embryo development. Thus, care should be taken when preparing dishes.

Similar rises in media osmolality were recorded when 3 mL of media was left in 30 mm dishes for 30–60 min in a nonhumidified environment without oil overlay (5%–14% increase), a condition that might be encountered during oocyte retrieval or other procedures [38]. In these cases, media should be warmed within a closed test tube to prevent evaporation and then aliquoted into the dish immediately before use, rather than warming the media for extended periods within the dish. When warming media within a dish, condensation can be seen on the lids, a clear indication that evaporation has occurred and osmolality has thus increased. If an osmometer is available, initial testing can be performed to determine whether media osmolality is altered after routine dish preparation. If elevations are detected, procedures should be modified to avoid osmolality increase. Although airflow in the sterile hood is preferable for sterility during dish preparation, preparation should be performed on an unheated surface if possible. In addition, if using small volumes of media, alteration of microdrop preparation technique may be explored, including use of a "wash drop," where media are removed and fresh media are added after oil overlay. Another easy modification to help prevent osmolality shifts due to media evaporation includes implementing a protocol limiting the number of dishes prepared at one time before oil overlay is added (Appendix 3C).

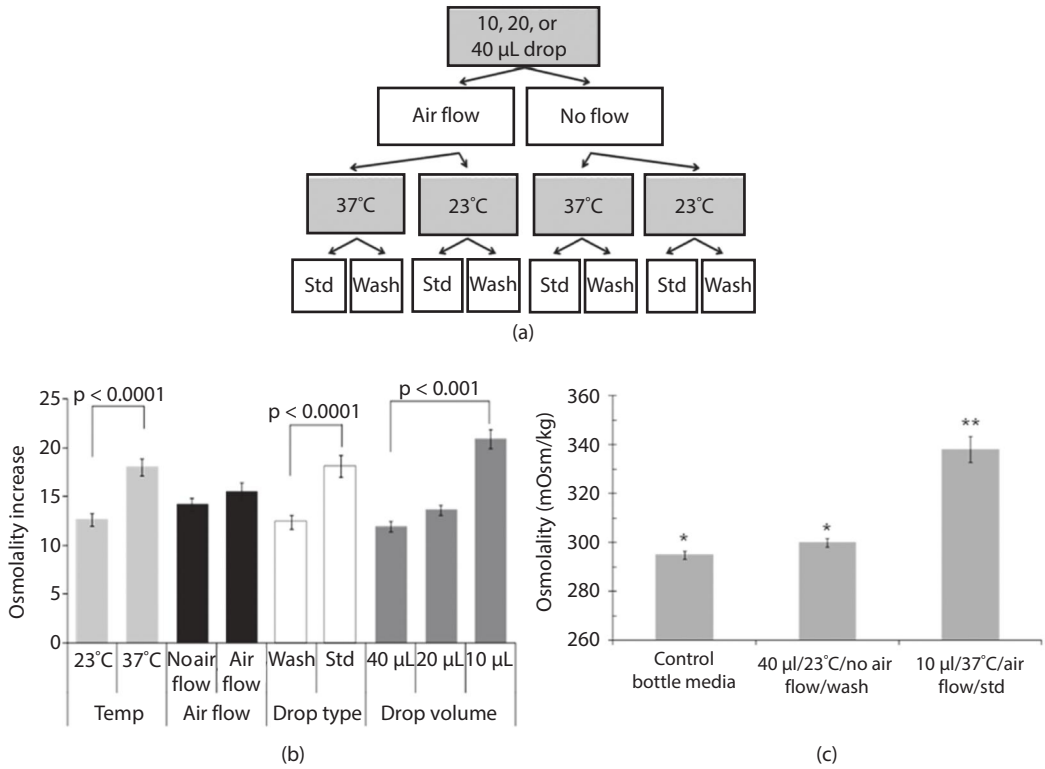

FIGURE 3.1 Conditions present during culture dish preparation can result in evaporation and affect media osmolality, impairing subsequent embryo development. (a) Various conditions tested for affect on media osmolality. (b) Impact of individual conditions on media osmolality. Temperature, drop volume, and drop preparation techniques all significantly increased media osmolality. (c) Demonstration of how combining several suboptimal preparation conditions can cause an osmoality increase high enough to impair embryo development (>300 mOsm). Different superscript symbols represent significant differences ($p < 0.05$).

APPENDIX 3C: CULTURE DISH PREPARATION

Purpose: To prepare embryo culture dishes in a manner so as to avoid evaporation and the resultant detrimental elevations in media osmolality that can impair subsequent embryo development.

Equipment and Materials

Airflow hood
Embryo culture dishes
Serological pipettes
Pipetman/pipettors
Pipette tips
Culture medium/protein
Mineral oil

Procedure

A. To help ensure sterility, all procedures should be performed within the confines of the airflow hood. Procedures should be performed away from the front of the hood, toward the center, and all items and packaging should be opened and closed within the hood when possible to ensure sterility. If the surface within the airflow hood is heated, dishes should be prepared on the unheated portion of the work surface.
   1. Set out all necessary pipettes, culture dishes, media, and oil into the airflow hood.
   2. Prepare media/protein as necessary based on the procedure.
      a. If protein is presupplemented, media are ready to use.
   3. When media are ready, lay out two to four culture dishes.
      a. If more dishes are to be made, these can also be set aside from their storage bags, but no more than two to four dishes should ever be prepared with media at any one time to avoid excess evaporation.
   4. Prepare two to four dishes by aliquoting the appropriate amount of medium and then immediately cover the dishes with the appropriate amount of mineral oil.
      a. Amounts of media and oil will vary based on individual lab protocols.
      b. If using microdrops (volumes <100 μL), it is recommended that no more than two dishes be made at any given time before adding oil overlay. It is also recommended that "wash" drops be used, where approximately half of the total final drop volume is first placed on the dish, covered with oil, and the remaining half of the drop volume is then added.

         Care should be taken not to form too many microdrops per plate. Limiting drop number to fewer than eight helps ensure rapid processing and avoids evaporation.
      c. If using four-well dishes or other larger volume methods (volumes >500 μL), up to four dishes may be made, adding the entire media volume to each well, before oil overlay.

B. If an osmometer is available, prepared media can be tested to confirm that osmolality is not elevated under laboratory preparation conditions. This need not be repeated each time, but may be useful during initial procedure implementation, during new technician training, or for routine monitoring. Osmolality of media from prepared dishes should be compared with control media out of the bottle. Differences in osmolality should be <10 mOsm.

NOTE: For other laboratory procedures that do not use oil overlay, such as oocyte retrieval and washing, embryo transfer, or cryopreservation, care must also be taken to avoid evaporation and increases in osmolality. For these procedures, media should be warmed within a closed test tube, rather than warming within a plate on a warmed surface. This avoids evaporation. Any time condensation is observed on the lid of a dish, evaporation has occurred. Larger volumes of media can be used to combat this and care should be taken to use the lid when possible due to the confounding effect of the airflow hood on facilitating evaporation, as well as heat loss.

Routine monitoring of osmolality after dish preparation can help ensure procedures are being followed and may be especially important in larger labs that make up numerous dishes on a daily basis, or when training new personnel to ensure proper technique.

Gas Monitoring and pH

Another aspect of culture media that deserves special attention with regard to culture system QC is pH. Although embryos have membrane-bound transporters that regulate their internal pH and permit them to develop a range of media pHs, improper media pH can stress embryos as they try to compensate [39–41]. Furthermore, some cell types, such as sperm, oocytes, and frozen-thawed embryos, lack robust intracellular pH regulators and are thus especially sensitive to media pH [42–45]. Therefore, adherence to an appropriate and narrow pH range is prudent.

The pH of culture media is established primarily via the balance of sodium bicarbonate in the medium and CO_2 levels from the incubator. Because bicarbonate levels are often set by the commercial manufacturer, pH is most easily adjusted via altering incubator CO_2 concentrations. Although daily checks of CO_2 concentration in incubators are often performed using Fyrite or any another measuring system, this is a poor substitute for actually measuring pH.

CO_2 measurement is a poor substitute for actually measuring pH.

Not all CO_2 measurement devices are accurate, and they can vary in their readings [46,47] (Figure 3.2). In addition, not all media are formulated in the same manner, and they may have differing bicarbonate concentrations. As a result, different media may yield different pH even if used in the same incubator. Furthermore, different protein supplements and varying amounts used can affect pH, either by impacting bicarbonate concentrations through dilution, or because protein supplements themselves are slightly acidic (Figure 3.3).

Finally, location of a particular laboratory at high altitude can impact the amount of CO_2 needed to achieve a desired pH, as labs at higher elevation require higher CO_2 levels due to the decreased atmospheric pressure. As a result, a single CO_2 concentration cannot be used reliably between laboratories to give the same medium pH. Thus, although daily measurement of incubator CO_2 concentration may be suitable to track deviations in

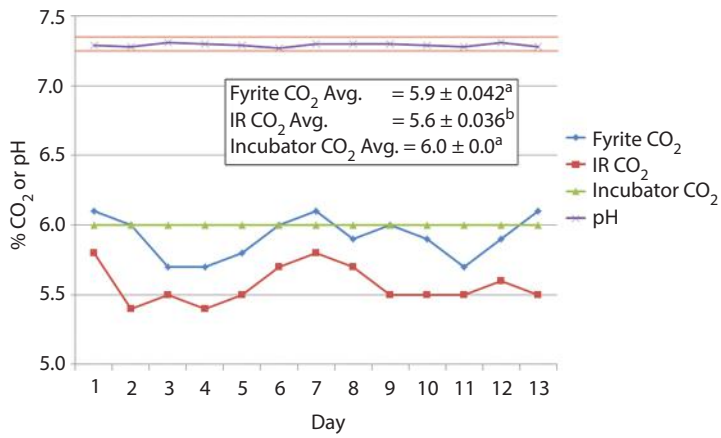

FIGURE 3.2 Different CO_2 measuring devices can yield different CO_2 readings, so pH should be mesured on all incubators to help determine the optimal CO_2 value. Simply relying on a CO_2 measuring device to set a specific CO_2 value could result in improper pH and improper growth conditions. Different superscripts represent a statistically significant difference in average CO_2 readings, $p < 0.05$.

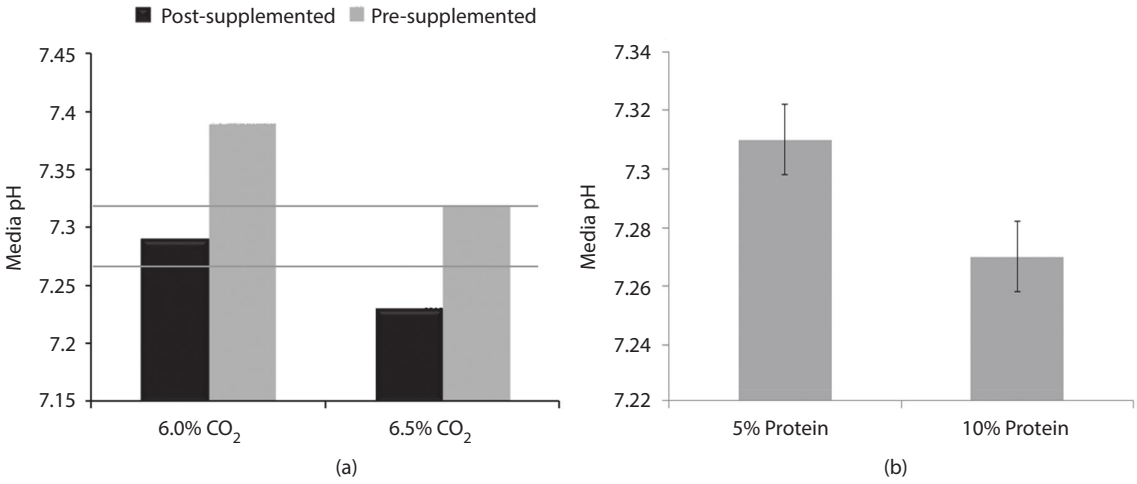

FIGURE 3.3 Different media can yield different pH values in the same incubator. (a) A medium presupplemented with protein by the manufacturer yields a different pH in the same incubator from exactly the same medium supplemented with the same protein and concentration by the lab. Supplementation of protein by the lab resulted in a dilution in media component concentrations, including bicarbonate, thereby lowering the pH at the same CO_2 concentration. (b) Similarly, differing amounts of protein can change the pH of the same medium in the same incubator by the dilution effect and also by the the fact that protein supplements are slightly acidic. Higher protein supplementation by the lab results in a lower pH value in the same incubator. As a result, all media should be tested for pH in each incubator to determine the optimal CO_2 concentrations required to obtain the desired pH.

incubator function from day to day, at some point pH should be measured to ensure that the incubator gas concentration is set correctly for a particular lab. At a minimum, pH measurement should be done on all new lots of media, but more routine monitoring may also be useful. Although there is no agreed upon "optimum" pH [40], and no proven need to change pH during culture has been demonstrated [40], following manufacturers' recommendations is prudent, and maintaining a narrow acceptable range is essential to reduce variability within the laboratory. A common acceptable pH range is 7.2–7.4, although a narrower target range of around 7.25–7.35 ensures less variation in culture conditions and tighter QC (Figure 3D.2).

A crucial aspect of pH and QC entails accurate measurement of the variable (Appendix 3D and Figure 3D.1). pH measurement itself can vary; thus, careful attention should be paid to measure pH using the correct methods. For example, temperature not only affects accuracy of a pH meter but also changes the actual pH of certain buffered media. Thus, the impact of temperature should be considered when taking pH measurements. In addition, some pH meters or electrodes may differ in their readings compared with other instruments (Figure 3.4); thus, establishment of baseline function of a particular device and an initial validation before clinical application is helpful when beginning pH measurements. Failure to validate pH measuring devices and probes could result in improper CO_2 values being set, thereby creating a potentially compromising growth environment for embryos. Validation should be performed again when probes are replaced on a regular basis to ensure proper functioning. Glass, double-junction, KCl-filled electrodes are often recommended for use with culture media due to protein content and organic buffers that can eventually clog the junction of the electrode. Other "in-incubator" pH systems are also available that measure pH inside the incubator or in real time, although, as mentioned, the accuracy of these newer systems should be validated before clinical implementation.

Temperature Control

Temperature is another environmental variable controlled within the lab that is crucial to the culture system and should be routinely monitored. It is also well known that temperature can affect various aspects of gamete and embryo function, most notably, meiotic spindle stability [48–50] and possibly embryo metabolism [51].

APPENDIX 3D: pH MEASUREMENT

Purpose: To measure pH accurately to confirm adequate culture conditions and aid in proper incubator settings (CO_2 levels).

Materials and Equipment

Snap top test tube
pH meter
pH electrode (semimicro, glass, double-junction KCl-filled recommended)
ATC probe (optional)
pH standards (7 and 10)
Electrode storage solution (KCl)
Warming block (37°C)

Procedure

A. For culture media used in the incubator, aliquot the medium being tested into a loosely capped test tube and place the test tube into the incubator. The same medium and protein content that are used clinically should be used for pH testing. Volume of medium will vary depending on tube size used and size of the pH probe or device, but 3–5 mL is usually adequate. Place tube loosely capped into each incubator and allow >12 hr to ensure adequate temperature and gas equilibration.
B. Immediately before measuring pH, the meter and probe should be calibrated according to manufacturer's instructions.
    1. It is important that temperature is accounted for to obtain the most accurate readings possible. Thus, the pH meter should be set to ~37°C, or an external ATC probe should be used. If an ATC probe is used, it should be placed into an ~37°C warming block. A standard benchtop pH meter and a semimicro-sized, double-junction glass KCl–filled electrode is recommended for use due to protein content of culture media and for use with organic buffers. This helps prevent clogging of the junction and ensures rapid and efficient readings. However, other electrodes will suffice in many cases, although care may be needed in cleaning and restoring electrodes to ensure rapid response and accurate readings. Regardless of the electrode, proper storage conditions and cleaning of electrodes are required for optimal performance. In this case, electrodes should be stored in a 3M KCl solution, not water, and the electrode should remain filled with 3M KCl. Before calibration and use, ensure electrode is filled with proper solution.
    2. It is helpful if there is a tight fit or seal between the electrode and the walls of the test tube. This can be accomplished by fitting a rubber gasket around the electrode to fill the gap when placed into the test tube to help stabilize the reading. Alternatively, a small hole can be made in a test tube cap and the electrode slipped through this hole. The cap/electrode can then be fitted onto the test tube to create a seal. This setup can be used during electrode storage, and if the same-size test tubes are used, the cap/electrode can be easily fitted over the test sample test tubes to create a seal and help stabilize pH readings.
    3. It is important to use freshly aliquoted calibration standards before each calibration and measurement to ensure accurate calibration, because pH of standards can drift after extended exposure to air. Use of a two-point calibration with standards of pH 7 and 10 is sufficient, although a three-point calibration using pH 4 can also be used if desired. Standards should be aliquoted into test tubes, capped, and then warmed in a water bath or heating block to ~37°C.

C. After equilibration of the medium and calibration of the pH meter, quickly remove a test sample tube from the incubator and snap the cap closed. Quickly move the tube to the pH meter that is adjacent to the incubator and place the pH electrode into the medium. This should be done first thing in the morning before any incubator openings to ensure accurate pH readings. This is made easier if the pH meter is set up near the incubators. Allow the reading to stabilize and record the reading. Repeat for each incubator and each medium used in that particular incubator. The readings should stabilize in <5–10 s.

Results

A. Record reading on pH log sheet.
   1. If pH readings in each incubator are in range (acceptable range set by lab based on manufacturer's recommendations, i.e., 7.25–7.35), no further action is required.
   2. If pH of a particular incubator is out of range, the incubator CO_2 levels should be adjusted according to manufacturer's instructions to raise or lower pH. Raising CO_2 levels lowers the pH and lowering CO_2 levels raises the pH. Adjust CO_2 accordingly and repeat pH measurement the next day or until values fall within the specified range.

NOTE:

A. pH measurements can be performed on a weekly or daily basis, based on lab protocols. Weekly measurement may be more practical when one considers cost of culture media and other variables.
B. Importantly, if testing a new lot of media, perform the pH reading in a side-by-side manner with the old verified lot. If the pH of the new lot is out of range and cannot be easily brought within range by a small adjustment of CO_2 levels, repeat to verify before contacting the media company to request a new lot of media. In addition, all new lots of culture media should have been pH verified before clinical implementation.
C. Handling media with HEPES or MOPS should never be placed inside the incubator. When measuring pH of these media, warm to 37°C in a water bath or warming block for >30 min in a capped test tube before measuring pH. Changes in temperature change the pH of these buffered media.

FIGURE 3D.1 Example setup of a pH meter and electrode for measurement of culture media pH. A warming block is used to account for the impact of temperature and is set to ~37ºC. The electrode is placed through the cap to prevent excessive gas exchange that could affect readings. The electrode/cap is removed from the storage solution tube, calibrated, and then quickly placed into the tube of medium for measurement.

pH Recording Form

Month:

Date	Tech	Media/ lot #	Calibration 6.98–7.01 9.88–10.01 Slope >98	Temp 3.65°C–37.5°C	Inc #1 7.25–7.35	Inc #2 7.25–7.35	Inc #3 7.25–7.35	Inc #4 7.25–7.35	Corrective action/ comment
					Fert:______ Culture:___	Fert:______ Culture:___	Fert:______ Culture:___	Fert:______ Culture:___	
					Fert:______ Culture:___	Fert:______ Culture:___	Fert:______ Culture:___	Fert:______ Culture:___	
					Fert:______ Culture:___	Fert:______ Culture:___	Fert:______ Culture:___	Fert:______ Culture:___	
					Fert:______ Culture:___	Fert:______ Culture:___	Fert:______ Culture:___	Fert:______ Culture:___	
					Fert:______ Culture:___	Fert:______ Culture:___	Fert:______ Culture:___	Fert:______ Culture:___	

FIGURE 3D.2 Sample recording sheet for routine pH measurements.

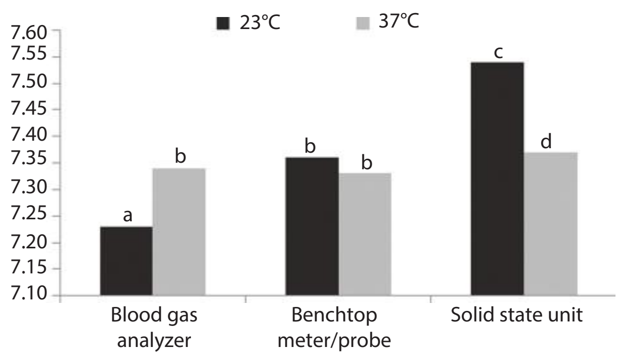

FIGURE 3.4 Validation of a pH meter is required before clinical implementation to verify accuracy. Failure to validate a pH meter could result in the improper CO_2 setting on an incubator, thereby providing an improper pH and possibly compromising growth conditions. Three pH measuring devices were compared using the same medium at two different temperatures. Different superscript letters represent significant differences ($p < 0.05$).

Thus, one aspect of temperature monitoring entails the laboratory incubator. The majority of IVF labs set incubator temperature at 37.0°C, with this value being presumably based on human core body temperature. However, it should be noted that this may not be entirely accurate. Regarding body temperature, Cox in 1998 reported that for decades it was thought that the normal body temperature was 98.6°F [52,53]. This number was calculated from a study in Germany that reported normal body temperature at 37°C. What was not known was that this number was an average rounded to the nearest degree. In other words, it was accurate only to two significant digits, not the three we have with 98.6. Scientists today know that normal is actually 98.2°F (±0.6°F), that is to say anything in the range of 97.6°F–98.8°F should be considered normal. Furthermore, it is thought that the temperature of

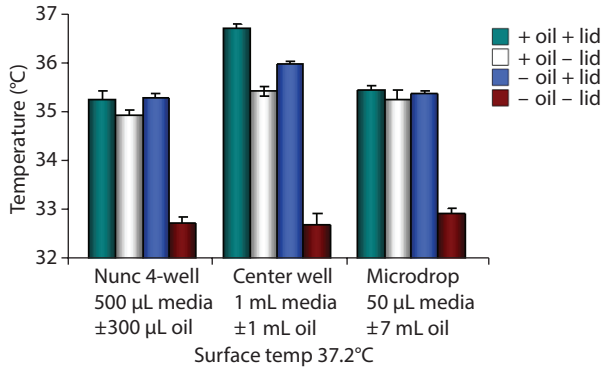

FIGURE 3.5 Temperature within a culture dish on a warmed surface can be impacted by various factors in the lab. The type of dish and its surface contact with the warmed surface, the presence of a lid, and the presence of an oil overlay can all impact the temperature of culture media within the confines of a sterile airflow hood. Surface temperature may need to be slighlty higher than the target temperature to achieve the correct temperature within the dish itself.

the human follicle is ~2.3°C cooler than core body temperature and that the fallopian tube from animal models carries a temperature gradient ~1.5°C cooler [54–59]. As a result, whether strict adherence to a temperature set point of 37°C within the incubator is required is questionable. The question has been poised "of whether human IVF and related procedures should be carried out at, say, 35.5°C–36°C rather than at 37°C" [51]. Use of a 1.5ºC lower temperature would presumably lower the metabolic rate of the embryo by ~15% and may result in a more "quiet" metabolism, thereby possibly benefiting embryo development [51]. Indeed, a recent preliminary study demonstrated that culture of human embryos at 36°C had no appreciable negative effect on blastocyst development or chromosomal compliment compared with 37°C, though no benefit was noted and no impact on outcomes was examined [60]. At least one study suggests that a temperature <37°C may improve outcomes, when increased pregnancy rates were obtained from incubators with a temperature of 36.96°C ± 0.13°C compared with those with a temperature of 37.03°C ± 0.13°C [25]. However, with such a narrow margin and limited accuracy of thermometers, it is not clear how meaningful this observation is. More detailed analysis of the optimal temperature for IVF is required.

In spite of the optimal temperature at which to culture embryos being debatable, a strict adherence to a narrow acceptable temperature range should be followed in the lab to reduce variability. Toward this end, surface temperatures in particular require careful monitoring. Different working surfaces in the laboratory, including microscope stages, may be warmed to reduce media temperature excursions outside the incubator for observation. Importantly, different warming surfaces may yield differing temperatures and should be monitored [49]. Similarly, different dishes may vary in their surface contact due to the conformity of the dish bottom. This can affect heat exchange and thus requires a differential surface temperature to achieve the desired temperature within the dish or media (Figure 3.5).

In addition, when used in sterile airflow hoods, volume of media and presence or absence of oil overlay or lids can also affect heat transfer and temperature (Figure 3.5). Similar findings have been reported previously [61]. Thus, a calibrated thermocouple should be used to measure temperature inside the various dishes used on the warmed surface and the temperature can then be adjusted to give the desired media temperature. For example, if aiming for 36°C–37°C in culture media, the surface temperature may have to be raised to 37°C–38°C. In addition, temperature within the incubator can also vary slightly from shelf to shelf. Thus, some have suggested that determining whether variation exists may be prudent, and preferential placement of dishes on a particular shelf may be helpful in optimizing incubator management [25]. As an added note, use of milled aluminum plates or tube holders can be used inside the incubator or on heated work surfaces to maintain thermal stability during repeated openings and closings [61].

Lab temperatures should be monitored daily using calibrated thermometers. This can be achieved through use of a National Institute of Standards and Technology (NIST) traceable device that has been verified for accuracy, or by comparing equipment to a calibrated NIST device, making sure to note any offsite or discrepancy to permit compensation when setting equipment temperatures.

Incubator Management

On a final note, one of the most important aspects of QC in the culture system is incubator management. Because gametes and embryos spend the majority of their time within the laboratory incubator, and the incubator controls multiple environmental variables, proper management of the incubator is an extremely important factor to consider in maximizing efficacy of the IVF lab. Even the most cutting-edge incubator with the more current technology can be made inefficient if managed improperly.

One of the most important aspects of QC in the culture system is incubator management.

Incubator management involves more than just selecting an appropriate incubator, setting it up, ensuring that it is off-gassed to reduce VOCs, measuring and setting proper gas levels (proper pH), and monitoring air quality and temperature, as mentioned previously. Proper incubator management also entails careful attention to caseload and workflow to help maintain a stable growth environment. IVF patients should be spread out among various incubators for a variety of reasons. Practically, having several incubators in which to spread out patients avoids catastrophic affects if patients are all placed within a single unit and it fails. Furthermore, spreading out of patients among several incubators also prevents excessive entry into the same incubator, thus helping to ensure environmental stability during the culture period. It was demonstrated that reducing door opening from six to four times over a 6-day period on a small-box incubator resulted in significantly improved blastocyst formation (53% vs. 43%) and "good" quality blastocysts (60% vs. 51%), although no differences in Day 3 embryo quality, implantation, or clinical pregnancy rates were observed [62]. Thus, IVF cases should be evenly distributed between all available incubators to avoid overuse or excessive openings of an individual incubator.

A specific number of incubators required within the IVF lab is difficult to recommend but is obviously based on incubator type and capacity and caseload and is influenced by cost. A minimum of two culture incubators is required, and the optimal number will be based on the weekly caseload of patients, rather than on the annual patient number. One can appreciate that if two laboratories both perform 300 cases annually, but one batches these patients into 2 weeks each month, then the laboratory that does not batch patients will likely require more incubators if they wish to keep the same incubator workflow (same number of patients per incubator, same number of openings and closings) as the lab that does not batch.

Regardless of how many incubators are present within a laboratory, some regular method of efficiency should be assessed to determine proper functions and management (Appendix 3E and Figure 3E.1). Tracking how many patients are placed into each incubator on a monthly basis is useful to monitor workflow and prevent overcrowding. Another useful indicator to monitor efficacy is to track embryo development and pregnancy per incubator. A useful threshold is >50% blastocyst conversion; this threshold will vary from patient to patient, but an overall average of >50% across all patients is a QC good indicator. Blastocyst quality should also be considered, although quality will vary based on individual grading criteria. Individual thresholds should be set and monitored on a monthly basis to track performance. These values can then be compared between incubators to validate proper management and functioning. If variation in the patient population is problematic, examination of the better prognosis patients, such as younger patients or the donor population, may be more insightful in determining whether a true problem exists in the culture system within a specific incubator or whether problems lie in the population itself.

APPENDIX 3E: DAILY INCUBATOR QC FORM

Incubators

.....Limits.....
5.5%–6.5% CO_2
4–6% O_2
Temp. 36.5°C–37.2°C

Month:

Day	Tech.	Daily –#1						DAILY	Weekly	Monthly	Comments/actions
		CO_2		O_2		Temp		H_2O in pans (√)	Change H_2O & Oil	Hygrometer (>80)	
		Inc Display	Measure	Inc Display	Measure	Inc Display	Therm				
1											
2											
3											
4											
5											
6											
7											
8											
9											
10											
11											
12											
13											
14											
15											
16											
17											
18											
19											
20											
21											
22											
23											
24											
25											
26											
27											
28											
29											
30											
31											

# of patients:

% Blastocyst formation:

FIGURE 3E.1 Sample recording sheet for daily or monthly incubator QC. One sheet can be placed on each incubator. A "comments" section can be used to record weekly pH values or indicate corrective actions taken during regular QC procedures. The number of patients, blastocyst conversion rates, or both may be tabulated at the end of each month for each incubator to aid in QC.

Conclusions

Proper QC is essential to optimize function of the IVF lab and to maximize reproductive outcomes. Although purchase of high-quality materials and equipment can aid in improving culture conditions, proper oversight and implementation are crucial. Despite having the same equipment and media in place, two laboratories can have dramatically different outcomes because several variables within the culture system are controlled directly within the individual lab. Examples include pH, osmolality, air quality, and incubator workflow. However, another variable that needs to be examined includes variation between technicians to ensure consistency in lab practices and approaches. This not only applies to procedures such as embryo grading, Intracytoplasmic sperm injection (ICSI), and catheter loading but also to how daily QC readings are taken [47], how QC assays are performed, and how media and dishes are prepared. Subtle deviations may introduce an environmental stressor into the culture system or miss a slight variation that could affect outcome.

REFERENCES

1. Morbeck DE. Importance of supply integrity for in vitro fertilization and embryo culture. *Semin Reprod Med* 2012; 30(3): 182–190.
2. Lee BE, Boone WR, Brackelsberg PO and Carmichael RA. Development of screening systems for evaluation of materials used in mammalian embryo transfer. *Theriogenology* 1988; 30(3): 605–612.
3. Scott LF, Sundaram SG and Smith S. The relevance and use of mouse embryo bioassays for quality control in an assisted reproductive technology program. *Fertil Steril* 1993; 60(3): 559–568.
4. Esterhuizen AD, Bosman E, Botes AD, Groenewald OA, Giesteira MV, Labuschagne GP, et al. A comparative study on the diagnostic sensitivity of rodent sperm and embryos in the detection of endotoxin in Earle's balanced salt solution. *J Assist Reprod Genet* 1994; 11(1): 38–42.
5. Rinehart JS, Bavister BD and Gerrity M. Quality control in the in vitro fertilization laboratory: Comparison of bioassay systems for water quality. *J In Vitro Fert Embryo Transf* 1988; 5(6): 335–342.
6. van den Bergh M, Baszo I, Biramane J, Bertrand E, Devreker F and Englert Y. Quality control in IVF with mouse bioassays: A four years' experience. *J Assist Reprod Genet* 1996; 13(9): 733–738.
7. Gardner DK, Reed L, Linck D, Sheehan C and Lane M. Quality control in human in vitro fertilization. *Semin Reprod Med* 2005; 23(4): 319–324.
8. Punt-van der Zalm JP, Hendriks JC, Westphal JR, Kremer JA, Teerenstra S and Wetzels AM. Toxicity testing of human assisted reproduction devices using the mouse embryo assay. *Reprod Biomed Online* 2009; 18(4): 529–535.
9. Morimoto Y, Hayashi E, Ohno T, Kawata A, Horikoshi Y and Kanzaki H. Quality control of human IVF/ICSI program using endotoxin measurement and sperm survival test. *Hum Cell* 1997; 10(4): 271–276.
10. Fleetham JA, Pattinson HA and Mortimer D. The mouse embryo culture system: Improving the sensitivity for use as a quality control assay for human in vitro fertilization. *Fertil Steril* 1993; 59(1): 192–196.
11. Davidson A, Vermesh M, Lobo RA and Paulson RJ. Mouse embryo culture as quality control for human in vitro fertilization: The one-cell versus the two-cell model. *Fertil Steril* 1988; 49(3): 516–521.
12. Khan Z, Wolff HS, Fredrickson JR, Walker DL, Daftary GS and Morbeck DE. Mouse strain and quality control testing: Improved sensitivity of the mouse embryo assay with embryos from outbred mice. *Fertil Steril* 2013; 99: 847–854.e2.
13. Wolff HS, Fredrickson JR, Walker DL and Morbeck DE. Advances in quality control: Mouse embryo morphokinetics are sensitive markers of in vitro stress. *Hum Reprod* 2013; 28(7): 1776–1782.
14. Morbeck DE, Khan Z, Barnidge DR and Walker DL. Washing mineral oil reduces contaminants and embryotoxicity. *Fertil Steril* 2010; 94(7): 2747–2752.
15. Thomas T. Culture systems: Air quality. *Methods Mol Biol* 2012; 912: 313–324.
16. Sharmin R and Ray MB. Application of ultraviolet light-emitting diode photocatalysis to remove volatile organic compounds from indoor air. *J Air Waste Manag Assoc* 2012; 62(9): 1032–1039.
17. Chapuis Y, Klvana D, Guy C and Kirchnerova J. Photocatalytic oxidation of volatile organic compounds using fluorescent visible light. *J Air Waste Manag Assoc* 2002; 52(7): 845–854.

18. Hall J, Gilligan A, Schimmel T, Cecchi M and Cohen J. The origin, effects and control of air pollution in laboratories used for human embryo culture. *Hum Reprod* 1998; 13(Suppl 4): 146–155.
19. Cohen J, Gilligan A and Willadsen S. Culture and quality control of embryos. *Hum Reprod* 1998; 13(Suppl 3): 137–144; discussion 145–137.
20. Cohen J, Gilligan A, Esposito W, Schimmel T and Dale B. Ambient air and its potential effects on conception in vitro. *Hum Reprod* 1997; 12(8): 1742–1749.
21. Boone WR, Johnson JE, Locke AJ, Crane MM, 4th and Price TM. Control of air quality in an assisted reproductive technology laboratory. *Fertil Steril* 1999; 71(1): 150–154.
22. Khoudja RY, Xu Y, Li T and Zhou C. Better IVF outcomes following improvements in laboratory air quality. *J Assist Reprod Genet* 2013; 30(1): 69–76.
23. Merton JS, Vermeulen ZL, Otter T, Mullaart E, de Ruigh L and Hasler JF. Carbon-activated gas filtration during in vitro culture increased pregnancy rate following transfer of in vitro-produced bovine embryos. *Theriogenology* 2007; 67(7): 1233–1238.
24. Guris J, Janssens R and Vercammen M. Air quality managment. In: *Practial Manual of In Vitro Fertilization* (eds. Nagy Z, Varghese A and Argarwal A). New York: Springer, 2012, pp. 17–27.
25. Higdon HL, 3rd, Blackhurst DW and Boone WR. Incubator management in an assisted reproductive technology laboratory. *Fertil Steril* 2008; 89(3): 703–710.
26. Schimmel T, Gilligan A, Garrisi G, Espositi B, Cecchi M, Dale B, et al. Removal of volatile organic compounds from incbuators used for gamete and embryo culture. *Fertil Steril* 1997; 68(Suppl 1): s165.
27. Mayer J, Nechchiri F, Weedon V, Jones E, Kalin H, Ochniger S, et al. Prospective randomized crossover analysis of the impact of an IVF incbuator air filtration system (coda, genx) on clinical pregnancy rates. *Fertil Steril* 1999; 72(Suppl 1): s42.
28. Baltz JM and Tartia AP. Cell volume regulation in oocytes and early embryos: Connecting physiology to successful culture media. *Hum Reprod Update* 2010; 16(2): 166–176.
29. Hammer MA and Baltz JM. Beta-alanine but not taurine can function as an organic osmolyte in preimplantation mouse embryos cultured from fertilized eggs. *Mol Reprod Dev* 2003; 66(2): 153–161.
30. Richards T, Wang F, Liu L and Baltz JM. Rescue of postcompaction-stage mouse embryo development from hypertonicity by amino acid transporter substrates that may function as organic osmolytes. *Biol Reprod* 2010; 82(4): 769–777.
31. Moravek M, Fisseha S and Swain JE. Dipeptide forms of glycine support mouse preimplantation embryo development in vitro and provide protection against high media osmolality. *J Assist Reprod Genet* 2012; 29(3): 283–290.
32. Swain JE, Cabrera L, Xu X and Smith GD. Microdrop preparation factors influence culture-media osmolality, which can impair mouse embryo preimplantation development. *Reprod Biomed Online* 2012; 24(2): 142–147.
33. Anas MK, Hammer MA, Lever M, Stanton JA and Baltz JM. The organic osmolytes betaine and proline are transported by a shared system in early preimplantation mouse embryos. *J Cell Physiol* 2007; 210(1): 266–277.
34. Dawson KM and Baltz JM. Organic osmolytes and embryos: Substrates of the Gly and beta transport systems protect mouse zygotes against the effects of raised osmolarity. *Biol Reprod* 1997; 56(6): 1550–1558.
35. Dawson KM, Collins JL and Baltz JM. Osmolarity-dependent glycine accumulation indicates a role for glycine as an organic osmolyte in early preimplantation mouse embryos. *Biol Reprod* 1998; 59(2): 225–232.
36. Hammer MA and Baltz JM. Betaine is a highly effective organic osmolyte but does not appear to be transported by established organic osmolyte transporters in mouse embryos. *Mol Reprod Dev* 2002; 62(2): 195–202.
37. Hammer MA, Kolajova M, Leveille M, Claman P and Baltz JM. Glycine transport by single human and mouse embryos. *Hum Reprod* 2000; 15(2): 419–426.
38. Lane M, Mitchell M, Cashman KS, Feil D, Wakefield S and Zander-Fox DL. To QC or not to QC: The key to a consistent laboratory? *Reprod Fertil Dev* 2008; 20(1): 23–32.
39. Swain JE. Optimizing the culture environment in the IVF laboratory: Impact of pH and buffer capacity on gamete and embryo quality. *Reprod Biomed Online* 2010; 21(1): 6–16.
40. Swain JE. Is there an optimal pH for culture media used in clinical IVF? *Hum Reprod Update* 2012; 18(3): 333–339.
41. Swain JE and Pool TB. New pH-buffering system for media utilized during gamete and embryo manipulations for assisted reproduction. *Reprod Biomed Online* 2009; 18(6): 799–810.

42. Lane M, Lyons EA and Bavister BD. Cryopreservation reduces the ability of hamster 2-cell embryos to regulate intracellular pH. *Hum Reprod* 2000; 15(2): 389–394.
43. Phillips KP and Baltz JM. Intracellular pH regulation by HCO3-/Cl- exchange is activated during early mouse zygote development. *Dev Biol* 1999; 208(2): 392–405.
44. Phillips KP, Petrunewich MA, Collins JL and Baltz JM. The intracellular pH-regulatory HCO3-/Cl- exchanger in the mouse oocyte is inactivated during first meiotic metaphase and reactivated after egg activation via the MAP kinase pathway. *Mol Biol Cell* 2002; 13(11): 3800–3810.
45. Hamamah S, Magnoux E, Royere D, Barthelemy C, Dacheux JL and Gatti JL. Internal pH of human spermatozoa: Effect of ions, human follicular fluid and progesterone. *Mol Hum Reprod* 1996; 2(4): 219–224.
46. Johnson JE, Boone WR, Lee ST and Blackhurst DW. Using Fyrite to monitor incubator carbon dioxide levels. *J Assist Reprod Genet* 1995; 12(2): 113–117.
47. Boone WR, Johnson JE, Lee ST, Detry MA and Blackhurst DW. Sources of variation in measurements of carbon dioxide levels inside incubators. *J Assist Reprod Genet* 1996; 13(7): 606–608.
48. Sun XF, Wang WH and Keefe DL. Overheating is detrimental to meiotic spindles within in vitro matured human oocytes. *Zygote* 2004; 12(1): 65–70.
49. Wang WH, Meng L, Hackett RJ, Oldenbourg R and Keefe DL. Rigorous thermal control during intracytoplasmic sperm injection stabilizes the meiotic spindle and improves fertilization and pregnancy rates. *Fertil Steril* 2002; 77(6): 1274–1277.
50. Wang WH, Meng L, Hackett RJ, Odenbourg R and Keefe DL. Limited recovery of meiotic spindles in living human oocytes after cooling-rewarming observed using polarized light microscopy. *Hum Reprod* 2001; 16(11): 2374–2378.
51. Leese HJ, Baumann CG, Brison DR, McEvoy TG and Sturmey RG. Metabolism of the viable mammalian embryo: Quietness revisited. *Mol Hum Reprod* 2008; 14(12): 667–672.
52. Dewdney, A. K., 200% of Nothing: An Eye Opening Tour Through the Twists and Turns of Math Abuse and Innumeracy. New York: Wiley, 1993.
53. Elert G et al., Temperature of a healthy human body (body temperature), The Physics Factbook, http://www.hypertextbook.com/facts.
54. Grinsted J, Kjer JJ, Blendstrup K and Pedersen JF. Is low temperature of the follicular fluid prior to ovulation necessary for normal oocyte development? *Fertil Steril* 1985; 43(1): 34–39.
55. David A, Vilensky A and Nathan H. [Temperature changes in different parts of the rabbit oviduct. Preliminary report]. *Harefuah* 1971; 80(4): 180–182.
56. Hunter RH, Bogh IB, Einer-Jensen N, Muller S and Greve T. Pre-ovulatory graafian follicles are cooler than neighbouring stroma in pig ovaries. *Hum Reprod* 2000; 15(2): 273–283.
57. Hunter RH, Grondahl C, Greve T and Schmidt M. Graafian follicles are cooler than neighbouring ovarian tissues and deep rectal temperatures. *Hum Reprod* 1997; 12(1): 95–100.
58. Hunter RH and Nichol R. A preovulatory temperature gradient between the isthmus and ampulla of pig oviducts during the phase of sperm storage. *J Reprod Fertil* 1986; 77(2): 599–606.
59. Hunter RH. Temperature gradients in female reproductive tissues. *Reprod Biomed Online* 2012; 24(4): 377–380.
60. Hong K, Forman E, Lee H, Ferry K, Treff N and Scott R. Optimizing the temperature for embyo culture in IVF: A randomized controlled trial (RCT) comparing standard culture temperature of 37C to the reduced more physiologic temperature of 36C. *Fertil Steril* 2012; 98(3): s167.
61. Cooke S, Tyler JP and Driscoll G. Objective assessments of temperature maintenance using in vitro culture techniques. *J Assist Reprod Genet* 2002; 19(8): 368–375.
62. Zhang JQ, Li XL, Peng Y, Guo X, Heng BC and Tong GQ. Reduction in exposure of human embryos outside the incubator enhances embryo quality and blastulation rate. *Reprod Biomed Online* 2010; 20(4): 510–515.

4

Morphological Selection of Gametes and Embryos: Sperm

Pierre Vanderzwalmen, Magnus Bach, Olivier Gaspard, Bernard Lejeune, Anton Neyer, Françoise Puissant, Maximilian Schuff, Astrid Stecher, Sabine Vanderzwalmen, Barbara Wirleitner, and Nicolas H. Zech

Importance of Spermatozoa Morphology in Fertility

Intracytoplasmic sperm injection (ICSI) introduced more than 20 years ago was a tremendously helpful tool to overcome the infertility of couples when conventional in vitro fertilization (IVF), partial zona dissection, or subzonal sperm injection treatments had failed [1]. The injection of a single spermatozoon into the ooplasm provided an apt answer to severe male infertility diagnosis indicated by low sperm count, poor sperm motility, or both, or to infertility due to morphology deficiency. Interestingly, since the introduction of ICSI, less attention has been devoted to the sperm's morphology in itself. In addition, it is even more remarkable that after the introduction of ICSI, even though human spermatozoa exhibit a wide range of shapes, several studies found no correlation between the injection of sperm with normal or abnormal morphology and ICSI outcomes [2,3]. However, such observations were most probably biased by the selection performed by the embryologist who tried to select the best "normal-looking" motile spermatozoa before ICSI, which does not always reflect the quality of the whole semen population.

The assessment of sperm morphology by Kruger's strict criteria is routinely applied and widely accepted as the best method of prediction for male fertility potential and highlights the concept that sperm morphology is a very important parameter in the analysis of the whole population of a semen sample [4]. Of all semen parameters, sperm morphology turns out to be the best predictor of a man's fertilizing potential [5].

But the situation is completely different when we move from the diagnostic level toward the laboratory practice of ICSI where we have to select only one spermatozoon for injection.

Although there is still a controversy as to whether morphological defects of spermatozoa even have an effect on fertilization or subsequent embryonic development [6], it becomes more and more accepted that abnormally shaped spermatozoa from patients diagnosed with terato- and asthenozoospermia have a significantly increased frequency of aneuploidy, a higher DNA fragmentation index (DFI), and an increased rate of mitochondrial dysfunction [7]. The importance of morphologically normal sperm selection is reinforced when facing the reproductive outcomes in terms of fertilization, embryo development, pregnancy rates, and abortion rates when the oocyte injections can be done only with abnormally shaped spermatozoa, that is, sperm with elongated, tapered, or amorphous heads; broken necks; or cytoplasmic droplets [8].

In view of ICSI bypassing the natural barriers of reproduction, it seems reasonable to develop optimized sperm selection techniques.

With the implementation of restrictive laws regulating the number of embryos for transfer, methods of gamete and embryo selection are of paramount importance. If we keep in mind that ICSI bypasses the natural barriers of reproduction and that an abnormal spermatozoon bears the danger of transferring putative negative effects on to the offspring, it might be reasonable to develop optimized selection techniques. Now, for almost a decade, therefore, more attention has been directed towards physiological selection methods based on the biochemical ability of the spermatozoa to bind either to solid hyaluronic acid or to zona pellucida before intracytoplasmic injection [9].

In addition, the importance of sperm morphology is being studied [8], with several novel microscopic approaches, such as differential interference contrast microscopy [10], digital holographic microscopy [11], and atomic force microscopy [12], currently being used or in development to allow a more detailed observation of the different parts of the sperm head (nucleus and acrosome), midpiece, and tail.

Bartoov et al. [10] introduced, 10 years ago, an innovative, noninvasive technique for a more precise morphological evaluation of motile spermatozoa. The so-called motile-sperm organelle-morphology examination (MSOME) changed the perception of how a spermatozoon suitable for injection should appear. In fact, MSOME permits not only simple observation in terms of a sperm's size and shape but also a detailed examination in real time of the subtle subcellular morphology and abnormalities, such as nuclear defects. The MSOME technique allowed a stricter discrimination of spermatozoa, with normal nuclei defined by an oval shape with a smooth configuration, including a normal nuclear content [10,13].

With the replacement of the standard bright-field or the Hoffman modulation contrast (HMC) optics by the Nomarski differential interference contrast (DIC) optics, a better three-dimensional view of the sperm head became available. Bright-field or HMC can reveal major abnormalities of the spermatozoon's aberrations in head shape and at the level of the midpiece and tail. With Nomarski interference contrast, a more in-depth evaluation of the quality of semen that provides substantial information about the normalcy of the head, neck, and midpiece is possible. In consequence, this method of spermatozoa evaluation and selection for ICSI indication generated the intracytoplasmic morphologically selected sperm injection (IMSI) technique [14,15].

The aim of the first part of this chapter is to give the reasons to select spermatozoa free of nuclear and neck–midpiece defects or those from patients suffering from globozoospermia syndrome. In addition, a brief overview of the putative nature of nuclear vacuoles according to the present status of knowledge and their consequences on embryo development is presented. In the second part of this chapter, we depict the different spermatozoa classification systems and the technical procedures to select spermatozoa so as not to impair oocyte quality.

Tangible Arguments to Select Sperm Free of Defects

One decade after the first application of MSOME and IMSI, can we still consider these as useful techniques?

Sperm Head Vacuoles: An Additional Sperm Defect That Can Be Better Highlighted with Nomarski Optics

The meticulous approach in sperm selection applying the Nomarski DIC optics allows the detection of subtle sperm head nuclear abnormalities that were designated as vacuoles by Bartoov et al. [10] (Figure 4.1a). These nuclear defects are otherwise not evident at a 400× magnification with HMC microscopy [15–17] (Figure 4.1b).

In fact, we had to wait for the introduction of Nomarski optics to be concerned about the presence of large and small vacuoles and then consider them as potential defects. Before the introduction of MSOME and IMSI, there was to our knowledge no report of the presence of vacuoles and analysis of their location, origin, structure, and effect on reproductive outcome after the conventional ICSI procedure.

Spermatozoa might contain heterogeneous vacuoles varying in number, size, and content. To simplify this matter, we often only refer to the term "vacuole" in any circumstance. But is vacuole the appropriate terminology? From a biological point of view, vacuoles are vesicles surrounded by a membrane. However, this structural abnormality that we airily term vacuole might more likely represent a kind of depression in the nuclear part of the head. Some of these so-called vacuoles are in fact deep, such as crater or hollow. Watanabe et al. [18] suggested that vacuoles are hollows where in the plasma membrane falls into the nucleus, and Westbrook et al. [19] even talked about nuclear crater formation in the sperm head. Toshimori [20] differentiates between large vacuoles with amorphous substances or membranous structures inside, and small vacuolous patterns without any structures inside.

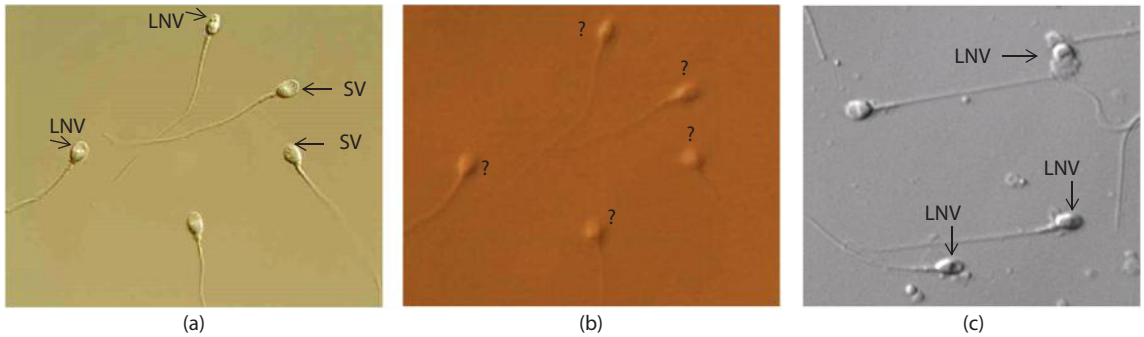

FIGURE 4.1 Observation of spermatozoa with HMC and DIC microscopy (Nomarski). (a) Nomarski at 6000× magnification. (b) Conventional HMC at 6000× magnification. (c) Conventional HMC at 600× after adjustment of the polarizer. SV, small vacuole; LNV, large nuclear vacuole.

Boitrelle et al. [12,21] reported that the plasma membrane was sunken, but intact, both large and small vacuoles were identified as an abnormal, "thumbprint"-like nuclear concavity covered by acrosomal and plasma membranes.

Reasons to Select Vacuole-Free Sperm

Pathological Character of Nuclear Vacuoles

One crucial question to investigate concerns the significance of vacuoles. Vacuoles are like liquid bubbles that can be seen in the sperm's head, where the nucleus is located, and that have been correlated with DNA anomalies. Considering the publications of Berkovitz et al. [15], Cayli et al. [22], and Hazout et al. [23], it is most likely that vacuoles reflect molecular defects that are responsible for anomalies of sperm chromatin packaging and abnormal chromatin remodeling during sperm maturation; such defects, in turn, may render spermatozoa more vulnerable to DNA damage. According to different studies, the integrity of the chromatin is related to the presence or absence of vacuoles in the head of spermatozoa and the loss of chromatin compaction renders the exposed DNA more prone to reactive oxygen species [24–26].

Several DNA and chromatin staining assays, including aniline blue, chromomycin A3, and acridine orange, were applied to assess more precisely the integrity of the DNA in vacuolated spermatozoa. Interestingly, several studies found highly statistically significant differences in the DNA integrity between spermatozoa with or without vacuoles [27].

According to the growing body of literature on this subject, it is now more and more accepted that the presence of large nuclear vacuoles (LNVs) is correlated with failures of chromatin condensation [7,28,29]. It is reported in selected teratozoospermic populations that sperm vacuoles were exclusively of nuclear origin and preferentially located toward the anterior part of the sperm head [30]. Chromatin condensation defects were the main alterations observed in spermatozoa with large vacuoles [7,12,21,28,30–32]. The chromatin in sperm with large vacuoles was atypically decondensed, showing a high degree of immaturity.

Indeed, chromatin condensation is a crucial step in protecting the paternal genome during the transit from the male to the oocyte before fertilization (epididymal transit) [33]. Rousseaux et al. [34] demonstrated a new keystone in DNA compaction in humans and murines. They postulated that histones are replaced by transitional proteins called bromodomains before protamination takes place. Structural abnormalities of the nucleus include incomplete or impaired chromatin condensation and nuclear vacuoles and inclusions. Karyolytic changes or the presence of large intranuclear lacunae or vacuoles are the morphological manifestations of underlying biochemical alterations.

Early embryogenesis is a critical time for epigenetic regulation, and these epigenetic modulation processes are sensitive to environmental factors [35,36]. Epigenetic patterns are usually faithfully maintained during development.

However, this maintenance sometimes fails, resulting in the disturbance of epigenetic processes representing the basis of numerous human disorders. It is known that before histone replacement by protamines, the nucleosomes are destabilized by hyperacetylation, resulting in rise in the DNA methylation levels [37,38]. These potential epigenetic mechanisms could be implied in chromatin condensation failures [39].

Poor chromatin condensation may expose the spermatozoon's nuclear DNA to damage (e.g., DNA fragmentation) during its journey through both the male and female genital tracts [40,41], and large vacuoles were found to be associated with DNA fragmentation [7,28]. However, other studies failed to establish a strong link between large vacuoles and DNA fragmentation [12,18,30,32].

This could explain the differences in terms of DNA fragmentation between different men. A disorder in spermiogenesis may result in uncondensed and vulnerable chromatin, and according to exposure to the level of oxidative stress conditions, differences in DNA fragmentation can be noticed [35].

Vacuoles and Reproductive Outcome

The importance of selecting normal spermatozoa becomes obvious when comparing the reproductive outcomes in terms of fertilization, embryo development, and pregnancy and abortion rates when oocyte injections are done with morphologically normal sperm and spermatozoa exhibiting different subcellular defects.

Selection of sperm devoid of sperm head vacuoles has multiple benefits.

Vacuoles and Embryo Development

The size and the number of sperm nuclear vacuoles, most accurately identified under Nomarski optics, negatively affect blastocyst development. In successive studies [42–45], the existence of LNVs together or not with abnormal shape was shown to reduce the percentage of good-quality blastocysts after culture until Day 5. Following the outcome of each embryo after injection of spermatozoa, it was clearly demonstrated that the use of spermatozoa with no vacuoles or fewer than two small vacuoles can be associated with significantly higher blastocyst rates compared with injecting spermatozoa with more than two small vacuoles or one large vacuole with or without abnormal shape. Such observations reinforce previous studies suggesting early and late paternal effects on initial embryonic development [46–48].

As mentioned, it seems that nuclear vacuoles are related to sperm DNA damage and might therefore negatively affect human embryo development [47]. In addition, it is well known that the integrity of sperm chromatin plays a key role in embryo development [25]. DNA helices in defective chromatin remodeling during spermiogenesis would be more vulnerable to physical and chemical stress such as reactive oxygen species [26]. Subsequent attack by reactive oxidative species may cause sperm's DNA fragmentation and might even affect later blastocyst development [26,49] and pregnancy outcomes in a negative manner [47,50,51].

Vacuoles and Pregnancy and Miscarriage Rates

Berkovitz et al. [52] were the first to carry out a more specific analysis on the impact of sperm cells with normal nuclear shape but with large vacuoles on two matched IMSI groups of 28 patients each. Spermatozoa with strictly defined normal nuclear shape but large vacuoles were selected for injection and compared with a control group that included normal nuclear shape spermatozoa lacking vacuoles. No difference in the fertilization and early embryo development up to Day 3 was reported. However, injection of spermatozoa with strictly normal nuclear shape but large vacuoles appeared to significantly reduce pregnancy outcomes (18% vs. 50%) and seemed to be associated with early miscarriage (80% vs. 7%).

Other studies showed that selection of normally shaped spermatozoa with a vacuole-free head was positively associated with pregnancy and lower abortion rates after Day 3 embryo transfers in couples with previous and repeated implantation failures [13,14,42,52,53] and in patients with an elevated degree of DNA-fragmented spermatozoa [23].

Knez et al. [44] showed that there was no significant difference in the pregnancy rates after IMSI and ICSI procedures and blastocyst transfer. However, after ICSI, more pregnancies were terminated by spontaneous

abortion, whereas after IMSI there were no spontaneous abortions. One explanation could be that the IMSI procedure permits selection of spermatozoa without defects and thus provides more "healthy" blastocysts without chromosomal abnormalities, possibly in spite of very comparable development and morphology to ICSI-derived blastocysts.

Vacuoles, Health of Babies Born, and Incidence of Malformations

Still, there are concerns about the long-term safety of injecting spermatozoa carrying vacuoles. We have to be cautious, especially in the light of Aitken's work [54] on the putative negative effects of sperm DNA fragmentation for the next generation. Depending on the level of sperm nuclear DNA fragmentation, oocytes may partially repair fragmented DNA, producing blastocysts capable of implanting and producing live offspring. However, the incomplete repair may lead to long-term pathologies. The data of Fernández-Gonzalez et al. [55] gained on the basis of a mouse model indicate that the use of DNA-fragmented spermatozoa in ICSI can generate effects such as aberrant growth, premature aging, abnormal behavior, and tumors derived from the mesenchymal lineage that emerge only in later life.

To date, there have not been sufficient numbers of published studies concerning the health of children born after ICSI to draw any firm conclusions about the long-term safety of this procedure. However, it is important to emphasize that animal data are absolutely unequivocal on this point and clearly indicate that DNA damage in the male germ line is potentially hazardous for the embryo and therefore for the resulting offspring [56]. According to Cassuto [39], sperm nucleus morphological normalcy, assessed at high magnification, could decrease the prevalence of major fetal malformations in ICSI children.

Midpiece Selection

MSOME permits not only the observation of nuclear vacuole defects but also other abnormalities that may result in infertility. Ugajin et al. [57] showed that they were able to clearly differentiate between a straight-shaped and tapering-shaped midpiece (Figure 4.2). The tapering-shaped midpiece is related to abnormal centrosomal function as a consequence of aberrant microtubule organization [57]. According to Van Blerkom and Davis [58], the centriole is, after the nucleus, the most important sperm organelle for initiation of the intraooplasmic fertilization

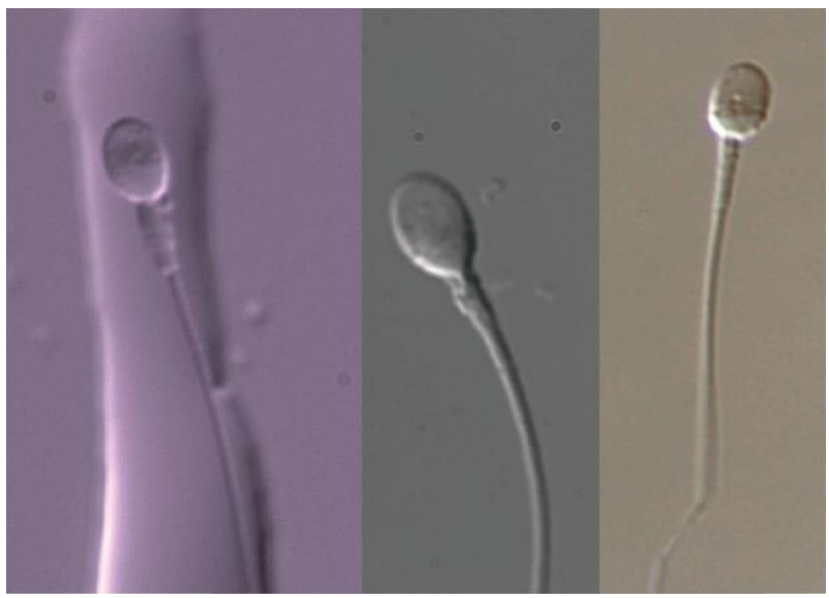

FIGURE 4.2 Tapering-shaped (a), intermediate-shaped (b), and straight-shaped (c) midpiece.

process, being responsible for the formation of the sperm aster. The centrosomes play a crucial role in fertilization [59], and their dysfunction may cause fertilization failure due to lack of a sperm aster [60,61]. The injection of selected sperm with a morphologically straight midpiece by IMSI may result in choosing sperm with functional centrosomes, thereby positively influencing fertilization rates and embryo development after ICSI [57].

MSOME Selection in Globozoospermia to Circumvent Artificial Activation

Globozoospermia is a male-factor infertility involving several abnormalities of sperm remodeling during spermiogenesis that can lead to formation defects or premature elimination of acrosomal structures. Fertilization capacity after ICSI is low [62], mainly due to a lack of sperm-specific phospholipase C (PLCζ) [63] that is responsible for inducing Ca^{2+} oscillations essential for oocyte activation.

Presently, 21 births have been reported after ICSI followed by artificial Ca^{2+} oscillations induction via the use of artificial oocyte activation protocols by exposing oocytes to certain chemical agents (ionophore) [64–67]. Another approach proposed by Kashir et al. [68] and Gatimel et al. [67] is to apply MSOME to maximize the efficacy of ICSI and IMSI. MSOME increases the efficacy of fertilization by selecting spermatozoa with superior oocyte activation ability. Sermondade et al. [69] selected spermatozoa that exhibited a small acrosomal bud that was not visible using conventional sperm selection methodology. Gatimel et al. [67] identified spermatozoa with some sparse oval forms, revealing the presence of Golgi residues. These studies showed that some globozoospermic spermatozoa possess an acrosomal bud that contains a sufficient amount of PLCζ that is not significantly different from fertile controls and that correlates to successful oocyte activation and fertilization without the need for artificial oocyte activation with exogenous chemical agents.

Evaluation of Sperm Head Shape

At high magnification (6300×), Utsuno et al. [70] decomposed sperm head shapes of motile spermatozoa into four quantitative parameters: ellipticity, anteroposterior symmetry, lateral symmetry, and angularity. Stepwise forward multiple logistic regression analysis showed a statistically significant increase of the percentage of DNA fragmentation in spermatozoa with abnormal ellipticity, angularity, and LNVs. This may ensure the advantage of morphological assessment of spermatozoa at high magnification.

IMSI in 2014: Still a Debate

As mentioned, there is a real benefit to select morphological spermatozoa free of vacuoles. But, for different reasons, there is undeniable evident skepticism about this method of spermatozoa selection. Controversial publications led to the hesitation to apply IMSI. What are the main indications for IMSI? How can we assess the benefit of IMSI?

Superiority of IMSI versus ICSI—But for Which Indications?

When should we propose IMSI instead of ICSI? In principle, all patients can benefit from using IMSI; however, it is especially useful after several previous implantation failures, in cases of severe teratozoospermia, for patients having experienced an unexplained abortion, and definitely in cases with no blastocysts of or low blastocyst rate(s) in previous IVF attempts. However, the superiority of IMSI over ICSI is still a matter of debate. To date, randomized and well-powered studies to confirm a benefit of IMSI are limited, and they even depict conflicting results [71].

Controversial conclusions have been drawn, especially in terms of fertilization, top-quality embryo rates, and pregnancy rates between IMSI and ICSI. Some studies have shown that IMSI improves reproductive outcomes in cases of male-factor infertility and previous failed ICSI attempts in terms of implantation and clinical pregnancy rates compared with conventional ICSI [14,16,23,42,44,72–77]. Alternatively, IMSI and conventional ICSI seemed to provide comparable laboratory and clinical results when an unselected infertile population was evaluated [78,79] or when IMSI was applied as the first treatment option [80].

Full Benefit of IMSI Is Attained with Blastocyst Culture

Even if the superiority of IMSI over ICSI is still a matter of debate, we have to recognize that the type of spermatozoa selected for injection influences the outcome in terms of embryo development, pregnancy, miscarriage, and malformation.

One of the main benefits of IMSI is the improvement in embryo quality and the higher rate of blastocysts obtained per cycle when morphologically good-quality spermatozoa are selected [42–45].

The type of spermatozoa selected for injection influences the outcome in terms of embryo development, pregnancy, miscarriage, and malformation.

The full benefit of a better spermatozoa selection is highlighted if we are able to produce one more blastocyst per cycle. In fact, more blastocysts provide a higher chance for the patient to become pregnant in successive vitrified embryo transfer cycle(s), thus increasing the cumulative pregnancy rate. Moreover, when using IMSI, the abortion ratios are reduced by 50%, increasing as a consequence the full-term gestation possibilities.

Also, prolonged embryo culture to the blastocyst stage (5 days) can serve as a strong diagnostic tool, reflecting indications of male and female infertility and yielding useful information regarding the implantation potential of the human embryo [44].

Explaining the Discrepancies between Studies

Different conclusions may be drawn to explain the absence of differences observed by some studies. For example, for several studies, embryo transfer is performed on Day 2 or Day 3. It is fair to mention that the selection of embryos with the higher developmental potential and implantation capacity is almost impossible at this stage, even with new technologies such as the time lapse. In fact, embryo selection on Day 2 or Day 3 completely neglects the paternal effect that becomes important only after embryonic genome activation (EGA) on Day 3. It was previously shown that such “late paternal effect” negatively influences preimplantation embryo development and clinical outcomes without any detectable impairment in zygote development, such as cleaving speed or embryo quality at this stage [48,72].

Another possible explanation for these conflicting results could be the way in which conventional ICSI is performed in an individual laboratory, and how experienced the embryologists are in performing the ICSI procedure and in particular the selection of spermatozoa for injection. Collecting sperm using a 20× or 40× objective is quite common. However, at this low-magnification, morphological defects of the sperm head can be hardly detected [81].

But with a well-aligned microscope equipped with 40× Hoffman contrast optics and optimal adjustment of both the optical beam and the polarizer, detection of sperm head alterations is possible. In addition, with a 1.5-fold increase in the magnification, it is practicable to observe LNV at 600× magnification (Figure 4.1c). However a more accurate and simple detection of small vacuoles is attained with Nomarski optics.

From our experience, we realized after some months of application of MSOME-IMSI that it was possible to observe nuclear defect even with a classical objective. When we started to analyze in a sibling study the rate of blastocysts after IMSI or ICSI, we observed a significant difference of almost 25% in favor of IMSI. With increasing experience and being aware of the presence of a vacuole, the probability to select, with the conventional ICSI microscope, spermatozoa free of a vacuole was increased. This has as a consequence an increase in the rate of blastocysts after ICSI and attenuation in the difference between both techniques.

The conclusions of such observations are that regardless of potential indications of IMSI, we have to select the best spermatozoa possible and exclude those carrying nuclear defects for all male infertility patients. Of course, not all spermatozoa with a nuclear vacuole will have a negative impact on the developmental rate, but if morphologically normal spermatozoa are present in the suspension, it is mandatory to try to select them independently of the technique that is available.

Thus, we have to do all we can to select the best spermatozoa. There are absolutely no indications to select bad-quality spermatozoa if good spermatozoa are present in the prepared semen sample. Are there still

indications where improved sperm selection before fertilization is not necessary or low-magnification microscopy using HMC is more than enough? Most probably this is not the case.

Technical Aspects

Several reservations concerning technical aspects serve as arguments not to apply this method of spermatozoa selection:

1. Too sophisticated system? Too complicated to perform.
2. Lack of standardized sperm selection criteria according to MSOME (classification).
3. Time-consuming aspect during spermatozoa selection.
4. Prolonged selection time of male gametes at the expense of oocyte aging.
   a. Problems in managing assisted reproductive technology (ART) laboratory
   b. High cost

The aim of our work is first to use this technology in a user-friendly way and second to classify the semen and provide in real time a spermocytogram (MSOME), and for the IMSI technique to select spermatozoa in a manner that does not impair oocyte quality.

Materials

Basic Materials

Observation at high magnification (MSOME) or sperm selection (before oocyte injection) is performed on an inverted light microscope equipped with DIC/Nomarski DIC optics, with dry or immersion 63× or 100× magnification objectives lens. In our IVF units, we use a Leica 6000 (Leica Microsystems, Germany) equipped with 63× and 100× DIC objectives.

Dry objectives instead of immersion are more convenient when dishes or slides are moved or replaced for each oocyte injection. Fast motion or dynamic movements between drops induce air bubble formation between the objective lens and the dish, preventing the visualization of the semen sample. The use of dry objective permits an easy handling of the dishes, in particular when a new dish is used for each oocyte injection.

Additional Materials

Using a variable zoom lens (HC Vario C-mount; Leica Microsystems) and subsequent magnification of the image with a high-definition digital video camera makes it possible to evaluate spermatozoan morphology on a monitor at magnifications between 6600× and 12,000× in real time or after spermatozoa immobilization. Despite all the available equipment and computer software, there is not a high priority to perform such observation and selection of spermatozoa using high magnification (>6000×) in conjunction with digital image capture systems to analyze spermatozoa in detail after their capture and visualization on a color monitor screen.

Practical and technical aspects of sperm selection need to be considered to facilitate the workflow while performing IMSI.

For IMSI, inverted microscopes are equipped with the classical ICSI equipment (Narashige or Eppendorf micromanipulators and injectors). Calculation of the total magnification on the screen monitor depends on several technical specifications of the objective, the magnification selector of the microscope, the variable zoom lens, the camera chip diagonal dimension, and the television monitor diagonal dimension.

MSOME: A Useful Tool for Routine Laboratory Semen Analysis

Morphological Normalcy of Spermatozoa Assessed by MSOME

Based on electron microscopy, and high-magnification optic microscopy, Bartoov et al. [10] defined the morphological normalcy of motile-sperm nucleus according to the shape and chromatin content. The shape has to be smooth, symmetric, and oval, with average length and width limits estimated to 4.75 µm ± 0.28 µm and 3.28 µm ± 0.20 µm, respectively (Figure 4.3).

The chromatin mass has to be homogeneous and should contain no extrusions or invaginations, with a maximum of one vacuole involving <4% of the nuclear area. The acrosome and post-acrosomal lamina are considered abnormal if absent, partial, or vesiculated. An abaxial neck with the presence of disorders or cytoplasmic droplets as well as the presence of broken, short, or double and coiled tail is considered abnormal.

Establishment of an MSOME Sperm Classification

According to Bartoov et al. [10], normal spermatozoa should not contain nuclear vacuole(s) exceeding >4% of the nuclear area. Saidi et al. [82] and Perdrix et al. [83] classified the relative area of the vacuole into three groups: (1) <5.9%–6.5%; (2) between 6.5% and 13% or between 5.9% and 12.4%; and (3) >13% or 12.4%, respectively. For Franco et al. [28], LNVs in spermatozoa were defined by the presence of vacuoles occupying ≥50% of the sperm nuclear area.

Under those circumstances where no normal spermatozoa in the semen sample can be found, the only alternative is then to select the morphologically "second-best spermatozoa." Hence, it is essential to know from the second-choice spermatozoa with vacuoles, abnormal shape, or both as to which spermatozoa we have to select. It seemed that the establishment of a classification system of the spermatozoa according to different types of abnormalities was mandatory for the selection of spermatozoa in a more tangible way and also to analyze their influence on further outcomes.

To estimate the impact of specific sperm defects on embryo development and further outcomes in an accurate way, different groups established models of sperm classification according to the normalcy of the shape and the presence and size of vacuoles [42,43]. For example, Vanderzwalmen et al. [42] classified spermatozoa into

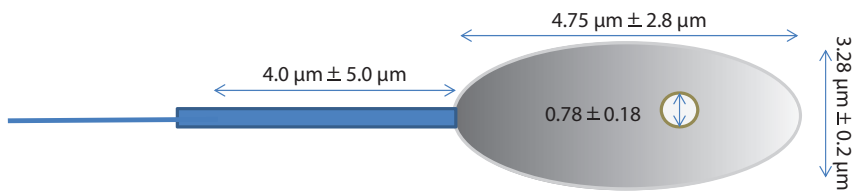

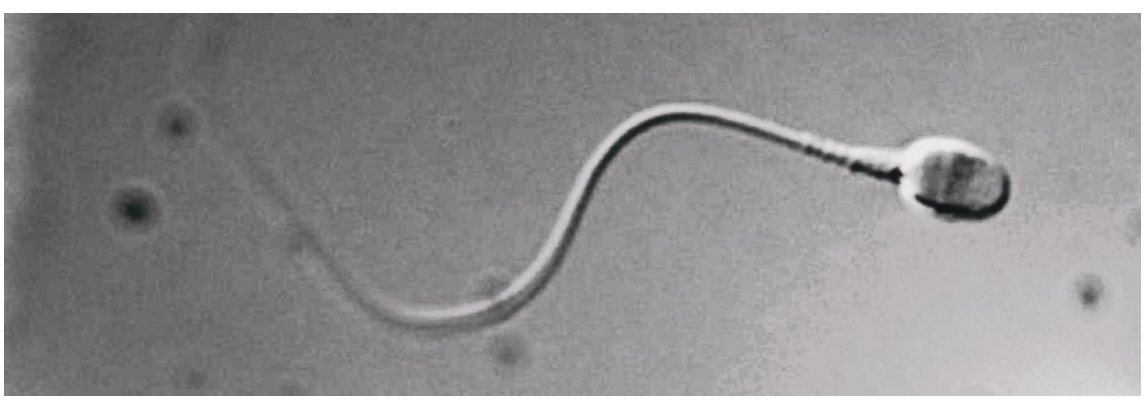

FIGURE 4.3 Representation of a normal spermatozoon according to Bartoov criteria.

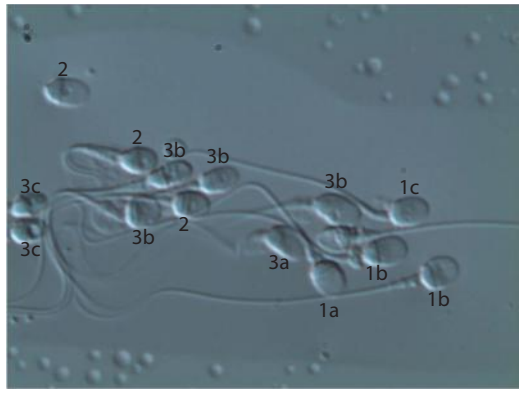

FIGURE 4.4 Spermatozoa vacuolization classification according to Vanderzwalmen et al. [42], observed with Nomarski optics 63× dry objective. Grade I spermatozoa with normal head shape without vacuole (1a), with one vacuole (1b), and with maximum of two small vacuoles (1c). Grade II spermatozoa with large nuclear vacuole (LNV) (2). Grade III spermatozoa with abnormal shape without vacuole (3a), small vacuoles (3b), and LNV (3c).

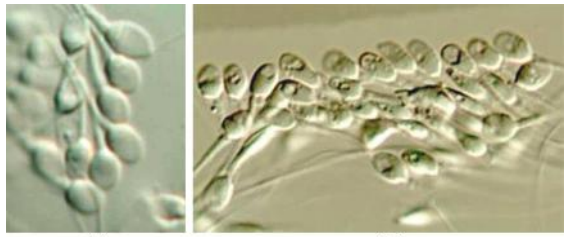

FIGURE 4.5 Spermatozoa vacuolization pattern. (a) High frequency of grade I spermatozoa (fertilization after conventional insemination). (b) Severe teratozoospermia (100 spermatozoa grade III).

three grades according to the presence and size of vacuoles: Grade I, normal shape and a maximum of two small vacuoles; Grade II, normal shape and more than two small vacuoles or at least one large vacuole; Grade III, abnormal head shapes with or without large vacuoles in conjunction with other abnormalities at the level of the base (Figures 4.4 and 4.5) [42].

Cassuto et al. [43] established a detailed classification scoring scale ranging between 6 and 0 points according to the normalcy of the head (2 points if normal), the symmetry of the base (1 point if normal), and the absence of vacuole (3 points if absent). Three grades of scoring were therefore established: grade 1, high-quality spermatozoa with calculated score of 4–6; grade 2, medium-quality spermatozoa with calculated score of 1–3; and grade 3, low-quality spermatozoa with calculated score of 0.

MSOME for Routine Laboratory Semen Analysis

To assess the usefulness of the evaluation of sperm morphology by MSOME, two studies were undertaken in a first instance by Bartoov et al. [10,13] that estimated the correlation between MSOME and the World Health Organization (WHO) routine method. More recently, Oliveira et al. [84] compared the MSOME evaluation with the Tygerberg classification criteria.

Both works conclude that the MSOME criteria appear to be much more restrictive, presenting significantly lower sperm normalcy percentages for the semen samples compared with those found after routine analysis by WHO criteria and the Tygerberg classification. In addition, MSOME represented a much stricter evaluation, because the use of Nomarski optics enabled the identification of vacuoles that could not be described with the same accuracy with other methods.

These studies point toward a benefit in sperm morphology and quality evaluation by including MSOME among the criteria for routine laboratory semen analysis before ICSI or conventional IVF procedures. A previous MSOME spermocytogram revealing a high percentage of vacuoles may be judicious to propose directly IMSI as the best therapy for ICSI candidates. Furthermore the additional information gained by MSOME may help to avoid fertilization failure in IVF cycles.

Proposed Cutoff Threshold for Further Treatment Decisions

With the aim to define a predictive value of sperm normalcy using MSOME on the outcome of combined IVF-ICSI, Wittemer et al. [85] undertook a study including 55 couples with previous failure of implantation after intrauterine insemination (IUI) treatments. In their next attempt, a combination of conventional IVF and ICSI was proposed for each couple. They concluded that below a threshold of 8% of morphological normal spermatozoa observed by MSOME, ICSI must be performed instead of conventional IVF to avoid the risk of fertilization failure. Cassuto (2011, personal communication) observed that if <42% of score 6 spermatozoa (equivalent to our grade I classification) are present in the semen sample, ICSI-IMSI has to be performed instead of conventional IVF.

Falagario et al. [86] identified a cutoff of 20, 28% of sperm nuclear vacuolization (SNV) on the total of sperm in a seminal sample as a physiological threshold. In their study, they observed that patients undergoing ICSI, grouped according to SNV, showed similar percentages of fertilization and embryo development after Day 2 embryo transfer but that more pregnancies were achieved with a higher implantation rate when SNV was ≤ 20, (28%). They concluded that SNV rate could be introduced as an easy diagnostic evaluation before performing an ICSI–IMSI cycle.

Sperm Preparation for Morphological Observation

For MSOME, observation of the spermatozoa may be done on the native semen or after the sperm washing procedure on a three-layer gradient of pure sperm (Nidacon, Sweden), as described previously [87]. It should be stressed that MSOME was applied exclusively to motile spermatozoa that under low-light microscopy magnification have a high potential to be selected for ICSI.

How to Perform MSOME

In certain situations, when we have to decide quickly after the oocyte pick-up (OPU) whether IVF or ICSI-IMSI has to be performed, a rapid assessment of the morphology may be a good decision. If MSOME was part of a previous exam (e.g., spermocytogram), assessment of the morphology is done in a more sophisticated way with the microchannel capture technique.

Rapid Morphological Assessment

To receive a rapid qualitative evaluation of the semen sample, a fast morphological assessment is performed using a microscope coverglass (24 × 60 mm). Elongated drops (~5 µL–10 µL) of 3%–10% polyvinyl pyrrolidone (PVP) solutions are placed on the coverglass (Figure 4.6a). An aliquot of (1 µL–10 µL) native or washed semen sample is transferred on the border of one elongated drop (Figure 4.6b). In case of too low sperm concentration or too low motility, drops of semen sample are placed in the three elongated drops of 3% PVP.

When spermatozoa start to swim, the evaluation of the morphology of motile spermatozoa is done in real time. According to the initial concentration, 50–100 spermatozoa are observed, classified, and recorded in a file (Figure 4.7).

Morphological Examination Using the Microdrops Capture Channel

In cases where quantitative evaluation of the semen sample is needed for research purposes, elongated drops of culture medium are placed into a glass-bottomed dish (GWST 5040; WillCo, World Precision Instruments Wells BV, the Netherlands) and covered with mineral oil (Irvine Scientific, Ireland). The number of elongated drops depends on the semen quality. With reduced sperm quality (severe oligoasthenozoospermia), more elongated drops are prepared.

After the washing step, the sperm suspension is deposited on the border at one end of the elongated drop. When motile spermatozoa start to swim along the edge of the elongated drop, sperm capture channels are created

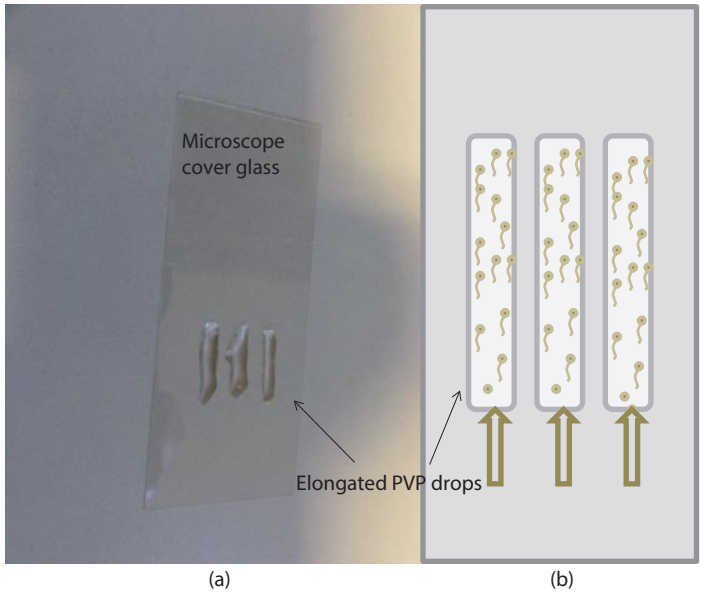

FIGURE 4.6 (a) Preparation of the slide with PVP drops for MSOME. (b) Arrow indicates where the microdrop of semen is deposited.

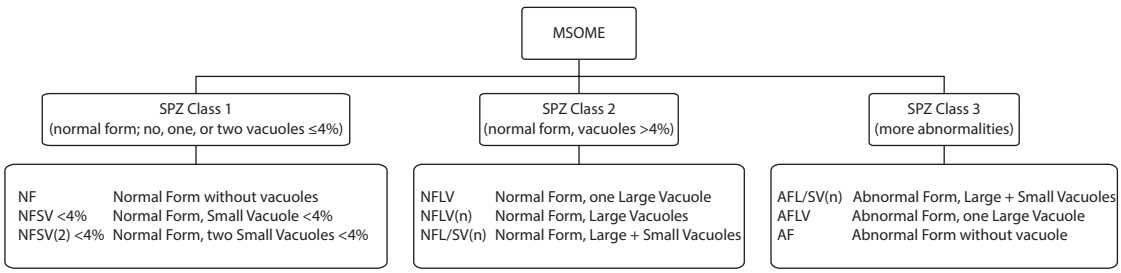

FIGURE 4.7 Flow chart reporting the percentages of spermatozoa according to the different vacuolization patterns.

by pulling channels from the drop with a microinjection pipette ICSI pipette (Microtech, Czech Republic) that is fixed on the micromanipulator [88] (Figure 4.8).

A proper setup of the dish for selecting and capturing sperm facilitates the routine application of IMSI.

Motile spermatozoa enter the small bays and accumulate at the end, where they stop their progressive movement due to a restriction of the free moving space.

A total of eight channels per elongated drop are created and examined (Figure 4.8). Because the majority of the spermatozoa present at the end of the channel show no progressive motility, it is possible to follow them and take several pictures. Morphological assessment of the spermatozoa may be performed in real time under the microscope at magnifications between 630× and 1000×.

A subsequent analysis is conducted on the monitor screen after taping the channel using time-lapse recording (Leica Application Suite magnification optics; Leica). Nevertheless, static sperm imaging only allows evaluation of the visible part of sperm and might leave some morphological alterations undetected.

A minimum of 100 spermatozoa were analyzed and documented on a specific file (Figure 4.7).

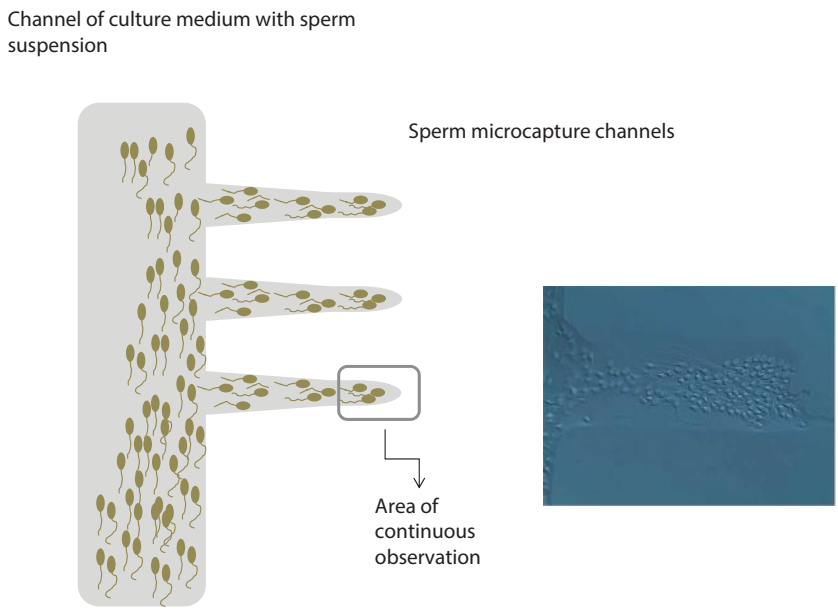

FIGURE 4.8 Application of the sperm-microcapture channels, where spermatozoa accumulate for MSOME.

Assessment with a Transparent Celluloid Form

Bartoov et al. [13] advised assessing the normalcy of spermatozoa by superimposing a fixed transparent celluloid form on the motile examined gametes. This fixed, transparent, celluloid form represents a sperm nucleus fitting the criteria of normalcy of the head (average length, 4.75 µm ± 0.28 µm; average width, 3.28 µm ± 0.20 µm). The correct sperm size, calculated by the ratio of expected normal sperm size to the actual size, can be visualized on the monitor screen. The nuclear shape is documented as abnormal if it varies in length or width by 2x standard deviation from the normal mean axes values [13]. This way of analyzing the morphology is extremely precise. The disadvantage of this technique is that it is very time-consuming and difficult in practice to compare the spermatozoa fitting the criteria of normalcy with moving spermatozoa.

IMSI

Sperm Preparation before IMSI

Before IMSI, only washed semen was used after density-gradient centrifugation on one to three layers of pure sperm (Nidacon, Sweden) [87]. The number of layers depended on the initial sperm concentration.

Two Strategies to Perform IMSI

Three criticisms about IMSI are frequently argued. The first concerns the prolonged period of time for oocytes out of the incubator during spermatozoa selection. The second criticism is that the prolonged selection time of male gametes may be at the detriment of oocyte and promote oocyte aging. Finally, some argue that exposing the spermatozoa for a longer period at 37°C increases the rate of vacuoles. To reduce the time of the oocytes out of the incubator, two approaches were implemented, as presented below.

First Approach: Sperm Selection and Oocyte Injection on Two Different Microscopes

The spermatozoa are selected using the Nomarski optic, and oocyte injection is performed with a conventional ICSI microscope. With such a strategy, the oocytes are not present in the dish during selection of the spermatozoa. After selection, the dish is incubated for 15–30 min to stabilize the temperature, pH, or both.

In cases of severe teratozoospermia, taking into account that more time for sperm selection is needed, we plan the selection at least around the time of OPU. With such a policy, oocyte injection can be performed 2–3 hr after OPU (38–40 hr post–human chorionic gonadotropin [hCG] administration) on the ICSI station, thereby avoiding oocyte aging. Another advantage of this approach concerns the organization of the laboratory work. In cases of several IMSI, the IMSI station is occupied only for the selection process and not for the injection phase. Also with this approach, the IMSI microscope is not occupied for an excessive period, and the oocytes are removed from the incubator only for the injection step.

Another possibility is to select the spermatozoa in a glass-bottomed dish and place them directly in a conventional ICSI dish.

Preparation of IMSI Dishes Under sterile conditions, several drops are deposited in the glass-bottomed dishes (Figure 4.9).

Sperm Selection PVP Drops (A) On the left side of the dish, place one to three elongated drops of 7.5%–10% PVP (~5 µL–10 µL). In this drop, selection of the spermatozoa is performed. The number of drops depends on the quality of the semen that was assessed in a previous MSOME analysis or on the number of metaphase II (MII) oocytes, which are needed for injection. The aim is that the spermatozoa that we select stay in the PVP drop for a period that does not exceed 15 min. Moreover, according to this rule, several elongated drops and even IMSI dishes should be prepared if many MII oocytes are present.

Sperm Aliquots Drops (B) Under each sperm selection drop (A), a drop of ~10 µL of human tubal fluid (HTF)-HEPES (IVFonline, Canada) containing 6% human synthetic albumin (HSA) (Irvine Scientific) is deposited.

Host-Selected Spermatozoa Microdrops (C) Adjacent to the elongated drops of PVP (A), very small drops (<1 µL) (C) of HTF-HEPES containing 6% HSA are deposited with a small stripper pipette. The microdrops will host the spermatozoa that were selected in drop A until oocyte injection.

Sperm Immobilization Drops (D) A small drop of 10% PVP in which sperm immobilization will take place is deposited in the upper part of the dish.

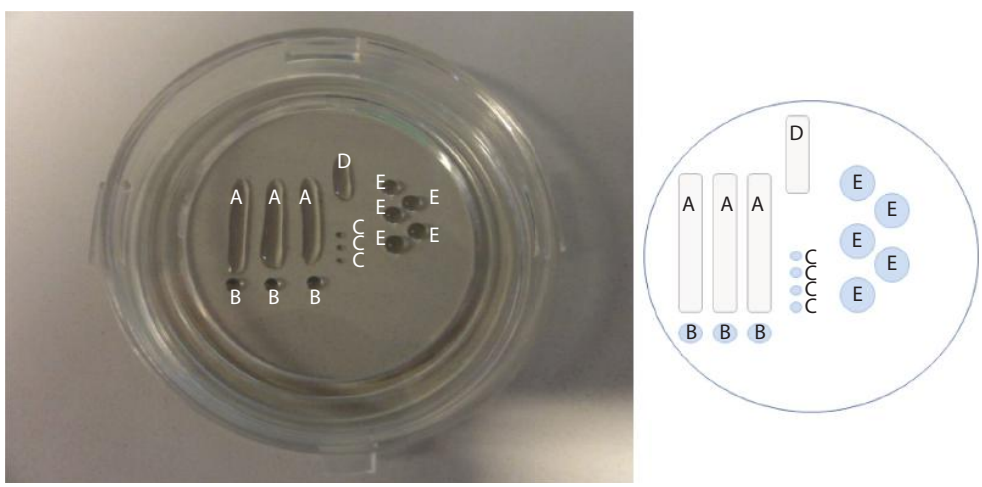

FIGURE 4.9 Position of the drops in an IMSI dish (A, D) 7.5%–10% PVP. (B, C, E) Culture medium. (A) Sperm selection PVP drops. (B) Sperm aliquot drops. (C) Host-selected spermatozoa microdrops. (D) Sperm immobilization drops. (E) Oocytes injection drops.

Oocytes Injection Drops (E) The right side of the dish contains five drops of HTF-HEPES containing 6% HSA in which oocyte injection will take place following the policy of IMSI procedure.

All drops were covered with sterile mineral oil (Irvine Scientific).

Method of Spermatozoa Selection and Injection The entire selection process is performed at room temperature. At the beginning of IMSI, a small aliquot of washed sperm (1 µL–10 µL according to the semen sample quality) is transferred into drop B (Figure 4.10a) and a small bridge is formed between drop B and drop A (Figure 4.10b). The motile spermatozoa swim into the PVP drop and the morphologically normal spermatozoa (or the best second class) are selected with an ICSI pipette and transferred into a small drop of culture media (drop C) (Figure 4.10c). They are selected at a magnification of 1000×.

After collecting spermatozoa (if possible, 1.5 times the number of oocytes to inject), the dish is removed from the IMSI station and placed on a 37°C heating stage for temperature recovery (~30 min).

After this period of incubation at 37°C, the oocytes are placed into the culture media (E), and ICSI is performed using a conventional Hoffman microscope at 400× magnification (Figure 4.10d). Motile spermatozoa are aspirated from the preselected host drop (C) and immobilized in the PVP drop (D) before injection.

Second Approach: Sperm Selection and Oocyte Injection on the IMSI Station

When the purpose of the study is to follow the outcome of embryo development in relation to the type of injected spermatozoon (photodocumentation of the injected spermatozoon), a maximum of two oocytes are placed directly in the IMSI dish (Figure 4.11). A minimum of two dishes are prepared as presented previously, except that sperm host drops are not present before starting such an approach, the quality of the spermatozoa should be assessed to be sure that the time spent to select one class I or II spermatozoa will not exceed 2 min.

This procedure is performed at 37°C. At the beginning of the IMSI procedure, a small aliquot of washed sperm (1 µL–10 µL) is transferred into drop B and a small bridge is formed between drop B and the elongated selection drop. The motile spermatozoa swim in the PVP drop, and the motile spermatozoa are morphologically selected at a magnification of 1000× (Figure 4.11a) before immobilization in drop D (Figure 4.11b). Use of a variable

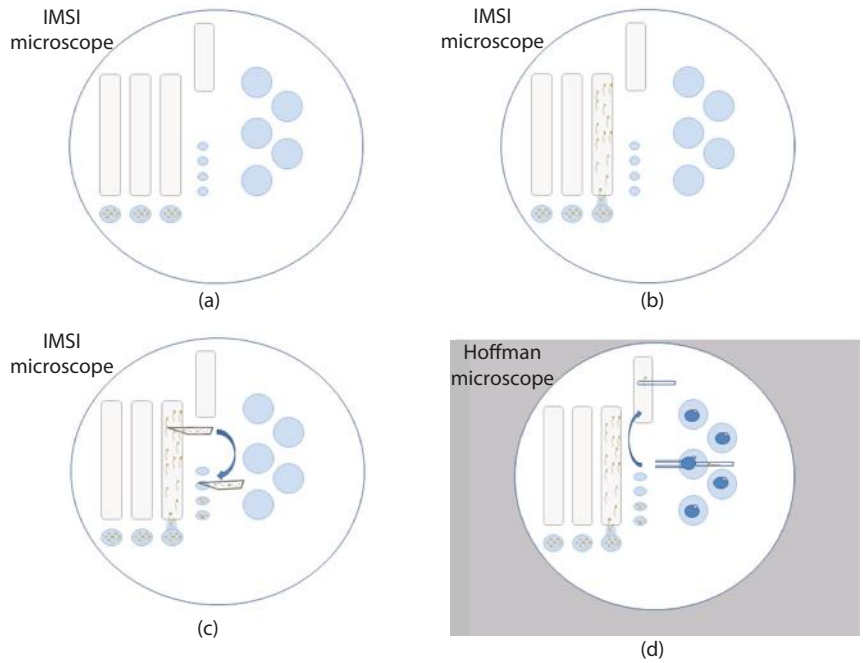

FIGURE 4.10 IMSI. (a–c) Description of the different steps for sperm selection on the IMSI microscope followed by (d) oocyte injection on the Hoffman ICSI microscope.

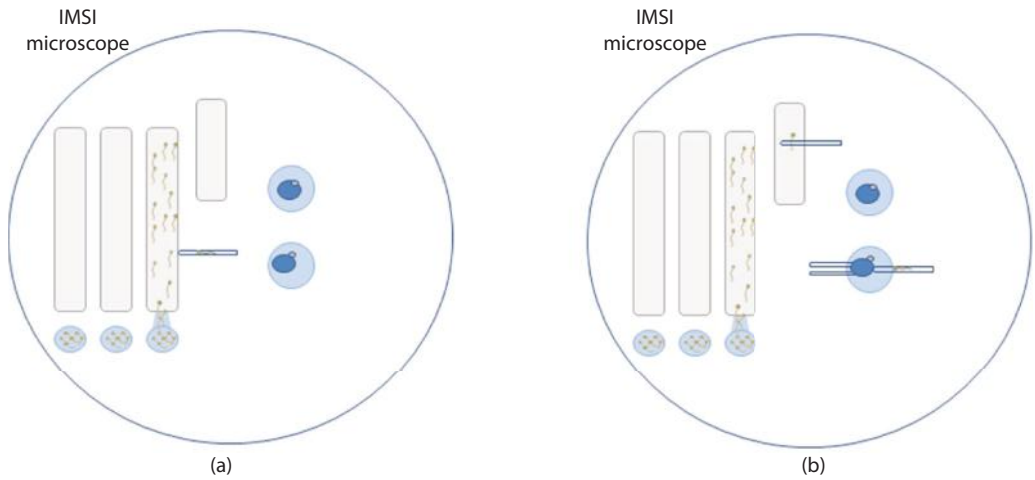

FIGURE 4.11 IMSI. Description of the different steps for sperm selection (a) and oocyte injection on the IMSI microscope (b).

zoom lens (HC Vario C-mount; Leica) allows for the reevaluation (after immobilization) of the morphology on the monitor at magnifications between 6600× and 12,000× and the performance of photodocumentation for a subsequent analysis. Injections are performed directly after immobilization in the same dish. After IMSI, single drop culture (in a petri dish or with the time-lapse technology) is performed.

The next two oocytes are placed in a new IMSI dish prewarmed on the heating stage. The previous IMSI dish is then placed on a heating stage at 37°C until the next injection selection and injection step. This technique is easy to apply with dry objectives, so that no problem with oil occurs when changing dishes.

Time Spent to Select Spermatozoa

Regarding time allotted to select spermatozoa, the primary intention is to choose normal-shaped spermatozoa without any vacuoles (grade I) for injection into the oocytes. Depending on the degree of impaired sperm morphology, the mean time required for selecting the best sperm ranged between 2 and 15 min. However, when it is obvious after 15 min of sperm examination that spermatozoa of a normal morphology cannot be found, the second-best spermatozoa with the least number of vacuoles, other abnormalities, or a combination is selected for injection.

In such situations, it might be difficult to decide whether to stop the search for a normal spermatozoon or to proceed. It might take 15 min and even longer; of course, this also depends on the number of oocytes that have to be injected and on the number of patients that have to be treated.

Temperature for Sperm Evaluation or Selection

Another crucial question is whether the duration of sperm selection and the temperature might influence vacuole formation. A study by Peer et al. [89] demonstrated that after 2 hr of incubation at 37°C in culture media, the incidence of spermatozoa with vacuolated nuclei was significantly higher compared with incubation at 21°C. Peer and colleagues suggested that prolonged (≥2 hr) sperm manipulations for ART should be performed at 21°C rather than 37°C. Schwarz et al. [90] reported a significant increase in SNV in washed sperm but not in swim-up sperm. They concluded that the mode of sperm preparation does influence SNV and that vacuolization is unaffected by temperature in motile sperm isolated by swim-up.

Several experiments were conducted in our centers to analyze the formation of vacuoles in real time. We implemented a time-lapse recording approach on selected Grade I spermatozoa incubated for 24 hr at 37°C. Compared with the control group, no changes in the morphology of the spermatozoa were observed. No vacuoles appeared.

Even when the same experiment was conducted on spermatozoa with vacuoles, no changes in the size and shape of the spermatozoa after 24 hr incubation at 37°C were found [88].

Conclusions

One of the most essential questions is not under which technical conditions the selection of spermatozoa should be recommended but rather whether we have to consider to select the best spermatozoa and, if possible, exclude those carrying defects.

For this reason, MSOME and IMSI were developed. MSOME appears to be a powerful method to improve our understanding of human spermatozoa, and IMSI is now routinely used in ART practices.

However, the clinical use of MSOME and IMSI remains unclear in the fields of male infertility diagnosis and ARTs. Answers to a lot of questions are pending or unclear for the following issues: (1) the terminology of vacuoles, their classification, and their location on the sperm head; (2) vacuole origin and formation; (3) application of MSOME-IMSI for specific indications, such as teratozoospermia or to a large population; (4) the application of IMSI instead of IVF in cases of unexplained infertility; and (5) oocyte repairing factors. Nevertheless, it is increasingly obvious that large vacuoles reflect a pathological situation, most probably correlated with sperm chromatin immaturity. In addition, we have to be aware that this technique is challenging and has to be performed under the best working conditions so as to not impair the quality of oocytes.

The introduction of IMSI made embryologists aware that in times of ICSI the selection of sperm has to be given proper attention.

The introduction of IMSI has the advantage that embryologists realize that more attention has been given to sperm selection even in cases of classical ICSI. The application of IMSI leads to more and better quality blastocysts and thus it increases the chance of selecting the proper embryo for transfer with the highest implantation potential. The full benefit of using MSOME as an additional tool to ICSI procedure manifests when it is performed in combination with Day 5 embryo culture of all fertilized oocytes. Also, knowing the excellent results obtained with vitrification should not be underestimated.

Even though there are only few reports in the human species on the abnormal outcome generated by spermatozoa carrying vacuoles, a higher and better-resolution technique has to be added as an additional tool for ICSI, knowing the possible consequence of sperm DNA damage for the offspring. Presently, one study reports higher de novo malformation after ICSI selection than after IMSI selection [39].

REFERENCES

1. Palermo G, Joris H, Devroey P, Van Steirteghem A. Pregnancies after intracytoplasmic injection of single spermatozoon into an oocyte. *Lancet*. 1992; 340: 17–18.
2. Nagy ZP, Liu J, Joris H, et al. The result of intracytoplasmic sperm injection is not related to any of the three basic sperm parameters. *Hum. Reprod*. 1995; 10: 1123–1129.
3. Svalander P, Jakobsson AH, Forsberg AS, Bengtsson AC, Wikland M. The outcome of intracytoplasmic sperm injection is unrelated to 'strict criteria' sperm morphology. *Hum. Reprod*. 1996; 11: 1019–1022.
4. Vawda A, Gunby J, Younglai E. Semen parameters as predictors of in-vitro fertilization: The importance of strict criteria morphology. *Hum. Reprod*. 1996; 11: 1445–1450.
5. Nikolettos N, Kiipker W, Demirel C, et al. Fertilization potential of spermatozoa with abnormal morphology. *Hum. Reprod.* 1999; 14(Suppl 1): 47–70.
6. Host E, Ernst E, Lindenberg S, Smidt-Jensen S. Morphology of spermatozoa used in IVF and ICSI from oligozoospermic men. *Reprod. Biomed. Online.* 2001; 3: 212–215.
7. Garolla A, Fortini D, Menegazzo M, et al. High power magnification microscopy and functional status analysis of sperm in the evaluation and selection before ICSI. *Reprod. Biomed. Online.* 2008; 17: 610–616.

8. De Vos A, Van De Velde H, Joris H, et al. Influence of individual sperm morphology on fertilization, embryo morphology, and pregnancy outcome of intracytoplasmic sperm injection. *Fertil. Steril*. 2003; 79: 42–48.
9. Ebner T, Filicori M, Tews G, Parmegiani L. A plea for a more physiological ICSI. *Andrologia*. 2011; 44: 1–18.
10. Bartoov B, Berkovitz A, Eltes F. Selection of spermatozoa with normal nuclei to improve the pregnancy rate with intracytoplasmic sperm injection. *N. Engl. J. Med*. 2001; 345: 1067–1068.
11. Coppola G, Di Caprio G, Wilding M, et al. Digital holographic microscopy for the evaluation of human sperm structure. *Zygote*. 2013; 7: 1–9.
12. Boitrelle F, Ferfouri F, Petit JM, et al. Large human sperm vacuoles observed in motile spermatozoa under high magnification: Nuclear thumbprints linked to failure of chromatin condensation. *Hum. Reprod*. 2011; 26: 1650–1658.
13. Bartoov B, Berkovitz A, Eltes F, Kogosowski A, Menezo Y, Barak Y. Real-time fine morphology of motile human sperm cell is associated with IVF-ICSI outcome. *J. Androl*. 2002; 23: 1–8.
14. Bartoov B, Berkovitz A, Eltes F, et al. Pregnancy rates are higher with intracytoplasmic morphologically selected sperm injection than with conventional intracytoplasmic injection. *Fertil. Steril*. 2003; 80: 1413–1419.
15. Berkovitz A, Eltes F, Yaari S, et al. The morphological normalcy of the sperm nucleus and pregnancy rate of intracytoplasmic injection with morphologically selected sperm. *Hum. Reprod*. 2005; 20: 185–190.
16. Berkovitz A, Eltes F, Lederman H, et al. How to improve IVF-ICSI outcome by sperm injection. *Reprod. Biomed. Online*. 2006; 12: 634–638.
17. Dorphin B, Lefevre M, Gout C, Oger P, Yazbeck C, Rougier N. Fine localization and characterization of some abnormalities observed in human sperm heads by interferential differential contrast. *Hum. Reprod.* 2010; 25: P–043.
18. Watanabe S, Tanaka A, Fujii S, Mizunuma H. No relationship between chromosome aberrations and vacuole-like structures on human sperm head. *Hum. Reprod*. 2009; 24: i94–i96.
19. Westbrook VA, Diekman AB, Klotz KL, et al. Spermatid-specific expression of the novel X-linked gene product SPAN-X localized to the nucleus of human spermatozoa. *Biol. Reprod*. 2000; 63; 469–481.
20. Toshimori K. Dynamics of the Mammalian Sperm Head. Advances in Anatomy, Embryology and Cell Biology Volume 204, 2009, pp. 45–51.
21. Boitrelle F, Albert M, Petit J-M, et al. Small human sperm vacuoles observed under high magnification are pocket-like nuclear concavities linked to chromatin condensation failure. *Reprod. Biomed. Online*. 2013; 27: 201–211.
22. Cayli S, Jakab A, Ovari L, et al. Biochemical markers of sperm function: Male fertility and sperm selection for ICSI. *Reprod. Biomed. Online*. 2003; 7: 462–468.
23. Hazout A, Dumont-Hassan M, Junca AM, Cohen Bacrie P, Tesarik J. High-magnification ICSI overcomes paternal effect resistant to conventional ICSI. *Reprod. Biomed. Online*. 2006; 12: 19–25.
24. Gopalkrishnan K, Padwal V, Meherji PK, Gokral JS, Shah R, Juneja HS. Poor quality of sperm as it affects repeated early pregnancy loss. *Arch. Androl*. 2000; 45: 111–117.
25. Hammadeh M, Nkemayim D, Georg T, Rosenbaum P, Schmidt W. Sperm morphology and chromatin condensation before and after semen processing. *Arch. Androl*. 2000; 44: 221–226.
26. Mahfouz R, Sharma R, Thiyagarajan A, et al. Semen characteristics and sperm DNA fragmentation in infertile men with low and high levels of seminal reactive oxygen species. *Fertil. Steril*. 2010; 94: 2141–2146.
27. Perrin A, Huong Nguyen M, Douet-Guilbert N, Morel F, De Braekeleer M. Motile sperm organelle morphology examination: Where do we stand 12 years later? *Expert Rev. Obstet. Gynecol*. 2013; 8: 249–260.
28. Franco J, Baruffi R, Mauri A, Petersen C, Oliveira J, Vagnini L. Significance of large nuclear vacuoles in human spermatozoa: Implications for ICSI. *Reprod. Biomed. Online*. 2008; 17: 42–45.
29. Franco J, Mauri A, Petersen C, et al. Large nuclear vacuoles are indicative of abnormal chromatin packaging in human spermatozoa. *Int. J. Androl*. 2012; 35: 1–6.
30. Perdrix A, Travers A, Chelli MH, et al. Assessment of acrosome and nuclear abnormalities in human spermatozoa with large vacuoles. *Hum. Reprod*. 2011; 26: 47–58.
31. Boitrelle F, Ferfouri F, Salama S, et al. Nature of sperm-head vacuoles and results and indications of IMSI (intracytoplasmic morphologically selected sperm injection). *Andrologie*. 2011; 21: 234–239.
32. Cassuto NG, Hazout A, Hammoud I, et al. Correlation between DNA defect and sperm-head morphology. *Reprod. Biomed. Online*. 2012; 24: 211–218.
33. Ward WS. Function of sperm chromatin structural elements in fertilization and development. *Mol. Hum. Reprod.* 2010; 16: 30–36.

34. Rousseaux S, Petosa C, Müller CW, Müller CW, Khochbin S. A novel key element in post-meiotic male genome reprogramming. *Med. Sci*. 2010; 26: 130–132.
35. Aitken RJ, De luliis GN. Origins and consequences of DNA damage in male germ cells. *Reprod. Biomed. Online.* 2007; 14: 727–733.
36. Koppers AJ, De Iuliis GN, Finnie JM, McLaughlin EA, Aitken RJ. Significance of mitochondrial reactive oxygen species in the generation of oxidative stress in spermatozoa. *J. Clin. Endocrinol. Metab*. 2008; 93: 3199–3207.
37. Palermo GD, Neri QV, Takeuchi T, Squires J, Moy F, Rosenwaks Z. Genetic and epigenetic characteristics of ICSI children. *Reprod. Biomed. Online*. 2008; 17: 820–833.
38. Miller D, Brinkworth M, Iles D. Paternal DNA packaging in spermatozoa: More than the sum of its parts? DNA, histones, protamines and epigenetics. *Reproduction.* 2010; 139: 287–301.
39. Cassuto G. Low birth defects by deselecting abnormal spermatozoa before ICSI. *Reprod. Biomed. Online*. 2014; 28: 47–53.
40. Aitken RJ, Koppers AJ. Apoptosis and DNA damage in human spermatozoa. *Asian J. Androl*. 2011; 13: 36–42.
41. Oliva R, de Mateo S. Medical implications of sperm nuclear quality. In: *Epigenetics and Human Reproduction* (eds. Rousseaux S, Khochbin S). Berlin: Springer-Verlag, 2011, pp. 45–55.
42. Vanderzwalmen P, Hiemer A, Rubner P, et al. Blastocyst development after sperm selection at high magnification is associated with size and number of nuclear vacuoles. *Reprod. Biomed. Online*. 2008; 17: 617–627.
43. Cassuto NG, Bouret D, Plouchart JM, et al. A new real-time morphology classification for human spermatozoa: A link for fertilization and improved embryo quality. *Fertil. Steril*. 2009; 92: 1616–1625.
44. Knez K, Zorn B, Tomazevic T, Vrtacnik-Bokal E, Virant-Klun I. The IMSI procedure improves poor embryo development in the same infertile couples with poor semen quality: A comparative prospective randomized study. *Reprod. Biol. Endocrinol*. 2011; 9: 123–130.
45. Knez K, Tomazevic T, Vrtacnik-Bokal E, Virant-Klun I. Developmental dynamics of IMSI-derived embryos: A time-lapse prospective study. *Reprod. Biomed. Online*. 2013; 27: 161–171.
46. Shoukir Y, Chardonnens D, Campana A, Sakkas D. Blastocyst development from supernumerary embryos after intracytoplasmic sperm injection: A paternal influence. *Hum. Reprod*. 1998; 13: 1632–1637.
47. Tesarik J, Greco E, Mendoza C. Late but not early paternal effect on human embryo development is related to sperm DNA fragmentation. *Hum. Reprod*. 2004; 19: 611–615.
48. Tesarik J. Paternal effects on cell division in the preimplantation embryo. *Reprod. Biomed. Online*. 2005; 10: 370–375.
49. Seli E, Gardner DK, Schoolcraft WB, Moffatt O, Sakkas D. Extent of nuclear DNA damage in ejaculated spermatozoa impacts on blastocyst development after in vitro fertilization. *Fertil. Steril*. 2004; 82: 378–383.
50. Larson KL, DeJonge CJ, Barnes AM, Jost LK, Evenson DP. Sperm chromatin structure assay parameters as predictors of failed pregnancy following assisted reproductive techniques. *Hum. Reprod*. 2000; 15: 1717–1722.
51. Nasr-Esfahani MH, Salehi M, Razavi S, et al. Effect of sperm DNA damage and sperm protamine deficiency on fertilization and embryo development post-ICSI. *Reprod. Biomed. Online.* 2005; 11: 198–205.
52. Berkovitz A, Eltes F, Ellenbogen A, Peer S, Feldberg D, Bartoov B. Does the presence of nuclear vacuoles in human sperm selected for ICSI affect pregnancy outcome? *Hum. Reprod*. 2006; 21: 1787–1790.
53. Junca AM, Cohen-Bacrie P, Hazout A. Improvement of fertilisation and pregnancy rate after intracytoplasmic fine morphology selected sperm injection. *Fertil. Steril*. 2004; 82(Suppl 2): S173.
54. Aitken R. Origins and consequences of DNA damage in male germ cells. *Reprod. Biomed. Online*. 2007; 14: 727–733.
55. Fernandez-Gonzalez R, Nuno Moreira P, Perez-Crespo M, et al. Long-term effects of mouse intracytoplasmic sperm injection with DNA-fragmented sperm on health and behavior of adult offspring. *Biol. Reprod.* 2008; 78: 761–772.
56. Berkovitz A, Eltes F, Paul M. The chance of having a healthy normal child following intracytoplasmic Morphologically-selected sperm injection (IMSI) treatment is higher compared to conventional IVF-ICSI treatment. *Fertil. Steril.* 2007; 88: S20.
57. Ugajin T, Terada Y, Hasgawa H, Nabeshima H, Suzuki K, Yaegashi N. The shape of the sperm midpiece in intracytoplasmic morphologically selected sperm injection relates sperm centrosomal function. *J. Assit. Reprod. Genet.* 2010; 27: 75–81.
58. Van Blerkom J, Davis P. Evolution of the sperm aster after microinjection of isolated human sperm centrosomes into meiotically mature human oocytes. *Hum. Reprod*. 1995; 10: 2179–2182.

59. Schatten H, Sun QY. The role of centrosomes in mammalian fertilization and its significance for ICSI. *Mol. Hum. Reprod*. 2009; 15: 531–538.
60. Rawe V, Olmedo S, Nodar F, Doncel G, Acosta A, Vitullo A. Cytoskeletal organization defects and abortive activation in human oocytes after IVF and ICSI failure. *Mol. Hum. Reprod.* 2000; 6: 510–516.
61. Rawe V, Terada Y, Nakamura S, Chillik C, Olmedo S, Chemes H. A pathology of the sperm centriole responsible for defective sperm aster formation, sygamy and cleavage. *Hum. Reprod*. 2002; 17: 2344–2349.
62. Dam AH, Feenstra I, Westphal JR, Ramos L, van Golde RJ, Kremer JA. Globozoospermia revisited. *Hum. Reprod. Update.* 2007; 13: 63–75.
63. Cox L, Larman MG, Saunders CM, Hashimoto K, Swann K, Lai FA. Sperm phospholipase Czeta from humans and cynomolgus monkeys triggers Ca2+ oscillations, activation and development of mouse oocytes. *Reproduction.* 2002; 124: 611–623.
64. Kashir J, Heindryckx B, Jones C, De Sutter P, Parrington J, Coward K. Oocyte activation, phospholipase C zeta and human infertility. *Hum. Reprod. Update.* 2010; 16: 690–703.
65. Montag M, Köster M, van der Ven K, Bohlen U, van der Ven H. The benefit of artificial oocyte activation is dependent on the fertilization rate in a previous treatment cycle. *Reprod. Biomed. Online*. 2012; 24(5): 521–526.
66. Stecher A, Bach M, Neyer A, Vanderzwalmen P, Zintz M, Zech NH. Case report: Live birth following ICSI with non-vital frozen-thawed testicular sperm and oocyte activation with calcium ionophore. *J. Assist. Reprod. Genet*. 2011; 28: 411–414.
67. Gatimel N, Léandri D, Foliguet B, Bujan L, Parinaud J. Sperm cephalic vacuoles: New arguments for their non acrosomal origin in two cases of total globozoospermia. *Andrology*. 2013; 1: 52–56.
68. Kashir J, Sermondade N, Sifer C, et al. Motile sperm organelle morphology evaluation-selected globozoospermic human sperm with an acrosomal bud exhibits novel patterns and higher levels of phospholipase C zeta. *Hum. Reprod*. 2012; 27(11): 3150–3160.
69. Sermondade N, Hafhouf E, Dupont C, et al. Successful childbirth after intracytoplasmic morphologically selected sperm injection without assisted oocyte activation in a patient with globozoospermia. *Hum. Reprod.* 2011; 26: 2944–2949.
70. Utsuno H, Oka K, Yamamoto A, Shiozawa T. Evaluation of sperm head shape at high magnification revealed correlation of sperm DNA fragmentation with aberrant head ellipticity and angularity. *Fertil. Steril*. 2013; 99: 1573–1580.
71. Perdrix A, Rives N. Motile sperm organelle morphology examination (MSOME) and sperm head vacuoles: State of the art in 2013. *Hum. Reprod. Update*. 2013; 19: 527–541.
72. Greco E, Scarselli F, Fabozzi G, et al. Sperm vacuoles negatively affect outcomes in intracytoplasmic morphologically selected sperm injection in terms of pregnancy, implantation, and live-birth rates. *Fertil. Steril.* 2013; 100: 379–385.
73. Antinori M, Licata E, Dani G, et al. Intracytoplasmic morphologically selected sperm injection: A prospective randomized trial. *Reprod. Biomed. Online.* 2008; 16: 835–841.
74. Nadalini M, Tarozzi N, Distratis V, Scaravelli G, Borini A. Impact of intracytoplasmic morphologically selected sperm injection on assisted reproduction outcome. *Reprod. Biomed. Online*. 2009; 19: 45–55.
75. Balaban B, Yakin K, Alatas C, Oktem O, Isiklar A, Urman B. Clinical outcome of intracytoplasmic injection of spermatozoa morphologically selected under high magnification: A prospective randomized study. *Reprod. Biomed. Online.* 2011; 22: 472–476.
76. Setti SA, Ferreira RC, Paes de Almeida Ferreira Braga D, de Cássia Sávio Figueira R, Iaconelli A, Jr, Borges E, Jr. Intracytoplasmic sperm injection outcome versus intracytoplasmic morphologically selected sperm injection outcome: A meta-analysis. *Reprod. Biomed. Online.* 2010; 21: 450–455.
77. Delaroche L, Yazbeck C, Gout C, Kahn V, Oger P, Rougier N. Intracytoplasmic morphologically selected sperm injection (IMSI) after repeated IVF or ICSI failures: A prospective comparative study. *Eur. J. Obstet. Gynecol. Reprod. Biol.* 2013; 167: 76–80.
78. De Vos A, Van de Velde H, Bocken G, et al. Does intracytoplasmic morphologically selected sperm injection improve embryo development? A randomized sibling-oocyte study. *Hum. Reprod*. 2013; 28: 617–626.
79. Mauri A, Petersen C, Oliveira J, Massaro F, Baruffi R, Franco JG, Jr. Comparison of day 2 embryo quality after conventional ICSI versus intracytoplasmic morphologically selected sperm injection (IMSI) using sibling oocytes. *Eur. J. Obstet. Gynecol. Reprod. Biol.* 2010; 150: 42–46.

80. Leandri RD, Gachet A, Pfeffer J, et al. Is intracytoplasmic morphologically selected sperm injection (IMSI) beneficial in the first ART cycle? A multicentric randomized controlled trial. *Andrology*. 2013; 5: 692–697.
81. Montag M, Toth B, Strowitzki T. Sperm selection in ART. *J. Reproduktionsmed. Endokrinol.* 2012; 9: 485–489.
82. Saidi R, Rives N, Gruel E, Mazurier S, Mousset-Simeon N, Mace B. New classification of spermatocytogram at high magnification. *Med. Reprod. Gyn. Endo.* 2008; 10: 315–324.
83. Perdrix A, Saïdi R, Ménard JF, et al. Relationship between conventional sperm parameters and motile sperm organelle morphology examination (MSOME). *Int. J. Androl*. 2012; 35: 491–498.
84. Oliveira JB, Massaro FC, Mauri AL, et al. Motile sperm organelle morphology examination is stricter than Tygerberg criteria. *Reprod. Biomed. Online*. 2009; 18: 320–326.
85. Wittemer C, Pujol A, Boughali H, et al. The impact of high-magnification evaluation of sperm on ART outcome. *Hum. Reprod*. 2006; 22(Suppl 1): i59–i60.
86. Falagario D, Brucculeri A, Depalo R, Trerotoli P, Cittadini E, Ruvolo G. Sperm head vacuolization affects clinical outcome in ICSI cycle. A proposal of a cut-off value. *J. Assist. Reprod. Genet.* 2012; 29: 1281–1287.
87. Van der Zwalmen P, Bertin-Segal G, Geerts L, Debauche C, Schoysman R. Sperm morphology and IVF pregnancy rate: Comparison between Percoll gradient centrifugation and swim-up procedures. *Hum. Reprod*. 1991; 6: 581–588.
88. Neyer A, Vanderzwalmen P, Bach M, Stecher A, Spitzer D, Zech N. Sperm head vacuoles are not affected by in-vitro conditions, as analysed by a system of sperm-micro capture channels. *Reprod. Biomed. Online*. 2013; 26: 368–377.
89. Peer S, Eltes F, Berkovitz A, Yehuda R, Itsykson P, Bartoov B. Is fine morphology of the human sperm nuclei affected by in vitro incubation at 37C? *Fertil. Steril*. 2007; 88: 1589–1594.
90. Schwarz C, Köster M, van der Ven K, Montag M. Temperature-induced sperm nuclear vacuolization is dependent on sperm preparation. *Andrologia*. 2012; 44(Suppl 1): 126–129.

5

Morphological Selection of Gametes and Embryos: Oocyte

Başak Balaban and Thomas Ebner

Introduction

Assessment of oocyte morphology and determination of its correlation with quality and viability and with the clinical outcome is a difficult task, as the underlying mechanisms that change its appearance are multifactorial and complex. Optimal oocyte morphology (Figure 5.1) is defined as an oocyte with spherical structure enclosed by a uniform zona pellucida (ZP), with a uniform translucent cytoplasm free of inclusions and a size-appropriate polar body (Pb) [1,2]. However, metaphase II (MII)-stage oocytes retrieved from patients after ovarian stimulation are known to show significant morphological variations that may affect the developmental competence and implantation potential of the derived embryo.

More than half of the oocytes collected can contain at least one morphological abnormality, and this abnormality may be correlated with the asynchrony between nuclear and cytoplasmic maturation of the MII oocyte, playing an important role in its viability and in the clinical outcome. Morphological variations of the oocytes may also result from other intrinsic factors, such as age and genetic defects, or extrinsic factors, such as stimulation protocols, culture conditions, and nutrition. Conflicting results have been published regarding the effect of morphological variations of the oocyte on embryo development and implantation.

This chapter reviews the correlation of morphological abnormalities of the MII oocyte and the clinical outcome, the effect on genetic disorders, the predictive value of specific abnormalities, and whether any of these parameters can be used in all the scoring systems applied in in vitro fertilization (IVF) laboratories.

Morphological abnormalities of the oocyte are discussed under two different subgroups: cytoplasmic abnormalities and extracytoplasmic abnormalities [1–4].

Cytoplasmic Abnormalities

Cytoplasmic abnormalities of MII oocytes include different types and degrees of cytoplasmic granulations (slightly diffused or excessive whole/centrally located granulation) and appearance of refractile bodies, smooth endoplasmic reticulum clusters (sERCs), or vacuolization in the ooplasm. Detection of cytoplasmic variations was first termed as cytoplasmic dysmorphism by Van Blerkom and Henry in 1992 [5] and since then has been used as a selection method to assess the viability and implantation potential of the derived embryos.

Morphological Appearance of the Cytoplasm

Although the appearance of cytoplasm was considered a potential predictive factor for the success of clinical outcome, different definitions and grouping of multiple morphological features in various published studies make a comparative analysis difficult. The terms that were used in the literature are dark cytoplasm [6–8], dark cytoplasm–granular cytoplasm [9], dark cytoplasm with slight granulation [10], dark granular appearance of the cytoplasm [11], and diffused cytoplasmic granularity [12]. The high subjectivity of the definition of these types of granulations in various laboratories provides limited predictive value for the clinical outcome. Despite the fact

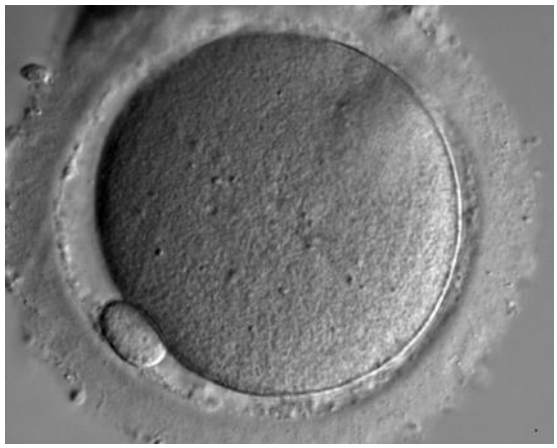

FIGURE 5.1 Normal mature oocyte.

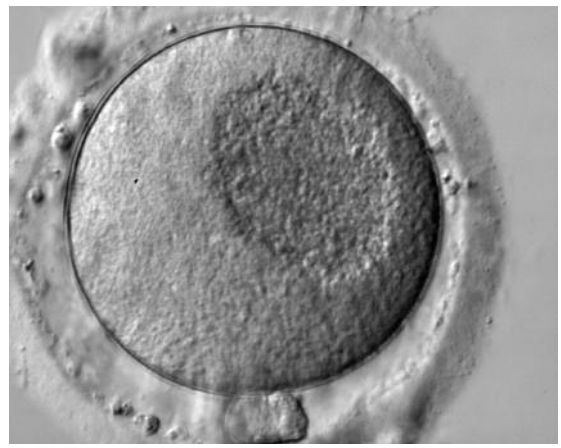

FIGURE 5.2 Oocyte with dense cytoplasmic granularity.

that the majority of the clinical trials examining the effect of dark granular cytoplasm as an individual feature showed no detrimental effect on the viability of the derived embryo [6,9–11], and even may be associated with higher fertilization when compared with the group of oocytes with total absence of granularity [13], controversial results were also published [7,8,12]. Variations published in these articles may be correlated with the subjectivity of the definition, because diffused slight cytoplasmic granularity, also called as dark cytoplasm, can be ill defined and could differ by different modulation of the optical path in phase contrast microscopies in various laboratories. Homogeneity of the cytoplasm is expected (Figure 5.1); however, the biological significance of nonhomogeneity is unknown, and based on current evidence, it may represent only variability between oocytes rather than a dysmorphism of developmental significance [1].

Centrally Located Granulation of the Cytoplasm

Condensed granulation that is centrally located within the cytoplasm with a clear border (Figure 5.2) is unlike various degrees of diffused granulation described above because it is easily distinguishable with a significantly darker appearance than normal cytoplasm that could be clearly visible by any modulation type of the optical path in different phase contrast microscopies. It had first been defined by Serhal et al. [14] with a detrimental effect on the outcome of intracytoplasmic sperm injection (ICSI), and was later named centrally located granular cytoplasm (CLCG) by Kahraman et al. [15]. It was indicated that CLCG is a rare morphological feature of the oocyte that is diagnosed as a large, dark, spongy, granular area in the cytoplasm and that the severity is based on both the diameter of granular area and the depth of the lesion.

Even though fertilization rate and embryo quality were not affected in the study by Kahraman et al. [15], poor ongoing pregnancy chance correlated with high aneuploidy (52.3%), and abortion rates (54.5%) were obtained by the transfer of embryos derived from oocytes with severe CLCG. A study by Meriano et al. [16] defined CLCG oocytes as organelle clustering and determined that this certain abnormality is the only repetitive dysmorphism in consecutive cycles and is a negative predictor of pregnancy and implantation rates in intracytoplasmic injection cycles. Even though more research is needed to define the subcellular and molecular mechanisms of organelle clustering, hypoxia of the follicle was shown to be correlated with oocytes of such poor developmental competence [17]. It has also been demonstrated that MII oocytes that exhibited severe cytoplasmic disorganization had a lower intracytoplasmic pH and ATP content as well as increased incidence of aneuploidy and chromosomal scattering [18,19], findings that were later confirmed by Kahraman et al. [15]. Yakin et al. [20] had also shown that the embryos that were derived from oocytes with severe cytoplasmic abnormalities where CLCG oocytes were included had a higher rate of aneuploidy (60.0%) compared with a group of embryos derived from oocytes with normal morphological appearance (41.9%). However, the results were not statistically different, most likely based on

the insufficient number of embryos included in the comparison. The same group demonstrated that cryopreserved Day 3 cleavage-stage embryos derived from oocytes with severe cytoplasmic abnormalities where CLCG oocytes consisted the majority of the experimental group had a significantly lower cryosurvival rate. Even if these embryos survived, they had lower rates of blastocyst formation, and none of the blastocysts obtained were of good quality or were able to successfully complete the hatching process [10]. Based on the evidence proof, it is important to inform patients about such morphological defects of the MII oocyte, and the reduced implantation outcome and increased risk of aneuploidy with the resultant embryos [1].

Refractile Bodies

Refractile bodies (Figures 5.3 and 5.4) are cytoplasmic inclusions that can be dark incorporations, fragments, spots, dense granules, lipid droplets, and lipofuscin. Transmission electron microscopy studies and Schmorl staining have shown that refractile bodies >5 μm in diameter showed the conventional morphology of lipofuscin inclusions that consisted of a mixture of lipids and dense granule materials [21]. Lipofuscin bodies in human oocytes can be detected throughout meiotic maturation (GV, germinal vesicle; MI, metaphase I; and MII), a situation that is different from that of other cytoplasmic abnormalities in humans, such as sERCs that appear only in mature MII-stage oocytes.

The average diameter of a recognizable refractile body under bright-field microscopy is approximately 10 μm [22]. In the majority of published articles, cytoplasmic abnormalities are examined jointly, whereas data on the individual predictive value of refractile bodies on clinical outcome are limited. According to some investigations, cytoplasmic inclusions did not appear to affect fertilization, embryo quality, and implantation rates [5,8]. Rienzi et al. [12] also showed that refractile bodies do not detrimentally affect fertilization and normal pronuclear morphology rates. In contrast, Xia [23] and Otsuki et al. [21] reported decreased fertilization and embryo development. It is most likely that controversial results might be correlated to the factors that are still unknown, and one possible confounding factor could be the differing diameters of refractile bodies. Only one study in the literature has examined precisely the relationship between the sizes of the refractile bodies and the developmental competence of oocytes, and this study found that lipofuscin inclusions were associated with reduced fertilization and unfavorable blastocyst development only when their diameter is >5 μm. This study also showed that the size of refractile bodies is not correlated with the age of the woman, or with different stimulation protocols, and that the embryo developmental outcome was not significantly affected by stimulation regimes [21]. According to the outcome found by Otsuki et al. [21], the aging of oocytes during inactive phases of oogenesis may not be involved with lipofuscinogenesis; instead, the accumulation of lipofuscin may occur during the growth phase

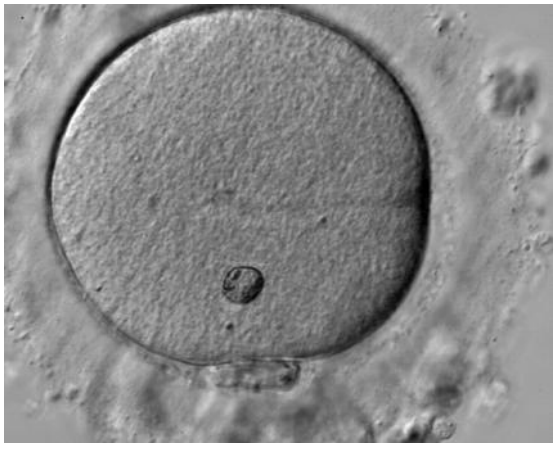

FIGURE 5.3 Presumably telophase I oocyte with dominant refractile body (15 μm).

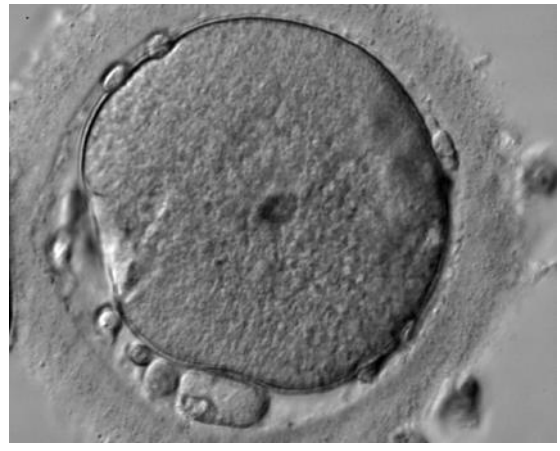

FIGURE 5.4 Oocyte with central refractile body and granule in the perivitelline space.

of the oocytes when dominant follicles are being recruited into the preovulatory pathway. The occurrence of large lipofuscin bodies in normal aging may also be related to conditions of the developing ovarian follicles, such as perifollicular blood circulation and follicular fluid composition. Other explanations may be related to oxidative stress [24], proteolytic degradation [25], or lipid metabolism as a source of energy supply [26]. Further research is needed to investigate whether any of these possibilities are involved in refractile bodies that are mainly correlated with lipofuscinogenesis in human oocytes.

Vacuoles

Vacuoles are membrane-bound cytoplasmic inclusions filled with fluid (Figure 5.5) that is virtually identical with perivitelline space (PVS) liquid [27]. Their sizes and numbers may vary, and it is assumed that vacuoles arise either spontaneously [27] or by fusion of preexisting vesicles derived from smooth endoplasmic reticulum (sER), Golgi apparatus, or both [28].

The incidence of vacuoles in MII oocytes varies from 3.1% [11] to 12.4% [29]. However multiple vacuolization is a less likely seen phenomenon, with approximately 1%–1.5% [6,7,30]. De Sutter et al. [6] reported a severely reduced fertilization rate in vacuolated oocytes (40%) compared with oocytes without any vacuoles. Ebner et al. [30] also reported a significantly decreased fertilization with oocytes containing single vacuoles (51.6%) and multiple vacuoles (43.8%) compared with oocytes without vacuoles (65.3%). Rienzi et al. [12] demonstrated significantly reduced fertilization rate for vacuolated oocytes; however, pronuclear morphology and embryo quality were not detrimentally affected. Only one study [30] had a subgroup analysis examining the effect of the size of the vacuoles on fertilization rates and found that the group of oocytes that fertilized normally contained vacuoles with diameters of <9.8 μm ± 3.7 μm, a value that was significantly smaller than the diameter of vacuoles that the unfertilized oocytes contained (17.6 μm ± 9.0 μm). A cutoff value of 14 μm for vacuole diameter was noted, above which fertilization did not occur. This study showed that a larger vacuole or multiple vacuoles may cause a much more detrimental effect to the oocyte than a small vacuole, because a larger portion of the cytoskeleton (e.g., microtubules) cannot function as it is supposed to function. Van Blerkom et al. [27] also suggested that large vacuoles might displace the MII spindle from its polar position and, in turn, result in fertilization failure, cleavage abnormalities, an abnormal cytokinesis pattern, or various combinations of these effects. Even though the presence of few small vacuoles (5 μm–10 μm in diameter) that are fluid filled but transparent are unlikely to be of biological consequence, observation of large vacuoles >14 μm in diameter should be noted [1]. Besides the deficiency on fertilization rates, it has also been shown that blastocyst formation, good quality, and hatching blastocyst rates can significantly decrease after ICSI of vacuolated oocytes. The percentage of aneuploid embryos can also be affected by the use of vacuolated oocytes (41.9%)

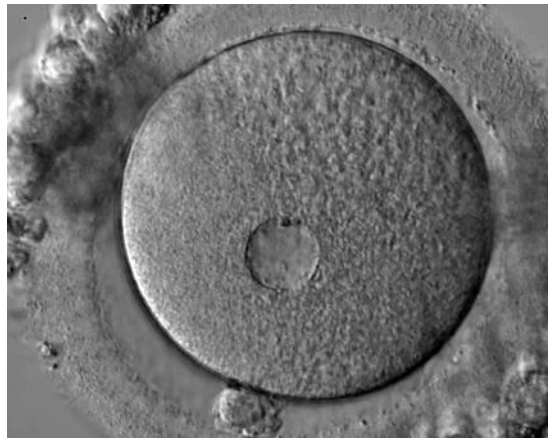

FIGURE 5.5 Vacuolized MII oocyte.

compared with embryos that are derived from oocytes with normal morphology (60.0%) [20]. Vacuolization in MII oocytes can also decrease cryosurvival rates and subsequent embryonic development of the derived cryopreserved embryos [10].

sER Clusters

The presence of sERCs in the cytoplasm of MII oocytes is one of the most important cytoplasmic defects and demands careful examination (Figure 5.6). A correlation between the presence of sERCs in MII oocytes and the clinical outcome was first published by Otsuki et al. [31]. They reported that in approximately 10% of the cycles, cytoplasmic localization of translucent vacuoles similarly sized as pronuclei exists at the MII stage of human oocytes after the denuding procedure for ICSI. This incidence was 5% for the study by Mateizel et al. [32], whereas it was 7% for the study by Braga et al. [33]. However, it is most likely that the number of oocytes with sERCs can be underestimated, because it has been shown by transmission electron microscopic analysis that there are at least three forms of sERCs: large (18 μm); medium (10 μm–17 μm), which can be classified by light microscopy; and small (2 μm–9 μm), which are not visible under the conditions used in clinical embryology laboratories for examination. sERCs can easily be distinguished from fluid-filled vacuoles because they are not separated from the rest of the ooplasmic volume by a membrane, and are seen as translucent vacuoles. Even though the mechanism responsible for sERCs is still unknown, there are some human and animal studies assuming that it could be correlated to some functional and structural alterations of the sER during oocyte maturation, such as an increase in the sensitivity of the IP3 receptor for Ca^{2+} [34], increased storage of Ca^{2+} that is released during oscillation [35], changes in the structure from a sheet-like form to a spherical form in starfish oocytes [36], and distribution of the sER in mouse oocytes [37]. In human oocytes, the localization of mobilizable Ca^{2+} was detected in the small vesicles beneath the plasma membrane of sER. Otsuki et al. [31] compared the clinical outcome of patients with oocytes containing sERCs and patients with retrieved oocytes without sERCs and examined whether any confounding parameters, such as stimulation methods and hormonal levels, can affect the outcome. Fertilization rate and embryo quality were not detrimentally affected; however, significantly lower clinical pregnancy and implantation and significantly higher biochemical pregnancy were observed for sERC-positive cycles. Due to the limited number of samples tested, no significant differences were found between the study groups when stimulation protocols were compared. However, the number of sERC-positive oocytes obtained by the short protocol was about three times larger than that by the long protocol. Serum estradiol levels on the day of hCG administration were significantly higher in sERC-positive cycles. This study had clearly shown that the viability of an embryo is significantly reduced with the presence of sERCs. Even though the embryo is derived from an oocyte without any clusters, its implantation potential

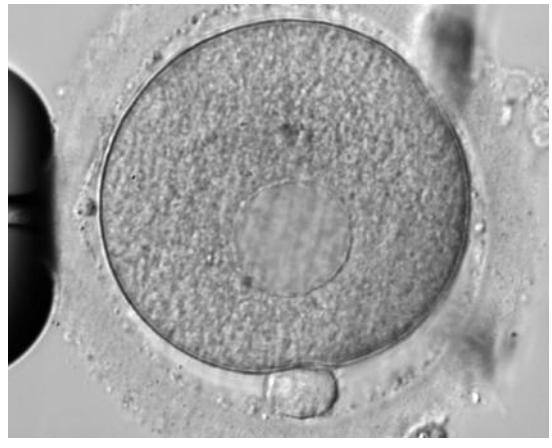

FIGURE 5.6 Oocyte with an aggregation of the smooth endoplasmic reticulum.

is detrimentally affected if the oocyte is from the cohort of oocytes where at least one oocyte is with clusters. Besides the viability of the derived embryos, the most important issue with the presence of sERCs had been the neonatal safety based on evidence proof in the literature. In the Otsuki study [31], only one pregnancy derived from gametes with sER defect has been reported at which the baby was diagnosed with Beckwith–Wiedemann syndrome.

Ebner et al. [38] showed that the occurrence of sERCs is significantly related with longer duration and higher dosage of the stimulation. Fertilization and blastocyst formation rate were significantly lower for oocytes with sERCs compared with oocytes without sERCs. Take-home baby rate was significantly lower in the group with sERCs and miscarriage rate was significantly higher in the same group of patients. Pregnancies in women with affected gametes had a significantly higher incidence of obstetric problems. Birth weight of babies born in the group with sERCs was significantly lower, and there were two unexplained neonatal deaths reported in the group with affected gametes, whereas there were no deaths reported in the group without sERCs. Malformation rate was similar in both groups, with one case of diaphragmatic hernia reported in the group with sERCs. Similar findings reported by Ebner [38] and Otsuki et al. [31] support the idea that this phenomenon is the manifestation of an intrinsic oocyte defect caused by a suboptimal ovarian stimulation [27], and perhaps as a result of overstimulation. Following other studies reporting multiple malformations [39] and ventricular septal defects [39] after the transfer of embryos originating from oocytes with sERCs, it was strongly recommended that oocytes with this feature should not be inseminated, and even that the sibling oocytes should be carefully examined [1]. However, a study [32] in which 394 sERC-positive cycles and 6845 sERC-negative cycles were retrospectively analyzed led the investigators to further research because this study reported that there was no difference in the rate of major malformations between sERC-positive cycles (5.3%) and sERC-negative cycles 82.1%). Three new borns, from single embryo transfer with frozen-thawed embryos originating from sERC-positive oocytes were delivered and presented no major malformations. Taking into account this controversial data on neonatal outcome, fate of babies born from oocytes with this feature should be very carefully evaluated and reported.

Extracytoplasmic Abnormalities

A variety of extracytoplasmic anomalies exist that in part negatively influence fertilization (consistency and thickness of the zona, Pb1 decay, and debris within the PVS), blastulation (thickness of zona, Pb1 fragmentation), and pregnancy (thickness of zona, Pb1 morphology, debris in PVS). Characteristics of the ZP and the PVS are most probably associated with the health of the developing follicle, for example, its vascularization and oxygen content. Any disturbance during growth might severely alter oocyte morphology, resulting in a pool of gametes with different prognoses.

Dysmorphic ZP

As a result of the mutual dependence between somatic cells (e.g., cumulus cells) and the egg, it is likely that any disturbance negatively affecting the follicle will have a comparable impact on the oocyte itself. Among the conceivable changes in oocyte performance, it is possible that the secretion or patterning of the ZP from the secondary follicle onward could be altered or interrupted [40,41]. This could either result in dysmorphism that can be seen under a light microscope (Figure 5.7) or in more subtle changes of the three-dimensional structure of the ZP.

Definitely, the most severe form of impaired growth of the ZP is its complete absence. Normally, up to four zona proteins [42,43] build up the three-dimensional matrix of the outer protective shell. Filaments are constructed of repeating zona protein (ZP) 2 and 3 units that are cross-linked by ZP1 [44], thus contributing to the structural integrity of the ZP. Experiments in mice lacking the ZP1 gene showed that secreting only ZP2 and ZP3 results in a thinner (Figure 5.8), more loosely organized ZP [45]. In contrast, disruption of ZP2 and ZP3 led to the absence of the a-cellular coat, resulting in infertility [46].

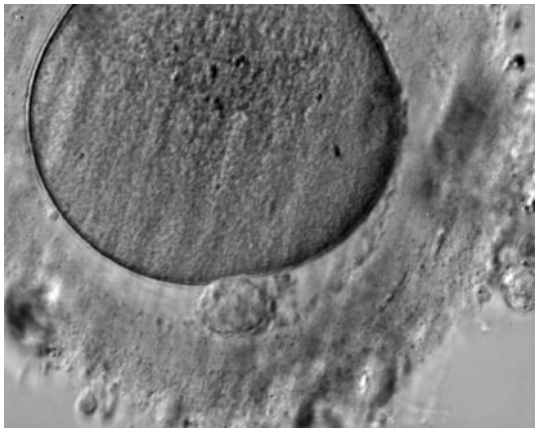

FIGURE 5.7 Extremely thick zona pellucida (>30 μm) at the 6 o'clock position.

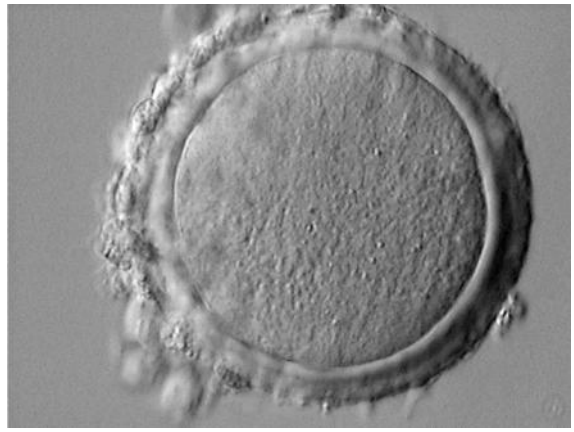

FIGURE 5.8 Immature oocyte showing extremely thin zona pellucida.

In humans, a defect in gene expression was shown to cause a failure in glycoprotein matrix, even though the ovum itself showed intact corona cells [47]. In such rare cases, the ovum fails to fertilize in conventional IVF. In ICSI, there is a considerable risk of exposing the gametes to mechanical stress during the denudation process. Studies [47,48] showed that in patients with zona-free eggs, pregnancies can be achieved by simply leaving the coronal cell layer attached, because it acts as a supporting structure keeping the oocyte in shape during injection.

From conventional IVF, it is known that thicker zonae (e.g., >20 μm) are associated with lower fertilization rates [49]. This has been linked to patient and stimulation parameters [50]. In ICSI, however, a thicker zona neither interferes with subsequent fertilization nor with implantation because assisted hatching can be applied.

The multilaminar structure of the ZP can also be analyzed quantitatively using polarized light microscopy [51]. Although variation exists in the thickness of zona layers around individual eggs and between members of a cohort, it is evident that the inner zona layer is the most dominant part of the zona [41,51]. It has been reported that the birefringence of the inner zona is directly proportional to its thickness [41,52,53].

Shen et al. [41] found an almost 30% higher mean light retardance in conception cycles compared with non-conception cycles, indicating that stimulated cycles may yield oocytes of affected quality. There are two retrospective studies that have suggested a relationship between ZP birefringence (inner layer) and preimplantation development. Montag et al. [53] noted a higher rate of good-quality embryos on Day 3 (but not on Day 2) in an oocyte group with high zona birefringence (41.7%) compared with a cohort with low birefringence (24.4%). Others [52] observed a difference in progression to the blastocyst stage. The lower the measured retardance, the lower the blastocyst formation (Figures 5.9 and 5.10).

Discoloration

Irrespective of the actual thickness of the ZP, ovarian stimulation sometimes generates gametes showing a ZP that appears dark or brownish under a light microscope (Figure 5.11). Mostly, the egg itself is affected. It is reported that the presence of a discolored ZP is a common phenomenon, at 9.5%–25.7% [6,9,29,54].

That said, it is not completely clear that dark or brown zonae/oocytes occur for the same reasons. These oocytes have been termed "brown eggs" because they were found to be dark with a thick ZP, a rather small PVS (sometimes filled with debris), and granular cytoplasm [11]. Esfandiari et al. [11] prospectively compared the

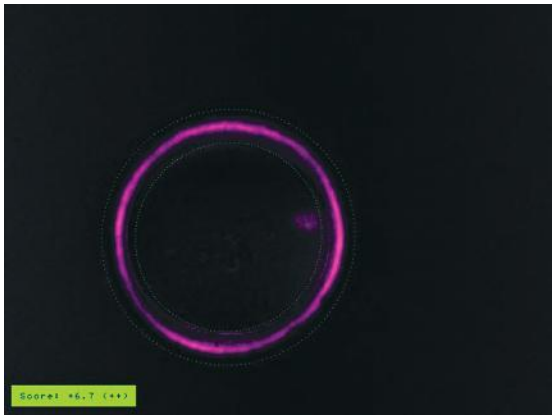

FIGURE 5.9 Zona imaging of oocyte with optimal zona pellucida and spindle with lower birefringence (3 o'clock position).

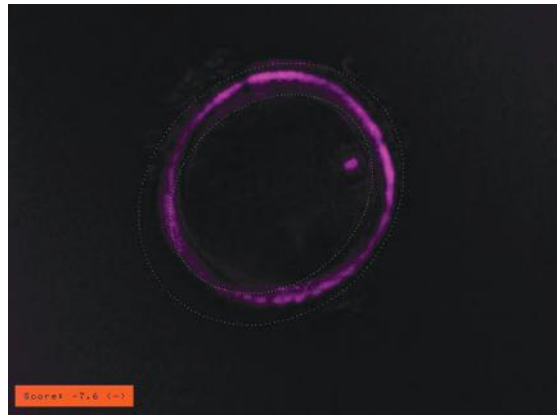

FIGURE 5.10 Zona imaging of oocyte with heterogeneous zona pellucida but optimal spindle (2 o'clock position).

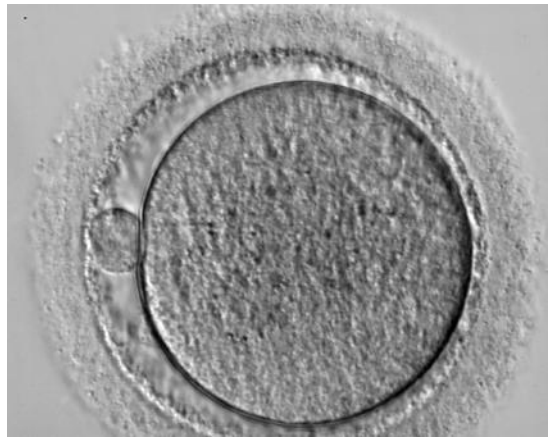

FIGURE 5.11 Brownish oocyte showing intact first polar body and perivitelline space granularity.

outcome of brown gametes with that of gametes of normal appearance. Although the zona in discolored eggs was thicker than that of control gametes, in conventional IVF the fertilization rate was similar. The same was true for the fertilization after ICSI, embryo quality, implantation rate, and clinical pregnancy rate. However, because of the thick zonae, brown oocytes were subjected to laser-assisted hatching significantly more often than the control group.

Shape Anomalies

Even if the thickness or color of the ZP is inconspicuous, it is not automatic that the shape of the gametes is spherical. Indeed, there is evidence that extremely ovoid eggs exist [55]. Such gametes have been shown to be fertilizable and may lead to the birth of a healthy baby. However, a major problem with these reports is that the degree of the shape anomaly was not quantified, and rather more imprecise descriptions have been given (e.g., cucumber shaped).

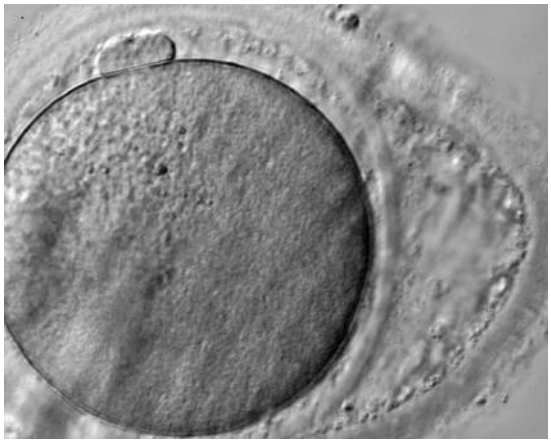

FIGURE 5.12 Spherically shaped oocyte with ovoid zona pellucida.

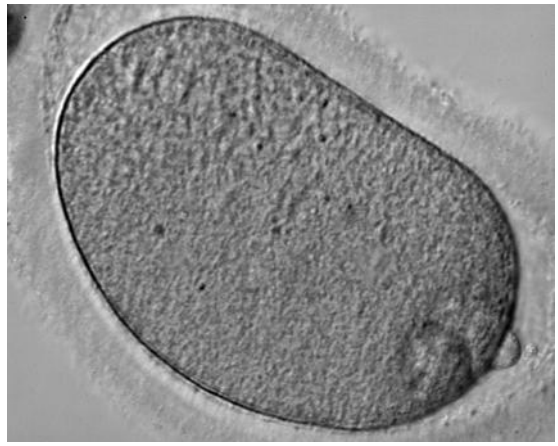

FIGURE 5.13 Ovoid oocyte with first polar body at 4 o'clock position (out of focus).

Our group successfully measured ovoid oocytes [56] and calculated a roundness index (RI, length divided by width). Actually, two indices were determined to assess whether the whole oocyte was affected (showing an ovoid ooplasm and zona) or only the ZP was of ovoid shape (with the ooplasm being perfectly round) (Figures 5.12 and 5.13). Special care was taken to detect splitting of the innermost zona layer that might keep ooplasm in a round shape (whereas the zona is ovoid). The latter dysmorphism was shown to be associated with implantation failure [41].

The degree of shape anomaly was neither correlated to fertilization nor embryo quality [57], and thus was in line with previous data [55]; interestingly, two types of cleavage pattern were observed on Day 2. Either ovoid gametes cleaved normally like a tetrahedron (a crosswise arrangement of four cells with three blastomeres lying side by side) or, if the ovoid zona failed to exert its shaping function, they resulted in a rather flat array of four blastomeres. Because the abnormal pattern reduces the number of cell-to-cell contact points from six to five or four, compaction and blastulation of the corresponding embryos may be delayed [56,58].

Two possible mechanisms may account for the occurrence of ovoid oocytes. First, mechanical stress during oocyte puncture, denudation processes, or both could deform the egg. This unwanted occurrence would create ovoid gametes with both ooplasm and zona being affected. In these artificially damaged gametes, a tendency toward recovery within a day has been suggested [56]. Thus, for the majority of ovoid ova, it can be assumed that the deformation is a preexisting anomaly generated during maturation within the follicle.

Perivitelline Space

The size of the PVS is closely related to the maturational phase of the oocyte. Whereas at the GV stage (prophase I) the expansion of PVS is minimal, it begins to increase after the resumption of meiosis. In detail, at MI, the PVS can clearly be detected, and after completion of maturation (MII) its full size is reached.

Several studies have noted that up to 50% of all ova show a large PVS [12,23]. In oocytes with a larger PVS (Figure 5.14), a lower fertilization rate was observed (67%) compared with gametes with a normally sized gap (85%) [23]. This is more or less in line with the results of an Italian group [12] who showed that a large PVS is detrimental to fertilization and zygote morphology. Interestingly, patient parameters such as female age and indication did not seem to influence PVS performance [23], but the ratio of estradiol to testosterone (and to progesterone) did [57].

Data from in vitro- and in vivo-matured oocytes indicate that a large PVS may be ascribed to overmature eggs [59,60]. Such eggs have shrunk in relation to the ZP, presenting a large gap between them. A large PVS

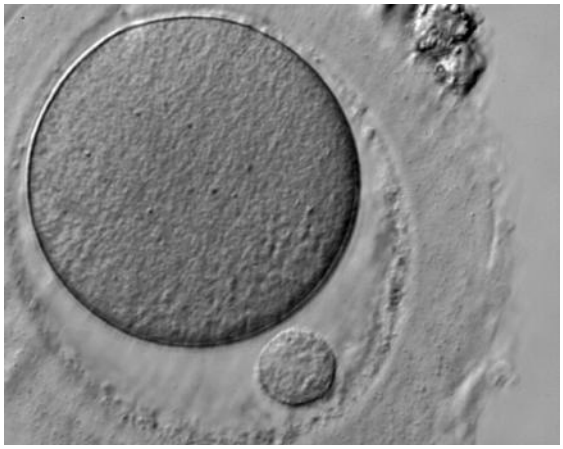

FIGURE 5.14 Metaphase II oocyte with large perivitelline space.

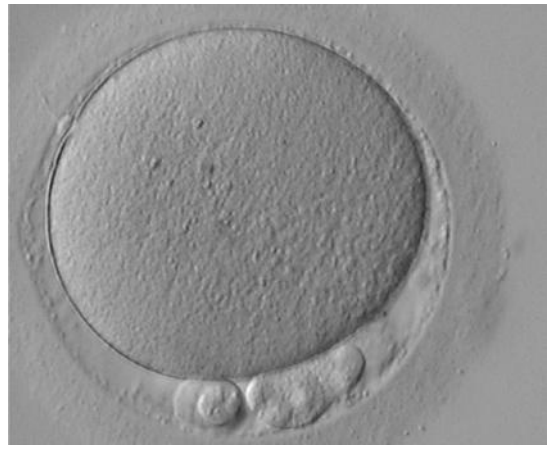

FIGURE 5.15 Oocyte with large fragmented first polar body.

would also occur if a larger portion of cytoplasm is extruded together with the haploid chromosomal set during first Pb formation. This would result in a large first Pb and a large PVS.

First Pb Morphology

For a long time, it was thought that Pb1 extrusion marks the completion of nuclear maturation ending in a MII oocyte. But by using polarized light microscopy, it has been demonstrated that some oocytes showing a Pb1 were actually in telophase I (Figure 5.3) and not in MII [61,62]. Otsuki et al. [63] found a chromosome aggregation phase that occurred not only from GV breakdown to MI but also from telophase I to MII. If ICSI is performed, although chromosomes are unaligned, it may result in failed fertilization or three pronuclear zygotes due to abnormal chromosomal segregation.

The impact of Pb1 morphology on outcome is still discussed controversially. Although some Pb1s in humans remain intact for >20 hr after ovulation (Figures 5.1, 5.6, and 5.14), they generally have a shorter lifetime [64]. Taking this time dependency into consideration, it might be hypothesized that Pb1 morphology provides adequate information on the actual postovulatory age of the corresponding egg [60].

Ebner et al. [54] tried to focus exclusively on the status of the Pb1. Ova showing an intact Pb1 gave rise to higher rates of implantation and pregnancy [65], probably due to an increase in blastocyst formation [66]. However, these data are still a matter of debate [12,54,66–70].

Apparently, the benefit of selecting oocytes according to the morphology of the Pb1 is somewhat reduced with increasing time span between ovulation induction and ICSI, because studies with different schedules could not find a relationship between constitution of the Pb1 and subsequent ICSI outcome [67,69,70]. In these data sets, the percentage of oocytes with fragmented Pbs (Figure 5.15) was higher [23,67,69,70] than that reported in the work of Ebner et al. [54] in which Pbs were scored 2 hr after collection. This is in line with the finding that of all intact Pb1, 13% were already fragmented at a second inspection 3 hr later [70]. For practical reasons and to minimize the risk of ovarian aging in vitro [33], ICSI should be finished within 42 hr post-ICSI [71].

Data from Hungary [69] suggest that a large Pb1 is the worst case (Figure 5.16). When large Pb1s were extruded, embryos with multinucleated blastomeres were significantly ($p < 0.001$) more frequent (26.7%) than in all other Pb1 classes (~8%). It has been postulated that the extrusion of an abnormally large Pb1 is due to dislocation of the meiotic spindle [72]. This would in part explain the observed impact on fertilization and embryo development [12,54,67].

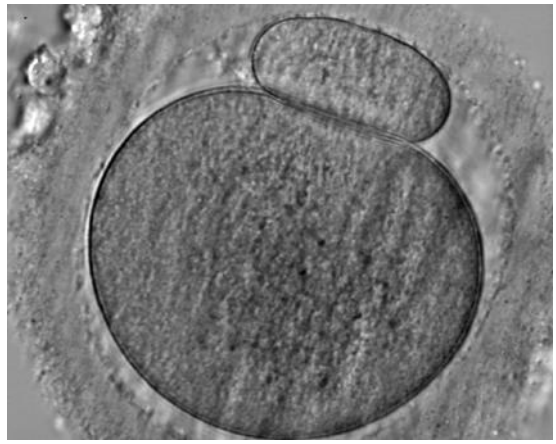

FIGURE 5.16 Oocyte with large first polar body.

Debris in the PVS

Sometimes, it is difficult to distinguish between heavily fragmented Pb1s and debris within the PVS (Figures 5.4 and 5.11). Two hypotheses have been proposed to explain the origin of the latter dysmorphism. One hypothesis is derived from ultrastructural data indicating the presence of an extracellular matrix comprised of granules and filaments in the space between oolemma and ZP because the matrix is identical to that found between cumulus cells and the corona radiata [73,74].

The second hypothesis is based on the existence of coronal cell processes passing the ZP and reaching the egg early in maturation. It is suggested that after withdrawal of these processes, some remnants remain within the PVS [75].

The findings of Hassan-Ali et al. [76] support the latter theory because they found a close relationship between the frequency of PVS granularity and maturation. In detail, they never detected debris in prophase I eggs, but they found debris in 4% of the MI and in 34.3% of MII gametes. They were also able to show that the presence of PVS granules was dependent on gonadotropin dose. If <30 ampoules were used to stimulate the patient, 17.4% of the eggs were positive for this anomaly compared with 45.4% in high-dose patients (>45 ampoules). Fertilization rate, cleavage rate, and embryo quality were found to be unaffected by the presence of coarse granules in the PVS [76,77]; however, rates of implantation and pregnancy seem to be affected [77], because transfer of embryos derived from PVS granule-free oocytes increased implantation rate by 5% and pregnancy rate by 21%.

Conclusions

The endpoint for evaluating morphological abnormalities of MII oocytes is to be able to correlate them with oocyte quality and viability and in correlation increase the overall efficiency of human-assisted reproduction in terms of clinical success and safety of offspring. High heterogeneity of the published material and subjectivity of the evaluation of morphological deviations of MII oocytes may provide only limited take-home messages on the predictive value of outcome parameters for successful results. A meta-analysis [78] examining the clinical results of 40 relevant articles on previously described extracytoplasmic and cytoplasmic abnormalities showed that there was no clear tendency to a general increase in predictive value of morphological features and that these contradicting findings underline the importance of more intensive and coordinated research that could lead to objective criteria with better predictive value to determine the viability of derived embryos. Rapidly developing continuous research on new biomarkers of oocyte quality may perhaps be used in addition or as

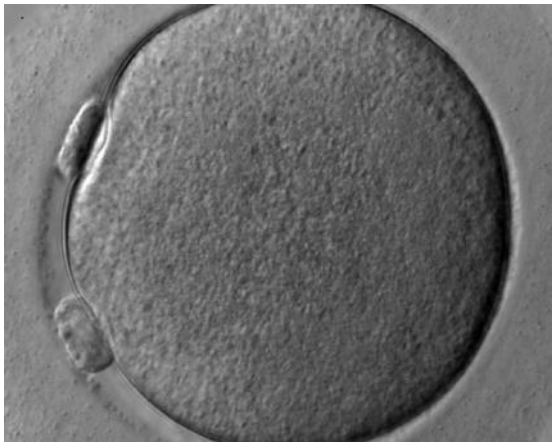

FIGURE 5.17 Diploid giant MII oocyte showing two first polar bodies.

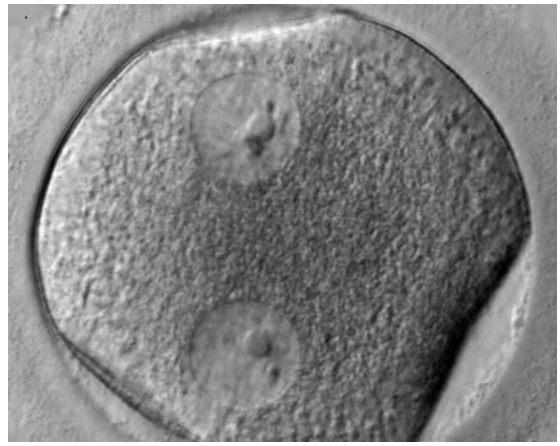

FIGURE 5.18 Diploid prophase I oocyte showing two germinal vesicles.

an alternative to morphological assessment in the future; however, current, limited, predictive value of morphology should not be underestimated considering that it still remains the sole method of choice for selection until a more effective technology can substitute for it in routine practice in various clinical IVF laboratories worldwide. Beyond the predictive value of oocyte morphology, it must not be forgotten that information linking dysmorphism with genetic disorders is of great value and scarce because these disorders are directly correlated with the health of the offspring in ART applications [79]. According to a common hypothesis [5], the majority of extracytoplasmic anomalies occur late in maturation because they are associated with fertilization and developmental failure rather than with aneuploidy (e.g., giant eggs). However, evidence-based data clearly demonstrate that some specific severe cytoplasmic defects are correlated with chromosomal aneuploidy and genetic disorders as described above. It is obvious that some anomalies, for example, the so-called giant eggs [80,81] with an almost double-sized diameter (Figures 5.17 and 5.18), show a diploid chromosomal set that contributes to digynic triploidy. Other studies [82] analyzed embryos genetically according to their Pb classes. No correlation was observed between Pb shape and genetic constitution; however, the only Pb group bearing a theoretical risk of chromosomal disorder, considering the larger volume of ooplasm in large polar bodies (Figure 5.16), was not analyzed.

REFERENCES

1. ALPHA Scientists in Reproductive Medicine, ESHRE Special Interest Group of Embryology. Istanbul consensus workshop on embryo assessment: Proceedings of an expert meeting. *Reprod Biomed Online* 2011;22:632–646.
2. Rienzi L, Balaban B, Ebner T, Mandelbaum J. The oocyte. *Hum Reprod* 2012;27:i2–i21.
3. Balaban B, Urman B. Effect of oocyte morphology on embryo development and implantation. *Reprod Biomed Online* 2006;12:608–615.
4. Ebner T. Is oocyte morphology prognostic of embryo developmental potential after ICSI? *Reprod Biomed Online* 2006;12:507–512.
5. Van Blerkom J, Henry G. Oocyte dysmorphism and aneuploidy in meiotically mature human oocytes after ovarian stimulation. *Hum Reprod* 1992;7:379–390.
6. De Sutter P, Dozortsev D, Qian C, et al. Oocyte morphology does not correlate with fertilization rate and embryo quality after intracytoplasmic sperm injection. *Hum Reprod* 1996;11:595–597.
7. Loutradis D, Drakakis P, Kallianidis K, et al. Oocyte morphology correlated with embryo quality and pregnancy rates after intracytoplasmic sperm injection. *Fertil Steril* 1999;72:240–244.
8. Ten J, Mendiola J, Vioque J, de Juan J, Bernabeu R. Donor oocyte dysmorphisms and their influence on fertilization and embryo quality. *Reprod Biomed Online* 2007;14:40–48.

9. Balaban B, Urman B, Sertac A, et al. Oocyte morphology does not affect fertilization rate, embryo quality and implantation rate after intracytoplasmic sperm injection. *Reprod Biomed Online* 1998;13:3431–3433.
10. Balaban B, Ata B, Isiklar A, et al. Severe cytoplasmic abnormalities of the oocyte decrease cryosurvival and subsequent embryonic development of cryopreserved embryos. *Hum Reprod* 2008;23:1778–1785.
11. Esfandiari N, Burjaq H, Gotlieb L, et al. Brown oocytes: Implications for assisted reproductive technology. *Fertil Steril* 2006;86:1522–1525.
12. Rienzi L, Ubaldi FM, Lacobelli M, et al. Significance of metaphase II human oocyte morphology on ICSI outcome. *Fertil Steril* 2008;90:1692–1700.
13. Wilding M, Di ML, D'Andretti S, et al. An oocyte score for use in assisted reproduction. *J Assist Reprod Biomed Online* 2007;24:350–358.
14. Serhal PF, Ranieri DM, Kinis A, et al. Oocyte morphology predicts outcome of intracytoplasmic sperm injection. *Hum Reprod* 1997;12:1267–1270.
15. Kahraman S, Yakin K, Donmez E, et al. Relationship between granular cytoplasm of oocytes and pregnancy outcome following intracytoplasmic sperm injection. *Hum Reprod* 2000;15:2390–2393.
16. Meriano JM, Alexis J, Visram–Zaver S, et al. Tracking of oocyte dysmorphisms for ICSI patients may prove relvant to the outcome in subsequent patient cycles. *Hum Reprod* 2001;16:2118–2123.
17. Van Blerkom J, Antczak M, Schrader R. The developmental potential of the human oocyte is related to the dissolved oxygen content of follicular fluid: Association with vascular endothelial growth factor levels and perifollicular blood flow characteristics. *Hum Reprod* 1997;12:1047–1055.
18. Van Blerkom J, Davis PW, Lee J. ATP content of human oocytes and developmental potential and outcome after in vitro fertilization and embryo transfer. *Hum Reprod* 1995;10:1047–1055.
19. Van Blerkom J. The influence of intrinsic and extrinsic factors on the developmental potential and chromosomal normality of the human oocyte. *J Soc Gynecol Invest* 1996;3:3–11.
20. Yakin K, Balaban B, Isiklar A, et al. Oocyte dysmorphism is not associated with aneuploidy in the developing embryo. *Fertil Steril* 2006;88:811–816.
21. Otsuki J, Nagai Y, Chiba K. Lipofuscin bodies in human oocytes as an indicator of oocyte quality. *J Assist Reprod Genet* 2007;24:263–270.
22. Veeck LL. *Atlas of the Human Oocyte and Early Conceptus*. Baltimore: Williams & Wilkins, 1991, pp. 121–166.
23. Xia P. Intracytoplasmic sperm injection. Correlation of oocyte grade based on polar body, perivitelline space and cytoplasmic inclusions with fertilization rate and embryo quality. *Hum Reprod* 1997;12:1750–1755.
24. Marzabadi MR, Sohal RS, Brunk UT. Mechanisms of lipofuscinogenesis: Effect of the inhibition of lysosomal proteinases and lipases under varying concentrations of ambient oxygen in cultured rat neonatal myocardial cells. *APMIS* 1991;99:416–426.
25. Iyy GO, Roopsingh R, Kanai S, et al. Leupeptin causes an accumulation of lipofuscin–like substances and other signs of aging in kidneys of young rats: Further evidence for the protease inhibitor model of aging. *Ann N Y Acad Sci* 1996;786:12–23.
26. Mitchell M, Armstrong DT, Robker RL, et al. Adipokines: Implications for female fertility and obesity. *Reproduction* 2005;130:583–597.
27. Van Blerkom J. Occurrence and developmental consequences of aberrant cellular organization in meiotically mature human oocytes after exogenous ovarian hyperstimulation. *J Electron Microsc Tech* 1990;16:324–346.
28. El Shafie M, Sousa M, Windt ML, et al. Ultrastructure of human oocytes: A transmission electron microscopic view. In: *An Atlas of the Ultrastructure of Human Oocytes. A Guide for Assisted Reproduction*. New York: Partheon Publishing, 2000, pp. 151–171.
29. Alikani M, Palermo G, Adler A, et al. Intracytoplasmic sperm injection in dysmorphic human oocytes. *Zygote* 1995;3:283–288.
30. Ebner T, Moser M, Sommergruber M, et al. Occurrence and developmental consequences of vacuoles throughout preimplantation development. *Fertil Steril* 2005;83:1635–1640.
31. Otsuki J, Okada A, Morimoto K, et al. The relationship between pregnancy outcome and smooth endoplasmic reticulum clusters in MII human oocytes. *Hum Reprod* 2004;7:1591–1597.
32. Mateizel I, Van Landuyt L, Tournaye H, et al. Deliveries of normal healthy babies from embryos originating from oocytes showing the presence of smooth endoplasmic reticulum clusters. *Hum Reprod* 2013.
33. Braga D, Setti A, Cassia R, et al. Influence of oocyte dysmorphisms on blastocyst formation. *Fertil Steril* 2013;100:748–754.

34. Goud PT, Goud AP, Van Oostveldt P, et al. Presence and dynamic redistribution of type I inositol 1,4,5–trisphosphate receptors in human oocytes and embryos during in-vitro maturation, fertilization and early cleavage divisions. *Mol Hum Reprod* 1999;5:441–451.
35. Carroll J, Jones KT, Whittingham DG. Ca^{2+} release and the development of Ca^{2+} release mechanisms during oocyte maturation: A prelude to fertilization. *Rev Reprod* 1996;1:137–143.
36. Jaffe LA, Tesaraki M. Structural changes in the endoplasmic reticulum of starfish oocytes during meiotic maturation and fertilization. *Dev Biol* 1994;164:579–587.
37. Mehlmann LM, Terasaki M, Jaffe LA, et al. Reorganization of the endoplasmic reticulum during meiotic maturation of the mouse oocyte. *Dev Biol* 1995;170:607–615.
38. Ebner T. Prognosis of oocytes showing aggregation of smooth endoplasmic reticulum. *Reprod Biomed Online* 2008;16:113–118.
39. Akarsu C, Caglar G, Vicdan K, et al. Smooth endoplasmic reticulum aggregations in all retrieved oocytes causing recurrent multiple anomalies: Case report. *Fertil Steril* 2009;92:1496e1–1496e3.
40. Epifano O, Liang LF, Familari M, et al. Coordinate expression of the three zona pellucida genes during mouse oogenesis. *Development* 1995;121:1947–1956.
41. Shen Y, Stalf T, Mehnert C, et al. High magnitude of light retardation by the zona pellucida is associated with conception cycles. *Hum Reprod* 2005;20:1596–1606.
42. Hughes DC, Barratt CLR. Identification of the true human orthologue of the mouse ZP1 gene: Evidence for greater complexity in the mammalian zona pellucida? *Biochem Biophys Acta* 1999;1447:303–306.
43. Lefiévre L, Conner SJ, Salpekar A, et al. Four zona pellucida glycoproteins are expressed in the human. *Hum Reprod* 2004;19:1580–1586.
44. Wassarman PM. Zona pellucida glycoproteins. *Ann Rev Biochem* 1998;57:415–442.
45. Rankin T, Talbot P, Lee E, et al. Abnormal zonae pellucida in mice lacking ZP1 results in early embryonic loss. *Development* 1999;126:3847–3855.
46. Liu C, Litscher ES, Mortillo S, et al. Targeted disruption of the mZP3 genes results in production of eggs lacking the zona pellucida and infertility in female mice. *Proc Natl Acad Sci USA* 1996;93:5431–5436.
47. Stanger JD, Stevenson K, Lakmaker A, et al. Pregnancy following fertilization of zona-free, coronal cell intact human ova. *Hum Reprod* 2001;16:164–167.
48. Ding J, Rana N, Dmowski WP. Intracytoplasmic sperm injection into zona-free human oocytes results in normal fertilization and blastocyst development. *Hum Reprod* 1999;14:476–478.
49. Bertrand E, Van den Bergh M, Englert Y. Does zona pellucida thickness influence the fertilization rate? *Hum Reprod* 1995;10:1189–1193.
50. Loret de Mola JR, Garside WT, Bussi J, et al. Analysis of the human zona pellucida during culture: Correlation with diagnosis and the preovulatory hormonal environment. *J Assist Reprod Genet* 1997;14:332–336.
51. Pelletier C, Keefe D, Trimarchi JR. Noninvasive polarized light microscopy quantitatively distinguishes the multilaminar structure of the zona pellucida of living human eggs and embryos. *Fertil Steril* 2004;81:850–856.
52. Rama Raju GA, Prakash GJ, Krishna KM, Madan K. Meiotic spindle and zona pellucida characteristics as predictors of embryonic development: A preliminary study using PolScope imaging. *Reprod Biomed Online* 2007;14:166–174.
53. Montag M, Schimming T, Zhou C. Validation of an automatic scoring system for prognostic qualitative zona imaging in human oocytes. *Hum Reprod* 2007;22(Suppl 1):i11.
54. Ebner T, Yaman C, Moser M, et al. Prognostic value of first polar body morphology on fertilization rate and embryo quality in intracytoplasmic sperm injection. *Hum Reprod* 2000;15:427–430.
55. Esfandiari N, Ryan EAJ, Gotlieb L, Casper RF. Successful pregnancy following transfer of embryos from oocytes with abnormal zona pellucida and cytoplasm morphology. *Reprod Biomed Online* 2005;11:620–623.
56. Ebner T, Shebl O, Moser M, et al. Developmental fate of ovoid oocytes. *Hum Reprod* 2008;23:62–66.
57. Xia P, Younglai EV. Relationship between steroid concentrations in ovarian follicular fluid and oocyte morphology in patients undergoing intracytoplasmic sperm injection (ICSI) treatment. *J Reprod Fertil* 2000;118:229–233.
58. Suzuki H, Togashi M, Adachi J, et al. Developmental ability of zona-free mouse embryos is influenced by cell association at the 4-cell stage. *Biol Reprod* 1995;53:78–83.
59. Mikkelsen AL, Lindenberg S. Morphology of in-vitro matured oocytes: Impact on fertility potential and embryo quality. *Hum Reprod* 2001;16:1714–1718.

60. Miao YL, Kikuchi K, Sun QY. Oocyte aging: Cellular and molecular changes, developmental potential and reversal possibility. *Hum Reprod Update* 2009;15:573–585.
61. Eichenlaub–Ritter U, Shen Y, Tinneberg HR. Manipulation of the oocyte: Possible damage to the spindle apparatus. *Reprod Biomed Online* 2002;5:117–124.
62. Montag M, Schimming T, Van der Ven H. Spindle imaging in human oocytes: The impact of the meiotic cell cycle. *Reprod Biomed Online* 2006;12:442–446.
63. Otsuki J, Nagai Y. A phase of chromosome aggregation during meiosis in human oocytes. *Reprod Biomed Online* 2007;15:191–197.
64. Ortiz ME, Lucero P, Croxatto HB. Postovulatory aging of human ova: II—Spontaneous division of the first polar body. *Gamete Res* 1983;7:269–276.
65. Ebner T, Moser M, Yaman C, et al. Elective transfer of embryos selected on the basis of first polar body morphology is associated with increased rates of implantation and pregnancy. *Fertil Steril* 1999;72:599–603.
66. Ebner T, Moser M, Sommergruber M, et al. First polar body morphology and blastocyst formation rate in ICSI patients. *Hum Reprod* 2002;17:2415–2418.
67. De Santis L, Cino I, Rabellotti R, et al. Polar body morphology and spindle imaging as predictors of oocyte quality. *Reprod Biomed Online* 2005;11:36–42.
68. Younis JS, Radin O, Mirsky N, et al. First polar body and nuclear precursor body morphology is related to the ovarian reserve of infertile women. *Reprod Biomed Online* 2008;16:851–858.
69. Fancsovits P, Tothne Z, Murber A, et al. Correlation between first polar body morphology and further embryo development. *Acta Biol Hung* 2006;57:331–338.
70. Ciotti PM, Notarangelo L, Morselli–Labate AM, et al. First polar body morphology before ICSI is not related to embryo quality or pregnancy rate. *Hum Reprod* 2004;19:2334–2339.
71. Van de Velde H, De Vos A, Joris H, et al. Effect of timing of oocyte denudation and microinjection on survival, fertilization and embryo quality after intracytoplasmic sperm injection. *Hum Reprod* 1998;13:3160–3164.
72. Verlhac MH, Lefebvre C, Guillaud P, et al. Asymmetric division in mouse oocytes: With or without MOS. *Curr Biol* 2000;10:1303–1306.
73. Dandekar P, Talbot P. Perivitelline space of mammalian oocytes: Extracellular matrix of unfertilized oocytes and formation of a cortical granule envelope following fertilization. *Mol Reprod Dev* 1992;31:135–143.
74. Dandekar P, Aggeler J, Talbot P. Structure, distribution and composition of the extracellular matrix of human oocytes and cumulus masses. *Hum Reprod* 1992;7:391–398.
75. Sathanathan H. Ultrastructure of the human egg. *Hum Cell* 1997;10:21–38.
76. Hassan-Ali H, Hisham-Saleh A, El-Gezeiry D, et al. Perivitelline space granularity: A sign of human menopausal gonadotropin overdose in intracytoplasmic sperm injection. *Hum Reprod* 1998;13:3425–3430.
77. Farhi J, Nahum H, Weissman A, et al. Coarse granulation in the perivitelline space and IVF–ICSI outcome. *J Assist Reprod Genet* 2002;19:545–549.
78. Rienzi L, Gajta G, Ubaldi F. Predictive value of oocyte morphology in human IVF: A systematic review of the literature. *Hum Reprod Update* 2011;17:34–45.
79. Sa R, Cunha M, Silva J, et al. Ultrastructure of tubular smooth endoplasmic reticulum aggregates in human metaphase II oocytes and clinical implications. *Fertil Steril* 2011;96:143–149.
80. Rosenbusch B, Schneider M, Gläser B, et al. Cytogenetic analysis of giant oocytes and zygotes to assess their relevance for the development of digynic triploidy. *Hum Reprod* 2002;17:2388–2393.
81. Balakier H, Bouman D, Sojecki A, et al. Morphological and cytogenetic analysis of human giant oocytes and giant embryos. *Hum Reprod* 2002;17:2394–2401.
82. Verlinsky Y, Lerner S, Illkevitch N, et al. Is there any predictive value of first polar body morphology for embryo genotype or developmental potential? *Reprod Biomed Online* 2003;7:336–341.

6

Morphological Selection of Gametes and Embryos: 2PN/Zygote

Martin Greuner and Markus Montag

Introduction

The question of the start of life is as old as life itself and nobody can really answer it.

> Life is the search from nothing for something.
>
> **— Christian Morgenstern**

The pronuclear (PN)-stage embryo is the first stage of life where the genetic material of both female and male is visible as pronuclei and when fertilization is initiated. Although it is possible to judge the morphology of the oocyte and the spermatozoa by itself, the PN stage is the first event that allows for morphology rating of the new life by various small details that are indicative for the future of the embryo.

> The basis of all is small. "*Omnia rerum principia parva sunt*."
>
> **— Marcus Tullius Cicero (106–43 BCE)**

There are numerous possibilities for noninvasive markers to evaluate the developmental potential of an embryo, but studies on transcriptomics [1], proteomics [2], and metabolomics [3] are still largely experimental. Thus, light microscopic morphological examination of the cells is still the most common routine in the laboratory for examining development from the oocyte to the embryo.

The challenge is that in the in vitro fertilization (IFV) program, only about 10% of the collected oocytes have the potential to develop into an embryo that can implant [4,5]. About 50%–70% [6] of the oocytes are aneuploid [7], and about 70% of the embryos, 44 hr after fertilization, present aneuploid blastomeres [8]. With reference to the success or failure of an assisted reproductive technique (ART) therapy, selection based on microscopic evaluation of morphology is essentially still the preferred method and essential.

After ovulation or ovum pick-up in therapy, the human oocyte has to be arrested in the second meiotic division (metaphase-II), usually characterized by the presence of a first polar body. The entry or the injection of the sperm into the oocyte initiates the biochemical activation of the oocyte by a sperm-specific protein called phospholipase C zeta [9,10] and leads to a change in the membrane potential, a rise of the intracellular Ca^{2+} level [10], and the second meiotic division. The second polar body containing the chromatids from one haploid chromosome set is extruded, and the female pronucleus is formed (Figure 6.1). During this process, the ooplasm rotates in a periodical way, and in parallel the sperm chromatin decondensates. The sperm cell also delivers the centriole that has a leading role in further development and control of microtubules that are important for the symmetry of the developing embryo [11]. These microtubules pull the haploid female pronucleus toward the male pronucleus. Both pronuclei finally migrate to the center of the cell and align [12–14]. Microtubules also mediate the organization of a mitochondrial clustering to the center of the cell in the area around the pronuclei. This could be the result of the different metabolic needs of the new life. The mitochondria are where ATP generation takes place, thus they are essential for further embryo development [13,15].

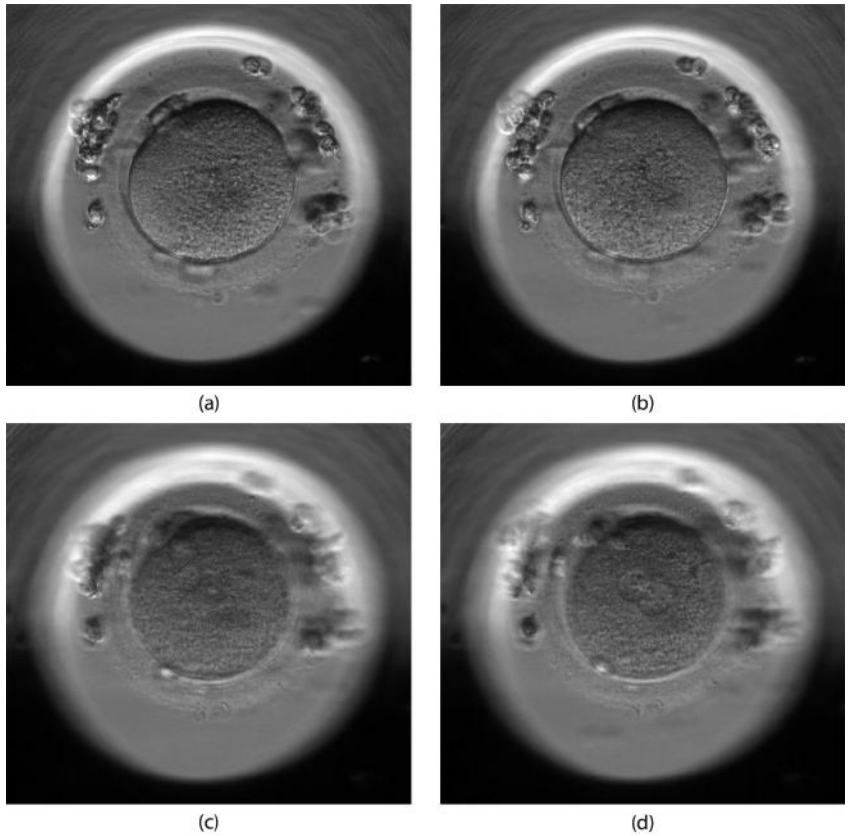

FIGURE 6.1 Time-lapse sequence showing the course of polar body extrusion. (a) 2.3 hr post-ICSI (pI). (b) 3.6 hr pI. (c) 6.7 hr pI. First appearance of pronuclei in the periphery. (d) 11.3 hr pI. Centralization of the pronuclei.

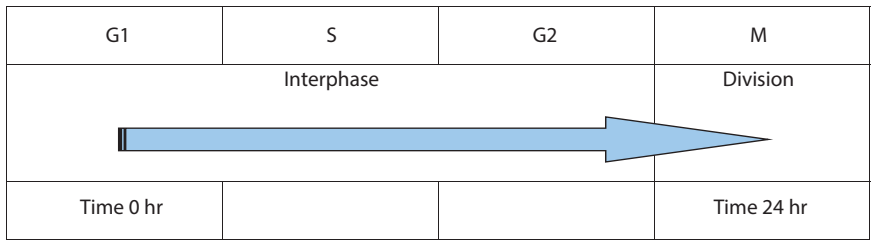

FIGURE 6.2 Cell cycle of an eukaryotic cell is divided into four stages. (From Alberts B et al., *Molekularbiologie der Zelle,* Zweite Auflage VCH Verlagsgesellschaft, Weinheim, 1990.)

The G1 phase starts approximately 2–3 hr after sperm entry, and pronuclei appear after 4–6 hr. This process is finished 18–22 hr after sperm entry or injection. Figure 6.2 [16] illustrates this cell cycle of an eukaryotic cell. A routine microscopic morphological examination [17–19] of the pronuclei is performed 16–18 hr after sperm entry. The judgment is done with reference to the number, size, and the symmetry of the pronuclei. Nuclear precursor bodies are formed in the pronuclei and constitute the nucleoli. Nucleoli are where pre-rRNA synthesis takes place. The symmetry and synchrony of the nuclear precursor bodies in the pronuclei can be used to evaluate the potential of the developing embryo [20–22].

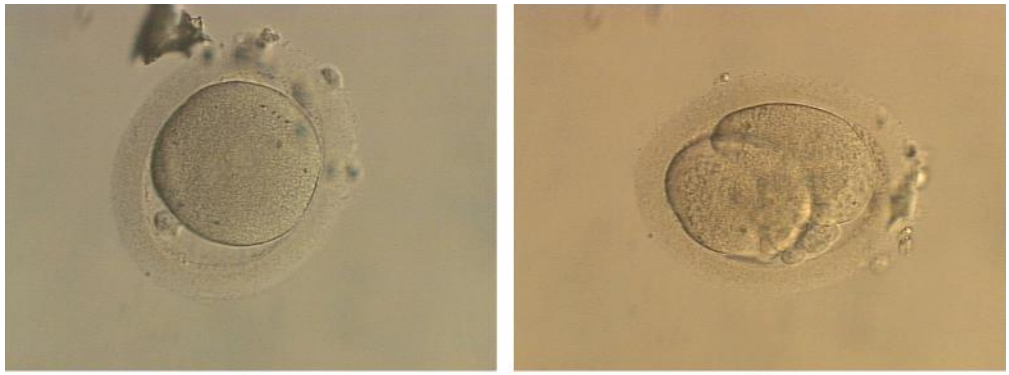

FIGURE 6.3 The pronuclear membrane breakdown (a) and early cleavage (b).

Anomalies in the cytoplasm of the PN-stage oocyte, such as vacuoles and refractile bodies, can negatively influence development of the embryo [23–25]. The appearance of a peripheral cytoplasmic translucency is seen in the majority of PN-stage oocytes and is discussed in the literature as another potential marker [14,26,27]. These criteria are most commonly used to evaluate the PN-stage oocyte.

The identical reduplication of the haploid chromosome set of each pronuclei takes place in the S phase within 6 hr after the G1 phase, followed by the onset of PN membrane breakdown and syngamy. With the fusion of the male and female genetic material, the fertilization cascade is finished, and embryo development starts by cellular division cycles. Figure 6.3 demonstrates this fusion and the start of the cellular division cycle.

The PN-stage judgment comprises (1) number of pronuclei; (2) size of pronuclei; (3) number, size, and distribution of nucleoli; (4) cytoplasmic halo; and (5) recommendations.

Number of Pronuclei

The occurrence of the pronuclei signals the initiation of the fertilization cascade. The number of pronuclei is an important indicator for aneuploidy. A normal fertilized cell presents with two centrally positioned, juxtaposed pronuclei.

A regular fertilized oocyte shows, in general, two pronuclei.

Existence and Number of Pronuclei

One day after oocyte retrieval (16–18 hr after sperm injection), it is possible to examine the pronuclei. Not all cells exhibit two pronuclei; there is the possibility of the appearance of only one or three and more pronuclei (Figure 6.4).

The judgment of the number of pronuclei is not always simple due to the three-dimensional spherical structure, with pronuclei being located somewhere inside this structure. To determine exactly the number and position of pronuclei, it is important to use a suitable optical mode, such as the Hoffmann modulation contrast optic, at a sufficiently high magnification (e.g., 40× objective). A simple stereomicroscope does not give sufficient resolution. Sometimes, it is very important to rotate the oocyte to identify pronuclei that are positioned above one another. Figure 6.5 illustrates this problem, where two pronuclei are positioned exactly above each other so that it looks like one PN cell. The same problem could appear by looking at a cell with three pronuclei (Figure 6.6). Depending on the orientation, such a cell could be judged as normal when looked at just once without turning.

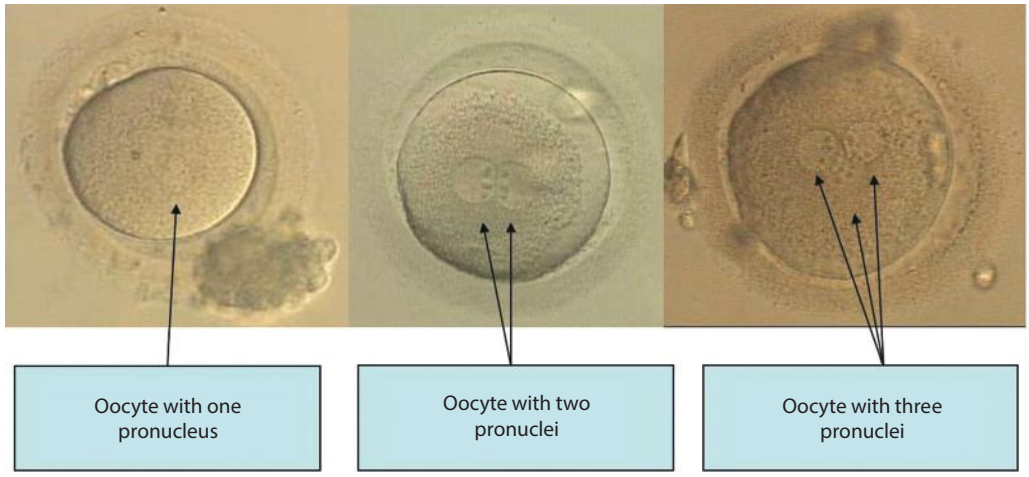

FIGURE 6.4 Oocyte with one, two, and three pronuclei.

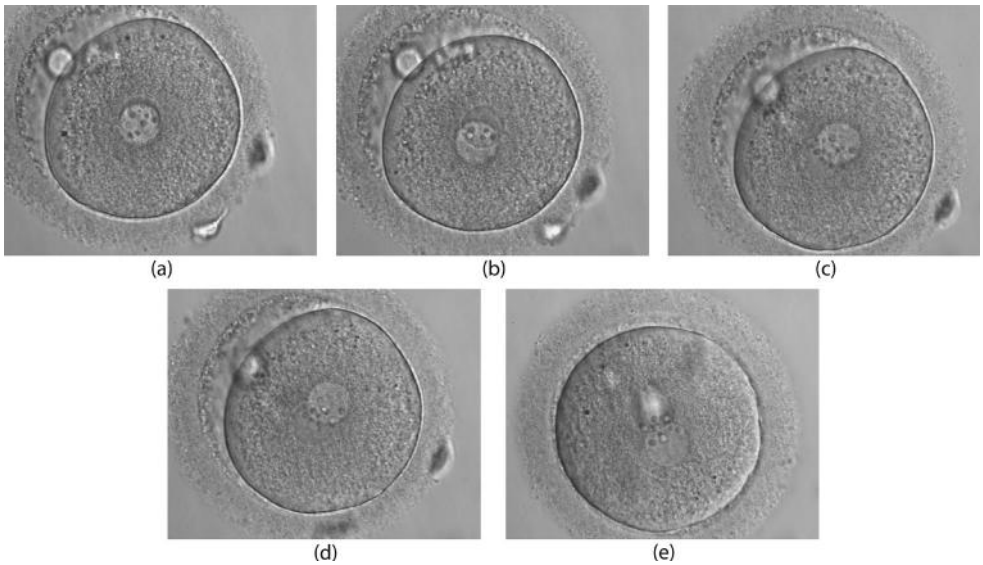

FIGURE 6.5 One cell seen in different positions, illustrating the difficulty in identifying the number of pronuclei. (a) This could be a cell with one pronucleus. (b-e) Rotation reveals the presence and position of two pronuclei.

Oocytes with One Pronucleus

An oocyte exhibiting 1PN has to be judged in a different way. Time-lapse sequences can show the development from PN appearance up to fusion. This allows identification of whether pronuclei appear in asynchrony or whether one pronucleus disappears earlier than the other pronucleus or whether pronuclei fuse prematurely. Also, cells that develop from the beginning with only one pronucleus can clearly be identified. Looking only once may not enable a correct judgment, and the potential of 1PN-stage oocytes depends on the fertilization method that determines, for example, the risk of aneuploidy.

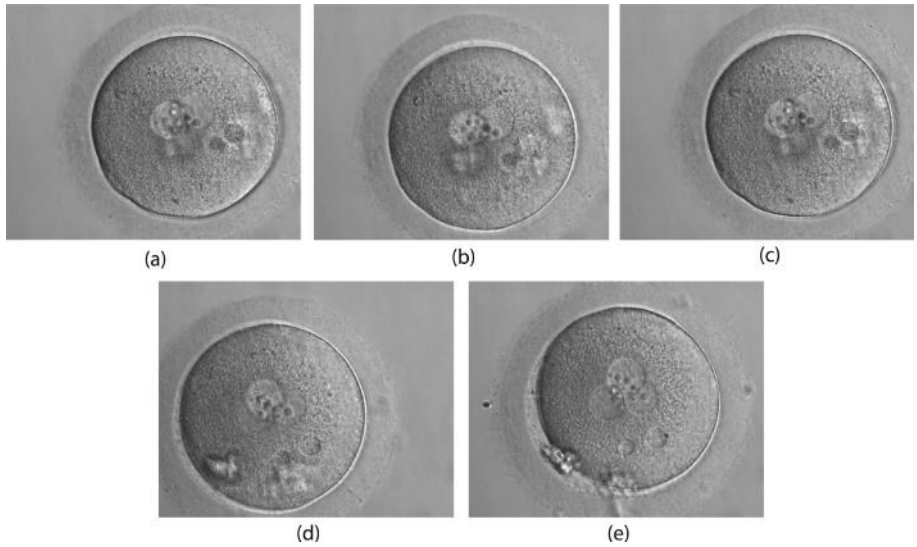

FIGURE 6.6 One cell in different positions to identify correctly the number of pronuclei. (a) This could be a cell with two pronuclei. (b-e) The same cell rotated to identify clearly three pronuclei.

In Vitro *Fertilization*

Oocytes with just one pronuclei (1PN stage) that develop after insemination of the cumulus-oocyte complex are not always aneuploid. Plachot et al. [28,29] showed that between 46% and 69% of these cells are haploid and that between 13% and 29% are diploid. Staessen et al. [30] analyzed even more cells (80.3%) to be diploid and found only 12.5% to be diploid. The asynchronous development of the cell can be a reason for 1PN-stage cells (early appearance or disappearance of one pronucleus) but parthenogenetic activation also could be a reason. Another possibility is the entry of a sperm that did not decondense or two pronuclei that fused. Balakier et al. [31] reported after fluorescent in situ hybridization (FISH) analyses that 50% of 1PN-stage oocytes were diploid. These results lead, in the routine work, to the question how to handle 1PN-stage oocytes after IVF when no other cells are available. A solution is to discuss with the patient the possible risk of aneuploidy of 1PN-stage oocytes after IVF. If the patient agrees to it, it is possible to have an embryo transfer. Staessen et al. [32] reported repeated birth from healthy children after transfer of 1PN-stage oocytes from IVF.

Intracytoplasmic Sperm Injection

The appearance of 1PN-stage cells after intracytoplasmic sperm injection (ICSI) is different from that of cells after IVF. Sultan et al. [33] could show that only 9.5% of these cells were diploid in comparison with 61.9% after IVF. Literature reveals that 1PN-stage oocytes after ICSI can be diploid but that the chance is just between 5.3% and 27.9% [30,34,35]. The risk of chromosomal anomalies (aneuploidy) in cells with just one pronucleus after ICSI is clearly higher than after IVF, leading to the recommendation not to transfer or freeze these cells.

Use of PN-stage oocytes with just ONE pronucleus	
IVF	ICSI
Diploid, 13%–80.5%	Diploid, 5.3%–27.9%
When no other cell is available, further culture and transfer can be performed after informing the patient about the possible risks	Further culture and transfer not recommended
No cryopreservation	No cryopreservation

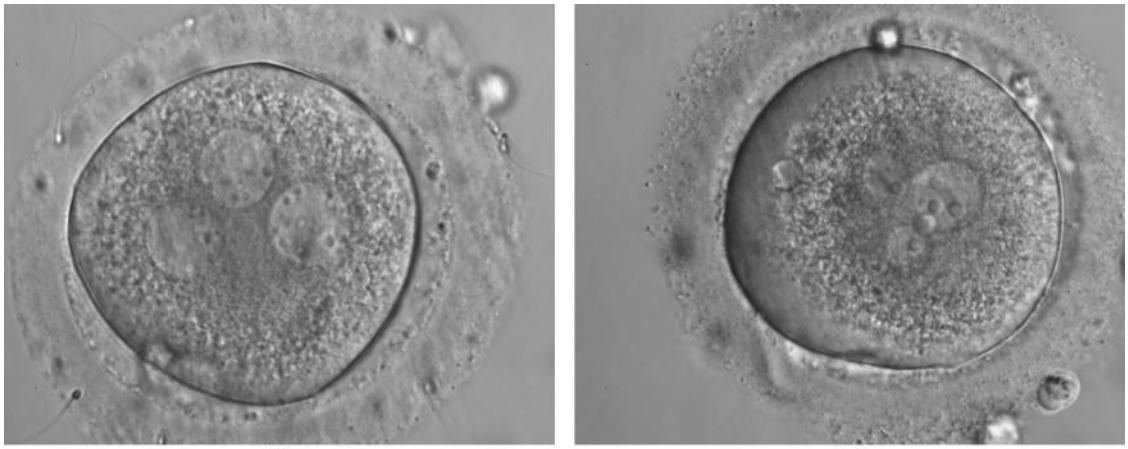

FIGURE 6.7 Cells with irregular fertilization or development with three and four pronuclei. (a) Oocyte with three pronuclei. (b) Oocyte with four pronuclei.

Three or More Pronuclei in an Oocyte

The appearance of three or more pronuclei in one oocyte (Figure 6.7) usually indicates an underlying error that has occurred during the developmental process. These cells are at high risk of being polyploid.

Three PN-stage cells have three haploid chromosome sets in comparison with the regular case with two haploid chromosome sets. If the redundant chromosome set originates from the maternal side, it is called digyny; if it is from the paternal side, it is called diandry. A triploid cell does normally not result in a pregnancy or miscarriage. In case of a pregnancy, the child dies after birth [36]. In IVF, the reason for diandry can be due to entry of two sperms into the oocyte [37]. The entry of a diploid sperm is very unlikely but possible. A possible explanation for digyny is failure of extrusion of the second polar body, and this is the most common reason for the presence of three pronuclei after ICSI [38].

PN-stage oocytes with three pronuclei or more after IVF or ICSI should be discarded and not be used for transfer or cryopreservation.

PN-Stage Cells with Two Pronuclei

PN Size and Position

After the entry or the injection of the sperm into the oocyte, the fertilization cascade is initiated. Within the next 2.5–4.5 hr, the second polar body is discharged and the PN formation starts. The sperm chromatin is very tightly packed with protamines, and these have to be exchanged with histones that are part of the decondensation process. At the same time, the maternal pronucleus is formed; it is slightly smaller than the paternal pronucleus. Both pronuclei grow in size during their development and move together in the center of the cell (Figure 6.8). The position is very important because the first cleavage furrow goes through the PN axis [39].

In most cases, variation in this sequential event shows a lower developmental potential. When one pronucleus is clearly smaller, as shown in Figure 6.9, the corresponding cells have a poor prognosis for initiating a successful pregnancy [17,40].

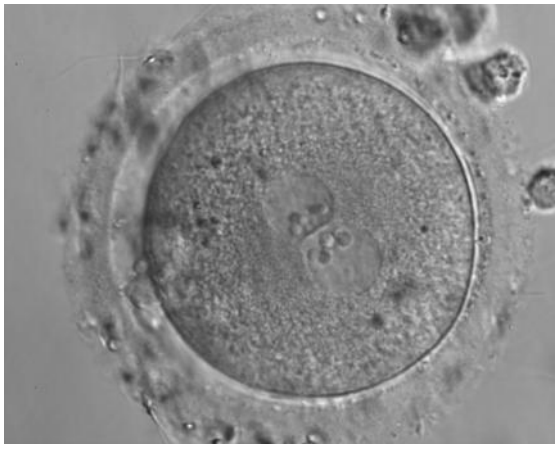

FIGURE 6.8 Pronuclear (PN)-stage oocyte with two regular pronuclei centrally positioned and of equal size (paternal pronucleus slightly larger).

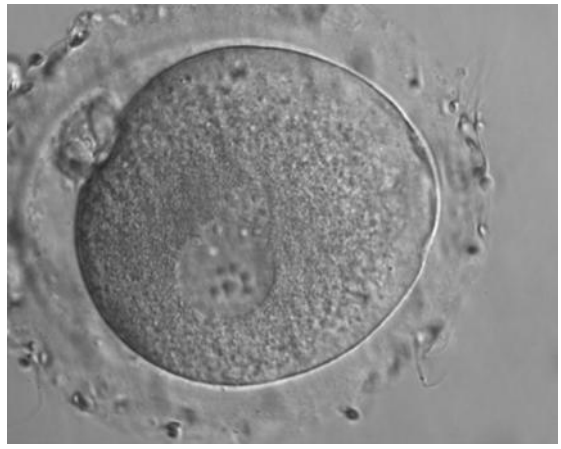

FIGURE 6.9 Pronuclear stage with uneven size of pronuclei.

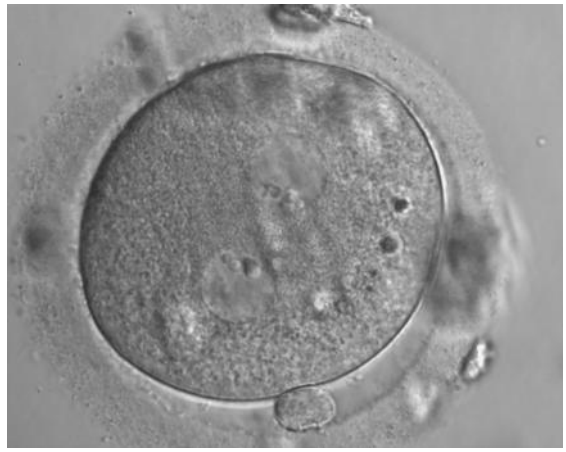

FIGURE 6.10 Pronuclei stage oocyte with two pronuclei not aligned in the center.

The pronuclei should be located side by side in the center of the cell. If this is not the case and if pronuclei are not aligned, as shown in Figure 6.10, further development is usually slow and irregular.

PN stage with two pronuclei that are not of the same size or that are not aligned at the center of the oocyte show a reduced development potential.

A reason for the low development potential could be the asymmetry in the cell. The first cleavage furrow is generally formed in the PN plane, and if pronuclei are located toward the edge of the oocyte, this can lead to problems and can be a potential reason for poor development [41]. In lower order animals, such as insects, worms, and reptiles, polarity is a well-established fact. In mammals, it is discussed whether it is asymmetry or polarity. Invertebrate and vertebrate oocytes present with a pronounced asymmetry in the position of the

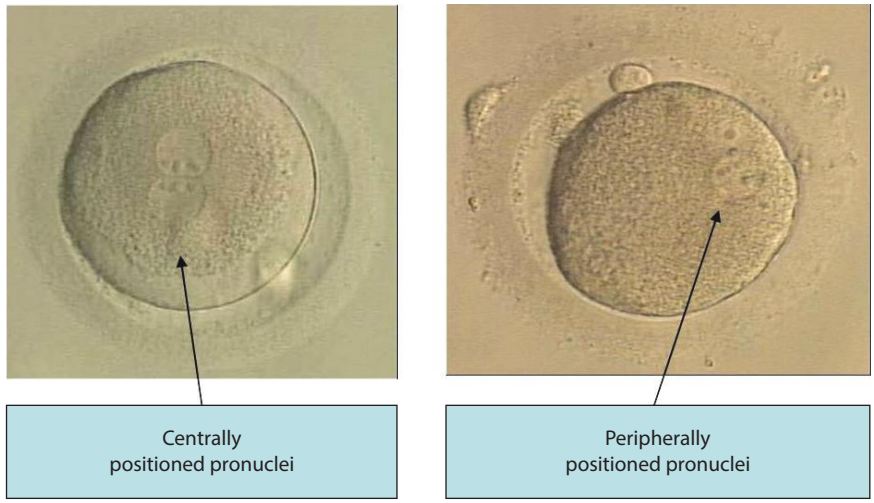

FIGURE 6.11 Location of the pronuclei in the oocyte: centrally or peripherally.

organelle distribution. If this is a manifestation of structural and molecular events and is invariable as well as irreplaceable, it is called polarity. The fact that it is possible to remove a blastomere from a human embryo shows that the polarity is not as strict as in lower order animals. Nevertheless, although in the human PN-stage asymmetry occurs, nonalignment of the pronuclei or asymmetry of the nucleolar precursor bodies is not a good sign.

However, it is very important to remember that PN scoring and PN appearance and disappearance is a time-dependent development and only time-lapse imaging can really see the dynamic structure of the development [42]. This dynamic can be the reason for the different opinions in the literature when pronuclei are located in the periphery of the cell, as demonstrated in Figure 6.11. Ebner et al. [27,43] showed a lower developmental potential for these cells. The relatively rare phenomenon of peripheral pronuclei could be a reason why it is not often found in the literature. Garello et al. [44] reported that this phenomenon is associated with failure or retarded embryo development, but his observations were based on only 19 cells. The problem of peripheral pronuclei is that the first cleavage furrow goes through the PN axis [39], and when the PN are peripherally located, this can result in an abnormal cleavage pattern, eventually leading to uneven two-celled embryos. Nevertheless, we also observed live birth after transfer of embryos derived from such oocytes. The prognostic value with regard to biological processes is not necessarily 100% correct. Still, it is important to identify the cells with the best statistical chances for achieving a pregnancy.

Number and Distribution of Nuclear Precursor Bodies (Nucleoli)

During the development of the pronuclei, the nucleolar precursor bodies appear. These are regions where rRNA synthesis and processing take place. They bind at repeated rDNA sequences of certain chromosomes and are responsible for the active transcription, processing, and protein packaging of ribosomal RNAs [45]. It is possible to determine the number and distribution of the nucleolar precursor bodies in pronuclei using Hoffmann contrast optics at 400× magnification. The underlying symmetry gives information about the development potential of the cell. Symmetry and balance are very important. The Alpha and ESHRE consensus paper (2012; [20,21]) has tried to define and classify PN scoring based on nucleolar precursor bodies. The consensus paper defined a good prognosis, when the nuclear precursor bodies show a symmetrical picture (range 1), but they mention that there are more specialized systems, such as Z-scoring [39]. Nonsymmetrical or other arrangements, including peripherally sited pronuclei, are rated as range 2, and cells with pronuclei with absent or just a single nuclear precursor body are rated abnormal.

The Alpha and ESHRE paper is a consensus and reflects the diversity in this topic in the literature. In routine work, it is often a problem that we just look once at a cell and we do not look at the development. This static observation can be the reason why different results from the same scoring system are reported. It has to be mentioned that some studies found no correlation between PN scoring and the developmental potential of the resulting embryo [46–51]. Nucleoli appear and disappear in a time-dependent way [52], and it is a good example how fast and symmetric development can be. This means that nucleolar patterns do rapidly change in a highly time-dependent manner in most oocytes during the alignment with the cleavage furrow between the two pronuclei and the gradual reduction of the number of nucleoli [53]. This can also been seen in time-lapse monitoring [42]. With this knowledge, it is obvious that the time of entry of the sperm into the oocyte and the maturational state itself play an important role. Nonsymmetrical formation of nucleolar precursor bodies reflects problems in the oocyte, but it does not necessarily mean that the cell cannot solve this problem. For the biologist, it is important to record and assess the right signals and symmetries to be able to compare the cells of one patient to identify those that are best suited for embryo transfer.

With ICSI, we know the exact time of entry of the sperm. Early development after IVF is in most cases slower because the sperm themselves have to find the way into the oocyte. In routine work, this is estimated to cause a delay in the range of 2 hr.

In our opinion, the Z-scoring model proposed by Scott et al. [14,17,39] is an easy scoring system that covers most of the other systems and variations presented in the literature [27,54–61]. According to Scott's work, the symmetric forms Z1 and Z2 show a high potential for initiating a pregnancy. It is very similar to the scoring system presented in the Alpha and ESHRE consensus paper (2011) [20,21].

PN Scoring According to Scott et al. [17,62]

Z1: Both pronuclei with equal numbers of nuclear precursor bodies (nucleoli) aligned at the PN junction

Z2: Both pronuclei with equal numbers of nuclear precursor bodies (nucleoli) scattered symmetrically

Z3: Both pronuclei with inequality of numbers or alignment of nuclear precursor bodies (nucleoli)

Z4: Both pronuclei of different size or not aligned in a central position in the cell

PN Scoring According to the Alpha and ESHRE Consensus Meeting 2011

Range 1: Symmetrical	Equivalent to Z1 and Z2
Range 2: Nonsymmetrical	Other arrangements, including peripherally sited pronuclei
Range 3: Abnormal	Pronuclei with 0 or 1 nuclear precursor body

Examples of these scoring systems are shown in Figure 6.12 [14,17,20,21,62].

The appearance and development of the nucleolar precursor bodies are time-dependent events and show how far the cell has progressed in the cell cycle. Symmetries are important in the development of cells, and the symmetric view of the Z1 and Z2 scores characterizes a PN stage with high potential. Figure 6.13 shows the time-dependent formation of the nucleoli in the pronuclei. For selection of the cells for transfer, a symmetric formation and pronounced progression in the cell cycle warrant a positive choice.

Timing of the development of the PN stage is influenced by the culture medium and by the culture conditions. This can be another reason for explaining the reported differences in the literature. However, for the decision of which cell has the greatest potential, it is important to compare all cells from one patient in a given cycle to others so as to choose the best cells. Asymmetric behavior of the cells can lead to a change in the stimulation regimes or the external conditions in the next cycle to reach better results.

Symmetry and Polarity

In nonmammalian species, the animal and the vegetal pole can be distinguished [44,63]. In the development of the mammalian cells, symmetries and polarization play an important role [41], but this role is not clearly understood yet. This is also reflected in the PN score, but it looks like symmetry and polarity

are essential in allvdevelopmental steps. It starts in the oocyte and continues through fertilization events until embryo development. Symmetry and polarity of the orientation of the polar body can play a role in embryo quality [44]. Polar bodies that are not situated next to each other and those that display a large angle between them are suggested to be of poorer quality [64]. A reason for this reduced quality could be a suboptimal orientation of the pronucleus that leads to cytoplasmic turbulence or uneven cleavage and fragmentation [22]. However, at least the first polar body is not affixed to the oolemma, hence timing can play an important role.

Presence of the So-Called Halo

The outer coat of the oocyte, the zona pellucida, is transparent. This is the reason why one can see the pronuclei as well as intracytoplasmic structures such as vacuoles and inclusion bodies. A cytoplasmic halo is formed when mitochondria and cytoplasmic components are pulled by microtubules from the periphery to the more central region [14]. Because of this pulling, the periphery gets cleared of granular structures, forming the so-called halo [65,66], as shown in Figure 6.14.

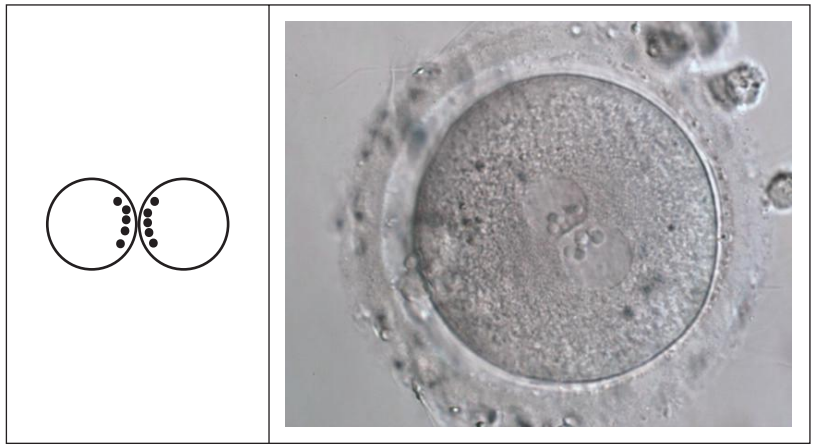

(a)

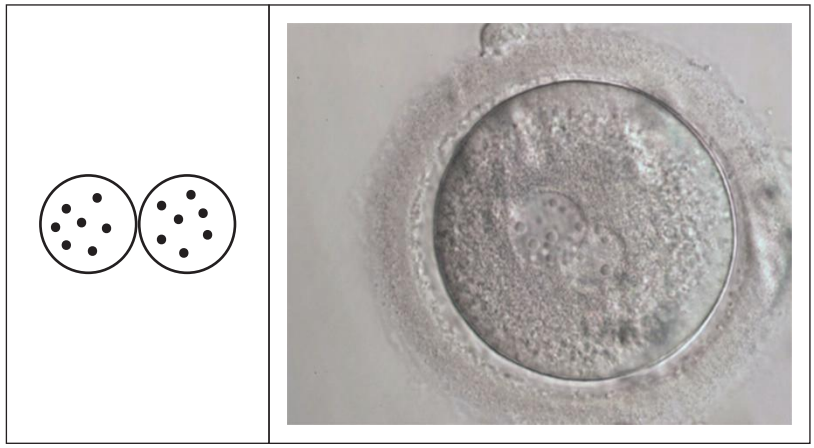

(b)

FIGURE 6.12 Scoring systems for pronuclear (PN) stages. (a) PN stage with Rang 1 (Z1) score (symmetrical). (b) PN stage with Rang 1 (Z2) score (symmetrical).

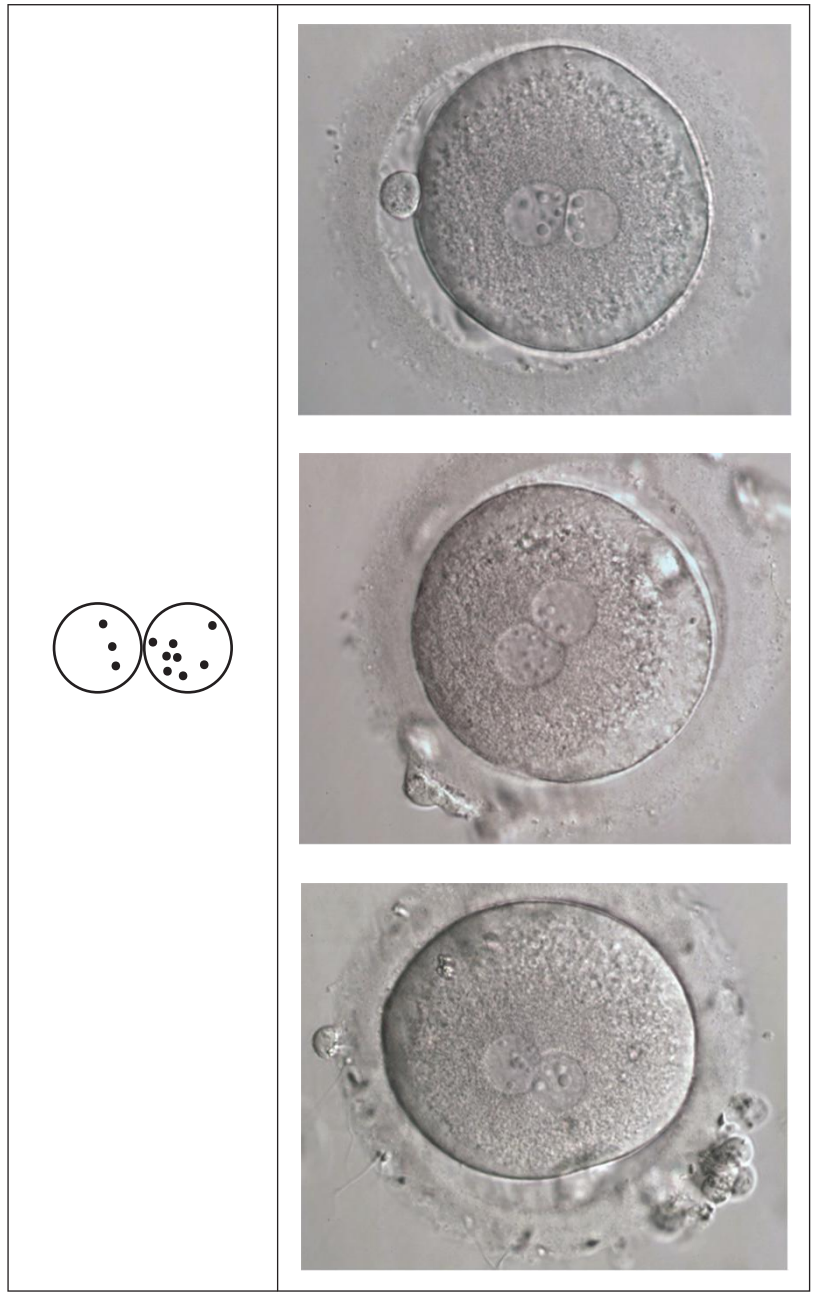

(c)

FIGURE 6.12 (*Continued*) Scoring systems for pronuclear (PN) stages. (c) PN stage with Rang 2 (Z3) score (nonsymmetrical).

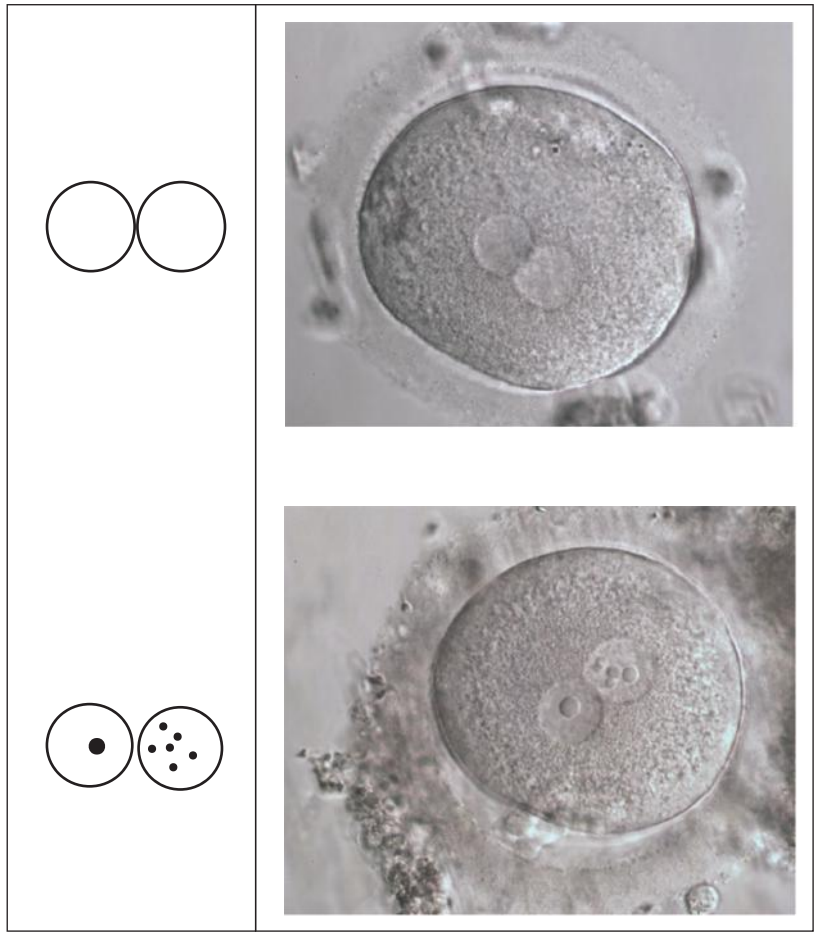

(d)

FIGURE 6.12 (*Continued*) Scoring systems for pronuclear (PN) stages. (d) PN stage with Rang 3 (abnormal, 0 or just 1 nuclear precursor body).

The phenomenon of a subplasmalemmal zone was first mentioned by Payne et al. [67]. Different reports exist about the importance and significance of this region in relation to the potential of the corresponding PN stage. Most of the cells (about 67.7%–88.7%) display a halo but in a different specificity [47,65,66]. We know that it appears because of the transport from mitochondria and cell toward the pronuclei [15], but the importance and the meaning of symmetrical and polar halos are not yet understood [14,47]. Ebner et al. [65] evaluated the halo as a positive sign, whereas Salumets et al. [47] found no influence and Zollner et al. [61] differentiated between normal halo as positive and concentric or extreme halos as negative. Our own study [68,69] found no influence by just looking to see whether there is a halo or not, but it could be that the halo also appears and disappears and it is just a momentum picture in the development of the cell. This could be the reason why the question toward the potential of the halo cannot be simply answered as yes or no. Time-lapse imaging should enable to gain more information in this regard.

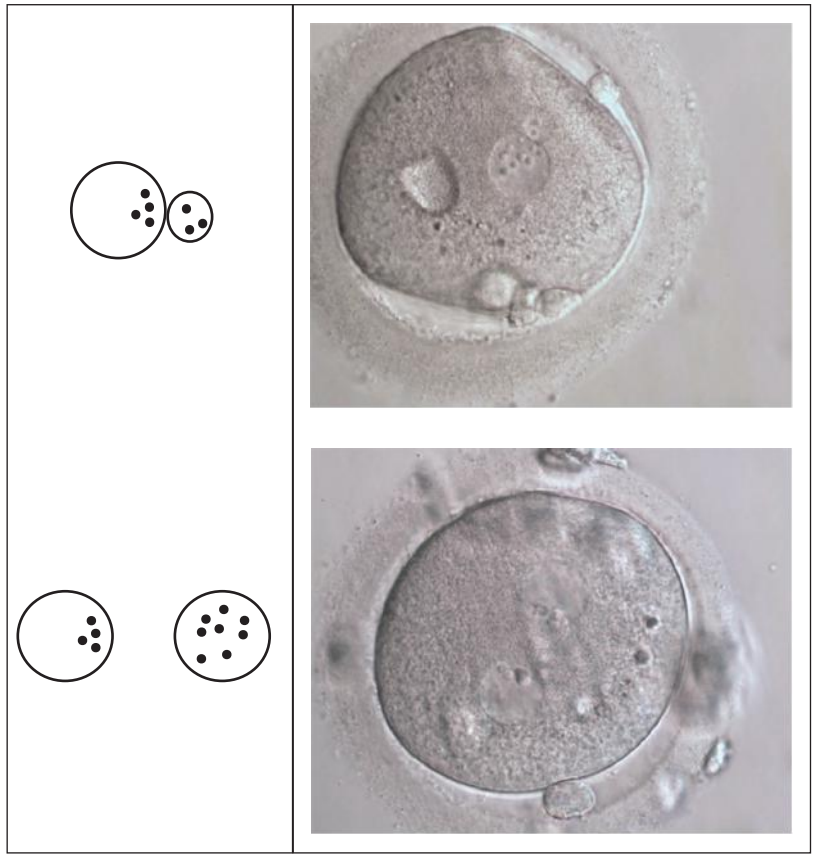

FIGURE 6.12 (*Continued*) Scoring systems for pronuclear (PN) stages. (e) PN stage with (Z4) score. PN of different sizes are not aligned in a central position in the cell. (Modified from Scott L, Smith S, *Hum Reprod* 13, 1003–1013, 1998; Scott L et al., *Hum Reprod* 15, 2394–2403, 2003; Scott L et al., *Hum Reprod* 22; 230–240, 2007; Alpha Scientists in Reproductive Medicine, ESHRE Special Interest Group of Embryology, *Reprod Biomed Online* 22, 2011, 632–646; Alpha Scientists in Reproductive Medicine, ESHRE Special Interest Group of Embryology, *Hum Reprod* 2011, 1–14.)

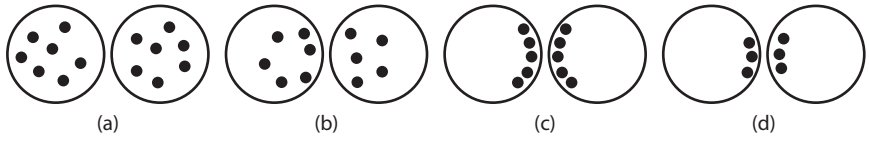

FIGURE 6.13 Time-dependent progression of the orientation of the nucleoli in the pronuclei of the pronuclear stage from (a) dispersed to (b) moving towards centre to (c) alignment at side of pronuclear contact to (d) fusion of nucleoli and further alignment.

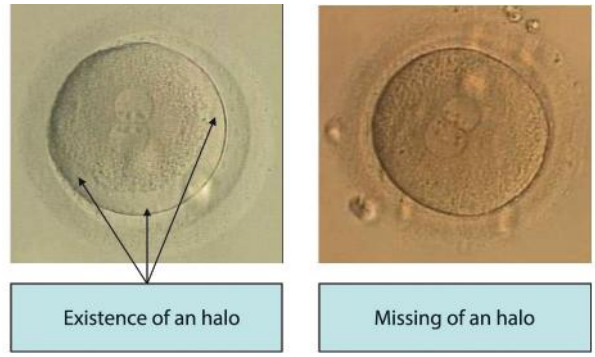

FIGURE 6.14 Occurrence of the halo effect.

REFERENCES

1. Devreker F. Uptake and Release of Glucose, Pyruvate and Lactate. In: ESHRE Campus Non-Invasive Embryo Quality Assessment. ed. ESHRE, Grimbergen, Belgium. 2005, pp. 77–91.
2. Brewis IA. Proteomics in reproductive research: The potential importance of proteomics to research in reproduction. *Hum Reprod* 1999; 14: 2927–2929.
3. Kere J, Hofmann B. Comprehensive molecular analysis of oocytes and embryos. *Hum Reprod* 2011; 26 (Suppl 1): i56.
4. Borini A, Lagalla C, Sciajno R, Distratis V, Bonu MA, Cattoli M, et al. Artificial reproductive technology achievements for optimizing embryo quality. *Ann N Y Acad Sci* 2004; 1034: 252–261.
5. Coticchio G, Sereni E, Serrao L, Mazzone S, Iadarola I, Borini A.What criteria for the definition of oocyte quality? *Ann N Y Acad Sci*. 2004;1034:132–144.
6. Geraedts J, Montag M, Magli C, Repping S, Handyside A, Staessen C, et al. Polar body array CGH for prediction of the status of the corresponding oocyte. Part I: Clinical results. *Hum Reprod* 2011; 26: 3173–3180.
7. Van Blerkom J. Epigenetic influences on oocyte development competence: Perifollicular vascularity and intrafollicular oxygen. *J Assist Reprod Genet* 1998; 15: 226–234.
8. Ziebe S, Lundin K, Loft A, Bergh C, Nyboe Andersen A, Selleskog U, et al. FISH analysis for chromosomes 13, 16, 18, 21, 22, X and Y in all blastomeres of IVF pre-embryos from 144 randomly selected donated human oocytes and impact on pre-embryo morphology. *Hum Reprod* 2003; 18: 2575–2581.
9. Saunders CM. PLC zeta: A sperm specific trigger of Ca^{2+} oscillations in eggs and embryo development. *Development* 2002; 129: 3533–3544.
10. Heytens E, Parrington J, Coward K, Young C, Lambrecht S, Yoon S-Y, et al. Reduced amounts and abnormal forms of phospholipase C zeta (PLCζ) in spermatozoa from infertile men. *Hum Reprod* 2009; 24: 2417–2428.
11. Palermo G, Munné S, Cohen J. The human zygote inherits its mitotic potential from the male gamete. *Fertil Steril* 1994; 9: 1220–1225.
12. Ebner T, Moser M, Tews G. Die Bedeutung der Morphologie der Oozyte hinsichtlich ihres weiteren Entwicklungspotentials [The significance of oocyte morphology regarding it's further developmental potential]. *J Reprod Endocrinol* 2006; 1: 17–23.
13. Van Blerkom J, Davis P, Merriam J, Sinclair J. Nuclear and cytoplasmic dynamics of sperm penetration, pronuclear formation and microtubule organization during fertilization and early preimplantation development in the human. *Hum Reprod Update* 1995; 1: 429–461.
14. Scott L, Smith S. The successful use of pronuclear embryo transfers the day following oocyte retrieval. *Hum Reprod* 1998; 13: 1003–1013.
15. Van Blerkom J, Davis P, Alexander S. Differential mitochondrial distribution in human pronuclear embryos leads to disproportionate inheritance between blastomeres: Relationship to microtubular organization, ATP content and competence. *Hum Reprod* 2000; 15: 2621–2633.

16. Alberts B, Bray D, Lewis J, Raff M, Roberts K, Watson J. *Molekularbiologie der Zelle* [Molecular Biology of the Cell. Weinheim: 2nd edition, VCH Verlagsgesellschaft, 1990]. Weinheim: Zweite Auflage VCH Verlagsgesellschaft, 1990.
17. Scott L, Alvero R, Leondiris M, Miler B. The morphology of human pronuclear embryos is positively related to blastocyst development and implantation. *Hum Reprod* 2000; 15: 2394–2403.
18. Hill GA, Freeman M, Bastias MC, Rogers BJ, Herbert CM, Osteen KG, et al. The influence of oocyte maturity and embryo quality on pregnancy rate in a program for *in vitro* fertilization-embryo transfer. *Fertil Steril* 1989; 52: 801–806.
19. Steer C, Mills C, Tan S, Campbell S, Edwards R. The cumulative embryo score: A predictive embryo scoring technique to select the optimal number of embryos to transfer in an in-vitro fertilization and embryo transfer programme. *Hum Reprod* 1992; 7: 117–119.
20. Alpha Scientists in Reproductive Medicine, ESHRE Special Interest Group Embryology. Istanbul consensus workshop on embryo assessment: Proceedings of an expert meeting. *Reprod Biomed Online* 2011; 22: 632–646.
21. Alpha Scientists in Reproductive Medicine, ESHRE Special Interest Group of Embryology. The Istanbul consensus workshop on embryo assessment: Proceedings of an expert meeting. *Hum Reprod* 2011; 26: 1270–1283.
22. Papale L, Fiorentino A, Montag M, Tomasi G. The zygote. *Hum Reprod* 2012; 27 (Suppl 1): i22–i4.
23. Kahraman S, Yain K, Dönmez E, Samli H, Bahce M, Cengiz G, et al. Relationship between granular cytoplasm of oocytes and pregnancy outcome following intracytoplasmic sperm injection. *Hum Reprod* 2000; 15: 2390–2393.
24. Ebner T, Moser M, Sommergruber M, Gaiswinkler U, Shebl O, Jesacher K, et al. Occurrence and developmental consequences of vacuoles throughout preimplantation development. *Fertil Steril* 2005; 83: 1635–1640.
25. Balaban B, Urman B. Effect of oocyte morphology on embryo development and implantation. *Reprod Biomed Online* 2006; 12: 608–615.
26. Sadler T. *Medizinische Embryologie*. New York: Georg Thieme Verlag Stuttgart, 1998, pp. 12–17.
27. Ebner T, Moser M, Sommergruber M, Tews G. Selection based on morphological assessment of oocytes and embryos at different stages of preimplantation development: A review. *Hum Reprod Update* 2003; 9 (3): 251–262.
28. Plachot M, Mandelbaum J, Junca A-M, de Grouchy J, Salat-Baroux J, Cohen J. Cytogenetic analysis and developmental capacity of normal and abnormal embryos after IVF. *Hum Reprod* 1989; 4 (Suppl 8): 99–103.
29. Plachot M, Crozet N. Fertilization abnormalities in human *in vitro* fertilization. *Hum Reprod* 1992; 7 (Suppl 1): 89–94.
30. Staessen C, Van Steirteghem AC. The chromosomal constitution of embryos developing from abnormally fertilized oocytes after intracytoplasmic sperm injection and conventional in-vitro fertilization. *Hum Reprod* 1997; 12: 321–327.
31. Balakier H, Squire J, Casper RF. Characterization of abnormal one pronuclear human oocytes by morphology, cytogenetics and in-situ hybridization. *Hum Reprod* 1993; 8: 402–408.
32. Staessen C, Janssenswillen C, Van den Abbeel E, Devroey P, Van Steirteghem AC. Avoidance of triplet pregnancies by elective transfer of two good quality embryos. *Hum Reprod* 1993; 8: 1650–1653.
33. Sultan KM, Munné S, Palermo GD, Alikani M, Cohen J. Chromosomal status of uni-pronuclear human zygotes following in-vitro fertilization and intracytoplasmic sperm injection. *Hum Reprod* 1995; 10: 132–136.
34. Staessen C, Janssenswillen C, Devroey P, Van Steirteghem AC. Cytogenetic and morphological observations of single pronucleated human oocytes after in-vitro fertilization. *Hum Reprod* 1993; 8: 221–223.
35. Plachot M, Selva J, Wolf JP, Bastit P, de Mouzon J. Consequences of oocyte dysmorphy on the fertilization rate and embryo development after intracytoplasmic sperm injection. A prospective multicenter study. *Gynecol Obstet Fertil* 2002; 10: 772–779.
36. Baraitser M, Winter RM. *Missbildungs Syndrome*. Bern: Hans Huber, 2001, pp. 10–11.
37. Rosenbusch B, Schneider M, Sterzik K. The chromosomal constitution of multipronuclear zygotes resulting from in-vitro fertilization. *Hum Reprod* 1997; 12: 2257–2262.
38. Grossmann M, Calafell JM, Brandy N, Vanrell JA, Rubio C, Pellicer A, et al. Origin of tripronucleate zygotes after intracytoplasmic sperm injection. *Hum Reprod* 1997; 12: 2762–2765.
39. Scott L. Pronuclear scoring as a predictor of embryo development. *Reprod Biomed Online* 2003; 6: 201–214.
40. Scott L. Morphological correlates of oocyte and embryo competence-identification. *Hum Fertility* 2002; 5: 206–214.
41. Scott L. Oocyte and embryo polarity. *Semin Reprod Med* 2001; 18: 171–183.

42. Montag M, Liebenthron J, Köster M. Which morphological scoring system is relevant in human embryo development? *Placenta* 2011; 32: S252–S256.
43. Beuchat A, Thévenaz P, Unser M, Ebner T, Senn A, Urner F, et al. Quantitative morphometrical characterization of human pronuclear zygotes. *Hum Reprod* 2008; 23 (9): 1983–1992.
44. Garello C, Baker H, Rai J, Montgomery S, Wilson P, Kennedy CR, et al. Pronuclear orientation, polar body placement, and embryo quality after intracytoplasmic sperm injection and in-vitro fertilization: Further evidence for polarity in human oocytes. *Hum Reprod* 1999; 14: 2588–2595.
45. Tesarik J, Kopecny V. Assembly of the nucleolar precursor bodies in human male pronuclei is correlated with early RNA synthetic activity. *Exp Cell Res* 1990; 191: 153–156.
46. Payne JF, Raburn DJ, Couchman GM, Price TM, Jamison MG, Walmer DK. Relationship between pre-embryo pronuclear morphology (zygote score) and standard day 2 or 3 embryo morphology with regard to assisted reproductive technique outcomes. *Fertil Steril* 2005; 84: 900–909.
47. Salumets A, Hyden-Granskog C, Suikkari A, Tiitinen A, Tuuri T. The predictive value of pronuclear morphology of zygotes in the assessment of human embryo quality. *Hum Reprod* 2001; 16: 2177–2181.
48. Weitzmann VN, Schnee-Riesz J, Benadiva C, Nulsen J, Siano L, Maier D. Predictive value of embryo grading for embryos with known outcomes. *Fertil Steril* 2010; 93: 658–662.
49. James A, Hennessy S, Reggio B, Wiemer K, Larsen F, Cohen J. The limited importance of pronuclear scoring of human zygotes. *Hum Reprod* 2006; 21: 1599–1604.
50. Nicoli A, Valli B, Di Girolamo R, Di Tommaso B, Gallinelli A, La Sala GB. Limited importance of pre-embryo pronuclear morphology (zygote score) in assisted reproduction outcome in the absence of embryo cryopreservation. *Fertil Steril* 2007; 88: 1167–1173.
51. Brezinova J, Oborna I, Svobodova M, Fingerova H. Evaluation of day one embryo quality and IVF-outcome – a comparison of two scoring systems. *Reprod Biol Endocrinol* 2009; 7: 9.
52. Tesarik J, Kopecny V. Development of human male pronucleus: Ultrastructure and timing. *Gamete Res* 1989; 24: 135–149.
53. Plachot M. Fertilization. *Hum Reprod* 2000; 15 (Suppl 4): 19–30.
54. Balaban B, Urman B, Isiklar A, Alatas C, Aksoy S, Mercan R, et al. The effect of pronuclear morphology on embryo quality parameters and blastocyst transfer outcome. *Hum Reprod* 2001; 16: 2357–2361.
55. Montag M, van der Ven H, German Pronuclear Morphology Study Group. Evaluation of pronuclear morphology as the only selection criterion for further embryo culture and transfer: Results of a prospective multicentre study. *Hum Reprod* 2001; 11: 2384–2389.
56. Nagy Z, Dozortsev D, Diamond M, Rienz L, Ubaldi F, Abdelmassih R, et al. Pronuclear morphology evaluation with subsequent evaluation of embryo morphology significantly increases implantation rates. *Fertil Steril* 2003; 80: 67–74.
57. Senn A, Urner F, Chanson A, Primi MP, Wirthner DW, Germont M. Morphological scoring of human pronuclear zygotes for prediction of pregnancy outcome. *Hum Reprod* 2006; 21: 234–239.
58. Tesarik J, Greco E. The probability of abnormal preimplantation development can be predicted by a single static observation on pronuclear stage morphology. *Hum Reprod* 1999; 14: 1318–1323.
59. Tesarik J, Junca A, Hazout A, Aubriot F, Nathan C, Cohen-Bacrie P, et al. Embryos with high implantation potential after intracytoplasmic sperm injection can be recognized by a simple, non-invasive examination of pronuclear morphology. *Hum Reprod* 2000; 15: 1396–1399.
60. Wittmer C, Bettahar-Lebuge K, Ohl J, Rongieres C, Nisand I, Gerlinger P. Zygote evaluation: An efficient tool for embryo selection. *Hum Reprod* 2000; 15: 2591–2597.
61. Zollner U, Zollner KP, Hartl G, Dietl J, Steck T. The use of a detailed zygote score after IVF/ICSI to obtain good quality blastocysts: The German experience. *Hum Reprod* 2002; 17: 1327–1333.
62. Scott L, Finn A, O'Leary T, McLellan S, Hill J. Morphologic parameters of early cleavage-stage embryos that correlate with fetal development and delivery: Prospective and applied data for increased pregnancy rates. *Hum Reprod* 2007; 22 (1): 230–240.
63. Edwards RG, Beard HK. Oocyte polarity and cell determination in early mammalian embryos. *Mol Hum Reprod* 1997; 3: 863–905.
64. Gianaroli L, Magli MC, Ferraretti AP, Fortini D, Grieco N. Pronuclear morphology and chromosomal abnormalities as scoring criteria for embryo selection. *Fertil Steril* 2003; 80: 341–349.

65. Ebner T, Moser M, Sommergruber M, Gaiswinkler U, Wiesinger R, Puchner M, et al. Presence, but not type or degree of extension, of a cytoplasmic halo has a significant influence on preimplantation development and implantation behaviour. *Hum Reprod* 2003; 18: 2406–2412.
66. Stalf T, Herrero J, Mehnert C, Manolopoulos K, Lenhard A, Gips H. Influence of polarization effects and pronuclei on embryo quality and implantation in an IVF program. *J Assist Reprod Genet* 2002; 19: 355–362.
67. Payne D, Flaherty SP, Barry MF, Mathews CD. Preliminary observations on polar body extrusion and pronuclear form score as a prognostic tool in IVF treatment. *Hum Reprod* 1997; 12: 705–708.
68. Greuner M. *Untersuchung morphologischer Kriterien der Gameten und Vorkernstadien zur Erzielung einer Schwangerschaft* [Investigation of morphological criteria of gametes and PN-stage oocytes for achieving a pregnancy]. Dissertation. Fakultät Charite, Universitätsmedizin Berlin, 2008.
69. Greuner M, Winkler S, Maxrath B, Montag M, Schmiady H. Charakterisierung des morphologischen Entwicklungspotenzials von der Oozyte bis zum Embryo [Characterization of the developmental potential from the oocyte to the embryo based on morphology assessment]. *J Reproduktionmed Endokrinol* 2012; 1: 13–19.

7

Morphological Selection of Gametes and Embryos: Embryo

Gayle Jones and M. Cristina Magli

Introduction

Fertilization occurs in vivo in the ampullary-isthmic region of the fallopian tube. In the subsequent days, the zygote undergoes successive cleavage divisions while traversing the fallopian tube, until 2–3 days after fertilization, and the embryo enters the uterus at the morula-blastocyst stage of development [1]. Until this century when quality commercial in vitro fertilization (IVF) media designed specifically to meet the needs of the growing embryo were introduced into IVF practice, embryos were traditionally transferred to the patient's uterus at the cleavage stage of development on Day 2 or Day 3 of in vitro culture at the four- to eight-cell stage of development.

Cleavage-stage embryos range from the two-cell stage to the morula stage when the embryo consists of more than eight cells and each blastomere is so closely juxtaposed so as to give the appearance of no individual internal cellular boundaries as a result of the formation of tight junctions between individual blastomeres. This light microscopic appearance at the morula stage is known as compaction. During cleavage, the embryo does not increase in size but undergoes successive reduction in blastomere size as cell numbers increase with each cleavage division. For the first 2 days of development, the embryo is under the control of stored maternal message inherited from the oocyte and it is not until the four- to eight-cell transition that the embryo is under the control of an activated embryonic genome [2]. Many embryos undergo developmental arrest between the four- to eight-cell stages at the time the embryonic genome becomes activated, and this embryonic block can be exacerbated by poor in vitro culture conditions.

It is imperative that critical morphological selection parameters are used to improve the chances of a successful pregnancy outcome.

Transferring embryos at the cleavage stage of development has the distinct disadvantage that most of the original zygotes undergo cleavage and are theoretically available for selection for transfer. It is therefore imperative that critical morphological selection parameters are used to improve the chances of a successful pregnancy outcome. A distinct advantage of transferring embryos at the cleavage stage of development, particularly on Day 2 at the four-cell stage, is that cryopreservation is very successful with pregnancy outcomes after transfer of thawed embryos equivalent to those achieved after transfer of fresh embryos, provided only good morphological quality embryos are selected for cryopreservation and there is no loss of blastomeres during the cryopreservation-thawing process [3].

Morphological criteria remain the gold standard for selection of embryos for transfer, and they have acquired greater significance as the global trend moves toward a single embryo transfer policy. Many morphological criteria and scoring systems have been proposed for the selection of the "best" cleavage-stage embryo for transfer. Embryos are scored based on cleavage kinetics, cell numbers and size of blastomeres, spatial orientation of blastomeres, pattern and extent of fragmentation, nuclear status, cytoplasmic anomalies, and in the case of morula-stage embryos the degree of compaction [4–25].

This chapter illustrates the various morphological characteristics of the two-cell to morula-stage embryo that have been used to select the best embryo for transfer and then links the characteristics to implantation potential, where known.

Cleavage Kinetics and Cell Numbers

It was recognized early in the history of IVF that the kinetics of cleavage, that is, the number of cells at a specific point in time postinsemination, was linked to implantation outcome [4]. Faster cleaving embryos were more likely to implant than slower cleaving embryos, with the exception of embryos showing very rapid cleavage [4]. Rapidly dividing embryos can result from tripronucleate zygotes that cleave from one to three cells and then to six cells within two cleavage divisions [26]. Furthermore, it has been demonstrated that embryos showing normal cleavage kinetics are more likely to be euploid than slower cleaving embryos and embryos showing very rapid cleavage kinetics [27–29].

The time of the first cleavage division to the two-cell stage has been linked to subsequent embryo quality and implantation rates [30–38]; however, some have claimed that this relationship holds true only for embryos generated in gonadotropin-releasing hormone (GnRH) agonist cycles and not for GnRH antagonist cycles [39,40].

It has recently been agreed that the timing for the observation of optimal cleavage rates that have been linked to the highest implantation potential should be two cells at 26 ± 1 hr postinjection or 28 ± 1 hr postinsemination (Figure 7.1a), four cells at 44 ± 1 hr (Figure 7.1b), eight cells at 68 ± 1 hr (Figure 7.1c), and morula at 92 ± 2 hr (Figure 7.1d) [24]. Transfer of four-cell embryos on Day 2 results in higher pregnancy rates than transfer of embryos with lower or higher cell numbers on Day 2 [22,41,42].

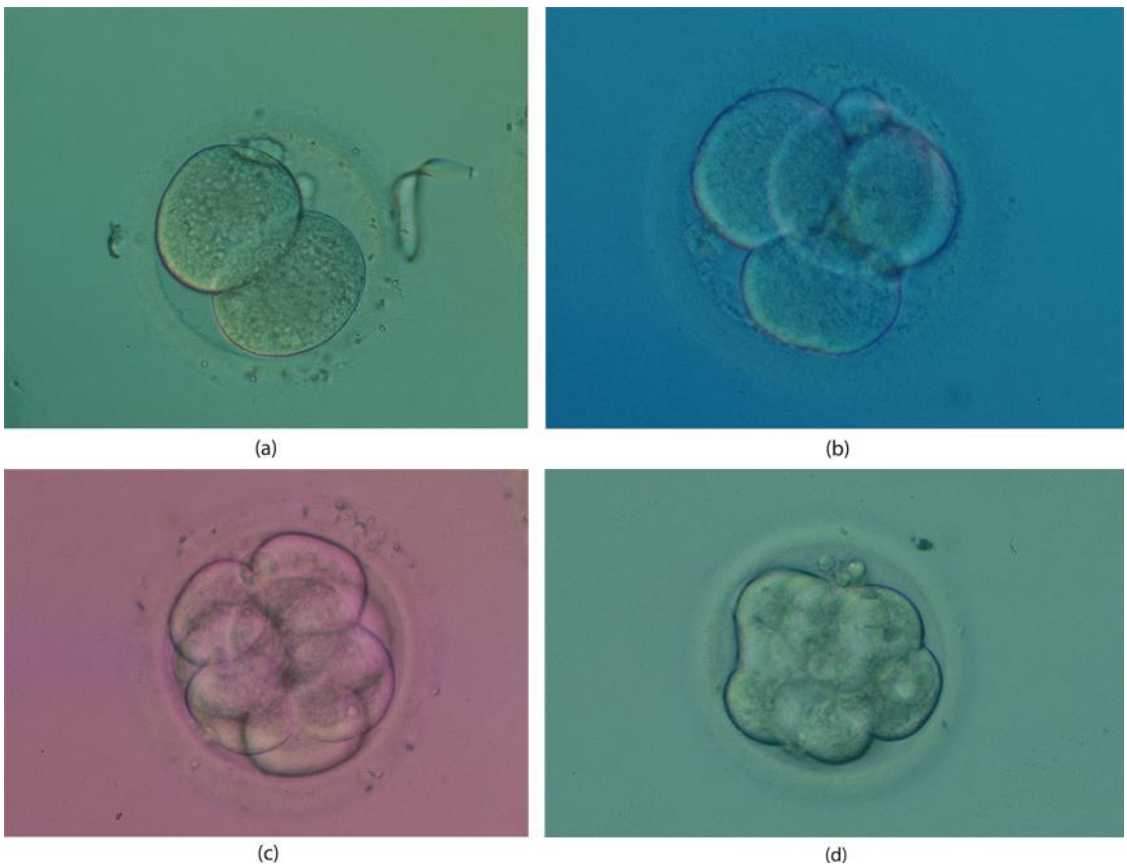

FIGURE 7.1 Examples of embryos showing normal cleavage kinetics and normal cytokinesis on Day 1 (a), Day 2 (b), Day 3 (c), and Day 4 (d). Original magnification, 300×.

Similarly, transfer of embryos with eight cells on Day 3 is associated with a higher pregnancy rate [12,43], and the transfer of slow-cleaving embryos on Day 3, with five or fewer cells, has been associated with early pregnancy loss [44]. It must be remembered that this information is based on nearly four decades of single light microscopic observations of embryo development on Days 1–4. The introduction of continuous observation through time-lapse microscopy may further refine our knowledge in this area in the coming decade, particularly the optimal timing between successive mitotic divisions.

Transfer of embryos on Day 3 with eight cells is associated with a higher pregnancy rate, and transfer of slow-cleaving embryos with five or fewer cells has been associated with early pregnancy loss.

Size of Blastomeres

Cell number is related to implantation outcome; so is cell size. Regular cytokinesis resulting in blastomeres of even size has been related to higher implantation rates when observed as early as the first cleavage division [45,46]. Subsequent cleavage divisions should also produce daughter cells of equivalent size, and poorer outcomes are associated with embryos whose daughter cells vary in diameter by more than one-third [6]. Regularity in blastomere size on Day 2 has been shown to correlate with higher implantation rates [8,9,22,47]. Irregular cytokinesis may also be associated with irregular nucleokinesis because multinucleation and chromosomal abnormalities have been observed at a higher frequency in embryos with blastomeres of uneven size [47,48].

Time-lapse imaging has demonstrated that embryos showing synchronous division on Day 2 with a time difference between the second and third mitosis (three cell to four cell) of no greater than 1 hr have a greater potential to develop to blastocyst and implant [49,50].

Irregular cytokinesis must be distinguished from asynchronous cleavage divisions, both of which result in embryos with blastomeres of uneven size. Embryos that undergo synchronous division should result in two cells, four cells, and eight cells after the first, second, and third cleavage divisions (or the first, third, and seventh mitosis), respectively (Figure 7.1). If there has also been regular cytokinesis, then all blastomeres in these embryos should be expected to be of the same size.

Regular cytokinesis results in blastomeres of even size that are related to higher implantation rates when observed as early as the first cleavage division.

Embryos that undergo asynchronous divisions result in three cells, fives cells, six cells, and seven cells on Day 2 and Day 3 (Figure 7.2). These embryos would therefore be expected to have a difference in cell size resulting from the cell that failed to undergo synchronous cleavage. A diagrammatic representation of normal and abnormal cell sizes for embryos that have undergone synchronous division, that is, two cell, four cell, and eight cell, are depicted in Figure 7.3, and asynchronous division, that is, three cell, five cell, six cell, and seven cell, are depicted in Figure 7.4.

Spatial Orientation of Blastomeres

There is polarization in the distribution of organelles, proteins, and molecular message within the oocyte [51–53]. Therefore, mitotic division results in differential inheritance of organelles and molecules in the developing embryo. This spatial arrangement of organelles and molecules can be further regulated by the execution of tangential cleavage planes in the second cleavage division (Figure 7.5) [54]. The first cleavage plane in mammalian embryos is meridional with the axis of division running from the position of the polar bodies (the animal pole) to the opposite pole (the vegetal pole), resulting in two equal-sized daughter cells with each inheriting similar

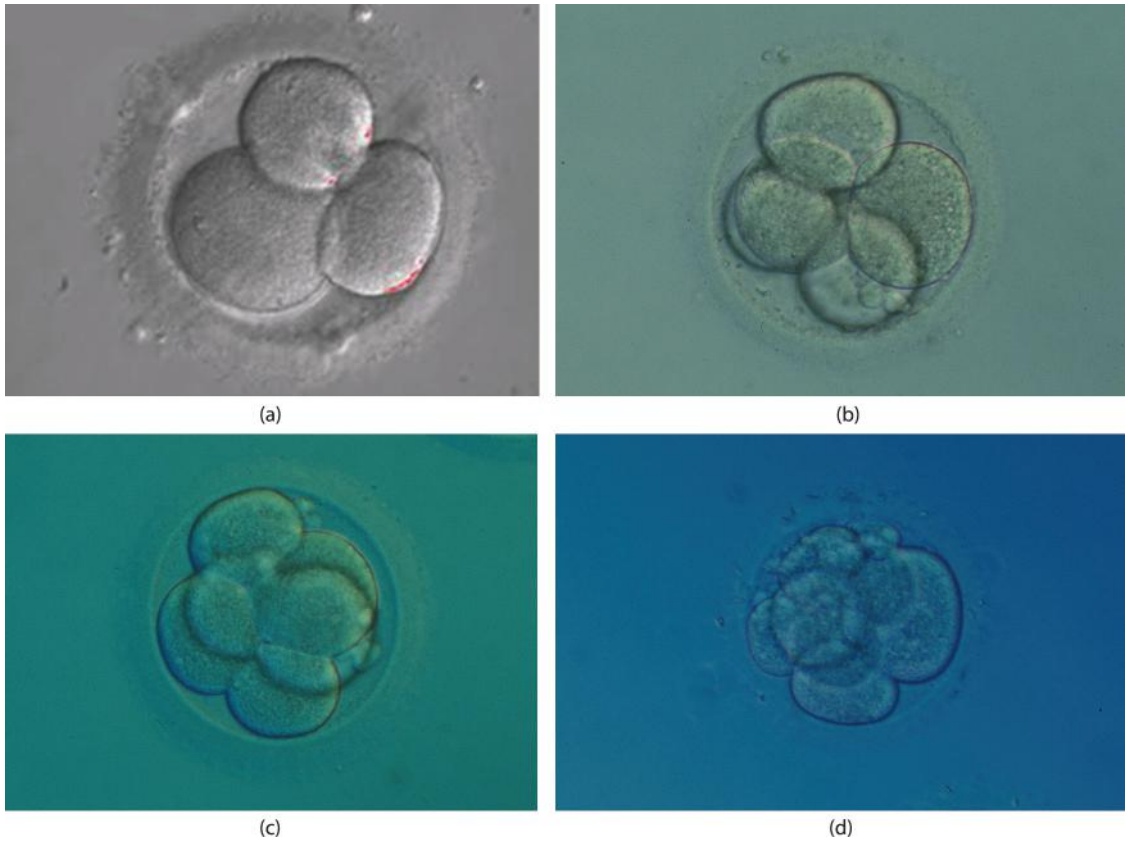

FIGURE 7.2 Examples of embryos showing asynchronous division but normal cytokinesis. (a) Three-cell embryo, one large blastomere and two smaller blastomeres. (b) Five-cell embryo, three large blastomeres and two smaller blastomeres. (c) Six-cell embryo, two large blastomeres and four evenly sized smaller blastomeres. (d) Seven-cell embryo, one large blastomere and six evenly sized smaller blastomeres. Original magnification, 300×.

distributions of animal and vegetal cytoplasm. The second cleavage plane is meridional, like the first cleavage plane, but the third cleavage plane is equatorial [54]. The resultant four-cell embryo has a tetrahedral appearance with a differential in distribution of animal and vegetal cytoplasm (Figure 7.5) [55].

Disturbances in these defined cleavage planes result in embryos with a nontetrahedral appearance, such as the clover-shaped embryo (Figure 7.6), and the resultant disturbance in distribution of animal and vegetal cytoplasm would theoretically have consequences on subsequent viability. Approximately 3% of embryos show a nontetrahedral appearance at the four-cell stage, and these embryos have decreased development to the blastocyst stage and a reduced implantation rate compared with embryos arising from a tetrahedral arrangement of cells at the four-cell stage [56].

Pattern and Extent of Fragmentation

Embryo fragmentation has long been included along with blastomere size and number as an important morphological criterion linked to embryo viability. Fragments are defined as anuclear, membrane-bound cytoplasmic structures found in the extracellular spaces between blastomeres or between the blastomeres and the zona pellucida in the perivitelline space. The extent of fragmentation is most often expressed as a percentage of the total volume of the embryo. In very fragmented embryo, it is often difficult to assess large anucleate fragments from

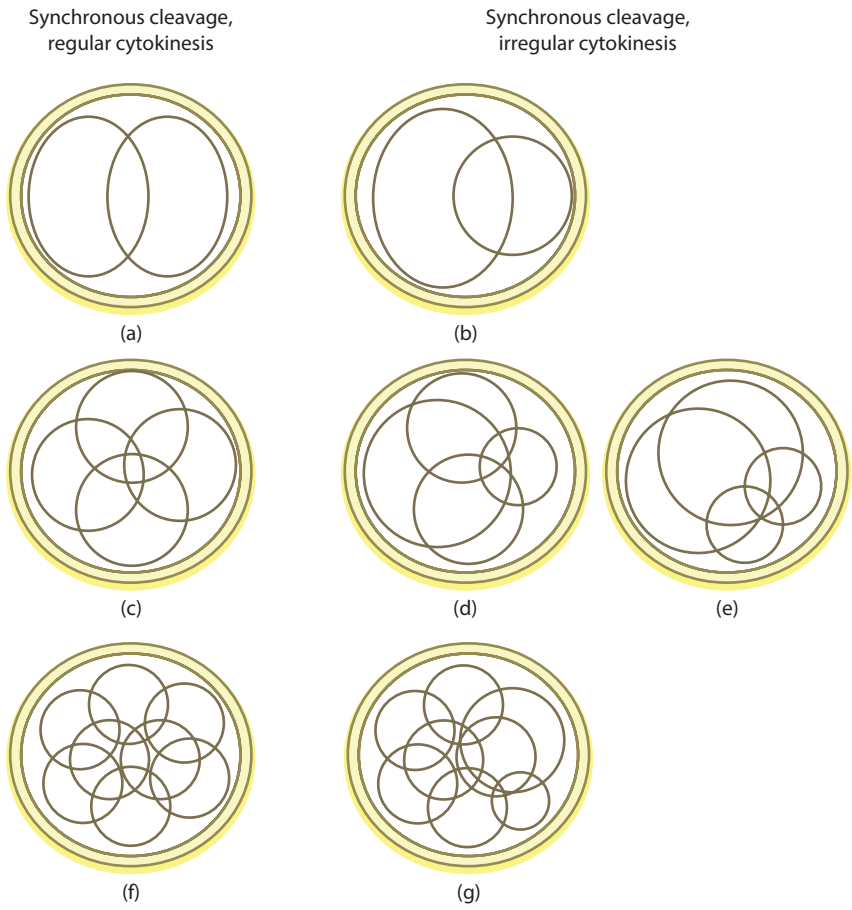

FIGURE 7.3 Diagrammatic representation of embryos on Days 1–3 that have undergone synchronous division with regular cytokinesis or irregular cytokinesis. (a) Two-cell embryo showing regular cytokinesis. (b) Two-cell embryo showing irregular cytokinesis. (c) Four-cell embryo showing regular cytokinesis. (d) Four-cell embryo showing irregular cytokinesis in one of the two originating blastomeres. (e) Four-cell embryo showing irregular cytokinesis in both of the originating blastomeres. (f) Eight-cell embryo showing regular cytokinesis. (g) Eight-cell embryo showing irregular cytokinesis in at least one of the originating blastomeres.

blastomeres, and it has been suggested that for Day 2 embryo fragments are defined as those <45 μm in diameter and for Day 3 embryos fragments are defined as those <40 μm in diameter [57], based on the observation that cytoplasmic structures of these sizes do not contain DNA. In addition, it must be remembered that when performing isolated assessments, the degree of fragmentation may appear to decrease from one observation to the next. This is because fragments or cytoplasmic blebbing often forms around the time of cleavage, and these cytoplasmic blebs or fragments are often transient structures that disappear by resorption or lysis with time [58,59].

Implantation and pregnancy rates have been reported to be low when embryos with a high degree of fragmentation are transferred on Day 2 [8,9] or Day 3 [43], particularly when the volume of fragmentation exceeds 25% of the total embryo volume. This observation would equate to the observation that thawed Day 2 embryos have a similar implantation potential to fresh embryos unless they suffer blastomere loss, that is, one cell of a four-cell embryo is equivalent to a 25% volumetric loss [3]. Regular embryos with a minor degree of fragmentation (<10%) however have similar implantation potential to embryos with no fragmentation [9,10]. The consensus document published by ALPHA Scientists in Reproductive Medicine and ESHRE Special Interest Group of Embryology suggests that fragmentation should be classified as mild (<10%; Figure 7.7a), moderate (10%–25%; Figure 7.7b), and severe (>25%; Figure 7.7c) [24].

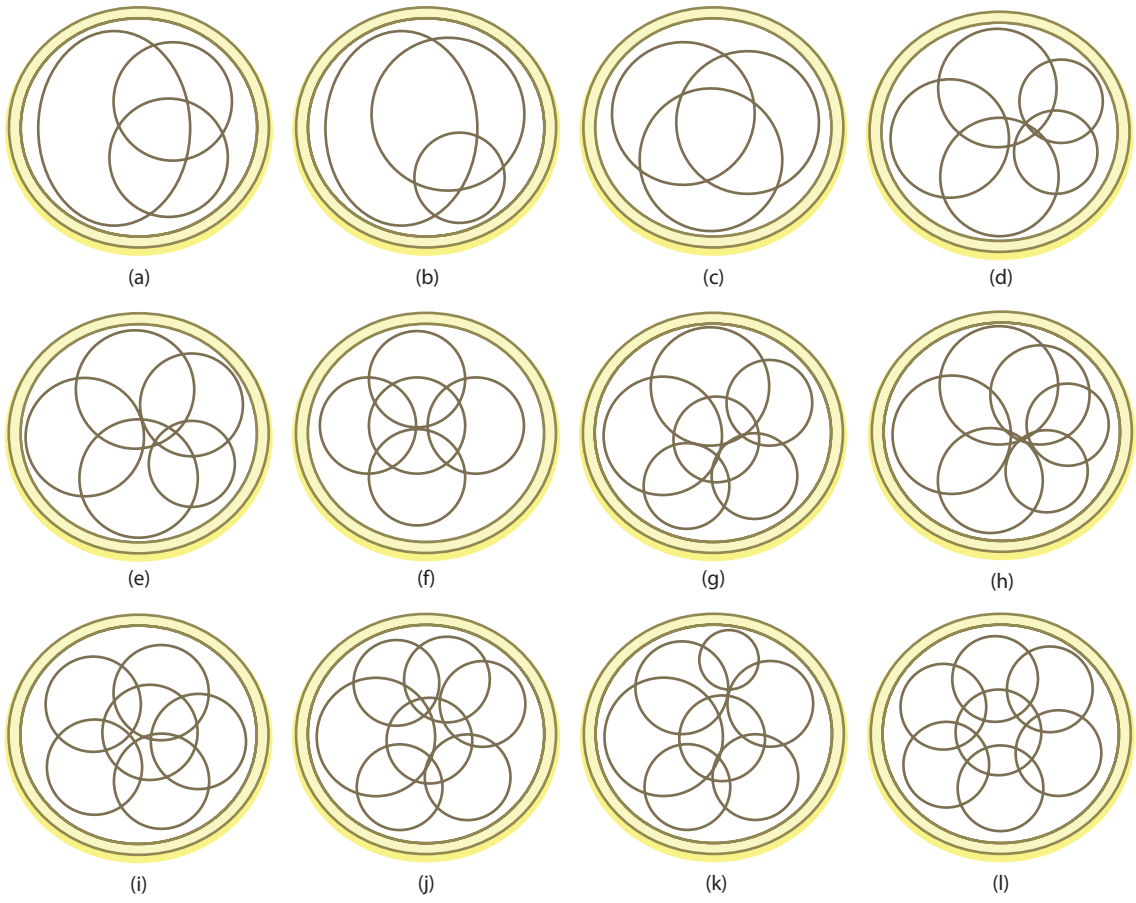

FIGURE 7.4 Diagrammatic representation of embryos on Days 2 and 3 that have undergone asynchronous division with regular cytokinesis or irregular cytokinesis. (a) Three-cell embryo showing regular cytokinesis in one of the two originating blastomeres. (b) Three-cell embryo showing irregular cytokinesis in one of the two originating blastomeres. (c) Three-cell embryo showing three equally sized blastomeres that is sometimes the result of the first mitotic division of a tripronucleate zygote. (d) Five-cell embryo showing regular cytokinesis in one of the four originating blastomeres. (e) Five-cell embryo showing irregular cytokinesis in one of the originating blastomeres. (f) Five-cell embryo showing irregular cytokinesis resulting in blastomeres of even size. (g) Six-cell embryo showing regular cytokinesis in two of the four originating blastomeres. (h) Six-cell embryo showing irregular cytokinesis in two of the four originating blastomeres. (i) Six-cell embryo showing irregular cytokinesis resulting in six blastomeres of even size. (j) Seven-cell embryo showing regular cytokinesis in three of the four originating blastomeres. (k) Seven-cell embryo showing irregular cytokinesis in one of the four originating blastomeres. (l) Seven-cell embryo showing irregular cytokinesis resulting in seven blastomeres of even size.

When the volume of fragmentation exceeds 25% of the total embryo volume, implantation and pregnancy rates have been reported to be low.

The reduction in implantation and pregnancy potential observed after the transfer of early cleavage stage embryos with a high degree of fragmentation (>25%) is likely to be due to the finding that these embryos, when cultured to the blastocyst stage, have a reduction in cell numbers in both the trophectoderm and inner cell mass. In contrast, embryos with mild-to-moderate fragmentation have a reduction in cell numbers in the trophectoderm only [60]. In addition, the rate of aneuploidy has been observed to increase with the degree of fragmentation [61–63].

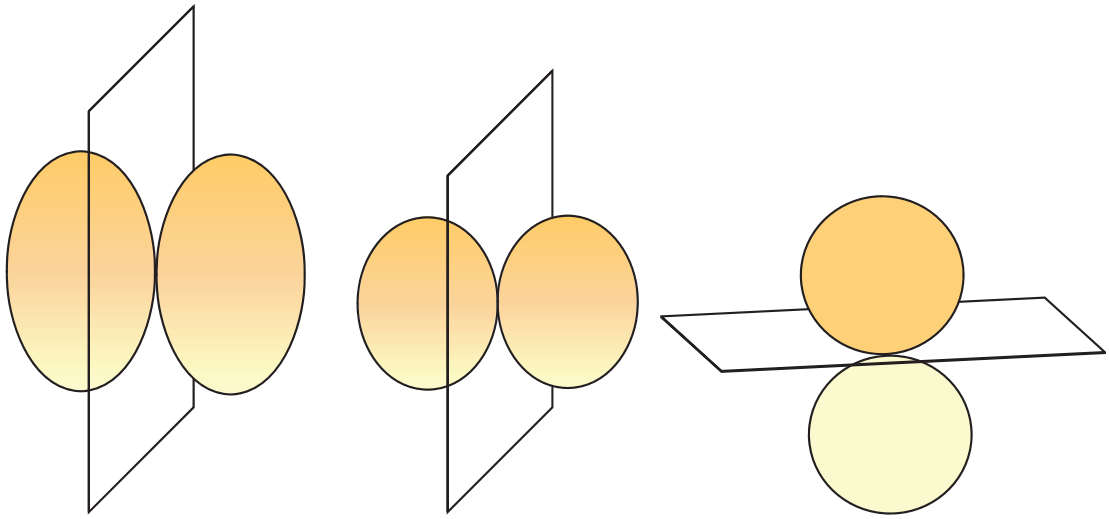

FIGURE 7.5 Diagrammatic representation of the first, second, and third mitotic divisions. (a) The first mitotic division is meridional; (b) the second mitotic division in one of the two originating blastomeres is meridional; and (c) the third mitotic division in the remaining blastomere is equatorial, resulting in a four-cell embryo with mixed inheritance patterns of organelles, proteins, and molecular message.

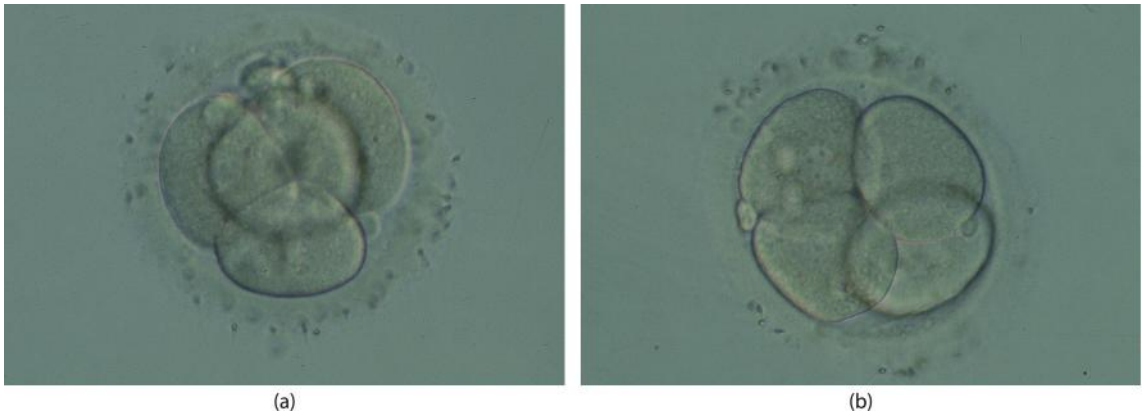

FIGURE 7.6 Examples of four-cell embryos showing different spatial distribution of blastomeres. (a) A four-cell embryo with tetrahedral arrangement of blastomeres expected as a result of the meridional and equatorial divisions. (b) A four-cell embryo showing a planar arrangement of blastomeres resulting in a clover-shaped embryo that may be reflective of disturbances in the normal cleavage patterns. Original magnification, 300×.

It has been suggested that the pattern of fragmentation is just as important as the extent of fragmentation to viability [10,53]. When the extent of fragments is similar but the fragments are scattered throughout the embryo rather than localized in one place in the perivitelline space, the implantation rate is compromised [10]. It has also been observed that there is a tendency toward a higher proportion of chromosomal errors in embryos with scattered fragments compared with embryos with localized fragments [62]. However, because time-lapse observations have shown that the position of fragments is dynamic, with fragments moving around and sometimes disappearing within the embryo, the consensus document published by ALPHA Scientists in Reproductive

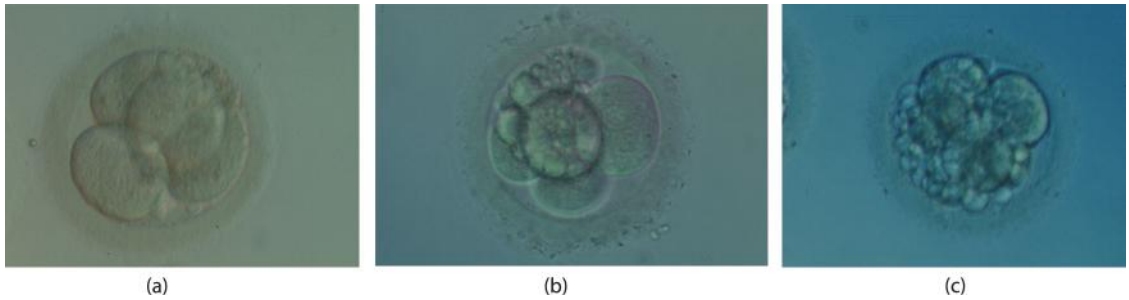

FIGURE 7.7 Examples of four-cell embryos showing different degrees of fragmentation. (a) Four-cell embryo with mild fragmentation, that is, <10% fragments. (b) Four-cell embryo with moderate fragmentation, that is, 10%–25% fragments. (c) Four-cell embryo with severe fragmentation, that is, >25% fragments. Original magnification, 300×.

Medicine and ESHRE Special Interest Group of Embryology concluded that no weight should be given to the spatial positioning of fragments in morphology scores [24].

Nuclear Status

It is not uncommon to observe a nucleus in one or more blastomeres during development, and this nucleation is dependent on the stage of the cell cycle at the time of observation, with the nucleus being visible only during interphase (Figure 7.8a). Because embryos are usually observed at a single discrete time point on any day of development, the incidence of multinucleation is probably underreported. In around one-third of all embryos, more than one nucleus can be observed within a single blastomere (Figure 7.8b) [64]. Multinucleation (two or more nuclei per blastomere) can be observed in embryos on Days 1–3; however, it is often more difficult to observe the nuclear status in embryos on Day 3 due to the smaller cell sizes [64]. The nuclei in a multinucleated blastomere may be of normal size (Figure 7.8b) or much smaller (micronuclei) (Figure 7.8c). Multinucleation is believed to arise through karyokinesis in the absence of cytokinesis; partial fragmentation of nuclei; or errors in chromosome segregation, packaging at mitosis, or both [65,66]. As a result, multinucleated embryos are associated with a high degree of chromosomal errors [47,62,63,66].

Embryo quality has been reported to be linked with nuclear status, with four-cell embryos on Day 2 and eight-cell embryos on Day 3 having a lower incidence of multinucleation than other cell numbers on these days [64]. Uneven cleavage has also been reported to be associated with a higher rate of multinucleation [47]. Transfer of

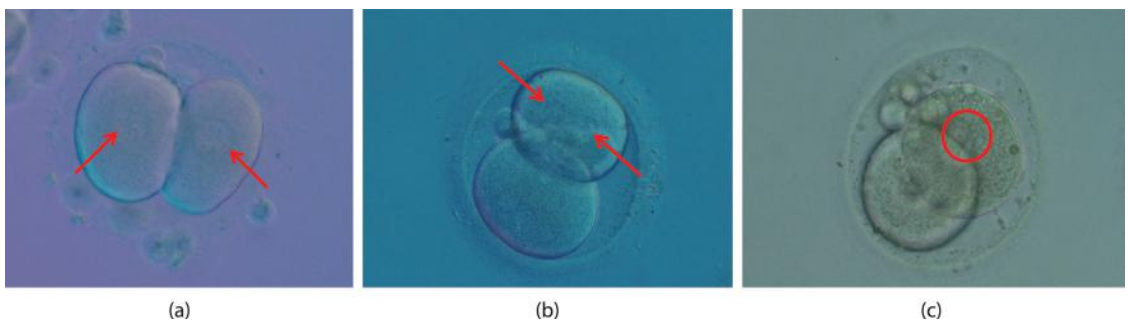

FIGURE 7.8 Examples of two-cell embryos showing different nucleation status. (a) Two-cell embryo showing a single nucleus in each blastomere (red arrows). (b) Two-cell embryo showing two nuclei in one blastomere (red arrows). (c) Two-cell embryo showing micronuclei in one blastomere (red circle delineates the micronuclei). Original magnification, 300×.

embryos with multinucleated blastomeres has been shown to result in lower implantation and pregnancy rates [47,64,67–70] and higher abortion rates [42].

It is generally agreed that embryos that have been identified, at some point in their development, to contain a multinucleated blastomere should not be selected for transfer if an alternative embryo is available [24]. However, it has been demonstrated that it is possible for binucleated cells on Day 1 to cleave to normal cells on Day 2 [66], and live births have been achieved, if less frequently, from the transfer of multinucleated embryos.

Cytoplasmic Anomalies

The cytoplasm of embryos is normally homogeneous in appearance and is normally pale and clear or slightly granular in appearance except perhaps around the time of cleavage, both before and immediately after, when significant organelle movement within the cytoplasm may result in a more granular appearance that may or may not be homogeneous at the time of observation. Several dysmorphisms have been identified in the cytoplasm of oocytes and cleavage-stage embryos and include cytoplasmic pitting, vacuoles, refractile bodies, plaques of smooth endoplasmic reticulum (sER), and the severe clustering of organelles that results in large areas, usually subcortical, of clear or "halo" cytoplasm [71]. With the possible exception of plaques of sER and severe clustering or centralization of organelles, there has been very little literature published on the impact of cytoplasmic dysmorphism on implantation outcome.

Cytoplasmic pitting is characterized by numerous tiny pits in the cytoplasm, resulting in a very granular appearance that may be associated with organelle reorganization, as mentioned above, before or immediately after cleavage. Studies have failed to identify any association between cytoplasmic pitting and implantation potential [14,72], but one study reported an increased incidence of early loss of gestational sacs after transfer of embryos showing cytoplasmic pitting [73].

Vacuoles are membrane-bound cytoplasmic inclusions filled with fluid [74]. Vacuoles can vary in size, number, and time of appearance during embryo development (see Chapter 5) [75]. Three different types of vacuoles can be identified: vacuoles arising within the oocyte, vacuoles artificially created during the intracytoplasmic sperm injection procedure, and vacuoles arising de novo during development [75]. Vacuolation de novo can occur throughout development but peaks at Day 4 of development when it is associated with developmental arrest [75]. It was observed that the later the vacuoles arose in the cytoplasm of the developing embryo, the greater the detrimental impact on blastocyst formation [75]. It has also been agreed that small vacuoles (<10 μm in diameter) have little consequence to development but that large vacuoles (>14 μm in diameter) can interfere with cleavage planes and result in reduction in development to the blastocyst stage [24].

Refractile bodies observed under bright-field microscopy are refractile due to the composition of lipid material and dense granules [76]. The lipid material has been demonstrated to be lipofuscin [77]. The presence of large refractile bodies (>5 μm in diameter) not only has an impact on fertilization but also results in significantly lower blastocyst developmental rates [77].

Plaques of sER can occasionally be identified in the cytoplasm of oocytes [78] and early cleavage-stage embryos [79]. Although similar in appearance, the localized accumulation of sER can be clearly differentiated from fluid-filled vacuoles at the light microscope level because they are translucent (see Chapter 5). The plaques can vary in size and can be as large as a pronucleus in diameter [78]. It has been reported that plaques of sER can perturb calcium signaling events and can have significant developmental consequences [24]. Once an oocyte that contains sER plaques is fertilized, there appears to be no impact on development to Day 4, but a significant reduction in the numbers of embryos developing to the blastocyst stage is noted [80]. Pregnancy outcomes after transfer of embryos from patients who produced oocytes with sER plaques are associated with a lower chance of successful pregnancy [78,80] regardless of whether the transferred embryo was derived from an oocyte containing an sER plaque. In addition, reports of fetal abnormalities [81] and in one case the birth of a child with the Beckwith–Wiedemann imprinting disorder [78] have been associated with patients who produce oocytes with sER plaques.

Occasionally, severe central clustering of organelles can be observed in one or more blastomeres of a cleavage-stage embryo, leaving a clear subcortical region or halo. It has been suggested that these blastomeres are destined to degenerate and that the resultant embryo has a reduced implantation potential [13,24].

Compaction

Up to Day 3 of development, each blastomere is a discrete entity, clearly distinguishable from the next blastomere. Between Day 3 and Day 4, tight junctions begin to form between neighboring blastomeres, and it becomes more difficult to distinguish one cell from the next. This process is known as compaction, and a completely compacted embryo is known as a morula. An ideal morula on Day 4 of development should contain between 16 and 32 cells, that is, it has undergone the fourth cleavage division or both the fourth and the fifth cleavage division [18] (Figures 7.1d and 7.9a). However, embryos can be observed on Day 4 that have initiated but not completed the compaction process, that is, partially compacted embryos (Figure 7.9b) or have failed to undergo the compaction process (Figure 7.9c).

The compaction process should begin on Day 3 at the eight-cell stage; however, compaction may be observed earlier in embryos with fewer than eight cells and this does not appear to have a negative impact on implantation potential [14]. A delay in the compaction process resulting in failure of, or partial compaction, on Day 4 may reflect a slight retardation in developmental kinetics, and given more time, these embryos may progress to complete compaction [18]. Alternatively, failure of, or partial compaction, in some embryos may be indicative of blastomeres with limited to no developmental potential, resulting in their exclusion from the compaction process and ultimately the formation of small compacted embryos with limited ability to form an inner cell mass of any appreciable size and viability when development progresses [18].

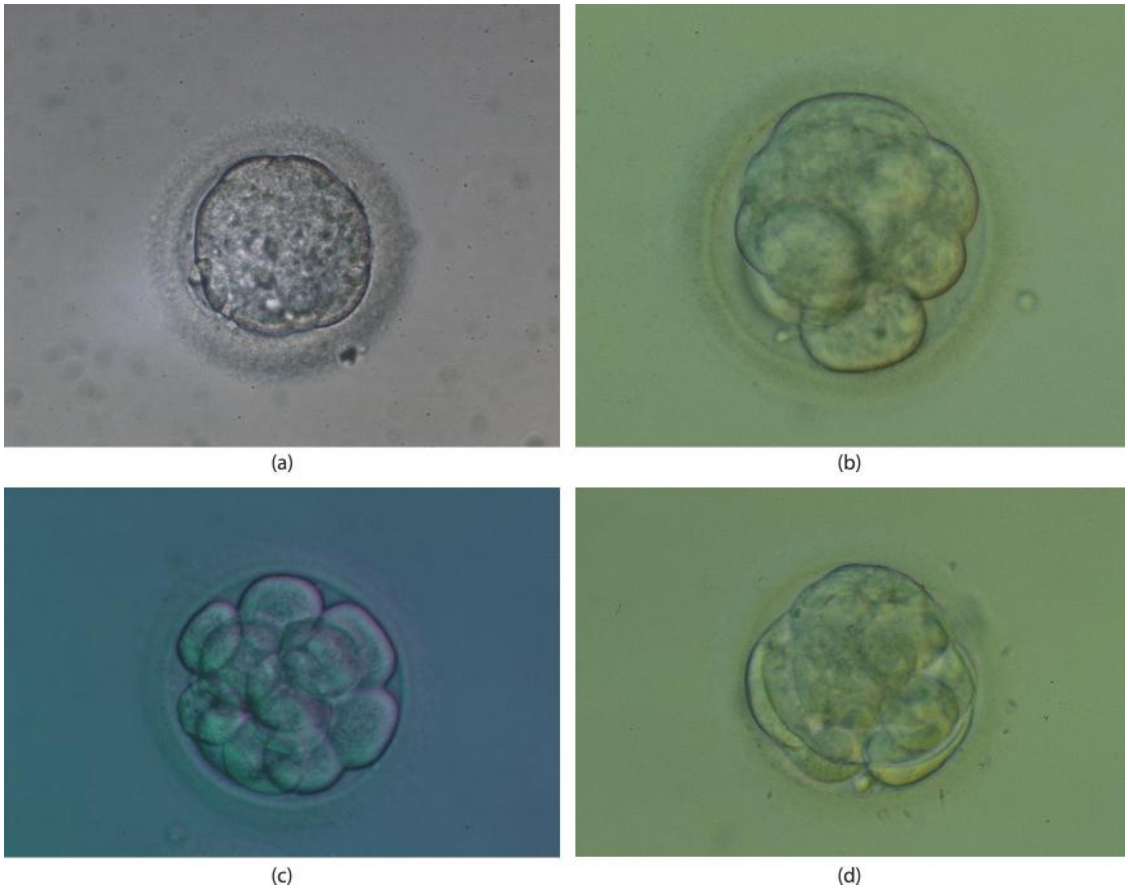

FIGURE 7.9 Examples of Day 4 embryos. (a) Fully compacted morula. (b) Partially compacted embryo. (c) Twelve-cell embryo showing little sign of compaction. (d) Cavitating morula. Original magnification, 300×.

Regardless of the reason for the incomplete or failed compaction, it is evident that this morphological feature is reflective of a reduction in viability that is most significant when compaction is completely absent. The consensus is that if more than half of the embryo is not involved in the compaction process by 92 ± 2 hr, these embryos have a reduced implantation potential [18,24]. Partially compacted embryos on Day 4 (at least half of the embryo is involved in the compaction process) have a similar implantation potential to fully compacted embryos, provided the embryo has entered the fourth cleavage division by Day 4 [23]; this finding concurs with our own observations (Vaxevanoglou, unpublished data).

Incomplete (more than half of the embryo is not involved in the compaction process by 92 ± 2 hr) or completely absent compaction is reflective of reduced viability, resulting in a reduced implantation potential.

Occasionally, advanced developmental kinetics can be observed on Day 4, with early signs of cavitation within the morula, the first step toward blastocyst formation (Figure 7.9d) [15,23,82]. These early cavitating embryos are associated with a very high implantation potential. Advanced developmental kinetics on Day 4 seems to confer an advantage to viability rather than being detrimental, as has been reported for early cleavage-stage embryos [8,9] where advanced developmental kinetics is more often associated with an increase in chromosomal abnormalities [27].

Conclusions

Morphology remains the gold standard for selecting the most viable embryo for transfer, and this is true for all stages of development. Genetic analysis of a Day 3 embryo or blastocyst-stage embryo can provide the additional advantage of selecting a chromosomally normal embryo, but biopsy for genetic analysis is not possible for embryos before Day 3.

Embryologists have reached consensus on the morphologic criteria that have the greatest predictive value in discriminating between viable and nonviable embryos on Days 2–4 (Tables 7.1 and 7.2) [24]:

1. The kinetics of development is probably the single most important predictor of normal development; therefore, it is essential that observations of embryo morphology are performed at fixed times as described in the consensus document. It is likely that in the next decade, continuous time-lapse observation of embryo morphology that is now available within incubators will reveal the ideal time intervals between successive cleavage divisions and further refine the predictive value of cleavage kinetics.

TABLE 7.1

Consensus Scoring System for Day 2 and Day 3 Embryos in Addition to the Ideal Cell Numbers at 44 ± 1 hr and 68 ± 1 hr Postinsemination

Grade	Rating	Description
1	Good	• <10% fragmentation • Stage-specific cell size • No multinucleation
2	Fair	• 10%–25% fragmentation • Stage-specific cell size for majority of cells • No multinucleation
3	Poor	• Severe fragmentation (>25%) • Cell sizes are not stage specific • Evidence of multinucleation

Source: ALPHA Scientists in Reproductive Medicine, ESHRE Special Interest Group of Embryology, *Hum Reprod* 26, 1270–1283, 2011.

TABLE 7.2

Consensus Scoring System for Day 4 Embryos

Grade	Rating	Description
1	Good	• Entered into fourth round of cleavage, i.e., >8 cells • Evidence of compaction that involves virtually all the embryo volume
2	Fair	• Entered into fourth round of cleavage, i.e., >8 cells • Compaction involves the majority of the embryo volume
3	Poor	• Disproportionate compaction involving less than half of the embryo with more than half of the embryo remaining as discrete blastomeres

Source: ALPHA Scientists in Reproductive Medicine, ESHRE Special Interest Group of Embryology, *Hum Reprod* 26, 1270–1283, 2011.

2. Blastomere size should be stage appropriate, that is, reflecting normal cytokinesis.
3. Fragmentation volume but not pattern was agreed to affect viability, particularly when it equated to approximately 25% or more of the embryo volume.
4. Multinucleation is best observed on Day 2, most likely due to the association of a high incidence of chromosomal error with multinucleation.
5. Day 4 embryos should have entered the fourth round of cleavage and should be compacted or compacting.
6. It must be remembered, however, that despite decades of linking embryo morphology to pregnancy potential, the predictive value of any one morphologic criterion remains low. The predictive value for pregnancy potential can be improved by combining several criteria and can be further improved by combining the observations over successive days of development (see Chapters 5, 6, and 8). However, morphological criteria improve the chances of selecting the best embryo within a cohort for transfer, but the chances of pregnancy remains a statistical probability rather than a certainty.

REFERENCES

1. Croxatto HB, Diaz S, Fuentaealba B, et al. Studies on the duration of egg transport in the human oviduct. I. The time interval between ovulation and egg recovery from the uterus in normal women. *Fertil Steril* 1972; 23: 447–458.
2. Braude P, Bolton V, Moore S. Human gene expression first occurs between the four- and eight-cell stages of preimplantation development. *Nature* 1988; 332: 459–461.
3. Edgar DE, Bourne H, Speirs AL, et al. A quantitative analysis of the impact of cryopreservation on the implantation potential of human early cleavage stage embryos. *Hum Reprod* 2000; 15: 175–179.
4. Cummins JM, Breen TM, Harrison KL, et al. A formula for scoring human embryo growth rates in in vitro fertilization: Its value in predicting pregnancy and in comparison with visual estimates of embryo quality. *J In Vitro Fert Embryo Transf* 1986; 3: 284–295.
5. Claman P, Armant DR, Seibel MM, et al. The impact of embryo quality and quantity on implantation and the establishment of viable pregnancies. *J In Vitro Fert Embryo Transf* 1987; 4: 218–222.
6. Puissant F, Van Rysselberge M, Barlow P, et al. Embryo scoring as a prognostic tool in IVF treatment. *Hum Reprod* 1987; 2: 705–708.
7. Steer CV, Mills CL, Tan SL, et al. The cumulative embryo score: A predictive embryo scoring technique to select the optimal number of embryos to transfer in an in-vitro fertilization and embryo transfer programme. *Hum Reprod* 1992; 7: 117–119.
8. Giorgetti C, Terriou P, Auquier P, et al. Embryo score to predict implantation after in-vitro fertilization: Based on 957 single embryo transfers. *Hum Reprod* 1995; 10: 2427–2431.
9. Ziebe S, Petersen K, Lindenberg S, et al. Embryo morphology or cleavage stage: How to select the best embryos for transfer after in vitro fertilization. *Hum Reprod* 1997; 12: 1545–1549.

10. Alikani M, Cohen J, Tomkin G, et al. Human embryo fragmentation in vitro and its implications for pregnancy and implantation. *Fertil Steril* 1999; 71: 836–842.
11. Gerris J, De Neubourg D, Mangelschots K, et al. Prevention of twin pregnancy after in vitro fertilization or intracytoplasmic sperm injection based on strict embryo criteria: A prospective randomized clinical trial. *Hum Reprod* 1999; 14: 2581–2587.
12. Van Royen E, Mangelschots K, De Neubourg D, et al. Characterization of a top quality embryo, a step towards single-embryo transfer. *Hum Reprod* 1999; 14: 2345–2349.
13. Veeck LL. Preembryo grading and degree of cytoplasmic fragmentation. In: *An Atlas of Human Gametes and Conceptuses: An Illustrated Reference for Assisted Reproductive Technology*. New York: Parthenon Publishing, 1999, pp. 46–51.
14. Desai NN, Goldstein J, Rowland DY, et al. Morphological evaluation of human embryos and derivation of an embryo quality scoring system specific for day 3 embryos: A preliminary study. *Hum Reprod* 2000; 15: 2190–2196.
15. Huisman GJ, Fauser BC, Eijkemans MJ, et al. Implantation rates after in vitro fertilization and transfer of a maximum of two embryos that have undergone three to five days of culture. *Fertil Steril* 2000; 73: 117–122.
16. Fisch JD, Rodriguez H, Ross R, et al. The Graduated Embryo Score (GES) predicts blastocyst formation and pregnancy rate from cleavage-stage embryos. *Hum Reprod* 2001; 16: 1970–1975.
17. De Placido G, Wilding M, Strina I, et al. High outcome predictability after IVF using a combined score for zygote and embryo morphology and growth rate. *Hum Reprod* 2002; 17: 2402–2409.
18. Tao J, Tamis R, Fink K, et al. The neglected morula/compact stage embryo transfer. *Hum Reprod* 2002; 17: 1513–1518.
19. Ebner T, Moser M, Sommergruber M, et al. Selection based on morphological assessment of oocytes and embryos at different stages of preimplantation development: A review. *Hum Reprod Update* 2003; 9: 251–262.
20. Baczkowski T, Kurzawa R, Głabowski W. Methods of embryo scoring in in vitro fertilization. *Reprod Biol* 2004; 4: 5–22.
21. Rienzi L, Ubaldi F, Iacobelli M, et al. Significance of morphological attributes of the early embryo. *Reprod Biomed Online* 2005; 10: 669–681.
22. Holte J, Berglund L, Milton K, et al. Construction of an evidence-based integrated morphology cleavage embryo score for implantation potential of embryos scored and transferred on day 2 after oocyte retrieval. *Hum Reprod* 2007; 22: 548–557.
23. Feil D, Henshaw RC, Lane M. Day 4 embryo selection is equal to Day 5 using a new embryo scoring system validated in single embryo transfers. *Hum Reprod* 2008; 23: 1505–1510.
24. ALPHA Scientists in Reproductive Medicine, ESHRE Special Interest Group of Embryology. The Istanbul consensus workshop on embryo assessment: Proceedings of an expert meeting. *Hum Reprod* 2011; 26: 1270–1283.
25. Prados FJ, Debrock S, Lemmen JG, et al. The cleavage stage embryo. In: *Atlas of Human Embryology: From Oocytes to Preimplantation Embryos* (eds. Magli MC, Jones GM, Lundin K, van den Abbeel E). *Hum Reprod* 2012; 27(Suppl 1): i22–i49.
26. Kola I, Trounson A, Dawson G, et al. Tripronuclear human oocytes: Altered cleavage patterns and subsequent karyotypic analysis of embryos. *Biol Reprod* 1987; 37: 395–401.
27. Magli MC, Gianaroli L, Munné S, et al. Incidence of chromosomal abnormalities from a morphologically normal cohort of embryos in poor-prognosis patients. *J Assist Reprod Genet* 1998; 15: 297–301.
28. Munné S. Chromosome abnormalities and their relationship to morphology and development of human embryos. *Reprod Biomed Online* 2006; 12: 234–253.
29. Finn A, Scott L, O'leary T, et al. Sequential embryo scoring as a predictor of aneuploidy in poor-prognosis patients. *Reprod Biomed Online* 2010; 21: 381–390.
30. Shoukir Y, Campana A, Farley T, et al. Early cleavage of in-vitro fertilized human embryos to the 2-cell stage: A novel indicator of embryo quality and viability. *Hum Reprod* 1997; 12: 1531–1536.
31. Sakkas D, Shoukir Y, Chardonnens D, et al. Early cleavage of human embryos to the two-cell stage after intracytoplasmic sperm injection as an indicator of embryo viability. *Hum Reprod* 1998; 13: 182–187.
32. Bos-Mikich A, Mattos AL, Ferrari AN. Early cleavage of human embryos: An effective method for predicting successful IVF/ICSI outcome. *Hum Reprod* 2001; 16: 2658–2661.
33. Lundin K, Bergh C, Hardarson T. Early embryo cleavage is a strong indicator of embryo quality in human IVF. *Hum Reprod* 2001; 16: 2652–2657.

34. Fenwick J, Platteau P, Murdoch AP, et al. Time from insemination to first cleavage predicts developmental competence of human preimplantation embryos in vitro. *Hum Reprod* 2002; 17: 407–412.
35. Salumets A, Hydén-Granskog C, Mäkinen S, et al. Early cleavage predicts the viability of human embryos in elective single embryo transfer procedures. *Hum Reprod* 2003; 18: 821–825.
36. Hammoud I, Vialard F, Casasnovas P, et al. How viable are zygotes in which the PN are still intact at 25 hours? Impact on the choice of embryo for transfer. *Fertil Steril* 2008; 90: 551–556.
37. Fu J, Wang XJ, Wang YW, et al. The influence of early cleavage on embryo developmental potential and IVF/ICSI outcome. *J Assist Reprod Genet* 2009; 26: 437–441.
38. Lee MJ, Lee RK, Lin MH, et al. Cleavage speed and implantation potential of early-cleavage embryos in IVF or ICSI cycles. *J Assist Reprod Genet* 2012; 29: 745–750.
39. Yang WJ, Hwu YM, Lee RK, et al. Early cleavage does not predict treatment outcome following the use of GnRH antagonists in women older than 35. *Fertil Steril* 2007; 88: 1573–1578.
40. Yang WJ, Hwu YM, Lee RK, et al. Early-cleavage is a reliable predictor for embryo implantation in the GnRH agonist protocols but not in the GnRH antagonist protocols. *Reprod Biol Endocrinol* 2009; 7: 20.
41. Thurin A, Hardarson T, Hausken J, et al. Predictors of ongoing implantation in IVF in a good prognosis group of patients. *Hum Reprod* 2005; 20: 1876–1880.
42. Scott L, Finn A, O'Leary T, et al. Morphologic parameters of early cleavage-stage embryos that correlate with fetal development and delivery: Prospective and applied data for increased pregnancy rates. *Hum Reprod* 2007; 22: 230–240.
43. Racowsky C, Stern JE, Gibbons WE, et al. National collection of embryo morphology data into Society for Assisted Reproductive Technology Clinic Outcomes Reporting System: Associations among day 3 cell number, fragmentation and blastomere asymmetry, and live birth rate. *Fertil Steril* 2011; 95: 1985–1989.
44. Hourvitz A, Lerner-Geva L, Elizur SE, et al. Role of embryo quality in predicting early pregnancy loss following assisted reproductive technology. *Reprod Biomed Online* 2006; 13: 504–509.
45. Ciray HN, Karagenç L, Ulug U, et al. Early cleavage morphology affects the quality and implantation potential of day 3 embryos. *Fertil Steril* 2006; 85: 358–365.
46. Hesters L, Prisant N, Fanchin R, et al. Impact of early cleaved zygote morphology on embryo development and in vitro fertilization-embryo transfer outcome: A prospective study. *Fertil Steril* 2008; 89: 1677–1684.
47. Hardarson T, Hanson C, Sjögren A, et al. Human embryos with unevenly sized blastomeres have lower pregnancy and implantation rates: Indications for aneuploidy and multinucleation. *Hum Reprod* 2001; 16: 313–318.
48. Magli MC, Gianaroli L, Ferraretti AP. Chromosomal abnormalities in embryos. *Mol Cell Endocrinol* 2001; 183: 29–34.
49. Wong CC, Loewke KE, Bossert NL, et al. Non-invasive imaging of human embryos before embryonic genome activation predicts development to the blastocyst stage. *Nat Biotechnol* 2010; 28: 1115–1121.
50. Meseguer M, Herrero J, Tejera A, et al. The use of morphokinetics as a predictor of embryo implantation. *Hum Reprod* 2011; 26: 2658–2671.
51. Antczak M, Van Blerkom J. Oocyte influence on early development: The regulatory proteins leptin and STAT 3 are polarized in mouse and human oocytes and differentially distributed within the cells of the preimplantation stage embryo. *Mol Hum Reprod* 1997; 3: 1067–1086.
52. Edwards RG, Beard HK. Oocyte polarity and cell determination in early mammalian embryos. *Mol Hum Reprod* 1997; 3: 863–905.
53. Antczak M, Van Blerkom J. Temporal and spatial aspects of fragmentation in early human embryos: Possible effects on developmental competence and association with the differential elimination of regulatory proteins from polarized domains. *Hum Reprod* 1999; 14: 429–447.
54. Gulyas BJ. A reexamination of cleavage patterns in eutherian mammalian eggs: Rotation of blastomere pairs during second cleavage of the rabbit. *J Exp Zool* 1975; 193: 235–248.
55. Edwards RG, Hansis C. Initial differentiation of blastomeres in 4-cell human embryos and its significance for early embryogenesis and implantation. *Reprod Biomed Online* 2005; 11: 206–218.
56. Ebner T, Maurer M, Shebl O, et al. Planar embryos have poor prognosis in terms of blastocyst formation and implantation. *Reprod Biomed Online* 2012; 25: 267–272.
57. Johansson M, Hardarson T, Lundin K. There is a cutoff limit in diameter between a blastomere and a small anucleate fragment. *J Assist Reprod Genet* 2003; 20: 309–313.

58. Hardarson T, Löfman C, Coull G, et al. Internalization of cellular fragments in a human embryo: Time-lapse recordings. *Reprod Biomed Online* 2002; 5: 36–38.
59. Van Blerkom J, Davis P, Alexander S. A microscopic and biochemical study of fragmentation phenotypes in stage-appropriate human embryos. *Hum Reprod* 2001; 16: 719–729.
60. Hardy K, Stark J, Winston RML. Maintenance of the inner cell mass in human blastocysts from fragmented embryos. *Biol Reprod* 2003; 68: 1165–1169.
61. Ziebe S, Lundin K, Loft A, et al. FISH analysis for chromosomes 13, 16, 18, 21, 22, X and Y in all blastomeres of IVF pre-embryos from 144 randomly selected donated human oocytes and impact on pre-embryo morphology. *Hum Reprod* 2003; 18: 2575–2581.
62. Magli MC, Gianaroli L, Ferraretti AP, et al. Embryo morphology and development are dependent on the chromosomal complement. *Fertil Steril* 2007; 87: 534–541.
63. Munné S, Chen S, Colls P, et al. Maternal age, morphology, development and chromosome abnormalities in over 6000 cleavage-stage embryos. *Reprod Biomed Online* 2007; 14: 628–634.
64. Van Royen E, Mangelschots K, Vercruyssen M, et al. Multinucleation in cleavage stage embryos. *Hum Reprod* 2003; 18: 1062–1069.
65. Pickering SJ, Taylor A, Johnson MH, et al. An analysis of multinucleated blastomere formation in human embryos. *Hum Reprod* 1995; 10: 1912–1922.
66. Staessen C, Van Steirteghem A. The genetic constitution of multinuclear blastomeres and their derivative daughter blastomeres. *Hum Reprod* 1998; 13: 1625–1631.
67. Jackson KV, Ginsburg ES, Hornstein MD, et al. Multinucleation in normally fertilized embryos is associated with an accelerated ovulation induction response and lower implantation and pregnancy rates in in vitro fertilization-embryo transfer cycles. *Fertil Steril* 1998; 70: 60–66.
68. Pelinck MJ, De Vos M, Dekens M, et al. Embryos cultured in vitro with multinucleated blastomeres have poor implantation potential in human in-vitro fertilization and intracytoplasmic sperm injection. *Hum Reprod* 1998; 13: 960–963.
69. Moriwaki T, Suganuma N, Hayakawa M, et al. Embryo evaluation by analysing blastomere nuclei. *Hum Reprod* 2004; 19: 152–156.
70. Saldeen P, Sundström P. Nuclear status of four-cell preembryos predicts implantation potential in in vitro fertilization treatment cycles. *Fertil Steril* 2005; 84: 584–589.
71. Van Blerkom J, Henry G. Oocyte dysmorphism and aneuploidy in meiotically mature human oocytes after ovarian stimulation. *Hum Reprod* 1992; 7: 379–390.
72. Rienzi L, Ubaldi F, Minasi MG, et al. Blastomere cytoplasmic granularity is unrelated to developmental potential of day 3 human embryos. *J Assist Reprod Genet* 2003; 20: 314–317.
73. Ebner T, Tews G, Sommergruber M, et al. Cytoplasmic pitting has a negative influence on implantation outcome. *J Assist Reprod Genet* 2005; 22: 239–344.
74. Van Blerkom J. Occurrence and developmental consequences of aberrant cellular organization in meiotically mature human oocytes after exogenous ovarian hyperstimulation. *J Electron Microsc Tech* 1990; 16: 324–346.
75. Ebner T, Moser M, Sommergruber M, et al. Occurrence and developmental consequences of vacuoles throughout preimplantation development. *Fertil Steril* 2005; 83: 1635–1640.
76. Veeck LL. Abnormal morphology of the human oocyte and conceptus. In: *An Atlas of Human Gametes and Conceptuses: An Illustrated Reference for Assisted Reproductive Technology*. New York: Parthenon Publishing, 1999, pp. 121–166.
77. Otsuki J, Nagai Y, Chiba K. Lipofuscin bodies in human oocytes as an indicator of oocyte quality. *J Assist Reprod Genet* 2007; 24: 263–270.
78. Otsuki J, Okada A, Morimoto K, et al. The relationship between pregnancy outcome and smooth endoplasmic reticulum clusters in MII human oocytes. *Hum Reprod* 2004; 19: 1591–1597.
79. Makabe S, Naguro T, Nottola SA, et al. Ultrastructural dynamic features of in vitro fertilization in humans. *Ital J Anat Embryol* 2001; 106(2 Suppl 2): 11–20.
80. Ebner T, Moser M, Shebl O, et al. Prognosis of oocytes showing aggregation of smooth endoplasmic reticulum. *Reprod Biomed Online* 2008; 16: 113–118.
81. Akarsu C, Cağlar G, Vicdan K, et al. Smooth endoplasmic reticulum aggregations in all retrieved oocytes causing recurrent multiple anomalies: Case report. *Fertil Steril* 2009; 92: 1496e1–1496e3.

8

Morphological Selection of Gametes and Embryos: Blastocyst

Thomas Ebner

Introduction

Morula or blastocyst stage marks the switch from a cell cluster of individual blastomeres to a relatively smooth mass with indistinguishable cell outlines capable of actively regulating its internal environment. Thus, any prolongation of in vitro culture will allow for a more accurate prediction of developmental capacity. Other potential advantages of blastocyst culture include synchronization between developmental stage of the embryo and the uterine milieu, reduction of multiple pregnancy rate, or indirect selection of chromosomal anomalies.

Prolonged culture to blastocyst stage (Days 4–6 of preimplantation development) is certainly not a new approach. Some 20 years ago, acceptable blastocyst formation rates as high as 40% were already reported [1]; however, associated pregnancy data indicate that blastocyst development does not automatically correspond to implantation potential. Obviously, it is important to differentiate between the ability of a particular culture system (e.g., culture medium, embryo density, type of incubator, oxygen tension) to support blastocyst formation in vitro and the potential of the said system to give rise to a viable blastocyst [2].

Change from a cleavage stage to a blastocyst transfer program requires a proper adaption strategy.

If a clinical embryologist needs to address the problem of changing a cleavage-stage transfer program into a blastocyst program, it is recommended to start working with supernumerary embryos first. Once a successful Day 2 or Day 3 transfer has been performed, further culture of sibling embryos may indicate whether a given culture system is capable of creating blastocysts at all. It should be kept in mind that the quality of the leftover embryos should be comparable with that of embryos transferred to allow for proper prediction of culture system quality. Thus, good-prognosis patients with sufficient embryos in abundance (e.g., more than five, to seven) should preferably be considered for training purposes.

In cases where a regular blastocyst formation rate of 40%–50% is reached and the quality of the developed blastocysts appears appropriate, one could proceed to transfer (and/or cryopreserve) them. However, if the opposite scenario is encountered, every effort needs to be made to increase the rate of blastulation.

Old-fashioned methods such as coculture with Vero have become rather obsolete because the improved understanding of both the physiological changes in oviduct and uterus and the different metabolic needs of the cleavage-stage and the blastocyst-stage embryos led to the development of a new generation of sequential and global culture media. If a change of media supplier is a nonissue, it is good to know that almost all major players provide simple as well as complex media. However, if the decision is made to persevere with feeder cells, in situ coculture with attached cumulus cells (as the result of an incomplete denudation process) that turned out to be advantageous in terms of blastocyst formation [3] would be a more commonly used technique.

Apart from somatic cells, stimulatory effects may also derive from neighboring embryos. Thus, grouping embryos in culture (in contrast to single culture) would facilitate accumulation of autotrophic factors that in turn have been found to be beneficial for blastulation [4]. Obviously, this is a balancing act because optimal embryo density, for example, the maximum number of embryos in a given volume of culture medium, is uncertain, as is

the actual negative impact of decomposition products such as ammonium. To be on the safe side for blastocyst culture, most clinical embryologists tend to change the culture medium on Day 3, regardless of the type (global or sequential) of medium used.

Usually, the above mentioned minor changes in culture conditions should result in acceptable survival rates to Day 5. Only in the event of little avail would major changes of the laboratory setup need to be considered, provided that physical premises (e.g., pH, temperature) are fulfilled. One such adaption would be the use of lowered incubator oxygen tension (approximately 5% instead of 20%), a tension that has been reported to support development to blastocyst stage and live birth rate [5,6].

Low oxygen tension in the incubator has been reported to support development to blastocyst stage and live birth rate.

Assuming that a sufficient number of blastocysts of acceptable quality will finally be available, adequate scoring of the grown concepti is of particular importance for selecting the best candidates for transfer. To avoid comparing apples and oranges in in vitro fertilization (IVF)-intracytoplasmic sperm injection (ICSI), timing of fertilization and embryo development is crucial. In this respect, an international consensus was reached [7] emphasizing that on Day 4, the first possible day of blastocyst formation, morphological scoring should be done at 92 ± 2 hr postinsemination. Typically, on the fifth day of in vitro culture (116 ± 2 hr), preimplantation development should culminate in the formation of the blastocyst. Once fully developed, human blastocysts consist of two different cell types: an outer layer of trophectoderm (TE) responsible for the accumulation of fluid in the blastocyst cavity and specialized for implantation and an inner cell mass (ICM) forming all three germ layers of the fetus.

Scoring of Blastocysts

Establishment of blastocyst transfer programs as a matter of routine came along with two key requirements: the need of an efficient cryopreservation program and an easily applicable blastocyst scoring system. In the early years of blastocyst grading, particular attention was focused on developmental stage, for example, degree of blastocyst expansion [8,9]. A more recent scoring system [10] took additional morphological parameters into consideration, namely, morphology of the ICM and TE. To summarize, according to the degree of expansion, blastocysts were scored using numbers in ascending order ranging from Grade 1 (Figure 8.1 [1]; blastocyst cavity less than half of the volume of the embryo) to Grade 6 (completely hatched blastocyst). Beginning with the full blastocyst stage (Figure 8.2; Grade 3), additional assessment of ICM and TE could be done (based on cell number and cohesion) to predict developmental competence.

For reasons of accuracy, the more detailed Gardner approach [10] gained acceptance and allowed for reducing the number of transferred blastocysts without limiting pregnancy rate [11]. A randomized prospective evaluation compared the two scoring systems [12]. Although similar numbers of blastocysts were transferred in comparable patient cohorts, the Gardner score turned out to be superior to the Dokras score in terms of implantation (37.6% vs. 25.0%) and multiple pregnancy (38.6% vs. 17.1%).

Blastocysts of different qualities can be grown per patient, making an optimized blastocyst scoring system indispensable.

Blastocyst Cell Number

A factor in common to both scoring systems is the emphasis on blastocyst expansion (e.g., the size of the blastocoel). Expansion of blastocyst on Day 5 or Day 6 ranges from retarded morula to expanded or even hatching blastocyst stage (Figure 8.3). Although most embryologists rely on visual judgment rather than measuring

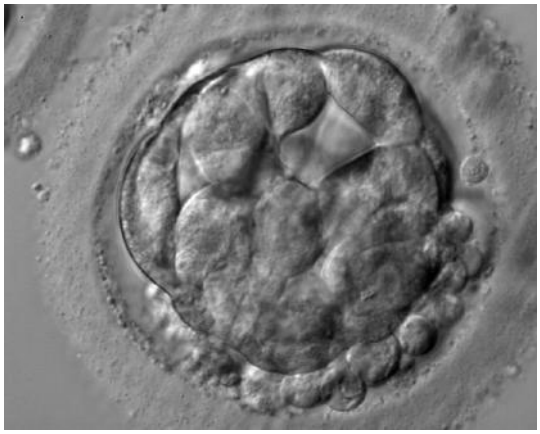

FIGURE 8.1 Early blastocyst with blastocoel taking up less than half of the volume. Fragments are extruded into the perivitelline space.

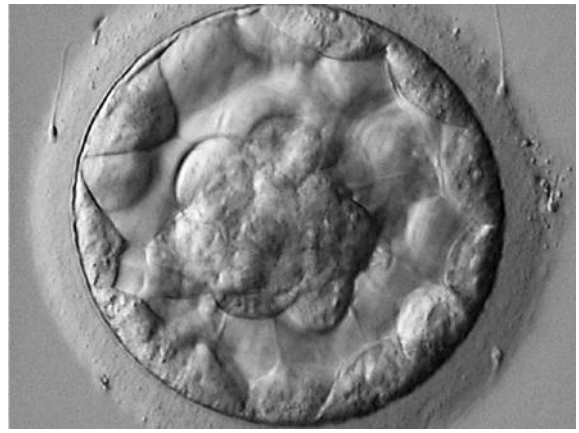

FIGURE 8.2 Full IVF blastocyst with optimal cell lineages (3AA).

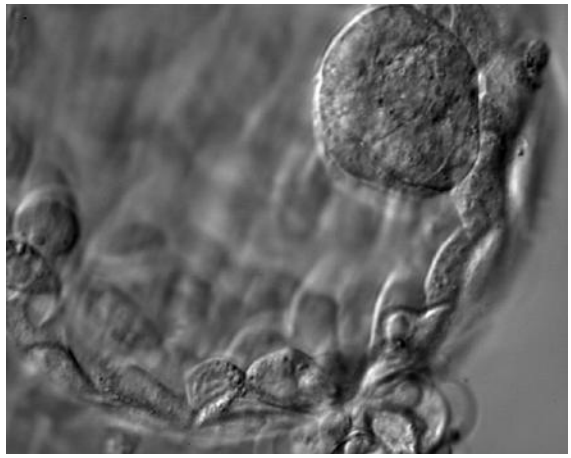

FIGURE 8.3 Optimal blastocyst showing hatching site close to the inner cell mass (5AA).

blastocyst diameter, Shapiro et al. [13] accurately measured blastocysts before transfer and found that the diameter of a transferred blastocyst was the most significant variable in predicting clinical pregnancy.

In this context, a high variability in cell numbers has been observed. The mitotic activity is considered to be a reliable indicator of blastocyst viability and developmental capacity [14]; however, to count the actual number of nuclei in a blastocyst, its cells have to be fixed.

Although it has been suggested [15] that noninvasive assessment of the total cell number (TCN) is possible under good microscopical optics, the majority of studies on TCN were performed using stained cells of spare blastocysts donated to research (often of reduced quality) and thus probably not representing the actual cell number of healthy blastocysts.

On Day 5, cell number of blastocysts ranged from 42 to 58 [1,16–18]. However, using sequential media, the rate of mitosis was found to be increased, for example, from 64 to 111 cells on Day 5 [19] and, on average, 167 cells on Day 6 [20]. It can be summarized that a full human blastocyst at Day 5 of development should exceed 60 cells and at least have its cell number doubled on Day 6.

Predictably, any process that severely reduces cytoplasmic volume of the embryo will cause a dramatic loss of cells at the blastocyst stage, if at all this stage is reached. Indeed, one report [21] describes that blastomere loss after cryopreservation resulted in significantly lower blastocyst cell numbers on Day 6 ($n = 45$) compared with blastocysts derived from fully intact cleavage-stage embryos after thawing ($n = 58$). Extensive fragmentation at earlier stages showed the same detrimental effect on TCN on Day 6 [22], for example, a significant decrease in cell count from 69 (embryos without fragmentation) to 29 (>25% fragmentation). Interestingly, for minimal and moderate levels of fragmentation, the reduction in cell number was largely confined to the TE, whereas a steady number of ICM cells were maintained. This finding suggests a homeostatic regulation of the lineage that gives rise to the fetus [22].

Cell Lineages

Hardy et al. [1] realized certain differences in the growth rate of both cell types. In general, mitotic rate of the TE is approximately 1.5 times higher than that of the ICM; however, compared with some other mammals, the overall proportion of the ICM is approximately 33% of all cells on Day 5 and 51% on Day 6 [1]. The striking peak on Day 6, with half of all cells in the blastocyst being part of the ICM, may be the result of increase in ICM growth rate between Day 5 and Day 6, a time when the number of TE cells is more or less unchanged. Because there is widespread cell death of even morphologically normal cells in both cell lineages [1], it is suspected that the preservation of cell number within cell lineages is regulated by apoptotic phenomena [23].

Inner Cell Mass

The health of a blastocyst is not only strongly dependent on the overall cell number [24] but also on the proper formation of both cell lineages. According to the scoring system of Gardner and Schoolcraft [10], the embryoblast is considered to be optimal (Grade A) if the ICM shows a tight package of numerous cells (Figures 8.2 through 8.4). Any reduction in number and contact affected the quality of this cell lineage; thus, loosely grouped cell accumulations are scored Grade B (Figures 8.5 through 8.7), whereas absence (Figures 8.8 through 8.10) or presence of only few cells randomly distributed within the cavity of the blastocyst are classified as Grade C.

Quantitative grading of the ICM emphasized the importance of its size and shape [25]. In contrast to blastocyst expansion and TE cell number, ICM size was significantly related to implantation. Blastocysts showing an ICM <3800 μm^2 showed lower implantation rates (18%) compared with blastocysts with an ICM >4500 μm^2 (45%).

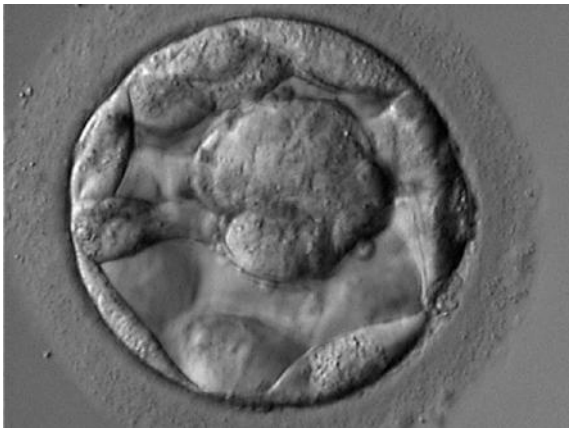

FIGURE 8.4 Full blastocyst with optimal inner cell mass and impaired trophectoderm (3AB).

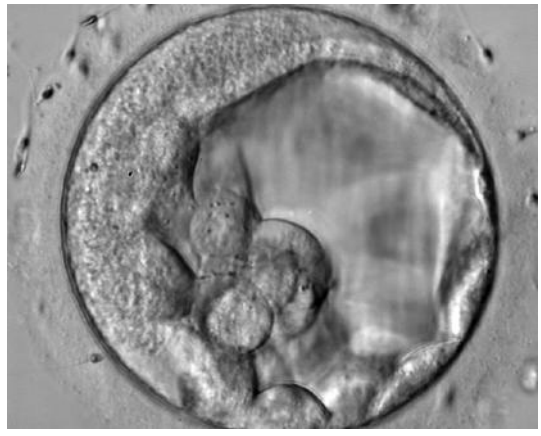

FIGURE 8.5 Suboptimal full blastocyst (3BC) developed after conventional IVF. Trophectoderm is not cohesive between 6 o'clock and 2 o'clock positions. Inner cell mass consists of few cells only.

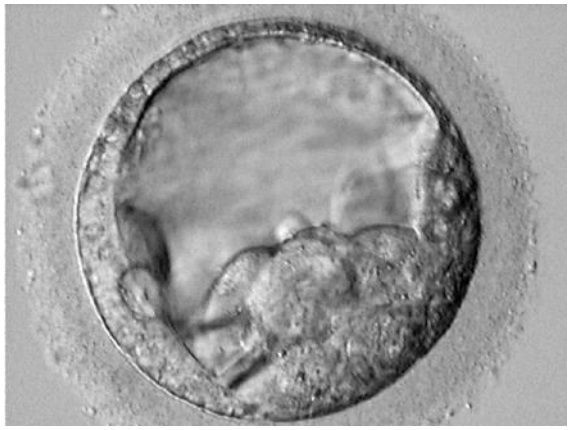

FIGURE 8.6 Full blastocyst with optimal inner cell mass but bad quality TE (3AC).

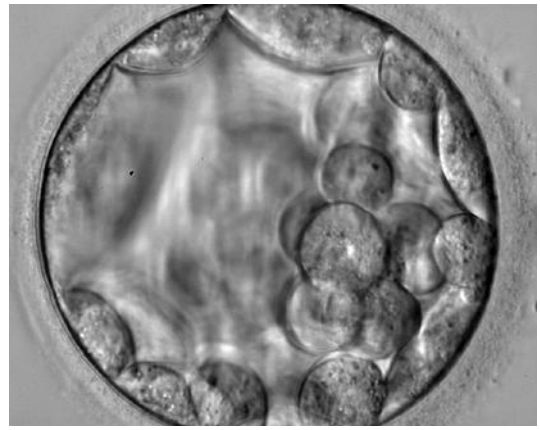

FIGURE 8.7 Expanded blastocyst with both cell lineages consisting of few cells (4BB).

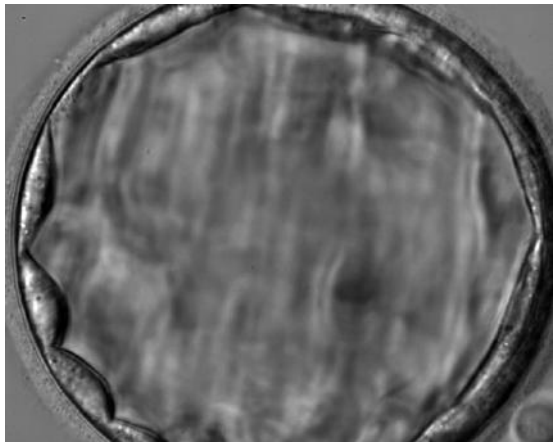

FIGURE 8.8 Hatching (5 o'clock position) blastocyst without inner cell mass and with reduced trophectoderm (5CB).

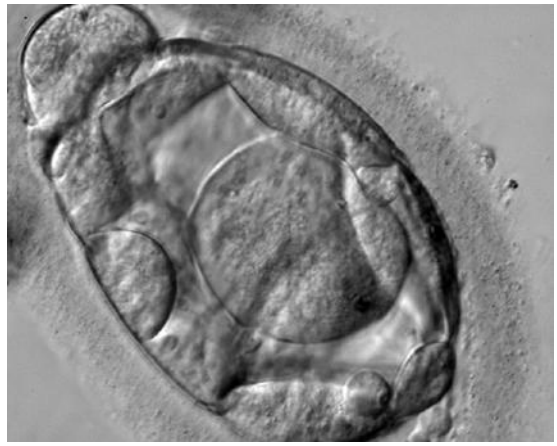

FIGURE 8.9 Ovoid full blastocyst with blastomeres extruded into perivitelline space (11 o'clock position) and blastocoel (3CB).

It has to be clarified that these studies [25] measured blastocysts of different sizes, for example, ranging from full to expanded stage. Recent data indicate that the size of the embryoblast is closely related to the degree of expansion [26]. This seems to be associated with a more peripheral location of the cell mass within the blastocyst cavity as the blastocyst expands, an increased cohesion within ICM cells, or both. The latter is further supported by the observation that at full blastocyst stage, the number of ICM cells can still be estimated, while at expanded stage, the number cannot be identified accurately. Taking these data into consideration, it was not surprising that Richter et al. [25] noticed a reduction in ICM size of Day 6 blastocysts compared with Day 5 blastocysts.

In addition, the above mentioned study [25] evaluated the possible influence of ICM shape on outcome by introducing the roundness index (RI), an index that represents the length-to-width proportion of the ICM (Figure 8.11). Extreme RI values of <1.04 (almost round) and >1.20 (too oval) had a worse prognosis (implantation rates of 7% and 33%, respectively) compared with those with intermediate RI. Implantation rates were highest for embryos with both optimal ICM size and shape.

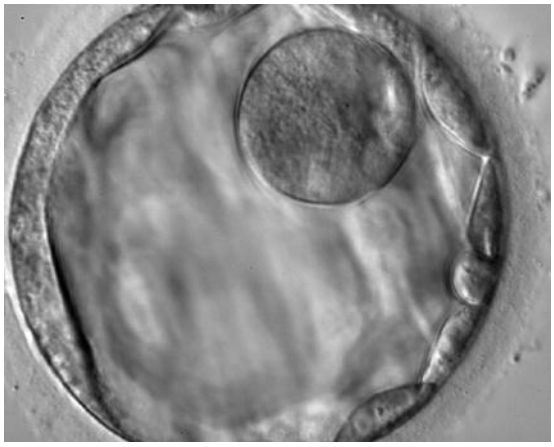

FIGURE 8.10 Expanded blastocyst of poor quality (4CB). Blastomere extruded into blastocoel should not be mixed up with inner cell mass.

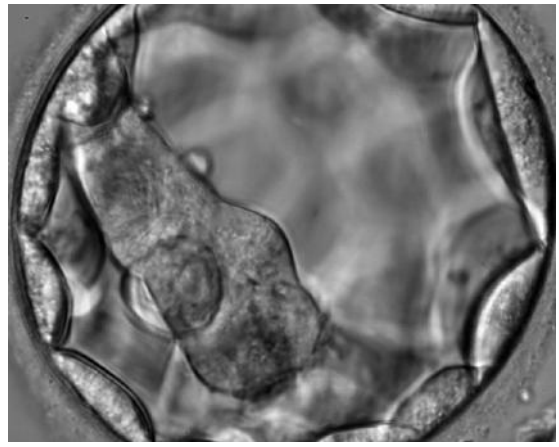

FIGURE 8.11 Expanded blastocyst of good quality (4AA) with ovoid inner cell mass (roundness index 2.0).

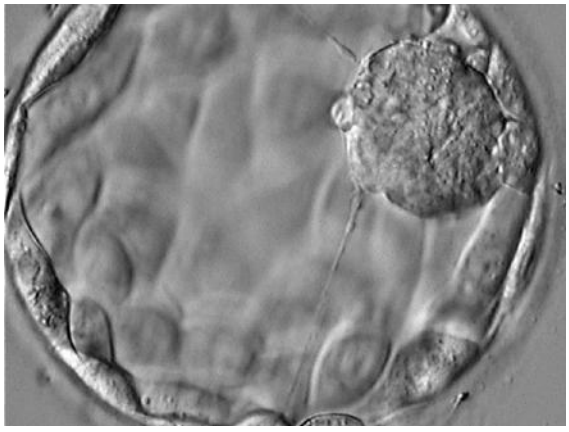

FIGURE 8.12 Expanded IVF blastocyst (4AA) with necrotic area in trophectoderm (8 o'clock position). Two cytoplasmic processes bridge the blastocoel.

FIGURE 8.13 Full blastocyst with both cell lineages consisting of few cells (3BB).

Striving to replace blastocyst with large ICM, embryologists should not forget that disproportionately oversized ICMs, for example, with apoptotic processes not working properly [22], could cause problems in maintaining healthy central cells because of the increased distance over which nutrients and oxygen have to diffuse or they could contribute to large-offspring syndrome [27].

Trophectoderm

TE can be classified in the same way as ICM [10]. The outer layer is considered to be optimal if it consists of numerous sickle-shaped cells (Figures 8.2, 8.11, and 8.12), forming a cohesive epithelium (Grade A). If number and cohesion of these cells are reduced or shows several gaps, the TE is scored B (Figures 8.4, 8.8, 8.10, 8.13, and 8.14). The worst-case scenario (Grade C) would be a TE consisting of very few larger cells with a low number of tight junctions (Figures 8.5 and 8.6).

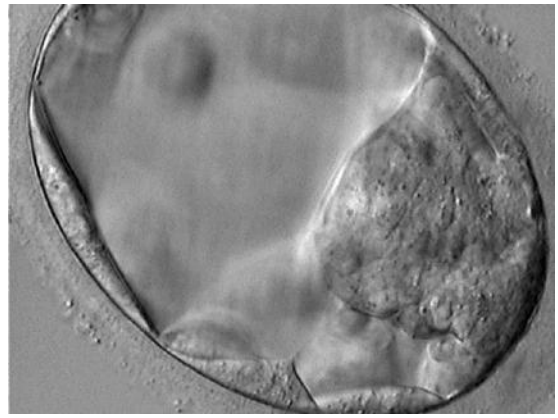

FIGURE 8.14 Expanded blastocyst of ovoid shape (4AB).

Recent studies suggest that of all blastocyst parameters, TE is the only significant independent predictor of live birth outcome.

Kovacic et al. [28] noted a 36% implantation rate in blastocysts showing an impaired trophoblast (e.g., flattened cells; no sickle-shaped cells; no junctions between TE cells; cells with granulation, pigmentation, vacuolization, or a combination), and other studies supported these findings [13]. Some studies [13,28] could not find any difference between the mean number of TE cells and the occurrence of a clinical pregnancy. One should keep in mind that they evaluated the number of TE cells in one single focal plane only, which might be an over- or underestimate of the actual quality of the TE. However, it can be hypothesized that any preliminary reduction in TE cell number could easily be compensated by the accelerated growth rate from Day 6 onward [1].

This is in contrast to the recent findings [29] that suggest that a decrease in the quality of TE had an almost linear relationship to a reduced rate of live births. In detail, all three morphological parameters had a significant effect on live birth; however, once adjusted for known significant confounders (e.g., female age, number of good-quality embryos, follicle-stimulating hormone [FSH] dosage), it was shown that TE was the only significant independent predictor of live birth outcome. In another retrospective study by the same working group [30] data from fresh single blastocyst transfers could be confirmed analyzing vitrified/warmed single blastocyst transfers. Others reported [31] that TE morphology is significantly related to the rates of ongoing pregnancy and miscarriage. Interestingly, the only data prospectively collected in a large multicenter trial revealed that it is rather the degree of expansion and hatching than the quality of both cell lineages that predicts outcome [32].

Bad-Quality Blastocysts

Only a limited number of papers analyzed the fate of bad-quality blastocysts [28,33]. This group of blastocysts with poor prognosis is usually associated with lower cell numbers and a higher degree of chromosomal disorders [33,34]. Bad-quality blastocysts consist of numerous different morphological subtypes, such as blastocysts with excessive fragmentation, excluded blastomeres, and necrotic cells, as well as trophoblast vesicles. Trophoblast vesicles are characterized by the absence of the ICM [35] and a rudimentary TE with only a minor number of cells (Figure 8.15). Transfer of trophoblast vesicles resulted in a disastrous live birth rate of approximately 7% [28].

The fate of all the other inferior blastocyst variations, although they may show acceptable ICMs or TEs, will also be compromised by excluded fragments, blastomeres, or both (Figures 8.1 and 8.16) [1]. These cellular remnants are accompanied by reduced cell numbers on Day 5 [22] and an impaired hatching process [36]. Live birth rate (approximately 17%) in these bad-quality blastocysts were found to be slightly higher than that of trophoblast vesicles [28].

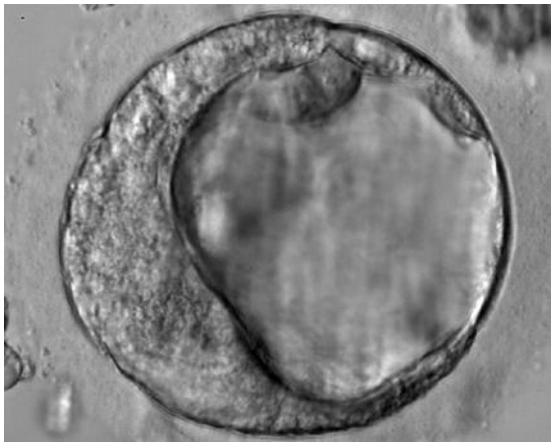

FIGURE 8.15 Pseudoblastocyst presumably consisting of <12 cells.

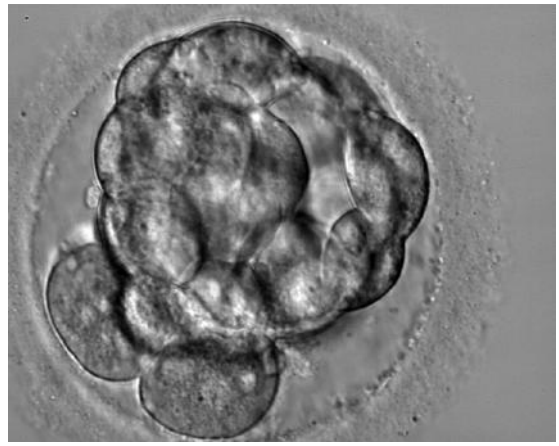

FIGURE 8.16 Early blastocyst showing exclusion of two blastomeres.

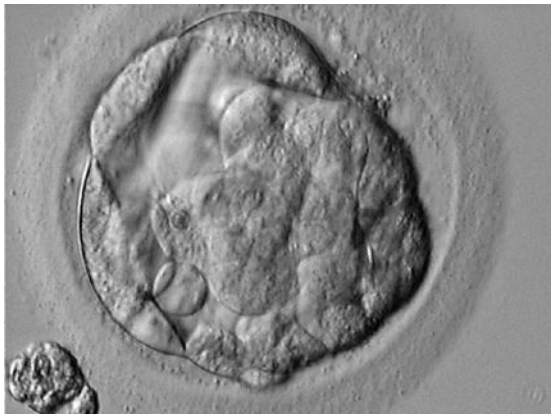

FIGURE 8.17 Transition of early to full blastocyst stage. The expansion of the blastocoel is more than half of the volume, and intended location of the inner cell mass can be estimated.

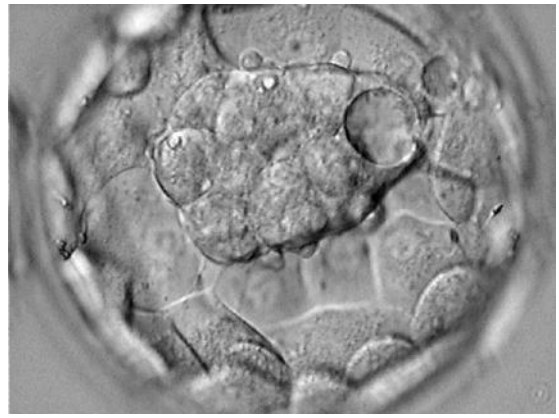

FIGURE 8.18 Expanded IVF blastocyst (4AA) with inner cell mass showing a large vacuole.

Transfer of blastocysts showing necrotic foci in one of the cell lineages (Figure 8.17) [2,3] is a common phenomenon (Figure 8.12). A study that assessed the actual location of such degenerative areas indicated that outcome was worse if the ICM was affected (23% live births) and slightly better if only the TE was affected (32.8%). Consequently, ICM compactness and multicellularity contributed more to vital implantation than TE cohesiveness [28].

Vacuolization of blastocysts could have a detrimental effect on developmental capacity as well (Figure 8.18). It has been reported that approximately one-third of Day 5 blastocysts showed vacuoles [37]. It appears that elimination of vacuoles from the ICM is a common scenario [37] because the majority of vacuoles could be located in the TE [37,38], indicating that embryos might develop strategies to minimize a negative impact of vacuolization on implantation behavior. Reports of pregnancies achieved after transfer of vacuolated blastocysts are rare; however, prognosis was much better if vacuolization was restricted to the TE [37].

Another important morphological characteristic is the presence of cytoplasmic extensions (Figure 8.12) bridging the blastocyst cavity at the full or later stages (Grades 3–6). These processes are commonly present in half of the junctional TE cells spanning the boundary between the polar and the mural region of TE and are

directed toward the surface of the ICM [39]. These cytoplasmic strings are thought to be related to the flow of cells from the polar to the mural TE; consequently, they tend to withdraw as the cells reach their final location. Interestingly, variations in both shape (from broad triangles to string-like projections) and length (some fail to reach the ICM surface) have been observed [39]. Persistence of cytoplasmic processes up to hatching stage possibly marks blastocysts of developmental lability.

Interestingly, blastocysts of ovoid shape (Figures 8.9 and 8.14) seem to have the same genetic risk and implantation potential as their round counterparts. The only striking finding is a delayed growth in these blastocysts deriving from ovoid oocytes due to a reduced number of cell–cell contacts at four-cell stage [40].

Spontaneous Hatching

Regardless of its respective quality, every blastocyst surviving until expanding stage is forced to escape from its zona pellucida (ZP) to not face total arrest of development. In vitro spontaneous hatching of the human embryo is rather supported by the tremendous increase of internal pressure caused by both a gradual accumulation of fluid and preferential proliferation of TE. The degree to which calcium-activated K^+ channels are involved in the process of hatching is currently under discussion [41].

In the absence of the uterine milieu, the hatching process usually starts with small vesicles protruding through the ZP. It should be kept in mind that this blebbing does not necessarily indicate the precise location of subsequent hatching [38]. Once a small opening has been created, the TE starts to herniate and, governed by TE projections, a larger opening is created by mechanical forces. Additional help may come from blastocyst "breathing" [38], a sequence of collapses and reexpansions considered to assist final extrusion from the ruptured ZP (Figure 8.19).

In humans, hatching occurs at various regions of the ZP. Although some studies suggest that blastocysts show hatching sites mainly close to the ICM [35], Sathananthan et al. [36] postulated that most of the blastocysts hatch from the abembryonic pole. Considering the proportions within a blastocyst, the likelihood of blastocysts hatching from the smaller embryonic site is much lower than the chance of herniating near the rather extensive mural TE. A recent study [42] supports the latter theory because out of all hatching blastocysts (Grade 5), <40% showed a zona breach close to the embryonic pole.

It seems that human blastocysts have a developmental benefit if they hatch adjacent to the ICM, irrespective of whether it is focused on fresh [42] or thawed blastocysts [43]. Because this area corresponds to the cells (syncytiotrophoblast) that will later drive invasion into the endometrium, theoretically, hatching close to the ICM would accelerate contact between those TE cells that are supposed to draw the blastocyst into the uterine wall and the endometrium. This mutual interaction between blastocyst and uterus may be impaired or delayed if herniation takes place opposite the ICM, if hatching difficulties occur, or both.

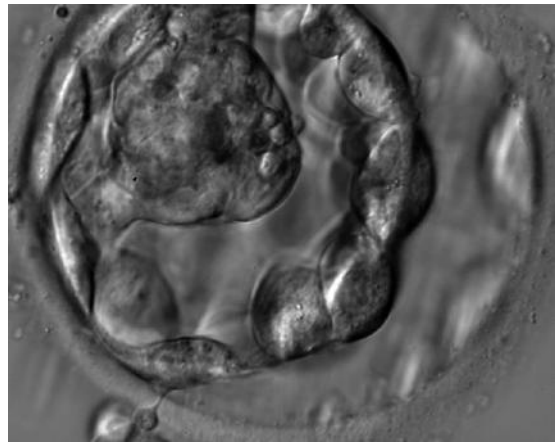

FIGURE 8.19 Hatching (7 o'clock position) blastocyst of optimal quality (5AA) during collapsing phase (breathing).

Conclusions

Blastocyst culture as the method of choice for all patients is a balancing act and could result in inacceptable rates of cycle cancellation. However, it should be kept in mind that prolonged culture to the blastocyst stage might be associated with negative scenarios.

First, an almost threefold incidence of monozygotic twinning (5.6% vs. 2%) was observed in blastocyst transfers compared with cleavage-stage transfers [44]. Others identified blastocyst culture as the major risk in terms of monozygotic twinning, whereas embryo freezing, type of stimulation protocol used, ICSI fertilization, or zona removal did not influence its incidence [45]. The other suggested risk with blastocyst culture is a theoretical change in methylation patterns, resulting in affected birth weights. A couple of studies found a significantly lower birth weight in children born from blastocyst transfer compared with cleavage-stage transfer [46,47]. These results have not been unchallenged [48]. Interestingly, the opposite was indicated when the birth weights of children were analyzed according to the length of embryo culture [49]. With increasing time in culture from Day 2 to Day 6, an increase in the proportion of large for gestational age (LGA) babies was found.

However, one prerequisite for optimizing blastocyst culture, transfer, and cryopreservation is to develop a better understanding of morphological criteria to adequately predict implantation potential of a certain blastocyst.

Identifying the blastocyst with the highest implantation potential paves the way to single embryo transfer.

Usually, several blastocysts of different qualities can be grown per patient, making an optimized blastocyst scoring system indispensable. With the current trend toward a significant reduction of the number of embryos considered for transfer, every effort should be made to filter out the blastocyst with the highest implantation potential.

Thus, it is recommended to weigh the morphological criteria at the blastocyst stage as follows: quality of the ICM, quality of the TE, expansion (e.g., blebbing out of the zona at the embryonic pole), and few anomalies (excluded blastomeres, vacuoles, necrotic foci, cytoplasmic strings). There is increasing evidence that the impact of the TE on live birth is at least the one of the ICM. In order to identify the actual potential of TE, multilayer analysis is recommended. If semiautomatic grading of human blastocysts [50] is the way to proceed may be questioned.

REFERENCES

1. Hardy K, Handyside AH, Winston RM. The human blastocyst: Cell number, death and allocation during late preimplantation development in vitro. *Development* 1989; 107: 597–604.
2. Gardner DK, Lane M. Culture and selection of viable blastocysts: A feasible proposition for human IVF? *Hum Reprod Update* 1997; 3: 367–382.
3. Ebner T, Moser M, Sommergruber M, et al. Incomplete denudation of oocytes prior to ICSI enhances embryo quality and blastocyst development. *Hum Reprod* 2006; 21: 2972–2977.
4. Ebner T, Shebl O, Moser M, et al. Group culture of human zygotes is superior to individual culture in terms of blastulation, implantation and life birth. *Reprod Biomed Online* 2010; 21: 762–768.
5. Kovacic B, Vlaisavljević V. Influence of atmospheric versus reduced oxygen concentration on development of human blastocysts in vitro: A prospective study on sibling oocytes. *Reprod Biomed Online* 2008; 17: 229–236.
6. Meintjes M, Chantilis SJ, Douglas JD, et al. A controlled randomized trial evaluating the effect of lowered incubator oxygen tension on live births in a predominantly blastocyst transfer program. *Hum Reprod* 2009; 24: 300–307.
7. Alpha Scientists in Reproductive Medicine. Istanbul consensus workshop on embryo assessment: Proceedings of an expert meeting. *Reprod Biomed Online* 2011; 32: 632–646.
8. Dokras A, Sargent IL, Ross C, et al. The human blastocyst: Its morphology and HCG secretion in vitro. *Hum Reprod* 1991; 6: 1143–1151.

9. Dokras A, Sargent IL, Barlow DH. Human blastocyst grading: An indicator of developmental potential. *Hum Reprod* 1993; 8: 2119–2127.
10. Gardner DK, Schoolcraft WB. In vitro culture of human blastocysts. In: *Towards Reproductive Certainity: Infertility and Genetics Beyond 1999* (eds. Jansen R, Mortimer D). Carnforth: Parthenon Press, 1999, pp. 378–388.
11. Gardner DK, Lane M, Stevens J, et al. Blastocyst score affects implantation and pregnancy outcome: Towards a single blastocyst transfer. *Fertil Steril* 2000; 73: 1155–1158.
12. Balaban B, Yakin K, Urman B. Randomized comparison of two different blastocyst grading systems. *Fertil Steril* 2006; 85: 559–563.
13. Shapiro BS, Daneshmand ST, Garner FC, et al. Large blastocyst diameter, early blastulation, and low preovulatory serum progesterone are dominant predictors of clinical pregnancy in fresh autologous cycles. *Fertil Steril* 2008; 90: 302–309.
14. Brinsko SP, Ball BA, Miller PG, et al. In vitro development of day 2 embryos obtained from young, fertile mares and aged, subfertile mares. *J Reprod Fertil* 1994; 102: 371–378.
15. Bongso A. Defining blastocyst quality. In: *Handbook on Blastocyst Culture* (ed. Bonso A). Singapore: Sydney Press Indusprint, 1999, pp. 62–79.
16. Winston NJ, Braude PR, Pickering SJ, et al. The incidence of abnormal morphology and nucleocytoplasmic ratios in 2–, 3– and 5–day human pre-embryos. *Hum Reprod* 1991; 6: 17–24.
17. Van Blerkom J. Development of human embryos to the hatched blastocyst stage in the presence or absence of a monolayer of Vero cells. *Hum Reprod* 1993; 8: 1525–1539.
18. Vlad M, Walker D, Kennedy RC. Nuclei number in human embryos co-cultured with human ampullary cells. *Hum Reprod* 1996; 11: 1678–1686.
19. Dumoulin JCM, Derhaag JG, Bras M, et al. Growth rate of human preimplantation embryos is sex dependent after ICSI but not after IVF. *Hum Reprod* 2005; 20: 484–491.
20. Fong CY, Bongso A. Comparison of human blastulation rates and total cell number in sequential culture media with and without co-culture. *Hum Reprod* 1998; 14: 774–781.
21. Archer J, Gook DA, Edgar DH. Blastocyst formation and cell numbers in human frozen-thawed embryos following extended culture. *Hum Reprod* 2003; 18: 1669–1673.
22. Hardy K, Stark J, Winston RML. Maintenance of the inner cell mass in human blastocysts from fragmented embryos. *Biol Reprod* 2003; 68: 1165–1169.
23. Hardy K, Stark J. Mathematical models of the balance between apoptosis and proliferation. *Apoptosis* 2002; 7: 373–381.
24. Matsuura K, Hayashi N, Takiue C, et al. Blastocyst quality scoring based on morphologically grading correlates with cell number. *Fertil Steril* 2010; 94: 1135–1137.
25. Richter KS, Harris DC, Daneshmand ST, et al. Quantitative grading of human blastocyst: Optimal inner cell mass size and shape. *Fertil Steril* 2001; 76: 1157–1167.
26. Ebner T, Vanderzwalmen P, Shebl O, et al. Morphological aspects of human blastocysts and the impact of vitrification. *J Reprod Med Endocrinol* 2011; 8: 13–20.
27. Leese HJ, Donnay I, Thompson JG. Human assisted conception: A cautionary tale. Lessons from domestic animals. *Hum Reprod* 1998; 13 (Suppl 4): 184–202.
28. Kovacic B, Vlaisavljevic V, Reljic M, et al. Developmental capacity of different morphological types of day 5 human morulae and blastocysts. *Reprod Biomed Online* 2004; 8: 687–694.
29. Ahlström A, Westin C, Reismer E, et al. Trophectoderm morphology: An important parameter for predicting live birth after single blastocyst transfer. *Hum Reprod* 2011; 27: 89–96.
30. Ahlström A, Westin C, Reismer E, et al. Prediction of live birth in frozen-thawed single blastocyst transfer cycles by pre-freeze and post-thaw morphology. *Hum Reprod* 2013; 28: 1199–1209.
31. Honnma H, Baba T, Sasaki M, et al. Trophectoderm morphology significantly affects the rates of ongoing pregnancy and miscarriage in frozen-thawed single-blastocyst transfer cycle in vitro fertilization. *Fertil Steril* 2012; 98: 361–367.
32. Van den Abbeel E, Balaban B, Ziebe S, et al. Association between blastocyst morphology and outcome of single-blastocyst transfer. *Reprod Biomed Online* 2013; 27: 353–361.
33. Hardarson T, Caisander G, Sjögren A, et al. A morphological and chromosomal study of blastocysts developing from morphologically suboptimal human pre-embryos compared with control blastocysts. *Hum Reprod* 2003; 18: 399–407.

34. Alfarawati S, Fragouli E, Colls P, et al. The relationship between blastocyst morphology, chromosomal abnormality, and embryo gender. *Fertil Steril* 2011; 95: 520–524.
35. Ménézo YJR, Kaufmann R, Veiga A, et al. A mini-atlas of the human blastocyst in vitro. *Zygote* 1999; 7: 61–65.
36. Sathananthan H, Menezes J, Gunasheela S. Mechanisms of human blastocyst hatching in vitro. *Reprod Biomed Online* 2003; 7: 228–234.
37. Ebner T, Moser M, Sommergruber M, et al. Occurrence and developmental consequences of vacuoles throughout preimplantation development. *Fertil Steril* 2005; 83: 1635–1640.
38. Veeck LL, Zaninovic N. Human blastocysts in vitro. In: *An Atlas of Human Blastocysts* (eds. Veeck L, Zaninovic N). London: Parthenon Publishing, 2003, pp. 99–137.
39. Gardner RL. Flow of cells from polar to mural trophectoderm is polarized in the mouse blastocyst. *Hum Reprod* 2000; 15: 694–701.
40. Ebner T, Shebl O, Moser M, et al. Developmental fate of ovoid oocytes. *Hum Reprod* 2008; 23: 62–66.
41. Lu YC, Ding GL, Yang J, et al. Small-conductance calcium-activated K (+) channels 3 (SK3) regulate blastocyst hatching by control of intracellular calcium concentration. *Hum Reprod* 2012; 27: 1421–1430.
42. Ebner T, Gruber I, Moser M. Location of herniation predicts implantation behaviour of hatching blastocysts. *J Turk Ger Gynecol Assoc* 2007; 8: 184–188.
43. Miyata H, Matsubayashi H, Fukutomi N, et al. Relevance of the site of assisted hatching in thawed human blastocysts: A preliminary report. *Fertil Steril* 2010; 94: 2444–2447.
44. Milki AA, Jun SH, Hinckley MD, et al. Incidence of monozygotic twinning with blastocyst transfer compared to cleavage-stage transfer. *Fertil Steril* 2003; 79: 503–506.
45. Kawachiya S, Bodri D, Shimada N, et al. Blastocyst culture is associated with an elevated incidence of monozygotic twinning after single embryo transfer. *Fertil Steril* 2011; 95: 2140–2142.
46. Källén B, Finnström O, Lindam A, et al. Blastocyst versus cleavage stage transfer in in vitro fertilization: Differences in neonatal outcome? *Fertil Steril* 2010; 94: 1680–1683.
47. Nakashima A, Araki R, Tani H, et al. Implications of assisted reproductive technologies on term singleton birth weight: An analysis of 25,777 children in the national assisted reproduction registry of Japan. *Fertil Steril* 2013; 99: 450–455.
48. Fernando D, Halliday JL, Breheny S, et al. Outcomes of singleton births after blastocyst versus nonblastocyst transfer in assisted reproductive technology. *Fertil Steril* 2012; 97: 579–584.
49. Mäkinen S, Söderström-Anttila V, Vainio J, et al. Does long in vitro culture promote large for gestational age babies? *Hum Reprod* 2013; 28: 828–834.
50. Santos Filho E, Noble JA, Poli M, et al. A method for semi-automatic grading of human blastocyst microscope images. *Hum Reprod* 2012; 27: 2641–2548.

9

Noninvasive Techniques: Gamete Selection—Sperm

Victoria Sánchez, Joachim Wistuba, and Con Mallidis

Introduction

The ultimate aim of any sperm selection method is to provide the best-quality sperm possible so as to maximize the outcome of whatever assisted reproductive technology (ART) procedures are to be undertaken. For artificial insemination and in vitro fertilization (IVF), the main requirement is the provision of a sample enriched with progressive motile sperm, because these techniques are dependent on the ability of sperm to find and penetrate the oocyte by themselves. To this end, several preparatory techniques have been developed, the most used of which have been detailed in the preceding chapter.

With the advent of intracytoplasmic sperm injection (ICSI), many of the elements of the aforementioned techniques were circumvented; consequently, the onus for sperm selection shifted from motility to other parameters more influential for ICSI itself, namely, sperm morphology, content, function, and nuclear DNA integrity. The purpose of this chapter is not to list every technique that has been developed or trialed but rather to present the most common clinically used of these methods to describe their underlying principle, detail the procedure, and discuss the advantages and disadvantages of each. As an adjunct, an exciting new use of a relatively old technique that holds the potential of noninvasive and nondestructive sperm selection is also presented.

Microscopy Beyond Morphology

Since Antoni van Leeuwenhoek first trained his microscope on the secretion "born from the seed of the genitals of animals" [1], the microscope has been central to the evaluation of semen. In the ensuing centuries, a multitude of publications have focused on the microscopic description of sperm and their qualities, with morphology being the predominant criterion considered by embryologists for their selection of sperm to be used in ICSI. The importance of sperm morphology and its associations with ARTs is dealt in depth in Chapter 4; here we describe a feature beyond morphological "normalcy."

Polarization Microscopy

Background

In contrast to the evaluation of oocytes with polarizing light, where it has been used to locate the spindle and assess the thickness of the zona pellucida, the use of polarizing light to appraise sperm quality is a relatively new development. The principle behind such measurements is that the nucleoprotein filaments together with the arrangement and orientation of the acrosome affect the birefringence, that is, the refractive index based on polarization and direction of propagated light, in such a way that it is indicative of the sperm's health and maturity [2]. Because these aspects are associated with nuclear (n)DNA integrity, birefringent appearance has been suggested as a further selection criterion of sperm, and as such many studies have incorporated polarized light microscopy into their conventional ICSI system [2–6].

BOX 9.1 APPLYING POLARIZATION MICROSCOPY FOR SPERM SELECTION

Overview

A. Preparation
B. Examination
C. Selection

Instrumentation and Materials

- ICSI system normally used (e.g., inverted microscope, Hoffman contrast, motorized micromanipulators)
- Polarizing and analyzing lenses (20× or 63×)
- Polyvinylpyrrolidone solution (PVP) (7%)
- Mineral oil

Procedure

A. Preparation
  A.1. Obtain the sperm suspension by the method routinely used (e.g., swim-up, density gradient centrifugation).
  A.2. Dilute the resulting suspension to 3×10^6/mL.
  A.3. Place 1 µL of sperm suspension in 10 µL drops of PVP covered with oil.
  A.4. Incubate at room temperature for 30 min [5].
B. Birefringence examination
  B.1. Observe on the inverted microscope equipped with polarizing and analyzing lenses.
  B.2. Identify the birefringent sperm.
  B.3. Observe whether the birefringence is displayed in the complete head or only partially in the posta–crosomal region.
C. Sperm selection
  C.1. Select sperm with micromanipulators that
    – Are birefringent
    – Show partial birefringence (post–acrosomal region) because these are reacted and should be better for ICSI [4]
    – Do not have vacuoles

Pros and Cons

Pros	Cons
• Can be performed on living sperm • Using a 63× objective, vacuoles can also be distinguished in both birefringent and nonbirefringent sperm [4], thereby providing more information for selection • Acrosome-reacted sperm, reported to be beneficial for ICSI [4], can be identified • Identification of birefringent sperm is relatively easy and does not add significantly to workload	• Expensive equipment • Only a limited number of groups use and few studies performed on the method • Further validation of the method's clinical performance is still needed

Sperm Binding

Selection based on the ability or inability to bind various substances presents an attractive option because, in theory, the process does not interfere with structure, affect viability, or endanger the genetic contents of the sperm. The type of separation that is achievable is dependent on the properties of the binding substrate, such as the preference for mature sperm (hyaluronic acid [HA] [7]), apoptotic cells (Annexin V, Yo Pro 1), and an affinity for disrupted DNA (oligopeptide p53 [8]). A further advantage of the approach is that the underlying principle allows for its adaptation to several sorting techniques (e.g., magnet-activated cell sorting [MACS], flow cytometry, and glass wool filtration).

Magnet-Activated Cell Sorting

Background

Regardless of the binding substance used, the underlying aspects of MACS are similar, that is superparamagnetic microbeads that have been conjugated with the binding substrate are incubated with the sperm to allow for binding, and then the resulting amalgams are placed into a magnetic field that entraps the beads that have sperm bound to them. The sperm that do not bind and therefore are not restricted in their passage can be collected and are thus available for use (Figure 9.1).

MACS sperm selection before ART has been reported to improve pregnancy rates and to be safe and reliable [9], although the extent of the latter is not yet clear. The efficacy of the technique has reportedly been improved when it is used in combination with sperm preparation methods (e.g., density gradient), in that it achieves better sperm yields in terms of apoptosis, motility, vitality, and DNA integrity [10–12].

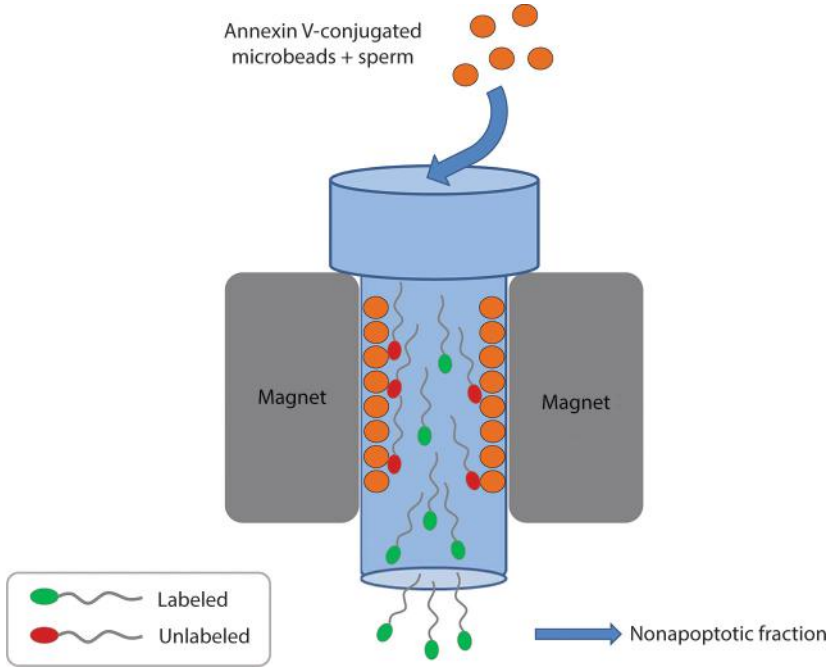

FIGURE 9.1 Schematic of the MACS system. A sperm suspension is incubated with Annexin V-conjugated microbeads and loaded onto the separation column that is exposed to a magnetic field. Apoptotic sperm that have externalized phosphatidylserine on the cell surface are bound to the microbeads (red) and thus remain in the column, leaving nonapoptotic sperm (green) to pass through and be collected.

BOX 9.2 APPLYING MACS

Although the following description is based on separation using Annexin V [9], as stated above, the basis of the protocol is similar for other binding substrates.

Overview

A. Setup
B. Labeling
C. Separation

Instrumentation and Materials

- MiniMACS™ Starting kit (e.g., Miltenyi Biotec GmbH, Germany)
  This kit contains
  - Separator
  - Multistand
  - Columns
  - Microbeads
- Degassed buffer (e.g., phosphate-buffered saline [PBS] supplemented with EDTA and bovine serum albumin [BSA]; see MACS Miltenyi Biotec GmbH product datasheet)

Procedure

A. Setup
  A.1. Adapt the MiniMACS separator to the MultiStand.
  A.2. Insert column to the front of the separator (column wings to the front).
  A.3. Place a collection tube under the column.
B. Cell magnetic labeling
  B.1. Obtain sperm suspension (e.g., by density-gradient preparation).
  B.2. Prepare microbead suspension.
    Incubate sperm suspension with 100 µL of superparamagnetic Annexin V-conjugated microbeads for 15 min at room temperature.
C. Separation
  C.1. Load the labeled suspension onto the column.
  C.2. Wash three times with degassed buffer by adding 500 µL each time (waiting until the reservoir is empty before adding the buffer).
  C.3. Collect nonlabeled (i.e., nonapoptotic) fraction passing through the column.
  C.4. Remove the column from the magnetic field.
  C.5. Place the column on another collection tube.
  C.6. Add 1 mL of buffer to the column.
  C.7. Flush out the labeled (apoptotic) fraction retained in the column by using the plunger provided in the kit.

Pros and Cons

Pros	Cons
• The apoptotic cell fraction can be separated	• Other cell types cannot be distinguished (e.g., immature germ cells, leukocytes)[a]
• It can be performed on living sperm	• Not suitable for samples with low sperm concentration

[a] Therefore, it has been suggested to be used together with density-gradient sperm preparation [11].

Fluorescence-Activated Cell Sorting

Background

Sorting by flow cytometry is a well-established technique dating back to the late 1960s, and it is based upon the detection of a fluorescent signal generated by a stain that has been incorporated into or onto a cell. As with MACS, numerous stains indicative of various properties (e.g., acridine orange, propidium iodide [nDNA status], Yo Pro 1 [apoptosis], Hoechst 33342 [vitality]) have been used either singularly or in combination in FACS [13]. Similarly to magnetic separation, the fundamental aspects of FACS are irrespective of the staining or binding substance.

BOX 9.3 APPLYING FACS

The following description is based on the separation strategy of Ribeiro et al. [13] using Yo Pro 1, a protocol that is adaptable for any of the other staining substrates.

Overview

A. Setup
B. Staining
C. Separation

Instrumentation and Materials

- Flow cytometer (in the cited paper, the instrument used was an influx flow cytometer (BD Biosciences) equipped with a solid-state laser (100 mW) for excitation at 355 nm, a blue laser (200 mW) for excitation at 488 nm, and a red laser (120 mW) for excitation at 640 nm. Analyses were performed using Sortware software from the same manufacturer)
- Yo Pro 1
- IVF medium or PBS
- BSA
- Penicillin and streptomycin

Procedure

A. Setup
  A.1. Prepare sperm suspension (e.g., swim-up).
  A.2. Centrifuge an aliquot of 0.3–1 × 10^6 spermatozoa for 10 min at 460*g*.
  A.3. Remove supernatant resuspend pellet in 1 mL of IVF medium or PBS.
B. Staining
  B.1. Add 1 µL of YO-PRO solution (final concentration, 0.2 µmol/L) to the sperm suspension.[a] Incubate at 37°C and 5% CO_2 for 15 min in the dark.
  B.2. Filter the stained suspension with Celltrics 100 mm filters (Partec).
C. Separation
  C.1. The settings used by Ribeiro et al. [13] for sorting were 100 µm nozzle; sample pressure, 19.5–20.5 psi; and event rate, 1000–9000 events per second.
  C.2. Sterile PBS containing 0.1% BSA, 50 U/mL penicillin, and 50 µL/mL streptomycin was used as sheath fluid.
  C.3. Sorted samples are collected in polystyrene round-bottomed tubes containing 1 mL of IVF medium.

[a] If more than one stain is to be used, it is added here.

Pros and Cons

Pros	Cons
• Large numbers of sperm can be sorted in a reasonable time • Objective selection • More than one stain can be used simultaneously	• Not suitable for samples with low sperm concentration • Requires expensive equipment • Exclusion of the stain from the sorted sperm not proven • Benefit to ART outcome as yet not established

Selection Using Micromanipulators

Two further procedures have been developed that use the binding ability of sperm themselves.

HA Binding

A major component of the cumulus for which only mature sperm have a receptor, HA is the basis of two commercially available separation methods: SpermSlow™ and the PICSI® system (both from Origio a/s, Denmark) (see Video 9.1). The rationale behind both approaches is that because only mature sperm have intact nDNA, the fraction that is bound to the acid must consist of sperm with high nDNA integrity. In practical terms, the HA solution in SpermSlow acts as an immobilizing agent, slowing down mature sperm so that they can be collected, whereas the PICSI system involves a dish precoated with a solid-state HA formulation; addition of the sample; and after an incubation step, the collection of the bound sperm using a micropippete. Although there is some evidence for the efficacy of the approach [7], at present its true clinical value is yet to be established [14].

Zona Pellucida Binding

Collection of sperm bound to the zona pellucida [15] is a more "physiological" use of sperm–oocyte binding, because it does not involve any direct intervention or treatment and is closer to "natural" conditions. However, access to and availability of suitable zonae are serious obstacles to the routine use of the method, as is the lack of verification of the technique's clinical worth.

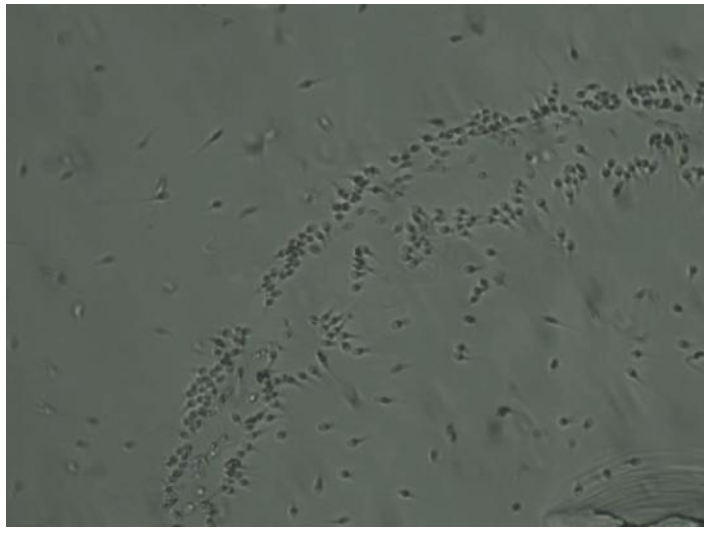

VIDEO 9.1 Binding of spermatozoa to solid HA in dish. (Video provided by Dr. Markus Montag, ilabcomm GmbH, Germany. Accessible on the "Downloads/Updates" tab at: http://www.crcpress.com/product/isbn/9781842145470.)

Electric Charge

Due to their concentrated, and relative to their size, large DNA content, sperm possess a high negative electric charge. Because this charge varies depending on chromosomal complement, it was initially used as a means of sperm sex selection [16]. More recently, variations in electrical charge have been shown to also be associated with chromatin compaction and DNA integrity [17]; as a consequence, methods have been developed that use these differences to separate and sort sperm.

Zeta Potential

The zeta (ζ) or electrokinetic potential is defined as the electric potential in the slip plane between a sperm membrane and its surroundings. Mature sperm possess a ζ between –16 and –20 mV [18] whereby they are able to adhere to positively charged substances such as the walls of plastic or glass tubes. The inference being that this adhering ability allows for the quick separation of sperm with intact (i.e., possessing high ζ values) from fragmented DNA (i.e., lower ζ values). The validation and use of this method have thus far been limited [19].

Electrophoresis

Background

The isolation of sperm based on their electrophoretic movement is based on the premise that the higher the electronegativity, the higher the sperm quality in terms of morphology, capacitation ability, and DNA integrity [20]. Marketed commercially as MicroFlow® or SpermSep® CS10 (Nusep Ltd., Australia), the system consists of a cartridge divided into two chambers that allow for the directional movement of cells when exposed to an electric potential. The chamber is divided by a 5 μm polycarbonate membrane that allows for the crossing of sperm but excludes larger contaminating cells (i.e., leukocytes and germ cells). Although the true efficacy of the system is yet to be established, a full-term pregnancy has been reported using electrophoretically isolated sperm from a male having high numbers of sperm with DNA damage [21].

BOX 9.4 APPLYING ELECTROPHORESIS FOR SPERM SELECTION

Overview

A. Setup
B. Separation

Materials

- SpermSep CS10 (NuSep Ltd.) [22]
- Electrophoresis buffer

Procedure

A. Setup
   A.1. Prepare the electrophoresis buffer 10 mM HEPES, 30 mM NaCl, and 0.2 M sucrose (osmolarity, 310 mOsm kg^{-1}; pH 7.4, adjusted with 2 M KOH)
   A.2. Autoclave the separation cartridge.
   A.3. Sterilize the electrophoresis buffer with a 0.22 μm filter.

A.4. Insert the separation cartridge into housing on the upper part of the SpermSep CS10.
A.5. Pipette 400 µL of electrophoresis buffer into the separation chamber.
A.6. Fill the buffer reservoir with 80 mL of electrophoresis buffer and place the reservoir housing into the front of the instrument.
A.7. Run the buffer pump for 1 min before the sperm separation.

B. Separation
B.1. Make sure that the separation unit is sealed.
B.2. Load 400 µL of the semen sample into the corresponding chamber using a sterile pipette.
B.3. Leave to equilibrate for 5 min.
B.4. Start the electrophoresis (constant current of 75 mA (18–21V) for 5 min).
B.5. After the separation, the sperm preparation is recovered from the separation chamber of the cartridge with an elongated sterile tip.

NOTE: If separated in the appropriate medium, the retrieved sperm can be used directly for IVF or ICSI. For intrauterine insemination (IUI), the separated suspension could be used if prostaglandins in seminal plasma have been removed or reduced to insignificant levels [22].

Pros and Cons

Pros	Cons
• Taking only 5 min, the separation run is very rapid in comparison with other methods • No centrifugation needed, thus no oxidative stress caused by the physical forces of centrifugation • Not associated with increased reactive oxygen species (ROS) or oxidative damage	• Recovery rates are low (approximately 20% [23]) • May not be suitable for severe oligozoospermic samples • Equipment and procedure outside of normal andrology laboratory practice [19] • Not clinically verified or validated

Future Perspectives

The rapid advances in miniaturization (e.g., labs on a chip), computerization, and optics have made accessible to biomedicine, instruments that were once the sole preserve of physics and chemistry researchers. Although not yet routine, these new methods provide opportunities for diagnosis and treatment that were previously unimaginable and possess aptitudes that could make the dependable and safe assessment, grading, and selection of live gametes a reality. One such technique that has already been introduced to reproductive investigations and holds the promise of possible selection of sperm for ART is Raman microspectroscopy.

Raman Microspectroscopy

Background

Raman spectroscopy is a relatively old method (i.e., the fundamental principle behind the technique was discovered in 1928) that has been recently "rediscovered" and used in biomedicine both as a research tool and as a diagnostic tool. Based on the inelastic scattering of light (i.e., the Raman effect), the process provides a "molecular fingerprint" of materials that when coupled with confocal microscopy allows for a detailed profiling of the chemical components of cells. Already used in numerous fields of medicine [24,25], the method has been shown to noninvasively and nondestructively analyze whole organs; tissue sections; and (more importantly for reproductive medicine) living cells. Preliminary work [26–29] has shown the power of this method to identify, classify, and localize nDNA damage in a single sperm, information that opens the way for the next step, the selection and use of this sperm for ART (Figure 9.2).

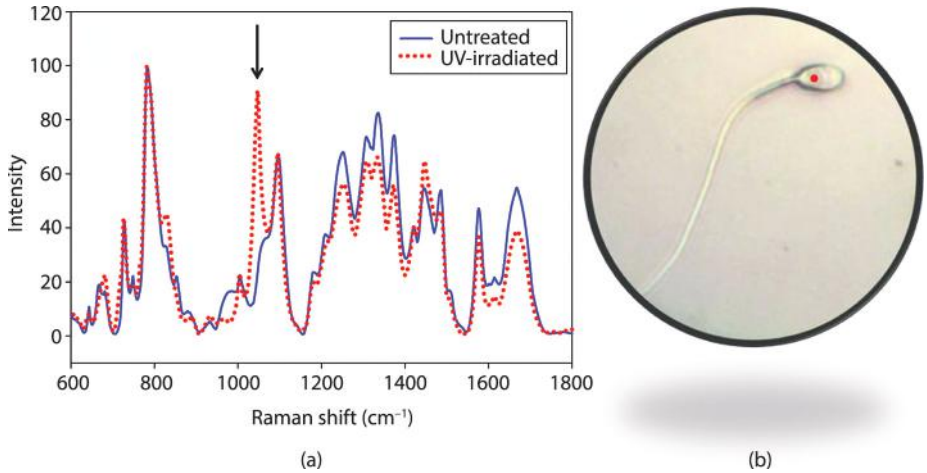

FIGURE 9.2 Raman spectroscopy for sperm. (a) Averaged Raman spectra from sperm (blue) and after ultraviolet (UV) irradiation (red). Arrow indicates main spectral feature in damaged sperm (peak at 1047 cm^{-1}). Spectra have been normalized, baseline-corrected, and smoothed. (b) Single-point Raman spectra are acquired from the post–acrosomal region of the sperm head. The red dot represents the position on which the laser is focused.

BOX 9.5 APPLYING RAMAN SPECTROSCOPY FOR SELECTING SPERM

The following method is based on the protocols optimized in Mallidis et al. [28] and Sanchez et al. [29] for the assessment of air-dried sperm using the LabRAM Aramis system (Horiba Scientific, France). The settings and procedure are similar to those that would be necessary for the evaluation of living sperm.

Overview

A. Sample preparation
B. Focus localization
C. Spectral acquisition
D. Spectral analysis

Materials

- Raman microspectroscopy system
- Suprasil slides
- PBS

Procedure

A. Preparation
   A.1. Obtain the sperm suspension to be analyzed.
   A.2. Wash in PBS (5 min, 600*g*).
   A.3. Smear 10 μL of the suspension onto a Suprasil slide.
   A.4. Let air-dry overnight.
B. Focus localization
   Normally, the visual focus does not correspond to the actual focus. Therefore, a Z-profile should be done to find the position in the Z-axis where the best possible signal can be obtained.
   B.1. Focus the sample.
   B.2. Select the cell to analyze.

B.3. Center it under the laser position.
B.4. Set that position to zero.
B.5. Make a quick map in the Z-axis, taking several spectra from ~3 µm below and up to ~3 µm above the current position.
B.6. Take note of the position with the best spectrum in terms of intensity and resolution.

C. Spectral acquisition
C.1. Settings (the following are optimized for the LabRAM Aramis and may differ depending on the system used):
- Laser: He-Ne 632.8 nm
- Filter: 100%
- Hole: 100 µm
- Slit: 100 µm
- Spectrometer: 1200 cm^{-1}
- Grating: 600 grooves per millimeter
- Objective: 100×
- Acquisition time: 2 × 30 s (2 × 5 for Z-maps)

C.2. Move the stage to the position selected after the Z-map.
C.3. Change the acquisition time to 2 × 30 s.
Take the spectrum.

D. Spectral analysis
D.1. Data processing:
- Baseline correction
- Normalization (e.g., to the maximum peak within the 600–1800 cm^{-1} spectral range)
- Set the lowest intensity to zero

Note: The procedures are performed using the software included as part of the microspectroscopic system. For example, in the LabRAM Aramis, the software provided is LabSpec5.

D.2. Depending on the information of interest (e.g., DNA damage), select a band to analyze (e.g., ~1095 cm^{-1}).
D.3. Select another band that remains stable in all measurements.
D.4. Extract from the software the peak intensity values corresponding to the selected peaks and calculate the ratios between them.

Pros and Cons

Pros	Cons
• Allows for profiling of specific sperm	• Equipment is expensive
• Provides detailed information on chemical composition	• Requires specialist knowledge
• Not restricted to nDNA assessment	• Results are complex
• Relatively quick and easy	• Needs validation and verification of clinical worth

Conclusions

The long-held dream of clinicians and scientists in reproductive medicine has been, and remains, the assessment, selection, and use of gametes that will provide not only good fertilization rates but also optimal embryo quality, implantation, and pregnancy rates, all of which ultimately lead to the birth of healthy children. In this endeavor, as noted in the preceding sections, numerous techniques have been developed to select the best possible sperm for ARTs. Although many of the described methods may be considered novelties and lack the robust verification and validation essential for routine clinical use, they nonetheless constitute a great improvement in the existing

TABLE 9.1

Overview of Different Technologies Used for Sperm Selection

Technique	Emerging	Used	Diagnostic	Therapeutic	Studies
Polarization microscopy		X	X	X	2–4
MACS		X	X	X	9, 30
FACS	X		X		13
PICSI		X	X	X	31
HA medium		X	X	X	32
Zona pellucida binding		X	X	X	15, 33, 34
Zeta potential		X	X	X	35
Electrophoresis		X	X	X	21, 21, 23
Raman microspectroscopy	X		X		26–29

Note: HA, hyaluronic acid.

selection process that is solely dependent on the subjective choice of the embryologists. The main disadvantage however is that although most of the techniques provide information on which sperm quality can be better classified, the practical aspects of the procedures either destroy or alter sperm in ways that render them unusable for ARTs (Table 9.1). Be that as it may, until the full potential of upcoming techniques based on advanced technology has been realized, the procedures described in this chapter, regardless of their limitations, represent the best options presently available to the ART clinic.

REFERENCES

1. Lewenhoeck A. De natis E Semine Genitali Animalculis. *Phil Trans* 1677.
2. Ghosh S, Chattopadhyay R, Bose G, Ganesh A, Das S, Chakravarty BN. Selection of birefringent spermatozoa under Polscope: Effect on intracytoplasmic sperm injection outcome. *Andrologia* 2012;44(Suppl 1):734–738.
3. Gianaroli L, Magli MC, Collodel G, Moretti E, Ferraretti AP, Baccetti B. Sperm head's birefringence: A new criterion for sperm selection. *Fertil Steril* 2008;90(1):104–112.
4. Gianaroli L, Magli MC, Ferraretti AP, Crippa A, Lappi M, Capitani S, et al. Birefringence characteristics in sperm heads allow for the selection of reacted spermatozoa for intracytoplasmic sperm injection. *Fertil Steril* 2010;93(3):807–813.
5. Petersen CG, Vagnini LD, Mauri AL, Massaro FC, Cavagna M, Baruffi RL, et al. Relationship between DNA damage and sperm head birefringence. *Reprod Biomed Online* 2011;22(6):583–589.
6. Collodel G, Iacoponi F, Mazzi L, Terzuoli G, Pascarelli NA, Moretti E. Light, polarizing, and transmission electron microscopy: Three methods for the evaluation of sperm quality. *Syst Biol Reprod Med* 2013;59(1):27–33.
7. Yagci A, Murk W, Stronk J, Huszar G. Spermatozoa bound to solid state hyaluronic acid show chromatin structure with high DNA chain integrity: An acridine orange fluorescence study. *J Androl* 2010;31(6):566–572.
8. Enciso M, Pieczenik G, Cohen J, Wells D. Development of a novel synthetic oligopeptide for the detection of DNA damage in human spermatozoa. *Hum Reprod* 2012;27:2254–2266.
9. Dirican EK, Ozgun OD, Akarsu S, Akin KO, Ercan O, Ugurlu M, et al. Clinical outcome of magnetic activated cell sorting of non-apoptotic spermatozoa before density gradient centrifugation for assisted reproduction. *J Assist Reprod Genet* 2008;25(8):375–381.
10. Said TM, Agarwal A, Zborowski M, Grunewald S, Glander HJ, Paasch U. Utility of magnetic cell separation as a molecular sperm preparation technique. *J Androl* 2008;29(2):134–142.
11. Said TM, Grunewald S, Paasch U, Glander HJ, Baumann T, Kriegel C, et al. Advantage of combining magnetic cell separation with sperm preparation techniques. *Reprod Biomed Online* 2005;10(6):740–746.
12. Said T, Agarwal A, Grunewald S, Rasch M, Baumann T, Kriegel C, et al. Selection of nonapoptotic spermatozoa as a new tool for enhancing assisted reproduction outcomes: An in vitro model. *Biol Reprod* 2006;74(3):530–537.
13. Ribeiro SC, Sartorius G, Pletscher F, de Geyter M, Zhang H, de Geyter C. Isolation of spermatozoa with low levels of fragmented DNA with the use of flow cytometry and sorting. *Fertil Steril* 2013;100:686–694.

14. Nijs M, Creemers E, Cox A, Janssen M, Vanheusden E, Van der Elst J, et al. Relationship between hyaluronic acid binding assay and outcome in ART: A pilot study. *Andrologia* 2010;42(5):291–296.
15. Liu F, Qiu Y, Zou Y, Deng ZH, Yang H, Liu de Y. Use of zona pellucida-bound sperm for intracytoplasmic sperm injection produces higher embryo quality and implantation than conventional intracytoplasmic sperm injection. *Fertil Steril* 2011;95(2):815–818.
16. Engelmann U, Krassnigg F, Schatz H, Schill WB. Separation of human X and Y spermatozoa by free-flow electrophoresis. *Gamete Res* 1988;19(2):151–160.
17. Chan PJ, Jacobson JD, Corselli JU, Patton WC. A simple zeta method for sperm selection based on membrane charge. *Fertil Steril* 2006;85(2):481–486.
18. Ishijima SA, Okuno M, Mohri H. Zeta potential of human X- and Y-bearing sperm. *Int J Androl* 1991;14(5):340–347.
19. Said TM, Land JA. Effects of advanced selection methods on sperm quality and ART outcome: A systematic review. *Hum Reprod Update* 2011;17(6):719–733.
20. Ainsworth C, Nixon B, Aitken RJ. Development of a novel electrophoretic system for the isolation of human spermatozoa. *Hum Reprod* 2005;20(8):2261–2270.
21. Ainsworth C, Nixon B, Jansen RP, Aitken RJ. First recorded pregnancy and normal birth after ICSI using electrophoretically isolated spermatozoa. *Hum Reprod* 2007;22(1):197–200.
22. Fleming S, Aitken J. Electrophoretic sperm separation. In: *Practical Manual of In Vitro Fertilization: Advanced Methods and Novel Devices* (eds. Nagy ZP, Varghese AC, Agarwal A, Springer Publishing, New York). 2012, p. 259.
23. Aitken RJ, Hanson AR, Kuczera L. Electrophoretic sperm isolation: Optimization of electrophoresis conditions and impact on oxidative stress. *Hum Reprod* 2011;26(8):1955–1964.
24. Caspers PJ, Lucassen GW, Puppels GJ. Combined in vivo confocal Raman spectroscopy and confocal microscopy of human skin. *Biophys J* 2003;85(1):572–580.
25. Downes A, Mouras R, Elfick A. Optical spectroscopy for noninvasive monitoring of stem cell differentiation. *J Biomed Biotechnol* 2010;2010:101864.
26. Huser T, Orme CA, Hollars CW, Corzett MH, Balhorn R. Raman spectroscopy of DNA packaging in individual human sperm cells distinguishes normal from abnormal cells. *J Biophotonics* 2009;2(5):322–332.
27. Meister K, Schmidt DA, Brundermann E, Havenith M. Confocal Raman microspectroscopy as an analytical tool to assess the mitochondrial status in human spermatozoa. *Analyst* 2010;135(6):1370–1374.
28. Mallidis C, Wistuba J, Bleisteiner B, Damm OS, Gross P, Wubbeling F, et al. In situ visualization of damaged DNA in human sperm by Raman microspectroscopy. *Hum Reprod* 2011;26(7):1641–1649.
29. Sanchez V, Redmann K, Wistuba J, Wubbeling F, Burger M, Oldenhof H, et al. Oxidative DNA damage in human sperm can be detected by Raman microspectroscopy. *Fertil Steril* 2012;98(5):1124–1129.e1–3.
30. Rawe VY, Boudri HU, Alvarez Sedo C, Carro M, Papier S, Nodar F. Healthy baby born after reduction of sperm DNA fragmentation using cell sorting before ICSI. *Reprod Biomed Online* 2010;20(3):320–323.
31. Nasr-Esfahani MH, Razavi S, Vahdati AA, Fathi F, Tavalaee M. Evaluation of sperm selection procedure based on hyaluronic acid binding ability on ICSI outcome. *J Assist Reprod Genet* 2008;25(5):197–203.
32. Parmegiani L, Cognigni GE, Bernardi S, Troilo E, Ciampaglia W, Filicori M. "Physiologic ICSI": Hyaluronic acid (HA) favors selection of spermatozoa without DNA fragmentation and with normal nucleus, resulting in improvement of embryo quality. *Fertil Steril* 2010;93(2):598–604.
33. Paes Almeida Ferreira de Braga D, Iaconelli A, Jr, Cassia Savio de Figueira R, Madaschi C, Semiao-Francisco L, Borges E, Jr. Outcome of ICSI using zona pellucida-bound spermatozoa and conventionally selected spermatozoa. *Reprod Biomed Online* 2009;19(6):802–807.
34. Black M, Liu de Y, Bourne H, Baker HW. Comparison of outcomes of conventional intracytoplasmic sperm injection and intracytoplasmic sperm injection using sperm bound to the zona pellucida of immature oocytes. *Fertil Steril* 2010;93(2):672–674.
35. Kheirollahi-Kouhestani M, Razavi S, Tavalaee M, Deemeh MR, Mardani M, Moshtaghian J, et al. Selection of sperm based on combined density gradient and Zeta method may improve ICSI outcome. *Hum Reprod* 2009;24(10):2409–2416.

10

Noninvasive Techniques: Gamete Selection—Oocyte

Laura Rienzi, Benedetta Iussig, and Filippo Maria Ubaldi

Introduction

Despite the recent advances in assisted reproductive techniques (ARTs), the embryo wastage remains dramatically high. In fact, it has been demonstrated that only a few of the embryos among those produced in vitro is actually able to implant, giving rise to pregnancy and live birth. As a consequence, the majority of ART-started cycles results in a negative outcome [1,2]. To increase the chances of success, many centers perform multiple embryo transfer, clearly at the expense of a higher incidence of multiple gestations. The ability to identify and select the embryos with the most developmental potential is considered one major goal of contemporary in vitro fertilization (IVF) worldwide, aiming for single embryo transfer (SET) without affecting the overall pregnancy rate.

Assessment of oocyte quality has gained increased consideration, leading to a blossoming of the literature.

To date, the morphological evaluation of cleavage-stage embryos and blastocysts remains the gold standard in ARTs, and it is routinely applied in IVF laboratories. However, because embryo viability seems to reflect the intrinsic developmental potential of the originating gametes, in the past few years, the assessment of oocyte quality has gained increased consideration, leading to a blossoming of the literature. In this regard, several morphological features have been proposed as earlier markers predictive of developmental competence and implantation. Nevertheless, the contradictory results obtained so far underline the importance of further research to reach a consensus as well as the parallel development of novel noninvasive tests for the assessment of oocyte quality [3].

Polarized Light Microscopy

To date, the first-line oocyte quality assessment relies on the morphological classification of the cumulus–corona–oocyte complex (CCOC) and, above all, on the correct identification of mature denuded eggs. This latter analysis is surely a primary goal for the choice of appropriate oocytes for insemination purposes, yet it is not devoid of difficulties and interpretational misunderstandings.

Usually, nuclear maturity is simply assessed by light microscopy through the visualization of the first polar body (IPB) extruded in the perivitelline space (PVS): oocytes displaying the IPB are presumably at the metaphase II (MII) stage (Figure 10.1) in which the homologous chromosomes are aligned at the spindle equatorial plate during meiosis II. It is well recognized that in stimulated cycles, 85% of the retrieved oocytes expose the IPB and are thus classified as MII, whereas 10% show an intracytoplasmic structure called the "germinal vesicle" (GV), characteristic of the prophase of meiosis I (PI) (Figures 10.2 and 10.3), and the last 5% lack both IPB and GV. These latter oocytes are generally classified as metaphase I (MI) [4], although they may have undergone GV breakdown but not yet progressed to the true MI stage (Figure 10.4).

However, it is now clear that the sole use of light microscopic analysis is inadequate, even for the seemingly simple classification of oocytes on the basis of nuclear maturity. For example, it has been demonstrated that some oocytes morphologically classified as MII are really immature, despite the presence of IPB in the PVS, being at the early

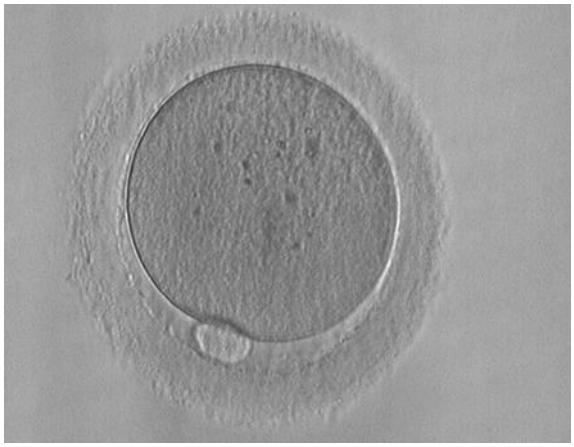

FIGURE 10.1 Denuded MII oocyte. An intact IPB is clearly visible in the PVS (400× magnification).

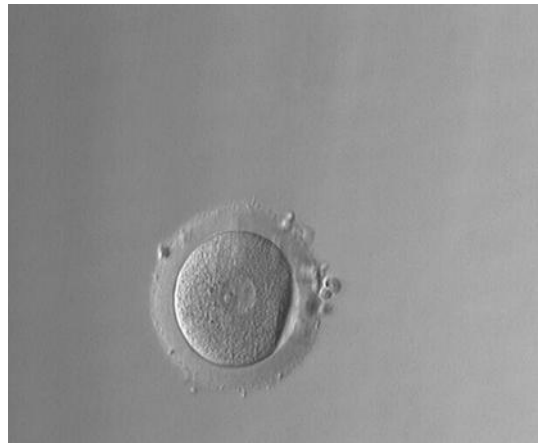

FIGURE 10.2 Denuded GV oocyte with a centrally placed nucleus and a prominent single nucleolus (200× magnification).

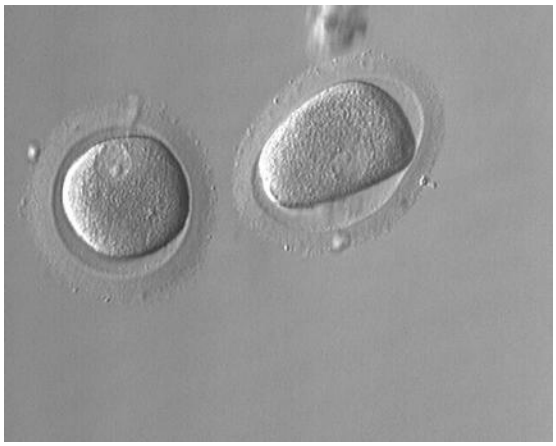

FIGURE 10.3 Denuded GV oocytes with eccentrically located nuclei and prominent nucleoli (200× magnification). The peripheral location of nuclei indicates that GVBD is probably imminent.

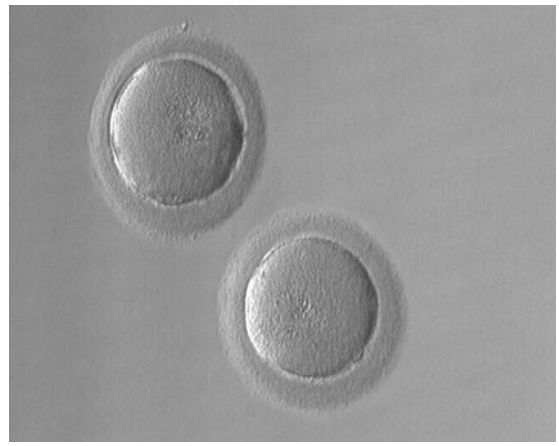

FIGURE 10.4 Denuded MI oocytes without any visible IPB in the typically narrow PVS (200× magnification).

telophase phase of meiosis I (TI). In these cases, additional information can be obtained by the visualization of the meiotic spindle (MS). This highly ordered microtubular structure is involved in the chromosome segregation process; thus, it is crucial for the correct completion of meiosis and subsequent fertilization. It is possible to use its ability to shift the plane of polarized light inducing a retardance (ability that makes it "birefringent") for the noninvasive spotting through polarized light microscopy combined with software for image processing (Figure 10.5) [5].

MS identification contributes to both qualitative and quantitative data. Importantly, the presence of the MS permits us to better assess nuclear maturity. For example, in the case of early telophase I the MS is clearly interposed between the IPB and the oocyte (Figure 10.6). About 80%–90% of MII present MS [6,7]; its absence has been related to lower fertilization rates and in vitro embryo development, although there are still insufficient data to demonstrate its correlation with an impairment of clinical pregnancy and implantation rates [8]. Even if the presence of the MS is reassuring, it should be noted that it seems to "disappear" in late telophase I, reforming only 40–60 min later [9,10]. Moreover, the microtubules are highly sensitive to both chemical and physical stresses, and suboptimal culture conditions can account for MS disappearance [5]. Finally, the MS may

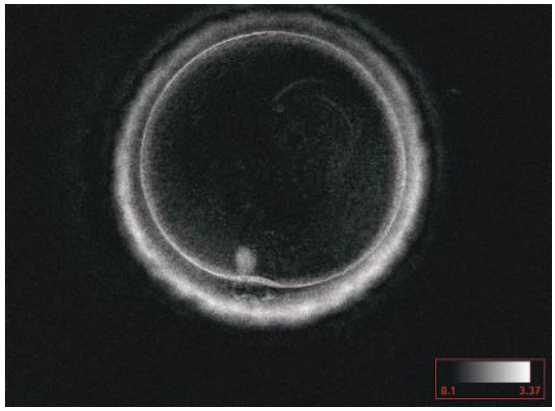

FIGURE 10.5 MII oocyte observed at polarized light microscopy (400× magnification). The birefringent MS is visible just below the extruded IPB at about the 6 o'clock position.

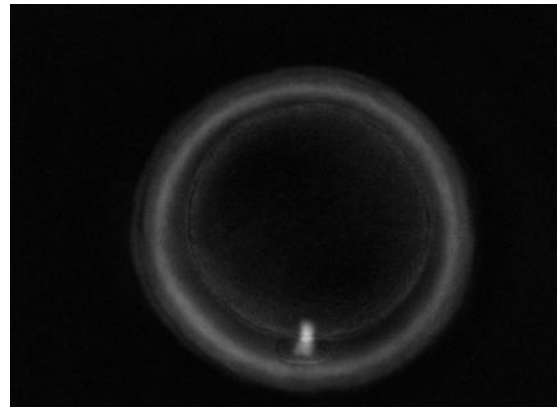

FIGURE 10.6 Telophase I oocyte observed at polarized light microscopy (400× magnification). The MS is visible at the 6 o'clock position. It is interposed between the extruded IPB and the ooplasm, indicating that the first meiotic division is not yet concluded.

be artifactually not visualized if the oocyte is not correctly orientated during the analysis [6,11], and it has been shown that its visualization is more probable if the time elapsed from human chorionic gonadotropin (hCG) administration is at least 38 hr [7]. This finding may be explained by the fact that it is likely that more oocytes are still in prometaphase II at time intervals closer to hCG administration [10].

Suboptimal culture conditions and oocyte handling can account for disappearance of the MS because microtubules are highly sensitive to both chemical and physical stresses.

The MS is not only fundamental for the chromosome segregation process but also is a key organelle in the creation of the IPB and the second polar body (IIPB). Its position at the very periphery of the cell [12] determines the true animal pole and the plane of the first cleavage [6] and thus the polar body (PB) extrusion site. However, the MS is not always perfectly aligned with the extruded PB (Figure 10.7). The IPB dislocation may be due to the manipulation occurring during the denuding process. It has been demonstrated that only displacements >90° are correlated with lower fertilization rates [11]. In fact, it should be hypothesized that in these cases the manipulation has been strong enough to possibly cause irreversible damage to the oocytes. Moreover, a displaced IPB may be a false indicator of the presence of the MS, which can be touched and injured by the micropipette during intracytoplasmic sperm injection (ICSI) [5,13].

Finally, it has been postulated that the degree of birefringence (directly proportional to the molecular organization of the structure and the density of microtubules) [14] may correlate with in vitro and clinical results [15–18], but data are still controversial [19].

Polarization microscopy allows detection of MSs as well as substructural features of the zona pellucida.

Just to complete the picture, it is noteworthy to mention that polarized light microscopy may also be applied to the analysis of other egg features considered important for oocyte selection and that usually are evaluated solely through light microscopy, such as zona pellucida (ZP) characterization [20]. The ZP is a trilaminar glycoprotein structure crucial in the protection of oocytes and embryos and in the fertilization process. Each ZP layer is characterized by different molecular arrangements and thereby exhibits different birefringence patterns;

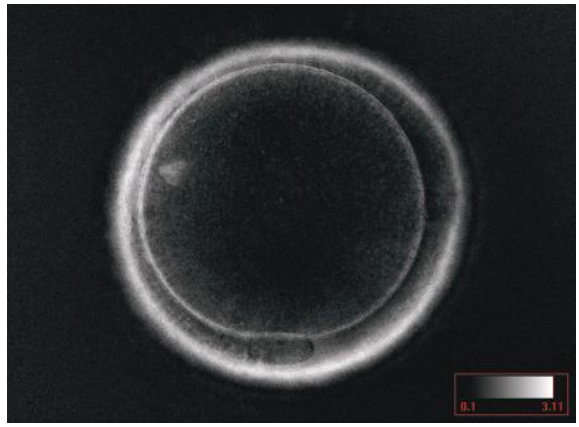

FIGURE 10.7 MII oocyte observed at polarized light microscopy (400× magnification). The MS is visible at the 9 o'clock position, and it is clearly dislocated about 90° from the IPB (placed at the 6 o'clock position).

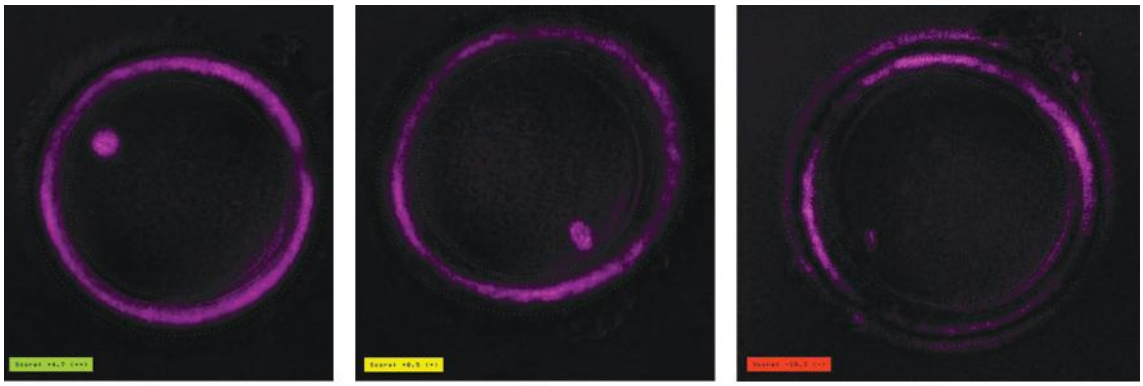

FIGURE 10.8 MII oocytes observed at polarized light microscopy (250× magnification) using automated zona scoring. The zona score is shown in the lower left corner and denotes oocytes with a good (a), medium (b), and bad (c) zona score. The score is dependent on the uniformity and the intensity of the birefringence of the inner zona layer. (c) also shows birefringence in the outer zona layer, which is a clear sign of an impaired zona formation during follicular development. (Images courtesy to Jana Liebenthron, University of Bonn, Germany.)

in particular, the inner and outer layers appear birefringent due to the highly organized orientation of the filaments [21]. The darkness, thickness, and retardance of the inner layer have been suggested by many studies to be markers of oocyte competence and prognostic of IVF success. Even if the data are not uniform, it seems that a regular and strong zona birefringence characterizes oocytes with better developmental potential [10]. Examples of different birefringence patterns of the ZP are shown in Figure 10.8, showing oocytes with a good (Figure 10.8a), medium (Figure 10.8b), and bad (Figure 10.8c) zona score. These measurements were performed with a polarization microscope and a build-in algorithm that enables automatic zona scoring [10].

The "Omics" Technologies

Most recently, the developing field of genomic, transcriptomic, proteomic, and metabolomic (the so-called "omics" technologies) seems to promise a completely new way of assessing oocyte (and embryo) quality and

competence. In fact, apart from morphology and polarized light microscopy assessment, these approaches offer promissory and powerful tools in the noninvasive investigation of the differences, at a molecular level, among eggs that are only apparently similar to each other.

The Genomic Analysis

The genomic analysis relies on the conceivable premise that there should exist genetic determinants for oocyte (and embryo) viability, such as an appropriate chromosome number and DNA integrity. The early identification and selection of oocytes with a correct chromosomal status should help in reducing the production and transfer of aneuploid embryos, thereby potentially improving IVF and clinical results. For many years, the method of choice for aneuploidy screening was fluorescence in situ hybridization (FISH), but FISH has been replaced by the more recent comparative genomic hybridization (CGH) technique that permits analysis of all the chromosomes throughout their length [22,23].

Whatever the technique of choice, it is essential to underline that the assessment of the chromosomal status of a cell requires undoubtedly its destruction; thus, it is considered a highly invasive procedure. In the context of reproductive medicine, the investigation of an oocyte DNA content renders it completely useless for subsequent ART purposes. The cytogenetic study of the IPB should overcome this limitation, because any chromosomal gain or loss in the PB is indicative of a reciprocal anomaly in the oocyte. Nevertheless, this approach does not take into account eventual errors occurring during meiosis II, after sperm penetration, nor the paternal effect. Even if the additional biopsy and study of the IIPB may add useful information, it is clear that (1) the nonimmediacy of the genetic results and (2) the extensive study of both IPB and IIPB are incompatible with early oocyte selection [22,23].

The Transcriptomic Approach

DNA content is not the whole story. In fact, the phenotype is made up by the conjunctive effect of the genomic constitution, epigenetic and environmental, acting on gene expression, protein synthesis, and metabolism [23].

The analysis of gene expression may provide useful insight into the way cells work and respond to stimuli under different conditions. The term "transcriptome" refers to the total amount of RNA in a cell, destined to protein synthesis as well as to RNA storage, and it comprises mRNA, rRNA, tRNA, and miRNA. Thus, the "transcriptomic" analysis analyzes the RNA content, both quantitatively and qualitatively [23,24].

Transcriptomic analysis can be performed on the oocyte itself, at the obvious expense of rendering it useless for subsequent IVF purposes once again, or more interestingly, on granulosa cells (GCs) or cumulus cells (CCs) [22–25]. During preantral-to-antral follicle transition, GCs commence differentiation into mural GCs (lining the follicle walls) and CCs, closely adherent to the oocyte. It is well recognized that GCs are major players in the follicular differentiation process that result in the creation of an optimal environment for the oocyte maturation and growth [26]. Moreover, CCs establish with the enclosed oocyte a complex cross-talk that promotes folliculogenesis as well as the acquisition of egg competence [27,28]. As a consequence, it is conceivable that the study of GC and CC functions may provide valuable information about oocyte quality and its ability to fertilize and develop into a viable implanting embryo: any observed abnormality in GCs' and CCs' molecular patterns may be either the cause or the consequence of an altered oocyte development [29]. Because in IVF treatments, after ovulation induction and ovum retrieval, GCs and CCs are usually discarded, they offer a valid, completely noninvasive alternative to standard morphological assessment and selection of eggs.

The transcriptomic analysis permits us to study the expression of individual defined genes (candidate-gene approach) as well as to characterize the transcriptomic profile. In the first option, the technology of choice is represented by quantitative reverse transcription-polymerase chain reaction (qRT-PCR), also known as real-time RT-PCR; as for the transcriptomic profiling, the microarrays lead the scene, resulting in the generation of a list of genes differentially expressed under different physiologic, pathologic, or experimental conditions [24]. With a combination of these approaches, it is hoped we can soon categorize the pattern of genes differentially expressed in GCs and CCs that surround healthy oocytes versus not-viable oocytes. To date, the genes already studied are involved in different cellular pathways and processes, such as the establishment of bidirectional communication between CCs and an oocyte [30], cumulus

expansion and mucidification [29–35], regulation of apoptosis [29,33,36–38], protection from oxidative stress and response to hypoxia [33,39,40], cell cycle/proliferation and DNA damage response [29,33,38], and lipid and carbohydrate metabolism [30,33,36,41].

Despite the results obtained so far being extremely intriguing and encouraging, the data are not uniform and need to be confirmed, validated, and tested in randomized trials to reach a consensus. One of the major problems facing the attempts to associate differentially expressed genes to known predictable outcomes is the difficulty in determining the threshold value for physiologic inter- and intrasample variances. Moreover, the studies currently available differ in size of study population (generally low), the technology used (characterized by different sensitivity and specificity values), and the referred outcomes (oocyte maturity, oocyte quality, oocyte aneuploidy, fertilization rate, cleavage and early cleavage rate, cleavage embryo quality, blastocyst rate, blastocyst quality, pregnancy rate, and implantation rate). Thus, the large amount of data collected seems to emphasize the notion that the true endpoint for every investigation should be pregnancy or, even better, live birth rate. In fact, although some identified factors may be considered prognostic for certain egg and embryo features, they may not be associated with other coupled characteristics, even if they are likewise correlated to further developmental potential. Moreover, it is clearly not coherent to propose novel early markers for oocyte competence prognostic for standard parameters already known to be inadequate predictors of IVF outcomes. Finally, when multiple embryo transfer is performed, data analysis is complicated by the fact that it is not possible to track the developmental fate of each embryo [24,25].

The omics technologies seem to promise a completely new way of assessing oocyte quality and competence.

The Proteomic and Metabolomic Frontier

Unfortunately, transcriptomic analysis does not reveal the real functional molecular status of a cell, because it does not take into account the possible posttranslational regulation of gene expression resulting in protein modification, degradation, or sequestration. It is believed that the protein content of a cell may be more clearly linked to the phenotype, thus bearing more useful information concerning cell viability [22,23]. The qualitative and quantitative protein profiling in clinical specimens is called “proteome,” and “proteomic” is the technology referred to proteome investigation. The ground-breaking advent of mass spectrometry promises to solve the technical problems related to conventional gel electrophoresis analysis and radiolabeling. However, the difficulty of the technique, the high costs, and the very little knowledge related to human (or even mammal) protein content renders this approach far from routine clinical applicability and more intensive search is needed [23].

The proteomic analysis should be carried on the oocyte itself, again at the expense of losing the precious gamete, or on the surrounding CCs and GCs. Unfortunately, very few articles have been published on this subject [42,43], and even a partial pattern profiling is lacking. The follicular fluid (FF) content has attracted much more interest from the scientific community, maybe due to the relatively easier way of obtaining the starting material and the supposed simpler protein pattern depicted in comparison with somatic cells [23]. As for CC and GC analysis, FF investigation oriented to oocyte quality determination takes an advantage from the interconnection between the egg and the provided microenvironment in which it happens to grow and mature. Indeed, recent publications tried to examine FF protein content to identify novel markers of IVF success [43–45].

Another frontier in omics technology for noninvasive assessment of the oocyte is represented by metabolomics, namely, the investigation of the complete content of small nonproteinaceous molecules in a given biological fluid, resulting from the action of different proteins and gene expression pathways [46,47]. In contrast to genomics and proteomics, metabolomics provides the immediate and punctual functional status of a biological system [46,47]. The contribution of metabolomics in oocyte selection is currently under investigation, both in FF and culture medium. In particular, it seems that the consumption of glucose and oxygen may be an interesting prognostic factor related to oocyte competence and IVF success [47–50].

Follicular Vascularity and Oxygenation

Another supposed critical factor affecting the maturation and growth of a competent oocyte, able to develop into a viable embryo, is the extent of perifollicular vascularity (PFV) and thus follicular oxygenation. Pulsed and power Doppler ultrasonography have been successfully used to measure the blood flow around maturing follicles in stimulated cycles, thus allowing us to determine differences among follicles apparently similar at a conventional ultrasound analysis [51–63]. According to the percentage of follicular circumference presenting visible blood flow, different PFV grades have been described: Grade 1, <25%; Grade 2, <50%; Grade 3, <75%; and Grade 4, >75%. Conventionally, Grade 1–2 follicles are referred as poorly vascularized, whereas Grade 3–4 follicles are highly vascularized [52]. Contradictory results failed to find any definite correlation between the extent of PFV and follicular maturity (expressed as follicular size, oocyte yield, and MII retrieval rate) as well as oocyte morphological assessment, fertilization rate, embryo quality, and cleavage status [51–54,56,57,59,62,64,65]. Nevertheless, tracking the developmental fate of oocytes and embryos derived from follicles with high-grade versus low-grade PFV showed that there seems to be a positive correlation between high PFV and pregnancy rates and live birth [52,54,57,58,60,61,64,65], even if some studies did not confirm this trend [62,63].

PFV could reflect the efforts to abate hypoxia increasing the intrafollicular dissolved oxygen concentration via gaseous diffusion as the antrum expands. It has been proposed that poorly vascularized and hypoxic follicles can eventually lead to higher oocyte aneuploidy rates by means of reduced ATP level and decreased intracellular pH (pHi). In fact, such an altered metabolic pattern seems to affect the organization and structural stability of the spindle, thus favoring chromosome displacement and segregation disorders that affect the embryos' further ability to develop and implant [55,56,66,67]. This finding is consistent with the results obtained by the cytogenetic analysis of noninseminated or unfertilized MII derived by highly vascularized versus poorly vascularized follicles [52,54].

To investigate the cellular basis for the apparent altered oocyte metabolism in cases of low PFV, some studies examined the structure and function of mitochondria [55,56], revealing that they were heterogeneously distributed in the cytoplasm of the majority of oocytes from poorly vascularized hypoxic follicles. As a consequence, some ooplasmic regions resulted in reduced metabolic activity. It has been speculated that this nonhomogeneous mitochondrial distribution may progress to asymmetric inheritance by the daughter cells after cleavage, causing embryo developmental arrest and demise. Nevertheless, the exact role of mitochondria remains to be elucidated.

Differences in PFV and follicular oxygenation could run in parallel with the production of angiogenic growth factors by the GCs. A correlation has been proposed between the grade of PFV and the presence of angiogenic growth factors in the FF. In particular, the role of vascular endothelial growth factor (VEGF) has been quite extensively studied because it is a strong promoter of vascularization expressed in human follicles by both cumulus and granulosa-lutein cells. Some studies suggested that the measurement of VEGF FF concentration could be used as an index of PFV and hypoxia [56,65,68,69], but contradictory results were obtained. Moreover, this is a time-consuming and expensive technique, and it has not yet been introduced in clinical practice.

Conclusions

Early selection of oocytes is considered a major goal of contemporary IVF worldwide, allowing the identification of the most competent gametes to inseminate. In turn, this would help in reducing the number of embryos produced in vitro and progress to SET. Unfortunately, standard morphological evaluation is not precise, and a consensus is still lacking. However, new noninvasive tools for oocyte selection are gaining increased interest from the scientific community, from the more classic polarized light microscopy analysis to the evaluation of PFV and, to conclude, the ground-breaking omics technology. The results obtained so far are really intriguing and encouraging, but it would be wise to raise some concerns. For polarized light microscopy analysis, the contradictory results underline the need of more intense study to reach a consensus. As to omics and, in part,

PFV evaluation, the high costs, the difficulty of the techniques, and the time required for testing are limiting their routine applicability. Moreover, even if these approaches are all considered "noninvasive," we still need more evidence for the safety of the techniques (i.e., the possible effect of additional time required for each oocyte outside the incubator or unindicated removal of CCs and, as a consequence, ICSI performance). Finally, prospective randomized studies are required to determine their predictive power, alone or in combination with other factors, so that further efforts enrich our current knowledge [24].

REFERENCES

1. Kovalevsky G, Patrizio P. High rates of embryo wastage with use of assisted reproductive technology: A look at the trends between 1995 and 2001 in the United States. *Fertil Steril* 2005; 84: 325–330.
2. Bromer JG, Seli E. Assessment of embryo viability in assisted reproductive technologies: Shortcomings of current approaches and the emerging role of metabolomics. *Curr Opin Obstet Gynecol* 2008; 20: 234–241.
3. Rienzi L, Vajta G, Ubaldi F. Predictive value of oocyte morphology in human IVF: A systematic review of the literature. *Hum Reprod Update* 2011; 17: 34–45.
4. Rienzi L, Ubaldi F. Oocyte retrieval and selection. In: *Textbook of Assisted Reproductive Technologies. Laboratory and Clinical Perspectives*, 3rd ed. (eds. Gardner DK, Weissman A, Howles CM, Shoham Z). London, UK: Informa Healthcare; 2009, pp. 85–101.
5. Oldenbourg R. Polarized light microscopy of spindles. *Methods Cell Biol* 1999; 61: 175–208.
6. Cooke S, Tyler JP, Driscoll GL. Meiotic spindle location and identification and its effect on embryonic cleavage plane and early development. *Hum Reprod* 2003; 18: 2397–2405.
7. Cohen Y, Malcov M, Schwartz T, et al. Spindle imaging: A new marker for optimal timing of ICSI? *Hum Reprod* 2004; 19: 649–654.
8. Petersen C. Relationship between visualization of meiotic spindle in human oocytes and ICSI outcomes: A meta-analysis. *Reprod Biomed Online* 2009; 18: 235–243.
9. Montag M, Schimming T, Van der Ven H. Spindle imaging in human oocytes: The impact of the meiotic cell cycle. *Reprod Biomed Online* 2006; 12: 442–446.
10. Montag M, Köster M, Van der Ven K, et al. Gamete competence assessment by polarizing optics in assisted reproduction. *Hum Reprod Update* 2011; 17: 654–666.
11. Rienzi L, Ubaldi F, Martinez F, et al. Relationship between meiotic spindle location with regard to the polar body position and oocyte developmental potential after ICSI. *Hum Reprod* 2003; 18: 1289–1293.
12. Maro B, Verlhac MH. Polar body formation: New rules for asymmetric divisions. *Nat Cell Biol* 2002; 4: E281–E283.
13. Silva CP, Kommineni K, Oldenbourg R, et al. The first polar body does not predict accurately the location of the metaphase II meiotic spindle in mammalian oocytes. *Fertil Steril* 1999; 71: 719–721.
14. Sato H, Ellis GW, Inoue S. Microtubular origin of meiotic spindle from birifrangence. Demonstration of the applicability of Wiener's equation. *J Cell Biol* 1975; 67: 501–517.
15. Trimarchi JR, Karin RA, Keefe DL. Average spindle retardance observed using the polscope predicts cell number in day 3 embryos. *Fertil Steril* 2004; 82 (Suppl 2): S268.
16. Shen Y, Stalf T, De Santis L, et al. Light retardance by human oocyte spindle is positively related to pronuclear score after ICSI. *Reprod Biomed Online* 2006; 6: 737–751.
17. Rama Raju GA, Prakash GJ, Krishna KM, et al. Meiotic spindle and zona pellucida characteristics as predictors of embryonic development: A preliminary study using Polscope imaging. *Reprod Biomed Online* 2007; 14: 166–174.
18. Kilani S, Cooke S, Kan A, et al. Are there non-invasive markers in human oocytes that can predict pregnancy outcome? *Reprod Biomed Online* 2009; 18: 674–680.
19. De Santis L, Cino I, Rabellotti E, et al. Polar body morphology and spindle imaging as predictors of oocyte quality. *Reprod Biomed Online* 2005; 11: 36–42.
20. Ebner T, Balaban B, Moser M, et al. Automatic user-independent zona pellucida imaging at the oocyte stage allows for the prediction of preimplantation development. *Fertil Steril* 2010; 94: 913–920.
21. Pellettier C, Keefe DL, Trimarchi JR. Non-invasive polarized light microscopy quantitatively distinguishes the multilaminar structure of the zona pellucida of living human eggs and embryos. *Fertil Steril* 2004; 81: 850–856.

22. Patrizio P, Fragouli E, Bianchi V, et al. Molecular methods for selection of the ideal oocyte. *Reprod Biomed Online* 2007; 15: 346–353.
23. Seli E, Robert C, Sirard MA. OMICS in assisted reproduction: Possibilities and pitfalls. *Mol Hum Reprod* 2010; 16: 513–530.
24. Huang Z, Wells D. The human oocyte and cumulus cells relationship: New insights from the cumulus cell transcriptome. *Mol Hum Reprod* 2010; 16: 715–725.
25. Uyar A, Torrealday S, Seli E. Cumulus and granulosa cell markers of oocyte and embryo quality. *Fertil Steril* 2013; 99: 979–997.
26. Adashi EY. Endocrinology of the ovary. *Hum Reprod* 1994; 9: 815–827.
27. Albertini DF, Combelles CM, Benecchi E, et al. Cellular basis for paracrine regulation of ovarian follicle development. *Reproduction* 2001; 121: 647–653.
28. Gilchrist RB, Lane M, Thompson JG. Oocyte-secreted factors: Regulators of cumulus cell function and oocyte quality. *Hum Reprod Update* 2008; 14: 159–177.
29. Zhang X, Jafari N, Barnes RB, et al. Studies of gene expression in human cumulus cells indicate pentraxin 3 as a possible marker for oocyte quality. *Fertil Steril* 2005; 83 (Suppl 1): 1169–1179.
30. Feuerstein P, Cadoret V, Dalbies-Tran R, et al. Gene expression in human cumulus cells: One approach to oocyte competence. *Hum Reprod* 2007; 22: 3069–3077.
31. McKenzie LJ, Pangas SA, Carson SA, et al. Human cumulus granulosa cell gene expression: A predictor of fertilization and embryo selection in women undergoing IVF. *Hum Reprod* 2004; 19: 2869–2874.
32. Cillo F, Brevini TAL, Antonini S, et al. Association between human oocyte developmental competence and expression levels of some cumulus genes. *Reproduction* 2007; 134: 645–650.
33. Van Montfoort APA, Geraedts JPM, Dumoulin JCM, et al. Differential gene expression in cumulus cells as a prognostic indicator of embryo viability: A microarray analysis. *Mol Hum Reprod* 2008; 14: 157–168.
34. Anderson RA, Sciorio R, Kinnell H, et al. Cumulus gene expression as a predictor of human oocyte fertilisation, embryo development and competence to establish a pregnancy. *Reproduction* 2009; 138: 629–637.
35. Gebhardt KM, Feil DK, Dunning KR, et al. Human cumulus cell gene expression as a biomarker of pregnancy outcome after single embryo transfer. *Fertil Steril* 2011; 96: 47–52.e2.
36. Assou S, Haouzi D, Mahmoud K, et al. A non-invasive test for assessing embryo potential by gene expression profiles of human cumulus cells: A proof of concept study. *Mol Hum Reprod* 2008; 14: 711–719.
37. Maraldi T, Riccio M, Sena P, et al. MATER protein as substrate of PKC epsilon in human cumulus cells. *Mol Hum Reprod* 2009; 15: 499–506.
38. Fragouli E, Wells D, Iager AE, et al. Alteration of gene expression in human cumulus cells as a potential indicator of oocyte aneuploidy. *Hum Reprod* 2012; 27: 2559–2568.
39. Matos L, Stevenson D, Gomes F, et al. Superoxide dismutase expression in human cumulus oophorus cells. *Mol Hum Reprod* 2009; 15: 411–419.
40. Ito M, Muraki M, Takahashi Y, et al. Glutathione S-transferase theta 1 expressed in granulosa cells as a biomarker for oocyte quality in age-related infertility. *Fertil Steril* 2009; 90: 1026–1035.
41. Hamel M, Dufort I, Robert C, et al. Identification of differentially expressed markers in human follicular cells associated with competent oocytes. *Hum Reprod* 2008; 23: 1118–1127.
42. Wang N, Zhang P, Guo X, et al. Comparative proteome profile of immature rat ovary during primordial follicle assembly and development. *Proteomics* 2009; 9: 3425–3434.
43. Atiomo WU, Khalid S, Ziauddin A, et al. Framework for a system approach to proteomic biomarker profiling in polycystic ovary syndrome. *Expert Rev Proteomics* 2009; 6: 469–499.
44. Estes SJ, Ye B, Qiu W, et al. A proteomic analysis of IVF follicular fluid in women <or=32 years old. *Fertil Steril* 2009; 92: 1569–1578.
45. Jarkovska K, Martinkova J, Liskova L, et al. Proteome mining of human follicular fluid reveals a crucial role of complement cascade and key biological pathways in women undergoing in vitro fertilization. *J Proteome Res* 2010; 5: 1289–1301.
46. Nagy ZP, Sakkas D, Behr B. Symposium: Innovative techniques in human embryo viability assessment. Non-invasive assessment of embryo viability by metabolomic profiling of culture media ('metabolomics'). *Reprod Biomed Online* 2008; 17: 502–507.
47. Revelli A, Delle Piane L, Casano S, et al. Follicular fluid content and oocyte quality: From single biochemical markers to metabolomics. *Reprod Biol Endocrinol* 2009; 7: 40.

48. Roberts R, Stark J, Iatropoulou A, et al. Energy substrate metabolism of mouse cumulus-oocyte complexes: Response to follicle-stimulating hormone is mediated by the phosphatidylinositol 3–kinase pathway and is associated with oocyte maturation. *Biol Reprod* 2004; 71: 199–209.
49. Preis KA, Seidel G, Jr, Gardner DK. Metabolic markers of developmental competence for in-vitro matured mouse oocytes. *Reproduction* 2005; 130: 475–483.
50. Scott L, Berntsen J, Davies D, et al. Human oocyte respiration rate measurement- potential to improve oocyte and embryo selection? *Reprod Biomed Online* 2008; 17: 461–469.
51. Nargund G, Bourne T, Doyle P, et al. Association between ultrasound indices of follicular blood flow, oocyte recovery, and preimplantation embryo quality. *Hum Reprod* 1996; 11: 109–113.
52. Chui DKC, Pugh ND, Walker SM, et al. Follicular vascularity – the predictive value of transvaginal power Doppler ultrasonography in an in-vitro fertilization programme: A preliminary study. *Hum Reprod* 1997; 12: 191–196.
53. Van Blerkom J, Antczak M, Schrader R. The developmental potential of the human oocyte is related to the dissolved oxygen content of follicular fluid: Association with vascular endothelial growth factor levels and perifollicular blood flow characteristics. *Hum Reprod* 1997; 12: 1047–1055.
54. Van Blerkom J. Can the developmental competence of early human embryos be predicted effectively in the clinical IVF laboratory? *Hum Reprod* 1997; 12: 1610–1614.
55. Van Blerkom J. Epigenetic influences on oocyte developmental competence: Perifollicular vascularity and intrafollicular oxygen. *J Assist Reprod Genet* 1998; 15: 226–234.
56. Van Blerkom J. Intrafollicular influences on human oocyte developmental competence: Perifollicular vascularity, oocyte metabolism and mitochondrial function. *Hum Reprod* 2000; 15: 173–188.
57. Bhal PS, Pugh ND, Chui DK, et al. The use of transvaginal power Doppler ultrasonography to evaluate the relationship between perifollicular vascularity and outcome in in-vitro fertilization treatment cycles. *Hum Reprod* 1999; 14: 939–945.
58. Bhal PS, Pugh ND, Gregory L, et al. Perifollicular vascularity as a potential variable affecting outcome in stimulated intrauterine insemination treatment cycles: A study using transvaginal power Doppler. *Hum Reprod* 2001; 16: 1682–1689.
59. Huey S, Abuhamad A, Barroso G, et al. Perifollicular blood flow Doppler indices, but not follicular pO2, pCO2, or pH, predict oocyte developmental competence in in vitro fertilization. *Fertil Steril* 1999; 72: 707–712.
60. Borini A, Maccolini A, Tallarini A, et al. Perifollicular vascularity and its relationship with oocyte maturity and IVF outcome. *Ann N Y Acad Sci* 2001; 943: 64–67.
61. Borini A, Tallarini A, Maccolini A, et al. Perifollicular vascularity monitoring and scoring: A clinical tool for selecting the best oocyte. *Eur J Obstet Gynecol Reprod Biol* 2004; 115 (Suppl): S102–S105.
62. Palomba S, Russo T, Falbo A, et al. Clinical use of the perifollicular vascularity assessment in IVF cycles: A pilot study. *Hum Reprod* 2006; 21: 1055–1061.
63. Palomba S, Russo T, Orio F, et al. Perifollicular vascularity assessment for selecting the best oocytes for in vitro fertilization programs in older patients. *Fertil Steril* 2008; 90: 1305–1309.
64. Robson SJ, Barry M, Norman RJ. Power Doppler assessment of follicle vascularity at the time of oocyte retrieval in in vitro fertilization cycles. *Fertil Steril* 2008; 90: 2179–2182.
65. Monteleone P, Artini PG, Simi G, et al. Follicular fluid VEGF levels correlate with perifollicular blood flow in normoresponder patients undergoing IVF. *J Assist Reprod Genet* 2008; 25: 183–186.
66. Gaulden M. The enigma of Down syndrome and other trisomic conditions. *Mutat Res* 1992; 269: 69–88.
67. Van Blerkom J, Davis P, Lee J. ATP content of human oocytes and developmental potential and outcome after in vitro fertilization and embryo transfer. *Hum Reprod* 1995; 10: 415–424.
68. Barroso G, Barrionuevo M, Rao P, et al. Vascular endothelial growth factor, nitric oxide, and leptin follicular fluid levels correlate negatively with embryo quality in IVF patients. *Fertil Steril* 1999; 72: 1024–1026.
69. Malamitsi-Puchner A, Sarandakou A, Baka SG, et al. Concentrations of angiogenic factors in follicular fluid and oocyte-cumulus complex culture medium from women undergoing in vitro fertilization: Association with oocyte maturity and fertilization. *Fertil Steril* 2001; 76: 98–101.

11

Noninvasive Techniques: Embryo Selection by Oxygen Respiration

Alberto Tejera, Belén Aparicio, Carmela Albert, Arancha Delgado, and Marcos Meseguer

Introduction

Assisted human reproduction is characterized by high variability in results regarding pregnancy and birth rates. In fact, in a cohort of fertilized oocytes from the same stimulation cycle, the developmental rate varies drastically, even though produced at the same time and under similar conditions [1]. This variability results in large differences in implantation potential of human embryos developed in vitro, despite similarities in observable parameters such as embryo developmental rates and morphology. Classic studies suggested that morphologic embryo quality is correlated with implantation rates, being the best predictor for the treatment outcome [2–4]. Therefore, there is no doubt that embryo morphology (determined by the number, size, and shape of blastomeres; the proportion of fragments; and the presence of multinucleated blastomeres) has some predictive value on development and implantation potential [5]. However, it is important to highlight that sometimes this conventional evaluation is not enough to get a successful pregnancy, and seemingly good morphology embryos do not always lead to implantation and birth. This could be explained by the lack of endometrial receptivity and the fact that many embryos cease to develop before implantation. For this reason, several noninvasive techniques have been proposed that may be able to detect alterations of culture environment surrounding oocytes and embryos to gain supplemental information regarding embryo viability [6–8].

Some noninvasive methods such as metabolomic profiling are still at the initial stages of development, awaiting verification in daily laboratory practice [9], but they could be applied in the future with further improvements [10,11]. One of these noninvasive methods, namely oxygen consumption (OC), show promise as a good indicator of overall metabolic activity [12] and may be a valuable parameter for evaluating embryo quality [13,14]. OC is directly related with the capacity of an embryo to produce ATP via oxidative phosphorylation, a process that uses 30% and 60%–70% of the oxygen consumed by the embryo at the early cleavage and blastocyst stages, respectively [15].

Cellular energy (ATP) is produced by glycolysis (anaerobic respiration) and oxidative phosphorylation (aerobic respiration). The energy created by the first pathway does not involve O_2 and produces a low amount of energy, owing to the incomplete metabolism of glucose (ΔG 47 kcal/mol glucose). The energy released from the aerobic process (second pathway) is higher (686 kcal/mol glucose) than with the anaerobic mechanism, and it is harnessed in the Krebs cycle coupled to the mitochondrial electron transport chain during oxidative phosphorylation [1,16–20]. Therefore, ATP production could be estimated by measuring OC, because oxidative phosphorylation is the major producer of ATP in mammalian early embryos [21–23], and measuring the OC pattern provides a good estimation of embryo metabolism.

The purpose of this chapter is to describe new and potentially useful aspects for the evaluation of the embryo implantation potential, focusing on OC as a tentative method for embryo selection. In the first section of this chapter, we evaluate the influence of different stimulation protocols on the oocyte OC as well as the influence of different oocyte dysmorphisms in respiration rates. The next step was to study how the fertilization process might be affected by oxygen uptake. In the second part of the chapter, we focus on embryos, measuring the OC during 3 days of culture until embryo transfer and evaluating its correlation with embryo development and reproductive outcome.

OC Measurements

Respiration or OC measurements need a special microsensor that is provided by the EmbryoScope version C (Unisense FertiliTech, Denmark) incubator as presented in Figure 11.1.

This incubator has controlled temperature and gas composition and an optional microsensor, facilitating automatic measurements of the OC for each individual oocyte or embryo based on a steady-state respirometer principle (Figure 11.1). OC rate measurements are performed by a Clark-type electrochemical O_2 sensor, and the time taken for O_2 measurements is 60 s per oocyte or embryo. Sensor calibration is automatic and is part of each measurement cycle. Calibration is performed by first submerging the microsensor in 0.1 M alkaline sodium ascorbate (0% O_2) and then in the medium inside the beaker (20% O_2).

The sensitivity and reproducibility of the technique enable accurate measurement of OC rates down to 0.05 nL/hr (0.6×10^{-15} fmol/s). The reproducibility analysis indicates a standard deviation of <0.01 nL/hr (0.083 fmol/s). The time between measurements is 60 min for four slides, for a 15 min cycle possible with a single slide.

The procedure is performed as follows: the oocyte or the embryo is placed at the bottom of a microwell (0.5 mm in diameter, 1.5 mm in depth) in the embryo slide containing a culture medium droplet of 25 µL of Quinn Advantage Cleavage medium (QACM) covered with an overlay of mineral oil to prevent evaporation. As the oocyte or embryo consumes O_2, the concentration at the bottom of the well is reduced, establishing a linear O_2 concentration gradient down through the well. This gradient is quantified by the O_2 sensor, and the OC rate can be estimated from the measured OC gradient within the well containing the sample, according to Fick's first law of diffusion. Thus, multiplying the gradient by the O_2 diffusion coefficient (3.37×10^{-5} cm^2/s at 37ºC and 9% salinity) and the cross-sectional area of the well (0.25 mm^2). The calculated OC rate for each sample is expressed in femtomoles of O_2 consumed per second, using O_2 solubility in the medium of 200.4 mmol/L at 37ºC and 9% salinity. The narrowness of the well prevents convection from taking place at a level that would influence the accuracy of the diffusion calculations.

OC by the oocyte or embryo reduces the concentration of O_2 at the bottom of the well, thereby establishing a linear measurable O_2 concentration gradient.

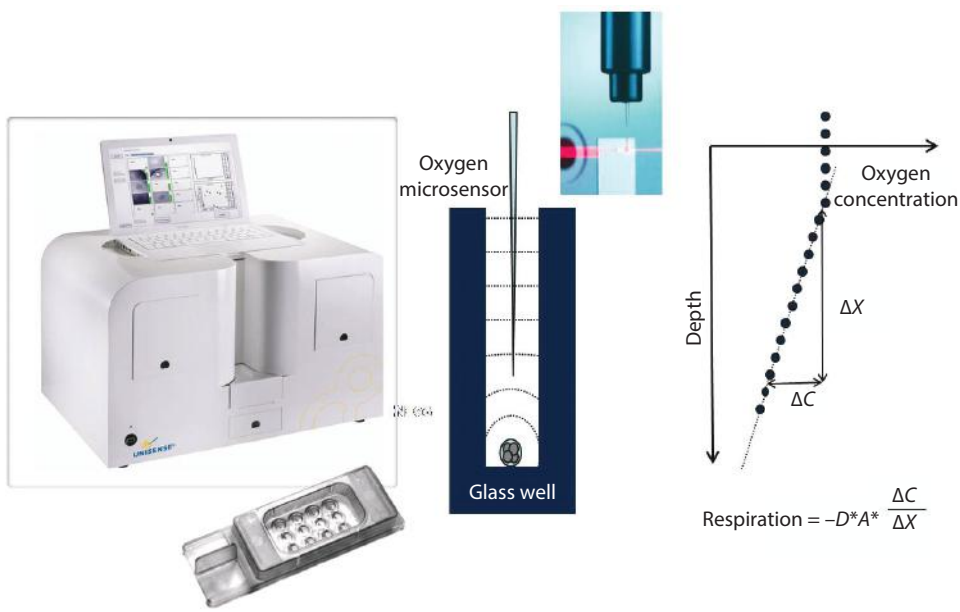

FIGURE 11.1 Schematic overview of incubator with a microsensor that can be used to measure the oxygen consumption through the gradient created by oocyte uptake, as explained in the text.

The injection-molded EmbryoSlide is impermeable to gaseous exchange, and the O_2 microelectrode is recalibrated automatically at the onset of each new measurement cycle. The interval between consecutive OC rate measurements for the same oocyte or embryo is 20 min.

Also, the incubator includes an imaging system that uses a low-intensity red light (650 nm) from a single light-emitting diode (LED) with short illumination times for image acquisition of 30 ms per image. The optics consists of a modified Hoffmann contrast with a 20× objective (Leica Place), providing optimal light sensitivity and resolution for the red wavelength. The digital images are collected by a highly sensitive charge-coupled device (CCD) camera (1280 × 1024 pixels) with a resolution of 3 pixels per μm, monochrome, 8-bit. The time between acquisitions is 15 min for four slides, and a 4 min cycle is possible for a single slide. The consequence is an image acquisition time per well including focusing that gives rise to a video recorded by a camera.

Oocyte Respiration

The contemporary classification of oocytes is routinely based solely on a qualitative evaluation of morphological criteria. For oocytes, polar body morphology [24]; cytoplasm appearance [25]; zona pellucida thickness, appearance, and birefringence [26,27]; and the position or shape of the spindle [28,29] have all been shown to correlate with viability. The predictive value of these individual parameters is still unresolved but is generally presumed to be limited. Animal experiments have shown that accurate measurement of different aspects of oocyte metabolic activity can predict embryo developmental potential [6–8].

The mitochondrial respiration component has been correlated with oocyte quality and subsequent embryo development [30–32], and a direct correlation between mitochondrial distribution and the subsequent development of mammalian embryos has been found in several species [30].

In the oocyte, mitochondria are probably the major energy-producing system (ATP production), many studies mention that low mitochondrial activity and number are associated with premature arrest of the oocyte, fertilization failure, and reduced embryo development [33–35].

If abnormal mitochondrial complement can compromise respiration [36–39], measuring O_2 uptake in single oocytes may indicate both defects on mitochondrial load or dysfunction and therefore O_2 uptake measurements might be useful for the selection of oocytes with better viability. To date, the different techniques developed to measure O_2 are unsuitable for clinical use because they are too invasive for embryos, they have low sensitivity, and they cannot measure OC without affecting embryo viability. A recent study [40] has demonstrated differences in oocyte quality based on morphology and reproductive outcome analysis for different ovarian stimulation regimens, such as urinary human menopausal gonadotropin (hMG), highly purified menotropin (HP-hMG), and recombinant follicle-stimulating hormone (rFSH). However, there is still little information available on metabolic markers of oocyte quality. One approximation of oocyte quality was done by Scott et al. [41,42]. They worked with human oocytes, and although the material consisted of immature or nonfertilized oocytes, they observed differences on respiration rates depending on maternal age or basal FSH concentrations, two factors directly related with oocyte health.

In human oocytes, OC is a quality marker for oocyte competence and is affected by ovarian stimulation regimens.

In human oocytes, we have demonstrated that OC is a quality marker for human oocyte competence and is affected by ovarian stimulation regimens (Figure 11.2). Regarding OC and oocyte morphology, we can see that OC was not affected by the morphology of the oocytes. Oocytes with normal morphology had similar oxygen uptake compared with other oocyte phenotypes, such as clustered (clust) and granular (Gr), or with oocytes having large periviteline space (LPS), refractile bodies (RBs), multiple dysmorphism (M), or the first polar body fragmented (fPB) (Figure 11.3). Finally, the analysis between OC and the fertilization of oocytes showed a direct correlation between oocyte OC and normal fertilization. The average OC was approximately 10% higher for oocytes, before intracytoplasmic sperm injection (ICSI), that were subsequently successfully fertilized (i.e., with two visible pronuclei) compared with oocytes that failed to fertilize (Figure 11.4).

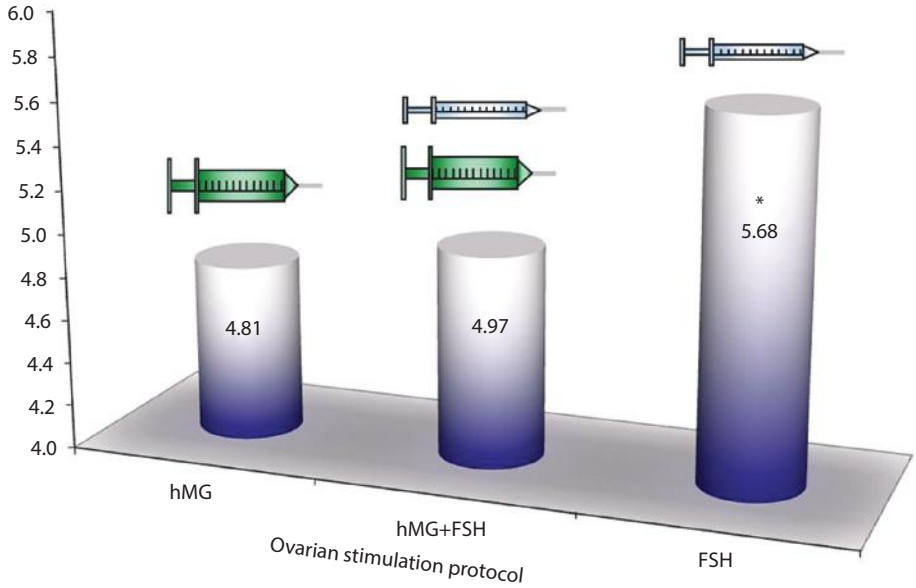

FIGURE 11.2 OC depending on stimulation protocol. Note the higher uptake when we stimulate the donor only with FSH, compared with stimulation with hMG or with a combination of FSH and hMG.

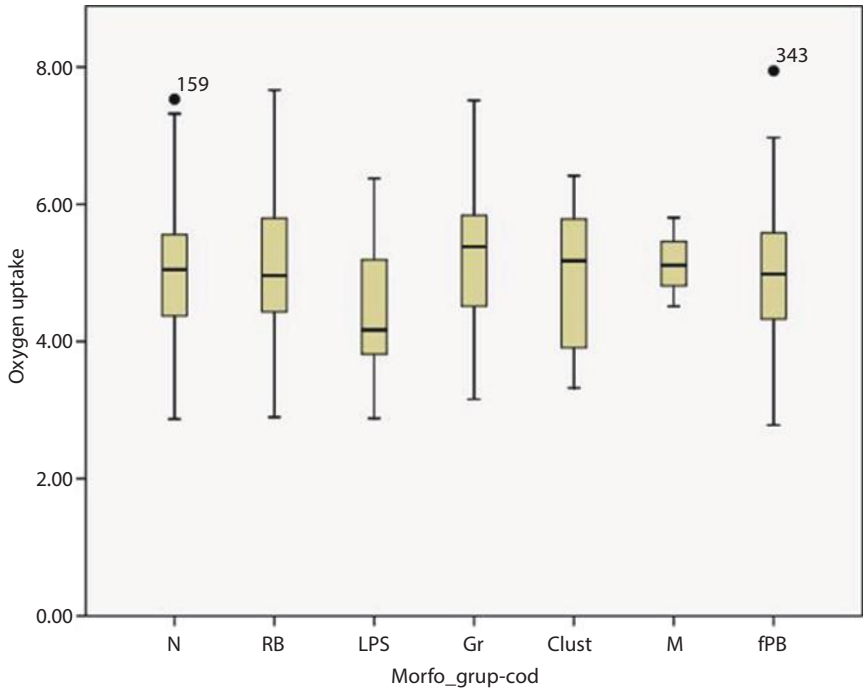

FIGURE 11.3 Box plot graphics of OC depending on oocyte morphology. Normal aspect (N), clustered (clust), granular (Gr), large periviteline space (LPS), refractile bodies (RB), multiple dysmorphism (M), or the first polar body fragmented (fPB). The levels of OC were very similar for the seven categories established with regard to oocyte phenotype.

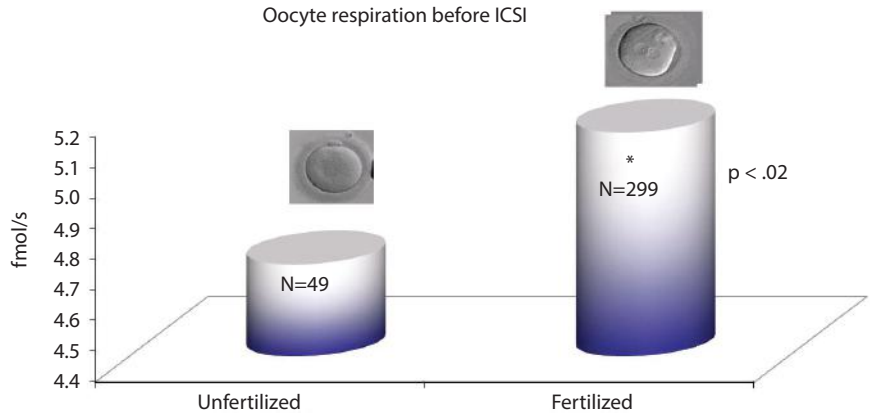

FIGURE 11.4 Analysis of OC and its influence on the fertilization process. The level of OC was higher for those oocytes correctly fertilized, whereas the unfertilized oocytes had lower values. (*) denotes a significant difference ($p < .05$).

Embryo Respiration

Until recently, the only instrument used for embryo evaluation was the inverted light microscope that provided information on morphological characteristics. Developmental and morphological information gained from microscopic assessment has been positively associated with in vitro fertilization (IVF) outcomes [3,4,43], including pregnancy and implantation rates, but as mentioned, we need new selection methods that allow prediction of embryo development potential by improving probabilities of achieving pregnancy for infertile couples [44]. The measurement of OC might be a valuable parameter for evaluating embryo quality [13,14]. Because paternal (sperm-derived) mitochondria do not survive after fertilization [45], the entire mitochondrial content of the developing fetus is derived from the oocyte. As it has been described, mitochondria are the main oxygen consumers in mammalian oocytes and early embryos [17,18,21,46,47]. Therefore, changes in mitochondrial activity should be directly reflected in the OC of the developing embryo.

It has been demonstrated that embryos change their metabolic preferences depending on their developmental stage [48], but to date it has not been described whether OC changes depend on the embryo developmental stage.

We have studied OC on embryo developmental stages from fertilization to embryo transfer, dividing the O_2 measurements into four groups based on quartiles with a similar number of measurements in each period: (1) from ICSI through pronucleus (PN) formation (<17.2 hr), (2) from PN formation through first cleavage (17.2–35.0 hr), (3) after first cleavage through second and third cleavages (35.1–52.0 hr), and (4) after 52 hr until moment of the embryo transfer (72 hr). The results revealed different levels of OC according to embryo stage, giving values for each quartile of 5.34 fmol/s (95% CI, 5.31–5.36), 5.17 fmol/s (95% CI, 5.15–5.20), 4.81 fmol/s (95% CI, 4.78–4.84), and 4.59 fmol/s (95% CI, 4.56–4.62; $p < .0001$), as shown in Figure 11.5.

Magnusson et al. [49] suggested that human embryos that consumed more oxygen developed into blastocysts more quickly than those with lower OC rates [49]. Other studies have demonstrated that embryos with appropriate OC have a high ability to develop into blastocysts. Yamanaka et al. [50] observed higher OC in advanced stages (hatching or hatched group) compared with the arrested or degenerated stages, as well as a higher consumption in fresh blastocysts than in vitrified, warmed blastocysts.

In our experience, the OC of embryos that achieve an ongoing pregnancy is higher compared with those that do not, showing the biggest differences in the last quartile (>52.1 hr post-ICSI), when the embryo has five or more cells (Figure 11.6). We observed the same pattern for embryos that implant compared with those that do not implant (Figure 11.7). Again, the biggest difference was observed in the last quartile. Therefore, results obtained

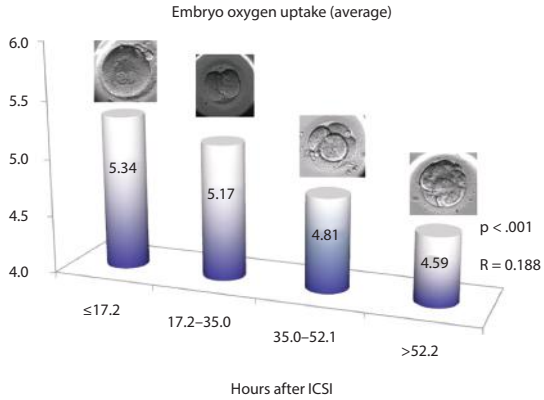

FIGURE 11.5 Time-dependent embryo OC. Averages in each of the four time ranges are presented. A significant linear correlation was found between embryo development and OC (Pearson correlation index = –0.188; p < .001).

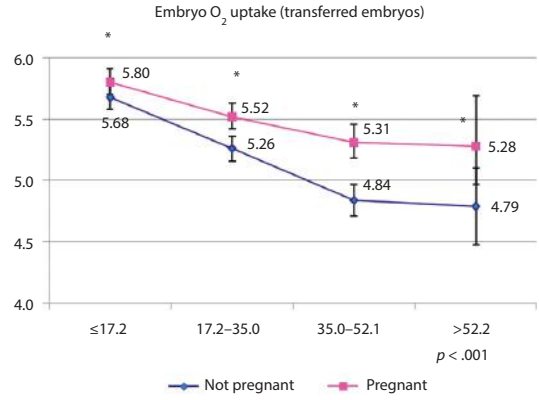

FIGURE 11.6 OC averages in each of the four time ranges for transferred embryos. (*) indicates a significant difference (p < .001) between transferred embryos that generated an ongoing pregnancy and embryos that did not generate an ongoing pregnancy at different time ranges.

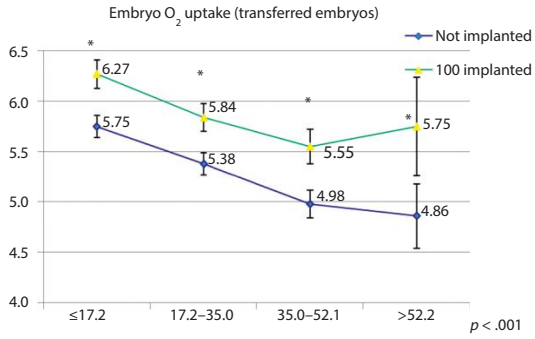

FIGURE 11.7 OC averages from transferred embryos in each of the four time ranges depending on implantation success. (*) indicates a significant difference (p < .001) between implanted embryos and nonimplanted embryos, with bigger differences from 52.1 hr post-ICSI.

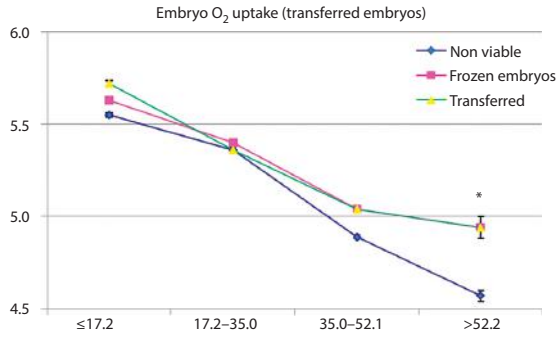

FIGURE 11.8 OC averages in each of the four time ranges depending on final embryo viability. (*) indicates significant difference (p < .001) between T/F and NV embryos.

in both analyses suggest that respiration patterns from 52 hr after ICSI and onward show the strongest correlation with implantation and ongoing pregnancy success.

Finally, we observed that the final destination of the embryo was well correlated with OC, with differences becoming more significant in the advanced stages of embryo cleavage. The OC values were very similar for the three categories nonviable (NV), frozen (F), and transferred (T) during the first hours of development. However, as cleavages continued, the differences in OC pattern became more pronounced between the better (T or F) and the poorer quality (NV) embryos, at 4.57 fmol/s for NV, 4.94 fmol/s for F, and 4.96 fmol/s for T from 52.2 hr and onward. Embryos with similar morphological features presented similar average OC values, displaying a correlation between quality and OC (Figure 11.8).

Time Lapse and Oxygen Uptake: Cytokinesis and Embryo Respiration

To understand the relationship between metabolism and embryo competence, we investigated the possible correlation between OC and cytokinesis, a key temporal event (cell cleavage). Studies have reported small peaks of OC (increases of 3%–10%) preceding cell division and lasting until 2 hr. Detection of the timing of the first cleavage is critical for subsequent evaluation of embryo quality and viability, because early cleavage is considered a significant predictor of developmental potential and has been associated with higher pregnancy and implantation rates [51–53].

Taking this into account, embryo OC rates were analyzed at time intervals according to cytokinesis timings (i.e., at the time in which the cleavage takes place or active period and the next measurement after the first division or inactive period). Initially, we analyzed these measurements in all embryos, for a further comparison between consumption of T and NV embryos, and finally, among the T embryos, in those that implanted or not.

We obtained a total of 3815 measurements during the cytokinesis (active phase) and 2204 measurements after this division (passive phase), and we observed a significant increase in OC levels when cytokinesis occurred, with values of 4.74 fmol/s (95% CI, 4.72–4.76) between cleavages (interphase period) and 5.14 fmol/s (95% CI, 4.72–4.76) during the cytokinesis period (Figure 11.9).

Silent and active cleavage periods show clear differences in OC.

Differences in OC between silent and active cleavage periods changed substantially among the different events from PN formation to cleavage to eight cells (Figure 11.10). When we analyzed OC between embryos with good and poor quality, we observed higher levels in the embryos with better quality in both phases (interphase and cytokinesis). The T embryos presented higher OC levels when cytokinesis occurred, 5.25 fmol/s (95% CI, 5.23–5.28) at interphase versus 5.43 fmol/s (95% CI, 5.33–5.52) at cytokinesis, compared with discarded embryos (arrested or bad-quality embryos), 5.09 fmol/s (95% CI, 5.01–5.05) versus 5.28 fmol/s (95% CI, 5.21–5.35), respectively (Figure 11.11).

Among the T embryos, we found that those that implanted presented a higher increase in OC during cytokinesis, 5.79 fmol/s (95% CI, 5.66–5.91) during interphase period versus 6.71 fmol/s (95% CI, 5.85–7.58) during cleavage period, than the embryos that failed to implant, 5.21 fmol/s (95% CI, 5.06–5.36) versus 5.28 fmol/s (95% CI, 5.15–5.41), demonstrating the existence of high OC demand in the cell cleavage in embryos with higher implantation potential (Figure 11.12).

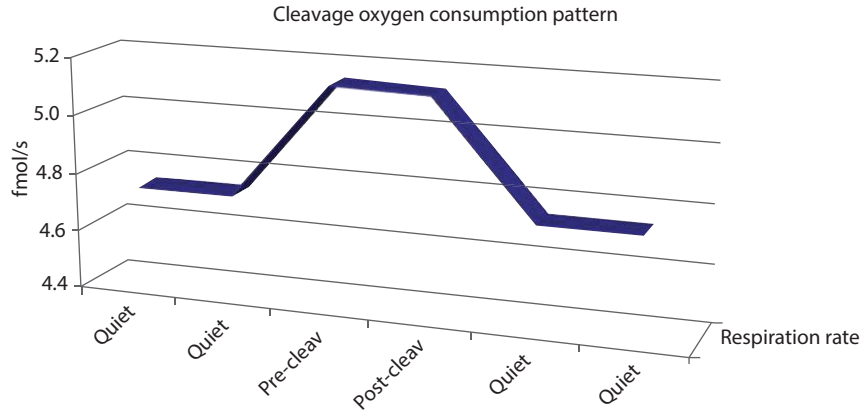

FIGURE 11.9 OC during the division timing. Note the peak corresponds to higher energy demand in the starting of second cell cycle.

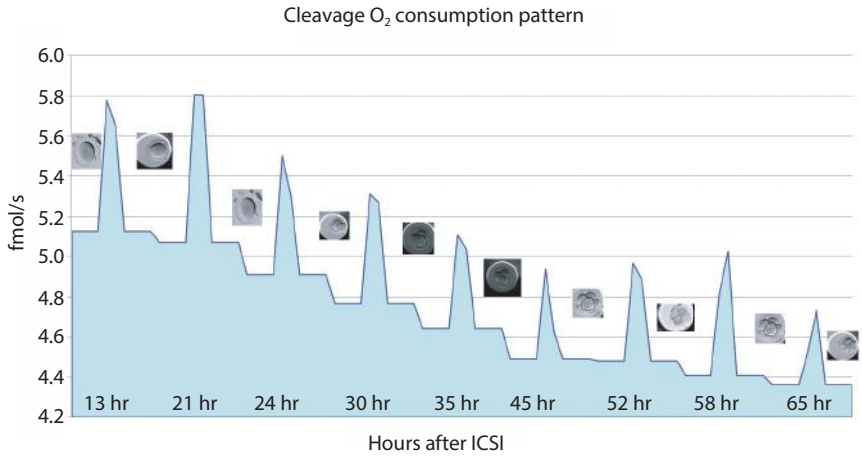

FIGURE 11.10 OC before and after each division. Note that the peak corresponds to higher energy demand in each embryo cleavage.

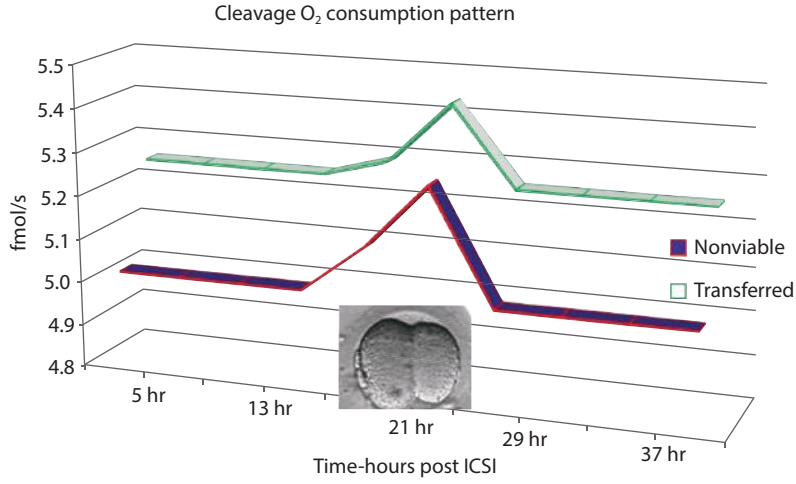

FIGURE 11.11 OC average between embryos with poor or good quality before and after cytokinesis. Note the higher values corresponding to transferred embryos (good quality), compared with lower values of nonviable embryos.

Limitations of the Measurement System

Even though we have seen that systems introducing OC measurements can be really useful in improving embryo selection in the laboratory, such systems do have some as yet not fully resolved limitations. We must take into account the fact that the study we have presented was developed using a C version of EmbryoScope and not the currently available medical device. Being then a prototype, several technical problems and limitations were present. This device had a capacity for four slides (12 embryos each) at the same time. It is important to highlight that the O_2 microelectrode was washed with different solutions and recalibrated automatically at the onset of each new measurement cycle (12 embryos). However, the same sensor was placed in different slides (embryos from different patients in their corresponding slides). Thus, in our study, we could analyze only one patient each time to avoid the same sensor handling different patients' media.

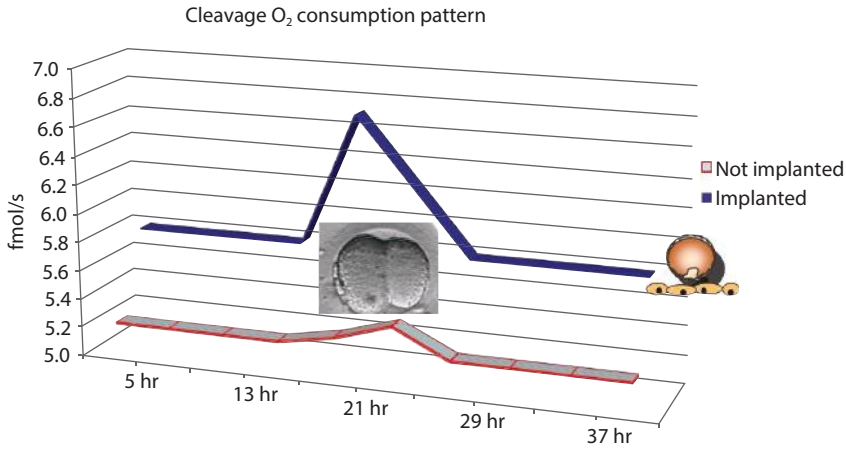

FIGURE 11.12 OC average between implanted or not implanted embryos before and after cytokinesis. Note the higher peak corresponding to implanted embryos, compared with lower peak of not implanted embryos (practically nonexistent peak).

Moreover, even though this version included a time-lapse unit, it was not possible to perform OC measurements and image analysis at the same time. Pictures were taken at different timings when OC measurements were performed. Having the measurements and time-lapse recordings, data analysis was complex. The software available did not combine both data, and then sophisticated Excel spreadsheets were mandatory to do data analysis. Regardless, the OC measurements were done just before and after each division and not during cytokinesis.

Future Perspectives: An Embryo Selection by OC?

It is important to highlight that even though morphological evaluation remains the primary method of embryo assessment, it is not always accurate enough and the good appearance of embryos does not always mean pregnancy and birth. Embryo selection based on OC could be a new option to improve the assisted reproduction outcome, where more than half of the cycles fail to succeed.

The results presented here show that the OC rate of T embryos that achieved an ongoing pregnancy was significantly higher than the OC rate of embryos that did not achieve it. The high peak observed during first division in implanted embryos could be regarded as an alternative method of embryo selection, based on our observations of reduced peaks in nonimplanted embryos. The higher OC differences observed in the advanced stages of cleavage embryos strengthens the hypothesis of embryo selection by OC: respiration patterns from 52 hr after ICSI and onward showed the strongest correlation with implantation and ongoing pregnancy success. Such differences, which increased as cleavage continued, could be indicating that progressive deficiencies in mitochondrial function are reflected in differences in embryo OC.

Regarding embryo viability, the OC values were very similar for all types of embryos during the first hours of development, but as cleavage continued, the differences in OC patterns became more pronounced between the better and the poorer quality embryos. These results corroborate the conclusions mentioned above and suggest that the measurements should be performed almost immediately before the embryo transfer (from 52 hr post-ICSI) if the intention is to perform the embryo selection by combining OC with standard embryo morphology.

Toward later cleavage stages, differences in OC patterns become more pronounced between better and poorer quality embryos.

The OC could be considered as an alternative to assess human embryo metabolomic profiling: OC is the main portion of metabolism in the growing embryo and the literature suggests that the metabolomic profile is a potential marker of embryo viability in the human model [54,55]. The combination of both methods (metabolism and time lapse), considered as noninvasive, offers an opportunity to learn more about the developmental competence of the embryo, without legal and ethical problems. Conventional morphological assessment will remain important, but the intrinsic subjectivity related to evaluation will be compensated by the additional noninvasive analysis, thereby increasing accuracy.

OC measurement could be applied in the near future in IVF laboratories as an alternative method for embryo selection based on the literature and our new findings, but prospective randomized control trials are mandatory to confirm its usefulness for embryo selection with a remarkable increase in the reproductive outcome.

REFERENCES

1. Wilding M, Coppola G, Dale B, Di Matteo L. Mitochondria and human preimplantation embryo development. *Reproduction* 2009;137(4):619–624.
2. Terriou P, Sapin C, Giorgetti C, Hans E, Spach JL, Roulier R. Embryo score is a better predictor of pregnancy than the number of transferred embryos or female age. *Fertil Steril* 2001;75(3):525–531.
3. Ziebe S, Petersen K, Lindenberg S, Andersen AG, Gabrielsen A, Andersen AN. Embryo morphology or cleavage stage: How to select the best embryos for transfer after in-vitro fertilization. *Hum Reprod* 1997;12(7):1545–1549.
4. Van Royen E, Mangelschots K, De Neubourg D, Valkenburg M, Van de Meerssche M, Ryckaert G, et al. Characterization of a top quality embryo, a step towards single-embryo transfer. *Hum Reprod* 1999;14(9):2345–2349.
5. Rienzi L, Ubaldi F, Iacobelli M, Romano S, Minasi MG, Ferrero S, et al. Significance of morphological attributes of the early embryo. *Reprod Biomed Online* 2005;10(5):669–681.
6. Rieger D, Loskutoff NM. Changes in the metabolism of glucose, pyruvate, glutamine and glycine during maturation of cattle oocytes in vitro. *J Reprod Fertil* 1994;100(1):257–262.
7. Lane M, Gardner DK. Selection of viable mouse blastocysts prior to transfer using a metabolic criterion. *Hum Reprod* 1996;11(9):1975–1978.
8. Houghton FD, Hawkhead JA, Humpherson PG, Hogg JE, Balen AH, Rutherford AJ, et al. Non-invasive amino acid turnover predicts human embryo developmental capacity. *Hum Reprod* 2002;17(4):999–1005.
9. Hardarson T, Ahlstrom A, Rogberg L, Botros L, Hillensjo T, Westlander G, et al. Non-invasive metabolomic profiling of Day 2 and 5 embryo culture medium: A prospective randomized trial. *Hum Reprod* 2012;27(1):89–96.
10. Nagy ZP, Sakkas D, Behr B. Symposium: Innovative techniques in human embryo viability assessment. Non-invasive assessment of embryo viability by metabolomic profiling of culture media (‘metabolomics’). *Reprod Biomed Online* 2008;17(4):502–507.
11. Seli E, Vergouw CG, Morita H, Botros L, Roos P, Lambalk CB, et al. Noninvasive metabolomic profiling as an adjunct to morphology for noninvasive embryo assessment in women undergoing single embryo transfer. *Fertil Steril* 2010;94(2):535–542.
12. Leese HJ. What does an embryo need? *Hum Fertil (Camb)* 2003;6(4):180–185.
13. Barnett DK, Bavister BD. What is the relationship between the metabolism of preimplantation embryos and their developmental competence? *Mol Reprod Dev* 1996;43(1):105–133.
14. Houghton FD, Thompson JG, Kennedy CJ, Leese HJ. Oxygen consumption and energy metabolism of the early mouse embryo. *Mol Reprod Dev* 1996;44(4):476–485.
15. Trimarchi JR, Liu L, Porterfield DM, Smith PJ, Keefe DL. Oxidative phosphorylation-dependent and -independent oxygen consumption by individual preimplantation mouse embryos. *Biol Reprod* 2000;62(6):1866–1874.
16. Wilding M, Dale B, Marino M, di Matteo L, Alviggi C, Pisaturo ML, et al. Mitochondrial aggregation patterns and activity in human oocytes and preimplantation embryos. *Hum Reprod* 2001;16(5):909–917.
17. Van Blerkom J. Intrafollicular influences on human oocyte developmental competence: Perifollicular vascularity, oocyte metabolism and mitochondrial function. *Hum Reprod* 2000;15(Suppl 2):173–188.
18. Van Blerkom J, Davis PW, Lee J. ATP content of human oocytes and developmental potential and outcome after in-vitro fertilization and embryo transfer. *Hum Reprod* 1995;10(2):415–424.

19. Pozzan T, Magalhaes P, Rizzuto R. The comeback of mitochondria to calcium signalling. *Cell Calcium* 2000;28(5–6):279–283.
20. Wilding M, Di Matteo L, Dale B. The maternal age effect: A hypothesis based on oxidative phosphorylation. *Zygote* 2005;13(4):317–323.
21. Houghton FD, Leese HJ. Metabolism and developmental competence of the preimplantation embryo. *Eur J Obstet Gynecol Reprod Biol* 2004;115(Suppl 1):S92–S96.
22. Shoubridge EA, Wai T. Mitochondrial DNA and the mammalian oocyte. *Curr Top Dev Biol* 2007;77:87–111.
23. Thompson JG, Partridge RJ, Houghton FD, Cox CI, Leese HJ. Oxygen uptake and carbohydrate metabolism by in vitro derived bovine embryos. *J Reprod Fertil* 1996;106(2):299–306.
24. Ebner T, Yaman C, Moser M, Sommergruber M, Feichtinger O, Tews G. Prognostic value of first polar body morphology on fertilization rate and embryo quality in intracytoplasmic sperm injection. *Hum Reprod* 2000;15(2):427–430.
25. Ebner T, Moser M, Tews G. Is oocyte morphology prognostic of embryo developmental potential after ICSI? *Reprod Biomed Online* 2006;12(4):507–512.
26. Shen Y, Stalf T, Mehnert C, Eichenlaub-Ritter U, Tinneberg HR. High magnitude of light retardation by the zona pellucida is associated with conception cycles. *Hum Reprod* 2005;20(6):1596–1606.
27. Shiku H, Shiraishi T, Ohya H, Matsue T, Abe H, Hoshi H, et al. Oxygen consumption of single bovine embryos probed by scanning electrochemical microscopy. *Anal Chem* 2001;73(15):3751–3758.
28. Madaschi C, de Souza Bonetti TC, de Almeida Ferreira Braga DP, Pasqualotto FF, Iaconelli A, Jr, Borges E, Jr. Spindle imaging: A marker for embryo development and implantation. *Fertil Steril* 2008;90(1):194–198.
29. Madaschi C, Aoki T, de Almeida Ferreira Braga DP, de Cassia Savio Figueira R, Semiao Francisco L, Iaconelli A, Jr, et al. Zona pellucida birefringence score and meiotic spindle visualization in relation to embryo development and ICSI outcomes. *Reprod Biomed Online* 2009;18(5):681–686.
30. Bavister BD, Squirrell JM. Mitochondrial distribution and function in oocytes and early embryos. *Hum Reprod* 2000;15(Suppl 2):189–198.
31. Squirrell JM, Lane M, Bavister BD. Altering intracellular pH disrupts development and cellular organization in preimplantation hamster embryos. *Biol Reprod* 2001;64(6):1845–1854.
32. Squirrell JM, Schramm RD, Paprocki AM, Wokosin DL, Bavister BD. Imaging mitochondrial organization in living primate oocytes and embryos using multiphoton microscopy. *Microsc Microanal* 2003;9(3):190–201.
33. Van Blerkom J. Mitochondria in human oogenesis and preimplantation embryogenesis: Engines of metabolism, ionic regulation and developmental competence. *Reproduction* 2004;128(3):269–280.
34. Van Blerkom J. Mitochondria in early mammalian development. *Semin Cell Dev Biol* 2009;20(3):354–364.
35. Dumollard R, Duchen M, Carroll J. The role of mitochondrial function in the oocyte and embryo. *Curr Top Dev Biol* 2007;77:21–49.
36. May-Panloup P, Chretien MF, Jacques C, Vasseur C, Malthiery Y, Reynier P. Low oocyte mitochondrial DNA content in ovarian insufficiency. *Hum Reprod* 2005;20(3):593–597.
37. May-Panloup P, Chretien MF, Malthiery Y, Reynier P. Mitochondrial DNA in the oocyte and the developing embryo. *Curr Top Dev Biol* 2007;77:51–83.
38. Reynier P, May-Panloup P, Chretien MF, Morgan CJ, Jean M, Savagner F, et al. Mitochondrial DNA content affects the fertilizability of human oocytes. *Mol Hum Reprod* 2001;7(5):425–429.
39. Muller-Hocker J, Schafer S, Weis S, Munscher C, Strowitzki T. Morphological-cytochemical and molecular genetic analyses of mitochondria in isolated human oocytes in the reproductive age. *Mol Hum Reprod* 1996;2(12):951–958.
40. Melo M, Bellver J, Garrido N, Meseguer M, Pellicer A, Remohi J. A prospective, randomized, controlled trial comparing three different gonadotropin regimens in oocyte donors: Ovarian response, in vitro fertilization outcome, and analysis of cost minimization. *Fertil Steril* 2010;94(3):958–964.
41. Scott L, Berntsen J, Davies D, Gundersen J, Hill J, Ramsing N. Symposium: Innovative techniques in human embryo viability assessment. Human oocyte respiration-rate measurement—potential to improve oocyte and embryo selection? *Reprod Biomed Online* 2008;17(4):461–469.
42. Scott L, Finn A, O'Leary T, McLellan S, Hill J. Morphologic parameters of early cleavage-stage embryos that correlate with fetal development and delivery: Prospective and applied data for increased pregnancy rates. *Hum Reprod* 2007;22(1):230–240.
43. Giorgetti C, Terriou P, Auquier P, Hans E, Spach JL, Salzmann J, et al. Embryo score to predict implantation after in-vitro fertilization: Based on 957 single embryo transfers. *Hum Reprod* 1995;10(9):2427–2431.

44. Baczkowski T, Kurzawa R, Glabowski W. Methods of embryo scoring in in vitro fertilization. *Reprod Biol* 2004;4(1):5–22.
45. Cummins JM. Fertilization and elimination of the paternal mitochondrial genome. *Hum Reprod* 2000;15(Suppl 2): 92–101.
46. Zweig MH, Campbell G. Receiver-operating characteristic (ROC) plots: A fundamental evaluation tool in clinical medicine. *Clin Chem* 1993;39(4):561–577.
47. Lopes AS, Lane M, Thompson JG. Oxygen consumption and ROS production are increased at the time of fertilization and cell cleavage in bovine zygotes. *Hum Reprod* 2010;25:2762–2773.
48. Botros L, Sakkas D, Seli E. Metabolomics and its application for non-invasive embryo assessment in IVF. *Mol Hum Reprod* 2008;14(12):679–690.
49. Magnusson C, Hillensjo T, Hamberger L, Nilsson L. Oxygen consumption by human oocytes and blastocysts grown in vitro. *Hum Reprod* 1986;1(3):183–184.
50. Yamanaka M, Hashimoto S, Amo A, Ito-Sasaki T, Abe H, Morimoto Y. Developmental assessment of human vitrified-warmed blastocysts based on oxygen consumption. *Hum Reprod* 2011;26(12):3366–3371.
51. Salumets A, Hyden-Granskog C, Suikkari AM, Tiitinen A, Tuuri T. The predictive value of pronuclear morphology of zygotes in the assessment of human embryo quality. *Hum Reprod* 2001;16(10):2177–2181.
52. Salumets A, Hyden-Granskog C, Makinen S, Suikkari AM, Tiitinen A, Tuuri T. Early cleavage predicts the viability of human embryos in elective single embryo transfer procedures. *Hum Reprod* 2003;18(4):821–825.
53. Fancsovits P, Toth L, Takacs ZF, Murber A, Papp Z, Urbancsek J. Early pronuclear breakdown is a good indicator of embryo quality and viability. *Fertil Steril* 2005;84(4):881–887.
54. Garrido-Gomez T, Dominguez F, Lopez JA, Camafeita E, Quinonero A, Martinez-Conejero JA, et al. Modeling human endometrial decidualization from the interaction between proteome and secretome. *J Clin Endocrinol Metab* 2011;96(3):706–716.
55. Dominguez F, Pellicer A, Simon C. The human embryo proteome. *Reprod Sci* 2009;16(2):188–190.

12

Noninvasive Techniques: Embryo Selection by Time-Lapse Imaging

Alison Campbell

Introduction

The ability to acquire sequential, photographic, time-lapse images of the developing preimplantation human embryo in vitro has recently provided clinical embryologists with a powerful noninvasive embryo monitoring and selection tool. Time-lapse imaging was used to study fertilization and early human embryo kinetics more than 15 years ago, but this technology is now available for the routine clinical in vitro fertilization (IVF) setting [1]. The first live birth after time-lapse imaging of embryos was reported by Pribenszky and colleagues in 2010, and since then time-lapse imaging of embryos has rapidly become a key topic and area of research in the field of human fertility [2]. This chapter focuses on practical aspects of time-lapse imaging for embryo selection. It covers some of the key findings that have been reported to date and considers the potential impact this exciting technology may have on our understanding of embryo development and on clinical IVF outcome.

Standard versus Time-Lapse Methodology in the Embryology Laboratory

Currently, embryo selection methods rely primarily on morphological evaluation of the embryo based on five or six single, conveniently scheduled observations during their in vitro development. Although these daily observations are recorded and considered, selection of the embryo(s) for transfer, or cryopreservation, tends to be weighted toward the morphology of the embryo just before embryo transfer, focusing on cell number and amount of fragmentation. Selection is often based on a simple embryo grading scheme or a graduated embryo scoring scheme that may also take into account several other variables such as static pronuclear morphology [3,4]. These observations are, in general, not photographic but are recorded by a scribed entry onto a laboratory worksheet, as a database entry, or both. Although this methodology is evidence based, and now guided by a consensus document, time-lapse technology has highlighted the limitations of this rather subjective approach to a crucial clinical decision [5,6].

It is logical that a static snap-shot method to accurately study a dynamic process, such as embryo development, may not be optimal; however, to date, IVF practitioners have worked within these limitations to study and improve embryo selection in the interest of their patients.

A static snap-shot method is not accurate to study a dynamic process such as embryo development.

Conventional light microscopical observations, unlike time-lapse imaging, cannot allow the precise timings of mitoses, or the observation of anomalous cleavage events of the in vitro preimplantation embryo, to be recorded. Furthermore, without time lapse, transient characteristics such as multinucleation can easily be missed when embryos are limited to a single daily observation. Many studies have demonstrated the detrimental effect of multinucleation on embryo implantation, pregnancy, and birth rates [7]. Time-lapse imaging and analysis ensure that such phenomena are observed and recorded, allowing embryo deselection, where appropriate.

Having thousands of time-lapse images available, compared with the usual four to six records of a static observation with conventional methods, may initially seem daunting to the embryologist responsible for embryo selection, but, with robust training and quality assurance, confidence and skills develop quickly and the inquiring mind of the embryologist is opened to this exciting approach.

The wealth of detail that can be observed and information gleaned from such time-lapse images is remarkable. As an example, even before the first cleavage, and within hours of insemination, polar body extrusion can be visualized, providing rapid reassurance that fertilization is likely underway. The dynamics and nature of the proceeding pronuclear formation and morphology now question the extent to which traditional pronuclear grading can assist in embryo selection.

Throughout the preimplantation embryo's development, from insemination to uterine transfer, new phenomena, observed using time-lapse imaging and analysis devices, are being defined and observed as the study of human preimplantation embryology takes on a new direction.

Essential Tools: The Time-Lapse Device

Several clinical time-lapse devices with automatic image capture and software for data collection and analysis are commercially available for IVF practice. Some use the standard incubator (e.g., Primo Vision, Vitrolife, Sweden and Eeva, Auxogyn, United States). Such systems use a single microscope objective within a unit placed inside the incubator chamber to capture images within one culture dish. These systems allow group culture conditions due to the design of the dishes provided with the devices. Each is modular, allowing multiple devices to be fitted within one incubator, with the number depending on the size of the incubator. Primo Vision uses Hoffman contrast integrated optics with green light-emitting diode (LED) (550 nm) illumination and can collect images through 11 focal planes. The Eeva system uses dark-field image capture, in a single focal plane, and automatic cell division tracking and uses software to analyze early embryo development, providing evidence-based quantitative data on each embryo's developmental potential to the blastocyst stage [8]. The Primo Vision system allows user-defined programming of the software to record morphokinetic variables. It also allows published or in-house–developed embryo selection algorithms to be used to rank embryos accordingly. Although widely available, these two systems are not yet cleared for clinical use in the United States.

Selection of a time-lapse system for clinical use is likely to be a task that all IVF centers will be faced with over the next few years to provide the optimum clinical outcome for their patients.

The most widely used integrated device available and in use worldwide is the EmbryoScope (FertiliTech, Denmark). Rather than using a conventional incubator, this device in itself is a nonhumidified incubator with internal circulation of ultraviolet (UV)-light sterilized air through a high-efficiency particulate air (HEPA) and volatile organic compound filtration system. The EmbryoScope has an in-built red LED (635 nm) illumination camera system that arguably allows the most stable and uninterrupted time-lapse imaging and culture. The EmbryoScope can image up to 72 embryos, through a maximum of nine equidistant focal planes. This system includes embryo selection modeling software and provides tools for knowledge building through retrospective analysis of embryo developmental data. A more recently developed device by ESCO Medical (Singapore) is an alternative time-lapse incubation system with capacity for up to 84 embryos from six patients. This system consists of six individually controlled and monitored culture compartments and also requires manual annotation of the acquired time-lapse images.

Selection of a time-lapse system for clinical use is likely to be a task that all IVF centers will be faced with over the next few years to provide the optimum clinical outcome for their patients. It is also likely to be a long-term investment. When deciding which system, or systems, to introduce, consideration should be given to potential impact of clinical outcome, opportunities for development and continuous improvement, device specification, focal planes, image quality and capacity, user friendliness, degree of validation conducted by the supplier and required in-house, certification and licensing (where required), limitations, space, and cost. Customer support, servicing, and training should also be taken into account because accessibility to these may be limited by clinic or supplier location.

Identification and Annotation of Dynamic Embryo Development

When using time lapse, the frequency of image acquisition can take place at variable time intervals set by the individual laboratory. At present 5, 10, 15, or 20 min intervals are most commonly used. As the technology advances, these time intervals may be moved closer, to acquire more detailed information, or even varied during the course of preimplantation embryo development to access more information during certain periods and less during periods of quiescence or where there is evidence of image capture being of lesser clinical impact.

Time-lapse images played, rewound, and paused sequentially as a video can be assessed automatically or semiautomatically by software, or manually. Embryologists and researchers can now study the movement (kinetics) and durations of developmental events alongside embryo morphology. The embryo's developmental patterns and appearance have been referred to as morphokinetics [9]. To date, several specific morphokinetic variables have been correlated to embryo viability, and the outcome measures considered have been blastocyst development, implantation, and live birth. As data from embryos transferred with a known outcome amasses, the most predictive morphokinetic variables for viable embryo selection can be identified. It should be noted, of course, that embryo quality and selection is just one of the several factors influencing IVF treatment success. Factors such as clinical history, embryo transfer procedure, and endometrial receptivity are also of great importance.

Unless the selected time-lapse system has fully automated image capture and analysis tools, some degree of user definability, in terms of morphokinetic variables to be recorded, may be required when establishing a clinical time-lapse service or research program.

Because there may be multiple practitioners in the laboratory involved with the assessment of time-lapse images, it is recommended that key variables for annotation are defined within the standard operating procedure and that these variables are routinely recorded. It is crucial that an early decision is made as to whether variables or morphological features that are not seen in a particular embryo (e.g., compaction or vacuolation) should be reported as "not seen" or whether not reporting them is sufficient to suggest that they were not observed.

Additional or novel variables can be added at a later date once the practitioners have gained familiarity and are able to annotate more swiftly. Annotation is the process of interpreting and recording morphokinetic events on visualizing the time-lapse images and entering this information into the time-lapse device software, where applicable. The introduction of time lapse should not been seen as a burden but rather as a tool that not only dramatically increases flexibility in the embryologists' working day but also has the potential to train, educate, and most importantly enhance clinical outcome. Because time-lapse images viewed as a video can be retrospectively studied and annotated, colleagues can work together to ensure the quality of annotation, discuss queries, and even go back to historical images to annotate new variables at a later date.

Guidelines and consensus are required for standard time-lapse imaging, and to date, without this agreement, several alternative definitions have already been used for the same variable and the approach and standard practice varied from clinic to clinic.

The most commonly used morphokinetic variables are established based on the basic principles of embryology and mitosis and include timing of pronuclear appearance and fading, increasing cell numbers (time to two, three, four, five, six cells, etc.) and times of embryo differentiation to the morula and blastocyst stages. Durations of mitotic cycles and synchronicity, as used in some of the published dynamic embryo selection algorithms, can then be calculated from these variables.

Annotation is the process of interpreting and recording morphokinetic events on visualizing the time-lapse images and entering this information into the time-lapse device software.

If there is a specific research interest, additional "user-defined" variables can be recorded. An example may be surrounding multinucleation. If the number, size, degree, appearance, fading, and dynamics of nuclei are of particular interest during embryo development, this information can be recorded. To facilitate downstream data analysis, it is important that strictly defined terms or phrases are used for these phenomena. An accepted consensus document defining such criteria would assist scientists in data sharing.

Table 12.1 summarizes the commonly used morphokinetic variables and provides basic descriptions and abbreviations for them. The abbreviations in bold may be considered core variables, several of which have been referred to in time-lapse–related clinical publications to date. It is recommended that they are routinely recorded when using time lapse in a clinical setting. This table is not exhaustive and is included as a guideline for users of time lapse. It has been adapted from a document, in preparation, by a team of time-lapse experts aiming to encourage users of time-lapse technologies in IVF to standardize practice for data to be amassed, experiences shared, and best practice reached. Anomalous and non-time-lapse–dependent variables have not been included but may be annotated at the embryologist's discretion and in line with standard operating procedure.

Assurance of Annotation Quality

Ensuring an accurate and objective record of dynamic, and often anomalous, embryo development can be challenging, whether using automatic detection software, the human eye, or even by committee. To amass data of high quality and a resource for embryo selection algorithm development to enhance clinical outcome, a quality assurance system should be introduced early on to ensure that embryologists' or practitioners' interpretations and annotations are objective and consistent. This exercise may be developed in-house or provided by the time-lapse device supplier. Even where there is a sole annotator, data should be compared over time to ensure that consistency and objectivity remain.

Several morphokinetic variables are at risk of subjective interpretation. The appearance of pronuclei and initiation of compaction are just two examples. Thorough training and the use of reference images and audit should be used to ensure annotation quality.

The Challenges of Annotation

Many of the morphokinetic variables within Table 12.1 (see also Figures 12.1 through 12.4) can readily be identified on studying the embryo's time-lapse images, whereas others can cause great discussion and debate. The current lack of an industry standard makes comparing practice and data difficult. An example of one annotation challenge may be fragmentation.

Fragmentation is a poorly understood but a very common and dynamic feature of human preimplantation IVF embryos that has been linked to aneuploidy [10,11]. Time lapse provides an opportunity for the dynamics of fragmentation to be studied in greater detail and has recently been used in a study by Chavez et al. [12] that suggested that most fragmented early cleavage-stage embryos were aneuploid. More recently, a preliminary study by Montgomery et al. [13] has shown an association between the timing and completion of compaction in fragmented embryos, and blastocyst ploidy.

Fragmented embryos with extended periods of compaction were significantly more likely to give rise to aneuploid blastocysts than embryos that completed compaction within 22 hrs of ICSI. Conventionally, fragmentation has been reported by an estimation of the proportion of the embryo affected, and ranges are used rather than specific values [5,6]. To share data and experience with other time-lapse practitioners, surrounding this common feature of human embryos, when annotating fragmentation, it is recommended that a percentage value and the number of cells at the time point of recording are used. There is currently no recommendation for the definition or standard recording of patterning or dynamic movement of fragmentation within the embryo, but there is a desire for such guidelines to be developed.

Outcome Measures

Successful live birth is the ultimate outcome after IVF treatment, and despite the limitations of any outcome measure, including live birth, this should be the primary outcome measure when considering the potential of a developing embryo.

TABLE 12.1

Summary of Morphokinetic Variables and Proposed Definitions

	Description
	Morphokinetic Variables
Time (t)	
t0	IVF or midtime of ICSI/IMSI
tPB2	The second polar body is completely detached from the ooplasm
tnPN	Fertilization status is confirmed
(tPN1a)	The first pronucleus is first visible
(tPN2a)	The second pronucleus is first visible
tPNf	All pronuclei have faded (see Figure 12.1)
t2-t9	Two (see Figure 12.2) to nine sequential, distinguished cells are present
tSC	The first two cells merge; initiation of compaction observed (see Figure 12.3)
tMx/w	Morula is formed or compaction goes no further; "x" corresponds to fully compacted, and "w" corresponds to partially compacted or cells excluded
tSB	The first sign of a cavity is observed as blastulation begins (see Figure 12.4)
tByz	Full blastocyst stage is reached; the last frame before the zona pellucida starts to thin; "y" corresponds to morphology of inner cell mass cells, and "z" corresponds to trophectoderm cells (see Figure 12.4)
tEyz	Initiation of expansion is confirmed; the zona pellucida starts to thin
tHNyz	Extrusion of cells from the zona pellucida is present
tHDyz	Blastocyst is fully hatched from the zona pellucida
	Calculated Variables
VP	tPNf-tPN1a (period of visible pronuclei)
Cell Cycle	
CC1	t2-tPB2 The end of the second meiosis to the formation of two discrete cells
CC2	The time for a two-cell embryo to form a four-cell embryo The two blastomeres (a and b) can be considered individually CC2a = t3-t2 CC2b = t4-t2
CC3	The time for a four-cell embryo to form an eight-cell embryo The four blastomeres can be considered individually CC3a = t5-t4 CC3b = t6-t4 CC3c = t7-t4 CC3d = t8-t4
Synchronization	
S2	The duration of the transition from two sister cells, each dividing to reach the four-cell stage t4-t3
S3	As above, but from four to eight cells t8-t5
Duration of Compaction (Morula Stage)	
tMx-tSC	Full compaction
tMy-tSC	Partial compaction
Blastocyst Stage	
tHN-tSB	Duration of blastulation

Note: Each time point defines the time-lapse frame in which the phenomena described are first observed or recorded.

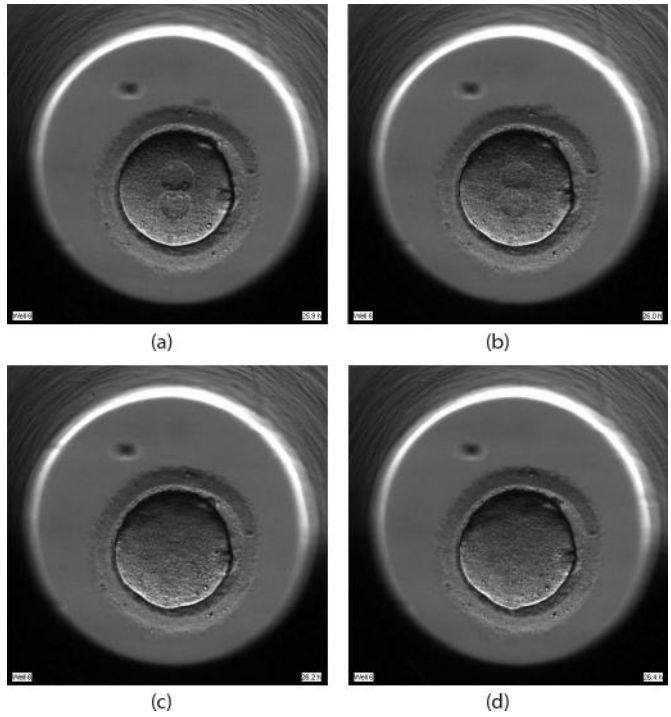

FIGURE 12.1 Sequential time lapse images of fading pronuclei. Image (c) is tPNf.

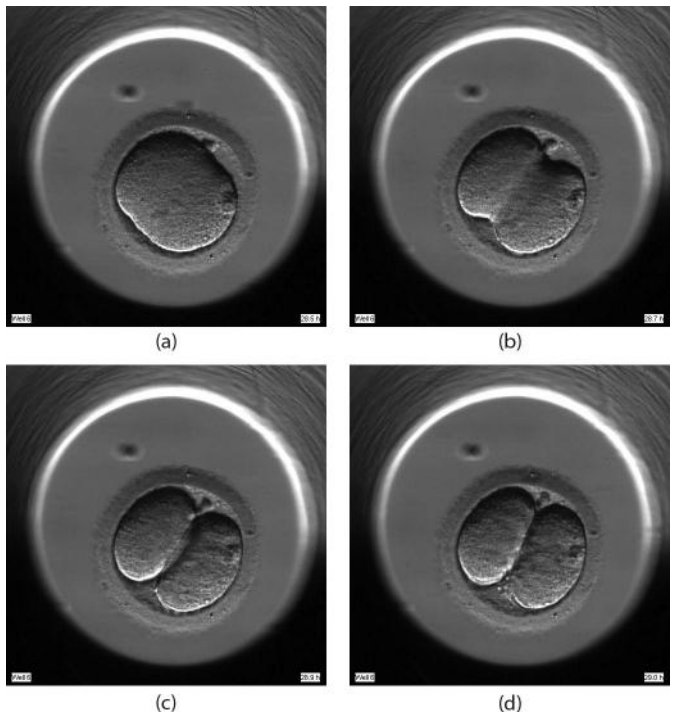

FIGURE 12.2 Sequential time lapse image of the first mitosis. Image (c) shows t2.

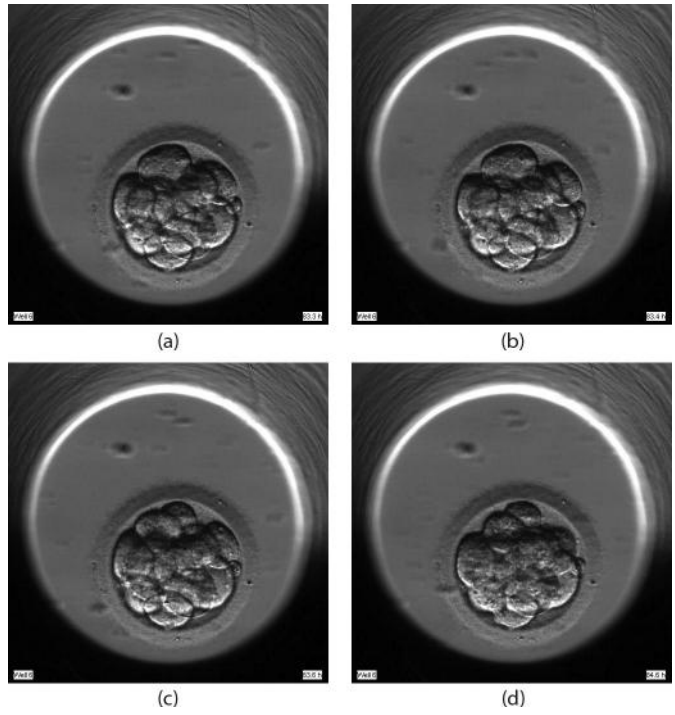

FIGURE 12.3 Initiation of compaction (tSC). More clearly seen with multiple focal planes. Image (c) shows tSC.

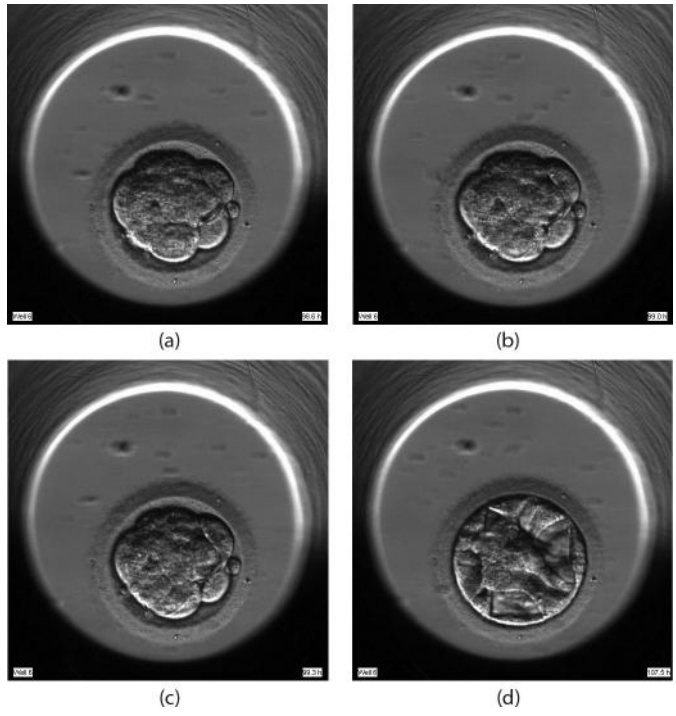

FIGURE 12.4 Initiation of blastulation (tSB). Images (b) and (c) show the increasing cavity and image (d) shows tB.

Due to the relatively recent introduction of time-lapse technology for IVF, the length of the gestational period, and the time required to acquire and collate obstetric outcome data from patients, alternative and less robust outcome measures have been used in published time-lapse studies. Blastulation, although of great scientific interest, has limited clinical value due to the high incidence of blastocysts that fail to implant or are aneuploid [8]. Clinical pregnancy, defined by the presence of a fetal heart on ultrasound scan, has also been used, but due to the early nature of these reported pregnancies, some pregnancies may be lost before term [14]. The difficulty remains that failed pregnancies or even failed implantations cannot necessarily always be attributed to the embryo; however, in terms of outcome measure, live birth arguably remains the most reliable indicator of the viability potential of the preimplantation embryo for IVF and time-lapse practitioners [15].

KID refers to transferred embryos with a known outcome.

What is commonly referred to as "known implantation data," or KID, are the morphokinetic data of a specific and transferred embryo that has a known outcome, with the outcome being either a negative pregnancy test, a gestational sac or fetal heart on ultrasound scan (at 6–8 weeks', gestation), or a live birth. Figure 12.5 describes

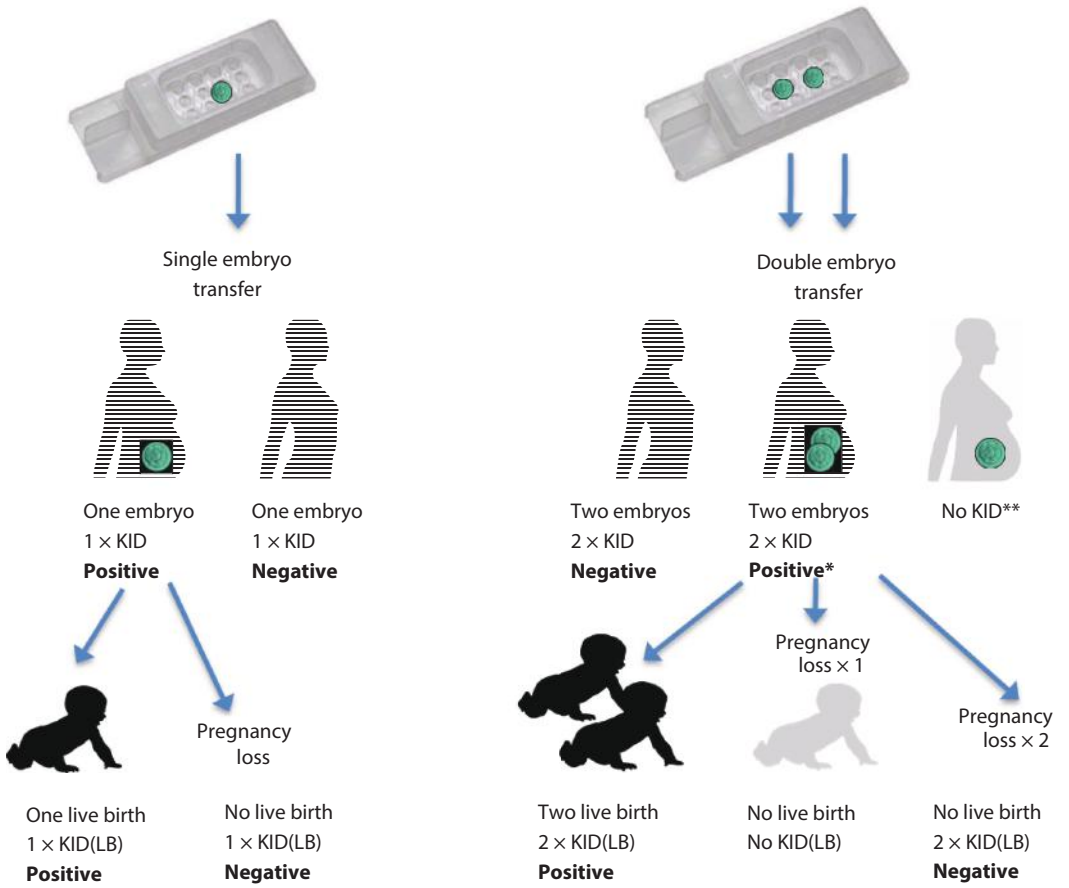

FIGURE 12.5 Known implantation data (KID). KID is the morphokinetic data of a specific, transferred embryo that has a known outcome. *Zygoticity of a twin pregnancy, following double embryo transfer, cannot be ascertained without genetic fingerprinting. Due to relatively low incidence of dizygotic twinning, practitioners, accepting this limitation, may include these data in KID analyses. **As implantation data cannot be deduced or used following a double embryo transfer resulting in a single implantation or birth, the KID ratio, or rate, is lower than the implantation rate per embryo transferred, commonly used for IVF data analyses.

how morphokinetic data may be used for analysis after embryo transfer. Data can be compared between embryos giving positive or negative implantation data (KID+ or KID–, respectively). All data can be used after a single embryo transfer, or a double embryo transfer with a negative outcome. Using data after multiple embryo transfer that has resulted in the same number of fetal hearts or babies born may be problematic without the use of genetic fingerprinting to ascertain the chrorionicity or zygoticity of the pregnancies. However, due to the very low incidence of monozygotic twinning, most analyses could justify the inclusion of these data.

Data Collection and Analysis

Data can be exported from the time-lapse devices for assessment and analysis, or they can be processed using integrated software tools. Provided the data are quality assured and complete, meaning that all relevant morphokinetic variables have been recorded according to standard policy, where they occurred, and that outcome of transferred embryos has been updated, there exists a powerful tool for retrospective analysis. The data should be carefully divided into groups for comparison and statistical analysis. Due to the ranges observed for each morphokinetic variable, it is recommended that median values are used as opposed to means. This way, extreme high or low outliers do not introduce a skew.

KID rates (or ratios) can be calculated for each significant variable for exclusion (deselection) and selection criteria to be identified and then used to develop embryo selection algorithms or models.

KID rates are calculated using the following formula: KID+/KID+ plus KID– × 100%.

Regular data review is recommended to continually improve embryo selection algorithms.

Selection and Deselection Criteria and Algorithms for Embryo Selection

Several time-lapse studies have linked kinetic markers to embryo viability. In a retrospective analysis of EmbryoScope-acquired time-lapse human embryo data, a significant association was previously demonstrated between the timing of pronuclear fading and the first three cleavage events, and successful implantation [16]. Another study, looking at early embryo development, showed an inverse relationship between the ability of embryos to develop to the blastocyst stage and the length of time for zygote division [17].

Time lapse identifies aberrant cleavage patterns.

More recently, a study by Rubio and colleagues [18] focused on the phenomenon of direct, or rapid, cleavage from a single cell to three cells in <5 hr. This study demonstrated the ability of time lapse to identify aberrant cleavage divisions and the reduced implantation potential when such embryos were transferred compared with embryos that did not exhibit this behavior. In a cohort of 1659 transferred embryos, the incidence of this "direct division" was 13.7%, and the known implantation rate of these embryos was statistically significantly lower than for embryos with a normal cleavage pattern (1.2% vs. 20.2%, respectively). Figure 12.6 shows a series of time-lapse images demonstrating this phenomenon within 0.5 hr.

This consecutive series of four time-lapse images, taken at about 10 min intervals, demonstrates the phenomenon of direct cleavage from one to three cells and would not be observed without time lapse and has been reported to be associated with reduced implantation potential [18].

Several embryo selection models, or algorithms, indicating the added value of using morphokinetic information when selecting embryos have now been published. The first by Wong and colleagues [8] identified three significant morphokinetic variables associated with the likelihood of blastulation. These variables and values (in parentheses) were P1, the duration of the first cytokinesis (within 33 min); P2, the interval between the first and the second cytokineses, that is, the total length of time at the two-cell stage (7.8–14.3 hr); and P3, the time between the second and third mitoses, that is, the total length of time at the three-cell stage or the synchrony of cleavage of the first two cells (within 5.8 hr). This work was used to develop the Eeva test (early embryo viability assessment) (Auxogyn).

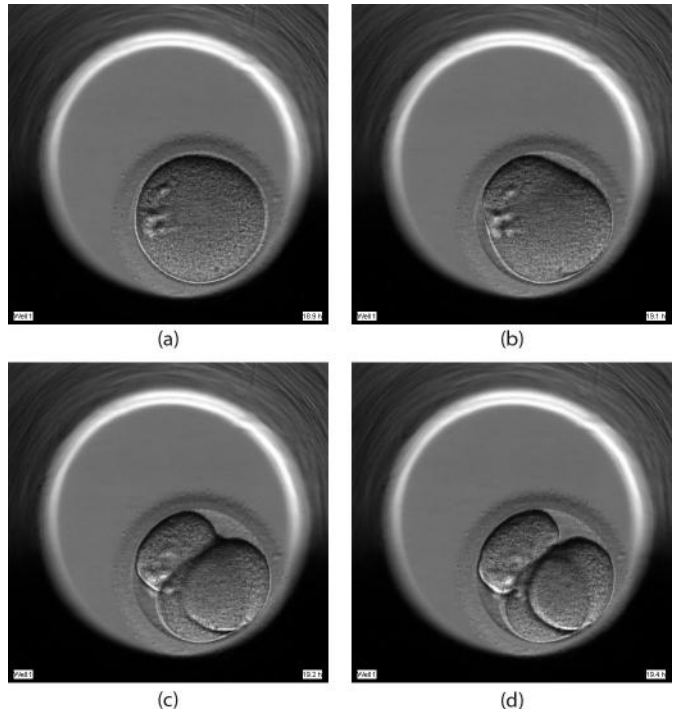

FIGURE 12.6 Rapid or direct cleavage from one to three cells.

The work of Meseguer et al. [9] used the EmbryoScope and looked beyond blastulation to implantation and pregnancy rates. By studying 247 transferred embryos with known implantation outcome, optimal ranges for specific morphokinetic variables were defined. By analyzing multiple preimplantation embryo developmental milestones and durations, a hierarchical model to classify embryos, according to the most significant morphokinetic variables, was developed. The timing of the cleavage to five cells (t5) in this study showed the highest correlation with positive implantation. This model first introduced exclusion criteria. These exclusion criteria were uneven blastomeres after the first cytokinesis, rapid or direct cleavage from one to three cells, and multinucleation at the four-cell stage. After the exclusion of embryos fulfilling these criteria, embryos were classified according to the timings of similar variables proposed by Wong et al. (P2 and P3 above), referred to as cc2 (within 11.9 hr) and S2 (within 0.76 hr), as well as t5 (48.8–56.6 hr post-intracytoplasmic sperm injection [ICSI]). Despite there being some similarities in the morphokinetic variables used within these published models, the timings differ and caution should be exercised when considering applying such models, developed in a different research or clinical setting, before robust validation is performed (as discussed below). It has been demonstrated that a published embryo selection model from one setting may not always effectively be transferred to another setting, but it may be useful with some modification, and after a validation process [19].

Time-lapse–based embryo selection models indicate the value of applied morphokinetics, but care has to be taken while transferring models from one clinical setting to another.

More recently, an aneuploidy risk classification model has been published [20]. Also, using the EmbryoScope, 20 morphokinetic variables and durations were recorded for blastocysts that then underwent trophectoderm biopsy and preimplantation genetic screening (PGS) for all chromosomes using array-comparative genomic

TABLE 12.2

Time-Lapse–Derived Model for Classification of Ploidy with Associated Probabilities of Aneuploidy

Aneuploidy Risk Class	Model	*n*	Probability of Aneuploidy (%)
Low	tB < 122.9 hr and tSB < 96.2 hr	36	37
Medium	tB < 122.9 hr and tSB ≥ 96.2 hr	49	69
High	tB ≥ 122.9 hr	12	97
All		97	61

hybridization (CGH) or single-nucleotide polymorphism (SNP) array. Two variables significantly correlated with embryo ploidy were used to develop an algorithm for embryo selection that classified embryos as having a low, medium, or high risk of aneuploidy. These variables were the start of blastulation (tSB) and the time to reach the full blastocyst stage (tB). Risk classifications were defined according to the time an embryo reached these two developmental milestones. Table 12.2 shows the probability of aneuploidy when embryos were partitioned according to their morphokinetic values for the two significant variables.

This model was later tested retrospectively, by the same researchers, on transferred blastocysts with known clinical outcome that had not undergone biopsy and PGS. Significant relative increases in positive fetal heart and live birth rates were demonstrated when an embryo retrospectively classified as low risk was transferred, compared with the overall rates after blastocyst transfer, indicating the potential clinical applicability of this noninvasive time-lapse algorithm for embryo selection.

Practitioners working with selection models where embryos are deselected or excluded should consider the supporting data to help with the decision process regarding the fate of such embryos. Considerations should be made as to whether the morphokinetic phenomena or timings observed during a particular embryo's development, deeming it deselected for transfer, preclude implantation entirely or are associated with reduced viability or potential. An embryo identified as having a high risk of aneuploidy or low potential to blastulate by a model, for example, may be the highest ranking embryo within a cohort and still give the patient a chance of a positive outcome, albeit small.

Transferability of Embryo Selection Algorithms

Whether such embryo selection algorithms can be directly transferrable between clinics remains to be demonstrated but based on reports that rates of embryo development can differ according to intrinsic or extrinsic factors, it is likely that they may not. Either way, it should be preferable for clinics to develop their own models for their specific patient populations, stimulation regimens, culture conditions, and according to their interpretation of time-lapse images.

Clinics introducing time-lapse methodologies are advised to do so with strict and standard practice throughout the process. Until we know the potential impact of subtle deviations from protocol, culture dishes or slides should be prepared in a standard and precise manner, and time-lapse images, where performed manually, should be assessed objectively and observations recorded (annotated) in the same way by all practitioners. Only this will allow centers to collate robust and complete data to develop in-house embryo selection models that can be fine-tuned as experience and data amasses.

Confounding Factors

There have been several reports on the impact, on embryo morphokinetics, of compounding factors that may be patient or clinic specific. Examples are gas composition during in vitro culture, age, female body mass index, and culture media [14,21–23].

A recent study, however, reported that morphokinetic parameters used for embryo selection were not affected between two different culture media analyzed [24]. Over the next few years, such questions surrounding confounding factors and those crucially asking whether algorithms for embryo selection are transferable will likely be a key focus for time-lapse study in the field of IVF. To make the most effective progress in this field, embryologists are urged to work together, sharing best and common practice to enable this shift in practice to take place most effectively.

Change Control

Due to the possible impact of intrinsic and extrinsic factors on morphokinetic timings, great care should be taken when a change to practice is being considered or made when using time-lapse systems. The impact of a controllable factor such as a change in media or plasticware, for example, on the precise timings of embryo development, should be understood and validated before full implementation, particularly if embryo selection models have been developed under specific conditions. As with all changes made in IVF laboratories, these changes should be justified, controlled, validated, and evaluated but now with the additional consideration of potential impact on morphokinetics, when using time-lapse imaging.

A Tool or a Rule? The Role of the Embryologist

As a clinical treatment, we are still in the relatively early stages of clinical implementation of time-lapse technology. We remain unclear as to whether published algorithms, developed using particular incubation conditions (such as gas mix and culture media), can be directly transferred between centers using not only alternative incubation but also potentially differing definitions and operating procedures for recording dynamic observations of embryo development. Although the expectation is that, eventually, agreement will be reached as to the most significant indicators of an embryo's potential to develop through to live birth, the specific timings may differ according to the variation in, for example, patient history, age, or incubation conditions, and this could result in clinics having numerous algorithms that can be applied for the purpose of embryo selection, according to these factors. In time, and with increasing data and experience, the optimal ranges for defined dynamic events such as the interval between the first and second cytokineses may be further fine-tuned, and additional novel morphokinetic markers of embryo viability will be identified.

The role of the embryologist remains key, despite the most sophisticated algorithm.

The role of the embryologist remains key. Even with sophisticated morphokinetic selection algorithms, the embryologist may need to overrule the algorithm should an embryo reaching all of the milestones within the optimal time ranges also have features considered detrimental, such as smooth endoplasmic reticulum clusters, large areas of cellular degeneration, or late-onset developmental arrest. The use of bright-field time-lapse devices provides embryologists with images already familiar to them and allows this facilitative interaction between the digital and the human eye.

Acknowledgments

I am grateful for permission to use and adapt the table of proposed definitions, currently being drafted for submission by The Embryo Morphokinetic Consensus Group; Inge Agerholm, Jesus Aguilar, Sandrine Chamayou, Nadir Ciray, Marga Esbert, Shabana Sayed, and Alison Campbell.

I thank Louise Kellam for assistance with image preparation for this chapter and my CARE Fertility colleagues.

REFERENCES

1. Payne D, Flaherty SP, Barry MF, et al. Preliminary observations on polar body extrusion and pronuclear formation in human oocytes using time-lapse video cinematography. *Hum Reprod* 1997; 12: 532–541.
2. Pribenszky C, Matyas S, Kovacs P, et al. Pregnancy achieved by transfer of a single blastocyst selected by time-lapse monitoring. *Reprod Biomed Online* 2010; 21: 533–536.
3. Cutting R, Morroll D, Roberts SA, et al. Elective single embryo transfer guidelines for practice British Fertility Society and Association of Clinical Embryologists. *Hum Fertil* 2008; 11: 131–146.
4. Fisch J, Rodriguez H, Ross R, et al. The graduated embryo score predicts blastocyst formation and pregnancy rate from cleavage stage embryos. *Hum Reprod* 2001; 16: 1970–1975.
5. Alpha Scientists in Reproductive Medicine, ESHRE Special Interest Group of Embryology. The Istanbul consensus workshop on embryo assessment: Proceedings of an expert meeting. *Hum Reprod* 2011; 26: 1270–1283.
6. Alpha Scientists in Reproductive Medicine, ESHRE Special Interest Group of Embryology. The Istanbul consensus workshop on embryo assessment: Proceedings of an expert meeting. *Reprod Biomed Online* 2011; 22: 632–646.
7. Van Royen E, Magelschots K, Vercruyssen M, et al. Multinucleation in cleavage stage embryos. *Hum Reprod* 2003; 18(5): 1062–1069.
8. Wong CC, Loewke KE, Bossert NL, et al. Non-invasive imaging of human embryos before embryonic genome activation predicts development to the blastocyst stage. *Nat Biotechnol* 2010; 28(10): 1115–1121.
9. Meseguer M, Herrero J, Tejera A, et al. The use of morphokinetics as a predictor of embryo implantation. *Hum Reprod* 2011; 26(10): 2658–2671.
10. Munne S, Cohen J. Chromosome abnormalities in human embryos. *Hum Reprod Update* 1998; 4: 842–855.
11. Alikani M, Calderon G, Tomkin G, et al. Cleavage anomalies in early human embryos and survival after prolonged culture in vitro. *Hum Reprod* 2000; 15: 2634–2643.
12. Chavez SL, Loewke KE, Han J, et al. Dynamic blastomere behaviour reflects human embryo ploidy by the four-cell stage. *Nat Commun* 2012; 3: 1251.
13. Montgomery S, Duffy S, Bowman N, et al. Does the duration of compaction differ in fragmented cleavage stage embryos that ultimately become euploid or aneuploidy blastocysts? Is this reflected in the timing of blastulation? ESHRE, London. *Hum Reprod* 2013; 28(Suppl 1): i1–i4.
14. Meseguer M, Rubio I, Cruz M, et al. Embryo Incubation and selection in a time-lapse monitoring system improves pregnancy outcome compared with a standard incubator: A retrospective cohort study. *Fertil Steril* 2012; 98: 1481–1489.
15. Campbell A, Fishel S, Bowman N, et al. Retrospective analysis of outcomes after IVF using an aneuploidy risk model derived from time-lapse imaging without PGS. *Reprod Biomed Online* 2013; 27: 140–146.
16. Herrero J, Alberto T, Ramsing NB, et al. Linking successful implantation with the exact timing of cell division events obtained by time-lapse system in the EmbryoScope. *Fertil Steril* 2010; 94(4): S149.
17. Cruz M, Perez-Cano I, Gadea B, et al. Time-lapse video analysis provides a correlation between early embryo division kinetics and subsequent blastocyst formation and quality. *Hum Reprod* 2011; 26: P-115.
18. Rubio I, Kuhlmann R, Agerholm I, et al. Limited implantation success of direct-cleaved human zygotes: A time-lapse study. *Fertil Steril* 2012; 98: 1458–1463.
19. Best L, Campbell A, Duffy S, et al. Session 57: Does one model fit all? Testing a published embryo selection algorithm on independent time-lapse data. *Hum Reprod* 2013; 28: i87–i90.
20. Campbell A, Fishel S, Bowman N, et al. Modelling a risk classification of aneuploidy in human embryos using non-invasive morphokinetics. *Reprod Biomed Online* 2013; 26: 477–485.
21. Liebenthron J, Montag M, Koster M, et al. Influence of age and AMH on early embryo development realised by time-lapse imaging. *Hum Reprod* 2012; 27: P-135.
22. Bellver J, Mifsud A, Grau N, et al. Similar morphokinetic patterns in embryos derived from obese and normoweight infertile women: A time-lapse study. *Hum Reprod* 2013; 28: 794–800.
23. Ciray HN, Aksoy T, Goktas C, et al. Time-lapse evaluation of human embryo development in single versus sequential culture media-a sibling oocyte study. *J Assist Reprod Genet* 2012; 29: 891–900.
24. Basile N, Morbeck D, García-Velasco J, et al. Type of culture media does not affect embryo kinetics: A time-lapse analysis of sibling oocytes. *Hum Reprod* 2013; 28: 634–641.

13

Noninvasive Techniques: Embryo Selection by Transcriptomics, Proteomics, and Metabolomics

Asli Uyar and Emre Seli

Introduction

The number of multiple births has increased >70% since 1980 [1], when approximately 40% of twin births and 80% of triplet and higher order births resulted from infertility therapy [2]. Multiple embryo transfers in in vitro fertilization (IVF) treatment particularly elevated the frequency of multiple pregnancies in this period. Although the desired outcome of infertility treatment is the birth of a single healthy infant, more than one embryo has commonly been transferred in IVF cycles to increase the likelihood of successful outcome. Subsequent multiple gestations, however, can lead to serious maternal and fetal health problems [3]. The overall cost of healthcare services provided for multiple pregnancies and resulting preterm births is estimated to exceed the cost of IVF itself [4–6]. Medical and financial complications associated with IVF multiple pregnancies became much more important as the prevalence of IVF treatment increased significantly within the past two decades.

To prevent potential negative implications of infertility treatment, regulatory legislation has been enacted in many countries to set limits on the number of embryos transferred [7]. In the meantime, investigators focused on selection of the most viable gametes and embryos in an attempt to reduce multiple pregnancies without compromising the pregnancy rates. Eventually, the average number of embryos transferred in nondonor IVF cycles during 2001–2010 has decreased from 3.1 to 2.3 in United States [8] and from 2.2 to 1.7 in United Kingdom [9]. However, elective single embryo transfers still constitute a minor portion of the transfer cycles because current ability to select the single most developmentally competent embryo is less than perfect.

Embryo Selection: From Morphology to Omics

Soon after the birth of the first IVF baby, controlled ovarian stimulation protocols provided maturation of multiple oocytes in a cycle that, in turn, enabled availability of multiple embryos for transfer. Since then, selection of the embryo(s) to be transferred has been a critical step affecting the success of the IVF treatment. From the early times of IVF to the present, embryo assessment strategies have mainly been based on timely morphological observations of embryos throughout the culture period. Morphology-based embryo selection has practical advantages in the clinical routine and has resulted in significant improvements in pregnancy rates [10]. The efficiency of morphological assessment has recently been further improved with the introduction of novel technologies that allow continuous monitoring of the embryo development in vitro and selection of embryos based on additional dynamic morphological parameters [11,12]. Nevertheless, the precision of morphological criteria remains less than desired, motivating investigators to pursue additional markers of embryo viability at the molecular level.

The molecular mechanisms underlying distinct biological conditions are mainly characterized by process-specific gene expression. Genes are expressed through transcription of the genetic code stored in DNA into RNAs and subsequent translation of messenger RNAs (mRNAs) into proteins. The human genome contains 3×10^9 base pair of nucleotides and approximately 30,000 genes. These genes generate ~200,000 transcripts and ~1 million proteins. In addition, human metabolome is estimated to have ~3000 metabolites, the small molecules (<1 kDa) including amino acids, lipids, nucleotides, and signaling molecules. The DNA, RNA, protein,

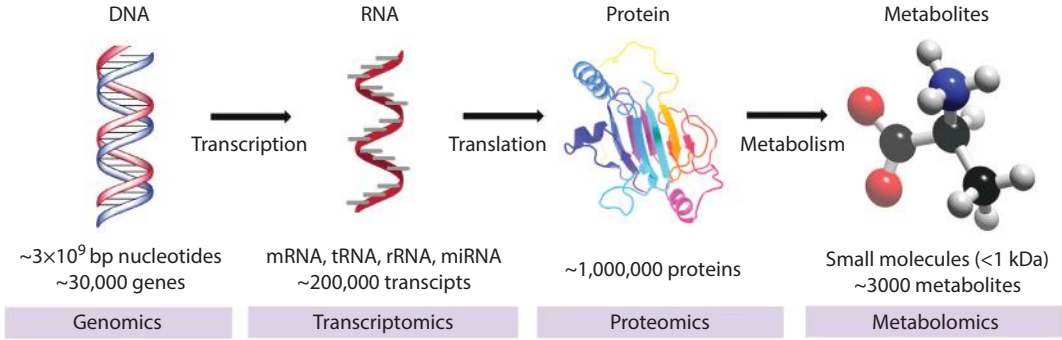

FIGURE 13.1 Omics approaches investigate the molecular constitution of biological samples at genomics, transcriptomics, proteomics, and metabolomics levels.

and metabolite constitutions of organisms are investigated by genomics, transcriptomics, proteomics, and metabolomics approaches, respectively (Figure 13.1). Omics research basically looks for answers to two questions: what distinct molecules and how many copies of each molecule exist in a biological sample? Within the past decade, the omics technologies have been used widely as potential novel embryo assessment tools in assisted reproduction (for review, see [13]).

The invasive genomic approach to embryo assessment, referred to as preimplantation genetic screening (PGS), allows the exclusion of aneuploid embryos through genetic profiling of biopsied cells. Although a recent meta-analysis showed that PGS with fluorescence in situ hybridization (FISH) is associated with lower pregnancy and live birth rates [14], PGS using more recent comparative genomic hybridization (CGH)-array or single nucleotide polymorphism (SNP)-array technologies has shown promising results [15,16].

Beyond the oocyte and embryo genome, RNA constitution of follicular somatic cells and protein and metabolite content of spent embryo culture media serve as potential indicators of embryo viability. This chapter covers an overview of the techniques and clinical applications of noninvasive transcriptomics, proteomics, and metabolomics approaches to embryo assessment.

Omics research basically looks for answers to two questions: what distinct molecules and how many copies of each molecule exist in a biological sample?

Embryo Selection by Transcriptomics

The term transcriptome refers to the entire set of RNA molecules in a particular cell or tissue, and includes mRNAs, transfer RNAs (tRNAs), ribosomal RNAs (rRNAs), microRNAs (miRNAs), and other noncoding RNAs. Specifically, the relative concentrations of individual mRNAs can be evaluated as an approximation to expression levels of the corresponding genes. Within the context of IVF, cumulus/granulosa cells transcriptome has been investigated widely as a noninvasive tool to assess oocyte quality as an indicator of embryo viability (for review, see [17]).

Folliculogenesis and Oocyte–Somatic Cell Interactions

The oocyte and its surrounding somatic cells grow and develop in a coordinated and mutually dependent manner [18]. At the initial stage of folliculogenesis, a single layer of flattened granulosa cells surrounds the perinatally formed primordial follicles. The oocyte in the primordial follicle remains arrested at the prophase of the first meiotic division until shortly before ovulation. Starting with puberty, selected primordial follicles grow and differentiate into primary follicles, where granulosa cells surrounding the oocyte become cuboidal.

The zona pellucida, a glycoprotein polymer capsule that separates the primary oocyte from the follicular cells, also develops at this stage. As follicles progress to the secondary stage, granulosa cells undergo mitosis, forming multiple layers around the zona pellucida. Subsequent early antral follicles are characterized by the formation and growth of fluid-filled cavities (antrum) adjacent to the oocyte.

Primordial, primary, and secondary stages of folliculogenesis occur independently of gonadotropic hormones, whereas follicular-stimulating hormone (FSH) secreted by the pituitary stimulates the transition from early antral to antral follicle stage [19]. In the human ovary, antral follicles compete with each other under the influence of FSH, and the majority of follicles that have fewer FSH receptors stop developing further and undergo atresia. Eventually, only one dominant follicle becomes the preovulatory follicle. In the preovulatory follicle, granulosa cells differentiate into two distinct cell types: the mural granulosa cells, lining the antrum and the follicle wall; and cumulus cells, immediately surrounding the oocyte. At this stage, luteinizing hormone (LH) surge initiates oocyte maturation and cumulus expansion occurs by the synthesis of hyaluronic acid within the cumulus mass. Synthesized hyaluronic acid is deposited into the extracellular matrix that binds to oocyte and cumulus cells together. The oocyte resumes meiosis and the ultimate mature cumulus–oocyte complex (COC) contains an oocyte arrested at the metaphase of the second meiotic division (MII) that is ready for ovulation and fertilization.

During folliculogenesis and oocyte maturation, the oocyte derives most of its substrates for energy metabolism and biosynthesis from the surrounding somatic cells [20,21]. The highly specialized cumulus cells within the COCs have transzonal cytoplasmic processes that penetrate through zona pellucida and form gap junctions [22]. Cumulus cells communicate with each other and with the oocyte through the gap junctions that allow bidirectional transfer of metabolites and signaling molecules [23]. The transfer of paracrine factors between the oocyte and the surrounding cumulus cells is of special importance for oocyte maturation. Initial observations on oocyte–cumulus cell interaction in relation to embryo viability demonstrated that oocytes obtained from follicles with impaired cumulus expansion have limited potential for implantation [24]. Consequently, cumulus/granulosa cell transcriptome has been analyzed in an attempt to identify potential biomarkers of embryo competence.

Technologies for Transcriptomic Analysis of Cumulus and Granulosa Cells

The common initial step in transcriptomics experiments is sample preparation that consists of the stages of cell and tissue collection; RNA isolation; concentration, purity, and integrity assessment; and reverse transcription of the RNA to complementary DNA (cDNA) molecules. Once the sample quality is ensured, quantification of relative mRNA levels is performed using either individual gene expression analysis tools or whole-genome transcription profiling technologies. This section provides an overview of the sample preparation methods and analytical techniques used for investigation of relationship between cumulus/granulosa cell transcriptome and oocyte/embryo competence.

Sample Preparation

Sampling of somatic components of the follicle poses specific challenges due to potential cross-contaminations or contamination with blood. Mechanical separation of COCs from contaminating cells is easier than that of granulosa cells. In addition, the effect of regional differences in the cumulus physiology can be minimized using laser capture technology. Granulosa cells need to be carefully separated from leukocytes because potential contamination with blood during follicular aspiration may alter the gene expression profile.

RNA must be purified immediately after tissue/cell isolation to prevent potential RNA degradation that would result in a rapid change in the transcript profile. RNases must be inactivated when the samples need to be stored before RNA isolation. After RNA isolation, concentration, purity, and integrity of RNA molecules must be confirmed using UV spectroscopic analyses [25], gel-based methods [26], or microfluidics technologies [27]. Then, mRNA molecules are reverse transcribed to cDNA before amplification and quantification. cDNA synthesis occurs by priming the total RNA with either one of the oligo(dT) random hexamers and gene-specific primers or a blend of these primers. Priming strategy has been shown to be an important factor affecting the results of mRNA quantification [28].

qRT-PCR and High-Throughput Transcriptomics

Since the discovery of the thermostable *Thermophilus aquaticus* (Taq) polymerase [29], polymerase chain reaction (PCR) has been used as an efficient and practical tool to detect the existence of a particular DNA (or cDNA) fragment in a biological sample. The PCR method allows exponential amplification of the target sequence by using a pair of primers, deoxynucleotides, and a polymerase enzyme. Each of the consecutive amplification cycles in PCR consists of three steps performed at specific temperatures: denaturation of double strands (~94°C), primer annealing to complementary parts on both strands (~65°C to 55°C), and primer extension (~72°C). The amount of starting material is doubled at the end of each cycle. After ~25 to 40 cycles, the resulting PCR product is analyzed on agarose gel containing a fluorescent DNA stain.

Transcriptomics studies make use of PCR after reverse transcription of mRNA molecules to cDNA. The combined method is called reverse transcription-polymerase chain reaction (RT-PCR) and is widely used for gene expression analysis. Because agarose gel–based analysis of RT-PCR products do not provide precise quantitative information, the quantitative reverse transcription-polymerase chain reaction (qRT-PCR), or the so-called real-time RT-PCR, has been developed for continuous measurement of PCR amplification, allowing reliable quantification of specific transcripts in a sample [30,31]. Currently, qRT-PCR is commonly used for quantitative gene expression analysis.

To account for potential variations between PCR reactions, gene expression results need to be normalized using endogenous controls. The most common control genes are beta-actin (β-Actin) or glyceraldehyde 3-phosphate dehydrogenase (GAPDH). Alternatively, mathematical models such as NormFinder [32] and GeNorm [33] exist that help with selection of the most suitable normalization genes among a set of candidate genes.

Within the past decade, gene expression research evolved from single-gene analysis to genome-wide transcription profiling with the advance of microarray technology. A microarray chip consists of single-stranded, ~25 base-length polynucleotide probes that are synthesized in fixed positions in the form of a two-dimensional array on a solid surface. Each probe is attached to a microscopic spot on the array and corresponds to the base sequence of a specific mRNA. The large number of probes on a single microarray chip enables simultaneous expression analysis for all known genes.

The microarray experimental procedure consists of labeling, hybridization, scanning, and data analysis stages (Figure 13.2). First, total RNA is isolated and then cDNA is synthesized by reverse transcription of mRNA. Amplified and biotin-labeled cRNA is obtained through in vitro transcription. Then, fragmented cRNAs are deposited over the array, allowing for hybridization of the labeled targets to the complementary probes. The amount of hybridization at each probe is expected to be proportional to the level of expression of the gene represented by that probe. Subsequently, the microarray chip is illuminated by a laser light. Gene expression is then quantified by means of fluorescence intensity that is captured by the scanners into an image.

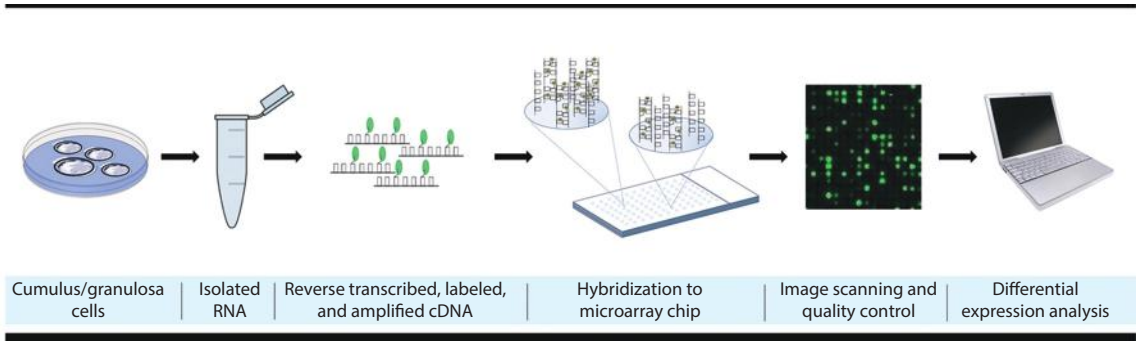

FIGURE 13.2 Major steps of a typical microarray experiment. Total RNA is extracted from the follicular cell samples, and mRNA is reverse transcribed into cDNA. Amplified and labeled samples are hybridized to a microarray slide, allowing the labeled targets to bind to their complementary oligonucleotides attached to the microscopic probes. The array is then washed and scanned to obtain the fluorescent image that is further processed to get the intensity values for differential expression analysis.

Recently, next-generation sequencing technologies have provided an alternative transcriptomics approach called RNA Sequencing (RNA-Seq) that appears to be a more precise detection and quantification of RNA transcripts [34,35]. The RNA-Seq procedure starts with the construction of a cDNA library from isolated RNA molecules. Long RNA molecules, such as mRNAs, need to be fragmented into smaller pieces (by hydrolysis or nebulization) to be compatible with the sequencing technology. The reverse-transcribed cDNA can also be fragmented by DNAse I treatment or sonication. Alternatively, recent direct RNA sequencing technology eliminates the need for prior conversion of RNA to cDNA [36].

By using the cDNA library constructed, short sequence reads (30–400 bp) are obtained by high-throughput sequencing of each molecule either from one end (single-end sequencing) or both ends (pair-end sequencing). The resulting reads are mapped to a reference genome or assembled de novo without a priori knowledge of the underlying genome. Each sequence read may correspond to a known exon, a splice variant, or a new candidate gene. The number of sequence reads that map to a particular transcript is expected to be proportional to its expression level. Hence, read counts are used for quantification of gene expression in RNA-Seq experiments.

Gene expression research evolved from single-gene analysis to genome-wide transcription profiling with the advance of microarray technology; however, next-generation sequencing technologies provide an alternative transciptomics approach called RNA sequencing that appears to be a more precise detection and quantification of RNA transcripts.

Typical RNA-Seq protocols require at least 1 μg of total RNA. However, this amount of starting material may not be available when studying small tissues such as oocytes. Recently, Antoniou and Taft [37] provided a protocol, specifically for Illumina, to prepare sequencing libraries from mouse oocytes and suggested that this protocol can also be used for follicular cells. Unfortunately, to date there are no publications applying RNA-Seq approach for analysis of follicular cells in the context of assisted reproduction.

Analysis of the data produced by both microarray and RNA-Seq technologies poses significant challenges because expression levels of thousands of genes are investigated simultaneously in a multistage experimental setting. Considering the underlying technological complexities, several bioinformatics methods have been proposed to provide reliable and efficient data analysis in transcriptomics studies.

Analysis of Transcriptomics Data

The raw microarray data obtained from the image files needs to be processed before differential expression analysis. The commonly applied robust multichip average (RMA) preprocessing method consists of background adjustment, quantile normalization, and probe set summarization stages [38–40]. Preprocessed data are then analyzed for differential expression. False discovery rate (FDR) corrected statistical analysis is proposed to prevent excessive Type I error (false-positive rate) during simultaneous testing of the null hypothesis (i.e., the expression levels are not different between the two experimental conditions) for each gene [41,42]. To conclude that a gene is differentially expressed, the data analysis should also consider biological significance (fold change rate) in addition to statistical significance (FDR corrected p-value). Commercial tools such as Partek Genomic Suite and Bioinformatics toolbox of Matlab exist for differential expression analysis of microarray data.

With regard to RNA-Seq data analysis, the depth of sequencing is a major concern because transcriptome coverage strongly depends on the sequencing depth. A small amount of sequencing data would be sufficient for the highly expressed genes where more reads are required for accurate quantification of low abundance targets. Analysis of RNA-Seq data requires advanced bioinformatics approaches for alignment of the reads to an existing genome or for assembly of the reads into a new genome. Despite the challenges, RNA-Seq has the advantage of being able to detect tissue-specific and currently unknown splice variants and polymorphisms.

The results of differential expression analysis of both microarray and RNA-Seq data may (1) reveal no difference between the populations of interest; (2) identify just a few genes up regulated or down regulated in either population; or (3) determine hundreds of differentially expressed genes requiring more sophisticated analyses for biological interpretation, that is, pathway analysis of microarray data.

Clinical Applications of Transcriptomics-Based Embryo Assessment

qRT-PCR and microarray analysis of cumulus and granulosa cell mRNAs have been applied to identify biomarkers associated with oocyte and embryo development and cycle outcome in women undergoing IVF. Studies using qRT-PCR are hypothesis-driven in nature. These studies propose that somatic cells surrounding viable oocytes have a different expression pattern for genes previously shown to be important for COC development, compared with cumulus and granulosa cells around nonviable oocytes. Many of these studies commonly investigated the genes that are up regulated in cumulus or granulosa cells in response to LH stimulation, such as epidermal growth factor (EGF)-like factors (amphiregulin [AREG], epiregulin [EREG], and betacellulin [BTC]) and their downstream regulators (prostaglandin synthase-2 [PTGS2], also termed cyclooxygenase-2 [COX2], tumor necrosis factor alpha-induced protein [TNFAIP6], hyaluronan synthase 2 [HAS2]), that are necessary for synthesis and stabilization of the extracellular matrix by cumulus cells, cumulus expansion, and subsequent ovulation. Others evaluated genes that mediate cell division and metabolism.

In the first study using qRT-PCR, McKenzie et al. [43] found HAS2, PTGS2, and GREM1 to be elevated in cumulus cells of oocytes that lead to high-grade embryos on Day 3. Subsequent studies confirmed the association between GREM1 expression and Day 3 embryo development [44,45] (Table 13.1). More recently, Gebhardt et al. [46] reported a significantly higher expression of PTGS2 and VCAN in cumulus cells obtained from oocytes that yielded a live birth.

In 2011, Wathlet et al. [47] used qRT-PCR to analyze cumulus cells for the expression of eight genes: Syndecan 4 (SDC4), PTGS2, VCAN, activated leukocyte cell adhesion molecule (ALCAM), GREM1, transient receptor potential cation channel—subfamily M member 7 (TRPM7), Calmodulin 2 (CALM2), and Inositol 1,4,5-trisphosphate 3-kinase A (ITPKA). Day 3 or Day 5 morphology correlated with all genes studied with the

TABLE 13.1

Potential Biomarker Genes of Oocyte and Embryo Competence Identified by Transcriptomic Analysis of Cumulus/Granulosa Cells

Transcript[a]	Study	Technique	Result
PTGS2 (COX2)	McKenzie et al. (2004)	qRT-PCR (Taqman assay)	↑ PTGS2 ∝ fertilization & Day 3 embryo morphology
	Feuerstein et al. (2007)	qRT-PCR (SYBR Green)	↑ PTGS2 ∝ PB formation
	Anderson et al. (2009)	qRT-PCR (SYBR Green)	↑ PTGS2 ∝ oocyte maturation
	Gebhardt et al. (2011)	qRT-PCR (SYBR Green)	↑ PTGS2 ∝ live birth
	Wathlet et al. (2011)	qRT-PCR (SYBR Green)	↑ PTGS2 ∝ oocyte maturation
GREM1	McKenzie et al. (2004)	qRT-PCR (Taqman assay)	↑ GREM1 ∝ fertilization & Day 3 embryo morphology
	Cillo et al. (2007)	RT-PCR	↑ GREM1 ∝ fertilization & Day 3 embryo morphology
	Anderson et al. (2009)	qRT-PCR (SYBR Green)	↑ GREM1 ∝ Day 2–3 embryo morphology
HAS2	McKenzie et al. (2004)	qRT-PCR (Taqman assay)	↑ HAS2 ∝ oocyte maturation
	Cillo et al. (2007)	RT-PCR	↑ HAS2 ∝ fertilization & Day 3 embryo morphology
PTX3	Zhang et al. (2005)	Microarray	↓ PTX3 ∝ fertilization & embryo quality
	Anderson et al. (2009)	qRT-PCR (SYBR Green)	↓ PTX3 ∝ cumulus expansion
TRPM7	Wathlet et al. (2011)	qRT-PCR (SYBR Green)	↑ TRPM7 ∝ Day 3 embryo morphology
	Wathlet et al. (2012)	qRT-PCR (SYBR Green)	↑ TRPM7 ∝ Day 3 embryo morphology
VCAN	Gebhardt et al. (2011)	qRT-PCR (SYBR Green)	↑ VCAN ∝ live birth
	Wathlet et al. (2011)	qRT-PCR (SYBR Green)	↓ VCAN ∝ oocyte maturation, ↑ VCAN ∝ pregnancy
RGS2	Feuerstein et al. (2012)	Microarray	↑ RGS2 ∝ blastocyst development & pregnancy
	Hamel et al. (2010)	qRT-PCR	↑ RGS2 ∝ pregnancy

Note: Symbols ↑, ↓, ∝ stands for higher level, lower level, and associated with, respectively. COX2, cyclooxygenase-2; GREM1, gremlin1; HAS2, hyaluronan synthase 2; PTGS2, prostaglandin synthase-2; PTX3, pentraxin 3; RGS2, regulator of G-protein signaling 2; TRPM7, transient receptor potential cation channel, subfamily M member 7; VCAN, versican.

[a] Only the transcripts identified by at least two studies have been listed in the table. All studies, except for Hamel et al. (2010), analyzed cumulus cells. RGS2, identified as a potential biomarker of pregnancy (Hamel et al. 2010), was studied in granulosa cells.

exception of VCAN. Predictive models were developed using multiple parameters, predicting pregnancy with a sensitivity of 70% and a specificity of 90%. Better cleavage-stage embryo prediction relied on TRPM7 and ITPKA expression and pregnancy prediction relied on SDC4 and VCAN expression.

The same group of investigators assessed 11 genes in a subsequent study and found no significant difference in cumulus cell expression of VCAN among the pregnant versus nonpregnant groups, whereas EphrinB2 (EFNB2) and ITPKA were up regulated and calcium/calmodulin-dependent protein kinase 1D (CAMK1D) showed the same trend in the pregnant group [48]. EFNB2, CAMK1D, and Stanniocalcin-2 (STC2) were used for the live birth prediction model.

An increasing number of unbiased studies used the microarray approach for oocyte viability assessment based on cumulus/granulosa cell transcriptome. In the first such study, Zhang et al. [49] compared pooled cumulus cells from oocytes that failed to fertilize with those derived from oocytes that developed into eight-cell embryos on Day 3, and they identified 160 genes differentially expressed between the two groups. They then applied qRT-PCR to quantify PTX3 and confirmed the association of PTX3 expression with oocyte development, contradictory to the results reported by Cillo et al. [44].

In another microarray study, van Montfoort et al. [50] compared gene expression in cumulus cells from eight oocytes resulting in early-cleavage embryos and from eight oocytes resulting in non-early-cleavage embryos. In total, 611 genes were differentially expressed between the groups. Among the genes found to be differentially expressed, cyclin D2 (CCND2), chemokine (C-X-C motif) receptor 4 (CXCR4), glutathione peroxidase 3 (GPX3), catenin delta 1 (CTNND1), 7-dehydrocholesterol reductase (DHCR7), disheveled, dsh homolog 3 (DVL3), heat shock 27 kDa protein 1 (HSBP1), and tripartite motif containing 28 (TRIM28) were reported to be the most significant genes, confirmed by subsequent qRT-PCR analysis.

Subsequently, Assou et al. [51] identified 630 genes as differentially expressed in cumulus cells from oocytes that lead to a pregnancy compared with oocytes that did not. Majority of these genes had higher expression levels in the pregnant group, suggesting transcriptional activation in cumulus cells of viable oocytes. The down regulation of nuclear factor IB (NFIB) and the up regulation of BCL-like protein 11 (BCL2L11) and phosphoenolpyruvate carboxykinase 1 (PCK1) in the pregnant group was further confirmed by qRT-PCR in the same study.

Most recently, Feuerstein et al. [52] collected 197 individual cumulus cell samples from 106 patients undergoing the ICSI procedure and investigated cumulus cell gene expression using 96 microarrays to determine genes associated with oocyte maturation and subsequent blastocyst development. After microarrays, these researchers performed a meta-analysis to test identified genes in other data sets available in Gene Expression Omnibus, and they selected eight genes from the 308 differentially expressed genes for further validation by quantitative polymerase chain reaction (qPCR). Three of these eight selected genes were validated as potential biomarkers (perilipin 2 [PLIN2], regulator of G-protein signaling 2 [RGS2], and angiogenin [ANG]). After correction for additional experimental parameters, including interpatient variability, only the expression level of RGS2 was confirmed to be related to oocyte developmental competence and clinical pregnancy.

Granulosa cell transcriptome has been analyzed in three consecutive studies by Hamel et al. [53–55] in correlation with pregnancy outcome. In the first study [53], the gene expression of granulosa cells was determined using both a custom-made cDNA microarray and an Affymetrix GeneChip®. The samples were investigated in two groups: the follicular cells from oocytes that resulted in a positive pregnancy and the follicular cells from oocytes resulting in embryos that failed to develop. Among the 115 genes identified as being differentially expressed, altered expression of 3-beta-hydroxystreoid dehydrogenase (HSD3β1), ferredoxin 1 (FDX1), serine (or cysteine) proteinase inhibitor clade E member 2 (SERPINE2), cytochrome P450 aromatase (CYP19A1), and cell division cycle 42 (CDC42) was significantly associated with pregnancy outcome. Building on the findings of this initial study, they subsequently identified phosphoglycerate kinase 1 (PGK1), RGS2, regulator of G-protein signaling 3 (RGS3), CDC42 [54], UDP-glucose pyrophosphorylase 2 (UGP2), and pleckstrin homology-like domain family A member 1 (PHLDA1) [55] as potential follicular markers associated with embryo quality resulting in a successful pregnancy.

Eventually, transcriptomic analysis of cumulus/granulosa cells enabled identification of various genes as potential biomarkers of oocyte and embryo competence; the most frequently studied of these genes are listed in Table 13.1.

Embryo Selection by Proteomics

Proteins are the key factors regulating the cellular functions within an organism. Proteome is the entire set of proteins expressed by a specific genome under certain environmental conditions at a certain time. Proteomic profiling is of primary importance to understand the complex nature of the biological processes. Although transcriptomics technologies are available to provide an estimation of gene expression by quantification of mRNAs within a sample, mRNA expression level of a particular gene does not always correlate with its protein expression [56]. Observed differences between mRNA and corresponding protein levels are mainly attributed to posttranscriptional mechanisms, substantial differences between proteins' in vivo half-lives, and a significant amount of experimental errors [57,58]. Recent advances in analytical proteomics techniques and related bioinformatics approaches enabled direct quantification of gene expression at the protein level.

Whereas transcriptomics provides an estimation of gene expression by quantification of mRNAs within a sample, proteomics aims at the actual protein expression of a biological sample.

Proteomics studies may be aimed at (1) profiling proteome content of a biological sample, (2) performing comparative protein expression analysis, (3) localizing and identifying posttranslational modifications, and (4) exploring protein–protein interactions [59]. Proteomics technologies could be applied to IVF for noninvasive assessment of embryonic secretome that includes the proteins produced by the embryos and secreted into the surrounding culture media [60,61]. Preliminary proteomics studies in this context hypothesized that secretome profiles of the culture media could potentially correlate with embryo viability [62–64]. Using mass spectrometry or protein array technologies, these studies reported altered expression of specific proteins associated with blastocyst development or implantation.

Analytical Proteomics Techniques

The basic mass spectrometer consists of an ionization source (matrix-assisted laser desorption ionization [MALDI], surface-enhanced laser desorption/ionization [SELDI], or electrospray ionization [ESI]), a mass analyzer (e.g., time-of-flight [TOF], ion trap, Orbitrap), and a mass detector. Mass analyzers are usually used in tandem (tandem mass spectrometry) to achieve higher degrees of ion separation and identification.

Mass spectrometry–based proteomics analyses are coupled with gel-based or gel-free protein separation techniques and provide high detection specificity without the need for antibodies [65].

In the widely used two-dimensional difference gel electrophoresis (2D-DIGE) method for protein separation, different protein mixtures are labeled with different fluorescent dyes and mixed and loaded together on a single gel for quantitative comparative protein expression analysis [66]. The proteins within the complex mixture are then separated by isoelectric focusing in the first dimension and by sodium dodecyl sulfate polyacrylamide gel electrophoresis (SDS-PAGE) that discriminates proteins based on molecular mass in the second dimension. The relative abundance of protein in each spot is determined by scanning the gel at the wavelengths of the fluorescent dyes, enabling differential expression analysis. The spots of interest are then further analyzed by mass spectrometers (e.g., MALDI-TOF/TOF) for identification of the corresponding proteins.

Different types of chromatographic separation techniques (commonly, high-performance liquid chromatography [HPLC]) are also used in proteomics analysis for gel-free protein separation. The basic principle behind these techniques is to separate solute proteins or peptides depending on their distributions between mobile and stationary phases. A typical example of combined liquid chromatography–mass spectrometry system is multidimensional protein identification technology (muDPIT) [67] as an efficient approach for protein identification lacking the ability to provide quantitative information. Alternative gel-free labeling technologies, such as isotope-coded affinity tag (ICAT), stable isotope labeling by amino acids (SILAC), and isobaric tags for relative and absolute quantification (iTRAQ), are also coupled with mass spectrometry, enabling quantitative proteomics analysis.

More recently, protein microarray technology is becoming a significant tool for quantitative and functional proteomics [68]. Protein microarrays consist of antibodies or other affinity reagents attached on a solid surface.

Each agent binds to its target protein in a complex mixture, and detected proteins are identified and quantified subsequently. Using protein arrays, it is possible to examine the expression of hundreds of proteins simultaneously. In contrast, protein arrays can provide data only on preselected proteins that were included in the chip design, whereas mass spectrometry techniques can potentially detect any protein [59].

Clinical applications of proteomics-based embryo assessment

Initial studies investigating protein expression in relation to embryo viability focused on identification of specific molecules produced by the embryo and secreted into the surrounding culture media. Embryos leading to successful pregnancies were shown to secrete higher levels of interleukin-1 (IL-1) alpha [69] and IL-1 beta [70], and embryos expressing soluble human leukocyte antigen G (HLA-G) had a better chance of implantation [71]. Also, significantly higher concentration of leptin was observed in competent blastocysts compared with the arrested blastocytes [72].

Preliminary data revealed correlation of protein secretion profiles with embryo competence and motivated a deeper investigation of human embryonic secretome. Using SELDI-TOF-MS, Katz-Jaffe et al. [62] successfully analyzed secretome of individual human embryos and observed distinctive secretome profiles at each successive 24 hr intervals of preimplantation embryo development. In the same study, significant up-regulation of an 8.5 kDa protein was observed in the secretome of developing blastocysts on Day 5. A subsequent protein identification process indicated that the best candidate for this potential biomarker was ubiquitin.

In another study, Dominguez et al. [63] used protein microarrays containing 120 antibody targets to analyze the secretome of the human blastocysts. Conditioned media were collected from implanted and nonimplanted embryos and from blank controls in a single embryo transfer program. Expressions of proteins such as CXCL13 (BCL, B lymphocyte chemoattractant), stem cell factor (SCF), and macrophage-stimulating protein-a (MSP-a) were significantly decreased and soluble tumor necrosis factor (TNF) receptor 1 (sTNFR1) was significantly increased in the media where the blastocyst was present in comparison with the control media. Moreover, when compared with nonimplanted blastocysts, granulocyte macrophage–colony-stimulating factor (GM-CSF) and CXCL13 were significantly reduced, therefore consumed at a higher rate by the implanted blastocysts.

A subsequent study by the same group [64] investigated comparative secretome of the conditioned media from implanted blastocysts in endometrial epithelial cell (EEC) coculture system versus sequential microdrop culture media. Protein array analysis indicated IL-6 as the most abundant protein in the implanted embryo coculture media, and this group suggested that the coculture system favors blastocyst development and implantation by the contribution of the factors secreted by EEC.

A summary of the initial proteomics analysis of embryonic secretome is given in Table 13.2. Despite the promising preliminary results, proteomics is still considered a limited source of information for assessing reproductive potential of embryos, possibly due to lack of sensitivity of proteomics platforms in this domain and to the complexity of the experimental and data analysis procedures. Nevertheless, rapid progression of proteomics technologies is likely to overcome such limitations in the near future.

TABLE 13.2

Potential Biomarker Proteins of Embryo Viability Identified in the Embryonic Secretome

Molecule	Study	Technique	Result
IL-1 beta	Baranao et al. (1997)	ELISA	↑ IL-1 beta ∝ pregnancy
HLA-G	Fuzzi et al. (2002)	ELISA	↑ HLA-G ∝ implantation
Ubiquitin	Katz-Jaffe et al. (2006)	SELDI-TOF-MS	↑ ubiquitin ∝ blastocyst development
CXCL13	Dominguez et al. (2008)	Protein array	↓ CXCL13 ∝ implantation
GM-CSF	Dominguez et al. (2008)	Protein array	↓ GM-CSF ∝ implantation

Note: Symbols ↑, ↓, ∝ stands for higher level, lower level, and associated with, respectively. CXCL13, C-X-C motif chemokine 13; ELISA, enzyme-linked immunosorbent assay; GM-CSF, granulocyte macrophage colony-stimulating factor; HLA-G, human leukocyte antigen G; IL, Interleukin; SELDI-TOF-MS, surface-enhanced laser desorption/ionization–time-of-flight–mass spectrometer.

Embryo Selection by Metabolomics

Metabolome is the entire set of small molecules (<1 kDa), including metabolic intermediates (amino acids, lipids, and nucleotides), hormones, signaling molecules, and secondary metabolites, within a biological sample. Metabolites are the final downstream products of gene expression, and their inventory provides a valuable database to explore genotype–phenotype relationships and genotype–environment interactions. Within the context of IVF, the changes in the levels of metabolites associated with carbohydrate metabolism and amino acid turnover were investigated as indicators of normal preimplantation embryo development.

Preimplantation Embryo Metabolism as an Indicator of Viability

Preimplantation embryo development has unique metabolic characteristics, because the preferred energy source for embryonic cellular metabolism changes during preimplantation development. Carbohydrate metabolism of preimplantation human embryos was mainly investigated in terms of pyruvate and glucose uptake and lactate production. Initially in 1989, Hardy et al. [73] reported higher pyruvate uptake in embryos that develop to blastocyst stage, soon after to be confirmed by Gott et al. [74]. Subsequently, Conaghan et al. [75] measured pyruvate uptake for the first time in relation to implantation and clinical pregnancy, and they demonstrated that embryo implantation after Day 2 and Day 3 transfers was inversely correlated with pyruvate uptake by two- to eight-cell embryos. Another study by Turner et al. [76] showed that embryos had a wide range of pyruvate uptake values, but this variation was reduced to an intermediate range in the embryos that implanted. More recently, Gardner et al. [77] investigated the pyruvate metabolism in relation to blastocyst development and suggested that pyruvate uptake on Day 4 was significantly higher by embryos that formed blastocysts compared with embryos that failed to develop before blastocyst stage. On the basis of these findings, pyruvate uptake seems to be correlated with blastocyst development, whereas its relationship to implantation or pregnancy outcome remains inconclusive.

Metabolome is the analysis of metabolites that are the final downstream products of gene expression, and in preimplantation embryo development, a distinct change in the levels of metabolites is expected to classify a "normal" development and a viable embryo.

Glucose uptake has also been measured in correlation with the embryo's developmental potential. According to initial findings, glucose uptake from Day 2 to Day 4 was similar for embryos that reached the blastocyst stage and those that were arrested during cleavage [73,74]. In contrast, Gardner et al. [77] showed a significant association between increased levels of glucose uptake on Day 4 and subsequent blastocyst formation and quality.

Besides the carbohydrates, amino acids are also key components of preimplantation embryo development because in vitro–developing embryos use and produce amino acids. The improvement in extended culture to the blastocyst stage has been achieved mainly by inclusion of amino acids into the culture medium [78,79]. Consequently, amino acid content of spent embryo culture media has been profiled to explore specific amino acid turnover patterns during preimplantation embryo development in correlation to blastocyst formation.

Initially, Houghton et al. [80] examined 18 amino acids during in vitro embryo development and showed that embryos that form a blastocyst displayed a different profile of amino acid metabolism than those that were arrested. Specifically, lower uptake of glutamine, arginine, and methionine and lower release of alanine and asparagine on Day 2 and Day 3 was found to be associated with blastocyst development. In the same study, lower uptake of serine and lower release of alanine and glycine by eight-cell- and morula-stage embryos correlated with blastocyst development. Moreover, consistent with the "quiet embryo hypothesis" [81], sum of depletion and appearance of the amino acids examined, that is, amino acid turnover, was shown to be lower in developing embryos compared with the arrested embryos.

In another study, Brison et al. [82] investigated the correlation of amino acid turnover with implantation and pregnancy outcomes when the embryos were selected according to routine morphological criteria and transferred

TABLE 13.3

Potential Biomarker Metabolites of Embryo Viability Identified in the Culture Media Metabolome

Metabolite	Study	Technique	Result
Pyruvate	Hardy et al. (1989)	Ultramicrofluorescence assay	↑ pyruvate uptake on Day 1–5 ∝ embryo development
	Gott et al. (1990)	Ultramicrofluorescence assay	↑ pyruvate uptake on Day 2–5 ∝ embryo development
	Conaghan et al. (1993)	Ultramicrofluorescence assay	↓ pyruvate uptake on Day 2–3 ∝ implantation
	Turner et al. (1994)	Ultramicrofluorescence assay	intermediate pyruvate uptake on Day 2 ∝ implantation of morphologically good embryos
	Gardner et al. (2001)	Ultramicrofluorescence assay	↑ pyruvate uptake on Day 4 ∝ blastocyst development
Glucose	Hardy et al. (1989)	Ultramicrofluorescence assay	↑ glucose uptake on Day 5 ∝ blastocyst development
	Gott et al. (1990)	Ultramicrofluorescence assay	↑ glucose uptake on Day 5 ∝ blastocyst development
	Gardner et al. (2001)	Ultramicrofluorescence assay	↑ glucose uptake on Day 5–6 ∝ blastocyst quality
Lactate	Gott et al. (1990)	Ultramicrofluorescence assay	↑ lactate production on Day 3–5 ∝ blasctocyst development
Glutamine	Houghton et al. (2002)	High-performance liquid chromatography	↓ glutamine uptake on Day 2–3 ∝ blastocyst development
Arginine	Houghton et al. (2002)	High-performance liquid chromatography	↓ arginine uptake on Day 2–3 ∝ blastocyst development
Methionine	Houghton et al. (2002)	High-performance liquid chromatography	↓ methionine uptake on Day 2–3 ∝ blastocyst development
Alanine	Houghton et al. (2002)	High-performance liquid chromatography	↓ alanine production on Day 2–3 ∝ blastocyst development ↓ alanine release at compacting 8-cell stage ∝ blastocyst development
Asparagine	Houghton et al. (2002)	High-performance liquid chromatography	↓ asparagine production on Day 2–3 ∝ blastocyst development
	Brison et al. (2004)	High-performance liquid chromatography	↑ asparagine level on Day 2 ∝ pregnancy & live birth
Serine	Houghton et al. (2002)	High-performance liquid chromatography	↓ serine uptake at compacting 8-cell stage ∝ blastocyst development
Glycine	Houghton et al. (2002)	High-performance liquid chromatography	↓ glycine release at compacting 8-cell stage ∝ blastocyst development
	Brison et al. (2004)	High-performance liquid chromatography	↓ glycine level on Day 2 ∝ pregnancy & live birth
Leucine	Brison et al. (2004)	High-performance liquid chromatography	↓ glycine level on Day 2 ∝ pregnancy & live birth
Glutamate	Seli et al. (2008)	Proton nuclear magnetic resonance	↑ glutamate level on Day 3 ∝ pregnancy & live birth

on Day 2. This study demonstrated that decreased glycine and leucine and increased asparagine levels in the culture media were associated with increased clinical pregnancy and live birth rates. A more recent study by Seli et al. [83] showed an association between increased glutamate levels in the culture media and clinical pregnancy and live birth.

Table 13.3 is a summary of the findings suggested by the studies investigating preimplantation embryo metabolism as an indicator of embryo viability.

Techniques for Metabolomic Analysis of Embryo Culture Media

Currently, a variety of analytical spectroscopic techniques are available for metabolomic analysis of biological samples. Here, we provide a brief overview of common techniques and related data analysis procedures.

Analytical Spectroscopic Techniques

Common analytical approaches applied for metabolomic analysis of embryo culture media can be categorized as nuclear magnetic resonance (NMR) spectroscopy, mass spectrometry, or vibrational spectroscopy.

NMR is a nondestructive analytical technique exploiting interaction of the magnetic moment of atomic nuclei with the external magnetic field. NMR provides information on metabolites containing elements with nonzero magnetic moments and has been efficiently used for biomarker analysis by enabling detection and quantification of specific metabolites within a biological fluid or tissue [84,85]. Limitations of NMR were attributed to requirement for large amounts of sample, higher costs, and lack of sensitivity for low-abundance targets favoring the method for analysis of high abundance metabolites.

Mass spectrometry operates by ion formation, separation of ions according to their mass-to-charge ratio (*m*/*z*), and detection of separated ions [86] and enables simultaneous characterization of several hundred metabolites with higher sensitivity compared with NMR approaches. Mass spectrometry is the most widely used analytical platform in metabolomics. The sensitivity and specificity of this common technique is further enhanced when coupled with chromatography or electrophoresis-based separation techniques.

The vibrational spectroscopy techniques include Raman and infrared (IR) approaches [87]. The main principle behind vibrational techniques is that, when a sample is exposed to an electromagnetic radiation, the chemical bonds within the molecules will absorb the energy and vibrate to a greater extent. The IR spectrum is the result of absorption of electromagnetic radiation by vibrating molecules when the sample is interrogated with an IR beam, whereas Raman spectroscopy measures the scattering of electromagnetic radiation by the vibrating molecules under exposure to a particular wavelength light (usually in the form of a laser).

The wavelength of the light used for radiation differs in the two IR spectroscopy techniques: near-infrared (NIR) and Fourier transform infrared (FTIR). NIR measures the spectra in the 14,000–4000 cm^{-1} region, whereas FTIR looks at the mid-IR part of the spectrum at 4000–600 cm^{-1}. NIR has the advantage of quantification with higher sensitivity in metabolomics research, whereas FTIR is a faster and higher throughput method.

Analysis of Metabolomics Data

Analysis of the metabolomics data is strongly related to the research objective, considering three main categories, namely targeted metabolite profiling, nontargeted profiling, and metabolic fingerprinting. Targeted analysis is based on detection and quantification of the metabolites for which chemical structures are known. In contrast, nontargeted profiling aims at quantification of all the peaks in the spectrum without associating the peaks to chemical structure of certain compounds. Metabolomic fingerprinting is also a nontargeted approach that considers the whole metabolic profile as a pattern.

Analysis of targeted metabolite profiling is relatively simple because only previously identified spectral regions are analyzed. In contrast, nontargeted profiling and metabolic fingerprinting are complex processes that may require bioinformatics support for efficient and accurate analysis of high dimensional metabolomics data [88].

A common preprocessing step in the analysis of metabolomics data is normalization. The multistage experimental setting underlying metabolomics studies is likely to introduce systematic variations in the resulting spectra. The main source of nonbiological variations in metabolomics embryo assessment is attributed to the culture environment. Spectral profiles of spent culture media (i.e., where individual embryo has been cultured) need to be normalized to that of blank samples (i.e., culture media incubated under the same conditions but without an embryo) to eliminate the possible impact of variations in culture conditions. Then, predictive models are developed using advanced statistical methods. To ensure the robustness of the model against center-specific variations, such models should be either developed using pooled multicenter data or validated in different centers. Once the success and robustness of a prediction model are established, it can be used as an embryo selection tool alone or in combination with other available criteria.

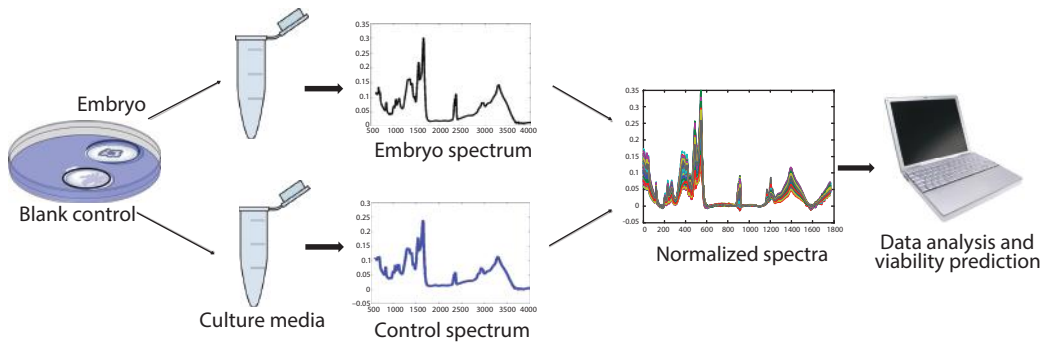

FIGURE 13.3 Metabolomic assessment of embryo viability through spectroscopic analysis of spent culture media.

Clinical applications of metabolomics-based embryo assessment

Efficiency of metabolomics-based embryo selection strategies was first evaluated in retrospective studies and then in subsequent randomized clinical trials (RCTs). The typical workflow of metabolomics-based embryo assessment is shown in Figure 13.3.

Proof-of-Principal Studies

In 2007, Seli et al. [89] reported the findings of a proof-of-concept study correlating spent culture media metabolome with embryo viability. In this initial study, Day 3 spent embryo culture media samples were analyzed using Raman spectroscopy, NIR spectroscopy, or both. The mean spectrum of embryos that failed to implant was compared with the mean spectrum of embryos that resulted in a live birth, and algorithms predictive of an embryo's reproductive potential were developed for Raman and NIR spectroscopy. Subsequently, Scott et al. [90] validated the Raman spectroscopy algorithm using spent culture media collected at a different center, where embryos were cultured in a different type and volume of culture medium.

In a subsequent study, Vergouw et al. [91] analyzed embryo culture media samples from single embryo transfer cycles using NIR spectroscopy and developed a new algorithm predictive of embryo implantation potential. They calculated a "viability score" for each embryo based on the NIR metabolomic profile of the corresponding culture medium and reported that increasing viability scores were correlated with an increasing ability of the embryo to implant. Subsequent studies with a large number of samples collected in SET cycles reported similar findings and suggested that the metabolomic profile of embryo culture medium was a parameter independent of morphology [92–94].

Commercialization Efforts and RCTs

The initial studies suggesting potential benefit from metabolomic profiling of spent culture media to determine embryo viability were retrospective and were performed in a single research laboratory using frozen and transported culture media samples. Because the promise of metabolomics approach is its potential use as a rapid on-site technology in the IVF laboratory, the algorithms developed needed to be tested using fresh samples at different clinical sites and RCT design.

A series of prototype and commercial instruments were built and tested for this purpose by a private company, Molecular Biometrics Inc., using an NIR system (ViaMetrics). Using the prototype instruments, two RCTs were conducted in centers performing SET [16,36]. In these studies, in the treatment arm, embryos with good morphology were identified followed by selection for transfer based on the metabolomic Viability Score™ generated by the commercial instrument. In the control arm, embryos were selected using standard morphological embryo assessment protocols.

In the first of these studies, Hardarson et al. [95] analyzed spent culture media from Day 2 and Day 5 SETs. Although not statistically significant, their findings suggested a potential benefit of NIR for the assessment

of embryos transferred on Day 2. In the NIR/morphology group ($n = 87$) and morphology alone group ($n = 83$), the pregnancy rates for Day 2 were 31% and 26.5%, respectively. In the same study, no benefit was found for selection on Day 5 ($n = 77$ for NIR/morphology and $n = 80$ for morphology alone groups). The second randomized trial performed by Vergouw et al. [36] reported similar findings in women undergoing SET on Day 3, and found no difference in live birth rates between NIR/morphology group ($n = 146$; live birth rate 29.5%) compared with the morphology alone group ($n = 163$; live birth rate 31.3%).

Conversely, Sfontouris et al. [96] performed an RCT using the commercial platform where two or three embryos were selected for transfer on the basis of NIR/morphology or morphology alone, and they showed an improvement in pregnancy rates in the NIR-assisted group. Implantation rates (IRs) were significantly improved in the NIR/morphology group ($n = 39$ patients; IR = 33/102 [32.4%]) compared with the morphology alone group [$n = 86$ patients; 55/257 [21.4%]).

Ultimately, the commercial version of the NIR instrument was withdrawn due to the wide variability in performance between clinics and the inconsistent results in clinical trials. The technology will hopefully be improved and tested again in the near future.

Summary and Conclusions

Current embryo assessment strategies that rely primarily on embryo morphology and cleavage rate do not provide adequate sensitivity or specificity to achieve desired pregnancy rates in women undergoing infertility treatment with IVF. Studies using emerging technologies to analyze cumulus/granulosa cell transcriptome or spent embryo culture media protein or metabolite content report promising results. However, the transcripts or proteins that have been identified as potential biomarkers of embryo viability or the metabolomic profiles associated with pregnancy outcome have not yet been adequately validated. Therefore, the use of these novel noninvasive technologies remains experimental, and their application to clinical practice awaits RCTs demonstrating benefit from their use, alone or in combination with morphological evaluation.

REFERENCES

1. Martin JA, Hamilton BE, Ventura SJ, Osterman MJK, Wilson EC, Mathews TJ. *Births: Final Data for 2010*. Hyattsville, MD: National Center for Health Statistics; 2012.
2. Practice Committee of American Society for Reproductive Medicine. Multiple gestation associated with infertility therapy: An American Society for Reproductive Medicine Practice Committee opinion. *Fertility and Sterility*. 2012;97(4):825–34.
3. Norwitz ER, Edusa V, Park JS. Maternal physiology and complications of multiple pregnancy. *Seminars in Perinatology*. 2005;29(5):338–48.
4. Ata B, Seli E. Economics of assisted reproductive technologies. *Current Opinion in Obstetrics & Gynecology*. 2010;22(3):183–8.
5. Bromer JG, Ata B, Seli M, Lockwood CJ, Seli E. Preterm deliveries that result from multiple pregnancies associated with assisted reproductive technologies in the USA: A cost analysis. *Current Opinion in Obstetrics & Gynecology*. 2011;23(3):168–73.
6. Velikonja U. The costs of multiple gestation pregnancies in assisted reproduction. *Harvard Journal of Law and Gender*. 2009;463:481–93.
7. Bromer JG, Seli E. Assessment of embryo viability in assisted reproductive technology: Shortcomings of current approaches and the emerging role of metabolomics. *Current Opinion in Obstetrics & Gynecology*. 2008;20(3):234–41.
8. Center for Disease Control and Prevention. ART. 2010. Available from: http://www.cdc.gov/art/
9. Human Fertilisation and Embryology Authority (HFEA). 2011. Available from: http://www.hfea.gov.uk
10. Sakkas D, Gardner DK. Noninvasive methods to assess embryo quality. *Current Opinion in Obstetrics & Gynecology*. 2005;17(3):283–8.

11. Wong CC, Loewke KE, Bossert NL, Behr B, De Jonge CJ, Baer TM, et al. Non-invasive imaging of human embryos before embryonic genome activation predicts development to the blastocyst stage. *Nature Biotechnology*. 2010;28(10):1115–21.
12. Meseguer M, Rubio I, Cruz M, Basile N, Marcos J, Requena A. Embryo incubation and selection in a time-lapse monitoring system improves pregnancy outcome compared with a standard incubator: A retrospective cohort study. *Fertility and Sterility*. 2012;98(6):1481–9.e10.
13. Seli E, Robert C, Sirard MA. OMICS in assisted reproduction: Possibilities and pitfalls. *Molecular Human Reproduction*. 2010;16(8):513–30.
14. Checa MA, Alonso-Coello P, Sola I, Robles A, Carreras R, Balasch J. IVF/ICSI with or without preimplantation genetic screening for aneuploidy in couples without genetic disorders: A systematic review and meta-analysis. *Journal of Assisted Reproduction and Genetics*. 2009;26(5):273–83.
15. Sher G, Keskintepe L, Keskintepe M, Maassarani G, Tortoriello D, Brody S. Genetic analysis of human embryos by metaphase comparative genomic hybridization (mCGH) improves efficiency of IVF by increasing embryo implantation rate and reducing multiple pregnancies and spontaneous miscarriages. *Fertility and Sterility*. 2009;92(6):1886–94.
16. Schoolcraft WB, Treff NR, Stevens JM, Ferry K, Katz-Jaffe M, Scott RT, Jr. Live birth outcome with trophectoderm biopsy, blastocyst vitrification, and single-nucleotide polymorphism microarray-based comprehensive chromosome screening in infertile patients. *Fertility and Sterility*. 2011;96(3):638–40.
17. Uyar A, Torrealday S, Seli E. Cumulus and granulosa cell markers of oocyte and embryo quality. *Fertility and Sterility*. 2013;99(4):979–97.
18. Gilchrist RB, Ritter LJ, Armstrong DT. Oocyte-somatic cell interactions during follicle development in mammals. *Animal Reproduction Science*. 2004;82–83:431–46.
19. Roche JF. Control and regulation of folliculogenesis—a symposium in perspective. *Reviews of Reproduction*. 1996;1(1):19–27.
20. Heller DT, Schultz RM. Ribonucleoside metabolism by mouse oocytes: Metabolic cooperativity between the fully grown oocyte and cumulus cells. *The Journal of Experimental Zoology*. 1980;214(3):355–64.
21. Brower PT, Schultz RM. Intercellular communication between granulosa cells and mouse oocytes: Existence and possible nutritional role during oocyte growth. *Developmental Biology*. 1982;90(1):144–53.
22. Albertini DF, Combelles CM, Benecchi E, Carabatsos MJ. Cellular basis for paracrine regulation of ovarian follicle development. *Reproduction*. 2001;121(5):647–53.
23. Tanghe S, Van Soom A, Nauwynck H, Coryn M, de Kruif A. Minireview: Functions of the cumulus oophorus during oocyte maturation, ovulation, and fertilization. *Molecular Reproduction and Development*. 2002;61(3):414–24.
24. Veeck LL. *An Atlas of Human Gametes and Conceptuses: An Illustrated Reference of Assisted Reproductive Technology*. New York: The Pathenon Publishing Group; 1999.
25. Manchester KL. Use of UV methods for measurement of protein and nucleic acid concentrations. *Biotechniques*. 1996;20(6):968–70.
26. Sambrook J, Russel DW. *Molecular Cloning: A Laboratory Manual*. 3rd ed. Cold Spring Harbor, NY: Cold Spring Harbor Laboratory Press; 2001.
27. Schroeder A, Mueller O, Stocker S, Salowsky R, Leiber M, Gassmann M, et al. The RIN: An RNA integrity number for assigning integrity values to RNA measurements. *BMC Molecular Biology*. 2006;7:3.
28. Stahlberg A, Hakansson J, Xian X, Semb H, Kubista M. Properties of the reverse transcription reaction in mRNA quantification. *Clinical Chemistry*. 2004;50(3):509–15.
29. Saiki RK, Gelfand DH, Stoffel S, Scharf SJ, Higuchi R, Horn GT, et al. Primer-directed enzymatic amplification of DNA with a thermostable DNA polymerase. *Science*. 1988;239(4839):487–91.
30. Higuchi R, Dollinger G, Walsh PS, Griffith R. Simultaneous amplification and detection of specific DNA sequences. *Biotechnology (NY)*. 1992;10(4):413–17.
31. Higuchi R, Fockler C, Dollinger G, Watson R. Kinetic PCR analysis: Real-time monitoring of DNA amplification reactions. *Biotechnology (NY)*. 1993;11(9):1026–30.
32. Andersen CL, Jensen JL, Orntoft TF. Normalization of real-time quantitative reverse transcription-PCR data: A model-based variance estimation approach to identify genes suited for normalization, applied to bladder and colon cancer data sets. *Cancer Research*. 2004;64(15):5245–50.

33. Vandesompele J, De Preter K, Pattyn F, Poppe B, Van Roy N, De Paepe A, et al. Accurate normalization of real-time quantitative RT-PCR data by geometric averaging of multiple internal control genes. *Genome Biology*. 2002;3(7):34–34.11
34. Mortazavi A, Williams BA, McCue K, Schaeffer L, Wold B. Mapping and quantifying mammalian transcriptomes by RNA-Seq. *Nature Methods*. 2008;5(7):621–8.
35. Wang Z, Gerstein M, Snyder M. RNA-Seq: A revolutionary tool for transcriptomics. *Nature Reviews Genetics*. 2009;10(1):57–63.
36. Ozsolak F, Platt AR, Jones DR, Reifenberger JG, Sass LE, McInerney P, et al. Direct RNA sequencing. *Nature*. 2009;461:814–18.
37. Antoniou E, Taft R. Gene expression in mouse oocytes by RNA-Seq. *Methods in Molecular Biology*. 2012;825:237–51.
38. Irizarry RA, Hobbs B, Collin F, Beazer-Barclay YD, Antonellis KJ, Scherf U, et al. Exploration, normalization, and summaries of high density oligonucleotide array probe level data. *Biostatistics*. 2003;4(2):249–64.
39. Bolstad BM, Irizarry RA, Astrand M, Speed TP. A comparison of normalization methods for high density oligonucleotide array data based on variance and bias. *Bioinformatics*. 2003;19(2):185–93.
40. Irizarry RA, Bolstad BM, Collin F, Cope LM, Hobbs B, Speed TP. Summaries of Affymetrix GeneChip probe level data. *Nucleic Acids Research*. 2003;31(4):e15.
41. Storey JD. A direct approach to false discovery rates. *Journal of the Royal Statistical Society: Series B*. 2002;64:479–98.
42. Storey JD, Tibshirani R. Statistical significance for genomewide studies. *Proceedings of the National Academy of Sciences of the United States of America*. 2003;100(16):9440–5.
43. McKenzie LJ, Pangas SA, Carson SA, Kovanci E, Cisneros P, Buster JE, et al. Human cumulus granulosa cell gene expression: A predictor of fertilization and embryo selection in women undergoing IVF. *Human Reproduction*. 2004;19(12):2869–74.
44. Cillo F, Brevini TA, Antonini S, Paffoni A, Ragni G, Gandolfi F. Association between human oocyte developmental competence and expression levels of some cumulus genes. *Reproduction*. 2007;134(5):645–50.
45. Anderson RA, Sciorio R, Kinnell H, Bayne RA, Thong KJ, de Sousa PA, et al. Cumulus gene expression as a predictor of human oocyte fertilisation, embryo development and competence to establish a pregnancy. *Reproduction*. 2009;138(4):629–37.
46. Gebhardt KM, Feil DK, Dunning KR, Lane M, Russell DL. Human cumulus cell gene expression as a biomarker of pregnancy outcome after single embryo transfer. *Fertility and Sterility*. 2011;96(1):47–52.e2.
47. Wathlet S, Adriaenssens T, Segers I, Verheyen G, Van de Velde H, Coucke W, et al. Cumulus cell gene expression predicts better cleavage-stage embryo or blastocyst development and pregnancy for ICSI patients. *Human Reproduction*. 2011;26(5):1035–51.
48. Wathlet S, Adriaenssens T, Segers I, Verheyen G, Janssens R, Coucke W, et al. New candidate genes to predict pregnancy outcome in single embryo transfer cycles when using cumulus cell gene expression. *Fertility and Sterility*. 2012;98(2):432–9.e4.
49. Zhang X, Jafari N, Barnes RB, Confino E, Milad M, Kazer RR. Studies of gene expression in human cumulus cells indicate pentraxin 3 as a possible marker for oocyte quality. *Fertility and Sterility*. 2005;83(Suppl 1):1169–79.
50. van Montfoort AP, Geraedts JP, Dumoulin JC, Stassen AP, Evers JL, Ayoubi TA. Differential gene expression in cumulus cells as a prognostic indicator of embryo viability: A microarray analysis. *Molecular Human Reproduction*. 2008;14(3):157–68.
51. Assou S, Haouzi D, Mahmoud K, Aouacheria A, Guillemin Y, Pantesco V, et al. A non-invasive test for assessing embryo potential by gene expression profiles of human cumulus cells: A proof of concept study. *Molecular Human Reproduction*. 2008;14(12):711–19.
52. Feuerstein P, Puard V, Chevalier C, Teusan R, Cadoret V, Guerif F, et al. Genomic assessment of human cumulus cell marker genes as predictors of oocyte developmental competence: Impact of various experimental factors. *PLoS One*. 2012;7(7):e40449.
53. Hamel M, Dufort I, Robert C, Gravel C, Leveille MC, Leader A, et al. Identification of differentially expressed markers in human follicular cells associated with competent oocytes. *Human Reproduction*. 2008;23(5):1118–27.
54. Hamel M, Dufort I, Robert C, Leveille MC, Leader A, Sirard MA. Genomic assessment of follicular marker genes as pregnancy predictors for human IVF. *Molecular Human Reproduction*. 2010;16(2):87–96.

55. Hamel M, Dufort I, Robert C, Leveille MC, Leader A, Sirard MA. Identification of follicular marker genes as pregnancy predictors for human IVF: New evidence for the involvement of luteinization process. *Molecular Human Reproduction*. 2010;16(8):548–56.
56. Gygi SP, Rochon Y, Franza BR, Aebersold R. Correlation between protein and mRNA abundance in yeast. *Molecular and Cellular Biology*. 1999;19(3):1720–30.
57. Greenbaum D, Colangelo C, Williams K, Gerstein M. Comparing protein abundance and mRNA expression levels on a genomic scale. *Genome Biology*. 2003;4(9):117.
58. Beyer A, Hollunder J, Nasheuer HP, Wilhelm T. Post-transcriptional expression regulation in the yeast Saccharomyces cerevisiae on a genomic scale. *Molecular & Cellular Proteomics*. 2004;3(11):1083–92.
59. Chandramouli K, Qian PY. Proteomics: Challenges, techniques and possibilities to overcome biological sample complexity. *Human Genomics and Proteomics*. 2009;2009: ii, 239204.
60. Katz-Jaffe MG, McReynolds S. Embryology in the era of proteomics. *Fertility and Sterility*. 2013;99(4):1073–7.
61. Garrido-Gomez T, Dominguez F, Simon C. Proteomics of embryonic implantation. *Handbook of Experimental Pharmacology*. 2010;(198):67–78.
62. Katz-Jaffe MG, Schoolcraft WB, Gardner DK. Analysis of protein expression (secretome) by human and mouse preimplantation embryos. *Fertility and Sterility*. 2006;86(3):678–85.
63. Dominguez F, Gadea B, Esteban FJ, Horcajadas JA, Pellicer A, Simon C. Comparative protein-profile analysis of implanted versus non-implanted human blastocysts. *Human Reproduction*. 2008;23(9):1993–2000.
64. Dominguez F, Gadea B, Mercader A, Esteban FJ, Pellicer A, Simon C. Embryologic outcome and secretome profile of implanted blastocysts obtained after coculture in human endometrial epithelial cells versus the sequential system. *Fertility and Sterility*. 2010;93(3):774–82.e1.
65. Scherp P, Ku G, Coleman L, Kheterpal I. Gel-based and gel-free proteomic technologies. *Methods in Molecular Biology*. 2011;702:163–90.
66. Unlu M, Morgan ME, Minden JS. Difference gel electrophoresis: A single gel method for detecting changes in protein extracts. *Electrophoresis*. 1997;18(11):2071–7.
67. Washburn MP, Wolters D, Yates JR, 3rd. Large-scale analysis of the yeast proteome by multidimensional protein identification technology. *Nature Biotechnology*. 2001;19(3):242–7.
68. MacBeath G. Protein microarrays and proteomics. *Nature Genetics*. 2002;32(Suppl):526–32.
69. Sheth KV, Roca GL, al-Sedairy ST, Parhar RS, Hamilton CJ, al-Abdul Jabbar F. Prediction of successful embryo implantation by measuring interleukin-1–alpha and immunosuppressive factor(s) in preimplantation embryo culture fluid. *Fertility and Sterility*. 1991;55(5):952–7.
70. Baranao RI, Piazza A, Rumi LS, Polak de Fried E. Determination of IL-1 and IL-6 levels in human embryo culture-conditioned media. *American Journal of Reproductive Immunology*. 1997;37(2):191–4.
71. Fuzzi B, Rizzo R, Criscuoli L, Noci I, Melchiorri L, Scarselli B, et al. HLA-G expression in early embryos is a fundamental prerequisite for the obtainment of pregnancy. *European Journal of Immunology*. 2002;32(2):311–15.
72. Gonzalez RR, Simon C, Caballero-Campo P, Norman R, Chardonnens D, Devoto L, et al. Leptin and reproduction. *Human Reproduction Update*. 2000;6(3):290–300.
73. Hardy K, Hooper MA, Handyside AH, Rutherford AJ, Winston RM, Leese HJ. Non-invasive measurement of glucose and pyruvate uptake by individual human oocytes and preimplantation embryos. *Human Reproduction*. 1989;4(2):188–91.
74. Gott AL, Hardy K, Winston RM, Leese HJ. Non-invasive measurement of pyruvate and glucose uptake and lactate production by single human preimplantation embryos. *Human Reproduction*. 1990;5(1):104–8.
75. Conaghan J, Hardy K, Handyside AH, Winston RM, Leese HJ. Selection criteria for human embryo transfer: A comparison of pyruvate uptake and morphology. *Journal of Assisted Reproduction and Genetics*. 1993;10(1):21–30.
76. Turner K, Martin KL, Woodward BJ, Lenton EA, Leese HJ. Comparison of pyruvate uptake by embryos derived from conception and non-conception natural cycles. *Human Reproduction*. 1994;9(12):2362–6.
77. Gardner DK, Lane M, Stevens J, Schoolcraft WB. Noninvasive assessment of human embryo nutrient consumption as a measure of developmental potential. *Fertility and Sterility*. 2001;76(6):1175–80.
78. Devreker F, Hardy K, Van den Bergh M, Vannin AS, Emiliani S, Englert Y. Amino acids promote human blastocyst development in vitro. *Human Reproduction*. 2001;16(4):749–56.
79. Lane M, Gardner DK. Nonessential amino acids and glutamine decrease the time of the first three cleavage divisions and increase compaction of mouse zygotes in vitro. *Journal of Assisted Reproduction and Genetics*. 1997;14(7):398–403.

80. Houghton FD, Hawkhead JA, Humpherson PG, Hogg JE, Balen AH, Rutherford AJ, et al. Non-invasive amino acid turnover predicts human embryo developmental capacity. *Human Reproduction*. 2002;17(4):999–1005.
81. Leese HJ, Baumann CG, Brison DR, McEvoy TG, Sturmey RG. Metabolism of the viable mammalian embryo: Quietness revisited. *Molecular Human Reproduction*. 2008;14(12):667–72.
82. Brison DR, Houghton FD, Falconer D, Roberts SA, Hawkhead J, Humpherson PG, et al. Identification of viable embryos in IVF by non-invasive measurement of amino acid turnover. *Human Reproduction*. 2004;19(10):2319–24.
83. Seli E, Botros L, Sakkas D, Burns DH. Noninvasive metabolomic profiling of embryo culture media using proton nuclear magnetic resonance correlates with reproductive potential of embryos in women undergoing in vitro fertilization. *Fertility and Sterility*. 2008;90(6):2183–9.
84. Nicholson JK, O'Flynn MP, Sadler PJ, Macleod AF, Juul SM, Sonksen PH. Proton-nuclear-magnetic-resonance studies of serum, plasma and urine from fasting normal and diabetic subjects. *The Biochemical Journal*. 1984;217(2):365–75.
85. Nicholson JK, Connelly J, Lindon JC, Holmes E. Metabonomics: A platform for studying drug toxicity and gene function. *Nature Reviews Drug Discovery*. 2002;1(2):153–61.
86. Dunn WB, Ellis DI. Metabolomics: Current analytical platforms and methodologies. *Trends in Analytical Chemistry.* 2005;24(4):285–94.
87. Ellis DI, Goodacre R. Metabolic fingerprinting in disease diagnosis: Biomedical applications of infrared and Raman spectroscopy. *The Analyst*. 2006;131(8):875–85.
88. Shulaev V. Metabolomics technology and bioinformatics. *Briefings in Bioinformatics*. 2006;7(2):128–39.
89. Seli E, Sakkas D, Scott R, Kwok SC, Rosendahl SM, Burns DH. Noninvasive metabolomic profiling of embryo culture media using Raman and near-infrared spectroscopy correlates with reproductive potential of embryos in women undergoing in vitro fertilization. *Fertility and Sterility*. 2007;88(5):1350–7.
90. Scott R, Seli E, Miller K, Sakkas D, Scott K, Burns DH. Noninvasive metabolomic profiling of human embryo culture media using Raman spectroscopy predicts embryonic reproductive potential: A prospective blinded pilot study. *Fertility and Sterility*. 2008;90(1):77–83.
91. Vergouw CG, Botros LL, Roos P, Lens JW, Schats R, Hompes PG, et al. Metabolomic profiling by near-infrared spectroscopy as a tool to assess embryo viability: A novel, non-invasive method for embryo selection. *Human Reproduction*. 2008;23(7):1499–504.
92. Seli E, Vergouw CG, Morita H, Botros L, Roos P, Lambalk CB, et al. Noninvasive metabolomic profiling as an adjunct to morphology for noninvasive embryo assessment in women undergoing single embryo transfer. *Fertility and Sterility*. 2010;94(2):535–42.
93. Ahlstrom A, Wikland M, Rogberg L, Barnett JS, Tucker M, Hardarson T. Cross-validation and predictive value of near-infrared spectroscopy algorithms for day-5 blastocyst transfer. *Reproductive Biomedicine Online*. 2011; 22(5):477–84.
94. Seli E, Bruce C, Botros L, Henson M, Roos P, Judge K, et al. Receiver operating characteristic (ROC) analysis of day 5 morphology grading and metabolomic Viability Score on predicting implantation outcome. *Journal of Assisted Reproduction and Genetics*. 2011;28(2):137–44.
95. Hardarson T, Ahlstrom A, Rogberg L, Botros L, Hillensjo T, Westlander G, et al. Non-invasive metabolomic profiling of day 2 and 5 embryo culture medium: A prospective randomized trial. *Human Reproduction*. 2012;27(1):89–96.
96. Sfontouris IA, Lainas GT, Sakkas D, Iliadis GS, Anagnostara K, Zorzovilis IZ, et al. Assessment of embryo selection using non-invasive metabolomic analysis as an adjunct to morphology indicates improvement in implantation and fetal cardiac activity rates. *Human Reproduction.* 2011;26(Suppl 1):86.

14

Invasive Techniques: Polar Body Biopsy

Markus Montag, Jana Liebenthron, and Maria Köster

Introduction

Polar body (PB) biopsy dates back to the 1990s when the technique was introduced by Verlinsky et al. [1] to diagnose chromosomal abnormalities. In contrast to preimplantation genetic diagnosis (PGD) of the embryo that was proposed earlier by Alan Handyside et al. [2], PB biopsy enabled a genetic diagnosis before the formation of the proper embryo, thereby establishing the term "preconception genetic diagnosis." PBs are by-products of the meiotic division. The first PB (PB1) is not required for successful fertilization or for normal embryonic development. The second PB (PB2), extruded from the oocyte after initiation of the fertilization cascade by the spermatozoa, is similarly not needed for subsequent embryo development. Furthermore, it is important to note that PB diagnosis gives direct information about the first and second PBs and therefore allows only an indirect diagnosis of the maternal genetic or chromosomal constitution of the corresponding oocyte. In contrast, analysis of blastomeres from the embryo gives a direct diagnosis for the embryo and allows for detection of both maternally and paternally derived genetic or chromosomal contributions.

Polar body diagnosis gives direct information about the first and second polar body and therefore allows only an indirect diagnosis of the maternal genetic or chromosomal constitution of the corresponding oocyte.

These clear diagnostic limitations of the PB were a major reason for the predominance of embryo biopsy at the six- to eight-cell stage on Day 3. PB biopsy was at that early times applied only in countries where embryo biopsy was not in line with legal requirements (e.g., Germany) [3] and by those groups who favored this technology for various other reasons [4]. The major diagnostic aims at that time were PGD, a technique implemented for diagnosing genetic diseases in known carriers before embryo transfer, and screening for chromosomal aneuploidies, defined by the term "preimplantation genetic screening" (PGS). PGS became a major indication for preimplantation diagnosis and was introduced in numerous laboratories worldwide (European Society of Human Reproduction and Endocrinology [ESHRE] PGD consortium data) with the hope to contribute to increased success rates in assisted reproduction.

However, since 2007 numerous randomized controlled trials reported that PGS by blastomere biopsy does not result in increased success rates [5–15], and several organizations published statements asserting that they no longer recommended using biopsy at the blastomere stage at least for PGS [16,17]. These reflections opened up new discussions concerning the stage of biopsy [18]. The two alternatives that were discussed in regard to blastomere biopsy were PB and trophectoderm (TE) biopsy [19]. Meanwhile, it was widely accepted that for PGS, both methods should be performed in combination with array-comparative genomic hybridization (CGH) for all chromosomes. Obviously, PB biopsy has known restrictions as only the female part can be investigated, but in view of aneuploidy screening to detect numerical chromosomal disorders that predominantly arise during meiosis in the oocyte [20], PB biopsy is a viable alternative.

This chapter gives an overview of the relevant technical details of PB diagnosis, with special emphasis on aneuploidy screening.

Zona Opening

PB biopsy requires access to the perivitelline space. For opening of the zona pellucida and subsequent removal of PBs, chemical, mechanical, and laser-assisted opening technologies have been proposed.

Chemical Opening

Acidic Tyrode's solution was initially used for opening of the zona pellucida by chemical means [21]. Although acidic Tyrode's solution can be applied at the embryo stage, there was an inhibitory effect on embryonic development when oocytes were exposed to acid Tyrode's solution [22]. Because both the oocyte and PB are sensitive to the effects of acid, zona drilling by acid Tyrode's solution is unsuitable for PB biopsy.

Mechanical Opening

The group in Chicago has established a very efficient mechanical technique [23] that is based on three-dimensional zona dissection and subsequent biopsy. The oocyte is first affixed to the holding capillary, and then a slit is made with a sharp needle close to the area where the PBs are located. After turning the oocytes by 90°, a second slit is made, creating a cross-like incision in the zona that allows access to the PBs (Figure 14.1). This method is very easy in experienced hands, but it requires multiple steps, including dissection, release, and rotation of the oocyte.

Laser-Assisted Opening

The easiest way of opening the zona pellucida is by a laser beam. The use of 1.48 µm diode laser drilling for PB biopsy was proposed in 1997 [24]. Animal experimentation showed the potential of this method for PB biopsy and for assisted hatching [25] and allowed investigation of its proper mode of application [2]. Such studies revealed that it is crucial to understand the effect of laser drilling and how the size and position of laser-drilled openings can influence further embryonic development, in particular, the type of hatching at the blastocyst stage [26]. Applying laser technology in an inappropriate way could be potentially deleterious and have an impact on overall success rate.

The easiest way of opening the zona pellucida is by a laser beam.

Laser-assisted biopsy then entered the field of PB [25,27] and embryo biopsy [28] and has helped in reducing the rate of biopsy damage and the time required for biopsy [29]. Due to its ease, laser-assisted biopsy is now also widely used for biopsy of blastomeres [28,30] and blastocyst cells [31], and its advantage compared with acid Tyrode's solution has been reported previously [29].

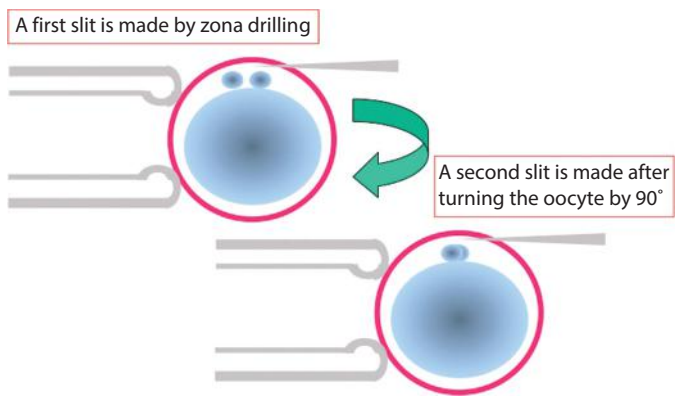

FIGURE 14.1 Schematic presentation of zona opening for subsequent mechanical biopsy.

Laser-Assisted Biopsy Procedure

For laser-assisted PB biopsy, the size of the drilled opening is usually in the range of 15–20 µm, but it can be easily adjusted to the diameter of the aspiration capillary (Figure 14.2). Because the capillary is introduced through the laser-drilled opening, there is no need for a sharp aspiration needle. This procedure allows the use of flame-polished, blunt-ended aspiration needles and greatly reduces the risk of damaging the PB, the blastomere, or the remaining oocyte or embryo, a major reason for why the biopsy procedure becomes safer, more accurate, and more reliable. It has even helped to significantly reduce the number of cells that cannot be reliably diagnosed as a result of technical problems during the biopsy procedure [3]. Another benefit of laser-assisted biopsy is that laser drilling and subsequent biopsy can be performed without changing the culture dish or the capillaries, in contrast to zona drilling that uses acid Tyrode's solution. This may help to prevent contamination of samples to be diagnosed by sensitive techniques such as polymerase chain reaction (PCR).

The simultaneous removal of the first and second PB is best accomplished if the oocyte is affixed to the holding capillary, with PB1 at the 12 o'clock position and PB2 to the right of PB1 but in the same focal plane. The reason for this positioning is the presence of a connective strand between PB2 and the oolemma of the oocyte. Further details regarding the timing of PB biopsy and possible consequences linked to the existence of spindle remnants within the connective strand are discussed below.

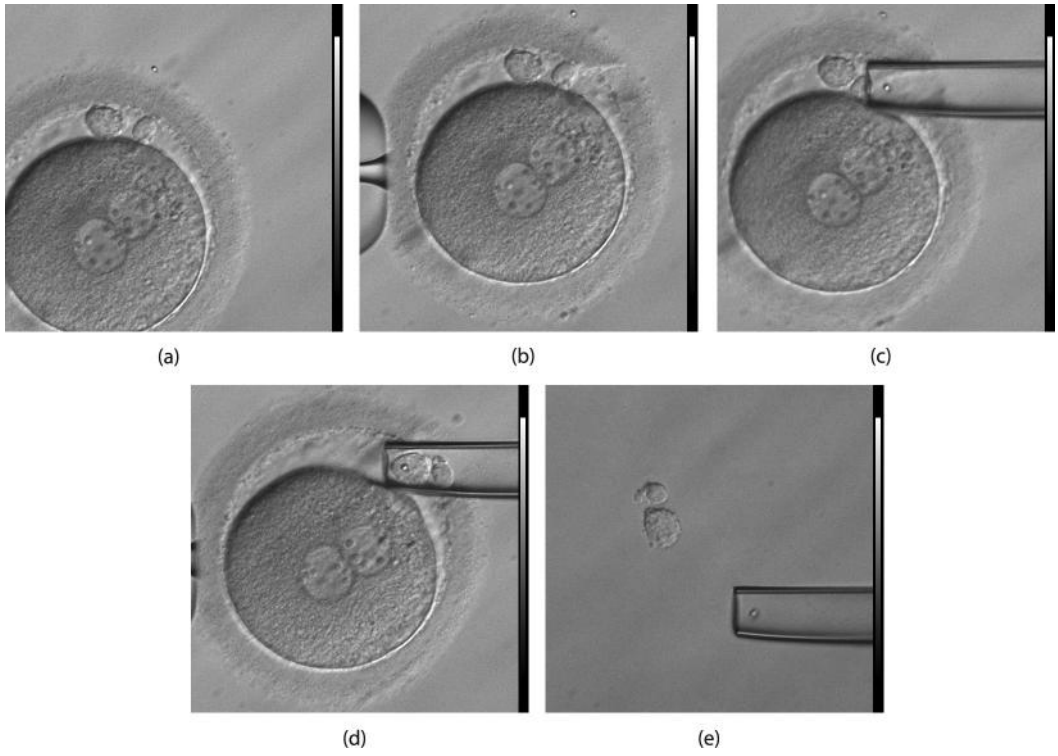

FIGURE 14.2 Laser-assisted polar body (PB) biopsy. For biopsy, the first and second PBs were aligned with a holding capillary so that the second PB faced the biopsy capillary (a). Using a noncontact 1.48 µm diode laser, an opening was introduced into the zona pellucida using two or three laser shots (b) through which the biopsy capillary could be easily introduced (c). The second PB is usually connected to the oolemma via a cytoplasmic strand. To remove the second PB without damaging the oocyte, it is not recommended to suck the second PB into the capillary; instead, the capillary is pushed slowly over the second PB and toward the first PB (d). Once the first PB enters the capillary, the strand between the second PB and the oolemma will break due to shear stress and both PBs can be easily removed (d), leaving the oocyte without any damage. PBs should be placed in one droplet for further processing for FISH analysis (e) or in two different droplets if a PCR-based analysis will be performed.

An opening is drilled at 2 o'clock or 3 o'clock, and the biopsy capillary is moved into the perivitelline space toward and then over the PBs. It is crucial to move the capillary further toward the other side of the perivitelline space to help in breaking the connective membrane strand linking PB2. This procedure is supported by using PB1 as a counterpart that, while moving into the capillary, will shear off the connective strand of PB2. At the proper time, both PBs can be easily removed simultaneously.

Timing of PB Biopsy

Polarization microscopy has shown that some oocytes presenting a PB1 may be still in telophase I due to the presence of a connective spindle strand between the PB1 and the oocyte (Figure 14.3) [32]. Spindle strands are remnants of the meiotic division, and they occur during extrusion of PB1 and PB2. Spindle fibers, also named the spindle bridge, are present only for a limited period that is usually 1–2 hr after extrusion of the first or second PB. During this time, chromosomal material from the oocyte is still attached to these spindle fibers. If PB biopsy is performed within a too short of a time after the formation of PB1 and PB2, there is a substantial risk to pull out chromosomal material during biopsy, thereby enucleating the oocyte. However, as mentioned, after dissolution of the spindle fibers the second PB still remains connected to the surface membrane of the oocyte and developing embryo by a connective membrane strand.

There is also an ongoing discussion as to whether biopsy of PB1 and PB2 should be done separately (sequential approach) or at the same time (simultaneous approach). Both approaches do work and have been tested in clinical practice. Simultaneous biopsy of the first and second PB requires only one manipulation, thereby reducing stress to the oocyte. A good time window is 8–14 hr after fertilization. A biopsy performed too early bears the risk of spindle remnants in the second PB, whereas a biopsy performed too late might affect the quality of PB1 caused by its disintegration or degeneration. Interestingly, the timing of biopsy of PB2 seems to influence amplification results in array-CGH. It was reported that biopsy of PB2 too early (4–6 hr post-intracytoplasmic sperm injection [ICSI]) may slightly lower the amplification efficiency. This effect disappeared after adjustment to later biopsy times (>8 hr post-ICSI) [33].

Timing of polar bodies is crucial for both sequential and simultaneous biopsies.

The timings proposed for simultaneous biopsy do equally apply to sequential biopsy. Sequential biopsy overcomes the potential problems of distinguishing PB1 and PB2 and of accurately separating PB1 and PB2 in case of fragmentation.

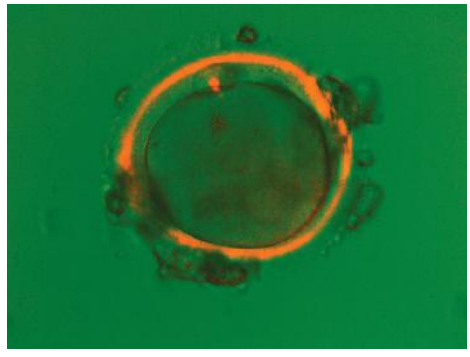

FIGURE 14.3 Presence of a meiotic spindle bridge between first polar body (PB1) and the oocytes. The presence of a connective spindle bridge can be assessed by polarization microscopy. Spindle fibers are displayed in red and characterize the corresponding oocyte as being in the transition phase from metaphase I to metaphase II. As long as spindle fibers are visible, chromosomes in the oocyte are attached, and the corresponding oocyte is in anaphase/telophase I. Removal of the PB1 shown would result in the withdrawal of chromatin material from the oocyte and could potentially lead to enucleation.

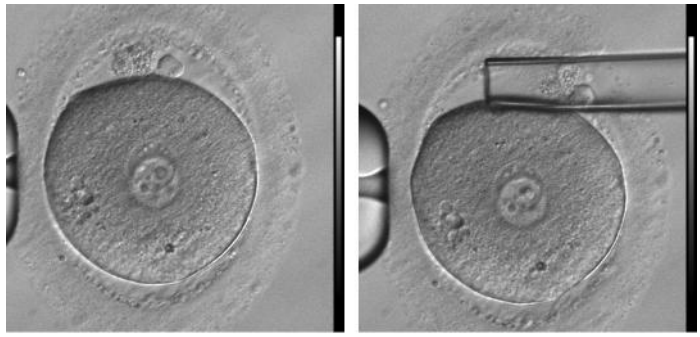

FIGURE 14.4 Degenerated PB1. A degenerated PB1 can be seen beside an intact PB2 (a). After opening the zona pellucida both PBs can be removed without further damage or loss (b).

Independent of the time of biopsy, degeneration of PBs (Figure 14.4) seems to be of minor importance for array-CGH, but it can be a problem for fluorescence in situ hybridization (FISH)-based analysis because it may contribute to diagnostic failures [34].

Potential Pitfalls of PB Biopsy

In all manipulation steps and zona opening techniques, it is important to drill only one opening. Especially if PB1 and PB2 are biopsied in a sequential approach at different times, it is tempting to introduce another opening to ease the procedure. However, the presence of two openings may cause problems at the time of hatching because the embryo could hatch through both openings simultaneously and therefore may get trapped within the zona [35].

Another important point is to generate a sufficiently large opening that allows consecutive hatching at the blastocyst stage. It has been shown experimentally in mouse embryos that smaller openings (<15 μm) cause trapping of the blastocyst at hatching, followed by degeneration [35].

Laser-drilled openings will stay permanently in the zona; therefore, gentle handling during subsequent transfer of oocytes to other media droplets and even during the embryo transfer is recommended.

In case of the presence of fragmented PBs, all fragments have to be removed. Usually fragments stick together; therefore, there is only a minor risk of mixing fragments from PB1 and PB2 (Figures 14.5 and 14.6). However, once fragments are transferred onto a slide for subsequent FISH analysis, there is a tendency for spreading and hence a potential risk to loose chromosomal material.

A position paper with relevant best-practice guidelines for PB biopsy for PGD and PGS has been published by ESHRE [36].

PB1 or PB2, or Both?

The reliability of PB biopsy is strongly dependent on the accuracy of the diagnosis of PB1 and PB2. This accuracy is indisputable for cases with structural chromosomal rearrangements and for the diagnosis of genetic disorders. For PGS, a recent study showed that PB1 is more prone to meiotic errors in younger women than PB2, but the opposite was found for older women [37]. Although one could conclude that for PGS PB1 is more important in younger women and PB2 in older women, there would be a relative risk for aneuploidy. Clinical studies on the concordance of PB1 and PB2 analyses and the corresponding oocyte gave direct proof for the need of analyzing both PB1 and PB2 [33,38].

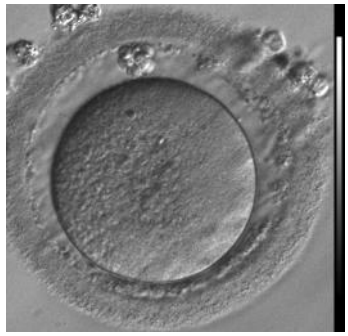

FIGURE 14.5 Attached fragments of PB1. During the course of fragmentation, the fragments stay together and remain loosely connected as long as the PB is located within the perivitelline space.

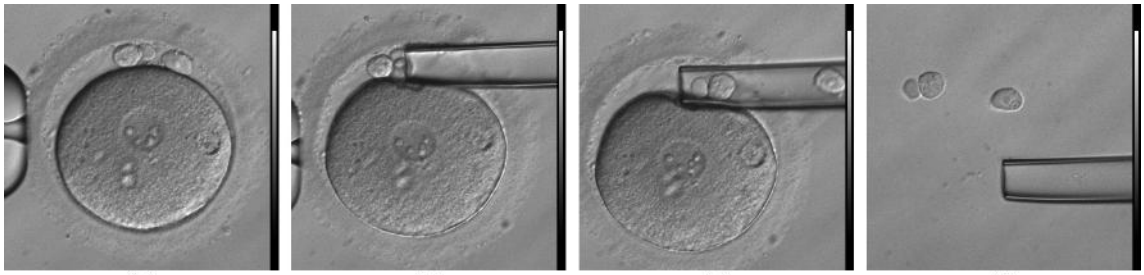

FIGURE 14.6 Biopsy of a fragmented PB1. (a) A fragmented PB1 is located beside an intact and smaller PB2. (b) The PBs remain together while the capillary is shifted over the PBs. (c) During final aspiration, the fragments stick together and (d) can be placed in a separate medium droplet without loosing the connectivity of the two fragments.

Transferring PBs for Subsequent Analysis (FISH and Array-CGH)

The way in which PBs are transferred for subsequent analysis by FISH or by array-CGH differs substantially; therefore, adequate procedures are required.

Transfer for FISH

Moving PBs into capillaries for transfer does require strict visual control. The best way to transfer PBs for FISH onto a glass slide is by using the biopsy capillary (Figure 14.7) [39]. After aspiration, both PBs are placed, under an inverted injection microscope, into a 0.1–0.2 μL drop of water located on a clean slide. PBs must be released at the bottom of the drop and directly on the glass surface, otherwise they will float in the droplet and rupture during evaporation, resulting in a loss of material. To follow the evaporation process, the slide has to be moved immediately to a stereomicroscope with good optical contrast and a reasonably high magnification (80–100×). PBs are small in diameter, and it is nearly impossible to find them on an unmarked slide. Therefore, the area with the PBs must be encircled after drying with a diamond or tungsten pen **on top of the slide** (Figure 14.8) [39]. When PBs from several oocytes are placed on one slide, it is recommended to connect all circles with a line drawn by the tungsten scribe. It is possible to visualize the tungsten mark in bright field as well as under fluorescence illumination. This allows identifying the position of the encircled PB and facilitates orientation at 100× oil immersion magnification by following the line from one circle to the next.

With experience, it is easy to distinguish PB1 and PB2 during evaluation of the FISH signals. Thus, both PBs can be placed in the same area. It is possible to allocate PBs from up to ten oocytes in individually encircled

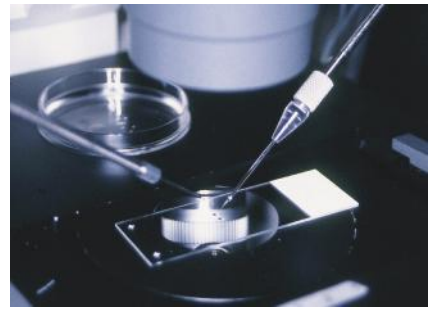

FIGURE 14.7 Transfer of isolated polar bodies (PBs) onto a slide. The transfer of isolated PBs from the dish (seen in the background) into the droplet on the slide must be performed on the microscope stage. The setup shown here allows sliding the dish used for biopsy backwards. Therefore, the aspiration capillary needs only to be lowered into the droplet for release of the PB. (Reprinted with permission from Montag M, *Textbook of Assisted Reproductive Techniques Volume One: Laboratory Perspectives*, 4th ed., Informa Healthcare, New York, 2012, pp. 336–345.)

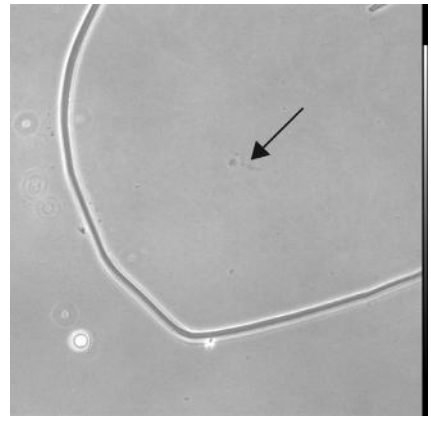

FIGURE 14.8 Identification of the polar body (PB) on the slide. This photograph is taken with a 10× phase contrast objective, and the diamond circle surrounding the PB can be partially seen. The PB appears gray (arrow). (Reprinted with permission from Montag M, *Textbook of Assisted Reproductive Techniques Volume One: Laboratory Perspectives*, 4th ed., Informa Healthcare, New York, 2012, pp. 336–345.)

spots within an area of 10 mm. By using a round coverslip with a diameter of 12 mm, the amount of hybridization probe needed can be minimized [39].

Transfer for Array-CGH

For any kind of molecular-based diagnosis, such as array-CGH, both PBs must be transferred into separate reaction tubes and in a defined volume that fits to the required amplification protocol [33]. Because array-CGH will be the most common application, this method is primarily described here. It is important to prefill reaction tubes with 2.1–2.3 µL of phosphate-buffered saline (PBS) and to transfer PBs with 0.2–0.4 µL of medium into this solution for obtaining a final maximum volume of 2.5 µL. Pipetting PBs in whatever volume directly into a dry test tube may result in loss of PBs and amplification failure. The transfer is best accomplished by using a plastic capillary with a fine tip, similarly to the capillaries used for oocyte denudation. Glass capillaries are not recommended because these can break, entrap the PB, and make the DNA inaccessible to amplification. Releasing the transferred medium at the sidewall of the PCR tube may result in PB sticking to the wall. Subsequent centrifugation will cause rupture of the PB and spread the DNA material along the wall, resulting in partial amplification and inaccurate diagnosis.

Transfer of polar bodies to slides or into tubes is one of the most crucial steps of the whole procedure.

For FISH, the use of a high-contrast stereomicroscope is recommended. PBs can be easily identified in the medium droplets and aspirated for transfer. It is advisable to rinse the capillary after transfer under visual control to verify that the PB has been placed in the reaction tube, because this process cannot be directly visualized due to the plastic material of the tubes. Needless to say, transferring PBs for subsequent single-cell DNA amplification has to be done in a manner (and using proper equipment) that avoids potential contamination.

What Is the Predictive Value of PB Diagnosis?

The discussion on the value of PGS has caused a growing interest in PB biopsy and diagnosis [18]. ESHRE has founded a task force on PGS and started a pilot study to evaluate the potential of PB biopsy and array-CGH for PGS [38]. The ESHRE pilot study has resulted in a series of clinical and fundamental publications [40], and the positive perception of this technology has prompted ESHRE to initiate a multicentric, randomized controlled trial using this technology. However, some studies based on PB biopsy and array-CGH reported a high or acceptable correlation for predicting of aneuploidy [38,41], and others questioned the accuracy of PB diagnosis due to the high incidence of postzygotic errors [42]. These studies were done on array-CGH, but recent data showed that quantitative PCR has a much higher accuracy compared with array-CGH [43]. Currently, we cannot exclude that the approach of analyzing DNA from a single PB may be more prone to methodological impact compared with TE biopsies with multiple cells.

Another topic that is controversially discussed is reciprocal chromosome aneuploidies in PBs. A recent study showed that this situation mostly gives rise to normal euploid embryos [44], and the birth of a healthy child has been reported from an oocyte with reciprocal aneuploid polar bodies [45]. So far, the general understanding is that reciprocal chromosome aneuploidies in PBs may give rise to mosaic embryos that should not be transferred [46].

Conclusions

PB biopsy has been proven as sufficiently effective for the diagnosis of structural and numerical chromosome aberrations in human oocytes by using FISH [27,47] and array-CGH [14]. Nevertheless, the use of PB biopsy and array-CGH for PGS is still a matter of debate due to cost effectiveness, the high incidence of postmeiotic aneuploidies that are undetectable by the PB approach [42], and the diagnostic procedure [43]. There is growing advocacy for TE biopsy and array-CGH as the new gold standard.

REFERENCES

1. Verlinsky Y, Ginsberg N, Lifchez A, et al. Analysis of the first polar body: Preconception genetic diagnosis. *Hum Reprod* 1990; 5: 826–9.
2. Handyside AH, Kontogianni EH, Hardy K, et al. Pregnancies from biopsied human preimplantation embryos sexed by Y-specific DNA amplification. *Nature* 1990; 244: 768–70.
3. Montag M, van der Ven K, van der Ven H. Erste klinische Erfahrungen mit der Polkörperbiopsie in Deutschland [First clinical experience with polar body biopsy in Germany]. *J Fertil Reprod* 2002; 4: 7–12.
4. Verlinsky Y, Cieslak J, Freidine M, et al. Pregnancies following pre-conception diagnosis of common aneuploidies by fluorescent in-situ hybridization. *Hum Reprod* 1995; 10: 1923–7.
5. Staessen C, Platteau P, Van Assche E, et al. Comparison of blastocyst transfer with or without preimplantation genetic diagnosis for aneuploidy screening in couples with advanced maternal age: A prospective randomized controlled trial. *Hum Reprod* 2004; 19: 2849–58.

6. Stevens J, Wale P, Surrey ES, et al. Is aneuploidy screening for patients aged 35 or over beneficial? A prospective randomized trial. *Fertil Steril* 2004; 82 (Suppl 2): 249.
7. Mastenbroek S, Twisk M, Van Echten-Arends J, et al. In vitro fertilization with preimplantation genetic screening. *N Engl J Med* 2007; 357: 9–17.
8. Blockeel C, Schutyser V, De Vos A, et al. Prospectively randomized controlled trial of PGS in IVF/ICSI patients with poor implantation. *Reprod Biomed Online* 2008; 17: 848–54.
9. Hardarson T, Hanson C, Lundin K, et al. Preimplantation genetic screening in women of advance maternal age decrease in clinical pregnancy rate: A randomized controlled trial. *Hum Reprod* 2008; 23: 2806–12.
10. Jansen RP, Bowman MC, de Boer KA, et al. What next for preimplantation genetic screening (PGS)? Experience with blastocyst biopsy and testing for aneuploidy. *Hum Reprod* 2008; 23: 1476–8.
11. Mersereau JE, Pergament E, Zhang X, et al. Preimplantation genetic screening to improve in vitro fertilization pregnancy rates: A prospective randomized controlled trial. *Fertil Steril* 2008; 90: 1287–9.
12. Staessen C, Verpoest W, Donoso P, et al. Preimplantation genetic screening does not improve delivery rate in women under the age of 36 following single-embryo transfer. *Hum Reprod* 2008; 23: 2818–25.
13. Meyer L, Klipstein S, Hazlett W, et al. A prospective randomized controlled trial of preimplantation genetic screening in the "good prognosis" patient. *Fertil Steril* 2009; 91: 1731–8.
14. Schoolcraft WB, Katz-Jaffe MG, Stevens J, et al. Preimplantation aneuploidy testing for infertile patients of advanced maternal age: A randomized prospective trial. *Fertil Steril* 2009; 92: 157–62.
15. Debrock S, Melotte C, Spiessens C, et al. Preimplantation genetic screening for aneuploidy in embryos after in vitro fertilization (IVF) does not improve reproductive outcome in women over 35: A prospective controlled randomized trial. *Fertil Steril* 2010; 93: 364–73.
16. Anderson R, Pickering S. The current status of preimplantation genetic screening: British Fertility Society Policy and Practice Guidelines. *Hum Fertil* 2008; 11: 71–5.
17. American Society for Reproductive Medicine (ASRM). Preimplantation genetic testing: A Practice Committee opinion. *Fertil Steril* 2008; 90 (Suppl): S136–43.
18. Geraedts J, Collins J, Gianaroli L, et al. What next for preimplantation genetic screening? A polar body approach! *Hum Reprod* 2010; 25: 575–7.
19. Harper J, Coonen E, De Rycke M, et al. What next for preimplantation genetic screening (PGS)? A position statement from the ESHRE PGD Consortium Steering Committee. *Hum Reprod* 2010; 25: 821–3.
20. Nicolaidis P, Petersen MB. Origin and mechanisms of non-disjunction in human autosomal trisomies. *Hum Reprod* 1998; 13: 313–19.
21. Gordon JW, Talansky BE. Assisted fertilization by zona drilling: A mouse model for correction of oligospermia. *J Exp Zool* 1987; 239: 347–81.
22. Malter HE, Cohen J. Blastocyst formation and hatching in vitro following zona drilling of mouse and human embryos. *Gamete Res*1989; 24: 67–80.
23. Cieslak J, Ivakhenko V, Wolf G, et al. Three-dimensional partial zona dissection for preimplantation genetic diagnosis and assisted hatching. *Fertil Steril* 1999; 71: 308–13.
24. Montag M, van der Ven K, Delacrétaz G, et al. Efficient preimplantation genetic diagnosis using laser assisted microdissection of the zona pellucida for polar body biopsy followed by primed in situ labelling (PRINS). *J Assist Reprod Genet* 1997; 14: 455–6.
25. Montag M, van der Ven K, Delacrétaz G, et al. Laser assisted microdissection of zona pellucida facilitates polar body biopsy. *Fertil Steril* 1998; 69: 539–42.
26. Montag M, Koll B, Holmes P, et al. Significance of the number of embryonic cells and the state of the zona pellucida for hatching of mouse blastocysts in vitro versus in vivo. *Biol Reprod* 2000; 62: 1738–44.
27. Montag M, van der Ven K, Dorn C, et al. Outcome of laser-assisted polar body biopsy. *Reprod Biomed Online* 2004; 9: 425–9.
28. Boada M, Carrera M, De La Iglesia C, et al. Successful use of a laser for human embryo biopsy in preimplantation genetic diagnosis: Report of two cases. *J Assist Reprod Genet* 1997; 15: 301–5.
29. Joris H, De Vos A, Janssens R, et al. Comparison of the results of human embryo biopsy and outcome of PGD after zona drilling using acid Tyrode medium or a laser. *Hum Reprod* 2003; 18: 1896–902.
30. Licciardi F, Gonzalez A, Tang YX, et al. Laser ablation of the mouse zona pellucida for blastomere biopsy. *J Assist Reprod Genet* 1995; 12: 462–6.

31. Veiga A, Sandalinas M, Benkhalifa M, et al. Laser blastocyst biopsy for preimplantation diagnosis in the human. *Zygote* 1997; 5: 351–4.
32. Montag M, Schimming T, van der Ven H. Spindle imaging in human oocytes: The impact of the meiotic cell cycle. *Reprod Biomed Online* 2006; 12: 442–6.
33. Magli MC, Montag M, Köster M, et al. Implementing polar body biopsy and chromosome copy number analysis by array comparative genomic hybridisation: Technical experiences from the ESHRE PGS Task Force pilot study. *Hum Reprod* 2011; 26: 3181–4.
34. Munné S, Dailey T, Sultan KM, et al. The use of first polar bodies for preimplantation diagnosis of aneuploidy. *Hum Reprod* 1995; 10: 1015–21.
35. Montag M, van der Ven H. Laser-assisted hatching in assisted reproduction. *Croat Med J* 1999; 40: 398–403.
36. Harton GL, Magli MC, Lundin K, et al. ESHRE PGD Consortium/Embryology Special Interest Group—best practice guidelines for polar body and embryo biopsy for preimplantation genetic diagnosis/screening (PGD/PGS). *Hum Reprod* 2011; 26: 41–6.
37. Fragouli E, Alfarawati S, Goodall NN, et al. The cytogenetics of polar bodies: Insights into female meiosis and the diagnosis of aneuploidy. *Mol Hum Reprod* 2011; 17: 286–95.
38. Geraedts J, Montag M, Magli MC, et al. Polar body array CGH for prediction of the status of the corresponding oocyte. Part I: Clinical results. *Hum Reprod* 2011; 26: 3173–80.
39. Montag M. Polar body biopsy and its clinical application. In: *Textbook of Assisted Reproductive Techniques Volume One: Laboratory Perspectives,* 4th ed. (eds. Gardner D, Weissman A, Howles C, Shoham Z). New York: Informa Healthcare, 2012, pp. 336–45.
40. Handyside AH, Montag M, Magli MC, et al. Multiple meiotic errors caused by predivision of chromatids in women of advanced maternal age undergoing in vitro fertilization. *Eur J Hum Genet* 2012; 20: 742–7.
41. Christopikou D, Tsorva E, Economou K, et al. Polar body analysis by array comparative genomic hybridization accurately predicts aneuploidies of maternal meiotic origin in cleavage stage embryos of women of advanced maternal age. *Hum Reprod* 2013; 28: 1426–34.
42. Capalbo A, Bono S, Spizzichino L, et al. Sequential comprehensive chromosome analysis on polar bodies, blastomeres and trophoblast: Insight into female meiotic errors and chromosomal segregation in the preimplantation window of embryo development. *Hum Reprod* 2013; 28: 509–18.
43. Treff NR. qPCR based CCS. *Reprod Biomed Online* 2013; 26 (Suppl 1): 55.
44. Forman EJ, Treff NR, Stevens JM, et al. Embryos whose polar bodies contain isolated reciprocal chromosome aneuploidy are almost always euploid. *Hum Reprod* 2013; 28: 502–8.
45. Scott RT, Jr, Treff NR, Stevens J, et al. Delivery of a chromosomally normal child from an oocyte with reciprocal aneuploid polar bodies. *J Assist Reprod Genet* 2012; 29: 533–7.
46. Kuliev A, Verlinsky Y. Meiotic and mitotic non-disjunction: Lessons from preimplantation genetic diagnosis. *Hum Reprod Update* 2004; 10: 401–7.
47. Verlinsky Y, Tur-Kaspa I, Cieslak J, et al. Preimplantation testing for chromosomal disorders improves reproductive outcome of poor-prognosis patients. *Reprod Biomed Online* 2005; 11: 219–25.

15

Invasive Techniques: Embryo Biopsy at the Cleavage Stage

Anick De Vos

Introduction

Cleavage-stage embryo biopsy of single blastomeres allows the analysis of male and female genetic contribution to the final embryo, by means of polymerase chain reaction (PCR) or fluorescence in situ hybridization (FISH) analysis at the single-cell level. One or two blastomeres are removed from the embryo in the morning of Day 3, at about 68–72 hr after microinjection. The embryos are preferably in the third mitotic division, presenting at least five cells or, more ideally, eight cells or more. Enough time for genetic or chromosomal testing is available if blastocyst transfer is performed on Day 5.

So far, cleavage-stage biopsy is the most widely used procedure (87.9% of all cycles reported by the European Society of Human Reproduction and Endocrinology (ESHRE) Preimplantation Genetic Diagnosis [PGD] Consortium), far exceeding polar body biopsy (11.7%) and blastocyst biopsy (0.4%) [1]. For many years, the method remained unchanged. Zona opening can be done mechanically; chemically by using acidic Tyrode's solution (AT); or, more recently, by using laser energy. Blastomere removal is mainly done by aspiration; however, extrusion and flow displacement are also used, but to a much lesser extent. Clinical application of cleavage-stage embryo biopsy resulted in the first pregnancies [2] and birth of a normal girl [3]. These achievements were based on the preclinical work [4] concluding that in vitro preimplantation development of biopsied human embryos is not adversely affected by the removal of one or two cells at the eight-cell stage. Since then, the number of in vitro fertilization (IVF) cycles, including embryo biopsy in view of PGD, has increased significantly [1,5].

This chapter presents an overview of all aspects of cleavage-stage embryo biopsy and aims to contain a very specific practical guide on how to perform the procedure. The following aspects are addressed: developmental stage and embryo inclusion criteria for biopsy, precautions to avoid contamination with maternal or paternal DNA, equipment for embryo biopsy, zona opening procedures, cellular removal and maximal mass reduction, compaction/decompaction, multinucleation and anucleates, dealing with cell lysis, postbiopsy development and finally, advantages and disadvantages of cleavage-stage embryo biopsy.

Developmental Stage and Embryo Inclusion Criteria for Biopsy

In cases where the paternal contribution to the embryo needs to be diagnosed, biopsy at preimplantation developmental stages is needed. Obviously, the developmental stage allowing maximum retrieval of cells at biopsy with a minimum reduction in pregnancy potential of the embryos after the procedure would be most appropriate. Two- and four-cell human embryos do not fit into this assumption. The best moment for embryo biopsy would then be the eight-cell stage, normally in the morning of Day 3. At this stage, all the cells are still totipotent as confirmed by lineage tracing [6], and the embryos are not yet compacting extensively.

Unfortunately, not all embryos are present in the eight-cell stage in the morning of Day 3 (Figure 15.1). Both delayed and advanced embryos are encountered. Embryos may also differ in quality according to the amount of anuclear fragments present. Blastomere sizes can deviate from the stage-specific division pattern; furthermore, vacuoles, granulation, and multinucleation may be present. It is recommended to establish biopsy criteria to determine which embryos should be included for biopsy (Table 15.1). Mostly, embryos with <50% anuclear

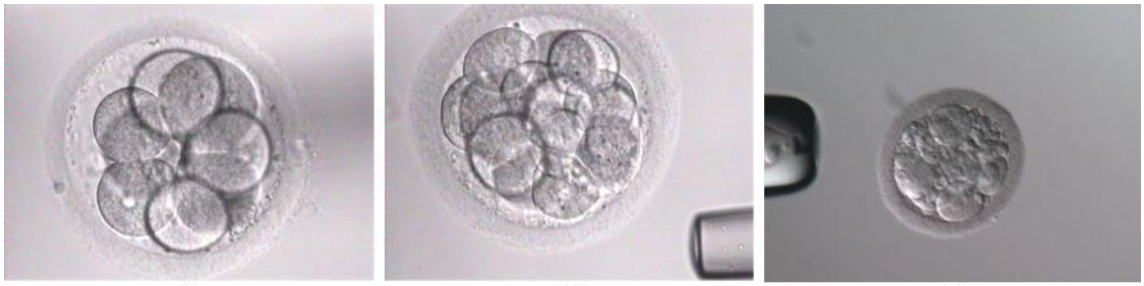

FIGURE 15.1 Cleavage-stage embryo biopsy is usually performed in the morning of Day 3. (a) Ideally, the embryos are in the eight-cell stage, having no fragmentation and showing stage-specific blastomere sizes. (b) An advanced-stage embryo on Day 3 with no fragmentation. (c) An embryo with more fragmentation (between 20% and 50%); however, it would still be included for embryo biopsy.

TABLE 15.1

Inclusion Criteria for Cleavage-Stage Embryo Biopsy

- Embryos resulting from 2-pronuclear (PN) oocytes (occasionally 1-PN embryos due to a missed second pronucleus at fertilization check, given a good morphological quality)
- ≥6 cell (occasionally 5-cell embryos, if <20% fragments and cell-stage specific)
- <50% anuclear fragments
- Preferably embryos with cell-stage-specific blastomere sizes; however, also those with cell-stage-aspecific blastomere sizes
- Preferably no granulation
- Preferably no vacuoles
- <50% multinucleated blastomeres present in the embryo

fragmentation and with at least six blastomeres are suitable for biopsy. Preferably, embryos have stage-specific cell sizes; however, stage-aspecific cell sizes would not represent an exclusion criterion for embryo biopsy. Occasionally, five-cell embryos could be included for one-cell removal if the embryos have <20% anuclear fragmentation and if the blastomere sizes are at least according to the division pattern (i.e., three larger and two small blastomeres). The number of cells to be removed (one or two) is dictated by the diagnostic protocol, wherein a secure result is crucial. Vacuoles and granulation are preferentially not present. Embryos with >50% of their blastomeres multinucleated are not included for embryo biopsy.

It is common practice to include only embryos resulting from 2-pronuclear (2-PN) normal fertilization. Occasionally, 1-pronuclear (1-PN) embryos could be included for embryo biopsy, given a good morphological quality and given that the diagnostic protocol can distinguish between a haploid embryo and a diploid one due to a missed second pronucleus at fertilization check.

On average, about 80% of all embryos resulting from 2-PN fertilization are suitable for embryo biopsy on Day 3. Obviously, biopsied embryos should be cultured singly in individual droplets, or even better in individual culture wells, thereby avoiding possible mixing of the embryos postbiopsy and diagnosis. Embryos are well rinsed postbiopsy to remove any trace of biopsy medium, which might be Ca^{2+}/Mg^{2+}-free medium, or acid in case of chemical zona opening. For this purpose, wash droplets are available in the culture dish.

Precautions to Avoid Contamination with Maternal or Paternal DNA

Intracytoplasmic sperm injection (ICSI) is recommended for all PCR cases to reduce the chance of paternal contamination from sperm attached to the zona pellucida [7]. In contrast, both ICSI and conventional IVF are acceptable for FISH cases [7].

TABLE 15.2

Precautions When Performing Cleavage-Stage Embryo Biopsy

- ICSI for all PCR cases; ICSI and IVF acceptable for FISH cases
- Careful oocyte denudation
- Careful embryo rinse after embryo biopsy (remove Ca^{2+}/Mg^{2+} traces present in the culture medium)
- Always replace aspiration pipette in cases of cell lysis
- Lysed cells are not used for PCR analysis (cf. maternal DNA contamination); for FISH analysis, the nucleus can occasionally be recovered
- Single embryo culture in individual droplets or individual culture dish wells
- Careful embryo rinse post–embryo biopsy (remove biopsy medium traces or acidic Tyrode in cases of chemical zona opening)

Cumulus cells may represent a source of maternal DNA contamination and may thus lead to misdiagnosis [8]. Therefore, extra care is taken at the moment of oocyte denudation to ensure that all these cells are removed from the zona pellucida.

Table 15.2 summarizes all precautions to be considered when performing cleavage-stage embryo biopsy.

Equipment for Cleavage-Stage Embryo Biopsy

Embryo biopsy is performed on an inverted microscope equipped with a warmed stage, as used for ICSI and embryo evaluations (Leica, Nikon, Olympus, and Zeiss represent well-known brands). This microscope should also be equipped with micromanipulators connected to oil-filled (or air-filled) microinjectors: one microinjector is for holding the embryo and the other microinjector is for aspiration of the blastomeres.

In case of mechanical or chemical zona opening, a double holder is needed. For mechanical zona opening, the second holder contains the microneedle used for partial zona dissection (PZD). No additional microinjector is needed in this case. For chemical zona opening, the second holder contains the micropipette with AT solution. Connection to a third microinjector is needed to aspirate and expel the acidic solution.

Microtools used for embryo biopsy (e.g., holding pipette, aspiration pipette, PZD needle, assisted hatching pipette; Table 15.3) are commercially available. Cook, Eppendorf, and Humagen microtools are well-established brands. The holding pipette (inner diameter, 17 μm) is used to hold the embryo during the biopsy procedure. A slightly larger inner diameter can be considered to provide greater stability and holding power for embryos during biopsy. Blastomere biopsy micropipettes or aspiration pipettes have an inner diameter of 28–32 μm and are used to remove the blastomeres by aspiration. PZD micropipettes or needles are pulled with a long, thin taper to a sharp point. These micropipettes can be used for mechanical zona opening by physically piercing and rubbing the zona pellucida. Assisted hatching pipettes have a blunt end with a typical inner diameter of 8–10 μm. They are used to create a hole in the zona pellucida using AT solution. For convenient manipulation in plastic Petri dishes, all pipettes display a 30° angle.

Instead of mechanical or chemical zona opening, a laser can be used to open the zona pellucida. Of course, a laser system represents quite expensive equipment. However, laser technology is considered less detrimental, extremely accurate, and simple and quick to use. Three main types of lasers are currently in use (Table 15.3): Octax Laser Shot (MTG GmbH, Germany), similar to the older version named Fertilase; Zilos-tk (Hamilton Thorne, United States); and Saturn 5 (Research Instruments, United Kingdom). All represent 1.48 μm infrared diode lasers, with laser power 100–150, 300, and 400 mW, respectively, and pulse lengths in the range of milliseconds or even microseconds.

Embryo biopsy is performed in Petri dishes, containing 25–50 μL droplets of HEPES-buffered human tubal fluid (HTF) medium supplemented with 0.5% human serum albumin or 10–20 μL droplets of Ca^{2+}/Mg^{2+}-free medium (G-PGD, Vitrolife) covered with mineral oil. When using Ca^{2+}/Mg^{2+}-free medium, embryos to be biopsied are rinsed twice through this medium (two separate droplets) before biopsy to remove calcium and magnesium

TABLE 15.3

Microtools for Embryo Biopsy and Laser Systems for Zona Opening

Holding pipette	Inner diameter 17 μm to hold the embryo
Aspiration pipette	Inner diameter 28–32 μm to aspirate blastomeres
PZD needle	For mechanical zona opening
Assisted hatching pipette	Inner diameter 8–10 μm for chemical zona opening
Laser systems	For laser zona opening Octax Laser Shot, MTG GmbH, Germany Zilos-tk, Hamilton Thorne, United States Saturn 5, Research Instruments, United Kingdom

traces present in the culture medium. Some centers manipulate with three to four biopsy droplets per dish, whereas other centers prefer to have only one single biopsy droplet and thus one embryo per Petri dish. For chemical zona opening, one additional droplet of AT solution (5 μL) is placed, allowing to prime the drilling pipette. AT solution is commercially available.

Zona Opening Procedures

Cleavage-stage embryo biopsy of human preimplantation embryos always involves two steps: opening of the zona pellucida and subsequent removal of cellular material by aspiration. Zona opening can be done in three ways: mechanical, chemical, or using laser energy.

Human zona pellucida opening procedures date from the late 1980s and early 1990s, when they were applied to help the hatching process of the embryo or to aid the fertilization process of the oocyte. At that time, zona penetration or opening was performed using only mechanical or chemical means. Mechanical zona opening for cleavage-stage embryo biopsy is applied clinically; however, in all data collections reported by the ESHRE PGD Consortium, the amount of cycles using mechanical zona opening ranged from only 1% to 10% of all cycles with PGD (Table 15.4). For many years, AT drilling was used in the majority of clinical biopsy cycles. In 2002, still two-thirds of the PGD cycles used AT to open the zona pellucida [9]. Since then, laser zona opening became more and more popular, reaching up to 60% of the clinical PGD cycles reported by the ESHRE PGD Consortium [1] (data collection XI, data up to 2008) at the expense of AT drilling (only 30% of all PGD cycles then).

Mechanical Zona Opening

To open the zona pellucida mechanically, PZD has been described and illustrated [10]. The zona pellucida is pierced with a sharp and closed microneedle through both sides. The size of the slit is determined by the distance between the first and second point at which the zona is pierced. With the microneedle piercing through the zona at both sides, the trapped area is then rubbed against the holding pipette until this area has been completely abraded. Usually, standardized slits of ±30–40 μm in length (2 μm in width) are created as such. The procedure in combination with embryo biopsy was described by Grifo et al. [11] for mouse embryos at the four- to eight-cell stages. When a second slit perpendicular to the first slit is created, a larger V-shaped opening can be obtained that is suitable for blastomere aspiration [12]. One advantage may be that the embryo remains protected until expansion because the zona flap created in this way closes after aspiration pipette removal. This is in contradiction to chemical zona opening, where an actual hole is created.

Opposite to the holding pipette, a double holder setup is used to contain the microneedle and the aspiration pipette at the same time. Mechanical opening of the human zona pellucida by piercing and rubbing is relatively simple and nontraumatic, and the risk of embryo damage at cleavage stages is also limited [13]. Nevertheless, the application of PZD for the purpose of removing cleavage-stage blastomeres for genetic diagnosis has been very limited in comparison with AT drilling and laser drilling (Table 15.4).

TABLE 15.4

Distribution of Zona Opening Procedures Used According to ESHRE PGD Consortium Data Collections (in Percentages of PGD Cycles)

Data Collection (up to Year)	II (2000)	III (2001)	IV (2001)	V (2002)	I (2003)	VII (2004)	VIII (2005)	IX (2006)	X (2007)	XI (2008)
Mechanical	1.3	1.1	5.3	5.4	6.1	8.2	9.9	9.7	9.2	8.9
AT drilling	79.4	69.4	64.5	60.7	55.0	47.1	41.7	35.8	32.5	30.5
Laser drilling	19.3	29.5	30.2	33.9	38.8	44.7	48.4	54.6	58.3	60.6

Note: AT, acidic Tyrode.

Chemical Zona Opening (AT Drilling)

Chemical zona drilling using AT (pH 2.3) represents a much cheaper option compared with the more sophisticated laser systems. Chemical zona drilling creates a larger, rounder hole in the zona pellucida, and the hole size is not always easy to control. It should be recognized that the human zona pellucida represents a stratified bilayered structure [14]. The outer layer of the zona is indeed easily dissolved, whereas the inner layer may vary greatly in its susceptibility to dissolution. When the inner layer is refractory to drilling, often a relatively large quantity of AT is needed to breach the zona pellucida. As a consequence, local acidification or even deposition of AT in the perivitelline space may occur and should be considered when evaluating the safety of this approach of zona opening. In addition to immediate cell lysis, subtle damage to cells due to acidic exposure may interfere with further development or implantation. To avoid acidic exposure of cells and thus reduce the blastomere lysis rate, drilling and blastomere aspiration using a single, larger drilling/biopsy pipette [15,16] seems not a good approach. Chemical zona drilling followed by blastomere aspiration is normally done with separate pipettes (one drilling pipette, inner diameter 8–10 μm, and one aspiration or biopsy pipette, inner diameter 28–32 μm) using a double holder setup [17]. An intact blastomere rate of up to 95% can be obtained [17].

Once the microtools are fixed and aligned on the inverted microscope, the embryo is visualized and fixed on the holding pipette. The drilling pipette is filled with a small amount of AT. Drilling is then performed by releasing acid onto the zona pellucida, preferentially between two blastomeres, or otherwise, in front of anuclear fragments. This approach should minimize the deleterious effect of the acid on the cells. Upon rupture of the zona pellucida, immediate aspiration is applied to remove excess acidic solution. Embryos can be washed by moving them to another area in the medium droplet, before continuing with blastomere aspiration. In cases of cell lysis, pipettes are always replaced in order to avoid DNA contamination to the next embryo. The present procedure is in itself extremely simple in terms of equipment; however, some technical skill is required when exposing the embryo to AT. The opening should be of appropriate size, while limiting the extent and duration of exposure of the embryo. The mean diameter of the gap thus created is about 20 μm (range, 10–36 μm). The rate of dissolution of the zona may vary between 30 s and 2 min.

In the early 2000s, representing 60%–80% of all PGD cycles reported by the ESHRE PGD Consortium [9], the use of AT drilling started to decline at the expense of laser zona drilling (Table 15.4), with laser zona drilling being certainly less detrimental [17] and extremely accurate, quick, and simple (taking only a few seconds to perform zona openings).

Laser Zona Opening

Within the infrared region, a 1.48 μm noncontact diode laser has been described for microdissection of mouse and human zona pellucida [18,19]. This system was used for cleavage-stage embryo biopsy [20], and its safety and efficacy were demonstrated on the basis of one single pregnancy. Joris et al. [17] later reported similar pregnancy rates obtained with laser drilling compared with AT drilling. Also, more intact blastomeres were obtained with laser drilling (up to 98% compared with 95% with AT). Additional studies compared the laser technology with AT solution for zona opening [21–23], concluding that laser represents a suitable alternative, being quick, easy, and safe, resulting in similar postbiopsy development. Safety evidence at the molecular level for laser

TABLE 15.5

Different Irradiation Times, According to Laser Power Specification, Have Been Used for Cleavage-Stage Embryo Biopsy

Laser System	Pulse Numbers, Pulse Length	Opening Diameter	References
Octax Laser Shot	Two, exceptionally three, pulses of 5–8 ms	20–30 µm	[17]
Zilos-tk	6–10 laser shots, 500 µs	20 µm	[29]
Zilos-tk	One or two laser pulses, 0.5 ms	Not specified	[30]
Zilos-tk	2–4 1 ms single pulses at 100% power	20–25 µm	[31]
Saturn 5	One laser shot, 1 ms	16.5 µm	[28]

zona pellucida perforation was obtained with mouse eight-cell embryos by measuring heats-shock protein transcription [24]. These reassuring data opened the way for a steady increase in the use of laser zona drilling for cleavage-stage biopsy (Table 15.4).

The laser uses high-energy light and consequently heat to dissolve or disintegrate the zona pellucida. The hole formation can be explained by a local photothermolysis of the protein matrix [25]. When the light from the laser comes in contact with the medium surrounding the embryo, heat is dissipated and transferred through the water of the medium, creating temperature gradients in increasing concentric circles from the laser beam [26,27]. It has been estimated that the temperature in the surrounding medium can increase to 60°C–80°C [25]. Thermal effects of the laser pulses around the embryo and on the blastomeres proper should be considered as a safety issue [28]. Blastomeres in the immediate vicinity of the laser beam should not be damaged. Therefore, exposure time should be limited, and a safe working distance away from blastomeres should be respected. A laser has three properties that determine its performance and hence its effect on the embryo and surrounding medium: wavelength, power, and pulse length. Typical wavelengths within the near-infrared light spectrum (2500–750 nm) are considered to be nonmutagenic in contrast to ultraviolet (UV) radiation. Laser power used for embryo biopsy ranges from 100 to 400 mW and is constant for each specific laser. Each increase or decrease in power will influence the hole diameter and also the temperature gradient through the medium and the embryo. Pulse length refers to the amount of time or duration of the laser beam. Pulse lengths range from 20 ms (Fertilase) to >1 µs (Saturn Zilos). A laser with a high power and short pulse length will produce smaller temperature gradients than a laser with low power and longer pulse lengths. A smaller temperature gradient will less likely compromise embryo development [28].

Exposure time with laser should be limited, and a safe working distance away from blastomeres should be respected.

The setup for laser zona pellucida drilling involves a laser beam that is tangentially guided to the zona pellucida of the embryo. The embryo is positioned to place a region of the zona pellucida on the aiming spot. The hole size can be chosen precisely by varying the irradiation time. Typically, a trench-like hole is produced. According to laser power specification, different irradiation times have been used (Table 15.5). Given pulse numbers and pulse lengths are indicative. According to any system used an individual approach has to be taken because pulse length is also dependent on, for example, medium, temperature, objective coating, and dishes. It is important to perforate the zona completely without harming the embryonic cells with the laser shot(s). The holes obtained with laser are more precise than the ones obtained with AT.

Cellular Removal, Maximal Reduction

Once the zona pellucida of the embryo has been opened, the blastomeres inside become freely accessible. Aspiration is most widely used to remove cells [1] (Table 15.6). The routine clinical use of flow displacement [32] has remained very limited (0.1% of all cycles reported by the ESHRE PGD Consortium). This method requires

TABLE 15.6

Distribution of Blastomere Removal Procedures Used According to ESHRE PGD Consortium Data Collection

ESHRE PGD Consortium Data Collection I-XI	No. of Cycles Reported	%
Cleavage aspiration	26,284	93.4
Cleavage extrusion	1834	6.5
Cleavage flow displacement	38	0.1

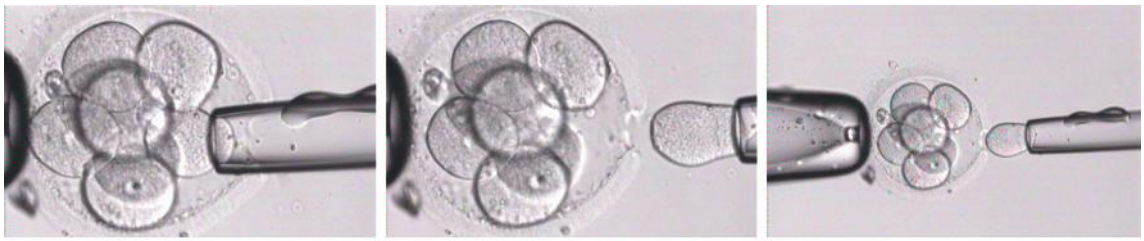

FIGURE 15.2 (a) For the removal of human blastomeres by aspiration, an aspiration pipette is introduced into the perivitelline space through the hole in the zona pellucida to reach a blastomere. (b, c) One blastomere is removed by gentle aspiration. Cells may be aspirated completely and then removed; alternatively, cells are only partially aspirated and pulled out (given full decompaction and thus no adherence to other blastomeres).

the production of two separate holes and considerable skill to displace the blastomere of choice by the injection of culture medium through the second opening. Blastomere removal by extrusion [33] is applied clinically, however, to a much lesser extent than blastomere aspiration (6.5% vs. 93.4% of all cycles reported by the ESHRE PGD Consortium). The blastomere is extruded through the opening by pushing against the zona pellucida at another site using a blunt pipette.

For the removal of human blastomeres by aspiration (Figure 15.2), an aspiration pipette (inner diameter, 28–32 μm) is introduced into the perivitelline space through the hole in the zona to reach a blastomere. Close location of the blastomeres respective to the opening allows limited penetration of the microtool. One or two blastomeres are removed by gentle aspiration. Cells may be aspirated completely and then removed; alternatively, cells are only partially aspirated and pulled out (given full decompaction and thus no adherence to other blastomeres).

Based on preclinical work [4], up to one-quarter of the embryo can be removed without impairment of its further in vitro development. However, there has been considerable discussion on whether the removal of two cells from a seven- or more-cell-stage embryo reduces its capacity to implant more than if only one cell were removed [34]. Of prime concern is that the diagnosis should be safe, that is, accurate and efficient, and misdiagnosis should be avoided at any price [8]. Recent evidence has accumulated that two-cell biopsy seems indeed more detrimental than one-cell biopsy. Indirect evidence came from cryopreservation analogy [35], assuming that cell loss from biopsy can be compared with cell loss after thaw of frozen cleaved embryos. A disproportionate reduction in implantation potential according to the cell number lost has been described previously [35]. Direct evidence was obtained from a prospective randomized clinical trial [36] and from a prospective cohort study of single blastocyst transfers [37]. Removal of two blastomeres (Figure 15.3) decreases the likelihood of blastocyst formation compared with the removal of one blastomere. However, delivery rates with live birth per started cycle were not significantly different (20.2% with one-cell biopsy and 17.2% with two-cell biopsy) [36]. In a prospective cohort of single blastocyst transfers, the clinical outcome from one-cell biopsy was significantly better (37.4% live birth per transfer) than that of two-cell biopsy (22.4%) and comparable with when no intervention on Day 3 was performed on the eight-cell embryos (35.0%) [37]. However, more recently, randomized single

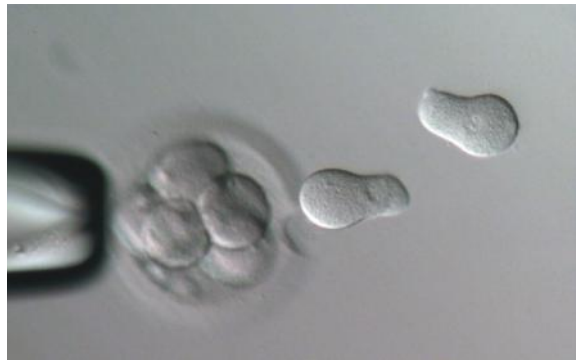

FIGURE 15.3 Removal of two blastomeres with a clear single nucleus present in each of the two blastomeres.

blastomere biopsy of one Day 3 embryo and its transfer together with a nonbiopsied sibling embryo showed that mostly the nonbiopsied embryo implanted (11/13) and led to the delivery [31]. In contrast, trophectoderm biopsy at the blastocyst stage had no meaningful impact on the developmental competence of the embryo as measured by implantation and delivery rates [31].

Removal of two blastomeres decreases the likelihood of blastocyst formation compared with the removal of one blastomere.

Regarding cleavage-stage biopsy, the biopsy of one cell is recommended, given sufficient safeguards for a correct diagnosis rather than the biopsy of two cells, at the expense of the implantation potential. Technical improvements at the diagnostic level have allowed similar diagnostic accuracy to be obtained on one blastomere compared with two blastomeres for certain indications or tests [38]. However, certain types of analysis (e.g., translocations, aneuploidy screening) will benefit from or will even continuously necessitate having two cells available for diagnosis. This is especially important because chromosomal mosaicism is commonly seen in cleavage-stage embryos. However, to alleviate chromosomal mosaicism at the cleavage stage, as well as the invasiveness of two-cell biopsy, several laboratories are shifting toward blastocyst trophectoderm biopsy (more cells available for diagnosis, safer than cleavage-stage biopsy [31]) in combination with array-CGH technology.

Compaction/Decompaction

Although full compaction does not occur before the 16- to 32-cell stage, membrane adhesion mechanisms [39] may render the biopsy procedure at the seven- or eight-cell stage rather difficult to perform because the blastomeres show a strong tendency to adhere to each other. Ca^{2+}/Mg^{2+}-free medium has been used to loosen the membrane adhesions between blastomeres [40,41], thereby allowing an easier removal of cells and resulting in less blastomere lysis and a shorter procedure time. Subsequent embryo development to the blastocyst stage was not affected by the choice of biopsy medium, even when embryos were exposed to Ca^{2+}/Mg^{2+}-free medium for 45 min [41]. Embryo biopsy may either be performed completely in decompaction medium, or otherwise, to limit the exposure time, embryos can be just preincubated for 5–10 min (normally sufficient for full decompaction) before the biopsy procedure.

Of course, the safety of embryo decompaction (using Ca^{2+}/Mg^{2+}-free medium) on further development, viability, and implantation should be critically evaluated. So far, there are no indications of an adverse effect; however, randomized controlled comparisons are lacking (Figure 15.4).

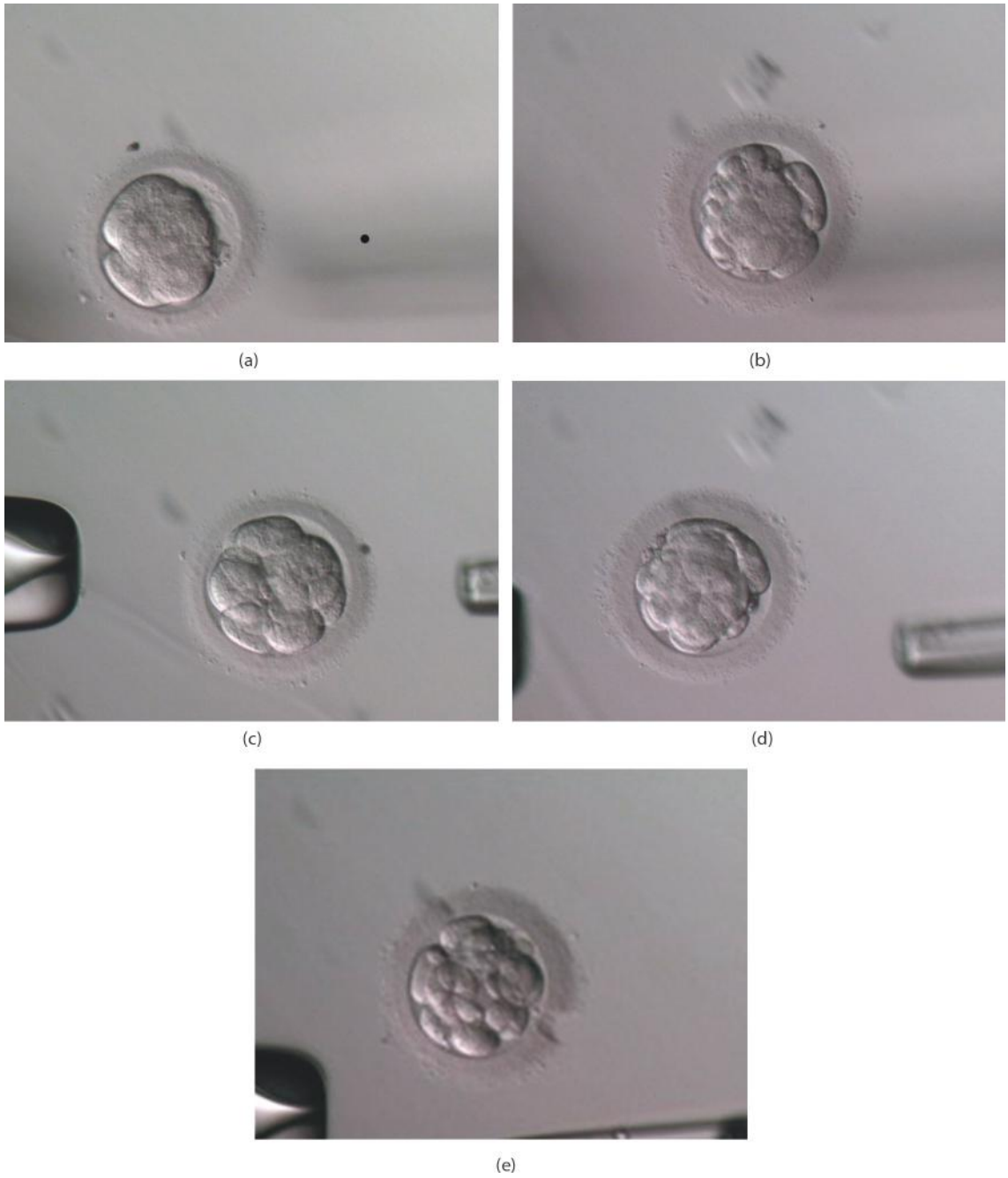

FIGURE 15.4 (a,b) Different degrees of embryo compaction can be observed in embryos to be biopsied. (c, d, e) To facilitate the biopsy procedure, Ca^{2+}/Mg^{2+}-free medium is used to loosen the membrane adhesions between blastomeres. (c) represents the same embryo as in panel (a) in a decompacted stage; (d,e) represent the same embryo as in panel (b), respectively in a less and further decompacted stage.

Multinucleation and Anucleates

To be suitable for genetic analysis either by FISH or by PCR, the removed blastomere(s) should contain one single, clearly visible nucleus (Figure 15.5 and 15.6a). Both multinucleation [42] and anucleate blastomeres (Figure 15.6b) [43,44] are frequently observed in cleavage-stage embryos. The knowledge that the chromosome constitution of multinucleated blastomeres is frequently different from that of their sibling blastomeres makes them unsuitable for PGD [45]. The presence of multinucleated blastomeres in human embryos has been correlated with chromosomal abnormalities [46]. Embryos with >50% of their blastomeres showing multinucleation are not considered for embryo biopsy, irrespective of the developmental stage at first detection.

Efficient embryo biopsy requires a careful assessment of the nuclear status by light microscopy to exclude both multinucleated and anucleate cells (Figure 15.6b) from genetic diagnosis. Sometimes, extreme granularity of the blastomeres may complicate this assessment. A mistaken interpretation of the nuclear status of a blastomere may then be anticipated if a FISH procedure follows because it would be noticed at fixation. One extra blastomere can be removed in these cases. A PCR procedure lacks this intermediate stage because cells are immediately transferred to PCR tubes and the amplification result is available only later.

Efficient embryo biopsy requires a careful assessment of the nuclear status by light microscopy to exclude both multinucleated and anucleate cells from genetic diagnosis.

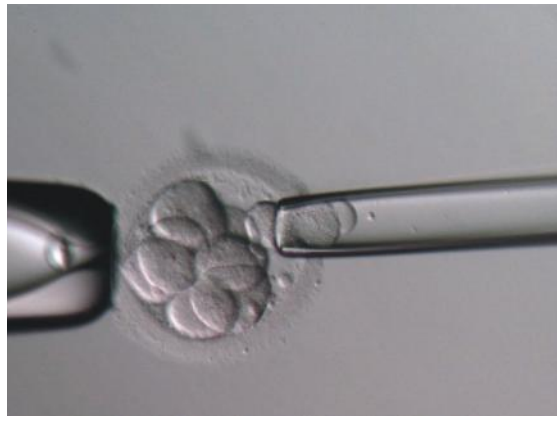

FIGURE 15.5 To be suitable for genetic analysis either by FISH or by PCR, the removed blastomere(s) should contain one single, clearly visible nucleus.

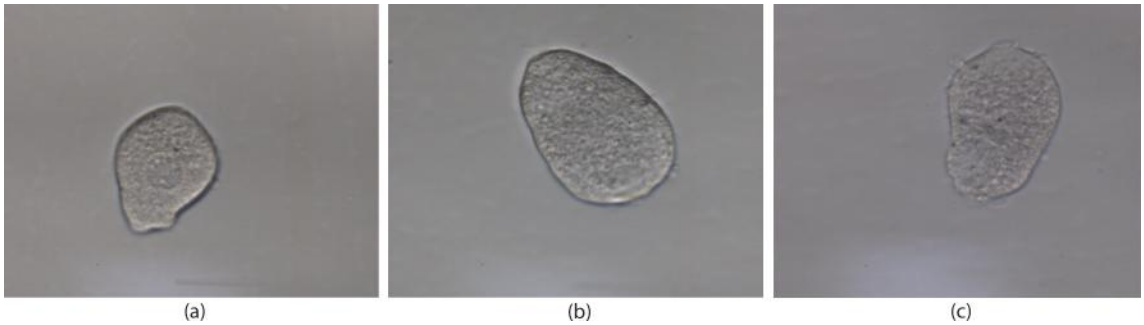

FIGURE 15.6 (a) Single-nucleated blastomere. (b) Anucleated blastomere. (c) Lysed blastomere.

Cell Lysis

Blastomere lysis rate (expressed per blastomere aspirated) represents a good quality control measure for the biopsy procedure. Cell lysis (Figure 15.6c) may occur at either step of the biopsy procedure. Cell lysis at the moment of zona opening may be related to the method used. Laser drilling has proven to result in fewer blastomere lysis (1.7%) compared with AT drilling (4.8%) [17]. Cell lysis when aspirating blastomeres may be related to excessive mechanical stress, resulting in cell blebbing, or related to strong adherence of blastomeres to each other [47] that may be avoided by means of Ca^{2+}/Mg^{2+}-free medium [41]. Lysed cells are not used for PCR analysis because contamination with maternal DNA cannot be excluded. Only occasionally, the nucleus can be recovered for FISH analysis. In cases of cell lysis, it is advised that the aspiration pipette be changed before continuing biopsy of other embryos as a safety measure to avoid cross-contamination.

Postbiopsy Development

Further embryo development should not be impaired as a result of the biopsy procedure. Embryo postbiopsy development can be evaluated on Day 4, where a doubling of cells, signs of compaction, or both represent a good progression. Otherwise, on Day 5, the quality of the inner cell mass and trophectoderm can be assessed (Figure 15.7). Extended culture to Day 5 of biopsied embryos results in typical eight-shaped artificially hatching blastocysts that might be in favor of implantation. Postbiopsy blastocyst formation has been well documented [36,48–51]. Embryo developmental characteristics may however be related to the genetic condition tested for [52,53].

In addition to in vitro development, further in vivo development postbiopsy may be reflected by the implantation rates obtained post-PGD. In this respect, large data collections are very much valued to serve as a standard reference of good laboratory and clinical practice. Live birth rates per cycle of 15.9% [54] and 15.0% [9] have been reported.

Advantages and Disadvantages

A clear advantage of cleavage-stage embryo biopsy over polar body analysis is that the paternal contribution to the embryo can be analyzed. In addition, enough time for diagnostic testing is available, especially when transferring embryos on Day 5. At present, supernumerary biopsied and diagnosed embryos can be effectively vitrified for later use, either on Day 4 [55] or in the blastocyst stage [56–58].

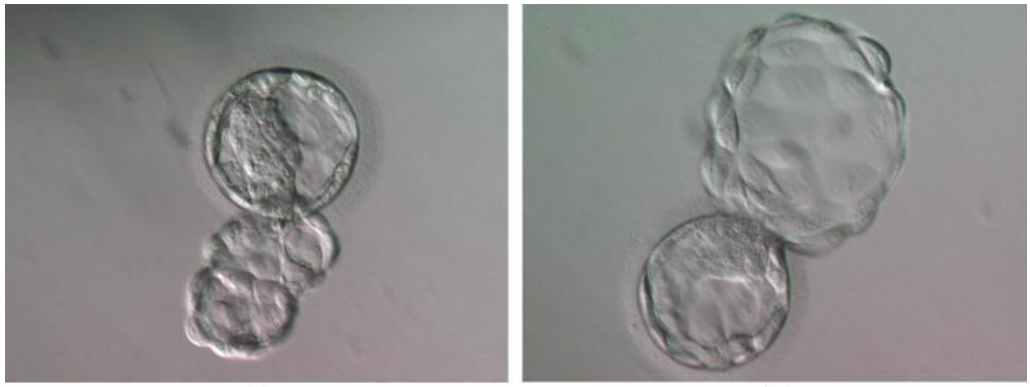

FIGURE 15.7 (a, b) Two examples of postbiopsy blastocyst formation on Day 5, allowing the evaluation of inner cell mass quality and trophectoderm quality. Biopsied embryos result in typical eight-shaped artificially hatching blastocysts.

At the cleavage stage, limited amounts of cellular material are available for genetic testing. However, PCR and FISH technologies are well established at the single-cell level. The invasive nature of the biopsy procedure on Day 3 should be recognized, and evidence exists that two-cell biopsy is more invasive than one-cell biopsy. Mosaicism at the cleavage stage remains a serious obstacle for chromosomal aneuploidy testing [59]. Removal of one cell does not interrogate mosaicism, thus more normal results are encountered, albeit with a lower predictive value. Two-cell analysis results in fewer embryos for transfer but with a higher predictive value.

REFERENCES

1. Goossens V, Traeger-Synodinos J, Coonen E, et al. ESHRE PGD Consortium data collection XI: Cycles from January to December 2008 with pregnancy follow-up to October 2009. *Hum Reprod* 2012; 27: 1887–1911.
2. Handyside AH, Kontogianni EH, Hardy K, Winston RM. Pregnancies from biopsied human preimplantation embryos sexed by Y-specific DNA amplification. *Nature* 1990; 344: 768–770.
3. Handyside AH, Lesko JG, Tarin JJ, Winston RM, Hughes MR. Birth of a normal girl after in vitro fertilization and preimplantation diagnostic testing for cystic fibrosis. *N Engl J Med* 1992; 327(13): 905–909.
4. Hardy K, Martin KL, Leese HJ, et al. Human preimplantation development in vitro is not adversely affected by biopsy at the 8-cell stage. *Hum Reprod* 1990; 5: 708–714.
5. Harper JC, Coonen E, De Rycke M, et al. ESHRE PGD Consortium data collection X: Cycles from January to December 2007 with pregnancy follow-up to October 2008. *Hum Reprod* 2010; 25: 2685–2707.
6. Mottla GL, Adelman MR, Hall JL, et al. Lineage tracing demonstrates that blastomeres of early cleavage-stage human pre-embryos contribute to both trophectoderm and inner cell mass. *Hum Reprod* 1995; 10: 384–391.
7. Harton GL, Magli C, Lundin K, et al. ESHRE PGD Consortium/Embryology Special Interest Group—Best practice guidelines for polar body and embryo biopsy for preimplantation genetic diagnosis/screening (PGD/PGS). *Hum Reprod* 2011; 26: 41–46.
8. Wilton L, Thornhill A, Traeger-Synodinos J, et al. The causes of misdiagnosis and adverse outcomes in PGD. *Hum Reprod* 2009; 24: 1221–1228.
9. Harper JC, Boelaert K, Geraedts J, et al. ESHRE PGD Consortium data collection V: Cycles from January to December 2002 with pregnancy follow-up to October 2003. *Hum Reprod* 2006; 21: 1887–1911.
10. Selva J. Assisted hatching. *Hum Reprod* 2000; 15: 65–67.
11. Grifo JA, Boyle A, Fischer E, et al. Preembryo biopsy and analysis of blastomeres by in situ hybridization. *Am J Obstet Gynecol* 1990; 163: 2013–2019.
12. Cieslak J, Ivakhnenko V, Wolf G, et al. Three-dimensional partial zona dissection for preimplantation genetic diagnosis and assisted hatching. *Fertil Steril* 1999; 71: 308–313.
13. Cohen J, Elsner C, Kort H, et al. Impairment of the hatching process following IVF in the human and improvement of implantation by assisting hatching using micromanipulation. *Hum Reprod* 1990; 5: 7–13.
14. Tucker MJ, Luecke NM, Wiker SR, Wright G. Chemical removal of the outside of the zona pellucida of day 3 human embryos has no impact on implantation rate. *J Assist Reprod Genet* 1993; 10: 187–191.
15. Chen SU, Chao KH, Wu MY, et al. The simplified two-pipette technique is more efficient than the conventional three-pipette method for blastomere biopsy in human embryos. *Fertil Steril* 1998; 69: 569–575.
16. Inzunza J, Iwarsson E, Fridström M, et al. Application of single-needle blastomere biopsy in human preimplantation genetic diagnosis. *Prenat Diagn* 1998; 18: 1381–1388.
17. Joris H, De Vos A, Janssens R, et al. Comparison of the results of human embryo biopsy and outcome of PGD after zona drilling using acid Tyrode medium or a laser. *Hum Reprod* 2003; 18: 1896–1902.
18. Germond M, Nocera D, Senn A, et al. Microdissection of mouse and human zona pellucida using a 1.48–microns diode laser beam: Efficacy and safety of the procedure. *Fertil Steril* 1995; 64: 604–611.
19. Germond M, Nocera D, Senn A, et al. Improved fertilization and implantation rates after non-touch zona pellucida microdrilling of mouse oocytes with a 1.48 microm diode laser beam. *Hum Reprod* 1996; 11: 1043–1048.
20. Boada M, Carrera M, De La Iglesia C, et al. Successful use of a laser for human embryo biopsy in preimplantation genetic diagnosis: Report of two cases. *J Assist Reprod Genet* 1998; 15: 302–307.
21. Chatzimeletiou K, Morrison EE, Panagiotidis Y, et al. Comparison of effects of zona drilling by non-contact infrared laser or acid Tyrode's on the development of human biopsied embryos as revealed by blastomere viability, cytoskeletal analysis and molecular cytogenetics. *Reprod Biomed Online* 2005; 11: 697–710.

22. Jones AE, Wright G, Kort HI, et al. Comparison of laser-assisted hatching and acidified Tyrode's hatching by evaluation of blastocyst development rates in sibling embryos: A prospective randomized trial. *Fertil Steril* 2006; 85: 487–491.
23. Geber S, Bossi R, Lisboa CB, et al. Laser confers less embryo exposure than acid tyrode for embryo biopsy in preimplantation genetic diagnosis cycles: A randomized study. *Reprod Biol Endocrinol* 2011; 9: 58.
24. Hartshorn C, Anshelevich A, Wangh LJ. Laser zona drilling does not induce hsp70i transcription in blastomeres of eight-cell mouse embryos. *Fertil Steril* 2005; 84: 1547–1550.
25. Rink K, Delacrétaz G, Salathé RP, et al. Non-contact microdrilling of mouse zona pellucida with an objective-delivered 1.48-microns diode laser. *Lasers Surg Med* 1996; 18: 52–62.
26. Douglas-Hamilton DH, Conia J. Thermal effects in laser-assisted pre-embryo zona drilling. *J Biomed Opt* 2001; 6: 205–213.
27. Tadir Y, Douglas-Hamilton DH. Laser effects in the manipulation of human eggs and embryos for in vitro fertilization. *Methods Cell Biol* 2007; 82: 409–431.
28. Taylor TH, Gilchrist JW, Hallowell SV, et al. The effects of different laser pulse lengths on the embryo biopsy procedure and embryo development to the blastocyst stage. *J Assist Reprod Genet* 2010; 27: 663–667.
29. Lanzendorf SE, Ratts VS, Moley KH, et al. A randomized, prospective study comparing laser-assisted hatching and assisted hatching using acidified medium. *Fertil Steril* 2007; 87: 1450–1457.
30. Sagoskin AW, Levy MJ, Tucker MJ, et al. Laser assisted hatching in good prognosis patients undergoing in vitro fertilization-embryo transfer: A randomized controlled trial. *Fertil Steril* 2007; 87: 283–287.
31. Scott RT, Upham KM, Forman EJ, et al. Cleavage-stage biopsy significantly impairs human embryonic implantation potential while blastocyst biopsy does not: A randomized and paired clinical trial. *Fertil Steril* 2013; 100: 624–30.
32. Pierce KE, Michalopoulos J, Kiessling AA, et al. Preimplantation development of mouse and human embryos biopsied at cleavage stages using a modified displacement technique. *Hum Reprod* 1997; 12: 351–356.
33. Levinson G, Fields RA, Harton GL, et al. Reliable gender screening for human preimplantation embryos, using multiple DNA target-sequences. *Hum Reprod* 1992; 7: 1304–1313.
34. Van de Velde H, De Vos A, Sermon K, et al. Embryo implantation after biopsy of one or two cells from cleavage-stage embryos with a view to preimplantation genetic diagnosis. *Prenat Diagn* 2000; 20: 1030–1037.
35. Cohen J, Wells D, Munné S. Removal of 2 cells from cleavage stage embryos is likely to reduce the efficacy of chromosomal tests that are used to enhance implantation rates. *Fertil Steril* 2007; 87: 496–503.
36. Goossens V, De Rycke M, De Vos A, et al. Diagnostic efficiency and accuracy, embryonic development and clinical outcome after the biopsy of one or two blastomeres for preimplantation genetic diagnosis. *Hum Reprod* 2008; 23: 481–492.
37. De Vos A, Staessen C, De Rycke M, et al. Impact of cleavage-stage embryo biopsy in view of PGD on human blastocyst implantation: A prospective cohort of single embryo transfers. *Hum Reprod* 2009; 24: 2988–2996.
38. Lewis CM, Pinel T, Whittaker JC, Handyside AH. Controlling misdiagnosis errors in preimplantation genetic diagnosis: A comprehensive model encompassing extrinsic and intrinsic sources of error. *Hum Reprod* 2001; 16: 43–50.
39. Campbell S, Swann HR, Seif MW, et al. Cell adhesion molecules on the oocyte and preimplantation human embryo. *Hum Reprod* 1995; 10: 1571–1578.
40. Santalo J, Grossmann M, Egozcue J. Does Ca^{2+}/Mg^{2+}-free medium have an effect on the survival of the preimplantation mouse embryo after biopsy? *Hum Reprod Update* 1992; 2: 257–261.
41. Dumoulin JC, Bras M, Coonen E, et al. Effect of Ca^{2+}/Mg^{2+}-free medium on the biopsy procedure for implantation genetic diagnosis and further development of human embryos. *Hum Reprod* 1998; 13: 2880–2883.
42. Van Royen E, Mangelschots K, Vercruyssen M, et al. Multinucleation in cleavage stage embryos. *Hum Reprod* 2003; 18: 1062–1069.
43. Hardy K, Winston RM, Handyside AH. Binucleate blastomeres in preimplantation human embryos in vitro: Failure of cytokinesis during early cleavage. *J Reprod Fertil* 1993; 98: 549–558.
44. Johansson M, Hardarson T, Lundin K. There is a cutoff limit in diameter between a blastomere and a small anucleate fragment. *J Assist Reprod Genet* 2003; 20: 309–313.
45. Munné S, Cohen J. Unsuitability of multinucleated human blastomeres for preimplantation genetic diagnosis. *Hum Reprod* 1993; 8: 1120–1125.
46. Kligman I, Benadiva C, Alikani M, Munne S. The presence of multinucleated blastomeres in human embryos is correlated with chromosomal abnormalities. *Hum Reprod* 1996; 11: 1492–1498.

47. De Vos A, Van Steirteghem A. Aspects of biopsy procedures prior to preimplantation genetic diagnosis. *Prenat Diagn* 2001; 21: 767–780.
48. Veiga A, Gil Y, Boada M, et al. Confirmation of diagnosis in preimplantation genetic diagnosis (PGD) through blastocyst culture: Preliminary experience. *Prenat Diagn* 1999; 19: 1242–1247.
49. Palmer GA, Traeger-Synodinos J, Davies S, et al. Pregnancies following blastocyst stage transfer in PGD cycles at risk for beta-thalassaemic haemoglobinopathies. *Hum Reprod* 2002; 17: 25–31.
50. Magli MC, Gianaroli L, Ferraretti A, et al. The combination of polar body and embryo biopsy does not affect embryo viability. *Hum Reprod* 2004; 19: 1163–1169.
51. Cieslak-Janzen J, Tur-Kapsa I, Iklevitch Y, et al. Multiple micromanipulations for preimplantation genetic diagnosis do not affect embryo development to the blastocyst stage. *Fertil Steril* 2006; 85: 1826–1829.
52. Findikli N, Kahraman S, Kumtepe Y, et al. Embryo development characteristics in Robertsonian and reciprocal translocations: A comparison of results with non-translocation cases. *Reprod Biomed Online* 2003; 7: 563–571.
53. Rubio C, Simon C, Vidal F, et al. Chromosomal abnormalities and embryo development in recurrent miscarriage couples. *Hum Reprod* 2003; 18: 182–188.
54. Verlinsky Y, Cohen J, Munné S, et al. Over a decade of experience with preimplantation genetic diagnosis: A multicenter report. *Fertil Steril* 2004; 82: 292–294.
55. Kahraman S, Candan ZN. Outcomes of vitrified-warmed day-4 embryos after day-3 cleavage-stage biopsy. *Reprod Biomed Online* 2010; 21: 636–641.
56. Escribá MJ, Zulategui JF, Galán A, et al. Vitrification of preimplantation genetically diagnosed human blastocysts and its contribution to the cumulative ongoing pregnancy rate per cycle by using a closed device. *Fertil Steril* 2008; 89: 840–846.
57. Zhang X, Trokoudes KM, Pavlides C. Vitrification of biopsied embryos at cleavage, morula and blastocyst stage. *Reprod Biomed Online* 2009; 19: 526–531.
58. Keskintepe L, Sher G, Machnicka A, et al. Vitrification of human embryos subjected to blastomere biopsy for preimplantation genetic screening produces higher survival and pregnancy rates than slow freezing. *J Assist Reprod Genet* 2009; 26: 629–635.
59. Los FJ, Van Opstal D, van den Berg C. The development of cytogenetically normal, abnormal and mosaic embryos: A theoretical model. *Hum Reprod Update* 2004; 10: 79–94.

16

Invasive Techniques: Blastocyst Biopsy

Steve McArthur

Introduction

The first report of the application of trophectoderm biopsy for the purpose of determining the genetics status of blastocyst-stage embryos was the sexing of rabbit embryos by Edwards and Gardner in 1967 [1]. Decades later and following in the wake of the development of human in vitro fertilization (IVF), Handyside and coworkers reported the first live birth after embryo biopsy in 1990 [2]. As preimplantation genetic diagnosis (PGD) developed, it was typical for biopsy to be performed to remove either the polar bodies or blastomeres. Polar body biopsy required the removal of the first and second polar bodies across Day 0 and Day 1 of development, the obvious restriction with polar body analysis being that only maternally carried genetic anomalies would be revealed. Blastomere biopsy occurred on Day 3 postfertilization when the embryo had progressed to the six- to eight-cell stage and typically resulted in the extraction of one or two blastomeres. Both polar bodies and blastomeres were analyzed by either polymerase chain reaction (PCR) or fluorescent in situ hybridization (FISH) techniques. PCR required the design of oligonucleotide primers to amplify allelic targets such a deletion or insertions in a single cell or polar body. FISH targeted and labeled chromosomes in a single cell, allowing detection of chromosomal aneuploidies and translocations. Recently, comparative genome hybridization (CGH) has displaced FISH for the purpose of chromosome aneuploidy and translocation analysis in PGD. To remove either the polar bodies or blastomeres from the embryo, the zona pellucida was breached by either mechanical means or by dissolving the protein with acid Tyrode's solution, and the embryo may or may not have been incubated for a period of time in a calcium- and magnesium-free medium to decrease cell-to-cell interactions and therefore make the biopsy of cells easier. During the late 1990s, the development of near-infrared lasers allowed for a more rapid and controllable opening if the zona pellucida.

Given that PGD relies upon embryo biopsy, an invasive procedure, it is critical that the impact of the biopsy procedure is reduced to the lowest level possible. The development of a fertilized oocyte through to a blastocyst (Figure 16.1) is the result of a process of selection that ultimately provides the embryo (interdependent on the quality of the culture conditions) with an improved prospect of implantation and survival through to live birth [3,4]. It is therefore conceivable that removal of 12%–25% of the embryos' biomass, as occurs with one- or two-cell biopsy on Day 3, will likely result in a decrease in the potential of the embryo to implant and progress through to a healthy live birth. There is evidence of a capacity within human embryos to withstand the damage of a Day 3 biopsy; there is a likelihood that embryos that may otherwise progress to implantation and a live healthy birth will be lost as a consequence of the detrimental impact of biopsy undertaken at this stage of embryo development. Blastocyst biopsy results in a significantly smaller loss of biomass, occurring when an embryo has >100 cells, and importantly it leaves the inner cell mass intact. Given that the inner cell mass will develop into the embryo proper, it is critical to minimize the effect of any invasive techniques on the component of the embryo.

Genea (formerly Sydney IVF) introduced a comprehensive blastocyst culture, transfer, and cryostorage methodology in the early 2000s that produced improved clinical pregnancy and health live baby rates, while also reducing miscarriage and multiple pregnancy rates [3–9]. The blastocyst culture system was based upon the ability to select the healthiest embryo from a patient's cohort for transfer and subsequent cryostorage of remaining blastocysts. The blastocyst culture methodology led to the development and routine clinical practice of blastocyst

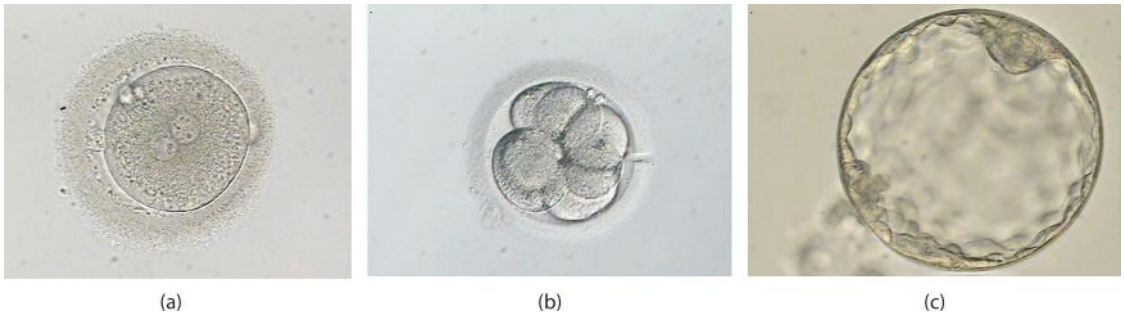

FIGURE 16.1 (a) In vitro development of a human blastocyst from 2-pronuclear stage through trophectoderm biopsy; (b) embryo hatching occurs on Day 3; (c) the embryo develops through the expanding blastocyst, with biopsy occurring on Day 5 or Day 6.

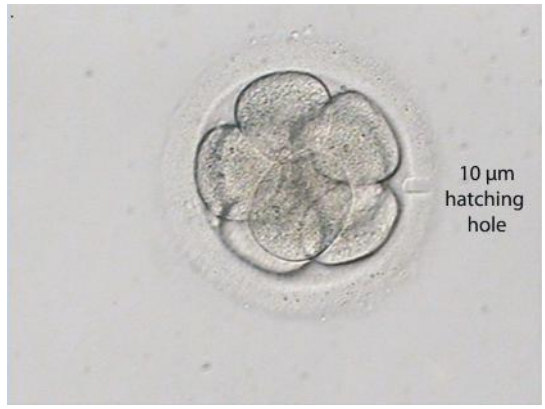

FIGURE 16.2 Image of Day 3 embryo after hatching (using a near-infrared laser) showing a 10 µm hole at the internal margin of the zona pellucida.

biopsy [3]. Biopsy at the blastocyst stage requires the zona pellucida to be breached on Day 3 of development by using a near-infrared laser (Figure 16.2) and allows for the extraction of 3–10 trophectoderm cells from an embryo generally made up of ≥100 cells. A step-by-step guide to embryo hatching is listed below.

Embryo hatching preceding blastocyst biopsy occurs either on Day 3 or on Day 5 or Day 6 of embryo development. In Genea laboratories, all embryo hatching occurs on Day 3 of development to ensure accessibility to a suitable hatching site with little risk of damaging any blastomeres. The development of this protocol occurred as a follow-on from the early PGD practice of embryo hatching and biopsy of Day 3 of development, when all embryos were hatched for analysis. In many cases of analysis failure, the embryos were reviewed on Day 5 or Day 6 and found to be hatching blastocysts with trophectoderm cells protruding from the Day 3 hatch site. It flowed into common practice once blastocyst biopsy was used for all embryo biopsy cases after 2003. Breaching the zona pellucida on Day 5 of development is practiced in many laboratories worldwide and was first reported in 2006 [10]. In this report, blastocysts were hatched at 116 hr post-fertilization and cultured for a further 4 hr to promote herniation of the trophectoderm. The 4 hr of further culture may be restrictive in allowing for the transfer of an embryo on the day of analysis; however, with the advent of array-CGH and vitrification of embryos for transfer in a subsequent cycle, this may no longer be an impediment. It is often speculated that breaching the zona pellucida on Day 3 may result in the inner cell mass being located external to the breach site. Experience at Genea shows that this situation does eventuate; however, given the ability to manipulate the position of the embryo on the microtools, this is no barrier to embryo biopsy.

BOX 16.1 EMBRYO HATCHING

1. The hole in the zona pellucida should be made adjacent to the polar body, if identifiable. Otherwise, hatch at a position where there is a space between the blastomeres.
2. The first pulse of the laser should be directed to the outer edge of the zona pellucida.
3. The third pulse of the laser should cut the internal wall of the zona pellucida in a direct line from the first laser pulse.
4. A hole in the internal margin of the zona of approximately 10 μm is created.
5. Embryos should then be washed before being placed back into culture dish.

Embryos hatched on Day 3 are cultured for another 2 days to allow for blastocoel expansion and extrusion of trophectoderm cells through the zona opening, thereby allowing for biopsy [5,9]. Embryos suitable for biopsy are placed in 5 μL drops of blastocyst culture medium under mineral oil. The embryo is held in position by a holding pipette, as used in intracytoplasmic sperm injection (ICSI) practice, and a 30 μm biopsy pipette is used to collapse the blastocyst and hold the cells that will be biopsied. Three to four shots of the laser set on a low power level reduce the cell-to-cell interactions, enabling multiple cells to be removed from the hatching trophectoderm. The cells remain as a single piece of tissue as the cells remain tightly coupled, thereby allowing the cells to be transferred easily in a single pipetting movement. The embryo is then returned to culture dish containing fresh blastocyst culture medium for further incubation while awaiting the results of the PGD analysis, at which point the embryo is transferred, cryostored, or disposed. The embryos are cultured individually postbiopsy in uniquely identified locations in the culture dish to ensure that embryo identity is maintained. The biopsied cells are washed and prepared for analysis by CGH, PCR, or FISH (FISH is no longer used in Genea laboratories). A step-by-step guide to trophectoderm biopsy procedure is listed in Box 16.2 and detailed in Figure 16.3.

The method for biopsy of a *fully hatched blastocyst* (Figure 16.4) is similar to that described for a standard blastocyst biopsy except there is no requirement to use the near-infrared laser for this biopsy method.

BOX 16.2 TROPHECTODERM BIOPSY

1. Ensure that the biopsy pipette tip and the leading edge of the trophectoderm are in focus.
2. Bring the biopsy pipette and touch the leading edge of the trophectoderm.
3. Draw a small number of trophectoderm cells carefully into the pipette by using suction until a good hold is achieved.
4. Stretch out the trophectoderm (at this point, the blastocoel cavity may collapse).
5. Adjust focus until the margins of the targeted cells are in focus, and then fire the laser at the intercellular junctions. Fire the laser three to five times across the width of the trophectoderm cells to be biopsied.
6. Using suction on the mouthpiece and the holding pipette joystick, pull the targeted cells away from the blastocyst.
7. Release the piece of trophectoderm from the biopsy pipette.
8. Where the stretched trophectoderm tissue does not readily separate from the remaining embryo, it is not recommended to fire the laser excessively because this may be detrimental to embryo recovery. In these cases, a more direct “cutting off” method may be used.
9. Gently release the embryo from the holding pipette while maintaining hold of cells in your biopsy pipette. Do not take further cells into your pipette because this may result in excess cells being biopsied. Ensuring that the holding and biopsy pipettes are in the same focal plane, rub the biopsy pipette across the end of the holding pipette. Take care not to damage the embryo protruding from the pipette as you carry out this step. If the first attempt is not successful, further attempts may be required.

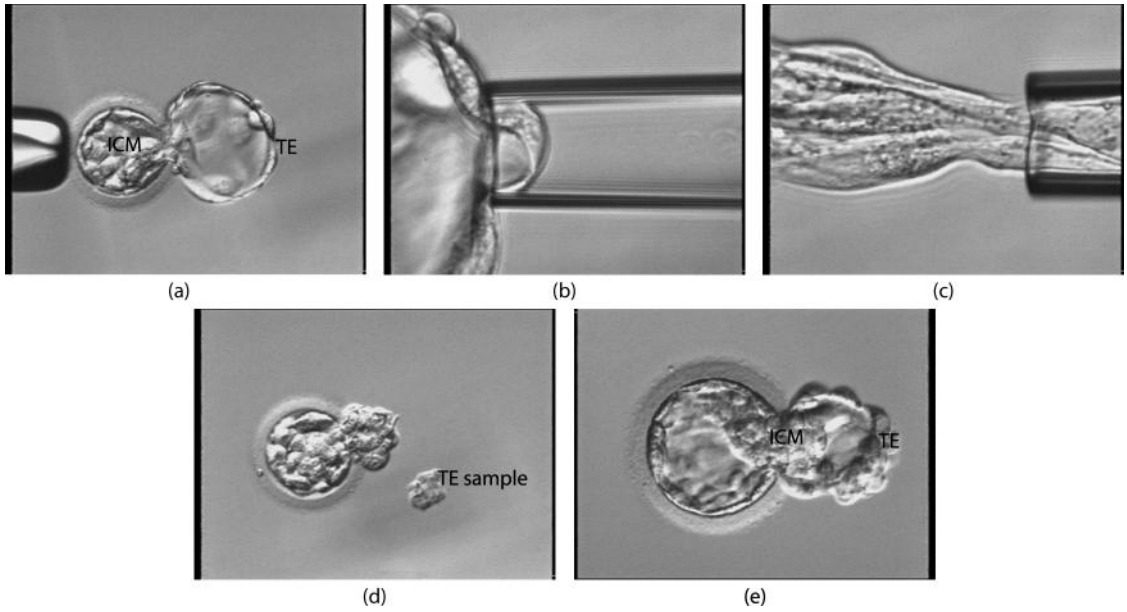

FIGURE 16.3 Photographs of blastocyst biopsy. (a) Blastocyst 2 days after laser-assisted hatching, consisting of herniating trophectoderm (TE) and inner cell mass (ICM). (b) Alignment of TE cells with biopsy pipette. (c) Three to ten cells aspirated from the TE while the ICM (destined to form the embryo proper) remains intact. (d) Blastocyst and TE sample. (e) Blastocyst approximately 90 min postbiopsy.

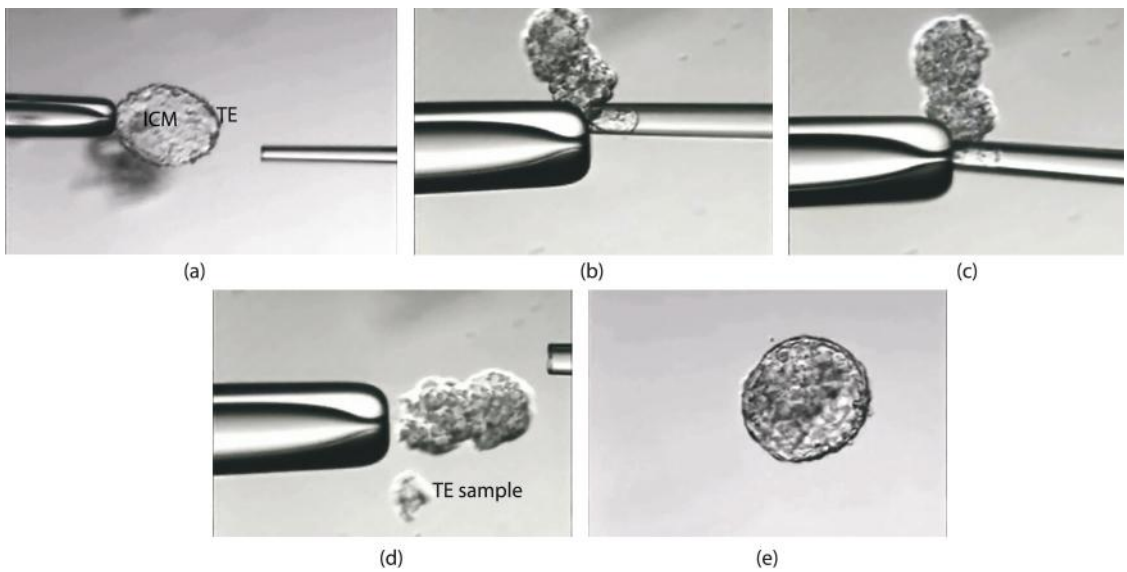

FIGURE 16.4 Images of fully hatched blastocyst biopsy. (a) Fully hatched blastocyst 2–3 days post–laser-assisted hatching; trophectoderm (TE) and inner cell mass (ICM) are labeled. (b) TE cells aspirated into biopsy pipette and contacted with holding pipette. (c) TE cells cut by shearing biopsy pipette against holding pipette. (d) Blastocyst and TE sample postbiopsy. (e) Blastocyst approximately 90 min postbiopsy.

In the method, steps 4–7 are removed, and the trophectoderm is biopsied as per step 8 by using the embryo-holding pipette as a shearing force to remove the trophoblasts drawn into the biopsy pipette in step 3 of the procedure.

Timing is critical to many aspects of IVF, with particular emphasis placed on the embryo transfer procedure. Embryo biopsy on Day 5 or Day 6 of development places time pressures on delivering analysis outcomes in time for an embryo transfer. To deliver the optimum number of embryos for biopsy, it is important to ensure coordination of all aspects of the IVF cycle, especially the timing of oocyte collection and insemination. It is ideal to undertake blastocyst biopsy on the morning of Day 5 or Day 6; therefore, it is suggested that oocyte collections are scheduled early in the theatre list to ensure early insemination time and maximum culture length through to the morning of Day 5 or Day 6. Blastocysts are routinely assessed for suitability for biopsy on the morning of Day 5 or Day 6 and between 12 PM and 1 PM on both days. Embryos not suitable for biopsy at the final check on Day 6 are excluded from the analysis.

The most advanced PGD technologies are reliant upon molecular biology techniques to provide material for analysis. Therefore, in a practical sense, having multiple cells and therefore multiple copies of DNA as targets for the amplification provides benefit to the quality of the amplification product generated compared with that provided by the single-copy DNA available from polar body or Day 3 embryo biopsy [8]. DNA amplification has inherent technical risks, such as amplification failure of the target DNA. The amplification risks in single cells (blastomeres) are likely to be higher than that seen in other sources of genetic material, such as polar bodies and lymphocytes [11]. Consequently, blastocyst biopsy allows increased confidence in diagnostic potential of PGD testing methods that require DNA amplification.

Use of PGD has increased in many clinics across the globe in the last decade. The 2010 report from the European Society of Human Reproduction and Endocrinology (ESHRE) PGD Consortium indicated that Day 3 biopsy accounted for 90% of embryo biopsies, whereas blastocyst biopsy accounted for just 0.4% [12]. At Genea clinics, PGD cycles now account for >15% of all cycles undertaken and the rate of uptake continues to increase. The increased use of PGD worldwide is not unexpected given reports of improved outcomes [13,14]. The technologies applied to cells biopsied from preimplantation embryos have grown in complexity as the uptake of PGD has expanded.

Chromosome enumeration, historically undertaken using FISH techniques, has in recent times been replaced by CGH techniques, allowing for the complete karyotyping of the preimplantation embryo. In the decade or so since the first reports of CGH and a live birth from the analysis of an embryo via the technique [15,16], there have been many advances in molecular analysis technology. CGH on metaphase chromosomes spread on glass slides has been replaced by molecular or microarray-CGH based on whole-genome amplification [17]. The complete karyotyping of an embryo has ensured that embryos are not transferred with aneuploidies previously undetected due to the limitations of FISH technologies. Figure 16.5 compares aneuploidies detected by microarray-CGH

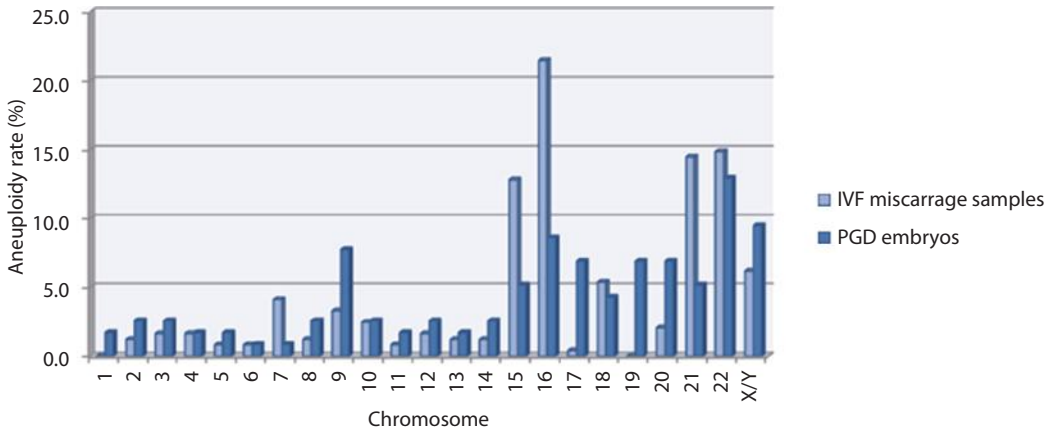

FIGURE 16.5 Comparison of chromosome aneuploidy rates between embryos biopsied on Day 5 or Day 6 with those detected in miscarriage samples post-IVF treatment. (Data courtesy of Genea Fertility, Sydney, Australia.)

with aneuploidies identified in miscarriage samples after an IVF cycle. Many of the aneuploidies detected by microarray-CGH would not have been revealed by FISH analysis, and subsequently such embryos would have been transferred.

The improvements in pregnancy and live birth outcomes associated with PGD have been attributed to the ability to produce a comprehensive chromosome karyotype of an individual embryo. Pregnancy and live birth outcomes have also improved with the advent of vitrification technologies postvitrification being introduced during the mid-2000s, and groups now report outcomes postembryo warming equivalent and in many clinics better than those achieved with a fresh embryo transfer [18]. Using blastocyst biopsy with microarray-CGH poses a challenge in achieving a fresh embryo transfer that is not otherwise an issue when either polar body biopsy or Day 3 embryo is applied. It is therefore important to be able to ensure that pregnancy and birth outcomes are maintained and improved with the application of more advanced PGD technologies combined with blastocyst biopsy. Wells et al. [19] reported on a strategy combining PGD and microarray-CGH analysis with vitrification of biopsied embryos before obtaining an analysis outcome. After analysis and assignment of the chromosomal status of the embryo, a normal embryo is identified and transferred in a subsequent cycle. The combination of blastocyst culture–biopsy techniques, vitrification, and advanced molecular technologies offers patients excellent clinical outcomes.

The last decade has shown that trophectoderm biopsy on Day 5 or Day 6 of embryo development delivers high implantation and live birth rates compared with both polar body and Day 3 blastomere biopsy. Improved implantation rates combined with a reduced impact of known embryological phenomena, such as mosaicism, have resulted in a wider move away from polar body and blastomere biopsy. The advent and use of whole-genome amplification technologies ensure that more detailed information is delivered from the PGD process, further adding to the implantation potential of embryos and consequently increasing the likelihood of success for patients accessing PGD technologies combined with blastocyst biopsy.

REFERENCES

1. Edwards RG, Gardner RL. Sexing of live rabbit blastocysts. *Nature* 1967;214(5088):576–7.
2. Handyside AH, Lesko JG, Tarín JJ, Winston RM, et al. Birth of a normal girl after in vitro fertilization and preimplantation diagnostic testing for cystic fibrosis. *N Engl J Med* 1992;327(13):905–9.
3. Henman M, Catt JW, Wood T, Bowman MC, et al. Elective transfer of single fresh blastocysts and later transfer of cryostored blastocysts reduces the twin pregnancy rate and can improve the in vitro fertilization live birth rate in younger women. *Fertil Steril* 2005;84(6):1620–7.
4. Jansen RPS. Benefits and challenges brought by improved results from in vitro fertilization. *Intern Med J* 2005;35(2):108–17.
5. de Boer KA, Catt JW, Jansen RPS, Leigh D, et al. Moving to blastocyst biopsy for preimplantation genetic diagnosis and single embryo transfer at Sydney IVF. *Fertil Steril* 2004;82(2):295–8.
6. Jansen RPS. Female age and the chance of a baby from one in-vitro fertilization treatment. *Med J Aust* 2003;178:258–61.
7. Jansen RPS, Bowman MC, de Boer KA, Leigh DA, et al. What next for preimplantation genetic screening (PGS)? Experience with blastocyst biopsy and testing for aneuploidy. *Hum Reprod* 2008;23(7):1476–8.
8. McArthur SJ, Leigh D, Marshall JT, de Boer KA, et al. Pregnancies and live births after trophectoderm biopsy and preimplantation genetic testing of human blastocysts. *Fertil Steril* 2005;84(6):1628–36.
9. McArthur SJ, Leigh D, Marshall JT, Gee AT, et al. Blastocyst trophectoderm biopsy and preimplantation genetic diagnosis for familial monogenic disorders and chromosomal translocations. *Prenat Diagn* 2008;28(5):434–42.
10. Kokkali G, Traeger-Synodinos J, Vrettou C, Stavrou D, et al. Blastocyst biopsy versus cleavage stage biopsy and blastocyst transfer for preimplantation genetic diagnosis of β-thalassaemia: A pilot study. *Hum Reprod* 2007;22(5):1443–9.
11. Rechitsky S, Strom C, Verlinsky O, Amet T, et al. Allele dropout in polar bodies and blastomeres. *J Assist Reprod Genet* 1998;15:253–7.
12. Harper JC, Coonen E, De Rycke M, Harton G, et al. ESHRE PGD Consortium data collection X: Cycles from January to December 2007 with pregnancy follow-up to October 2008. *Hum Reprod* 2010;25:2685–707.

13. Forman EJ, Hong KH, Ferry KM, Tao X, et al. In vitro fertilization with single euploid blastocyst transfer: A randomized controlled trial. *Fertil Steril* 2013;100(1):100–7.
14. Treff NR, Ferry KM, Zhao T, Su J, et al. Cleavage stage embryo biopsy significantly impairs embryonic reproductive potential while blastocyst biopsy does not: A novel paired analysis of cotransferred biopsied and non-biopsied sibling embryos. *Fertil Steril* 2011;96(3):S2.
15. Wells D, Fragouli E, Stevens J, Munne S, et al. High pregnancy rate after comprehensive chromosomal screening of blastocysts. *Fertil Steril* 2008; 90:S80.
16. Wilton L, Williamson R, McBain J, Edgar D, et al. Birth of a healthy infant after preimplantation confirmation of euploidy by comparative genomic hybridization. *N Engl J Med* 2001;345(21):1537–41.
17. Hu DG, Webb G, Hussey N. Aneuploidy detection in single cells using DNA array-based comparative genomic hybridization. *Mol Hum Reprod* 2004;10(4):283–9.
18. Roy T, Peura T, McArthur S. Effect of embryo development and grade on pregnancy outcomes following fresh and vitrified single blastocyst embryo transfer. *Fertil Steril* 2011;96(3):S44–5.
19. Wells D, Fragouli E, Stevens J, Munne S, et al. High pregnancy rate after comprehensive chromosomal screening of blastocysts. *Fertil Steril* 2008;90:S80.

17

Invasive Techniques: Aneuploidy Testing by FISH

Semra Kahraman and Çağrı Beyazyürek

Introduction

Preimplantation Genetic Diagnosis for Aneuploidy Testing

Preimplantation genetic diagnosis (PGD) is a preventive method to identify genetic disorders and chromosomal abnormalities in preimplantation embryos, thus giving couples the opportunity to avoid a pregnancy termination after the prenatal diagnosis of such disorders and abnormalities. With PGD, only embryos having a normal genotype and chromosomal constitution are selected for transfer to the uterus, providing the birth of a healthy baby. There are three main indication groups in which PGD could be applied: (1) aneuploidy screening for numerical chromosomal abnormalities, (2) diagnosis of structural chromosomal abnormalities in translocation and inversion carriers, and (3) diagnosis of genetic disorders or human leukocyte antigen (HLA) compatibility for a child in need of stem cell transplantation (Figure 17.1) [1–8].

Although first applications of the PGD technique were for selecting disease-free embryos for an X-linked single gene disorder [1], soon after the introduction of the fluorescence in situ hybridization (FISH) technique for chromosomal disorders [2], the number of PGD cycles rose rapidly to detect chromosomal abnormalities in embryos generated from patients undergoing in vitro fertilization (IVF) treatments for the purpose of improving success [9,10]. The most frequent reasons for aneuploidy testing are advanced maternal age, recurrent miscarriages, repeated implantation failures, previous fetal chromosomal abnormality, and severe male factor infertility.

Chromosomal Abnormalities in Preimplantation Embryos

Chromosomally normal human somatic cells contain 46 chromosomes (22 pairs of autosomes and 1 pair of gonosomes, thus 2n, n = 23) (Figure 17.2). Any deviation from this chromosome set is called as abnormality. Aneuploidy is known as abnormalities in chromosome number that can originate from an excess number of chromosomes (e.g., trisomy) or from missing chromosomes (e.g., monosomy), whereas haploidy (n) and triploidy (3n) are associated with the abnormalities of the whole chromosome set.

A significant proportion of human preimplantation embryos contain aneuploidy as one of the major causes of implantation failures, pregnancy losses, and abnormal live births [11]. Although the rate of aneuploidy increases with the maternal age, PGD reveals a high incidence of aneuploidy and mosaicism in both young and advanced maternal age patients [12,13].

The mechanisms of chromosomal abnormalities in embryos could be divided into two major categories according to the onset of formation as meiotic and postmeiotic. Although both mechanisms are common in preimplantation embryos, most of the aneuploidies originate from meiotic divisions in oogenesis [14–17], increasing with advancing maternal age. In normal meiosis, homologous chromosomes are separated in metaphase I (MI), and sister chromatids are separated in metaphase II (MII). Meiotic segregation errors in oocytes and polar bodies are formed either by premature separation of sister chromatids (PSSC) or nondisjunction of homologous chromosomes (Figure 17.3). Recent studies using single-nucleotide polymorphism arrays (SNP-arrays) in which the origin of individual alleles could be labeled and tracked demonstrate the former mechanism is responsible for almost all errors in the first meiotic division [16,17].

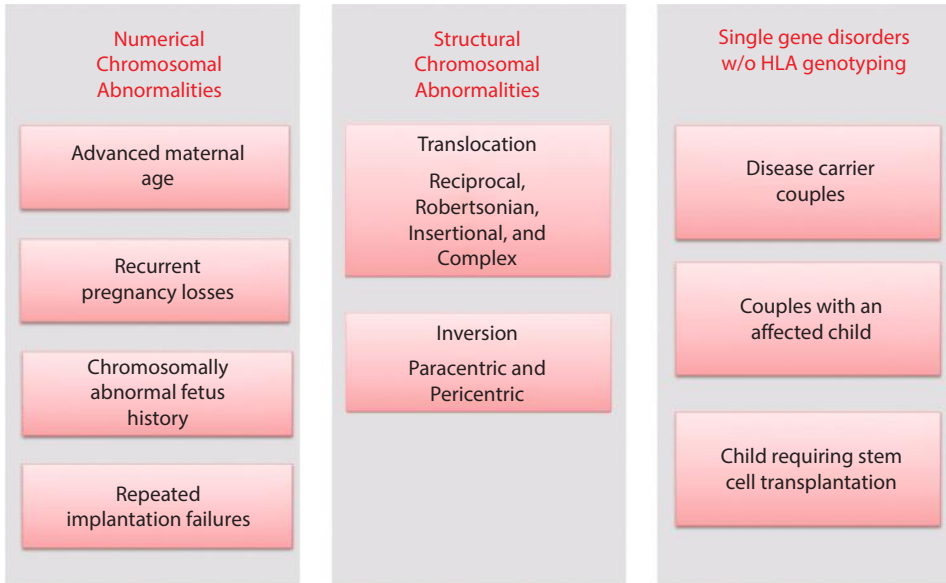

FIGURE 17.1 Main indication groups for PGD.

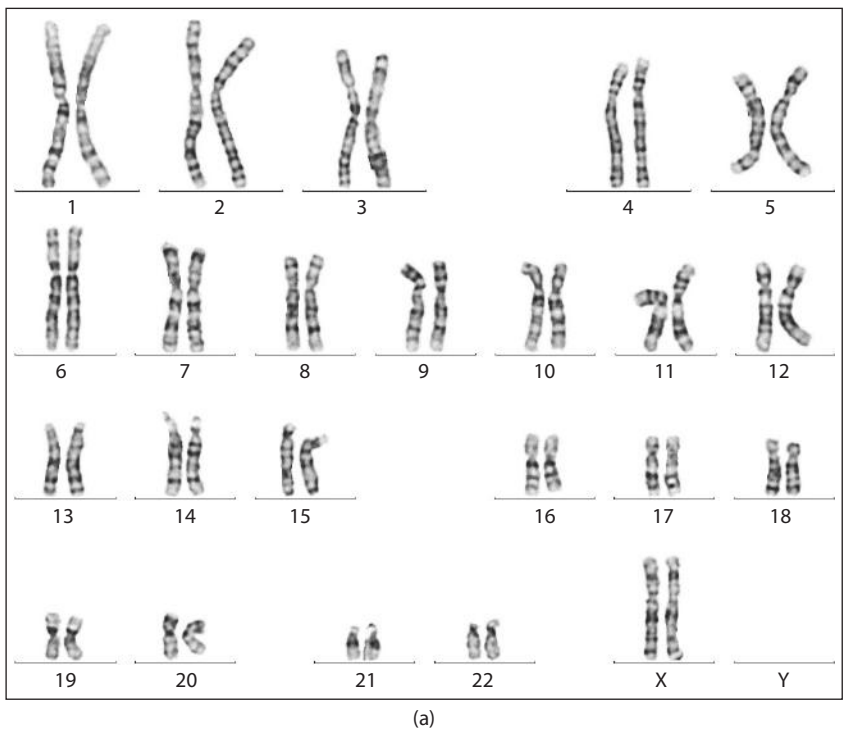

(a)

FIGURE 17.2 Normal set of chromosomes in human somatic cells. GTG banding image of chromosome sets in (a) normal female, 46,XX.

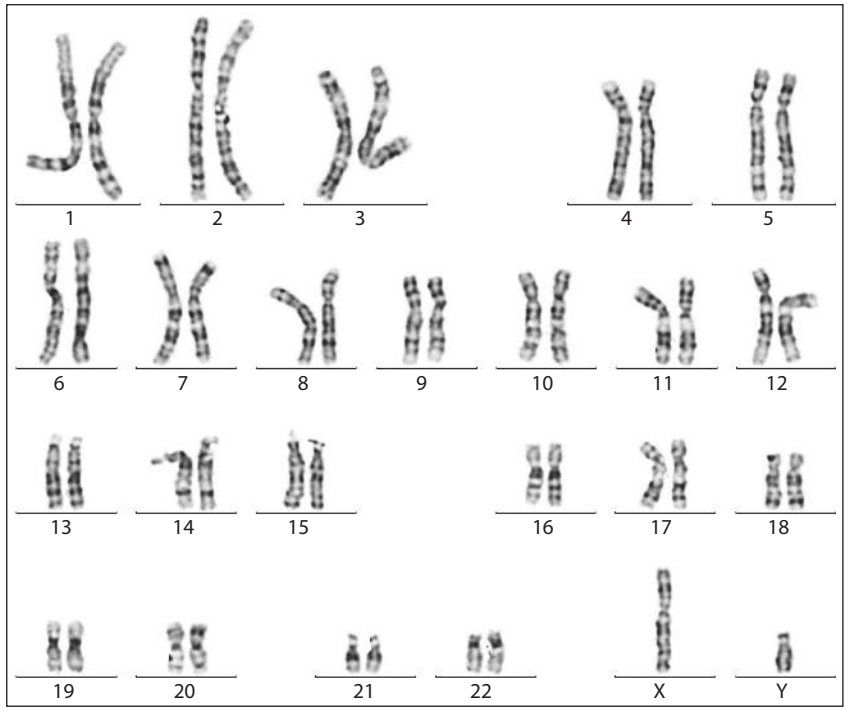

FIGURE 17.2 (*Continued*) Normal set of chromosomes in human somatic cells. GTG banding image of chromosome sets in (b) male, 46,XY, peripheral lymphocytes induced by conventional culturing and karyotyping techniques.

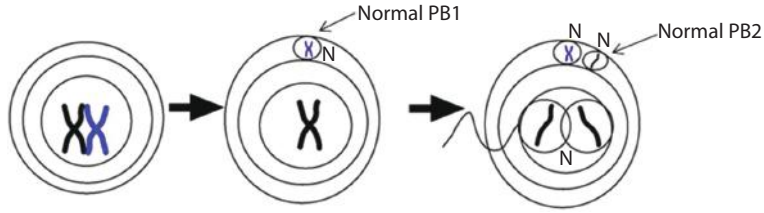

FIGURE 17.3 Normal meiosis. Chromosomal segregations in oocytes in two successive meiotic divisions.

Aneuploidy Testing by FISH

There are several methods for the detection of aneuploidy in embryos: FISH, array comparative genomic hybridization (a-CGH), SNP-arrays, and real-time polymerase chain reaction (RT-PCR).

In the FISH technique, DNA probes that are labeled with different colored fluorescent tags that are specific for chromosomal regions are hybridized to interphase nuclei or metaphase chromosomes. The advantage over conventional cytogenetic methods is that it can be applied to the interphase cell; thus, it is not necessary to culture cells to achieve metaphases. Because it is a rapid test and eliminates the need of culture, this technique is suitable for use in prenatal and preimplantation genetic diagnosis.

To date, the majority of PGD analyses for aneuploidy screening and rearrangements have been performed using FISH, which has still wider application among other techniques. Aneuploidy testing by FISH consists of the following steps: fixation of biopsied cells, pretreatment and probe application, denaturation, hybridization,

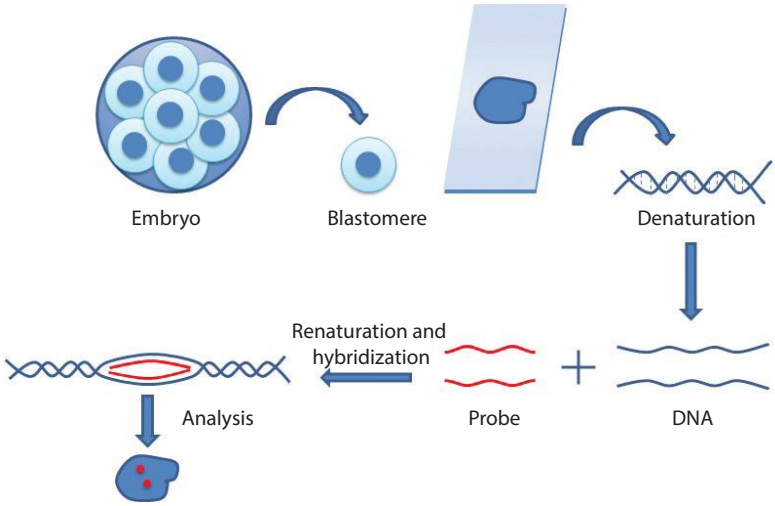

FIGURE 17.4 Steps of FISH.

stringent washing, and analysis after counterstain application (Figure 17.4) [2,18]. The most critical step for FISH is the cell fixation; each cell should be informative, and the loss of genetic material should be avoided [19].

Preparing for FISH

Fixation Methods

Mainly, there are two different methods of fixation of cells that are biopsied from embryos. Both involve the use of Carnoy's fixative that contains methanol:acetic acid in a 3:1 proportion. The methods differ by solutions used to swell and breakdown the cell membrane: a detergent-based (Tween 20) solution or a hypotonic buffer containing either KCl or bovine serum albumin (BSA) with sodium citrate. Although the former method requires less skill and is easier to handle, the resulting nuclear diameter is small and signal overlaps and FISH errors are more frequent. In contrast, the hypotonic method gives a larger diameter nucleus that decreases the probability of signal overlaps and nuclear loss during fixation.

BOX 17.1 FIXATION OF CELLS

Materials

Microscope slides (Superfrost)
Falcon tubes (TreffLab)
Glass Pasteur pipettes
Flame source
Mouth pipette (Drummond Scientific)
Carbide marker
Methanol (Sigma)
Glacial acetic acid (Sigma)
Sterile distilled H_2O
Sodium citrate (tribasic:dihydrate) (Sigma)
Albumin, bovine (Sigma)
Stereomicroscope (Olympus SZX12), inverted microscope (Olympus CK40)

Method

1. Fixative solution (3:1) should be prepared freshly just before fixation.
2. Hand-drawn glass pipettes with a 60 µL inner diameter are prepared by using a flame source.
3. Glass slides are cleaned with fixative solution.
4. The proper function of the mouth pipette is checked by aspirating of a little amount of hypotonic solution (6 mg/mL BSA, 1% sodium citrate). Another mouth pipette should be ready to avoid oil.
5. A small amount of hypotonic solution is aspirated into the pipette. The blastomere/trophectoderm tissue is aspirated and transferred into hypotonic solution, and then with another mouth pipette, the blastomere/trophectoderm tissue is taken onto the slide.
6. Just before the nucleus dries, one drop of fixative solution is added to digest the cytoplasm. The drop containing fixative can be added with a Pasteur pipette pulled in a flame, and the tip of the pipette has to be very narrow so the drop of fixative added is tiny.
7. At the time the fixative is dropped, the blastomere/trophectoderm tissue may move while the fixative and hypotonic are mixing on the slide. After a short distance, it will stop and attach to the slide. At this moment if needed, another drop of fixative can be added to lyse the cytoplasm completely.
8. The place of fixed chromatin is carefully marked using a carbide marker.
9. The sample number and case name are written on the slide, and slides are maintained at room temperature until hybridization.

In polar body fixation, distilled water is used instead of hypotonic solution. The rest of the method is as same as the fixation method for blastomeres and trophectoderm samples [26–29].

Pretreatment and Dehydration

Dehydration steps are common for polar body, blastomere and trophectoderm tissues, and they are done before hybridization to clean the fixed chromatin from the cytoplasm and fixative artifacts that remain after fixation. This step provides effective hybridization with a clean nucleus.

BOX 17.2 DEHYDRATION AND HYBRIDIZATION

Materials

Coplin jars
Ethyl alcohol (70%, 85%, 100%)

Method

1. The slides are immersed in solutions as follows: 1 min each in 70% ethanol, 85% ethanol, and 100% ethanol.
2. Slides are air-dried.

Probe mix and hybridization (first round)

Materials

Slide warmer (Hybrite-Vysis), microcentrifuge (Eppendorf), vortex (Velp)
2–10 µL micropipette (Eppendorf)
18 × 18 mm coverslips[a] (Isolab)
Parafilm
Direct labeled probes (Vysis): MultiVysion PB [26–29].

[a] The coverslips can be resized via cutting by a carbide marker according to the area size for hybridization.

FISH Method

Single-cell interphase FISH is a rapid, reliable, and efficient technique capable of detecting up 9–12 chromosomes in two or three rounds of hybridization on a single nucleus. Currently, fluorescent DNA probes for chromosomes X, Y, 13, 14, 15, 16, 17, 18, 21, and 22 are being used in PGD for aneuploidy screening because they are involved in >50% of all chromosomally abnormal miscarriages.

There are commercially available probe panels for aneuploidy screening. With the five-chromosome probe set, chromosomes 13, 16, 18, 21, and 22 can be screened simultaneously. The number of chromosomes screened could be increased to nine (Figure 17.5) with the addition of a panel with four chromosomes, 15, 17, X, and Y, and further to 12 with the addition of locus-specific probes for three more chromosomes, 9, 19, and 20. Evaluation of these chromosomes offers the selection of normal embryos for the most common aneuploidies found in chromosomally abnormal miscarriages. Alternatively, for translocations and other chromosomal rearrangements, different probe combinations are used that are specific for the type of abnormality (Figure 17.6).

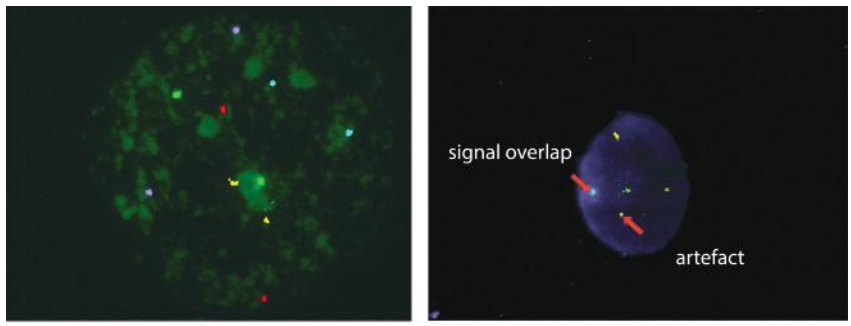

FIGURE 17.5 First and second round results of the same blastomere. (a) Normal for the first round study, including chromosomes 13, 16, 18, 21, and 22. Chromosome 13 (red), chromosome 16 (light blue), chromosome 18 (blue), chromosome 21 (green), and chromosome 22 (yellow). (b) Abnormal for the second round study, including chromosomes 15, 17, X, and Y. Chromosome 15 (yellow), chromosome 17 (aqua), chromosome X (green), and chromosome Y (blue). This blastomere was diagnosed as "monosomy 17." Notice that there is a signal overlap between aqua and one of the green signals. In addition, for the yellow signal, the signal at the bottom-middle is an artifact, evident from the color and the intensity. (Courtesy of Reproductive Genetics Laboratory, Istanbul Memorial Hospital, Istanbul, Turkey, 2009.)

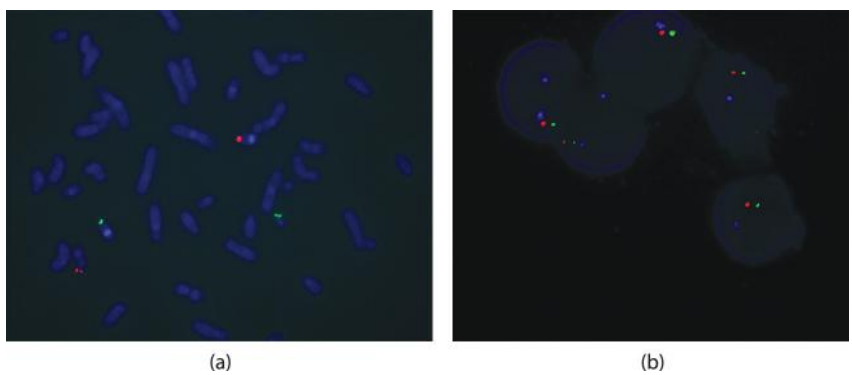

FIGURE 17.6 Preimplantation genetic diagnosis (PGD) for translocation carriers by FISH. (a) In this example, the patient was a carrier of a reciprocal translocation: 46,XY,t(17;22)(q23;q11.2). Probes were tested on patient's blood samples to ensure translocation and test the efficiency of probes. CEP 17 (spectrum aqua), Telomeric 17q (spectrum orange), and Telomeric 22q (spectrum green) probes were used on metaphase chromosomes obtained after peripheral blood culture. (b) Detection of unbalanced products by using same probe mixture on trophectoderm sample in the PGD study. This embryo was diagnosed as partial monosomy for 17q and partial monosomy for 22q and hence as unbalanced for translocation.

1. MultiVysion PB probe panel is ready to use.
2. Before hybridization, humidified paper towels are placed on the slide warmer and the slide warmer set up to 37°C.
3. The working probes are warmed up to 37°C, mixed by vortex, and centrifuged for a few seconds.
4. Then, 3 µL of probe mix is applied onto the marked area where the fixed chromatin is located.
5. A coverslip is carefully placed on the probe. It is important to avoid air bubbles.
6. The coverslip is sealed with parafilm or rubber cement.
7. Slides are placed onto the slide warmer (Hybrite), and the hybridization program starts with the denaturation step at 75°C for 5 min and the hybridization step at 37°C for 3 hr.

Washing and Counterstaining

NOTE: Because fluorophores that label the probes may fade under light, all steps after the hybridization should be performed under dim light.

BOX 17.3 WASHING AND COUNTERSTAINING

Materials

Waterbath (Memmert)
Coplin jars
Coverslips (24 × 60 mm) (IsoLab)
2–10 µL micropipette (Rainin)
0.45 µm Minisart filters (Sartorius)
Thermometer
20× standard saline citrate (SSC) (Vysis)
Nonidet P-40 (NP-40) (Vysis)
Antifade solution (Vysis)
4,6-Diamidino-2-phenylindole (DAPI) (Vysis)
Washing solution (0.4× SSC, 0.3% NP-40)

For wash solution, combine 10 mL of 20× SSC (pH 5.3) with 1.5 mL of NP-40 and add distilled water to the final volume of 500 mL. Adjust the pH to 7–7.5 with NaOH, and then filter with 0.45 µm filter before use.

Method

1. A Coplin jar is filled with wash solution and placed in the waterbath; another jar filled with wash solution stays at room temperature. The waterbath is warmed to 71°C, and the temperature of the solution is checked by a thermometer.
2. The parafilm and coverslip are carefully removed from the slide and immersed in 71°C wash solution for 3 min incubation.
3. After 3 min of incubation, slides are removed from the wash solution and placed in the Coplin jar containing wash solution at room temperature and incubated for a minute.
4. Slides are removed from wash solution, rinsed with distilled water, and allowed to dry vertically on a paper towel in a dark area.
5. After the slides have dried, 10 µL of DAPI or Antifade solution is added onto the hybridization area and the slide is covered with a 24 × 60 mm coverslip. For MultiVysion PB and MultiVysion 4CC probe panels, Antifade is used instead of DAPI because some probes have blue fluorophores.
6. Slides are covered with aluminum foil and evaluated as soon as possible by using a fluorescent microscope that contains appropriate filters for the probe fluorophores [26–29].

Evaluation of Signals

Evaluation of signals is performed in a dark area using a fluorescent microscope. This step is the most important step in the FISH-based PGD technique. Visualization of signals is performed using the appropriate single bandpass filters (red, fluorescein isothiocyanate [FITC], aqua, blue, gold, and DAPI).

There are some points that are very important in the signal evaluation:

1. Dual or triple bandpass filters are used to distinguish artifacts from specific signals.
2. Cross-hybridizations may occur between centromeric regions of repetitive sequences. The unspecific cross-hybridizations can be detected easily because their signal intensity is lower than that of the specific cross-hybridizations.
3. High-intensity signals may appear in other filters; aqua signals may leak in the blue filter and yellow signals may leak in green filter because they have excitation wavelengths close to each other depending on the choice of bandpass filters.
4. For a signal to be considered as "split," the centers of the two signals should not be far from two signal-size and the shapes should be similar to each other.
5. Because the evaluation is subjective, at least one witness is needed in the interpretation of the signals.
6. When there is no consensus for a signal, the chromosome that was doubted should be reevaluated after rehybridization with a new probe set (Figure 17.7).

BOX 17.4 APPLICATION OF PROBE MIX AND HYBRIDIZATION (SECOND ROUND)

Materials

Slide warmer (Hybrite-Vysis)
Incubator (Heraeus)
Microcentrifuge (Eppendorf)
Vortex (Velp)
2–10 µL micropipette (Rainin)
18 × 18 mm coverslips (Isolab)
Parafilm
MultiVysion 4 Color Custom probe set for chromosomes X, Y, 15, and 17 (Vysis)

Method

After the evaluation of the first round hybridization, the fixed blastomere chromatin is prepared for second round hybridization.

1. The coverslip is removed by placing slide under water faucet until it falls.
2. The slides are immersed in solutions as follows:
   a. 1 min in 70% ethanol
   b. 1 min in 85% ethanol
   c. 1 min in 100% ethanol
3. After the slides are dried, 3 µL of working probe (MultiVysion 4cc) is applied onto the chromatin.
4. A coverslip is carefully placed on the probe. It is important to avoid air bubbles.
5. The coverslip is sealed with parafilm or rubber cement.
6. Slides are placed onto the slide warmer (Hybrite-Vysis), and the hybridization program starts with the denaturation step at 75°C for 5 min and the hybridization step at 42°C for 1.5 hr.

Washing, Couterstaining, and Evaluation (Second Round)

1. Washing step is the same as in the previous section.
2. After the slides have dried, 10 µL of Antifade solution is added onto the hybridization area, and the slide is covered with a 24 × 60 mm coverslip. For 4cc probe panels, Antifade is used instead of DAPI because some probes have blue fluorophores.
3. Slides are covered with aluminum foil and evaluated as soon as possible with a fluorescent microscope that contains appropriate filters for the probe fluorophores. For the 4cc probe, chromosome 15 is seen in orange, chromosome 17 is seen in aqua, chromosome X is seen in green, and chromosome Y is seen in blue (Figure 17.5b) [26–29].

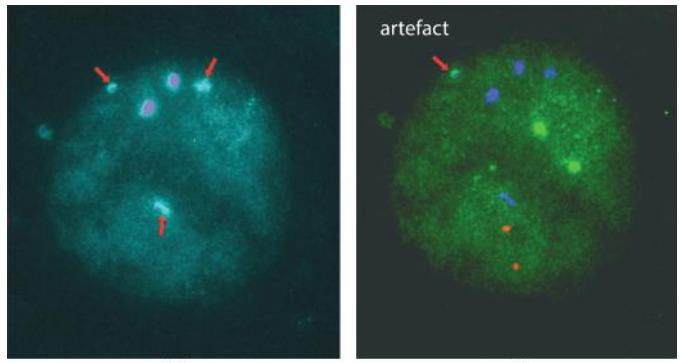

FIGURE 17.7 Distinguishing an artifact. (a) In aqua and blue filters, the cell seems to have three aqua (as shown by the arrows) and two blue signals. (b) In the triple filter, the signal in the 11 o'clock position remains but has a whitish color that is very different from the rest of the specific aqua signals. Thus, the cell was diagnosed as "normal." Chromosome 13 (red), chromosome 16 (light blue), chromosome 18 (blue), chromosome 21 (green), chromosome 22 (yellow). (Courtesy of Reproductive Genetics Laboratory, Istanbul Memorial Hospital, Istanbul, Turkey, 2009.)

Third Round Hybridization

1. After the evaluation of the second round hybridization, if there is a doubt in first and second analyses, the fixed blastomere chromatin can be reanalyzed with telomeric- and locus-specific probes. This situation is often present in embryos of 16qh polymorphism carriers (Figure 17.8).
2. If a probe mix is to be used for the third round, 1 µL of each probe and 7 µL of buffer are added to the mixture, and it can be stored at –20°C.
3. Probe application, hybridization conditions, and washing procedures are the same as described for the first round, except for the time for hybridization; it should be 6–14 hr.

There are some difficulties regarding the interpretation of signals in polar bodies, blastomeres, and trophectoderm samples. For polar bodies, the frequent problem would be the fragmentation of the first polar body (Figure 17.9) and the signal overlap and pulverization (Figure 17.10) due to the compact nature of the polar bodies. Because the first polar body contains "2n," it should have two signals for each chromosome, and second polar body should contain only one signal. Another difficulty is the discrimination of signal splitting in the first polar bodies. An interpretation of a split signal as two distinct signals may lead to the diagnosis of a trisomic embryo as normal (Figure 17.11).

In cleavage-stage embryo analysis, the most frequent difficulty that may be encountered is the low representative ability of a blastomere for the embryo due to mosaicism. A significant proportion of cleavage-stage embryos have mosaicism, representing the most frequent reason of misdiagnosis. In addition, because the diagnosis

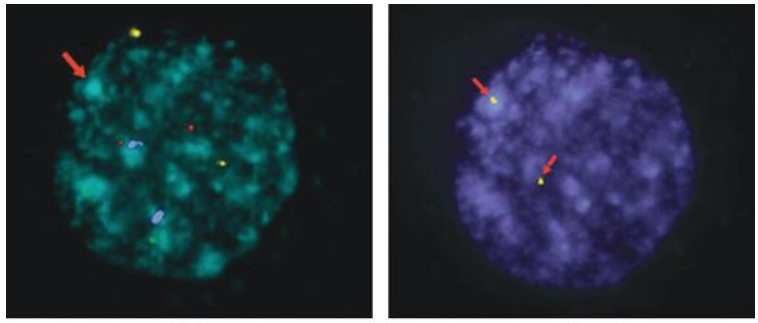

FIGURE 17.8 (a) For monosomic embryos such as monosomy 16, only one aqua signal specific for chromosome 16 is observed in the first round. (b) When additional third round hybridization is performed, specific for telomeres of chromosome 16 (Tel 16q, spectrum orange), it is identified that this blastomere is indeed normal for chromosome 16, thus "rescued."

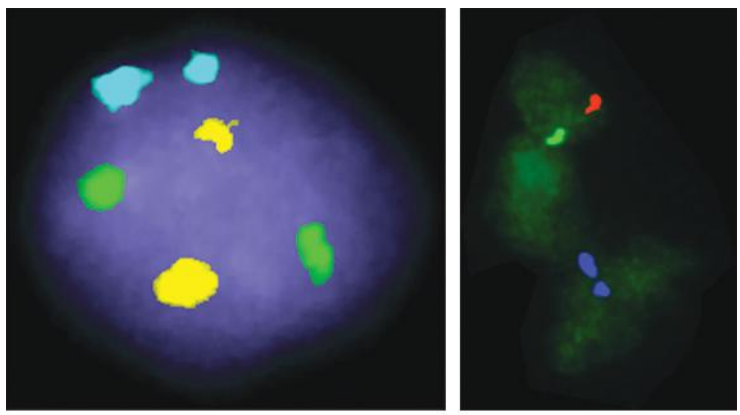

FIGURE 17.9 (a) An intact polar body that is easily interpretable. (b) Although this polar body is fragmented, it is interpretable, but caution should be taken to ensure that no other parts belonging to the polar body have been missed during fixation.

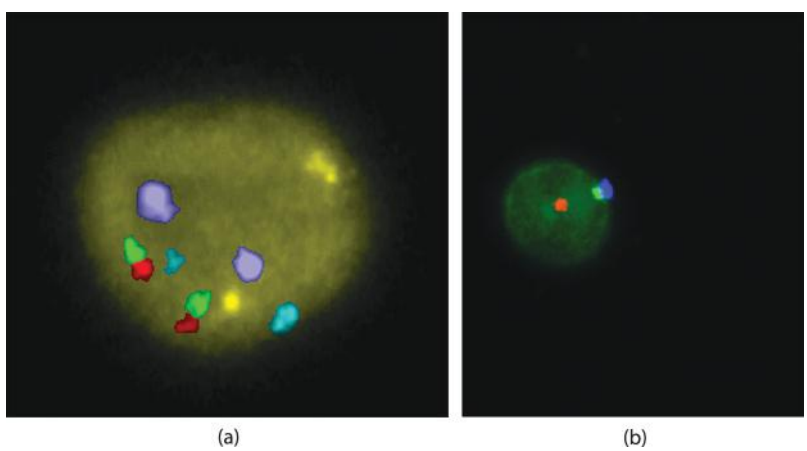

FIGURE 17.10 (a) This polar body has normal signals that were concentrated on the bottom-left side of the nucleus, resulting in partial overlaps. (b) This second polar body has a blue signal that was pulverized due to being located on the edge of the nucleus.

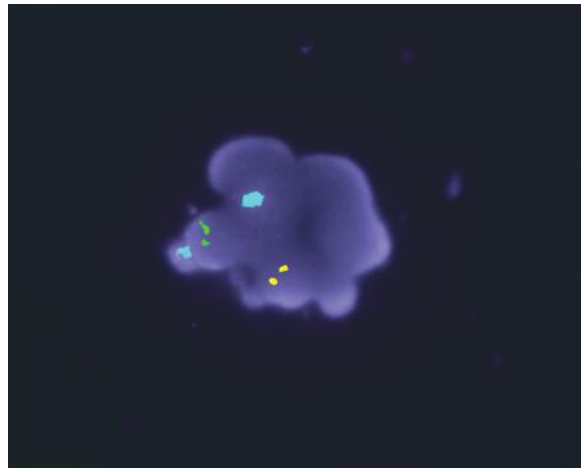

FIGURE 17.11 In this first polar body, the chromosome 22 (spectrum gold) signals are split and should be counted as one chromosome. This means one extra copy of chromosome 22 will remain in the oocyte unless a reciprocal aneuploidy occurs in the second division in this gamete.

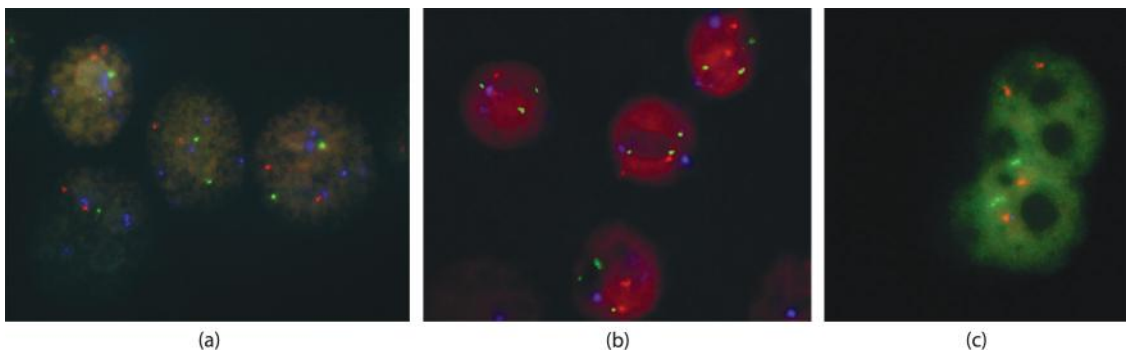

FIGURE 17.12 (a, b) Good spreading of cells after fixation of a trophectoderm tissue. Each cell has clear borders, and the nuclear quality is high, with no residual cytoplasm. (c) Cells overlapped, and the nuclear material was lost during fixation, probably due to excessive use of fixative.

depends only on one blastomere, the efficiency is limited by the efficiency of hybridization of that blastomere. In contrast, blastocyst-stage biopsy provides approximately five cells (Figure 17.12a, b), reducing the error rates and increasing the diagnosis rate by providing more nuclei for double-checking the evaluations. However, there are also difficulties in the interpretation of signals in trophectoderm tissues that may result in overlap of cells and residual cytoplasm due to improper fixation (Figure 17.12c).

Advantages and Disadvantages of FISH

Although it is a relatively low cost and less complex, FISH suffers from being subjective and error prone; thus, quality control guidelines should be followed for every step from fixation to signal interpretation.

The most important disadvantage of FISH is that it is not able to detect all abnormalities because the number of chromosomes that can be analyzed is limited. Comprehensive chromosomal screening methods such as a-CGH is able to detect aneuploidies related to all 23 pairs of chromosomes. In the a-CGH technique, DNA from a test sample (green) and a normal reference sample (red) is labeled differentially and hybridized to several

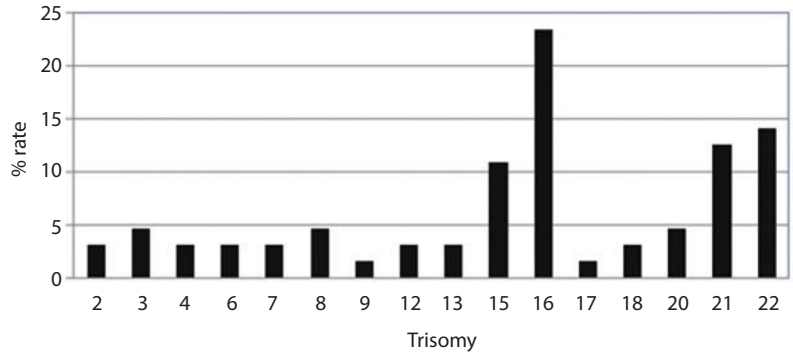

FIGURE 17.13 Summary of cytogenetic analysis of 410 abortus materials. The chart shows the rate of trisomic conceptions by the specific chromosome involved. (Courtesy of Istanbul Memorial Hospital.)

thousand probes that are imprinted on a glass slide. The fluorescence intensity of the test and the reference DNA is measured to calculate the copy number changes for each chromosome. The analysis lasts 12–24 hr.

Studies using a comprehensive chromosomal screening (e.g., CGH) technique on embryos demonstrated that abnormalities of the chromosomes that are not present in the FISH panel are also quite frequent [20]. Furthermore, FISH is not efficient in detecting all trisomies that end up with spontaneous abortions. Although the most frequent trisomy found is 16, trisomies of chromosomes 2, 3, 4, 6, 7, 8, 9, 12, and 20 could also be found in abortus materials that are not in the regular FISH panel. Approximately 30% of all trisomies would be undiagnosed with the nine-probe panel and 45% would be undiagnosed with the five-probe panel (Figure 17.13).

On the other hand, FISH technique has some advantages over other novel techniques. Comprehensive chromosomal screening methods are yet to be improved on some aspects on which FISH is still superior. For example, a-CGH is not able to detect all abnormalities, such mosaicism, polyploidy and haploidy, and cryptic translocations. SNP-array analysis [21–23] suffers from high noise and unspecific results. RT-PCR [24] is quite fast but it is limited to analysis of several chromosomes. Although next generation sequencing is the most promising technique among them, it is time-consuming and expensive, and the prices have to be reduced before it can enjoy wider application in clinical use [25]. Furthermore, all these recently developed techniques suffer from interpretational difficulties due to the large volume of data that is often beyond what is needed.

The future direction of PGD should be to obtain all required genetic information of the embryo with maximal accuracy at the earliest time possible. The technical limitations are gradually being reduced, and simultaneous screening of all chromosome pairs and identification of polyploidy and uniparental disomy, diagnosis of polygenic disorders and imprinting disorders, HLA genotyping, and copy number repeats are not too far. In the future, although FISH is going to be used less frequently, the routine use of comprehensive chromosomal screening and next generation sequencing methods will launch a new era of PGD.

REFERENCES

1. Handyside AH, Kontogianni EH, Hardy K, Winston RML. Pregnancies from biopsied human preimplantation embryos sexed by Y-specific DNA amplification. *Nature.* 1990;344:768–70.
2. Munné S, Weier HU, Stein J, Grifo J, et al. A fast and efficient method for simultaneous X and Y in situ hybridization of human blastomeres. *J Assist Reprod Genet*. 1993;10(1):82–90.
3. Scriven PN, Handyside AH, Ogilvie CM. Chromosome translocations: Segregation modes and strategies for preimplantation genetic diagnosis. *Prenat Diagn*. 1998;18(13):1437–49.
4. Verlinsky Y, Rechitsky S, Schoolcraft W, Strom C, et al. Preimplantation diagnosis for Fanconi anemia combined with HLA matching. *JAMA.* 2001;285(24):3130–3.
5. Kuliev A, Pakhalchuk T, Verlinsky O, Rechitsky S. Preimplantation genetic diagnosis for hemoglobinopathies. *Hemoglobin*. 2011;35(5–6):547–55.

6. Kahraman S, Benkhalifa M, Donmez E, Biricik A, et al. The results of aneuploidy screening in 276 couples undergoing assisted reproductive techniques. *Prenat Diagn.* 2004;24(4):307–11.
7. McArthur SJ, Leigh D, Marshall JT, Gee AJ, et al. Blastocyst trophectoderm biopsy and preimplantation genetic diagnosis for familial monogenic disorders and chromosomal translocations. *Prenat Diagn*. 2008;28(5):434–42.
8. Kahraman S, Beyazyurek C, Ekmekci CG. Seven years of experience of preimplantation HLA typing: A clinical overview of 327 cycles. *Reprod Biomed Online*. 2011;23(3):363–71.
9. Munné S, Sandalinas M, Escudero T, Velilla E, et al. Improved implantation after preimplantation genetic diagnosis of aneuploidy. *Reprod Biomed Online*. 2003;7(1):91–7.
10. Voullaire L, Collins V, Callaghan T, McBain J, et al. High incidence of complex chromosome abnormality in cleavage embryos from patients with repeated implantation failure. *Fertil Steril*. 2007;87(5):1053–8.
11. Hassold T, Hunt P. To err (meiotically) is human: The genesis of human aneuploidy. *Nat Rev Genet*. 2001;2(4):280–91.
12. Baart EB, Martini E, van den Berg I, Macklon NS, et al. Preimplantation genetic screening reveals a high incidence of aneuploidy and mosaicism in embryos from young women undergoing IVF. *Hum Reprod*. 2006;21(1):223–33.
13. Garrisi JG, Colls P, Ferry KM, Zheng X, et al. Effect of infertility, maternal age, and number of previous miscarriages on the outcome of preimplantation genetic diagnosis for idiopathic recurrent pregnancy loss. *Fertil Steril*. 2009;92(1):288–95.
14. Verlinsky Y, Ginsberg N, Lifchez A, Valle J, et al. Analysis of the first polar body: Preconception genetic diagnosis. *Hum Reprod*. 1990;5(7):826–9.
15. Verlinsky Y, Cieslak J, Ivakhnenko V, Evsikov S, et al. Chromosomal abnormalities in the first and second polar body. *Mol Cell Endocrinol*. 2001;183(Suppl 1):S47–9.
16. Christopikou D, Handyside AH. Questions about the accuracy of polar body analysis for preimplantation genetic screening. *Hum Reprod*. 2013;28(6):1732–3.
17. Handyside AH, Montag M, Magli MC, Repping S, et al. Multiple meiotic errors caused by predivision of chromatids in women of advanced maternal age undergoing in vitro fertilisation. *Eur J Hum Genet.* 2012;20(7):742–7.
18. Griffin DK, Handyside AH, Harper JC, Wilton LJ, et al. Clinical experience with preimplantation diagnosis of sex by dual fluorescent in situ hybridization. *J Assist Reprod Genet*. 1994;11(3):132–43.
19. Velilla E, Escudero T, Munné S. Blastomere fixation techniques and risk of misdiagnosis for preimplantation genetic diagnosis of aneuploidy. *Reprod Biomed Online*. 2002;4(3):210–17.
20. Wilton L. Preimplantation genetic diagnosis and chromosome analysis of blastomeres using comparative genomic hybridization. *Hum Reprod Update*. 2005;11(1):33–41.
21. Handyside AH. PGD and aneuploidy screening for 24 chromosomes by genome-wide SNP analysis: Seeing the wood and the trees. *Reprod Biomed Online*. 2011;23(6):686–91.
22. Brezina PR, Benner A, Rechitsky S, Kuliev A, et al. Single-gene testing combined with single nucleotide polymorphism microarray preimplantation genetic diagnosis for aneuploidy: A novel approach in optimizing pregnancy outcome. *Fertil Steril*. 2011;95(5):1786.
23. van Uum CM, Stevens SJ, Dreesen JC, Drüsedau M, et al. SNP array-based copy number and genotype analyses for preimplantation genetic diagnosis of human unbalanced translocations. *Eur J Hum Genet*. 2012;20(9):938–44.
24. Treff NR, Scott RT, Jr. Four-hour quantitative real-time polymerase chain reaction-based comprehensive chromosome screening and accumulating evidence of accuracy, safety, predictive value, and clinical efficacy. *Fertil Steril*. 2013;99:1049–53.
25. Desai AN, Jere A. Next-generation sequencing: Ready for the clinics? *Clin Genet*. 2012;81(6):503–10.
26. Verlinsky Y, Kuliev A. 2000. An Atlas of Preimplantation Genetic Diagnosis. Section 4, 31–39. Parthenon Publishing Group. New York, USA.
27. Abdelhadi I, Colls P, Sandalinas M, Escudero T, et al. Preimplantation genetic diagnosis of numerical abnormalities for 13 chromosomes. *Reprod Biomed Online*. 2003;6(2):226–31.
28. Munné S, Gianaroli L, Tur-Kaspa I, Magli C, et al. Substandard application of preimplantation genetic screening may interfere with its clinical success. *Fertil Steril*. 2007;88(4):781–4.
29. Colls P, Escudero T, Cekleniak N, Sadowy S, et al. Increased efficiency of preimplantation genetic diagnosis for infertility using "no result rescue". *Fertil Steril*. 2007;88(1):53–61.

18

Invasive Techniques: Aneuploidy Testing by Array-CGH

Alan R. Thornhill, Christian Ottolini, Gary Harton, and Darren Griffin

Introduction

Aneuploidy is the term used to describe gross chromosomal imbalance in an organism or embryo, presenting as either additional (e.g., trisomy) or missing (e.g., monosomy) chromosomes. Aneuploidy arises during cell division when chromosomes fail to separate equally between the two new daughter cells [1]. Aneuploidy may be present in all the cells of the body and extra embryonic membranes, or it may be represented in a conceptus having both normal and aneuploid cells (so-called mosaicism). The consequences of aneuploidy constitute a wide phenotypic spectrum from early embryonic arrest to mild infertility, with the best-known being Down syndrome (trisomy 21) and first trimester spontaneous abortion (mostly trisomies and monosomy X). The origins of aneuploidy lie in the meiotic divisions (principally in the ovary) and the early cleavage divisions of the preimplantation embryo. Arising by either nondisjunction, precocious separation of sister chromatids, or anaphase lag [1], the impact of aneuploidy on families can be devastating, for example, when faced with pregnancy loss, stillbirth, or a severely affected child. In all cases, aneuploidy results in an unfavorable outcome for the family in question and is undoubtedly a major contributing factor to the relatively low fecundity of humans compared with other species.

The concept of preimplantation genetic screening (PGS) for aneuploidy in oocytes or preimplantation embryos to both lower the risk of the above-mentioned phenotypic consequences and improve in vitro fertilization (IVF) success rates is not new. Indeed it was proposed alongside the earliest developments of preimplantation genetic diagnosis [2]. The ability to do this effectively has required rapid evolution of diagnostic technologies to combine speed, accuracy, and reliability. To date, only direct analysis of chromosome copy number has been applied clinically because indirect approaches (e.g., metabolomic analysis of embryonic products or detailed morphokinetic analysis using time-lapse imaging technology) have yet to be convincingly associated with aneuploidy incidence.

Explanations for the failure of a fluorescence in situ hybridization (FISH) approach on blastomeres from cleavage-stage embryos to demonstrate a clinical benefit in a large randomized controlled trial [3] and in subsequent trials (see meta-analysis [4]) are well documented [5]. Potential reasons proposed for the reported failure include the safety of biopsy, the importance of low error rates on the diagnostic efficiency of PGS [6], and the need to detect all chromosomes simultaneously for aneuploidy. Notwithstanding the ability now to detect all 24 chromosomes by FISH using successive rounds of hybridization [7], the issues of mosaicism, signal interpretation, clinical trial data, and the development of microarray-based methods for detecting 24 chromosome copy number are now signaling the demise of FISH-based cleavage-stage embryo biopsy approaches to PGS. Microarray-based tests are now the standard, and these tests have been made possible through the advancement of whole-genome amplification (WGA) technology. Despite the undoubtedly superior technical capabilities of array comparative genomic hybridization (aCGH) compared with FISH, and several prospective clinical trials showing benefit and widespread clinical use of aCGH, the policy position regarding PGS among both professional and regulatory bodies is regrettably out of date and refers only to the historic and flawed FISH approach [8,9].

The classical approaches to embryo biopsy for preimplantation genetic diagnosis (polar body, cleavage stage, trophectoderm [10–12] and reviewed in [13]) are all in current clinical application for PGS, with first

polar body (PB1) [14], combined PB1 and second polar body (PB2) [15], and trophectoderm biopsy [16] increasingly finding favor. The more well-established cleavage-stage approach, although once thought to be harmless [17], is now considered to reduce implantation potential, especially when two cells are biopsied [3,18], and should ideally be used only after conducting a cost–benefit analysis. The invasive nature of embryo or oocyte biopsy means that PGS has historically been targeted to specific high-risk patient groups (e.g., advanced maternal age, repeated implantation failure, recurrent pregnancy loss, and elevated sperm aneuploidy levels [common in patients presenting with severe male factor infertility]). More recently, PGS has been used to improve the effectiveness of elective single embryo transfer in good prognosis patients to reduce multiple birth rates while maintaining high success rates [19]. The complex spectrum of chromosome abnormalities in the human preimplantation embryo has yet to be fully described, and diagnostic procedures can be expensive to implement. Moreover, embryo biopsy is invasive; thus, a robust cost–benefit analysis is essential to achieve widespread patient benefit through the use of PGS [20]. This chapter explores the current methodologies used to perform PGS using aCGH and provides a description of alternative and future approaches.

Biopsy Strategies

Several different strategies have been proposed and used to detect aneuploidy using aCGH in oocytes and embryos. The relative merits of each are listed in Table 18.1. PB1 biopsy alone and combined PB1 and PB2 strategies have both been used clinically for PGS. However, it is increasingly evident that PB1 alone has limited applicability for PGS because up to 30% of aneuploidy of maternal origin will not be diagnosed if only PB1 is analyzed [26]. Because precocious separation of sister chromatids appears to be the predominant cause of maternal meiotic aneuploidies [26,27], PB2 must be biopsied to accurately identify all maternal aneuploidies and to ensure even abnormal segregations in PB1 are not corrected in the second meiotic division. The timings of both PB1 and PB2 biopsy are critical to the efficiency of diagnosis. This was relevant when aneuploidy screening using the FISH approach was used [28] and is equally critical when using aCGH [29].

Theoretically, blastocyst-stage biopsy is the optimal stage for aneuploidy screening because it partially negates the problem of mosaicism and gives maximum aneuploidy information from maternal, paternal, and postzygotic events at the latest possible stage of embryo development possible in current in vitro culture systems. In addition, the biopsy of three or more cells virtually eliminates the problem of allelic dropout (ADO) after WGA [30]. Historically, it has been viewed as a downside that embryos may need cryopreservation after trophectoderm biopsy while awaiting genetics results. However, it is becoming increasingly apparent that vitrification is a viable strategy to maintain or even potentially increase live birth rates after biopsy [31]. Furthermore, embryo vitrification may be considered for all PGS cases to overcome logistic issues with sample transportation and diagnostic timings. It should be noted that TE biopsy does not eliminate the problem of mosaicism. Furthermore, it is possible that some embryos failing to reach blastocyst stage in vitro may be viable in vivo [32].

Principles of aCGH

Originally designed for molecular karyotyping of tumor cells [33], CGH is a method whereby the chromosomal genotype of an unknown DNA sample can be inferred according to its relative ability to competitively hybridize with reference DNA of known genotype to either (1) metaphase chromosomes from a karyotypically normal reference male (metaphase CGH) or (2) a series of specified DNA sequences at specified spots or positions on a glass slide (aCGH). A schematic representation of the principles of CGH is shown in Figure 18.1. Like its more time-consuming predecessor, metaphase CGH, which has been used for clinical PGS [34,35], aCGH is a relatively DNA-hungry technique and commonly requires nanogram to microgram amounts of DNA for optimal performance. It is estimated that a single blastomere contains approximately 6 pg of DNA; therefore, it is essential to perform WGA before the aCGH procedure itself. Although aCGH can be performed using either

TABLE 18.1

Advantages and Disadvantages of Different Biopsy Strategies for PGS of Aneuploidy

Biopsy Stage	Advantages	Disadvantages
TE biopsy	Fewer embryos are ultimately tested reducing diagnostic costs. Only the highest quality embryos (suitable for embryo transfer [ET]) are tested. Fresh ET on Day 6 (or Day 7) is possible in many cases. Maternal, paternal, and postzygotic errors can be detected. Multicellular samples result in better amplification rates than single cell and enable detection of mosaicism. Mosaicism may not be major issue for TE biopsy due to low prevalence of mosaic diploid/aneuploid blastocysts and the high detection rate of clinically relevant mosaicism. Aneuploidy detected at the earlier stages may not affect the blastocyst [21,22].	Blastocyst culture potentially not suitable for all patients. Some viable embryos may not reach blastocyst in vitro. Higher "no biopsy" rate compared with PB biopsy and cleavage-stage biopsy. Depending on availability of local diagnostic services, vitrification of all biopsied blastocysts may be required. Significance of mosaicism is unclear.
Cleavage-stage (blastomere) biopsy	Fresh ET from Day 4 onward is possible in many cases. Maternal, paternal, and post zygotic errors detected.	High rates of mosaicism are present in even good-quality cleavage-stage embryos [23]. Inability to distinguish between aneuploidy mosaic and uniformly aneuploid embryos leads to false-positive results and subsequent discard of potentially chromosomally normal viable embryos. Biopsy of one or two cells affects implantation rate [18].
PB biopsy	Removal of PBs from a human oocyte has no deleterious effect on subsequent embryo, fetal, and infant development as neither is required for successful fertilization or embryogenesis [24]. Detection of constitutive embryonic aneuploidies of maternal origin without confounding mosaicism. Majority of patients will have a biopsy. Screening of whole cohort of oocytes provides comprehensive diagnostic information. May be suitable to patients for whom blastocyst culture is typically unsuccessful. Flexibility of fresh ET timing, in many cases from Day 2 onward. High concordance with zygote aneuploidy [14] and cleavage-stage aneuploidy [25].	Biopsy of first and second polar bodies is relatively labor-intensive (many oocytes may not even develop into therapeutic quality embryos). Extensive testing may be expensive. Does not allow the detection of aneuploidies of paternal origin or those arising after fertilization in the embryo.

bacterial artificial chromosome (BAC) DNA clones or specific oligonucleotides across the genome, this chapter focuses on the BAC clone approach because this approach has been validated and used in >300,000 clinical preimplantation genetic samples to date. The current 24Sure™ microarray contains 2900 unique BAC clones spaced approximately 1 Mb apart that have been extensively validated in >2000 postnatal clinical array experiments to exclude copy number polymorphisms. In addition, the exact genomic location of each probe has been confirmed by reverse painting of labeled single chromosome preparations onto arrays, FISH mapping, and sequencing verification. aCGH for preimplantation testing has been pioneered by BlueGnome (Fulbourn, Cambridge, United Kingdom), and all reagents for WGA, labeling, hybridization, washing, reference DNA, microarray slides, and analytical software described below are available from BlueGnome except where noted.

aCGH for Chromosome Enumeration

After egg (PB1, PB2, or both), embryo (cleavage-stage), or blastocyst biopsy, the biopsied material is washed in a buffer, typically phosphate-buffered saline (PBS), with an additive such as polyvinyl alcohol (PVA) to reduce cell stickiness [36]. After washing, the biopsy material is picked up in a very small

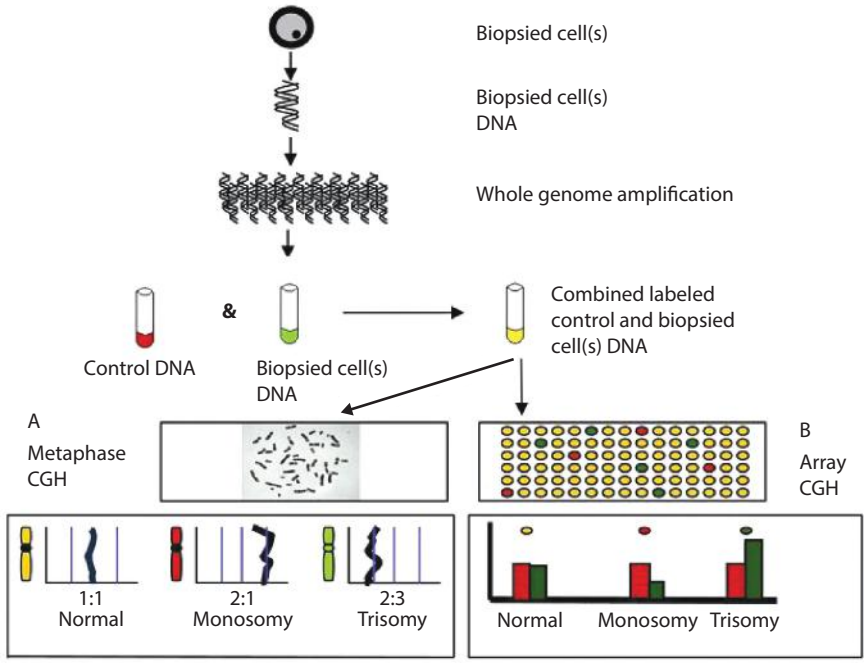

FIGURE 18.1 Schematic of comparative genomic hybridization.

volume (<2 μL) and placed into a sterile 0.2 mL Eppendorf tube for transport to the testing laboratory. A more detailed description of this process is given in Chapter 14. Most laboratories perform a quick centrifugation step to ensure that the cellular material and all of the fluid are collected at the bottom of the tube. Most labs then freeze each sample before transport to the testing lab; however, this is not essential, depending on the length of time the sample will be in transit before further processing. It is very important to note that the mineral oil that is typically used as an overlay on top of biopsy material destined for polymerase chain reaction (PCR) testing should never be used before WGA and aCGH because it inhibits the amplification process.

WGA and Labeling

Several different WGA methods have been used historically for aCGH, with the current, most often used method being SurePlex™ (Rubicon Genomics Inc., Ann Arbor, MI; and BlueGnome). After fragmentation of the sample DNA, self-inert degenerative primers are annealed at multiple sites along the genome. Extension then displaces downstream strands to generate multiple fragments spanning each region. The reaction produces large fragment sizes that are reproducible between samples and that are optimized for aCGH. Many of the other WGA techniques have been adapted for use in aCGH, but they were originally used for other purposes (e.g., single-locus PCR and mutation detection). SurePlex is suitable because of its simple, short protocol; highly representative amplification; and low allele dropout rates. In brief, after sample receipt in the lab, each tube is opened in a dedicated DNA amplification cleanroom, under laminar flow conditions, and the WGA reagents are added (SurePlex kit). Amplification is performed according to the manufacturer's instructions because these kits have been validated using single cells. For SurePlex, there is a 15 min cell lysis (DNA extraction) step, followed by the preamplification steps (90 min), and finally amplification (30 min). All of these steps are performed in a single tube, thereby reducing the likelihood of sample switches and contamination.

In addition, all of these steps require the use of a PCR thermal cycler machine because they are time and temperature dependent. Because the arrays are the most expensive consumable in the process, it is best to ensure amplification before taking the sample further through the process. After amplification, most laboratories run an agarose gel electrophoresis step to confirm amplification. A smear of high-molecular-weight DNA, observed on the gel after electrophoresis, is indicative of positive amplification, and all such samples may be taken forward to the fluorescent labeling steps. Low-molecular-weight DNA, or the absence of any smear, indicates poor or failed amplification. In such cases, it may be prudent to avoid running such samples on the microarrays. Successfully amplified WGA product is labeled through nick translation with either Cy3 (green) or Cy5 (red) fluorescence and purified.

Hybridization

Samples with unknown genotype (i.e., embryo biopsy) labeled in one fluorescent color and control reference DNA (typically a karyotypically normal male) labeled in the opposite color are separately denatured (to render them single stranded) at 74°C before being mixed together in equal proportions in hybridization buffer containing formamide and cot-1 human DNA before adding to each 24Sure microarray. Microarrays are hybridized at 47°C for at least 4 hr or overnight in a humidified chamber. The length of hybridization time varies depending on the number of samples in the lab on any given day, the time samples are received during the day, and the local staffing levels and shift patterns. During validation of the array in the lab, hybridization times as short as 3 hr and as long as 16 hr (overnight) were tested with no differences noted (BlueGnome, unpublished data). On the basis of these results, hybridization for at least 4 hr and no longer than 16 hr is deemed to be interchangeable (Reprogenetics Ltd., unpublished data).

Posthybridization Washing

After hybridization, each microarray is washed as follows: 10 min in 2× standard saline citrate (SSC)/0.05% Tween 20 at room temperature, 10 min in 1× SSC at room temperature, 5 min in 0.1× SSC at 60°C, and 2 min in 0.1× SSC at room temperature to remove unbound DNA.

Scanning

Each microarray slide is scanned using a dual-channel fluorescent laser scanner that creates TIFF images (e.g., ClearScan™, BlueGnome) for green fluorescence at 632 nm and for red fluorescence at 587 nm. Raw images are loaded automatically into BlueFuse™ software allowing for automated evaluation of fluorescent signals (ratio analysis).

Scoring

Each sample is scored by a trained technologist who assesses traces for all 24 chromosomes, noting all gains and losses as well as determining the sex of each sample. A second technologist then scores the sample blindly, with no knowledge of the initial score by the first technologist. A final score for each sample is assigned by comparing the two scores. Any discrepancies are noted and are adjudicated by a third technologist, the laboratory supervisor or director, or both. Single chromatid errors can be distinguished from whole chromosome errors through examination of the mean per-chromosome hybridization ratios (Figure 18.2) [27].

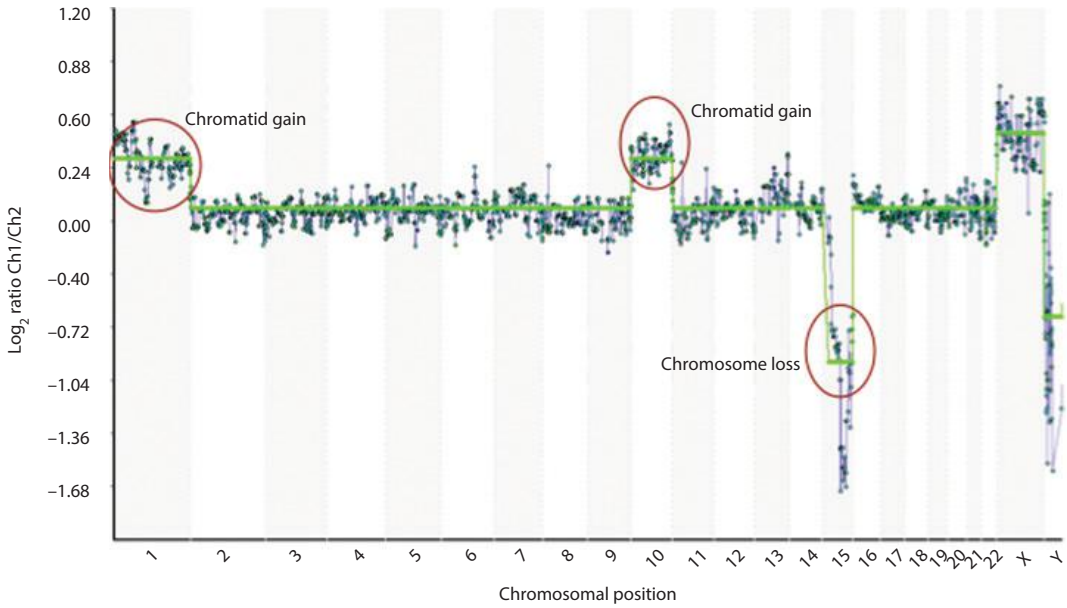

FIGURE 18.2 Determining chromatid versus chromosome loss in first polar body samples by aCGH. For most chromosomes (i.e., not the sex chromosomes or the aneuploid chromosomes), a clear and consistent 1:1 ratio is observed along the chromosome length. Because the polar body sample was cohybridized with male genomic DNA, a hybridization pattern representing a 2:1 ratio for the X chromosome and a "0:2" ratio for the Y chromosome is observed. This polar body clearly shows multiple aneuploidies with chromatid gains on chromosomes 1 and 10 (single chromatid gains are consistent with a 3:2 [or 1.5:1] ratio, i.e., approximately half that of the X chromosome shift) and a loss of whole chromosome 15 (similar to the shift seen for the absent Y chromosome).

Reporting

Once results for all samples from each patient are finalized, a diagnostic report is prepared, signed off by an appropriately qualified person (on site or remotely), and shared with the referring laboratory and physician before embryo transfer [36].

Validation

In extensive validation using single cells from known cell lines against the gold standard of karyotyping, 24Sure demonstrated 98% accuracy. In contrast to the use of cell lines, validation for embryo aneuploidy is difficult. To obtain reliable and robust results, one needs truth data (i.e., samples of known genotype). Although the same is true of human oocytes, in that they are of unknown genotype, the ability to biopsy both the PB1 and PB2 from the oocyte provides the opportunity to obtain relatively robust validation data comparing results from so-called "trios" of both polar bodies and their corresponding oocyte. The expectation is to see reciprocal results (i.e., chromosomal gains and losses) from aneuploid polar body and oocyte (Figure 18.3). The presence of chromosomal mosaicism in human embryos makes it difficult to categorically identify embryos as having a single specific genotype. Thus, from a mosaic embryo, individual single-cell results may appear to be unrepresentative and multicellular results (e.g., from trophectoderm biopsy) potentially difficult to interpret (Figure 18.4) and therefore challenging to make decisions regarding embryo selection.

To date, 24Sure and 24Sure-plus™ arrays have been validated using several different cell types to evaluate both technical and biological performance, some examples of which are listed in Table 18.2. After clinical implementation, it is essential to maintain accuracy and overall quality assurance of the test(s) offered in your laboratory.

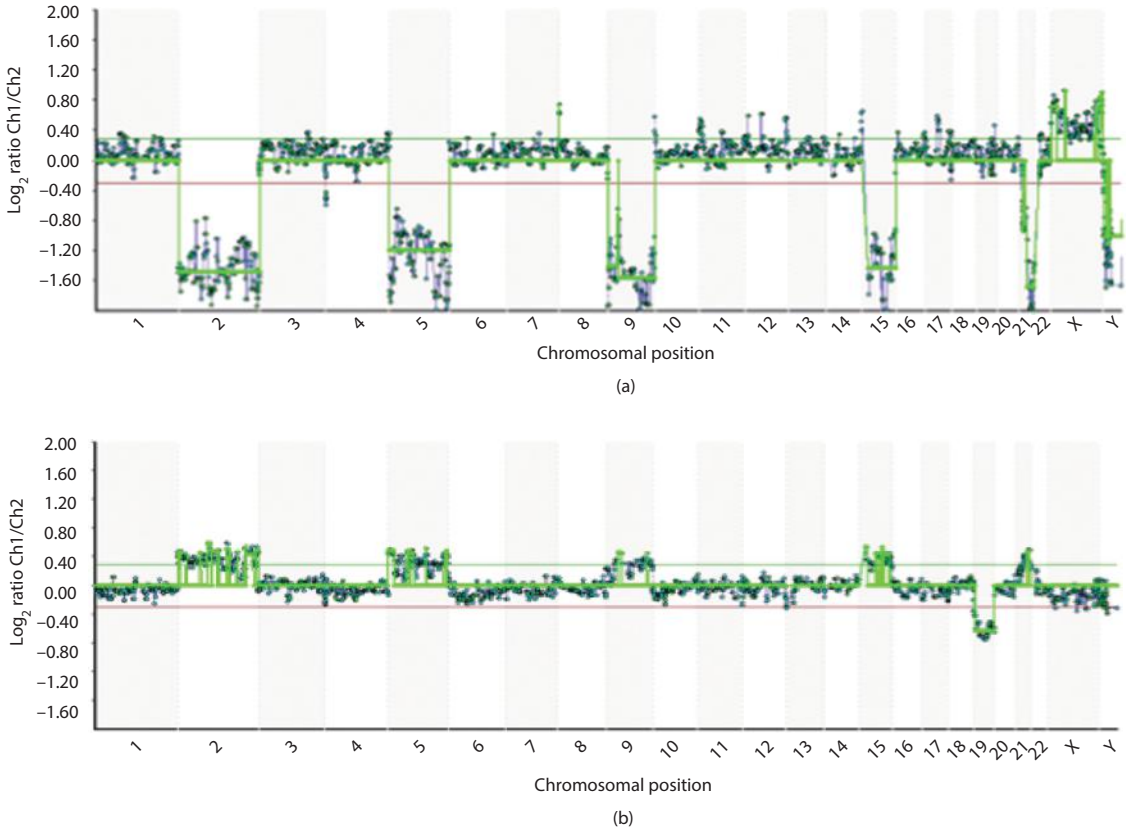

FIGURE 18.3 aCGH trace from second polar body and corresponding oocyte sample. Multiple aneuploidies (gains or losses) detected in (a) the PB2 (–2, –5, –9, –15, and –21) are seen in the reciprocal form in (b) the corresponding oocyte (+2, +5, +9, +15, +21, and also –19). Note the increased amplitude of the signal-to-noise ratio for the oocyte versus the polar body sample. In part, this is due to the quantity and quality of DNA available within the respective cells.

This task is often performed by means of internal quality control measures and external quality assessment (EQA) schemes. The sex chromosomes provide a good internal control by observing the X and Y chromosome deviation from the autosomes within a euploid DNA complement. This level of deviation can be used as a guide to assess aneuploid and euploid positions on the aCGH plot. For EQA, a scheme for single-cell aCGH is currently in development based on earlier single-cell PGD schemes [38], and in many countries such schemes are required for laboratory accreditation and to meet regulatory requirements.

High-Resolution aCGH for Detection of Chromosome Imbalance

Where aCGH is used to detect chromosomal imbalance in embryos derived from couples where at least one partner carries a balanced translocation, an assessment of (1) the likely unbalanced outcomes should be made by a qualified genetics professional and (2) the likely size of all unbalanced products should be performed. A prediction tool (available from BlueGnome) can be used to ensure the microarray has sufficient resolution to detect all potential products. For example, the current version of 24Sure-plus contains 4800 BAC clones and claims to be able to accurately detect products as small as 10 Mb (with possible detection to the 2.5 Mb resolution level in regions with good clone coverage). The protocol for use of 24Sure-plus is essentially the same as for 24Sure, with the primary difference being the higher resolution microarray slide used in

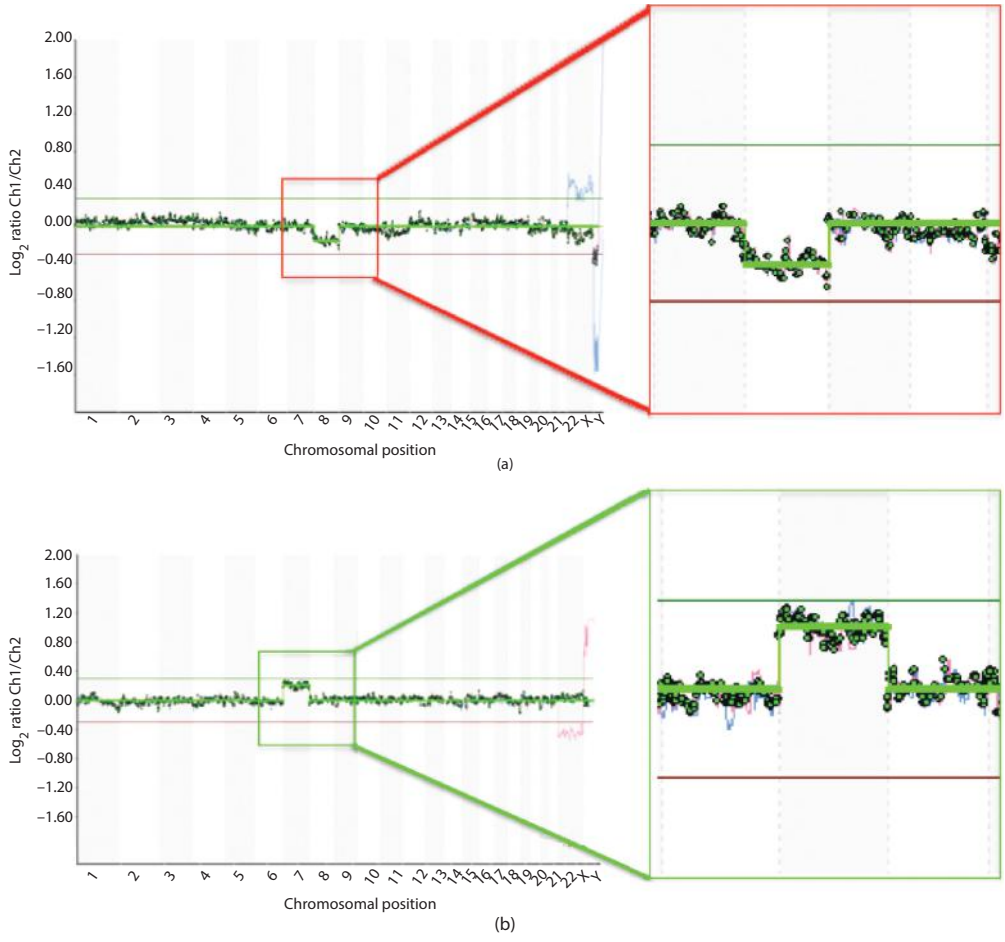

FIGURE 18.4 Detection of mosaicism in trophectoderm samples using aCGH. Trophectoderm samples from two different blastocysts show likely chromosomal mosaicism as follows: (a) euploid female except for mosaic monosomy 8 and (b) euploid male except for mosaic trisomy 7. Mosaicism is suspected because the signals for the remaining chromosomes are relatively uniform and the $\log_2$ ratio shift is uniform along the length of the chromosome but does not exceed the threshold (bottom red and top green line, respectively) required to call as a uniform aneuploidy. It is unclear whether the presence of these cells identifies this embryo as chromosomally abnormal and potentially nonviable for this reason. Note the generally high signal-to-noise ratio for this multicellular sample compared with that seen for polar body samples in Figure 18.2. (Data courtesy of Dr. Francesco Fiorentino, Genoma Laboratories, Rome, Italy.)

the 24Sure-plus test. Aside from improved accuracy and effectively eliminating the need to provide couple-specific test development, an additional benefit of using aCGH for translocation carriers is the simultaneous detection of aneuploidy for all the other chromosomes not involved in the translocation [39]. An example of the array trace showing reciprocal gains and losses in the predicted chromosomes (involved in the translocation) is shown in Figure 18.5.

Limitations of aCGH

aCGH is highly accurate (98%), and in competent hands it delivers a 98% result rate. Despite its proven accuracy, aCGH has clinically relevant limitations in the field of preimplantation genetics. For example, it cannot

TABLE 18.2

Formal Preclinical Validation of 24Sure BAC Microarrays

Cell/Sample Type	Known Genotype	Accuracy of aCGH Diagnosis (%)
Blinded euploid/aneuploid ovarian carcinoma cell lines (single cells) (Dr. Joyce Harper, UCL Centre for PGD, Personal Communication)	Various aneuploid lines	51/51 (100)
Blinded aneuploidic cell lines (single cells) (BlueGnome, unpublished data)	45, X; 47, XY +13; 47, XY +21; 47, XYY; 47, XXY	118/121 (98)
Human embryonic blastomeres (reanalyzed embryos) [37]	Various genotypes established by 12-color FISH	53/54 (98)
Human oocytes and polar bodies [15]	Various genotypes deduced by reciprocity between PB1/2 and corresponding oocyte	90% concordance in 226 trios (PB1/2 and oocyte)

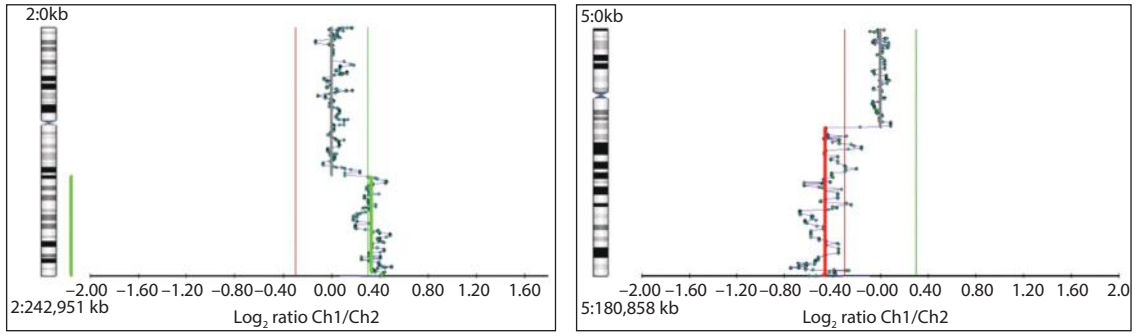

FIGURE 18.5 Detection of partial aneuploidies in embryonic samples from a reciprocal translocation carrier, t(2;5)(q21;q31), using array CGH. Embryos from reciprocal translocation carriers can be used to validate 24Sure detection of segmental aneuploidies because each affected embryo will have segmental aneuploidies based at two specific breakpoints. Detecting gains (chromosome 2q) and losses at these two specific breakpoints internally validates the accuracy of the test. In this case, one parent carried the translocation t(2;5)(q21;q31), resulting in gains and losses (chromosome 5q) of chromosomal material in the single blastomeres of affected embryos. Even though the deletion/duplications can be relatively small, the combination of a higher resolution microarray, known breakpoints, and their predicted meiotic products and a multicellular sample makes it relatively straightforward to detect reliably.

discriminate between maternal and paternal errors. Nor can it distinguish between meiotic and mitotic errors of chromosome segregation. For the purposes of the cycle in which the testing is being done, this is not so relevant. However, such additional information may provide clues as to how to treat the patient in the future. Finally, because aCGH is a method predicated on high-quality DNA and successful hybridization, the possibility exists that borderline results could be miscalled (as with FISH).

Future Opportunities

Although aCGH has become the gold standard for direct chromosome enumeration in embryos and oocytes, there are alternatives available. As with all competing technologies, there are advantages and disadvantages to each [40,41]. Comprehensive chromosomal screening using multiplex quantitative fluorescent PCR [42] may provide a cheaper alternative, but it is not currently commercially available, thereby restricting its use. Aneuploidy can also be detected with single-nucleotide polymorphism (SNP) arrays using a combination of loss of heterozygosity (monosomy), quantitation of specific SNP loci, and incongruous SNP calls compared with predicted Mendelian results with parental information that are incompatible with normal disomy [43–47]. Next generation

sequencing (NGS) promises to supersede all other methodologies [41], but currently it is cheaper than array-based methods only if large numbers of samples are processed simultaneously. At this time, NGS solutions are not commercially available.

Noninvasive Indirect Methods of Determining Aneuploidy

Weak correlations exist between the presence of embryonic aneuploidy and morphological aspects of embryo development after retrospective analysis [48,49]. Such findings have stimulated the field of morphokinetic analysis of embryos in an attempt to identify aneuploidy in a real-time clinical setting. Time-lapse imaging and analysis appear to demonstrate that morphological features and developmental timings of the embryo have some relationship to aneuploidy, with an algorithm based on the onset and duration of blastulation correlating well with implantation rates [50,51]. This finding, if confirmed in larger data sets and with appropriate subgroup analysis stratified by maternal age, provides some useful prioritization criteria but cannot, at present, replace the specificity and accuracy of aneuploidy testing using aCGH. Another promising morphokinetic approach is to assess dynamic fragmentation patterns within early embryos; but again, it currently does not identify specific aneuploidies and cannot be regarded as a threat to direct genetic analysis [52]. Indeed, to date, no morphokinetic parameter has been observed to discriminate between euploid and simple aneuploid (e.g., trisomy 21) embryos. Moreover, although there have been some useful predictors of viability related to specific metabolites, none so far has been linked specifically to aneuploidy rather than viability or been able to differentiate between general chromosomal aneuploidy and specific aneuploidy [53,54].

Summary and Essentials

At present, aCGH is considered the gold standard for detecting aneuploidy in single cells or multicellular samples from oocytes and embryos because of its reliability, reproducibility, and accuracy and the large worldwide experience with it. It is possible to obtain results within 12 hr after biopsy, making it accessible to most laboratories regardless of the biopsy stage selected. Although there remains some controversy over the benefit of PGS for specific patient indications, there appears to be a recent shift toward trophectoderm (multicellular) biopsy of the highest quality embryos from good prognosis patients in contrast to the historic focus on cleavage-stage biopsy of few, poor-quality embryos in poor prognosis patients. Irrespective of the approach taken, the following tips should be considered critical for effective use of this technology.

Quality of the IVF Laboratory

Overall quality of the IVF program is critical. Whenever an oocyte or embryo is subjected to a procedure outside of the incubator, there is a risk involved. Thus, a fundamental principle underpinning the use of aneuploidy screening is that the benefit gained should outweigh the harm, if any, caused. Thus, if the success rates of the program are already suboptimal, it is difficult to see any procedure providing sufficient benefit to rescue the cycle.

Embryo biopsy

Embryo biopsy has become simpler with the availability of the noncontact infrared laser that is common in many IVF laboratories (see Chapters 14 and 15). With this laser, it is relatively simple to perform oocyte or embryo biopsy, in many cases without apparent damage to the subject. However, after indiscriminate use,

invisible thermal damage might be caused that, although not immediately lethal, could have later consequences, compromising development and subsequent implantation. For this reason, it is vital to perform the embryo biopsy as quickly as possible with minimal exposure to laser energy to complete the task safely and effectively. The issue of embryo selection for biopsy is not straightforward because there is inevitably a balance between the cost and efficacy of biopsying all embryos in the cohort against the need for all information and the small chance that apparently delayed embryos (either at cleavage or blastocyst stages) may still have some implantation potential.

Sample Preparation and Transportation

Proper preparation of the biopsied sample, although mundane, is of critical importance. Focus on the sterility of the working area and solutions; precise volume of buffer in the microcentrifuge tube, with minimal carryover of embryo culture medium, which can reduce amplification efficiency; and subsequent storage of the sample preanalysis is paramount to ensure high diagnostic success rates. Particular care must be taken not to contaminate the sample with foreign DNA by means of good laboratory practice and appropriate apparel and dedicated cleanroom, equipment, and consumables for amplification steps. A negative control of the embryo media and collection buffer should always be taken at this point to check for the absence of contamination because aCGH is not able to identify the origin of any contamination. Although published protocols exist and diagnostic service laboratories generally provide their own standard operating procedures, a series of laboratory-specific validation experiments are extremely useful before offering the service clinically.

Whole-Genome Amplification

Many different methods are available and have been reported for use in preimplantation genetic testing. However, the specifications of the amplified DNA optimal for aCGH are DNA fragments of a specific size corresponding to the specific array type. For 24Sure BAC arrays, SurePlex (a PCR-based method) is used in preference to multiple displacement amplification (MDA).

aCGH Procedure

Hybridization is fairly robust but care should be taken to ensure microarray slides do not dry out before washing. The high-temperature, high-stringency wash posthybridization must be temperature controlled. Lower temperatures prevent the removal of nonspecific-labeled DNA from the array and generate noisy results. If the temperature is too high, too much of the labeled DNA will be stripped from the array and could result in too few probes per chromosome to accurately call the result, particularly for smaller chromosomes. Drying of the microarray slides is also critical; the most effective way is to mechanically remove wash buffer by centrifugation. If wash buffer is left to dry on the slides, it fluoresces and will reduce data quality. After drying, slides should be scanned immediately because in some circumstances the fluorescent dyes can be degraded by atmospheric ozone. Although the software is highly accurate, a combination of both automated and manual calling of results is recommended.

Target Population for Testing

Regardless of the testing method used, it is important to properly identify the appropriate patients who would benefit from the test. Indications for testing vary widely, and it is crucial for both providers and patients to understand the difference between using the test to provide diagnostic information (e.g., in the case where

there are very few embryos present but they are highly likely to be grossly aneuploidy) or information to enable selection of euploid embryos (e.g., to improve the likelihood of success in that embryo transfer cycle). Essentially, in the absence of comprehensive prospective randomized controlled clinical trials for each putative indication for PGS, clinics must conduct a cost–benefit exercise weighing the potential prognostic (selection) and diagnostic (closure or alternative therapy) benefits against the financial cost to the patient and biological cost to the biopsied embryo [20].

REFERENCES

1. Hassold T, and Hunt P. (2001). To err (meiotically) is human: The genesis of human aneuploidy. *Nat Rev Genet* **2**, 280–91.
2. Penketh R, and McLaren A. (1987). Prospects for prenatal diagnosis during preimplantation human development. *Baillieres Clin Obstet Gynaecol* **1**(3), 747–64.
3. Mastenbroek S, Twisk M, van Echten-Arends J, Sikkema-Raddatz B, Korevaar JC, Verhoeve HR, et al. (2007). In vitro fertilization with preimplantation genetic screening. *N Engl J Med* **357**, 9–17.
4. Mastenbroek S, Twisk M, van der Veen F, and Repping S. (2011). Preimplantation genetic screening: A systematic review and meta-analysis of RCTs. *Hum Reprod Update* **17**(4), 454–66.
5. Cohen J, and Grifo JA. (2007). Multicentre trial of preimplantation genetic screening reported in the New England Journal of Medicine: An in-depth look at the findings. *Reprod Biomed Online* **15**, 365–6.
6. Summers MC, and Foland AD. (2009). Quantitative decision-making in preimplantation genetic (aneuploidy) screening (PGS). *J Assist Reprod Genet* **26**, 487–502.
7. Ioannou D, Fonseka KGL, Meershoek EJ, Thornhill AR, Abogrein A, Ellis M, et al. (2012). Twenty four chromosome FISH in human IVF embryos reveals patterns of post-zygotic chromosome segregation and nuclear organization. *Chromosome Res* **20**, 447–60.
8. Anderson RA, and Pickering S. (2008). The current status of preimplantation genetic screening: British Fertility Society Policy and Practice Guidelines. *Hum Fertil (Camb)* **11**, 71–5.
9. American Society of Reproductive Medicine (ASRM) Practice Committee. (2008). Preimplantation genetic testing: A Practice Committee opinion. *Fertil Steril* **90**, S136–43.
10. Magli MC, Gianaroli L, Ferraretti AP, Toschi M, Esposito F, and Fasolino MC. (2004). The combination of polar body and embryo biopsy does not affect embryo viability. *Hum Reprod* **19**, 1163–9.
11. Cieslak-Janzen J, Tur-Kaspa I, Ilkevitch Y, Bernal A, Morris R, and Verlinsky Y. (2006). Multiple micromanipulations for preimplantation genetic diagnosis do not affect embryo development to the blastocyst stage. *Fertil Steril* **85**, 1826–9.
12. Kokkali G, Traeger-Synodinos J, Vrettou C, Stavrou D, Jones GM, Cram DS, et al. (2007). Blastocyst biopsy versus cleavage stage biopsy and blastocyst transfer for preimplantation genetic diagnosis of beta-thalassaemia: A pilot study. *Hum Reprod* **22**, 1443–9.
13. Thornhill AR, Ottolini C, and Handyside AH. (2012). Human embryo biopsy procedures. In *Textbook of Assisted Reproductive Technologies,* 4th edn. (eds. Gardner DK, Howles CM, Weissman A, and Shoham Z). London, UK: Informa Healthcare, pp. 197–211.
14. Wells D, Escudero T, Levy B, Hirschhorn K, Delhanty JD, and Munne S. (2002). First clinical application of comparative genomic hybridization and polar body testing for preimplantation genetic diagnosis of aneuploidy. *Fertil Steril* **78**, 543–9.
15. Geraedts J, Montag M, Magli MC, Repping S, Handyside A, Staessen C, et al. (2011). Polar body array CGH for prediction of the status of the corresponding oocyte. Part I: Clinical results. *Hum Reprod* **26**(11), 3173–80.
16. Schoolcraft WB, Fragouli E, Stevens J, Munne S, Katz-Jaffe MG, and Wells D. (2010). Clinical application of comprehensive chromosomal screening at the blastocyst stage. *Fertil Steril* **94**, 1700–6.
17. Hardy K, Martin KL, Leese HJ, Winston RM, and Handyside AH. (1990). Human preimplantation development in vitro is not adversely affected by biopsy at the 8-cell stage. *Hum Reprod* **5**, 708–14.
18. Cohen J, Wells D, and Munne S. (2007). Removal of 2 cells from cleavage stage embryos is likely to reduce the efficacy of chromosomal tests that are used to enhance implantation rates. *Fertil Steril* **87**, 496–503.
19. Yang Z, Liu J, Collins GS, Salem SA, Liu X, Lyle SS, et al. (2012). Selection of single blastocysts for fresh transfer via standard morphology assessment alone and with array CGH for good prognosis IVF patients: Results from a randomised pilot study. *Mol Cytogenet* **5**, 24.

20. Ottolini C, Griffin DK, and Thornhill AR. (2012). The role of aneuploidy screening in human preimplantation embryos. In *Aneuploidy in Health and Disease* (ed. Storchova Z). InTech. ISBN 978-953-51-0608-1, pp. 217–44.
21. Capalbo A, Bono S, Spizzichino L, Biricik A, Baldi M, Colamaria S, et al. (2013). Sequential comprehensive chromosome analysis on polar bodies, blastomeres and trophoblast: Insights into female meiotic errors and chromosomal segregation in the preimplantation window of embryo development. *Hum Reprod* **28**(2), 509–18.
22. Capalbo A, Wright G, Elliott T, Ubaldi FM, Rienzi L, and Nagy ZP. (2013). FISH reanalysis of inner cell mass and trophectoderm samples of previously array-CGH screened blastocysts shows high accuracy of diagnosis and no major diagnostic impact of mosaicism at the blastocyst stage. *Hum Reprod* **28**(8), 2298–307.
23. Mertzanidou A, Wilton L, Cheng J, Spits C, Vanneste E, Moreau Y, et al. (2013). Microarray analysis reveals abnormal chromosomal complements in over 70% of 14 normally developing human embryos. *Hum Reprod* **28**(1), 256–64.
24. Gianaroli L. (2000). Preimplantation genetic diagnosis: Polar body and embryo biopsy. *Hum Reprod* **15**(Suppl 4), 69–75.
25. Christopikou D, Tsorva E, Economou K, Shelley P, Davies S, Mastrominas M, et al. (2013). Polar body analysis by array comparative genomic hybridization accurately predicts aneuploidies of maternal meiotic origin in cleavage stage embryos of women of advanced maternal age. *Hum Reprod* **28**(5), 1426–34.
26. Handyside AH, Montag M, Magli MC, Repping S, Harper J, Schmutzler A, et al. (2012). Multiple meiotic errors caused by predivision of chromatids in women of advanced maternal age undergoing in vitro fertilisation. *Eur J Hum Genet* **20**(7), 742–7.
27. Gabriel AS, Thornhill AR, Ottolini CS, Gordon A, Brown AP, Taylor J, et al. (2011). Array comparative genomic hybridisation on first polar bodies suggests that non-disjunction is not the predominant mechanism leading to aneuploidy in humans. *J Med Genet* **48**, 433–7.
28. Verlinsky Y, Cieslak J, Freidine M, Ivakhnenko V, Wolf G, Kovalinskaya L, et al. (1996). Polar body diagnosis of common aneuploidies by FISH. *J Assist Reprod Genet* **13**, 157–62.
29. Magli MC, Montag M, Koster M, Muzi L, Geraedts J, Collins J, et al. (2011). Polar body array CGH for prediction of the status of the corresponding oocyte. Part II: Technical aspects. *Hum Reprod* **26**(11), 3181–5.
30. Ling J, Zhuang G, Tazon-Vega B, Zhang C, Cao B, Rosenwaks Z, et al. (2009). Evaluation of genome coverage and fidelity of multiple displacement amplification from single cells by SNP array. *Mol Hum Reprod* **15**, 739–47.
31. Schoolcraft WB, and Katz-Jaffe MG. (2013). Comprehensive chromosome screening of trophectoderm with vitrification facilitates elective single-embryo transfer for infertile women with advanced maternal age. *Fertil Steril* **100**(3), 615–19.
32. Glujovsky D, Blake D, Farquhar C, and Bardach A. (2012). Cleavage stage versus blastocyst stage embryo transfer in assisted reproductive technology. *Cochrane Database Syst Rev* **7**, CD002118.
33. Kallioniemi A, Kallioniemi OP, Sudar D, Rutovitz D, Gray JW, Waldman F, et al. (1992). Comparative genomic hybridization for molecular cytogenetic analysis of solid tumors. *Science* **258**, 818–21.
34. Voullaire L, Slater H, Williamson R, and Wilton L. (2000). Chromosome analysis of blastomeres from human embryos by using comparative genomic hybridization. *Hum Genet* **106**, 210–17.
35. Wells D, and Delhanty JD. (2000). Comprehensive chromosomal analysis of human preimplantation embryos using whole genome amplification and single cell comparative genomic hybridization. *Mol Hum Reprod* **6**, 1055–62.
36. Harton GL, Magli MC, Lundin K, Montag M, Lemmen J, Harper JC, et al. (2011). ESHRE PGD Consortium/Embryology Special Interest Group—best practice guidelines for polar body and embryo biopsy for preimplantation genetic diagnosis/screening (PGD/PGS). *Hum Reprod* **26**(1), 41–6.
37. Gutierrez-Mateo C, Colls P, Sanchez-Garcia J, Escudero T, Prates R, Ketterson K, et al. (2011). Validation of microarray comparative genomic hybridization for comprehensive chromosome analysis of embryos. *Fertil Steril* **95**, 953–8.
38. Deans Z, Fiorentino F, Biricik A, Traeger-Synodinos J, Moutou C, De Rycke M, et al. (2013). The experience of 3 years of external quality assessment of preimplantation genetic diagnosis for cystic fibrosis. *Eur J Hum Genet* **21**(8), 800–6.
39. Alfarawati S, Fragouli E, Colls P, and Wells D. (2011). First births after preimplantation genetic diagnosis of structural chromosome abnormalities using comparative genomic hybridization and microarray analysis. *Hum Reprod* **26**, 1560–74.

40. Bisignano A, Wells D, Harton G, and Munné S. (2011). PGD and aneuploidy screening for 24 chromosomes: Advantages and disadvantages of competing platforms. *Reprod Biomed Online* **23**(6), 677–85.
41. Handyside AH. (2013). 24–chromosome copy number analysis: A comparison of available technologies. *Fertil Steril* **100**(3), 595–602.
42. Treff NR, Tao X, Ferry KM, Su J, Taylor D, and Scott RT, Jr. (2012). Development and validation of an accurate quantitative real-time polymerase chain reaction-based assay for human blastocyst comprehensive chromosomal aneuploidy screening. *Fertil Steril* **97**(4), 819–24.
43. Handyside AH, Harton GL, Mariani B, Thornhill AR, Affara N, Shaw MA, et al. (2010). Karyomapping: A universal method for genome wide analysis of genetic disease based on mapping crossovers between parental haplotypes. *J Med Genet* **47**, 651–8.
44. Johnson DS, Gemelos G, Baner J, Ryan A, Cinnioglu C, Banjevic M, et al. (2010). Preclinical validation of a microarray method for full molecular karyotyping of blastomeres in a 24-h protocol. *Hum Reprod* **25**, 1066–75.
45. Treff NR, Su J, Tao X, Levy B, and Scott RT, Jr. (2010). Accurate single cell 24 chromosome aneuploidy screening using whole genome amplification and single nucleotide polymorphism microarrays. *Fertil Steril* **94**, 2017–21.
46. Gabriel AS, Hassold TJ, Thornhill AR, Affara NA, Handyside AH, and Griffin DK. (2011). An algorithm for determining the origin of trisomy and the positions of chiasmata from SNP genotype data. *Chromosome Res* **19**, 155–63.
47. Brezina PR, Benner A, Rechitsky S, Kuliev A, Pomerantseva E, Pauling D, et al. (2011). Single-gene testing combined with single nucleotide polymorphism microarray preimplantation genetic diagnosis for aneuploidy: A novel approach in optimizing pregnancy outcome. *Fertil Steril* **95**, 1786.e5–8.
48. Munne S. (2006). Chromosome abnormalities and their relationship to morphology and development of human embryos. *Reprod Biomed Online* **12**, 234–53.
49. Alfarawati S, Fragouli E, Colls P, Stevens J, Gutierrez-Mateo C, Schoolcraft WB, et al. (2011). The relationship between blastocyst morphology, chromosomal abnormality, and embryo gender. *Fertil Steril* **95**, 520–4.
50. Campbell A, Fishel S, Bowman N, Duffy S, Sedler M, and Hickman CF. (2013). Modelling a risk classification of aneuploidy in human embryos using non-invasive morphokinetics. *Reprod Biomed Online* **26**(5), 477–85.
51. Campbell A, Fishel S, Bowman N, Duffy S, Sedler M, and Thornton S. (2013). Retrospective analysis of outcomes after IVF using an aneuploidy risk model derived from time-lapse imaging without PGS. *Reprod Biomed Online* **27**(2), 140–6.
52. Chavez S, Loewke K, Han J, Moussavi F, Colls P, Munne S, et al. (2012). Dynamic blastomere behaviour reflects human embryo ploidy by the four-cell stage. *Nature Comm* **3**, 1251.
53. Picton HM, Elder K, Houghton FD, Hawkhead JA, Rutherford AJ, Hogg JE, et al. (2010). Association between amino acid turnover and chromosome aneuploidy during human preimplantation embryo development in vitro. *Mol Hum Reprod* **16**, 557–69.
54. McReynolds S, Vanderlinden L, Stevens J, Hansen K, Schoolcraft WB, and Katz-Jaffe MG. (2011). Lipocalin-1: A potential marker for noninvasive aneuploidy screening. *Fertil Steril* **95**, 2631–3.

19

Summary: Comprehensive Summary of Main Points by Topic

Markus Montag

This chapter contains the key points and images from the preceding chapters for ease of quick reference.

Chapter 1: Handling Gametes and Embryos: Sperm Collection and Preparation Techniques

Verena Nordhoff, Con Mallidis, and Sabine Kliesch

The analysis of a semen sample is crucial for the treatment decision in an assisted reproduction technique (ART) and should be performed in the following order:

- Liquefaction
- Record of volume and appearance
- Measurement of the pH
- Motility assessment
- Identification of aggregation or agglutination
- Determination of vitality
- Evaluation of concentration and morphology

The right technique for sperm preparation can be determined only after appropriate analysis of the native semen sample. For ART, sperm preparation should select the most motile and morphologically normal spermatozoa.

The most common preparation techniques are as follows:

- Simple washing
- Swim-up
- Density-gradient centrifugation

Semen samples that possess sperm with parameters within the normal range are processed primarily by swim-up; samples with lower concentrations benefit from density-gradient centrifugation preparation.

Swim-up does not provide as high recovery rates as gradient centrifugation, but it is quick and easy to perform, and yields a population enriched with the best motile spermatozoa. Gradient centrifugation results in the retrieval of high numbers of motile spermatozoa; however, standardization of the method is difficult due to the inherent variation of semen samples.

Testicular or epididymal spermatozoa can be retrieved using standard surgical techniques. Sperm retrieval rates from testicular tissue depend on the surgical technique applied and the status of the testis and its underlying spermatogenic state. In cases of obstructive azoospermia, high retrieval rates are achieved. The method of choice for surgical sperm retrieval in nonobstructive azoospermia is a microsurgical method wherein focal areas with spermatogenic activity are selected. In nonobstructive cases where spermatogenic abnormalities are the expected cause, spermatozoa retrieval might be laborious and time-consuming and should always be handled with care.

TABLE 1.1

Comparison of Different Sperm Preparation Techniques

	Type of Ejaculate Quality	Pros	Cons
Washing (W)	Normozoospermia	Quick-and-easy technique Yields high numbers of spermatozoa	Only for sperm counts with high sperm numbers Not useful for samples with contamination with other cells, debris, or blood cells
Swim-up (SU)	Normozoospermia Moderate OAT	Quick and easy to perform High rates of highly progressive motile spermatozoa	Lower recovery rates compared with DG
Density gradient (DG)	Moderate-to-severe OAT	High numbers of motile spermatozoa Best removal of debris or other cell types occurring in the semen sample	Difficult to standardize High-molecular-weight compounds of unknown influence Costs more because DG solutions have to be purchased

Chapter 2: Handling Gametes and Embryos: Oocyte Collection and Embryo Culture

Lars Johansson

Oocyte retrieval should be performed in a way that avoids damaging the oocyte via too strong aspiration and exposure to suboptimal temperature.

Prepare only one dish at a time if microdrop cultures are to be used and avoid repeated retrieval of culture media from the vial or flask.

Use embryo-tested material for all steps.

The optimal temperature must be checked at the location of the oocyte (e.g., in a dish, tube).

Work fast, concentrate, and avoid too long exposure of cumulus–oocyte complex (COC)/oocytes to the environment.

Control and maintenance of proper pH and temperature are key to success.

TABLE 2.1

Classification of Cumulus Oophorous Complexes

Quality	Cumulus	Corona	Oocyte
Immature (I) (Figure 2.8)	Small, compact, grey, non-expanded	Dark ring around the zona pellucida	Not visible, if visible GV stage
Mature (M) (Figure 2.9–2.11)	Small, bright, expanded	Not fully radiated	Partially visible
Excellent (E) (Figure 2.12–2.13)	Large, bright, expanded	Radiated	Clear and visible
Overmature (O) (Figure 2.14–2.15)	Small, thin, patches of dark cells.	Light or dark	Visible, granular and dark
Atretic (A)	Patches of dark cells or absent	None or clumps	Dark

TABLE 2.2

Classification of Oocyte Maturational Stages

Stage	Polar Body	Nucleus
Germinal vesicle (GV)	None	Large halo with nucleoli
Meiosis I (MI)	None	None
Meiosis II (MII)	Present	None

TABLE 2.3

Timing of Procedures in Relationship to Injection of HCG (hpHCG)

Procedure	Egg Collection	Oocyte Vitrification	Insemination (IVF)	Denudation	ICSI
hpHCG	36–38	38–40	40–41	40–41	41–42

Chapter 3: Handling Gametes and Embryos: Quality Control for Culture Conditions

Jason E. Swain

- When optimizing in vitro fertilization (IVF) results in the laboratory, the devil is in the details.
- Poor air quality in the lab can compromise embryo development and outcome, but air quality in the incubator should also be addressed.
- CO_2 measurement is a poor substitute for actually measuring pH.

Proper quality control (QC) is essential to optimize function of the IVF lab and to maximize reproductive outcomes. Although purchasing of high-quality materials and equipment can aid improving culture conditions, proper oversight and implementation are crucial. Despite having the same equipment and media in place, two laboratories can have dramatically different outcomes because several variables within the culture system are controlled directly within the individual lab. Examples include pH, osmolality, air quality, and incubator workflow. However, another variable that needs to be examined includes variation between technicians to ensure consistency in lab practices and approaches. This applies not only to procedures, such as embryo grading, intracytoplasmic sperm injection (ICSI), or catheter loading but also to how daily QC readings are taken, how QC assays are performed, and how media and dishes are prepared. Subtle deviations may introduce an environmental stressor into the culture system or miss a slight variation that could affect outcome.

TABLE 3.1

Recommended Monitoring and Filter Exchange Schedules to Maintain or Improve IVF Lab Air Quality

Equipment	Recommended Maintenance
Heating, ventilating, and air-conditioning (HVAC)/air handler (positive pressure, if present)	Confirm daily
HVAC/air handler (HEPA filters, charcoal/permanganate filters)	Replace 3–6 months or as needed
Incubator HEPA filters	Replace 6–12 months
Incubator/gas line VOC filters	Replace 3–6 months
Laminar flow hood prefilters	Replace or clean annually or as needed
Laminar flow hood (flow rate inspection)	Inspect annually
Lab air quality assessment (particle counts, VOC levels)	Inspect annually

Note: Lab air exchange rates may be modified to improve certain variables, such as particle counts. Additional maintenance may be required to maintain air quality if other systems are in place (i.e., UV photocatalytic oxidation).

Chapter 4: Morphological Selection of Gametes and Embryos: Sperm

Pierre Vanderzwalmen, Magnus Bach, Olivier Gaspard, Bernard Lejeune, Anton Neyer, Françoise Puissant, Maximilian Schuff, Astrid Stecher, Sabine Vanderzwalmen, Barbara Wirleitner, and Nicolas H. Zech

Optimized sperm selection techniques are important in the era of ICSI because ICSI does bypass the natural barriers of conception. The introduction of intracytoplasmic morphologically selected sperm injection (IMSI) made embryologists aware that in times of ICSI, the selection of sperm has to be given proper attention.

The type of spermatozoa selected for injection influences the outcome in terms of embryo development, pregnancy, miscarriage, and malformation.

Large vacuoles reflect a pathological situation, probably correlated with sperm chromatin immaturity.

Practical and technical aspects of sperm selection need to be considered to facilitate the workflow while performing IMSI. In particular, a proper setup of the dish for selecting and capturing sperm facilitates the routine application of IMSI.

The application of IMSI leads to more and better quality blastocysts, and as a consequence, it increases the chance to select the proper embryo for transfer with the highest implantation potential.

A lot of questions are still pending and unclear:

(1) The terminology of vacuoles, their classification, and their location on the sperm head and their origin and formation

(2) The application of motile-sperm organelle-morphology examination (MSOME)–IMSI for specific indications such as teratozoospermia or to a large population

(3) The application of IMSI instead of IVF in cases of unexplained infertility

(4) The oocyte repairing factors

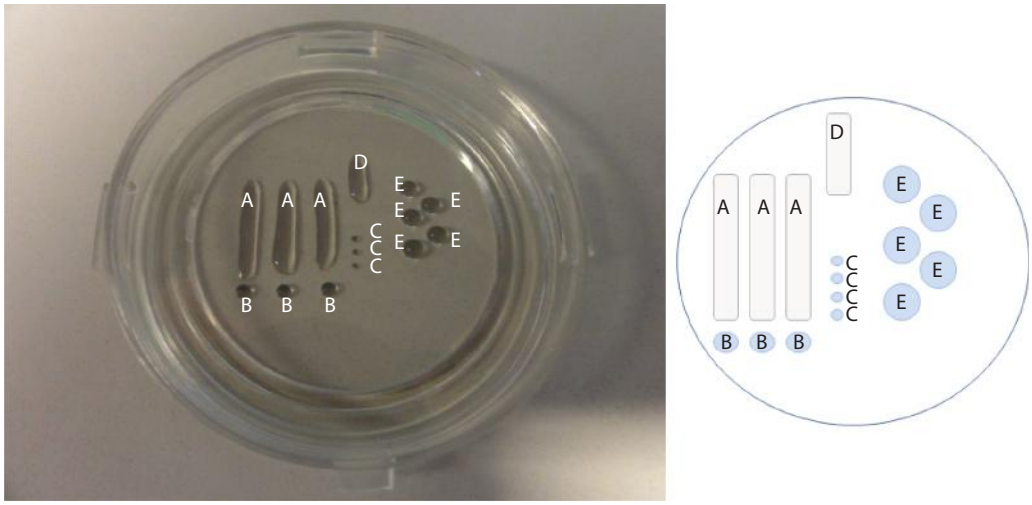

FIGURE 4.9 Position of the drops in an IMSI dish (A, D) 7.5%–10% PVP. (B, C, E) Culture medium. (A) Sperm selection PVP drops. (B) Sperm aliquots drops. (C) Host-selected spermatozoa microdrops. (D) Sperm immobilization drops. (E) Oocytes injection drops.

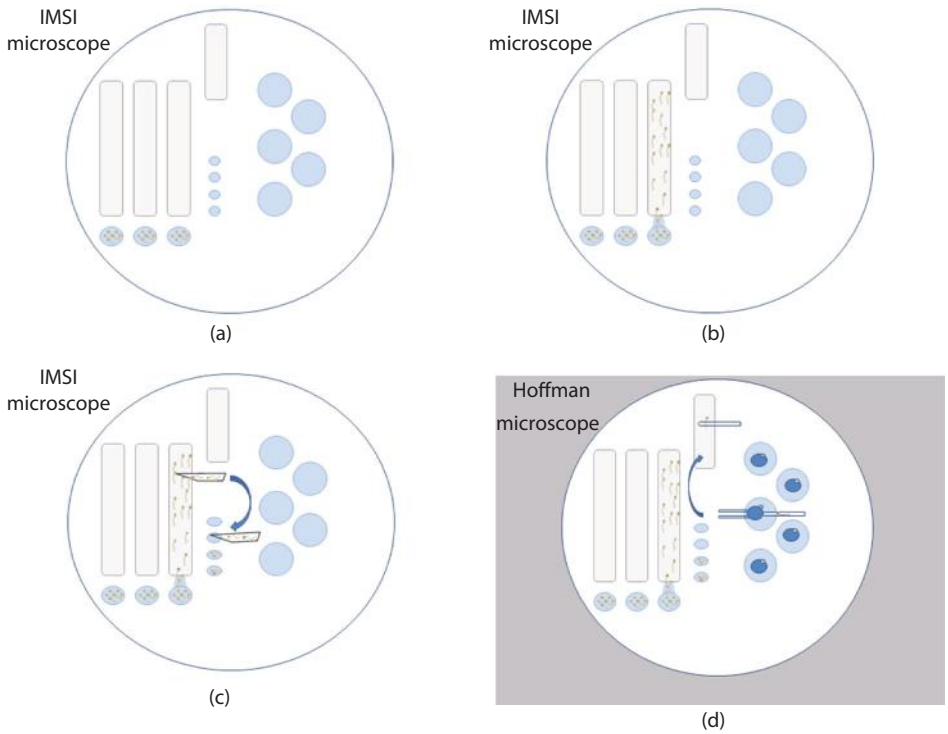

FIGURE 4.10 IMSI. (a–c) Description of the different steps for sperm selection on the IMSI microscope followed by (d) oocyte injection on the Hoffman ICSI microscope.

Chapter 5: Morphological Selection of Gametes and Embryos: Oocyte

Başak Balaban and Thomas Ebner

- Check the maturity stage of the oocyte after cumulus-corona removal.
- If the oocyte is at germinal vesicle (GV) stage, and if the patient does not have any other available mature oocytes, GV stage oocytes can be in vitro cultured for up to 24 hr. If the oocyte is in vitro matured, it could be used for microinjection procedure. However, the patient should be informed that the viability and the implantation potential of embryos derived from such oocytes are significantly lower than those of embryos derived from oocytes that are at metaphase II (MII) stage after oocyte collection. It is recommended to use only morphologically normal MII oocytes that are obtained after in vitro maturation of GV stage oocytes.
- If the oocyte is at metaphase I (MI) stage, it could be in vitro cultured and if MII stage is reached it could be used for microinjection. The patient should be informed that MI oocytes at the time of oocyte retrieval can have similar viability as MII oocytes if they can be in vitro matured for up to 6 hr post-collection. Same morphological recommendations for MII oocytes can be used for in vitro matured MI oocytes.
- If the oocyte is at MII stage, morphological deviations that should be examined with high priority are in the following order:
  - Oocytes that are large in size (giant oocytes), and oocytes that have a large first polar body should not be used for insemination because of the high risk of chromosomal abnormalities. If the patient has only such oocytes, preimplantation genetic screening for the derived embryo can be recommended.
  - Oocytes should be observed for the presence of smooth endoplasmic reticulum cluster(s) within the cytoplasm. The patient should be informed that embryos derived from such oocytes may have significantly reduced rates of healthy offspring.
  - Oocytes should be observed for the presence of vacuole(s) within the cytoplasm. Patients should be informed that MII oocytes with vacuole(s) ≥14 μm have a significantly lower chance of getting fertilized compared with oocytes with normal morphological appearance.
  - Oocytes should be observed for the presence of organelle clustering/centrally located condensed granulation within the cytoplasm. The patient should be informed that embryos derived from such oocytes may have a higher risk of chromosomal abnormalities.
  - Oocytes defined with other cytoplasmic deviations such as refractile bodies/cytoplasmic inclusions or with dark cytoplasm/dark cytoplasm–granular cytoplasm/dark cytoplasm with slight granulation/dark granular appearance of the cytoplasm/diffused cytoplasmic granularity should be documented.
  - Ovoid oocytes with ovoid zona and normally shaped oolemma, or ovoid zona and ovoid oolemma, should be observed because the blastocyst formation rate of embryos derived from such oocytes may be detrimentally affected and delayed.
  - Oocytes with extremely large perivitelline space (PVS) may result with reduced fertilization rates and higher degeneration rates after ICSI.
  - Dysmorphic zona pellucida, discoloration of the oocyte, first polar body morphology, and debris in PVS should be documented.

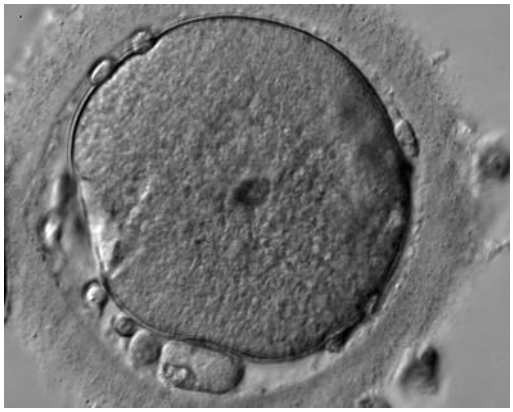

FIGURE 5.4 Oocyte with central refractile body and granule in the perivitelline space.

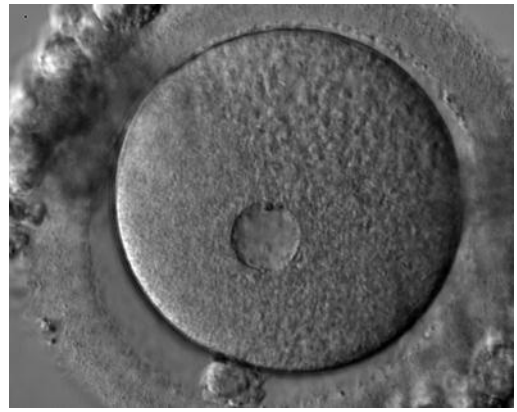

FIGURE 5.5 Vacuolized MII oocyte.

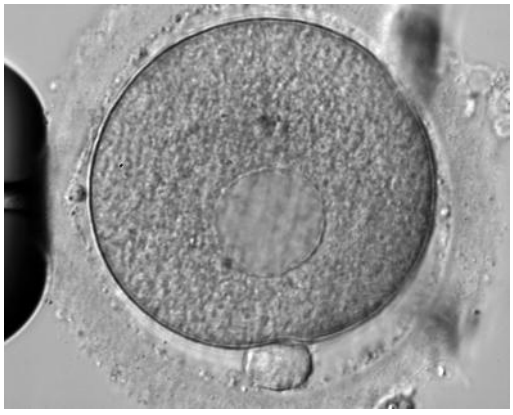

FIGURE 5.6 Oocyte with an aggregation of the smooth endoplasmic reticulum.

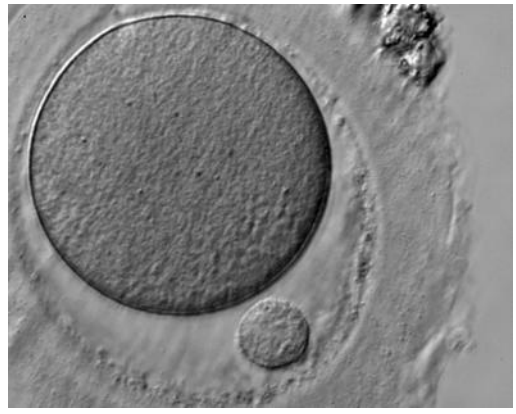

FIGURE 5.14 Metaphase II oocyte with large perivitelline space.

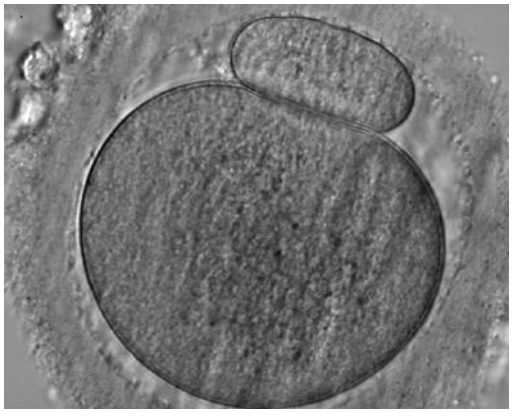

FIGURE 5.16 Oocyte with large first polar body.

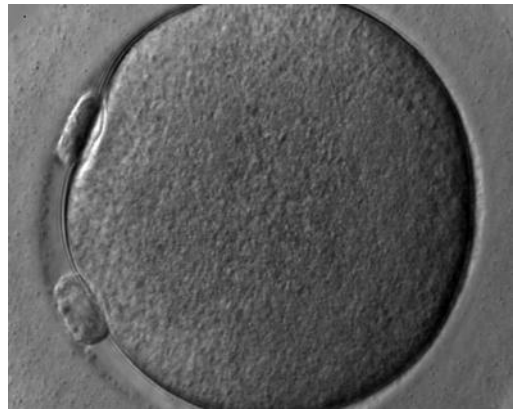

FIGURE 5.17 Diploid giant MII oocyte showing two first polar bodies.

Chapter 6: Morphological Selection of Gametes and Embryos: 2PN/Zygote

Martin Greuner and Markus Montag

- A regular fertilized oocyte shows in general two pronuclei.
- Pronuclear stage oocytes with three pronuclei or more after IVF or ICSI should be discarded and not be used for transfer or cryopreservation.
- Pronuclear stage with two pronuclei that are not of the same size or are not aligned in the center of the oocyte show a reduced development potential.
- Pronuclear stages with one pronuclei after ICSI should be discarded.
- Pronuclear stages with one pronuclei after IVF: if there are no other cells and the patient are informed about the situation it is possible to transfer them; however, there should be no cryopreservation.
- Criteria for the selection of the pronuclear stages as a function of the distribution of the nucleoli in the pronuclei.
- Always remember the development is time dependent and the correct timing is important.

It is not recommended to transfer or cryopreserve pronuclear stage oocytes with score Z4 or Rang 3.

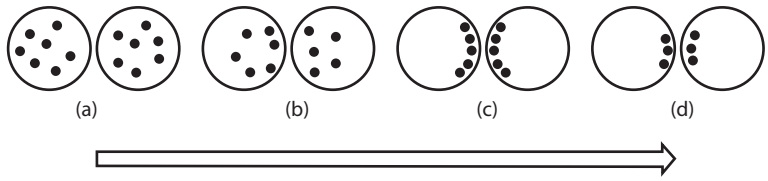

Rang 1/Z1-Score

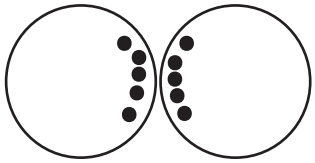

Rang 1/Z2-Score

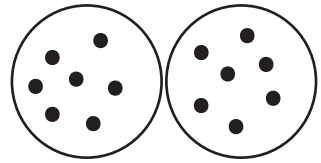

Rang 2/Z3-Score

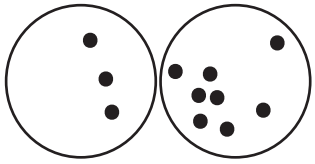

Z4-Score

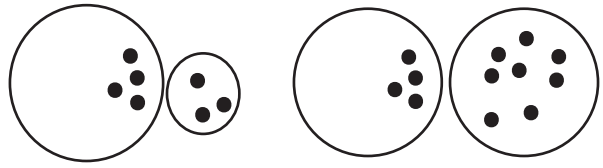

Rang 3 (ghost)

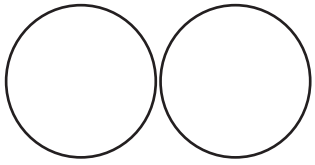

Rang 3 (bull eye)

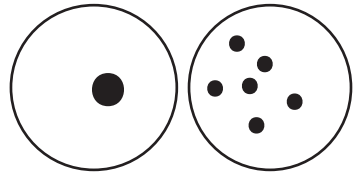

Chapter 7: Morphological Selection of Gametes and Embryos: Embryo

Gayle Jones and M. Cristina Magli

Day 1 At 26 ± 1 hr postinjection or 28 ± 1 hr postinsemination, the embryo should have completed the first mitotic division and resulted in a two-cell embryo with blastomeres of even size and have a single nucleus evident in each of the blastomeres. Embryos showing more than one nucleus per blastomere should be preferentially excluded from selection for transfer on subsequent days of development. At this stage, very little fragmentation is usually evident, and fragments observed at this time may be reabsorbed into the embryo, resulting in a different appearance on Day 2 of development.

Day 2 At 44 ± 1 hr postinsemination, the embryo should have completed the second round of cleavage, resulting in a four-cell embryo with blastomeres of even size and have a single nucleus evident in each of the blastomeres. Again, any embryos showing more than one nucleus per blastomere should be preferentially excluded from selection for transfer on this or subsequent days of development. Four-cell embryos showing ≥25% fragmentation should also be excluded from selection for transfer. Four-cell embryos showing more than one-third difference in cell size should be preferentially excluded from transfer on this and subsequent days of development. Embryos showing very rapid cleavage (more than five cells) or very slow cleavage (fewer than three cells) should be preferentially excluded from selection for transfer on this or subsequent days of development because rapid cleavage and slow cleavage have been linked to an increase in chromosomal aneuploidy. Three-cell or five-cell embryos at 44 ± 1 hr postinsemination showing stage-specific cell sizes may be suitable alternatives when no four-cell embryos are available for transfer, provided multinucleation has never been observed during development and fragmentation is minimal.

Day 3 At 68 ± 1 hr postinsemination, the embryo should have completed the third round of cleavage, resulting in an eight-cell embryo with blastomeres of even size. Eight-cell embryos showing ≥25% fragmentation or having a difference in size of more than one-third in any blastomere should be preferentially excluded from selection for transfer. Seven-cell embryos and nine-cell embryos at 68 ± 1 hr postinsemination, showing stage-specific cell sizes, may be suitable alternatives when no eight-cell embryos are available for transfer, provided multinucleation has never been observed during development and fragmentation is minimal. Very rapidly cleaving embryos and very slow cleaving embryos should be excluded from selection for transfer because these embryos are more likely to be chromosomally aneuploid. If an embryo is showing early signs of compaction, this is not detrimental to outcome.

Day 4 At 92 ± 1 hr postinsemination, the embryo should have entered the fourth round of cleavage, that is, be more than eight cells, and should be partially or preferably completely compacted. Embryos that have more than eight cells but that are showing no signs of compaction at 92 ± 1 hr postinsemination should be preferentially excluded from selection for transfer if a more ideal embryo is available. Embryos that have not entered the fourth round of cleavage should be excluded from transfer unless a more suitable embryo is unavailable for transfer. Embryos that are fully compacted and showing early signs of cavitation should be preferentially selected for transfer.

The criteria for each of the major morphological selection paramters are indicated in the heirarchical order for selection. The ideal embryo at each time of assessment is indicated in redand exclusion criteria are indicated in blue.

Time of Observation	Hierarchy for Selection				
	Cell Number	Cell Size	Fragmentation	Multinucleation	Compaction
26±1 hr postinjection or 28±1 hr postinsemination	• 2 cells • Syngamy • 2PN or >2 cells	• Stage-specific • Not stage-specific	• <10% • 10%–25% • >25%	• Single nucleus/ blastomere • No nucleus observed • >1 nucleus/ blastomere	• Cavitating
44±1 hr postinsemination	• 4 cells • 3 cells or 5 cells • <3 cells or >5 cells	• Stage-specific • Not stage-specific	• <10% • 10%–25% • >25%	• Single nucleus/ blastomere • No nucleus observed • >1 nucleus/ blastomere	• Completely compacted
68±1 hr postinsemination	• 8 cells • 7 cells or 9 cells • 6 cells or 10 cells • <6 cells or >10 cells	• Stage-specific • Not stage-specific	• <10% • 10%–25% • >25%	• Multinucleation observed in earlier development	• Partially compacted
92±1 hr postinsemination	• >8 cells • < 8 cells			• Multinucleation observed in earlier development	• No compaction

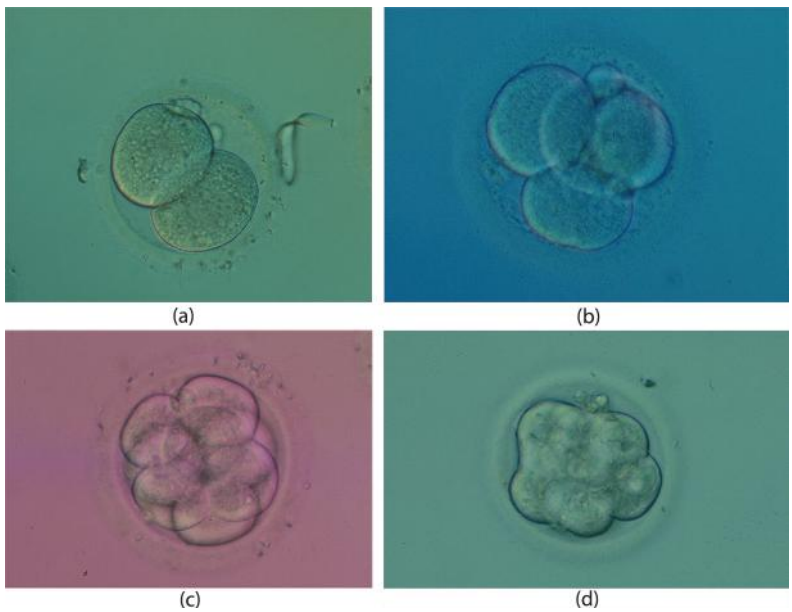

FIGURE 7.1 Examples of embryos showing normal cleavage kinetics and normal cytokinesis on Day 1 (a), Day 2 (b), Day 3 (c), and Day 4 (d). Original magnification, 300×.

Chapter 8: Morphological Selection of Gametes and Embryos: Blastocyst

Thomas Ebner

- If a clinical embryologist plans to change in vitro culture from a cleavage stage to a blastocyst transfer program, it is recommended to start working with supernumerary embryos to check whether culture conditions actually work properly. Thus, good prognosis patients with sufficient embryos in abundance should preferably be considered for training purposes.
- At least 40%–50% blastocyst formation rate should be used as KPI.
- In case blastocysts are available, an adequate scoring system is an absolute prerequisite.
  - It is of utmost importance to distinguish between trophoblastic vesicles ("pseudoblastocysts") and real blastocysts. Preceding cleavage behavior might give a clue.
  - The applied scoring scheme should at least deal with expansion as well as the quality of the inner cell mass and the trophectoderm.
  - There is growing evidence that in terms of live birth rate the quality of the trophectoderm outweighs the quality of the inner cell mass.
  - Additional morphological parameters should be noted, for example, presence of apoptotic areas, vacuoles, cytoplasmic strings, and exclusion of fragments and/or blastomeres.
- Spontaneous hatching is a positive predictor of implantation. Usually no artificial hatching is applied at blastocyst stage.
- Prolonged culture to Day 5 might be associated with the phenomenon of monozygotic twinning.
- An increase in birth weight has been observed in blastocyst transfers.

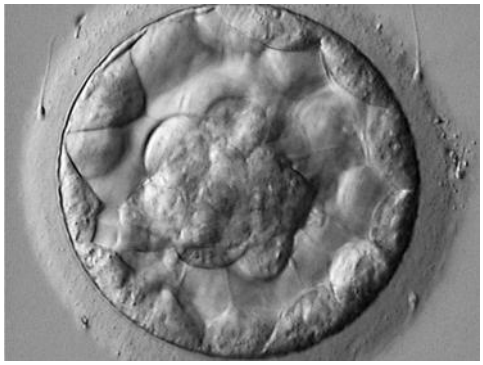

FIGURE 8.2 Full IVF blastocyst with optimal cell lineages (3AA).

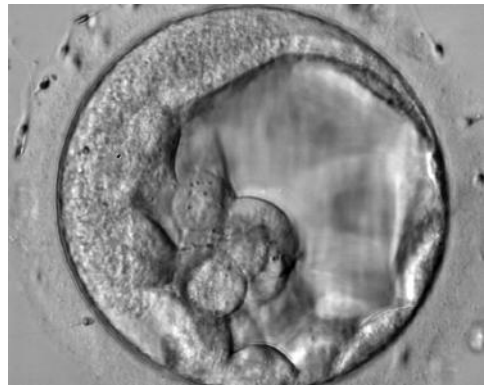

FIGURE 8.5 Suboptimal full blastocyst (3BC) developed after conventional IVF. Trophectoderm is not cohesive between 6 o'clock and 2 o'clock position. Inner cell mass consists of few cells only.

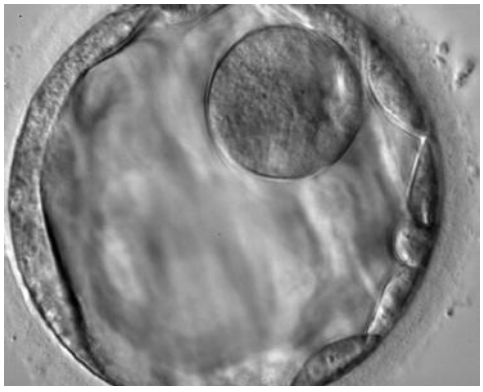

FIGURE 8.10 Expanded blastocyst of poor quality (4CB). Blastomere extruded into blastocoel should not be mixed up with inner cell mass.

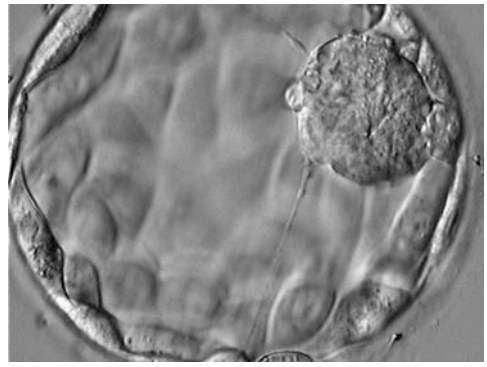

FIGURE 8.12 Expanded IVF blastocyst (4AA) with necrotic area in trophectoderm (8 o'clock position). Two cytoplasmic processes bridge the blastocoel.

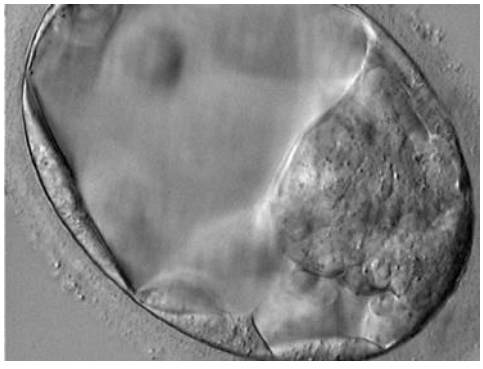

FIGURE 8.14 Expanded blastocyst of ovoid shape (4AB).

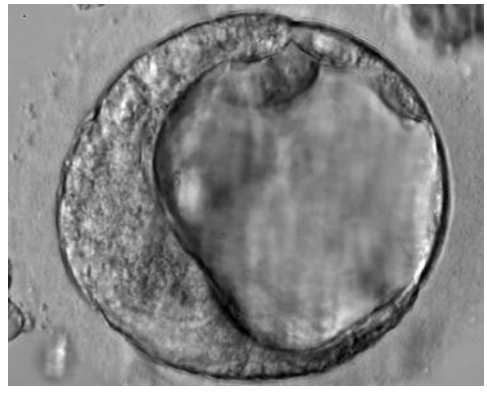

FIGURE 8.15 Pseudoblastocyst presumably consisting of <12 cells.

Chapter 9: Noninvasive Techniques: Gamete Selection—Sperm

Victoria Sánchez, Joachim Wistuba, and Con Mallidis

The ultimate aim of any sperm selection method is to provide the best quality sperm possible so as to maximize the outcome of whatever ART procedures are to be undertaken. For artificial insemination and IVF, the main requirement is the provision of a sample enriched with progressive motile sperm because these techniques are dependent upon the ability of sperm to find and penetrate the oocyte by themselves.

Numerous techniques have been developed to select the best possible sperm for ART. Although many of the described methods may be considered novelties and lack the robust verification and validation essential for routine clinical use, they nonetheless constitute a great improvement on the existing selection process that is solely dependent upon the subjective choice of the embryologists. The main disadvantage, however, is that although most of the techniques provide information upon which sperm quality can be better classified, the practical aspects of the procedures either destroy or alter sperm in such a way that renders them unusable for ART. Be that as it may, until the full potential of upcoming techniques based on advanced technology has been realized, the procedures described in this chapter, regardless of their limitations, represent the best options presently available to the ART clinic.

TABLE 9.1

Overview of Different Technologies Used for Sperm Selection

Technique	Emerging	Used	Diagnostic	Therapeutic	Studies
Polarization microscopy		X	X	X	2–4
MACS		X	X	X	9, 30
FACS	X		X		13
PICSI		X	X	X	31
HA medium		X	X	X	32
Zona pellucida binding		X	X	X	15, 33, 34
Zeta potential		X	X	X	35
Electrophoresis		X	X	X	21, 21, 23
Raman microspectroscopy	X		X		26–29

Note: HA, hyaluronic acid.

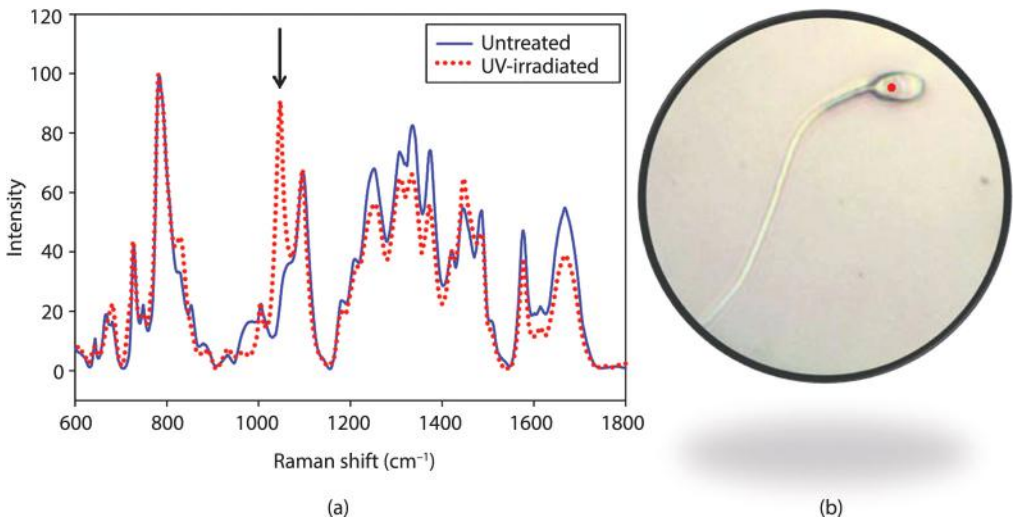

FIGURE 9.2 Raman spectroscopy for sperm. (a) Averaged Raman spectra from sperm (blue) and after ultraviolet (UV) irradiation (red). Arrow indicates main spectral feature in damaged sperm (peak at 1047 cm^{-1}). Spectra have been normalized, baseline-corrected, and smoothed. (b) Single-point Raman spectra are acquired from the post–acrosomal region of the sperm head. The red dot represents the position on which the laser is focused.

Chapter 10: Noninvasive Techniques: Gamete Selection—Oocyte

Laura Rienzi, Benedetta Iussig, and Filippo Maria Ubaldi

Early selection of oocytes is considered one major goal of contemporary IVF worldwide, allowing the identification of the most competent gametes to inseminate. In turn, this would help reduce the number of embryos produced in vitro and progress to single embryo transfer. Unfortunately, standard morphological evaluation is not precise, and a consensus is lacking. However, new noninvasive tools for oocyte selection are gaining increasing interest from the scientific community, from the more classic polarized light microscopy analysis to the evaluation of PFV and the ground-breaking OMICS technology. The results obtained so far are really intriguing and encouraging, but it would be wise to rise some concerns. For polarized light microscopy analysis, the contradictory results underline the need of more intense study to reach a consensus. For OMICS and, in part, PFV evaluation, the high costs, the difficulty of the techniques, and the time required for testing are limiting the routine applicability. Moreover, even if these approaches are all considered "noninvasive," we still need more evidence about the safety of the techniques (i.e., the possible effect of additional time required for each oocyte outside the incubator or unindicated removal of CCs and, as a consequence, ICSI performance). Finally, prospective randomized studies are required to determine their predictive power, alone or in combination with other factors, so that further efforts enrich our current knowledge.

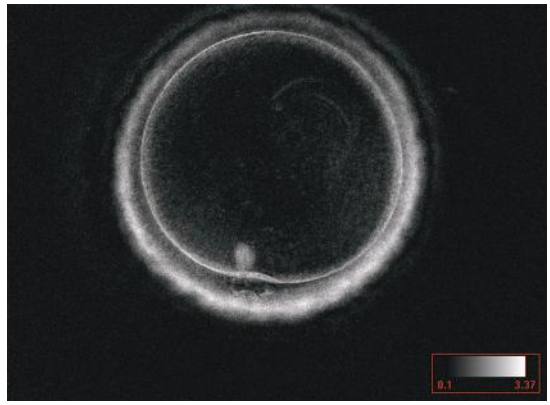

FIGURE 10.5 MII oocyte observed at polarized light microscopy (400× magnification). The birefringent MS is visible just below the extruded IPB at about the 6 o'clock position.

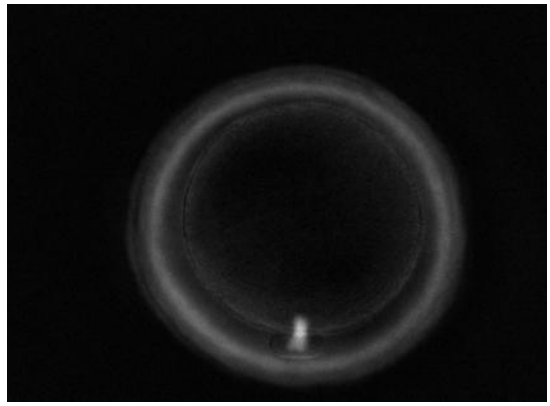

FIGURE 10.6 Telophase I oocyte observed at polarized light microscopy (400× magnification). The MS is visible at the 6 o'clock position. It is interposed between the extruded IPB and the ooplasm, indicating that the first meiotic division is not yet concluded.

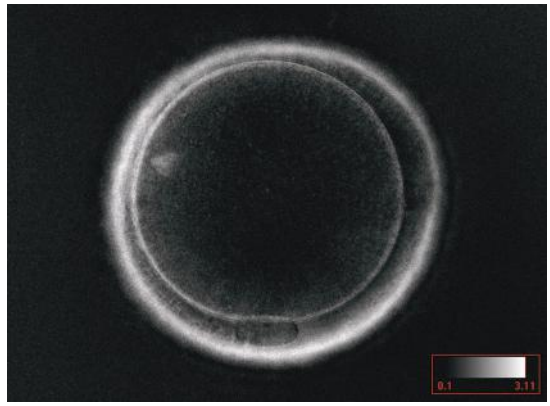

FIGURE 10.7 MII oocyte observed at polarized light microscopy (400× magnification). The MS is visible at the 9 o'clock position, and it is clearly dislocated about 90° from the IPB (placed at 6 o'clock position).

Chapter 11: Noninvasive Techniques: Embryo Selection by Oxygen Respiration

Alberto Tejera, Belén Aparicio, Carmela Albert, Arancha Delgado, and Marcos Meseguer

- Because the embryo development is directly related to a gamete's health, oxygen uptake could be a noninvasive marker of oocyte and embryo quality.
- Oocyte OC is affected by different ovarian stimulation regimens, and it increases 10% when we obtain a successful fertilization.
- OC levels vary depending on the embryonic stage.
- Best quality embryos show higher OC levels during embryo development, displaying a correlation between quality and OC.
- Higher levels of OC correlate with embryos that achieve implantation and give rise to ongoing pregnancy.
- There is a peak of OC during the first division, corresponding to a high energy demand period that is significantly higher in implanted embryos and defines cytokinesis as the best time period to consider OC as a marker of embryo quality.

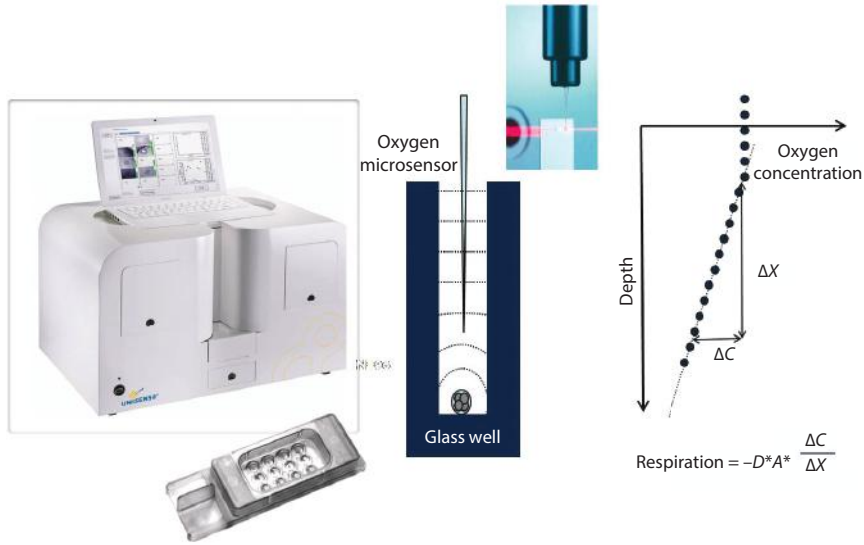

FIGURE 11.1 Schematic overview of incubator with a microsensor that can be used to measure the oxygen consumption through the gradient created by oocyte uptake, as explained in the text.

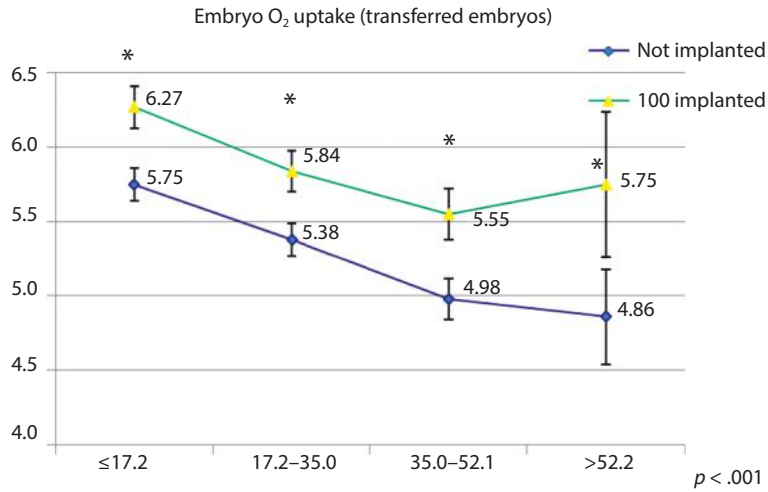

FIGURE 11.7 OC averages from transferred embryos in each of the four time ranges depending on implantation success. (*) indicates a significant difference ($p < .05$) between implanted embryos and nonimplanted embryos, with bigger differences from 52.1 hr post-ICSI.

Chapter 12: Noninvasive Techniques: Embryo Selection by Time-Lapse Imaging

Alison Campbell

Implementation and Routine Use of Time-Lapse Technology in IVF

Selection of a Time-Lapse System or Device

Before introducing a time-lapse system, the following should be considered to justify the decision: evidence base for positive impact on clinical outcome; opportunities for development and continuous improvement; device specification, for example, focal planes, image quality, and capacity; user friendliness; degree of validation conducted by the supplier and required in-house; certification and licensing (where required), limitations; space requirement; cost; customer support; servicing; and access to training.

Installation

Before installation, a detailed plan must be devised and approved that ensures that all requirements for installation of the equipment have been considered and that the laboratory and staff are prepared. Depending on the device selected, requirements may include gas supply, uninterrupted power supply (UPS), incubator capacity and accessibility, and space for additional hardware. A validation plan should be prepared to outline the process of qualifying the installation, operation, and performance of the time-lapse device before the introduction of time lapse for clinical use.

Practical Aspects

Standard operating procedure should be defined before the introduction of the time-lapse system for clinical use to which all users should acknowledge and adhere. As with any new technology, robust and rigorous training and quality assurance processes are required.

Dish or slide preparation methodologies must be established and practiced. The operating procedure should detail these methodologies, ensuring that the media and consumables to be used are appropriate and standardized.

Annotation guidelines, where required for nonautomated systems, must be defined strictly because it will be the accuracy of these guidelines downstream that could limit or support the development of embryo selection algorithms, based on the clinic's own data. This is crucial and buy-in of staff is essential. Users are encouraged to consider with care which morphokinetic variables, already defined or novel, should be routinely recorded and whether nonrecording assumes that a phenomenon was not seen. Table 12.1, within the body of the chapter, may assist with this task, and users are encouraged to follow consensus guidelines where they are available.

Time lapse allows great flexibility within the IVF lab. Monitoring of embryo development, traditionally performed at fixed times daily, can now be performed to suit the laboratory workflow. When manual annotation is required, it is advised that this annotation is performed regularly by a review of the images accumulated since the previous session of annotation. For flexible and efficient practice, annotation should be performed daily rather than at the end of the extended culture period, but users may find their own way of incorporating this annotation according to the workflow through their laboratories and find that it is dependent on the amount of morphokinetic variables to be recorded.

Quality Assurance and Review

Although the direct use of published algorithms for embryo selection may be desirable to new users, this practice may not be effective in varied settings, and as such, it is not recommended. The use of "known implantation data" from within the clinical setting is arguably the most robust method for developing embryo selection algorithms for in-house application. Regular review of time-lapse scientific literature is recommended, and communication with other time-lapse users may be beneficial, particularly during the early stages of implementation. Close monitoring of clinical results is necessary to ensure that the new technology is working well, and regular quality assurance activity will ensure that users are working in the same way.

TABLE 12.1

Summary of Morphokinetic Variables and Proposed Definitions

	Description
	Morphokinetic Variables
Time (t)	
t0	IVF or midtime of ICSI/IMSI
tPB2	The second polar body is completely detached from the ooplasm
tnPN	Fertilization status is confirmed
(tPN1a)	The first pronucleus is first visible
(tPN2a)	The second pronucleus is first visible
tPNf	All pronuclei have faded (see Figure 12.1)
t2-t9	Two (see Figure 12.2) to nine sequential, distinguished cells are present
tSC	The first two cells merge; initiation of compaction observed (see Figure 12.3)
tMx/w	Morula is formed or compaction goes no further; "x" corresponds to fully compacted, and "w" corresponds to partially compacted or cells excluded
tSB	The first sign of a cavity is observed as blastulation begins (see Figure 12.4)
tByz	Full blastocyst stage is reached; the last frame before the zona pellucida starts to thin; "y" corresponds to morphology of inner cell mass cells, and "z" corresponds to trophectoderm cells (see Figure 12.4)
tEyz	Initiation of expansion is confirmed; the zona pellucida starts to thin
tHNyz	Extrusion of cells from the zona pellucida is present
tHDyz	Blastocyst is fully hatched from the zona pellucida
	Calculated Variables
VP	tPNf-tPN1a (period of visible pronuclei)
Cell Cycle	
CC1	t2-tPB2 The end of the second meiosis to the formation of two discrete cells
CC2	The time for a two-cell embryo to form a four-cell embryo The two blastomeres (a and b) can be considered individually CC2a = t3-t2 CC2b = t4-t2
CC3	The time for a four-cell embryo to form an eight-cell embryo The four blastomeres can be considered individually. CC3a = t5-t4 CC3b = t6-t4 CC3c = t7-t4 CC3d = t8-t4
Synchronization	
S2	The duration of the transition from two sister cells, each dividing to reach the four-cell stage t4-t3
S3	As above, but from four to eight cells t8-t5
Duration of Compaction (Morula Stage)	
tMx-tSC	Full compaction
tMy-tSC	Partial compaction
Blastocyst Stage	
tHN-tSB	Duration of blastulation

Note: Each time point defines the time-lapse frame in which the phenomena described are first observed or recorded.

Chapter 13: Noninvasive Techniques: Embryo Selection by Transcriptomics, Proteomics, and Metabolomics

Asli Uyar and Emre Seli

Current embryo assessment strategies that rely primarily on embryo morphology and cleavage rate do not provide adequate sensitivity or specificity to achieve desired pregnancy rates in women undergoing infertility treatment with IVF. Studies using emerging technologies to analyze cumulus/granulosa cell transcriptome or spent embryo culture media protein or metabolite content report promising results. However, the transcripts or proteins that have been identified as potential biomarkers of embryo viability or the metabolomic profiles associated with pregnancy outcome have not yet been adequately validated. Therefore, the use of these novel noninvasive technologies remains experimental, and their application to clinical practice awaits randomized clinical trials demonstrating benefit from their use, alone or in combination with morphologic evaluation.

Key Messages

Omics research basically looks for answers to two questions: what distinct molecules and how many copies of each molecule exist in a biological sample?

Gene expression research evolved from single-gene analysis to genome-wide transcription profiling with the advance of microarray technology; however, next generation sequencing technologies provide an alternative transcriptomics approach called RNA Sequencing that appears to be a more precise detection and quantification of RNA transcripts.

Proteomics aims at (1) profiling proteome content of a biological sample, (2) performing comparative protein expression analysis, (3) localizing and identifying of posttranslational modifications, and (4) exploring protein–protein interactions.

Metabolome is the analysis of metabolites that are the final downstream products of gene expression, and in preimplantation embryo development, a distinct change in the levels of metabolites is expected to classify a "normal" development and a viable embryo.

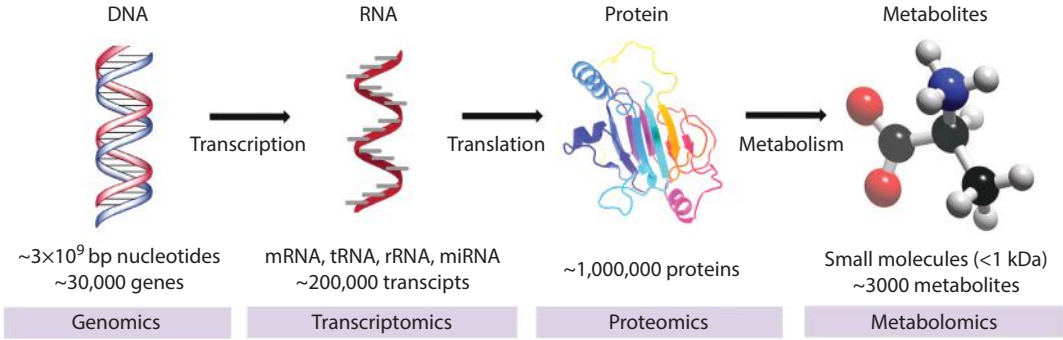

FIGURE 13.1 Omics approaches investigate the molecular constitution of biological samples at genomics, transcriptomics, proteomics, and metabolomics levels.

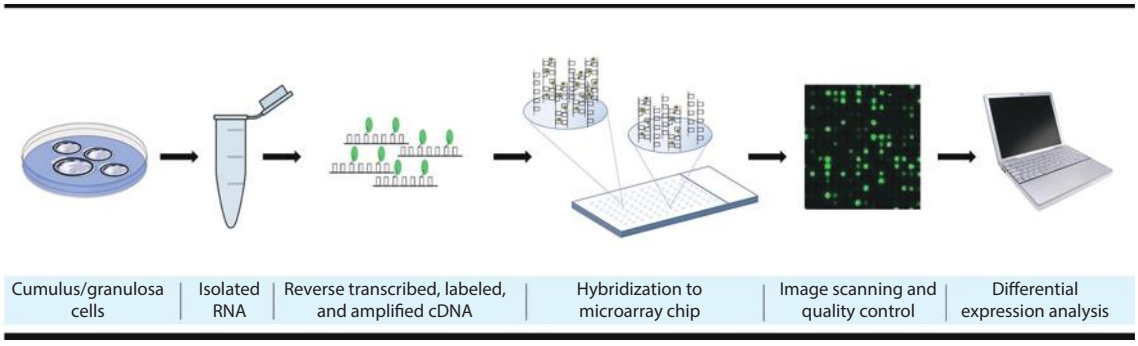

FIGURE 13.2 Major steps of a typical microarray experiment. Total RNA is extracted from the follicular cell samples, and mRNA is reverse transcribed into cDNA. Amplified and labeled samples are hybridized to a microarray slide, allowing the labeled targets to bind to their complementary oligonucleotides attached to the microscopic probes. The array is then washed and scanned to obtain the fluorescent image that is further processed to get the intensity values for differential expression analysis.

Chapter 14: Invasive Techniques: Polar Body Biopsy

Markus Montag, Jana Liebenthron, and Maria Köster

- Polar body diagnosis gives direct information about the first and second PB and therefore allows only an indirect diagnosis of the maternal genetic or chromosomal constitution of the corresponding oocyte.
- Polar body biopsy can be done by mechanical means using micropipettes for zona drilling or by using a laser for contact-free opening of the zona pellucida.
- The easiest and safest way of opening the zona pellucida is by laser.
- Although laser application seems easy, certain dead ends need to be avoided:
  - Openings in the zona pellucida should be large enough to enable undisturbed hatching at later stages.
  - Too small openings may trap the blastocyst during hatching.
  - Zona opening must be done at one site only: two openings will lead to blastocyst splitting or degeneration at the time of hatching.
- Timing of polar bodies is crucial for sequential as well as simultaneous biopsy.
- Too early biopsy in the presence of spindle remnants may lead to enucleation.
- Too late biopsy bears the risk of degeneration of PB1 and compromised quality of amplification (array-CGH) or signals (FISH).
- Transfer of polar bodies for subsequent analysis onto slides or into tubes is one of the most crucial steps of the whole procedure.
  - For FISH, always release polar bodies in the droplet on the slide at or close to the bottom to avoid floating and rupture.
  - For array-CGH, always release polar bodies in the fluid droplet on the bottom of the tube.
- Openings in the zona pellucida require precautions during all subsequent steps that involve pipetting or handling of the embryos.
- After zona opening, embryos do hatch earlier.
- Embryo transfer should be done smoothly due to the presence of the zona opening.

Summary
PB biopsy has been proven as sufficiently effective for the diagnosis of structural and numerical chromosome aberrations in human oocytes using FISH and array-CGH. Nevertheless, the use of PB biopsy and array-CGH for PGS is still a matter of debate due to cost effectiveness, the high incidence of postmeiotic aneuploidies that are undetectable by the polar body approach, and the debate on the accurate diagnostic procedure. There is growing advocacy for trophectoderm biopsy and array-CGH as the new gold standard.

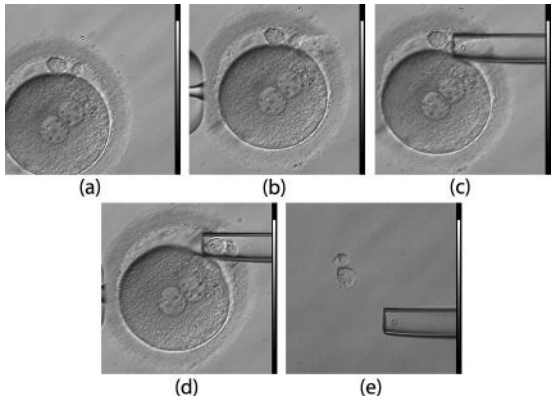

FIGURE 14.2 Laser-assisted polar body (PB) biopsy. For biopsy, the first and second PBs were aligned with a holding capillary so that the second PB faced to the biopsy capillary (a). Using a noncontact 1.48 µm diode laser, an opening was introduced into the zona pellucida using two or three laser shots (b) through which the biopsy capillary could be easily introduced (c). The second PB is usually connected to the oolemma via a cytoplasmic strand. To remove the second PB without damaging the oocyte, it is not recommended to suck the second PB into the capillary; instead, the capillary is pushed slowly over the second PB and toward the first PB (d). Once the first PB enters the capillary, the strand between the second PB and the oolemma will break due to shear stress and both PBs can be easily removed (d), leaving the oocyte without any damage. PBs should be placed in one droplet for further processing for FISH analysis (e) or in two different droplets if a PCR-based analysis will be performed.

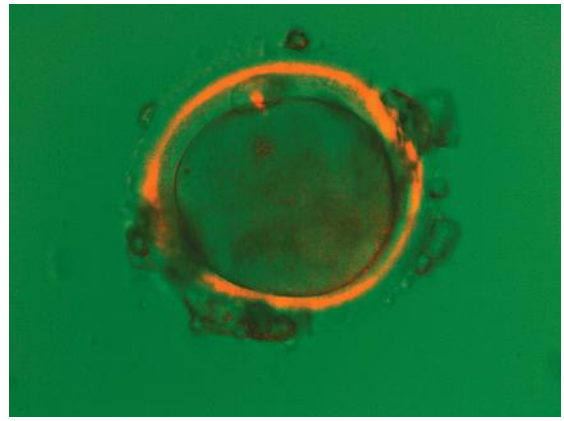

FIGURE 14.3 Presence of a meiotic spindle bridge between first polar body (PB1) and the oocytes. The presence of a connective spindle bridge can be assessed by polarization microscopy. Spindle fibers are displayed in red and characterize the corresponding oocyte as being in the transition phase from metaphase I to metaphase II. As long as spindle fibers are visible, chromosomes in the oocyte are attached, and the corresponding oocyte is in anaphase/telophase I. Removal of the PB1 shown would result in the withdrawal of chromatin material from the oocyte and could potentially lead to enucleation.

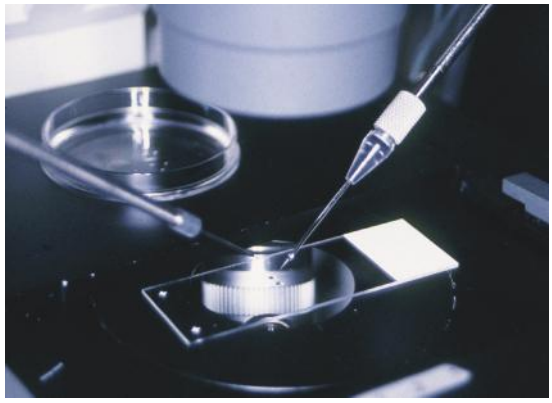

FIGURE 14.7 Transfer of isolated polar bodies (PBs) onto a slide. The transfer of isolated PBs from the dish (seen in the background) into the droplet on the slide must be performed on the microscope stage. The setup shown here allows sliding the dish used for biopsy backwards. Therefore, the aspiration capillary needs only to be lowered into the droplet for release of the PB. (Reprinted with permission from Montag M, *Textbook of Assisted Reproductive Techniques Volume One: Laboratory Perspectives*, 4th ed., Informa Healthcare, New York, 2012, pp. 336–345.)

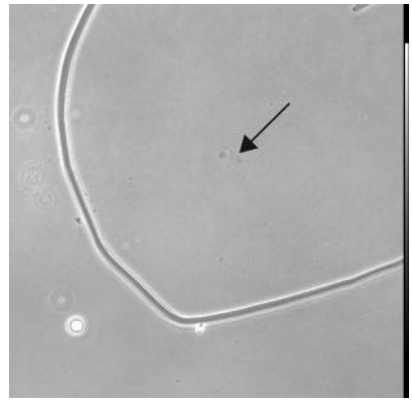

FIGURE 14.8 Identification of the polar body (PB) on the slide. This photograph is taken with a 10× phase contrast objective, and the diamond circle surrounding the PB can be partially seen. The PB appears gray (arrow). (Reprinted with permission from Montag M, *Textbook of Assisted Reproductive Techniques Volume One: Laboratory Perspectives*, 4th ed., Informa Healthcare, New York, 2012, pp. 336–345.)

Chapter 15: Invasive Techniques: Embryo Biopsy at the Cleavage Stage

Anick De Vos

- Cleavage-stage embryo biopsy still remains the most widely practiced method for embryo biopsy.
- Cleavage-stage embryo biopsy offers the advantage over polar body biopsy that the paternal contribution to the genetic content of the embryo can be analyzed.
- The use of ICSI avoids paternal contamination from sperm attached to the zona pellucida, whereas a careful oocyte denudation should avoid maternal contamination resulting from cumulus cells.
- One or two blastomeres are removed from the embryo in the morning of Day 3, at about 68–72 hr after microinjection, when the embryos are preferably in the eight-cell stage.
- It is common practice to include only embryos resulting from 2-pronuclear (2PN) normal fertilization. Embryos with <50% of anuclear fragmentation and with at least six blastomeres are suitable for biopsy. Preferably, the embryos have stage-specific cell sizes.
- Laser zona opening is most often used, although chemical zona opening using acidic Tyrode's solution or mechanical zona opening are still in use too.
- Aspiration is most widely used to remove the blastomeres.
- Ca^{2+}/Mg^{2+}-free biopsy medium can be used to facilitate the biopsy procedure by reducing the existing junctions between blastomeres.
- Care is taken to remove mononucleate intact blastomeres.
- Lysed cells are not used for PCR analysis because contamination with maternal DNA cannot be excluded. Occasionally, the nucleus can be recovered for FISH analysis. In cases of cell lysis, it is advised that the aspiration pipette is changed before continuing biopsy of other embryos as a safety measure to avoid cross-contamination.
- Postbiopsy, single embryo culture in individual droplets or individual culture dish wells is adopted to ensure tracking of blastomeres removed and easy identification of embryos postdiagnosis.
- Further embryo development should not be impaired as a result of the biopsy procedure.
- Supernumerary biopsied and diagnosed embryos can be effectively vitrified for later use.
- The invasive nature of the biopsy procedure on Day 3 should be recognized, and evidence exists that one-cell biopsy is less invasive than two-cell biopsy. Based on the observation and direct proof that blastocyst trophectoderm biopsy safeguards the developmental competence of the embryo even better, a shift toward blastocyst trophectoderm biopsy might be anticipated in the near future. As such, chromosomal mosaicism at the cleavage stage could be alleviated as well.

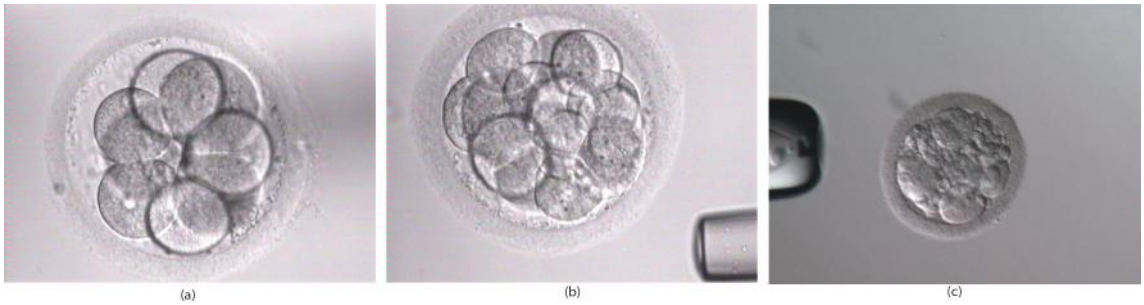

FIGURE 15.1 Cleavage-stage embryo biopsy is usually performed in the morning of Day 3. (a) Ideally, the embryos are in the eight-cell stage, having no fragmentation and showing stage-specific blastomere sizes. (b) An advanced-stage embryo on Day 3 with no fragmentation. (c) An embryo with more fragmentation (between 20% and 50%); however, it would still be included for embryo biopsy.

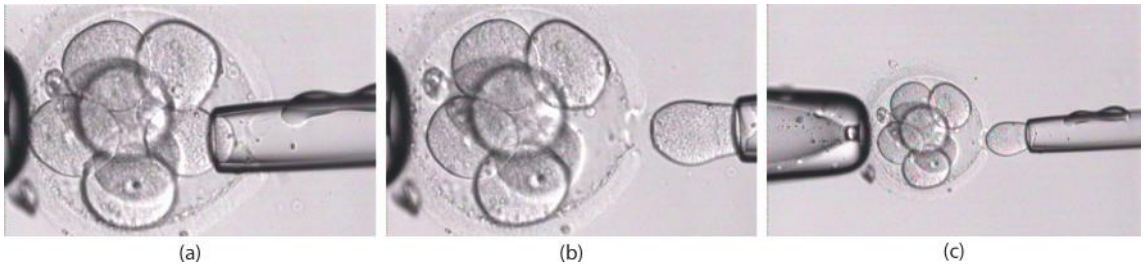

FIGURE 15.2 (a) For the removal of human blastomeres by aspiration, an aspiration pipette is introduced into the perivitelline space through the hole in the zona pellucida to reach a blastomere. (b, c) One blastomere is removed by gentle aspiration. Cells may be aspirated completely and then removed; alternatively, cells are only partially aspirated and pulled out (given full decompaction and thus no adherence to other blastomeres).

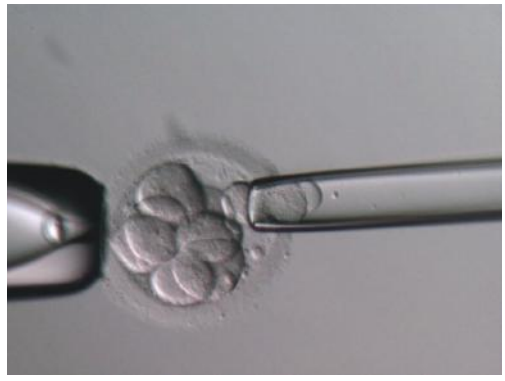

FIGURE 15.5 To be suitable for genetic analysis either by FISH or by PCR, the removed blastomere(s) should contain one single, clearly visible nucleus.

Chapter 16: Invasive Techniques: Blastocyst Biopsy

Steve McArthur

Blastocyst biopsy is preceded by embryo hatching on either Day 3 or on Day 5 or Day 6 of embryo development. Hatching on Day 3 of development ensures accessibility to a suitable hatching site with little risk of damaging any blastomeres.

Embryo Hatching

1. The hole in the zona pellucida should be made adjacent to the polar body, if identifiable; otherwise, hatch at a position where there is a space between the blastomeres.
2. The first pulse of the laser should be directed to the outer edge of the zona pellucida.
3. The third pulse of the laser should cut the internal wall of the zona pellucida in a direct line from the first laser pulse.
4. A hole in the internal margin of the zona of approximately 10 μm is created.
5. Embryos should then be washed before being placed back into culture dish.

Trophectoderm Biopsy

1. Ensure that the biopsy pipette tip and the leading edge of the trophectoderm are in focus.
2. Bring the biopsy pipette and touch the leading edge of the trophectoderm.
3. Draw a small number of trophectoderm cells carefully into the pipette using suction until a good hold is achieved.
4. Stretch out the trophectoderm (at this point, the blastocoel cavity may collapse).
5. Adjust focus until the margins of the targeted cells are in focus and fire the laser at the intercellular junctions. Fire the laser three to five times across the width of the trophectoderm cells to be biopsied.
6. Using suction on the mouthpiece and the holding pipette joystick, pull the targeted cells away from the blastocyst.
7. Release the piece of trophectoderm from the biopsy pipette.
8. Where the stretched trophectoderm tissue does not readily separate from the remaining embryo, it is not recommended to fire the laser excessively because this may be detrimental to embryo recovery. In these cases, a more direct “cutting off” method may be used.
9. Gently release the embryo from the holding pipette while maintaining hold of cells in your biopsy pipette. Do not take further cells into your pipette because this may result in excess cells being biopsied. Ensure the holding and biopsy pipettes are in the same focal plane, and rub the biopsy pipette across the end of the holding pipette. Take care not to damage the embryo protruding from the pipette as you carry out this step. If the first attempt is not successful, further attempts may be required.

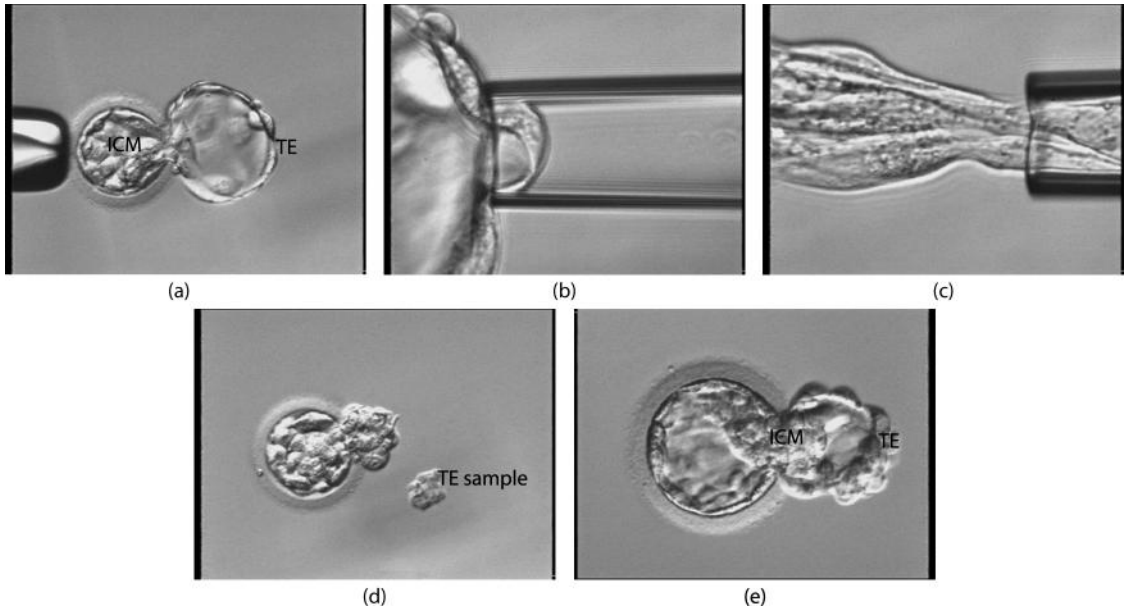

FIGURE 16.3 Photographs of blastocyst biopsy. (a) Blastocyst 2 days after laser-assisted hatching, consisting of herniating trophectoderm (TE) and inner cell mass (ICM). (b) Alignment of TE cells with biopsy pipette. (c) Three to ten cells aspirated from the TE while the ICM (destined to form the embryo proper) remains intact. (d) Blastocyst and TE sample. (e) Blastocyst approximately 90 min postbiopsy.

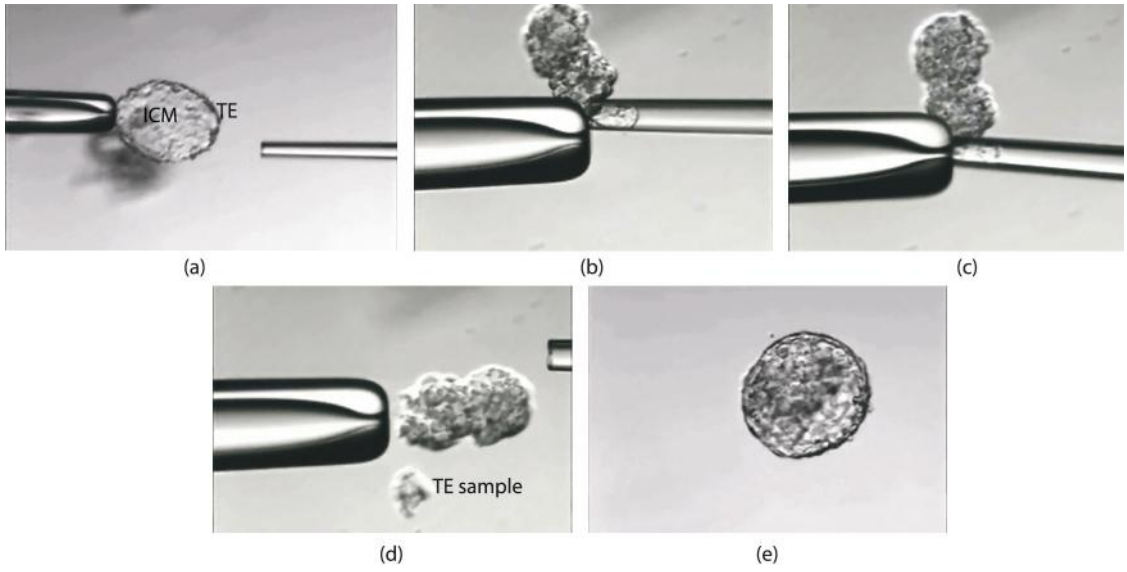

FIGURE 16.4 Images of fully hatched blastocyst biopsy. (a) Fully hatched blastocyst 2–3 days post–laser-assisted hatching; trophectoderm (TE) and inner cell mass (ICM) are labeled. (b) TE cells aspirated into biopsy pipette and contacted with holding pipette. (c) TE cells cut by shearing biopsy pipette against holding pipette. (d) Blastocyst and TE sample postbiopsy. (e) Blastocyst approximately 90 min postbiopsy.

Chapter 17: Invasive Techniques: Aneuploidy Testing by FISH

Semra Kahraman and Çağrı Beyazyürek

In the FISH technique, DNA probes that are labeled with different-colored fluorescent tags that are specific for chromosomal regions are hybridized to interphase nuclei or metaphase chromosomes.

Aneuploidy testing by FISH consists of the following steps: fixation of biopsied cells, pretreatment and probe application, denaturation, hybridization, stringent washing, and analysis after counterstain application.

The most critical step for FISH is the cell fixation; each cell should be informative and the loss of genetic material should be avoided.

The preferred method for fixation is by the hypotonic method that gives a larger diameter nucleus and decreased probability of signal overlap and nuclear loss.

Dehydration steps are common for blastomere and trophectoderm tissues and are done before hybridization to clean the fixed chromatin from the cytoplasm and any fixative artifacts that remain after fixation.

Denaturation prepares for effective hybridization and is mostly done with prelabeled, ready-to-use DNA probes.

Washing off unspecific bound probes is crucial to enable subsequent signal evaluation. The detection probes are labeled by fluorophores that may fade under light.

Evaluation of signals is performed in the dark area using a fluorescence microscope equipped with appropriate filters for the fluorophores used.

FISH can be performed at a relatively low cost, and the procedure is less complex. However, QC guidelines should be followed for every step from fixation to signal interpretation.

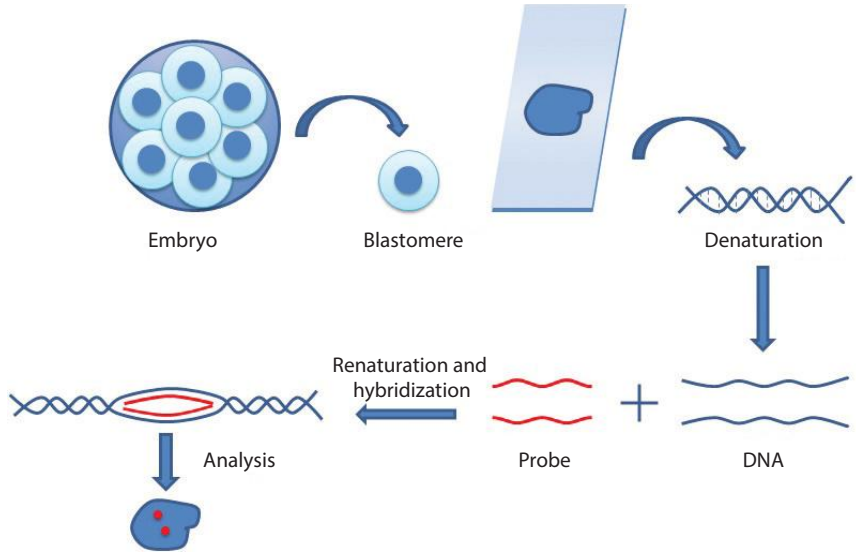

FIGURE 17.4 Steps of FISH.

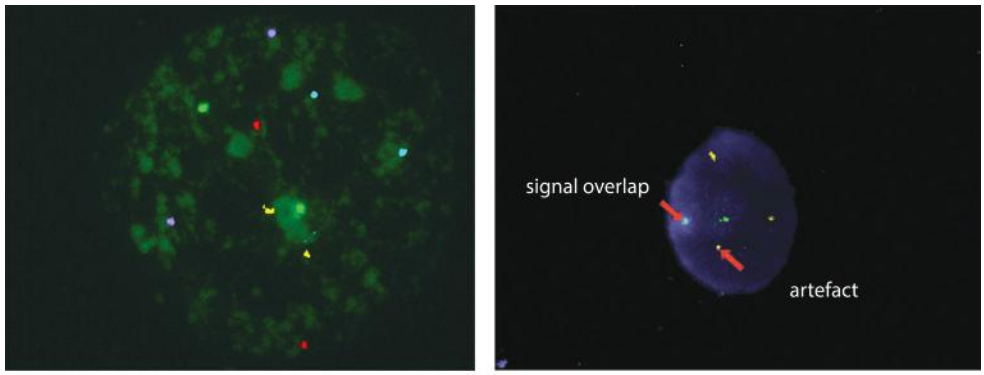

FIGURE 17.5 First and second round results of the same blastomere. (a) Normal for the first round study, including chromosomes 13, 16, 18, 21, and 22. Chromosome 13 (red), chromosome 16 (light blue), chromosome 18 (blue), chromosome 21 (green), and chromosome 22 (yellow). (b) Abnormal for the second round study, including chromosomes 15, 17, X, and Y. Chromosome 15 (yellow), chromosome 17 (aqua), chromosome X (green), and chromosome Y (blue). This blastomere was diagnosed as "monosomy 17." Notice that there is a signal overlap between aqua and one of the green signals. In addition, for the yellow signal, the signal at the bottom-middle is an artifact, evident from the color and the intensity. (Courtesy of Reproductive Genetics Laboratory, Istanbul Memorial Hospital, Istanbul, Turkey, 2009.)

Chapter 18: Invasive Techniques: Aneuploidy Testing by Array-CGH

Alan R. Thornhill, Christian Ottolini, Gary Harton, and Darren Griffin

Currently, array-CGH is considered the gold standard for detecting aneuploidy in single cells or multicellular samples from oocytes and embryos because of its reliability, reproducibility, and accuracy. In addition, it enjoys large worldwide experience (>250,000 clinical samples tested to date) and results can be obtained within 12 hr after biopsy.

A fundamental principle in applying aneuploidy screening is that the benefit gained should outweigh the harm, if any, caused. Thus, if the success rates of the program are already suboptimal, it is difficult to see any procedure providing sufficient benefit to rescue the cycle.

Noncontact laser technology is the primary choice for assisting oocyte and embryo biopsy. Proper preparation of the biopsied sample is of critical importance to ensure high diagnostic success rates, with a focus on the sterility of the working area and solutions, precise volume of buffer in the microcentrifuge tube, minimal carryover of embryo culture medium, and subsequent storage of the sample preanalysis.

Good laboratory practice, appropriate apparel, and a dedicated cleanroom, equipment, and consumables for amplification steps are mandatory.

A negative control of the embryo media and collection buffer should always be taken to check for the absence of contamination.

Laboratory-specific validation experiments are extremely useful before offering the service clinically.

For whole-genome amplification, a PCR-based method should be preferred to multiple displacement amplification (if working with 24Sure).

Care should be taken to ensure microarray slides do not dry out during hybridization and before washing. The high-temperature, high-stringency wash posthybridization must be temperature controlled.

Drying of the microarray slides is critical after washing, and the most effective way is to mechanically remove wash buffer by centrifugation.

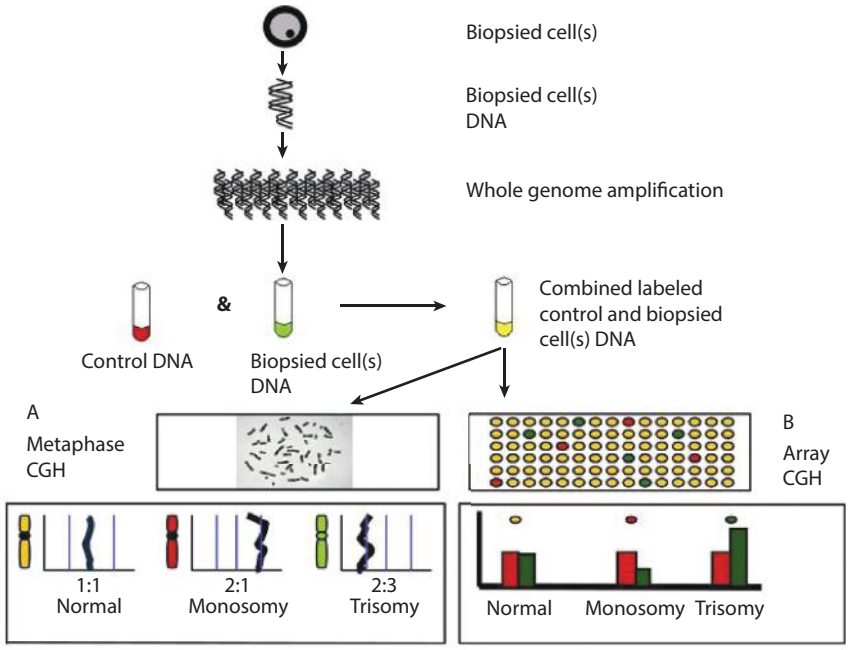

FIGURE 18.1 Schematic of comparative genomic hybridization.

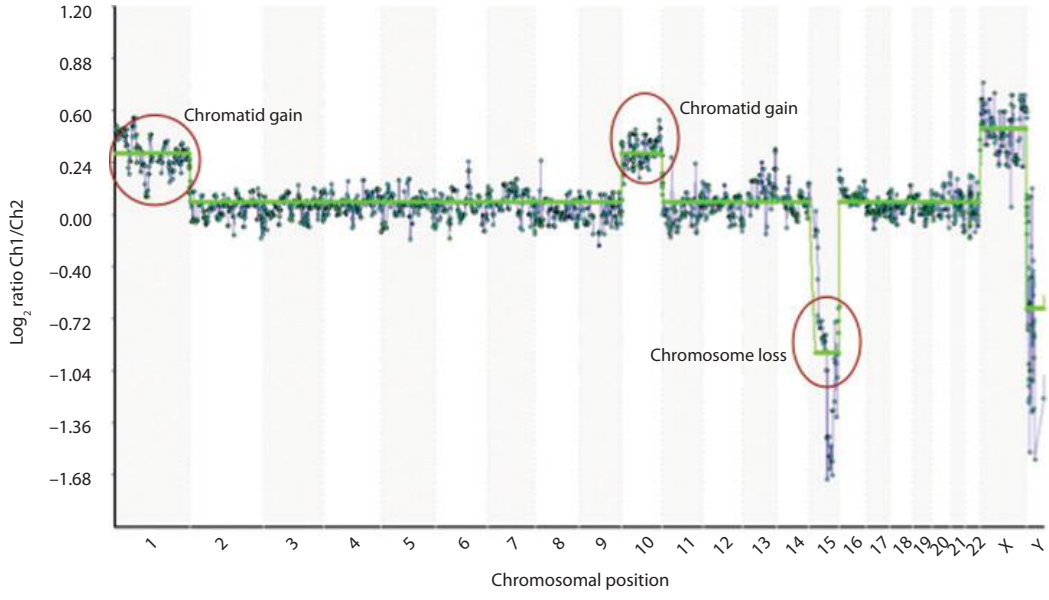

FIGURE 18.2 Determining chromatid versus chromosome loss in first polar body samples by aCGH. For most chromosomes (i.e., not the sex chromosomes or the aneuploid chromosomes), a clear and consistent 1:1 ratio is observed along the chromosome length. Because the polar body sample was cohybridized with male genomic DNA, a hybridization pattern representing a 2:1 ratio for the X chromosome and a "0:2" ratio for the Y chromosome is observed. This polar body clearly shows multiple aneuploidies with chromatid gains on chromosomes 1 and 10 (single chromatid gains are consistent with a 3:2 [or 1.5:1] ratio, i.e., approximately half that of the X chromosome shift) and a loss of whole chromosome 15 (similar to the shift seen for the absent Y chromosome).

REPRODUCTIVE MEDICINE

A PRACTICAL GUIDE TO SELECTING GAMETES AND EMBRYOS

Edited by
Markus Montag, PhD
iLabCoMM GmbH, International Reprolab Consulting
St. Augustin, Germany

Among the many recent advances in assisted reproduction therapies (ART), improved technologies for identifying viable oocytes, sperm, and embryos are of primary importance. Paradoxically, the latest advances presented at conferences and symposia are often slow to become part of the daily routine in IVF laboratories. Detailing established and developing techniques, *A Practical Guide to Selecting Gametes and Embryos* provides a user-friendly text of ready-to-use ARTs that can be utilized effectively in the lab.

In this volume, renowned embryologist and educator Markus Montag and his expert panel highlight sophisticated and proven selection strategies and emphasize the importance of proper lab practice in handling gametes and embryos.

Topics include

- Steps undertaken for the analysis of a semen sample
- Quality control and prevention of exposure to toxins in oocyte collection and embryo culture
- Morphological selection of gametes and embryos
- Both commonly used and innovative techniques for gamete and embryo selection, such as oxygen respiration and time-lapse imaging
- Invasive techniques, including polar body, embryo, and blastocyst biopsies as well as aneuploidy testing by FISH and array-CGH

Accompanied by numerous figures and descriptions, this guide to selecting gametes and embryos brings the insight of international authors with knowledge and expertise, highlighting practical tips and key points. The book offers a starting point for applying successful selection strategies for reducing the rate of high-risk multiple gestations while maintaining or increasing viable pregnancy rates.

CRC Press
Taylor & Francis Group
an informa business
www.crcpress.com

6000 Broken Sound Parkway, NW
Suite 300, Boca Raton, FL 33487
711 Third Avenue
New York, NY 10017
2 Park Square, Milton Park
Abingdon, Oxon OX14 4RN, UK

H100479
ISBN-13: 978-1-84214-547-0
90000
9 781842 145470